Thesis

2021

Khabat M. Ahmad

University Of Miskolc

Faculty of Earth Science and Engineering

Petroleum and Natural Gas Institute

"EFFECT OF MINERAL COMPOSITION OF THE CLAY CONTENT AND THE MICROSCOPIC TEXTURE OF THE POROUS RESERVOIR ROCKS ON THE PRODUCTIVITY OR INJECTIVITY OF THE HYDROCARBONS AND DEEP WATER WELLS"

Author's name: Khabat Mohammed Ahmad

Supervisor's name: Ass. Prof. Dr. Zoltán Turzó

Co-supervisor's name: Dr. Ference Kirstaly

Mikoviny Sámuel Doctoral School of Earth Sciences

Head of the Doctoral School: Prof. Péter Szűcs

Place: Miskolc, 2021

Supervisor's Certification

We certify that this thesis entitled (Effect of mineral composition of the clay content and the microscopic texture of the porous reservoir rocks on the productivity or injectivity of the hydrocarbon and deep water) was prepared under our supervision at the Department of Petroleum Engineering, Institute of Petroleum and Natural Gas, Faculty of Earth Science and Engineering, University of Miskolc in partial fulfilment of the requirements for the degree of Doctor of Philosophy in Petroleum Engineering.

Signature:

Supervisor: Ass. Prof. Dr. Turzó Zoltán

Date:

Signature:

Co- Supervisor: Dr. Ferenc Kristály

Date:

Signature:

Certification of Head of Doctoral School.

Prof. Dr. Mihály Dobroka

ACKNOWLEDGEMENT

I wish to express my deepest gratitude and appreciation to my supervisor, Dr. Zoltan Turzo, who showed me endless support and dedication despite his heavy load as a head of the institute and department in such times and current time as well. He always finds time to help and support me above and beyond his duties. Also, I would like to express my gratitude to the second supervisor Dr. Kirstaly Ference who was as a friend rather than a supervisor, I would like to thank for their continuous supervision, encouragement, kindness, friendly behavior and valuable help during my study. My endless thanks to Dr. Anita Jacob, head of *Research Institute of Applied Earth Science, University of Miskolc* and their staff, for giving me a chance to conduct petrophysical, initial permeability and core flood experiments at their laboratory. Thanks also go to the staff of the *Institute of Geology and Mineralogy* for their continuous support during XRD and SEM sample preparation and analysis. I would like to express special thanks for the administrative staff of *Institute of Petroleum and Natural Gas*. I am grateful to the entire staff and *Faculty of the Earth Science and Engineering* for sharing their knowledge and experience.

I would like to thank *Stipendium Hungaricum Scholarship* for their financial and academic support and for granting me this opportunity to complete my advance degrees. Special thanks to the Ministry of Higher Education- KRG- Iraq for giving me this chance to attend this study. Many thanks go to the MOL group- Hungary for providing adequate samples for my study.

Thank you to all of my friends for their continuous help, valuable advice, effective support and encouragement during the stages of my study.

Last but not least, I would like to thank my beloved wife, Shayan, and two daughters, Diyam and Diya, as without their dedication, help, love, patience and support the completion of my Ph.D. study would not be possible. My thanks and respects to beloved mother, brothers and sisters for their support and help.

This dissertation is dedicated to my wife, Shayan, my daughters. Thank you for loving me and taking care of me endlessly to go through my studies. I love you.

ABSTRACT

Variation of permeability related to fine particles migration is one of the most typical phenomenon that occurs in most oil and gas sandstone reservoirs. Fines migration is widespread in reservoir sandstones but frequently misinterpreted. It can be so difficult to identify and even more difficult to predict and interpret. This dissertation focuses on the change of permeability called "formation damage" as a result of fine particles migration (clay and non- clay minerals) related to changing pH and flow rate in core plugs from sandstone reservoir of Pannonian basin (Upper Miocene, Eastern Hungary). The main objective of core- flooding experiment was to investigate the effect of pH and the flow rate on stability of fine particles within the porous media. In addition, this study focused on the influence of amount of clay minerals, their size, type, composition and distribution as well as their effects on reduction of permeability and the degree of formation damage due to change of flow rate in the same pH rate. Furthermore, to study the effects of flow rate on permeability, three different flow rates have been used to investigate their influence on permeability variation. The selected core samples were examined by X-ray powder diffraction (XRD) for bulk mineralogy and clay mineral composition. The shape, position, distribution and type of clay minerals within the core samples were diagnosed by scanning electron microscopy and energy dispersive spectroscopy (SME- EDS). The basic petrophysical properties such as porosity and initial permeability were determined prior to experiments. The influence of pH and flow rate on permeability was examined through a series of laboratory coreflooding experiments, testing for different pH and flow rates (50; 100 and 200 ml/ h). This resulted in various changes to permeability from a substantial permeability decline at higher pH values to its increase at low pH. It had been shown that the total amount of clay fraction and its composition in the core samples had a significant effect on permeability along with pH and flow rate effects.

It is summarised that the results of this work could be extended to different petroliferous sandstone reservoirs.

Preface

This thesis is submitted to the *University of Miskolc* (UoM) for partial fulfilment of the requirements for the degree of philosophy doctor. The doctoral work has been performed at the *Faculty of Earth Science and Engineering*, *Institute of Petroleum and Natural Gas*, *Petroleum Engineering Department* under the supervision of *Asst. Prof. Dr. Zoltan Turzó* and *Dr. Ference Kristaly*. The research was sponsored by the Stipendium Hungaricum Scholarship/ Tempus Public Foundation.

During my study at the *University of Miskolc*, I am grateful for having been given the opportunity and experiences from wonderful people who offered their advices and inspirations. Nevertheless, without downplaying the role of others, on this occasion I will mention a few people who have contributed generously to my work.

At the top of my list, I would like to thank my supervisors, Asst. Prof. Dr. Zoltan Turzó and Dr. Ference Kristaly for the patient guidance, encouragement, and all the good discussions we have had through these years. I have been fortunate to have them as my supervisors who cared so much about my work and who responded to all my queries so promptly.

I would like to thank Peter at MOL who provided me with sandstone core plugs from one of the oil and gas reservoirs in the eastern part of Hungary and gave me opportunity to work with those cores. I would also like to thank the Head of Research Institute of Applied Earth Sciences Dr. Anita Jobbik for permitting me to conduct a part of my research at the Institute.

Special thanks go to Mr. Roland Docs and his colleagues who assisted me to conduct a part of research at the institute.

I would also like to thank Delia and her colleagues at the Institute of Mineralogy and Geology for their helping and recommendation during preparation the XRD and SEM samples.

I also would like to thank Professor Jeff Wilson and his wife Dr. L. Wilson for their recommendations and advising during the whole study.

Finally, I would like to thank my Wife Shayan and my family for their support and unconditional love.

Table of Contents

List of Tables

List of Figures

Chapter One

1.1 Introduction

Formation damage has become a frequent problem for petroleum reservoirs, ranging from exploration to output at different phases of reservoir development. The scale of the problem to the formation depends on the flow patterns, the rock characteristics, and the interaction between a rock as well as fluid. Wilson and Wilson (2014) defined formation damage "a decline in the initial permeability of the reservoir rock following various wellbore operations, which may be irreversible and which may have a serious economic impact upon the productivity of the reservoir". The percentage of formation damage is not only affected by fluid properties but is influenced by the rock characteristics and the interaction of rock-fluid as well. Formation damage will adversely affect both drilling operations and development, which directly effects on commercial feasibility Faergestad (2016). Formation damage is one of the consequences of oil and gas production. It refers to any process that decreases the permeability of the reservoir, and hence in a reduction in natural productivity of an oil and gas producing reservoir. This could occur through all activities involving production, drilling, hydraulic fracturing, and site preparation.

As stated in Amaefule (1988) "formation damage has become a costly problem for the oil & gas companies." Bennion (1999) defined the damage done by the formation as 'the weakening of the intangible and the uncontrollable, culminating in an indeterminate loss of the unidentifiable.' The reasons for damage to the structure include the invasion of objects, fine movement, pore deformation or collapse, and chemical precipitation. Wang (2005) defines formation degradation as "an unacceptable technical and financial issue that may appear in different phases of oil and natural gas extraction from underground reservoirs, including refining, drilling, work-over activities, and hydraulic fracturing." Formation damage may happen due to various conditions such as, chemical, mechanical, biological, physicochemical, hydrodynamic, and thermal interfaces of porous development, shear fluids Oluwagbenga (2015). Formation damage is one of the major challenges facing the oil and gas well; it is not a welcome situation or condition in the oil and gas industry. Laboratory and field studies indicate that almost every operation in the oil field is a potential source of damage to the formation hence reducing well productivity Krueger (1988).

Many factors are related to formation damage clay minerals content and physicochemical factors (pH, water salinity, flow rate, temperature and transport of fine clay particles within the reservoir rocks. The majority of rocks containing oil and gas produce clay minerals initially accumulated through sedimentation (detrital clay) or precipitated type fluid moving through the matrix (authigenic clay). Clay-mineral cement can even have different absorption effects because they take up different points inside the pore system. This loss of permeability is commonly referred to as formation damage and is related to the ionic composition and pH of the permeating fluids when caused by clays. The dependence of permeability on the composition of the flowing aqueous fluids is known as water sensitivity (Mohan, 1993).

The majority of formations, approximately 97% of all petroleum reservoirs, contain clay minerals. Theses clay minerals were either naturally occurring, originally deposited during sedimentation referred to as detrital clay, or precipitated from fluids within the matrix and referred to as authigenic clay. The presence of authigenic and detrital clays can cause loss of permeability by several mechanisms. The reaction of water with these clay minerals tends to cause fine particle dispersion and clay- swelling (Azari and Leimkuhler 1990). Inadequate prevention of these effects can lead to a significant loss in productivity by reducing reservoir permeability by more than 90%.

Most Sandstone formations contain a certain percentage of indigenous clays in their mineral composition which can potentially cause a severe reduction in reservoir permeability, due to swelling and/ or fine particle migration, hence, plugging interconnecting pore throats. Natural formations contain both swelling and non-swelling clays and the clay-related permeability loss due to foreign fluids in these formations can be attributed to more than one mechanism.

Reservoir rocks are susceptible to two general types of permeability damage. One type is due to the presence of swelling clays and dispersible clays, which results in mobilized clay particles in water-saturated rocks. Such clays are described as water-sensitive and damage resulting therefrom is described as water- sensitive damage. Another type of damage occurs due to particular production operations and is independent on mineralogy and texture of the rocks. Water- sensitive formation damage is a function of the type of clay mineral, distribution within the pore space, and fluid composition. All clay-water interactions such as clay-swelling and fine particle migration occur at pore- scale (Aksu 2015).

In addition to clay minerals, small particles which can lead to impairment of the permeability include quartz, carbonates and amorphous silica. These material easily can react with fluids injected within the porous media (Civan 1989).

Migration of fine particles, which usually consists of principally clay minerals, is often considered a major cause of formation damage. These clay minerals migrate as a consequence of Physico-chemical dispersion processes so, that fine particles physically break away during hydrodynamic flow. Eventually, the migration of those minerals may cause accumulation in pore throats, block fluid flow and thus reduce overall permeability. The role of individual clay minerals in causing formation damage through fines migration in North Sea sandstones was reviewed by Wilson et al. (2014) who concluded that kaolinite and illite, including mixed-layer illite/smectite (I/S), were the major culprits. Clay particles migration is the most common mechanism of permeability reduction in most sandstone formations because they contain little to almost no swelling clays.

One of the factors controlling the degree of formation damage is spatial clay distribution within the pore-structure, which for natural sandstones is related to the clay origin. Detrital, or allogenic clays originate as a dispersed matrix of sand/silt- size clay pellets, aggregated and clasts (Ali et al., 2010). Authigenic clays occur as loosely attached grain coatings, porous linings, porous fillings, pseudomorphous replacements, and fracture fillings, and have significant control over the quality of the reservoir. Despite their strong susceptibility to porous fluids, authigenic clays have a greater effect on the formation of damage than detrital clays that are heavily crowded in the rock conditions (Civan 2007).

Besides the type and spatial distribution of clay minerals, the fluid composition is another important variable that influences the degree of formation damage. A significant decrease in permeability usually occurs when water pumped is less saline than the formation water. Changes in the chemistry of the aqueous medium would change the amount of swelling and the type and number of exchangeable cations present between montmorillonite layers (Zhou, 1995).

Many factors are related to the formation damage due to clay minerals. These factors include Physico-chemical factors such as temperature, pH, water salinity, flow rate, clay mineralogy, and others, which affect the stability and transport of clay particles in the sandstone formation. The amount distribution pattern and morphology of clay minerals have significant effects on sandstone properties in terms of porosity, permeability, density, natural

radioactivity, electrical conductivity, the water content of petroleum fields, and reactivity to various enhanced oil recovery practice (Worden, 2003).

Specific clay-mineral cement may impact permeability differently since they fill-up different places inside the pore system. Clay minerals that are arranged tangentially to the grain surfaces have less of an effect on permeability than perpendicularly oriented clay minerals or clay minerals that sit within pores and pore throats. Thin clay layer on grain surfaces may have little effect on permeability unless they become interwoven in pore throats.

This study will attempt to characterize the clay mineralogy and other characteristics such as size, distribution, and location within the pores of selected reservoir sandstones. Together clay mineralogy and pore geometry give a better understanding of formation damage due to fines migration and swelling. An understanding of the complex pore geometry of sandstone reservoirs is a key to improved reservoir characterization. Recent advances in reservoir characterization have revealed the importance of mineralogical attributes that occur microscopically or at the pore level. Physicochemical methods will be applied for a more detailed characterization of migration starting with bulk rock mineralogy, including clay mineralogy, by X-ray diffraction (XRD).

However, quantitative assessment of the clay mineralogy of the rock is not the only important parameter concerning formation damage and other attributes such as chemical composition, morphology, location, and distribution of clay material must also be taken into account. These parameters will give a better understanding of formation damage. Scanning Electron Microscopy (SEM) will certainly enable a more complete picture to be obtained, particularly at the pore level where clay mineralogy will have the greatest impact on permeability and fluid flow (Al- Bazzaz and Kisr Engler, 2001).

In certain instances, disruption to the structure of petroliferous sandstone reservoir in the oil and gas fields is impossible to measure. This is attributed to the reservoir engineer's inability to collect precise samples and undertake comprehensive calculations on the region of concern, normally defined by a layer of rock covering the wellbore that is approximately several thousand meters just under the earth's surface. However, ongoing experiments and analysis over the years have allowed the creation of several strategies allowing the use of the available knowledge to achieve a much clearer understanding of the nature and degree of damage that various reservoirs might be susceptible to, thus changing working practices to seek and mitigate or reduce these mitigation factors. These data also included information

like log analysis, data from the special core analysis, information, and core data from fluid and PVT, cuttings.

1.2 Aim of the research

It is well- known that hydrocarbon-bearing siliciclastic reservoir rocks can be economically productive in the initial phases of exploitation but such productivity can quickly decline to a point where further exploitation is no longer economic. This is often attributed to "formation damage", a phenomenon which may have many causes. However, formation damage is most often attributed to dispersion and migration of fine migrated particles leading to their accumulation in and blocking of pore throats, thus resulting in decreases of permeability. Clay minerals, <2μm in diameter, are generally considered to comprise the majority of migrating particles, although fine-grained non- clay minerals for instance carbonates have also been implicated causing formation damage. In this investigation, it is intended to study the clay mineralogy of several Hungarian siliciclastic rocks of potential interest as hydrocarbon reservoirs and contrasting in their fabric and texture. In brief, the study will aim to: Investigate the influence of mineralogy on the permeability of typical sandstones of the Pannonian Basin, eastern Hungary as influenced by the effect of pH and flow rate.

a) Characterize the clay mineralogy of selected core samples by X-ray diffraction (XRD).
b) Characterize the texture and fabric of the selected samples by scanning electron microscope (SEM).
c) Determine the poro- perm (porosity and permeability) properties of the selected core samples in their initial state.
d) Determine the poro- perm properties of the selected cores, particularly concerning their permeability to water under various physicochemical conditions (water chemistry and flow rate).
e) Conduct experiments to determine whether formation damage effects can be ameliorated by treatments aiming to change the physicochemical conditions within the selected cores.
f) Following these experiments, conduct further SEM and XRD studies to seek evidence that fine particle migration is implicated in any adverse effects found on poro- perm properties.

g) Rationalize any differences found between the selected core samples of contrasting texture and fabric.
h) To describe the ongoing studies on the mechanisms of permeability reduction in sandstones containing swelling and non-swelling clays. To delineate the mechanisms of permeability reduction in reservoir sandstone due to changes of the aqueous composition, porosity, pore throat size distribution, and permeability.

Over the past decades, the scanning electron microscopy (SEM) has frequently been used as a tool in the study of reservoir rocks in terms of pore geometry, pore-size distribution, and presence of dispersed clays. The mineralogical analyses of the cores and the relative abundance of clay minerals were carried out by X-ray Diffraction (XRD).

The extent and severity of the formation damage depend on various factors, among which are initial porosity and permeability of the formation and the size of the invading particles. Therefore, different initial porosity and size of the invading particles are used to estimate the permeability and analyse the effects of the two factors on the permeability damage. Conclusive remarks and corresponding recommendations are presented at the end of this work.

1.3 Study Area

The Hosszúpályi gas field was discovered in 2001 and 13 reservoirs to found in Upper- Pannonian sandstone reservoir. Structurally is a faulted anticline with edge water drive reservoir type. This field was the biggest discovery in the past 20 years. It is located in the Northern Great Plain of the eastern part of the Great Hungarian Plain between the latitude 47° 23' 34.91" N and longitude 21° 43' 58.08" E (Fig 1.1). Its volumetric original gas in place (OGIP) was estimated at more than $5*10^9$ m^3 (Balogh, 2009). The upper permeability between 200- 2000 mD, lower permeability between 1- 50 mD. The porosity ranges between 17% to 23%. SPE Budapest Nov. 19, 2009. (http://webcache.googleusercontent.com/search?q=cache:JY_frvOrt_EJ:connect.spe.org/HigherLogic/System/DownloadDocumentFile.ashx%3FDocumentFileKey%3D8fc4e5cc-27cc-4584-9aef-1f966e5faa30%26forceDialog%3D1+&cd=1&hl=en&ct=clnk&gl=hu)

The focus of the study is on reservoirs zones encountered in three wells which include Hpi-D2; Hpi- D3; Hpi- D4, their respective location is listed in Table 1.0 and Fig. 1.1.

Figure 1.1: Location of the study area

(http://latitude.to/map/hu/hungary/cities/hosszupalyi/articles/page/2)

Table 1-1: Details of selected sandstone core plugs

Well Hpi-D2 depth (m)	Ordering Sample ID	Well Hpi-D3 depth (m)	Ordering Sample ID	Well Hpi-D4 depth (m)	Ordering Sample ID
1943.0	D- 2- 6	1868.9	D- 3- 2	1872.6	D- 4- 2
2140.3	D- 2- 5	1872.1	D- 3- 1	1874.0	D- 4- 1
2145.1	D- 2- 4				

1.4 Outline of the Chapter

This Ph.D. thesis begins by introducing general theory regarding formation damage and mostly referred to the presence of clay minerals and their stability in sandstone reservoir rocks at different salinity, pH, and flow rates.

This thesis is organized as follows:

Chapter one presents brief introduction to formation damage, the influence of clay minerals on stability on permeability impairment, especially underlying mechanisms of clay minerals instability and damage, which gives the background and objectives of the work. This is followed by a detailed literature review that describes mechanisms of formation damage and

the influence of physicochemical factors such as salinity, pH, and flow rate on the stability of clay minerals and their effects on permeability decline in sandstone reservoirs. Chapter two also describes some generalities of clay minerals and describes the effect of pH, and flow rate on the stability of clay minerals and their influence on petrophysical properties. The third is the heart of the work that gives a detailed description of the laboratory experiment, which includes a description of materials and apparatus, methodology, and procedures used. Chapter Four presents the results and discussion of the laboratory experiment and goes ahead to give a detailed discussion of the experimental results. Chapter Five lists the conclusions and recommendations for further future work.

1.5 List of Publications and Academic Activities:

1- EXPERIMENTS WITH X-RAY DIFFRACTION FOR SMECTITE PRESENCE ON MIXTURES WITH KNOWN COMPOSITION: IDENTIFICATION, QUANTIFICATION, AND LIMIT OF DETECTION FOR ARTIFICIAL "SANDSTONE", 70th Turkish International Conference, April 2017 (Oral Presentation). Khabat M. Ahmad[1,] Ference Kristály

2- An experimental study on the effect of High Temperature and High Pressure on the Properties of "GLYDRIL Water-Based Drilling Mud", 70th Turkish International Conference, April 2017 (Poster Presentation). Khabat M. Ahmad[1]

3- AN EXPERIMENTAL STUDY OF THE EFFECTS OF pH, SALT CONCENTRATION, AND TIME ON SANDSTONE PERMEABILITY CONNECTED CLAY MINERAL STABILITY, 31st International Oil and Gas Conference and Exhibition, Siofok, Hungary, 5-6 October 2017. *Khabat M. Ahmad, Ferenc Kristály[b], Zoltan Turzo[c]*

4- A laboratory study influence of pH, time, and non- swelling clay minerals effects on permeability in reservoir sandstone rocks, 5th INTERNATIONAL SCIENTIFIC CONFERENCE ON ADVANCES IN MECHANICAL ENGINEERING (ISCAME 2017) 12-13 October 2017 Debrecen, Hungary, Khabat M. Ahmad[1,] Ference Kristály.

5- Attending a Forum on November 2016 Miskolc University.

6- Attending a Forum on November 2017 Miskolc University.

7- EFFECTS OF CLAY MINERAL and Physico-Chemical variables on SANDSTONE Rock PERMEABILITY, Feb. 15, 2018, Khabat M. Ahmad[1], Zoltan Turzo[2], Ference Kristály, Roland Docs, http://ologyjournals.com/jogps/jogps_01_01_00006.pdf.

8- An experimental study to investigate the influence of temperature and pressure on the rheological characteristics of "Glydril" water-based muds. Journal of Oil, Gas, and Petrochemical Sciences, March 20, 2018, pp. 1- 10. http://ologyjournals.com/jogps/ (pp. 31- 35). *Khabat M. Ahmad, Zoltan Turzo[b], Gabriella Federer*

9- Laboratories study the effect of salinity, pH on permeability reduction in sandstone reservoirs, 5th Annual Student Energy Congress, International Conference ASEC 2018, 7th – 10th March 2018, Zagreb, Croatia.

10- INVESTIGATION THE ROLE OF FLOW RATE ON FINE PARTICLES MOBILIZATION AND INFLUENCING THE PETROPHYSICAL PROPERTIES OF SANDSTONE RESERVOIRS, EAST OF HUNGARY, Khabat M. Ahmad[1], Zoltan Turzo[2], Ference Kristály, Constantin Gh. Popa, Paper, and Poster Contest Xth Edition, 3- 6th, 2018. (Next activity).

11- Investigation of the role of flow rate on fine particles migration and influencing the petrophysical properties of sandstone reservoirs, east of Hungary, Khabat M. Ahmad[1], Zoltan Turzo[2], Ference Kristály, Interdisciplinary Doctoral Conference, 17 - 19th May 2018, Pecs, Hungary. (Next activity)

12- The Role of Flow Rate and Fluid Alkalanity on Fine Particles Movement and Influencing the Petrophysical Properties of Reservoir Sandstone, Khabat M. Ahmad[1], Zoltan Turzo[2], Ference Kristály, https:// www. garmian.edu.krd, http://passer.garmian.edu.krd/article_92575_a8830880677a4f53a7f05c857c2661b0.pdf, 29th Aug. 2019, Passer 2 (2019) 17- 21.

13- The Role of Flow Rate and Fluid Alkalanity on Fine Particles Movement and Influencing the Petrophysical Properties of Reservoir Sandstone, Khabat M. Ahmad[1], Zoltan Turzo[2], Ference Kristály, 6th Scientific Conference of Pure and Applied Sciences (SCPAS 2019) 10th to 11th April 2019, at Garmian University.

14- The influence of flow rate on formation damage at different pH, *Khabat M. Ahmad, Ferenc Kristály[b], Zoltan Turzo[c]*, Roland Dócs[d], GeoKurdistan IV International Conference 8th – 10th Oct. 2019.

Chapter Two

Literature Review

2.1Introduction:

The different topics discussed in this chapter which are essential to attain the objectives of this research work, these topics include mechanisms of formation damage, formation damage in sandstone, formation damage and clay stability, damage mechanisms of clay minerals, origins of clay minerals in sandstones, clay minerals, fines migrations, and petrophysical properties. This review will discuss the mechanism of formation damage generally and especially in sandstone reservoirs, the types of clay minerals, and their role in reservoir quality enhancement or reduction. Furthermore, an overview of the main petrophysical properties will be given and their importance in petroleum reservoir quality.

There are four primary mechanisms of formation of damage:

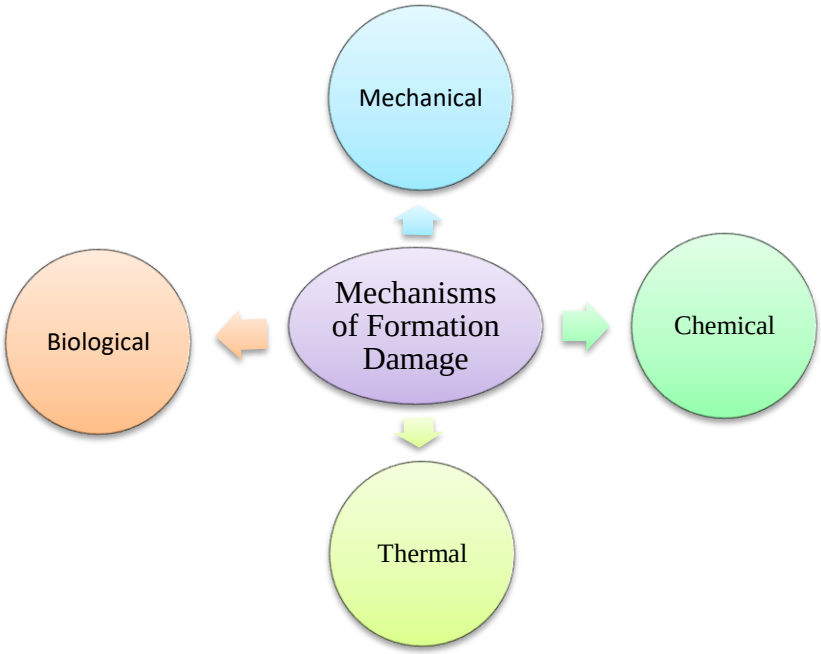

Figure 2.1: Flow chart of mechanisms of formation damage

2.2 Clay Minerals

Clay minerals are extremely fine particles, platy-shaped materials that may be presented in sedimentary rocks as aggregates of crystalline particles. The maximum dimension of typical clay particles is less than 0.005 mm or 5 μm (Mahmoud et al., 2011), which belong to the group of hydrous aluminum silicates and are usually considered to be less than 0.2μm in size. This is the realm of exceedingly small, crystalline particles dominated by planar arrays of SiO_4 and $Al(OH)_4$ structural units with adsorbed hydrated cations and water. These 'clay minerals' crystallize in the aqueous environment at the Earth's surface from the constituent ions released by the weathering of 'primary rock-forming minerals' such as olivines, pyroxenes, feldspars, mica, quartz, and others that were formed under extreme heat and pressure deep within the earth. Clay minerals possess fundamental soil properties such as cation exchange and the capacity to shrink and swell properties.

Clay minerals are hydrous aluminosilicates that belong to the phyllosilicate group of mineral Deer et al. (1988). The phyllosilicates are divided into 1:1- and 2:1- type minerals, based on the number of tetrahedral and octahedral sheets in the layer structure (Schulze, 2005). In addition to aluminum and silicon, they may also contain other cations, including alkali, alkaline earth, and transition metals. Clay minerals have a sheet-like structure in which the building blocks are either tetrahedral or octahedral linked to each other into planar layers by sharing oxygen ions between Si and Al ions of the adjacent tetrahedral or octahedral sheets (Bailey, 1980). The tetrahedral sheet results from the close packing of four O ions, with the space between them occupied by a Si^{4+} ion or, to a lesser extent, an Al^{3+} ion. The octahedra result from the close packing of six anions that are dominantly oxygen but also can include some hydroxyl (OH) ions. The Si and Al ions mainly occupy the space between the oxygen tetrahedra and octahedra respectively, but other cations, such as Fe, Mg, Ca, K are incorporated into the clay structure to ensure charge balance.

According to Gaupp (1993), there are five dominant groups of clay minerals in sandstones: kaolinite, illite, chlorite, smectite, and mixed-layer varieties. They are composed of tetrahedral and octahedral sheets which are bound together in layers that extend for tens to thousands of nanometres. Sandstone geochemistry and clay diagenesis involve multiple elements and not just alumina and silica. The oxides of iron, calcium, magnesium, and potassium are also crucial, as well as CO_2.

The interactions of clay minerals with aqueous solutions are the primary culprit for the damage of petroleum- bearing formations. The rock fluid interactions in sedimentary formations can be classified into two groups:

1- Chemical reactions resulting from the contact of rock minerals with incompatible fluids,
2- Physical processes are caused by extensive flow rates and pressure gradients.

Baptis and Sweeney (1954) used petroleum reservoir sands to measure air and water permeability, focusing on the type and amount of clay. They showed that sands containing kaolinite, illite, and mixed-layer clay (Illite/ Montmorillonite) were the most sensitive to water, while the sands with small amounts of kaolinite and illite were the least sensitive.

Among others, (Ohen and Civan, 1993) pointed out that fines migration and clay swelling are the primary reasons for formation damage measured as permeability impairment, pore filling clays, such as kaolinite, illite, chlorite, smectite and mixed- layer clay minerals, which are sensitive to aqueous solutions, could lead to formation damage. The majority of hydrocarbon producing formations contain clay minerals, and the reaction of low salinity fluid with these clay minerals tends to cause fine dispersion and clay swelling (Kaufman, 2008)

Clay minerals are especially susceptible to migration because of their physical size and surface properties. From further studies based on the work by Zhou et al. (1995) most clay minerals carry a negative surface charge when immersed in the aqueous solution of pH 5 and/or above. As a result of this negative charge, clay particles detach themselves from the matrix becoming susceptible to migration under hydrodynamic drag. From many laboratory tests and field cases, clay swelling has been continually proven to cause extreme damage to reservoir permeability.

Kaolinite and illite are non-swelling clays that tend to detach from the rock surface and migrate when water chemistry is conducive for release and dispersion. The migrating particles can get trapped in pore throats, thus causing a reduction in permeability. The depositional environment could be such that when the clay particles swell, they might cause the breakage of fines that are in contact with them. This mechanism is called swelling-induced migration. The three possible mechanisms of permeability reduction in sandstones

containing swelling and non-swelling clays are shown in Fig. 2.2. (Mohan and Vaidya, 1993).

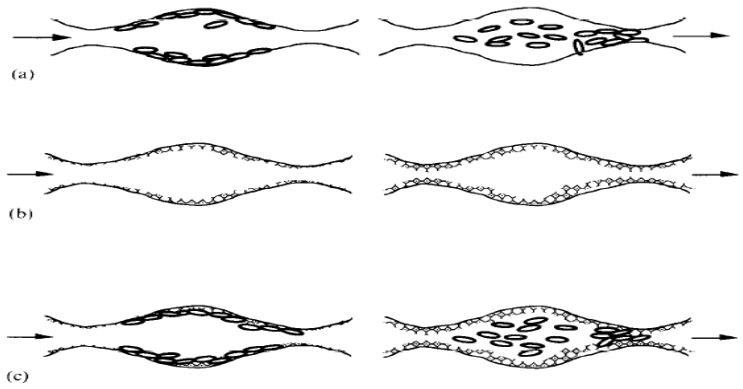

Fig. 2. 2: Mechanisms of permeability reduction

a- Fines Migration, **b**- Clay swelling, and c- Swelling-induced migration

Properties and damage processes of three clay groups can be classified as follows (Mahmoud et al., 2011):

1- Kaolinite has a two-layer structure, a small Cation Exchange Capacity (CEC), and is basically non-swelling clay but will easily disperse and move. Kaolinite platelets are thought to be some of the more common migratory clays. Damage from fines is located in the near-wellbore area within a 3-55 ft radius. Kaolinite can absorb some water, the adsorbed water is held tightly to the clay surface.
2- Montmorillonite (Smectite) has a three-layer structure, a large Cation Exchange Capacity (CEC) of 90 to 150 meq/ 100g and will readily adsorb Na^+, all leading to a high degree of swelling and dispersion. Smectite and smectite mixtures swell by taking water into their structure. The swollen clay can increase its volume up to 600%, significantly reducing permeability, by creating an impermeable barrier to flow. The removal of these clays can be accomplished HF treatment if the depth of penetration from the wellbore face is small. If the depth of penetration was large, the best treatment is to fracture the well to bypass the damage.
3- Illite has a three layers structure and is often interstratified with smectite. Therefore, illites combine the worst characteristics of the dispersible and the swellable clays. The illite is the most difficult to stabilize. Also, this type of clay can swell because, it adsorbs water. Osmotic swelling results from concentration imbalances between

the ions held at the exchange sites on the clays and the solute content of the contacting fluid.

2.2.1 Structure of Clay Minerals

Broadly speaking, clays are a subset of minerals that may be described as hydrous aluminum silicates. Clays generally form by the weathering and decomposition of igneous and other rocks MaCabe (1996), including shales. The term "clay" is applied both to materials having a particle size of fewer than 2 μm and to the family of minerals that has similar chemical compositions and common crystal characteristics.

Clay minerals consist of aluminosilicate layers, made up of Al-OH, Fe-OH, or Mg-OH octahedral sheets and Si-O tetrahedral sheets. These tetrahedral and octahedral; sheets can be arranged in two different ways: either in a 1:1 structure or a 2: 1 structure. The 1:1 structure consists of one tetrahedral and one octahedral sheet whereas 2:1 clay structure is made of two tetrahedral sheets that enclose one central octahedral sheet. These two types of clay structures are often denoted as T-O and T-O-T layers. The surfaces of the clay layers are negatively charged and the 2:1 layers can be neutralized by cations in the interlayer regions. Cations such as Na^{+} and Ca^{2+} are exchangeable under appropriate conditions. 2:1 smectite clays have an enormous potential to swell and are the subject of most of the clay swelling studies. The distance between two 2:1 layers, i.e. d_{001} spacing, is a function of the characteristics of the exchangeable cations, the composition of the solution. In the presence of water, interlayer exchangeable cations tend to hydrate and to increase the d_{001} spacing. This results in a volume expansion that is referred to as clay swelling (Grim, 1953).

The octahedral sheet contains magnesium or aluminum atoms in octahedral coordination with oxygen atoms and hydroxyl groups, while the tetrahedral sheet contains silicon atoms in tetrahedral coordination with oxygen atoms, as shown in Fig 2.3. The sheets making up the unit layer are covalently bonded together by sharing the oxygen atoms. Octahedral sheets link with one or two tetrahedral sheets, the resulting structure forming the precursor to different clay minerals. When some of the cations in this structure are substituted by other (usually lower valence) cations, different families of clay minerals are formed. Table 2.2 shows a major groups of clay minerals (Grim, 1953).

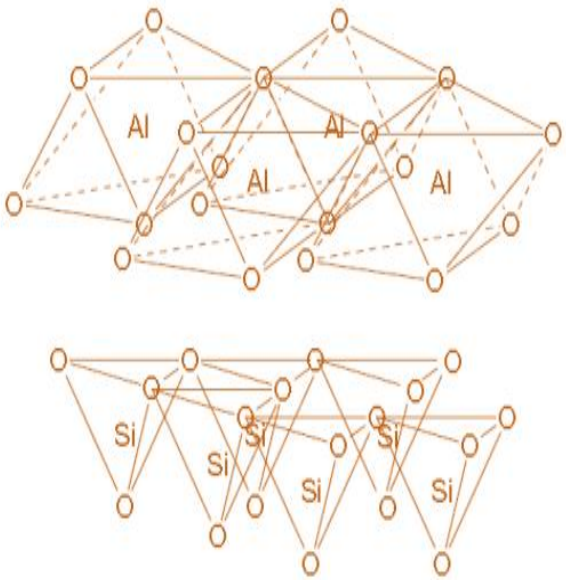

Fig. 2.3: Octahedral and tetrahedral layers in clays

Table 2. 1: Major groups of clay minerals (modified from Grim, 1953)

Group name	Member minerals	General formula	Remarks
kaolinite	kaolinite, dickite, nacrite	$Al_2SiO_5(OH)_4$	Members are polymorphs (composed of the same formula and different structure).
montmorillonite/ smectite	montmorillonite, pyrophillite, talc, vermiculite, sauconite, saponite, nontronite	$(CaNa,H)(Al,Mg,Fe,Zn)_2$ $-(SiAl)_4O_{10}(OH)_2 \cdot nH_2O$	n indicates varying level of water in mineral type.
illite	illite	$(K,H)Al_2(Si,Al)_4O_{10}(OH)_2 \cdot nH_2O$	n indicates varying level of water in mineral type.
chlorite	(i) amesite (ii) chamosite (iii) cookeite (iv) nimite	(i) $(Mg,Fe)_4Al_4Si_2O_{10}(OH)_8$ (ii) $(Mg,Fe)_3Fe_3AlSi_3O_{10}(OH)_8$ (iii) $LiAl_5Si_3O_{10}(OH)_8$ (iv) $(Ni,Mg,Fe,Al)_6AlSi_3O_{10}(OH)_8$	Each member mineral has separate formula; this group has relatively larger member minerals and is sometimes considered as a separate group, not as part of clays.

2.2.2 Types of Clay Minerals

The most common clay minerals found in sandstone reservoirs can be classified into five groups based on the features of crystalline structure. Research shows that different crystal structures of clay minerals to different behaviours of swelling and fines migration. Therefore, the knowledge of clay structure is necessary for a good understanding of mineral sensitivity.

2.2.2.1 Kaolinite [Al2Si2O5 (OH)4]

Kaolinite is one of the most common clay minerals. It occurs in abundance in soils that have formed from chemical weathering of rocks (aluminum silicate minerals like feldspar) (Fig. 2.4). Kaolinite is a non-swelling clay and the charges within the kaolinite structure are well balanced, and it, therefore, has a relatively low cation exchange capacity as shown in Table 3. The crystal structure is represented by a layered silicate (Si_2O_5) arrangement with one tetrahedral sheet linked through oxygen atoms to one octahedral sheet of alumina ($Al_2(OH)_4$). Kaolinites have very little isomorphous substitution in either the tetrahedral or octahedral sheets. The (T-O) 1:1 unit layer has little or no permanent charge because of o the low amount of substitution. Consequently, cation exchange capacity and surface areas are typically low. Soils high in kaolinite are generally less fertile than soils in which 2: 1 clay minerals dominate (Schulze, 2005). It has a low shrink-swell capacity and a low cation exchange capacity. It is soft, earthy, and usually white. The kaolinite group has three polymorphic members (kaolinite, dicktite, halloysite and nacrite) all with identical chemical compositions. The layers are bonded together by weak bonds existing between the silicate and alumina layers and occur as booklet shape and vermicules.

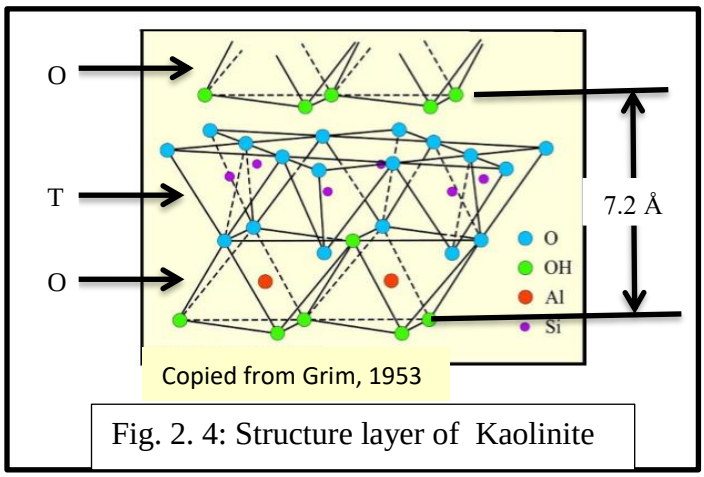

Fig. 2. 4: Structure layer of Kaolinite

Kaolinite is relatively stable, non- swelling, and not easy to hydrate; but easy to disperses and migrate under the action of external forces. During the migration of fine particles, these fines will block the pores or throats of the rock and then lead to a significant decrease in rock permeability. Authigenic clay minerals have more damaging effects on the reservoir because

they are formed by rock- fluid interactions in tightly packed sediments. Authigenic kaolinite together with some Illite material are the most common clay minerals encountered within the Sandstone reservoirs, (Beaufort et al., 1988). Kaolinite often occurs as pore-filling cement, however, the effects on the reservoirs are less pervasive unless it is changed to another form of clay minerals which is more damaging. According to Grim (1953) kaolinite is less common in ancient sediments than in younger sediments and thus inferred that it may have been converted to another form of clay minerals. Identification and separation of detrital kaolinite and authigenic kaolinite may be difficult, this difficulty can be mitigated using the XRD and SEM as detrital kaolinite is fine-grained and poorly crystallized when observed on thin section and SEM.

2.2.2.2 Illite: [(K,H3O)(Al,Mg, Fe)2(Si, Al)4O10[(OH)2 (H2O)]]

Illite is a K-rich dioctahedral clay mineral, also termed hydromica or hydromuscovite. It has a structure made up of tetrahedron-octahedron-tetrahedron (T-O-T) and termed a 2:1 structures (Fig. 2.7) (with a 10Å unit thickness, O-K-O interlayers connect two opposing tetrahedral layers. The interlayer K+ is required for charge balance accompanying the partial substitution of Al^{3+} for Si^{4+} in the tetrahedral sheet (Bailey S. , 1984). The O-K-O bonding is strong and prevents swelling behavior in illite and glauconite mica. Due to its small size, it usually requires XRD orSEM-EDS analysis for best identification. It is common in sediment, soils, argillaceous sedimentary rocks, and some low-grade metamorphic rocks. The cation exchange capacity is higher than that of kaolinite but lower than that of smectite. Illite can occur as flakes, filaments, or hair-like structures lining the pore walls (Fig. 2.5).

Through intergrating careful core preservation, critical- point drying, and SEM, it can be seen that illite has numerous morphologies, both natural and artificial (Raman, 1995). The petrophysical properties of reservoirs containing illite depend significantly on the technique of core preparation, but commonly, illite collapses upon air-drying resulting in porosity, high permeability, and low capillary pressure. Whenever illite gets in contact with fresh water, it increaes low porosity, low permeability, and high capillary pressure. Illite has also shown high vulnerability to migrate, it remains dispersed and is taken with the flowing fluid until the particles are trapped in pore restriction.

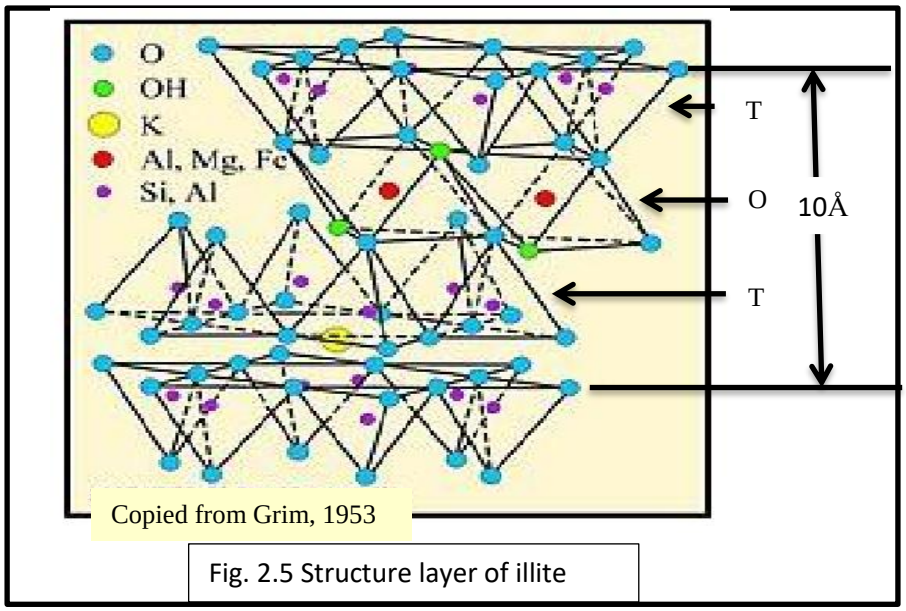

Fig. 2.5 Structure layer of illite

2.2.2.3 Chlorite (Mg, Al, Fe)12 [(Si, Al)8 O20](OH)16

Chlorite has a 2: 1: 1 structure comprising negatively charged 2: 1 layers. Tetrahedral- octahedral- tetrahedral layered with an additional octahedral sheet that is positively charged and is comprises of cations and hydroxyl ions (T-O-T). Chlorite group minerals are often derived from the alteration of ferromagnesium- rich minerals in metamorphic rocks and encompass a group of minerals characterized by a wide range of chemical and structural variation (Fig.2.6) (14Å).

Chlorite has a relatively small surface area and cation exchange capacity. It is a common metamorphic mineral, usually indicative of low-grade metamorphism, and is associated with hydrothermal ore deposits. Different Chlorite group minerals include: clinochlore (Mg-rich chlorite), chamosite (Fe-rich, nimite (Ni-rich), and pennantite (Mn-rich) are (Bayliss, 1975). The most common iron cations in chlorite are Fe^{2+} or Fe^{3+}, the most important is that iron-rich chlorite will react with acid and generate precipitates under acidic conditions this precipitation fills the pores in the rock and finally lead to severe damage in reservoirs. Iron-rich chlorite is an acidic- sensitive mineral. Chlorite can weather to form vermiculite or smectite, and the ease with which chlorites break down makes them sensitive indicators of weathering (Schulze, 2005).

The relation between chlorite cement and reservoir quality have been identified years ago, previous studies have shown that chlorite cement is a major cause of anomalous porosity and permeability, especially in deeper reservoirs sandstones (Bloch, 2002). Aside from the formation of chlorite from fluid-rock interaction in ferromagnesian rich rock, authigenic

smectites and kaolinite are also probably to be transformed into chlorite. The dissolution by acid could potentially lead to the formation of pre plugging iron hydroxide precipitation.

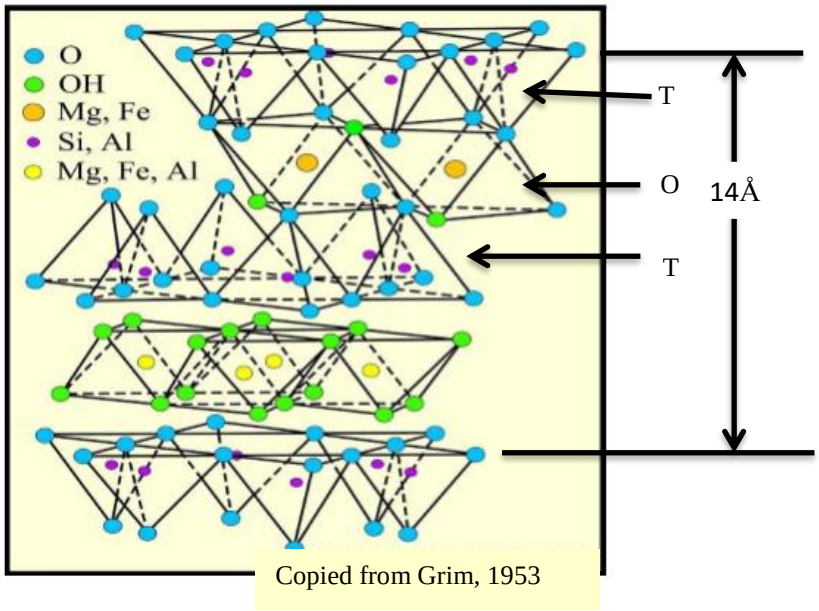

Fig. 2. 6: Structure Layer of Chlorite

2.2.2.4 Smectite [(0.5Ca, Na)0.7 (Al, Mg, Fe)4 (Si, Al)8 O20 (OH)4 . n(H2O)]

Smectite is a soft clay that typically forms in microscopic crystals. Smectite is a 2: 1 clay element placed between two tetrahedral sheets and one octahedral layer (T-O-T). Trioctahedral smectite has octahedral sites dominated by divalent metals (Fe^{2+}, Mg^{2+}), whereas dioctahedral smectite has octahedral sites dominated by trivalent metals (Fe^{3+}, Al^{3+}). The layer is balanced completely by exchangeable cations located in the interlayer space so that the whole structure is electrically neutral, and adjacent 2:1 layers are held together only by van der Waals force.

When smectite exposed to low ionic- strength aqueous solutions, the interlayer cations in smectite will adsorb a lot of water molecules to form the thick envelope of water film around clay particles. This process will cause a visible increase in the space between crystal layers and thus lead to clay swelling. Under the effect of fluid flow, moreover, smectite clay will split along the cleavages into thin layers. These fines will further coagulate and migrate with fluid flowing in rock pores (Zhao, 2017).

Interlayer cations are variably hydrated, resulting in the swelling characteristics of smectite clay minerals (9.6- 18Å). Smectites are defined by their tendency to swell when exposed to organic solvents, which can be absorbed between interlayers. Smectite usually occurs as

flakes curling up from an attachment zone on the detrital sand grain surface as shown in (Fig. 2.7). Smectites have non-equivalent substitutions of atoms that generate a negative charge on each layer surface, which is balanced by exchangeable interlayer cations. These cations are responsible for the differences in the physicochemical behavior of smectites such as water absorption and retention, plasticity, and swelling, among others (Schoonheydt and Johnston, 2013). Thus, smectites are recognized as the most heterogeneous class of minerals with a pronounced variety in reactivity. Montmorillonite has a very high cation exchange capacity (CEC).

Smectites are often progressively transformed to chlorite and illite through a mixed-layer structure, such as smectite/illite or smectite/ chlorite. Examples of this have been observed in the North Sea where most smectites occur in the shallowest of the reservoirs and subsequently transformed into other clay minerals as deeper depth. Smectite is most often unstable at temperatures greater than 60 ^{0}C and tends to convert to illite presumably because of their metastability, although smectite has been found in high- temperature environments. Smectites are characterized by properties of unique cation exchange capacity. They have been reported to be major contributors to reservoir damage when in contact with freshwater because of the large surface area and swelling capacity exhibited by smectite. The larger the surface area and swelling capacity of clay minerals, the more severe they tend to reduce the permeability of the reservoirs, the reservoirs that have a reasonable degree of smectite cement often display poor quality, the accommodation of interlayer water which causes smectite to swell always has a damaging effect on the porosity and permeability of reservoirs. Early formation of smectite before fluid migration in any reservoir impedes fluid flow by chocking the pore throats due to swelling when it comes in contacts with water.

Three different origins of authigenic smectite have been proposed, these include a reworking of weathering products in surficial soils and transient sediment deposits, marine alteration of volcanic minerals, early diagenesis smectite resulting from different authigenic processes during eo-diagenesis (Chamley, 1994). Authigenic smectite, especially nontronite have been formed by hydrothermal influence via mixing and cooling of hydrothermal brines with ocean water and by fixation of K. Detrital and authigenic smectite can occur in sandstones and they are a good source of transformation for other diagenetic processes including illitization, quartz cementation, and zeolite formation.

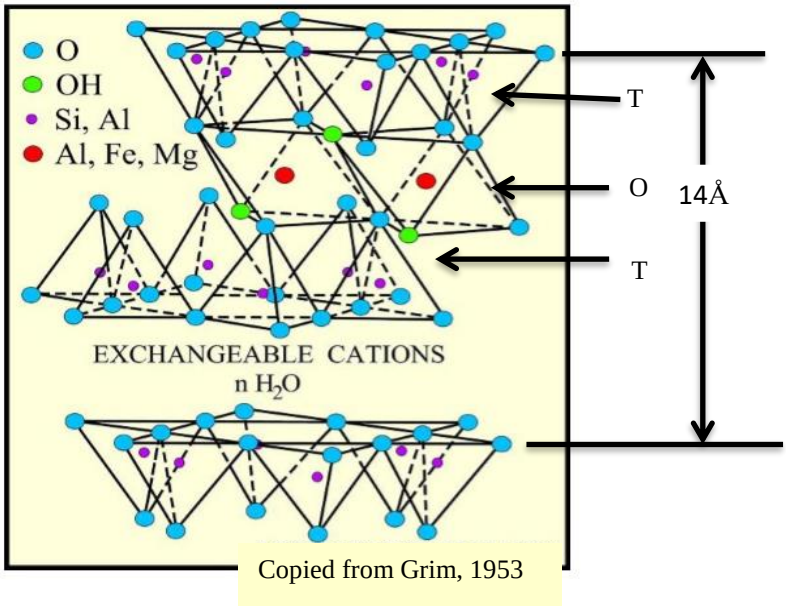

Fig. 2.7: Structure layer of Smectite

2.2.2.5 Interstratified Clay minerals

Interstratified clay minerals result from the interstratification of different mineral layers in a single structure such as illite- smectite, chlorite- smectite, illite- vermiculite, chlorite- vermiculite, illite- chlorite (Srodon, 1999). According to Velde (2008) interstratified clay minerals refer to remarkable phyllosilicate structures, characterized by a vertical staking sequence of two or more types of single layers which involved a 2:1, 2:1:1 and even 1:1 types. Interstratified clay minerals are common, and consist of clays that change from one type to another through a stacking sequence. Typical peaks for interstratified clay minerals between 11- 14 Å.

2.2.3 Occurrence of clay minerals in petroleum reservoirs:

The occurrence of clay minerals in petroleum reservoirs has great influences on the flowing of fluids. Based on the shape of the clay mineral aggregate in rock pores and the influences of clay minerals on petrophysical properties of reservoir rocks, the occurrence of clay minerals can be divided into three types, as shown in Fig. below.

1 Patch type (Discrete particle type)

Discrete types are shown in (Fig. 2. 8 a), means the occurrence of clay minerals, like "disperse patches," packs in the rock pores. Locally the pores become narrow and micropores between the clay particles are well developed. For instance kaolinite, a few needle-shaped mica, etc., are common. As a result, fines migration easily arises because of the effect of high- speed fluids.

2 Pore- lining type

Pore- lining types of clay minerals are shown in (Fig. 2.8b), in this occurrence clay minerals lining the pores, arranged parallel to the grain surface with the grains wrapped partially or fully. This type of occurrence belongs mainly to illite, chlorite, montmorillonite, etc. Fines migration generally is rare, but hydration and swelling are very common.

3 Pore- bridging type

In this occurrence, clay minerals, like hairy or fibrous clays such as illite and chlorite, easily form bridges in pores between grains (Fig.2.8c). The bridges in pores are easily broken off by the shock of fluids through the pores. As a result, fines migration occurs along with the flow of fluids. Micropores in such type of occurrence are easily developed. In this way, the resistance of fluid flowing through the rocks is much increased. The permeability of the rock to fluid is thus, remarkably decreased. In most cases, there is not only one type of occurrence of clay minerals in sandstone reservoirs. It is very common several occurrences coexist in reservoirs. It should be noted that the occurrence of clay minerals usually has a serious effect on the petrophysical properties of reservoir rocks.

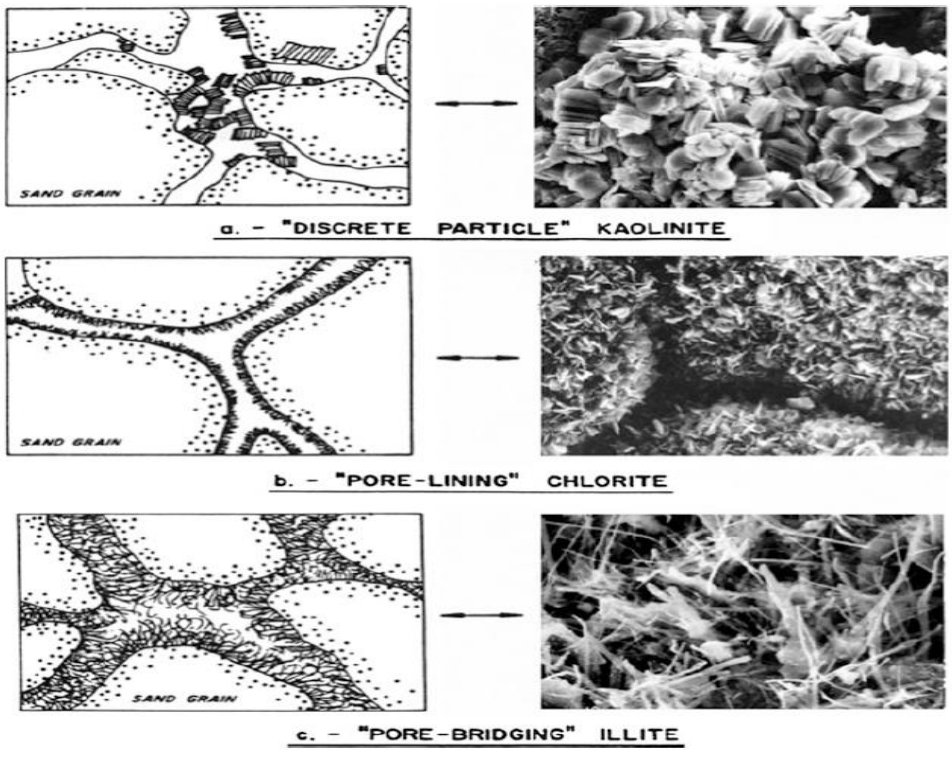

Fig. 2. 8: Occurrence of clay minerals in sandstone

Kaolinite is the most common clay minerals in sandstone reservoirs; it often fills in the pores. The potential impact of kaolinite on reservoirs is as follows:

a- Kaolinite fills intergranular pores, and thus turns original intergranular pores into tiny intercrystalline pores. Tiny intercrystalline pores contribute little to the permeability of rocks. Rock permeability is thus, visibly decreased.
b- The adhesion of kaolinite aggregate to the surface of the rock particles is weak. Under the shear stress of fluids through the rock, kaolinite aggregate easily crashes or falls off from the surface of rock particles, and move with fluid in rock pores. Consequently, the pores or throats of the rock could be severely blocked.

Illite is distributes on the surface of the rock particles, and thus affects rock permeability. It may bridge in pores and forms many micro-pores. The pore space of the rock becomes more complicated and its permeability is then compromised. Besides, when contacting with freshwater, fibrous illite may disperse or break to pieces and migrate with the fluid. The pores could be plugged by the fragments of illite. The permeability of the rock is significantly diminished.

Chlorite often covers the surface of rock particles or fills in pores. It is bridge- type growing in pores. In petroleum reservoirs, common chlorite is iron-rich. When contacting HCl acid, it releases iron ions and then generates colloidal precipitate of ferric hydroxide. The colloidal precipitates will plug pore- throats, and finally result in serious reservoir damage.

2.2.4 Clay Swelling

Clay swelling has been identified continuously as one of the major causes of the formation of damage in oil and gas reservoirs. Most of the clay swelling-related problems studied in the literature have been observed in the vicinity of the well-bore during drilling, completion, or workover (Sanai et al., 2016). Clay swelling is widely considered a major cause of formation damage in hydrocarbon reservoirs and can greatly reduce fluid flow in porous media.

Clay minerals may be divided based on types of their sheets, and electron charges of the layers. The most important clay minerals within the scope of permeability reduction study of the most sandstone reservoirs are kaolinite, smectite, illite, and chlorite (Grim, 1953). Generally, clay swelling issues happen when dealing with smectite or mixed-layer types. Adsorption of a thin layer of water on the external surfaces and between the layers together causes swelling. This adsorption is because of the negative charges existing on the clay unit layers. Many researchers have shown that this water film has formed a hydrogen bond with

the unit layers. The thickness of this water layer depended on the type of clay and existing exchangeable cations.

Exchangeable cations (Ca^{+2}, Mg^{+2}) may strengthen the cohesion of clay particles; because they do not participate in osmotic swelling and maintain a constant water layer thickness (see Figure 2.9). Clay swelling usually causes three major problems, severe permeability reduction and pore plugging, fine particle migration and accumulation, and entrapment of a large amount of fluid which is detected in petrophysical logs as high water saturation intervals. Generally, smectite tends to occur in shallow sandstone formations. Smectites are not usually observed in deep and high- temperature reservoirs (higher than 100-120 ^{0}C).

The commonest swelling clay is montmorillonite. Montmorillonite can swell up to 60 % of its initial bulk volume when absorbing water (Abbasi, 2001).

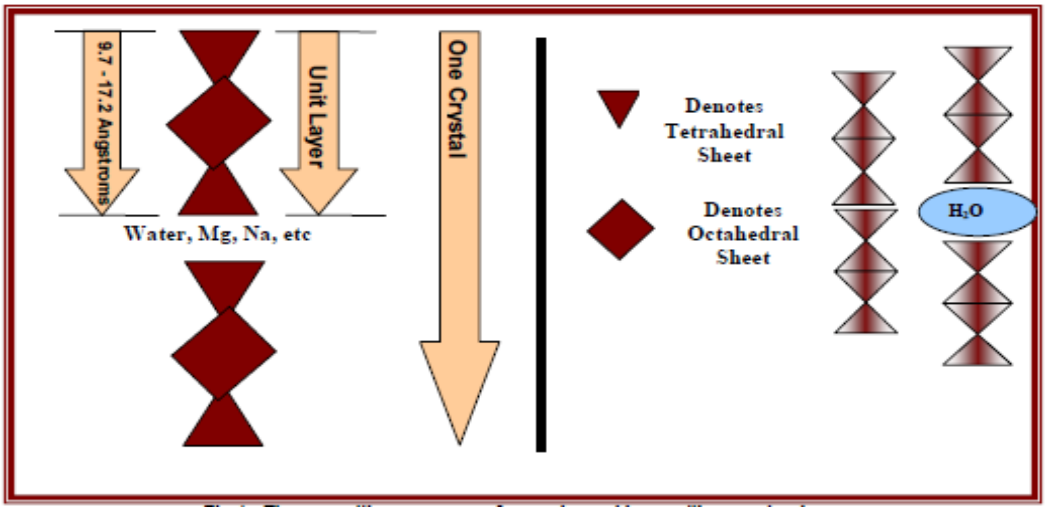

Fig. 2.9: The crystalline structure of smectite and its swelling mechanism (Abbasi, 2001)

Fig. 2.10 shows schematics of a swelling phenomenon in case of water- sensitive smectite-type clay. A negative charge on the 2:1 layers unbalances the structure and is connected by the placement of univalent, divalent, or trivalent cations (Na^+, K^+, Ca^{2+}, $Mg^{2+,}$ or Al^{3+}) in the interlayer space. Since water shows a polar behaviour, it can be placed in the gaps between the interlayer cation and clay sheet. The large size of the water molecules and the hydrated cation structure causes some physical expansion and enlargement. This expansion and swelling could reach five folds of clay initial bulk volume (Abbasi, 2001). The consequences of clay swelling in modern oil processing are more extreme as incompatible injection fluids come into contact with swelling clays found inside the rock matrices, resulting in dramatically decreased permeability to structure (Anderson et al., 2010).

Existing cations can be substituted with other cations once clay is exposed to solutions which contain cations. This property is called the cation exchange capacity (CEC) of the clay, which is defined as the maximum quantity of total cations that the clay is holding which is available for exchange with cation in an external solution at a given pH value (Moor and Renyolds, 1989). The cation exchange capacity (CEC) is one of the basic properties of clay minerals (Table 2.2). Grim (1942) determined the order of replaceability of the common cations in clays from most to least easy cations as:

$$Li^{+} > Na^{+} > K^{+} > Rb^{+} > Cs^{+} > Ca^{2+} > Sr^{2+} > Ba^{2+} > H^{+}$$

Table 2.2. Surface area and CEC of clay minerals (Eslinger and Pevear, 1988)

Type of mineral	Surface area [m^2/g]			CEC [meq/100 g]
	Internal	External	Overall	
Smectite	750	50	800	80-150
Illite	5	15	30	10-40
Kaolinite	0	15	15	1-10
Chlorite	0	15	15	<10

Swelling occurs when polar molecules, such as water or organic molecules, adsorb into the interlamellar space of the 2:1 smectite structure. The expansion of the interlayer and swelling is thought to be primarily influenced by the type of exchangeable cations present in the aqueous solutions that come into contact with the clay (Luckham and Rossi, 1999).

If the concentration of NaCl rises, the thickness of the clay substrate falls. In the presence of KCl, the same process was replicated, and a related pattern was observed although the level. However, the level of clay swelling in the presence of KCl was slightly lower (Pham and Nguyen, 2014). This prevention of clay swelling attributable to KCl‘s capacity to contract the electrical double layer and decrease the electrostatic repulsion between the clay particles indicated that osmotic swelling in K-montmorillonite is energetically inhibited when the water content is higher than the double layer hydrate level. Their study suggests that Na-smectites prefer expanded states (double layer, triple-layer, and fully expanded) to a single-layer hydrate, while K-smectites prefer the single-layer state over the double- layer state. The K^{+} cations form complexes that interact with the hexagonal ring oxygen atoms found on the clay surface and are essentially immobilized. In this area, the set K^{+} cations on either side of the interlayer space will share a water molecule. The neutralization of the negative clay surface charge by K^{+} cations inhibits further swelling.

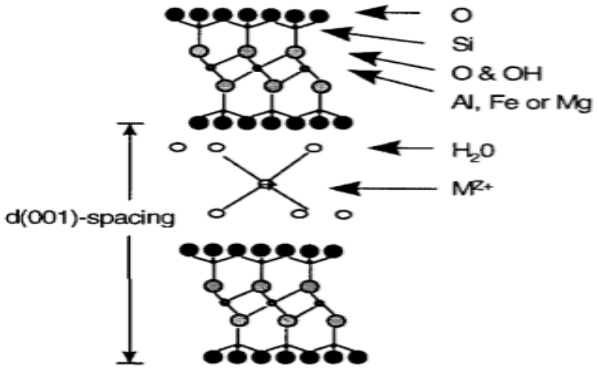

Fig. 2. 10: Crystalline structure of swelling clays M^{+2} represents exchangeable cations (Zhou et al., 1997).

The laboratory studies by many researchers have concluded that clay swelling primarily occurs by crystalline and osmotic swelling mechanisms. Crystalline swelling occurs within the clay minerals where multiple layers of water molecules constitute a limited amount of adsorbed water. Their swelling increases interlayer spacing (Fig 2.10). Osmotic swelling is restricted to certain clay minerals, such as smectite, that embrace interlayer exchangeable cations. If the cation concentration in the interlayer region exceeds that of the surrounding water, those water molecules can be dragged into the interlayer to equilibrate the charge balance. This type of swelling involves a much larger volume of water and therefore a more significant volume expansion occurs compared to crystalline swelling. As the salt concentration was varying, Mohan and Fogler noticed a discontinuity in the interplanar spacing value and described the area as the critical salt concentration. Crystalline swelling occurs above the critical salt concentration while osmotic swelling occurs below this point (Mohan and Fogler, 1997).

Crystalline Swelling and Osmotic Swelling

Swelling occurs through two distinct processes depending upon the type and concentration of cations present in the aqueous solution in contact with the clay. The magnitude of smectite swelling is much dependent on the composition of the solution with which it contacts. In our earlier study Zhou et al. (1996) suggested that water molecules are "saturated" in layers on the clay surface when swelling of smectite is inhibited by divalent for (example Ca^{2+}) and multi-valent (example Al^{3+}) cations. This also applies to monovalent cations at high concentrations. This type of swelling (limited d-spacing increase, structured water molecules on clay surface) has been called *Crystalline swelling*. The magnitude of crystalline swelling depends on the nature of exchangeable cations and crystalline chemistry of swelling clay.

Crystalline or microscopic swelling (sometimes called surface hydration) occurs under high brine concentrations or aqueous solutions high in divalent or multivalent ion concentrations. The initial entry of water forms surface complexes by hydrating the ions present in the interlayer spacing and forming hydrogen bonds to the clay surface oxygen atoms. Subsequent formation of additional monomolecular water layers on the clay surface can occur. Crystalline swelling results in relatively minimal swelling and the gross particle morphology is preserved. Osmotic swelling occurs in either dilute solution or solutions containing large quantities of Na^+ cations. The presence of Na^+ cations results in the formation of an electric double layer on the surface of the clay mineral contributing to repulsive forces between the platelets.

Swelling clays in the ***Osmotic swelling*** state does not have a single peak but has a range of d-spacing distribution. Norish (1964) suggested that in osmotically swollen samples, the interlayer d-spacing can be taken as the distance at which the first maxima occurs. The first maxima for the 0.15 M sample, at 45Å is a 300% increase from the 1.0 M NaCl solution sample. In osmotic swelling the concentration of cations between unit layers in a clay mineral is higher than the concentration of the cation in the surrounding water. Osmotic swelling occurs in about 20 times the size of the interlayer and the amount of clay Norish (1964). The discrepancy between the two swelling processes can be calculated by calculating the clay's interplanar distance at differing concentrations of salts.

The interplanar spacing value discontinuity was observed as the salt concentration was varied, and the area was described as the critical salt concentration (CSC). Crystalline swelling occurs at salt concentrations above the critical salt concentration while osmotic swelling occurs below this point. Despite these complexities, the osmotic swelling can be easily differentiated from crystalline swelling from the XRD traces. Osmotic swelling not only causes a much larger volume expansion but also makes smectites more mobile in hydrocarbon reservoirs as the smectite platelets move farther apart from each other. Thus, osmotic swelling of smectites would be much more damaging to a hydrocarbon reservoir than crystalline swelling (Zhou et al., 1997).

Distinguishing clay swelling damage from clay migration damage is always an interpretive problem. A steady, usually rapid decrease in permeability with decreasing salinity of the flowing fluids is generally a consequence of clay swelling; however, water sensitivity caused by particle migration will also be manifested in this fashion, but sometimes more irregularly.

Damage caused by particle plugging is detected by noting a temporary change (usually an increase) in permeability when fluid flow direction was reversed. The Berea and the Entrada sandstones produced dispersed clays before permeability decline occurred. This is considered to be the best available evidence for clay migration damage as opposed to clay swelling damage. In most, but not all, cases permanent loss of air permeability accompanied clay migration damage, especially in the less permeable cores. This was indicated by the difference between initial and final air permeability (Gray and Rex, 1966).

2.2.5 Fines Migration

Fines migration is a process involving the release, transport, and capture of fine clay and non- clay particles in a fluid-saturated porous media. Fine particles that may contribute to the permeability reduction include clay minerals, quartz, amorphous silica, and carbonates. According to Bradford (2002) fine particles typically may be made of many different materials such as organic, inorganic, but some of the more common materials are clay minerals. Fines migration phenomena were studied by Muecke (1979), who said that unconsolidated sandstone formations have very fine grain particles with different sizes and shapes and are unstable in porous media. He also found that the fluid systems considered to prevent damages by these fines to such formations not only should consider clay mineralogy but also can face the problems induced by other minerals and organic particles. This phenomenon has been observed in some sandstone reservoirs and is caused by clay dispersion (Gray, 1996). Using low salinity brine and high pH fluids or high fluid velocity are the most common causes of fine migration in the reservoir.

Fines migration with consequent permeability reduction is a widely recognized mechanism responsible for formation damage. Migration and retention of fine particles may cause a substantial reduction in good productivity (Khilar, 1984).

Migration damage may depend on the sizes of both clay minerals and pore restriction. The type and amount of clay minerals are not the only cut- off parameters in characterizing permeability reduction, but other physical parameters such as clay composition, size, location, and distribution must be taken into account. These parameters will give a better understanding of formation damage. These parameters can be explored with XRD and the SEM analyses make for a more comprehensives mineralogy. Mineralogical pore level characterization reveal the presence of various forms of clay minerals that may have an impact on permeability and fluid flow. Non- swelling clay minerals such as kaolinite, illite,

chlorite, and interstratified layer clays, may migrate their filling sites, which affect the petrophysical properties of oil and gas reservoirs as described by (Seemann, 1979).

All such fine particles are free to migrate through the pores along with any fluids that flows through the reservoir. If these fine particles migrate, but are not formed by the formation of produced fluids, they might be concentrated on pore restriction, causing the plugging of pore throats and severe decrease of permeability. Particle migration in porous media is a challenging issue of both scientific and industrial importance, particularly in the field of petroleum engineering. Experimental studies have shown that release of fine particles migrates with the flowing fluid, reducing permeability and causing damage to the formation. Obeservasion, results is also essential in order to predict the behaviour of the particle, such as attachment and release, and its effect on the formation damage during suspension in porous media. During the flow of suspension through a porous medium, fine particles attached to pore surfaces are released or detached under certain sets of conditions as described by Khilar and Fogler (1988).

Transport of fine particles in a porous media is followed by particle aggregation and a consequent reduction in permeability as described by (Shapiro et al., 2007). Particles migration may occur in a number of different situations. It may occur during primary production from a field, particularly from heavy oil, consolidated in a clay-rich reservoir. Khilar and Vaida (1990) clearly showed that Bandera sandstone contains very little to no swelling clay minerals and composed of a considerable amount dispersible clay minerals such as kaolinite, illite, and chlorite, which are susceptible to abrupt chnages in salinity and thereby formation damage.

Shepperd and Morris (1982) researched the role of clay minerals in the porosity and permeability characteristics in the Bridport Sand. They found that permeability reduction can be due to the adsorption and expansion of pore- lining clay. Just small spreads of mixed-layer illlite/smactite are adequate to block or partially block small pore throats here in this fine- grained reservoirs.

Gray and Rex (1966) studied the migration of dendritic micas, kaolinite, and illite. They found that fines migration occurs when salinity decreases, the concentration of divalent ions decreases, or substitution with univalent ions. Mungan (1965) and Gunter (1994) found that pH changes can result in fine migration, although incremental changes in salinity can decrease fine migration.

2.3 Origins of clay minerals in the sandstone formation

Generally, most sandstone contains clay minerals, which are an important factor to control the distribution and production of oil and gas, as clays can cause significant formation damage. Clay minerals may be present in the form of a detrital matrix and as a part of the rock fragment known as “allogenic” clays and as replacements or cement called “authigenic” clays. These clays are originated from various rock- fluid interactions in an existing pack of sediments, loosely attached deposits, and have greater formation damage potential. The diagenetic/ authigenic clays can be divided into three groups: pore- lining, pore filling, and pore- bridging, as shown in Fig. 2.11, the second group could be the detrital clay group. These clays originated during the formation of rocks, they are tightly packed and blended within the matrix, cause less potentially formation damage, and are usually seen as laminations in sandstones or shales (Schechter, 1992). The types, amounts of clay minerals, and their distribution in sandstones have a significant impact on permeability and rate of production.

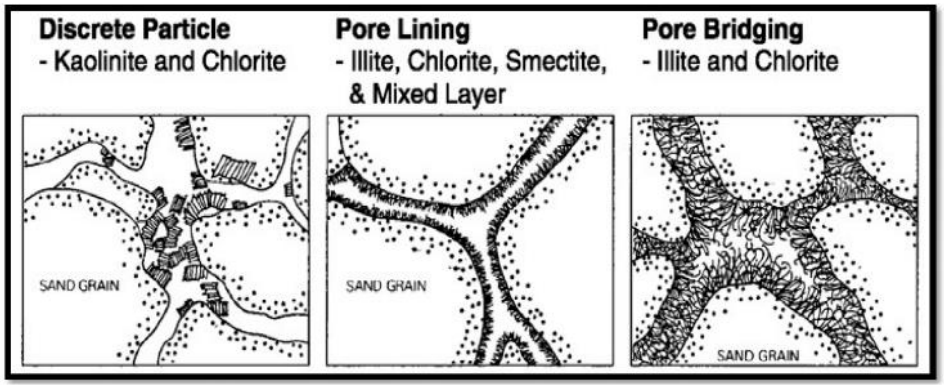

Fig. 2.11: Authigenic clays in the formation (Schechter, 1992)

Diagenetic clay minerals occur in sandstones by direct precipitation from pore fluids (Authigenesis), or by alteration of detrital silicates. Eodiagenesis includes all processes that occur at or near the sediment surface, where the upper-temperature limit is <70 ^{0}C, typically equivalent to approximately 2 km burial. Mesodiagenesis occurs during burial and includes all diagenetic processes following Eodiagenesis and through to the earliest stages of low-grade metamorphism. In many cases, this includes sediments buried to depths with equivalent temperatures of approximately 200- 250^{0}C.

Telodiagenesis occurs in inverted basins that have experienced an influx of surface waters (usually meteoric). Such water can cause significant geochemical changes.

There are eight main ways that clay minerals are incorporated into sandstones:

1- Clay-rich rock fragments formed in the hinterland (extraclassic);
2- Clay-rich clasts formed within the sedimentary basin (intraclastic);
3- Flocculated mud particles and faecal pellets;
4- Inherited clay rims on sand grains;
5- Post-depositional incorporation of detrital mud into the sandstone by bioturbation and clay infiltration;
6- Eogenetic reaction products in sandstones;
7- Monogenetic reactions in sandstones;
8- Telogenetic reactions in sandstones.

Upon increasing burial depth and temperature, Eogenetic kaolinite is transformed into dickite. This process is possibly aided by an increase in acidity of formation water. With burial and heating, dioctahedral smectite transforms to illite. Diagenetic illites formed at moderate temperatures (<90 ^{0}C) in sandstones have at least a minor component of smectite within them. The transformation of kaolinite to illite is prevalent at temperatures greater than about 70 ^{0}C but becomes pervasive at temperatures greater than about 130 ^{0}C.

Authigenic chlorite in sandstones may occur during mesodiagensis as a result of the break-down of volcanoclastic grains and Fe-Mg- rich detrital minerals such as garnet, biotite or amphibolite. This type of chlorite occurs as grain replacement. Chlorite occurs as coatings comprising small pseudo-hexagonal crystals, which are arranged perpendicular to the sand grain. Transformation of precursor Fe-rich clay minerals to chlorite occurs at burial depths greater than about (2-3 km) and temperatures (60- 100 ^{0}C). The precursor can be Fe-bearing berthierine, odinite, trioctahedral smectite, and kaolinite (Ehrenberg, 1993).

On the deposition, the primary sand comprises a mixture of minerals that were formed under a various conditions (for example temperature, pressure, oxidation state, and water composition). The main Eogenetic clay minerals such as kaolinite and smectite are formed by precipitation from pore walls, replacement of framework sand grains, and replacement of precursor detrital or diagenetic clay minerals. Alternatively, illite and chlorite are depositional rather than Eogenetic in origin.

Several studies in the past have addressed the subject of formation damage due to swelling and non-swelling clays. Natural formations contain both swelling and non-swelling clays

and the clay- related permeability loss due to foreign fluids in these formations can be attributed to more than one mechanism. The response of clays when in contact with water depends on the size, charge, and total amount of interlayer cations (Barshad, 1952).

Monagham et al. (1959) conducted laboratory studies of formation damage in sands containing clay; they prepared samples at the laboratory from crushed quartz with an average particle size of 1.5- 10 microns that was mixed separately with three API standard clay minerals, kaolinite, illite, and montmorillonite. They concluded that kaolinite, illite, and montmorillonite (individually or in combination) were found in several producing formations that suffer permeability reduction when contacted by freshwater.

Moore and Reynolds (1989) give a comprehensive summary and introduction to the literature on the subject. The consensus is that the permeability reduction of sandstones can be attributed either to clay swelling or fine clay migration or, a combination of these effects.

Gray and Rex (1966) determined that formation damage in sandstones caused by clay dispersion and migration. They selected samples from six localities; five core suites were oil reservoir rocks from Canada, the USA, and Colombia. The sixth, Berea sandstone is a building stone quarried in Ohio. The analytical work showed that these samples were indeed water sensitive, but they did not appear to be damaged by bulk swelling of montmorillonite or mixed layer clays. They showed that in the absence of montmorillonite, combined in mixed layer mica needles and small kaolinite, direct evidence from high permeability sandstones strongly suggests that the dispersion of mica needles and small kaolinite crystals is the main cause of fine clay migration damage in the suited sandstone studied.

Hurst and Archer (1986) studied some applications of clay mineralogy to reservoir description based on some previous works, they suggested that to understand the effect clay minerals have on reservoir characteristics, one must identify not only clay mineral types but describe threat origin, distribution, and surface textures. Their studies were based on a review of three previous works. Finally, they concluded that small variations of authigenic clay content can have a significant effect on the permeability reduction and show that distribution and texture of authigenic clay cement can determine the extent to which clay mineralogy influences reservoir characteristics.

Kia, and Fogler (1987) performed an experiment to study the effect of salt composition of fluid on clay-bearing Berea sandstones. Experiments were conducted using the core- flood

apparatus, a sandstone core, one inch in diameter and one inch in length, is a vacuum saturated for 3- 4 days in a given salt concentration. They concluded that the water sensitivities of Berea sandstone is due to a colloidal dispersion process involving the release of clay particles from pore walls. The particle detachment strongly depending on the concentration, type, and the valence of the ions present in the pre-treatment salt solution. Also, they observed that in case of calcium ions providing a full surface converge of clay-bearing sandstones, the formation damage will be eliminated. In the solution of mixed calcium and sodium ions, calcium ions are selectively adsorbed onto the surfaces of clay particles and a critical calcium surface coverage has existed above which the formation damage is greatly reduced. In the calcium form, the clay particles are always attracted the pore walls and therefore will not migrate and plug the pore throat causing formation damage.

Kumar (1988) studied on new approaches for mathematical modelling of formation damage due to the invasion of clay suspensions. They proposed a mathematical model that is based on a mass balance of particles. They applied their model on the experimental data obtained on 80 mm sandstone core plugs. They observed that their simulation consistently worked with the experimental data.

Chang and Civan (1992) declared that fluid introduced into the petroleum- bearing formations frequently causes formation damage due to the incompatibility of the formation. The processes contributing to formation damage include dissolution/ precipitation of minerals, fine particles release and capture, and formation swelling. When the pore throats of porous media are blocked, the porosity may remain nearly unchanged, but permeability can decrease significantly because the gates connecting the pores are shut off. This effect should be studied into permeability and porosity correlations.

Valdya and Fogler (1992) set up an experimental work to study the influence of pH and ion exchange on fines migration and formation damage, they adopted a series of experimental procedures for the experiments. A Berea sandstone sample (2.54 cm in diameter and 5.08 cm long) was vacuum saturated in 0.51 M NaCl (or other salt) solution and placed in the core holder. Next, an acidified brine solution (pH ≈ 2 – 3 and 1 M NaCl) was injected to remove carbonates; then the core was subjected to a flow of approximately 150 PV of 0.51 M NaCl at near-neutral pH to restore the core to sodium- saturated state. The core permeability at any time can be calculated by monitoring the pressure drops across the core at constant injection flow rate. Typical flow rates were (1.0 – 2.0 ml/ min or 0.33- 0.66 m/

s). They observed rapid and drastic decrease in permeability as a result of increasing pH from 2 to 9 and a water shock was recorded at a pH 11. They summarized the results of experiments obtained using different alkaline solutions. Both K^+ and NH_4^+ showed results to those obtained for Na^+, while no damage was observed with Ca^{+2} at pH > 12. Similarly, they observed that salinity reduction induces a pH increase, which amplifies the release of fines and leads to a decrease in permeability drastically. Overall they identified the conditions of low salinity and high pH as the conditions that cause drastic damage in Berea sandstone.

Ohen and Civan (1993) proposed that formation damage is an undesirable phenomenon encountered at any stage of well development operation and hydraulic fracturing using water-based fracturing fluids. Fines migration and clay swelling have been recognized as the major causes of formation damage observed as permeability impairment. The damage is especially more severe in poorly lithified and low permeability formations with an abundance of authigenic pore-filling clay minerals.

Dahab et al. (1993) studied the role of authigenic clays in permeability reduction; they adopted a series of experiments on fifteen sandstone and limestone cores from the north eastern part (Alkhafji) and the eastern part (Safaniya) of the Kingdom of Saudi Arabian reservoirs and five Berea sandstones. X-ray diffraction has been used to study the mineralogical analysis of the cores and the relative abundance of the clay minerals, Alkhafji cores contain the least amount of clay but Safaniya cores contain a higher percentage of montmorillonite than Berea sandstone cores. Permeability measurements were conducted at 1.000 psi overburden pressure and different temperatures (30, 50, 70, and 90 ^{0}C) for each core sample. The displacement runs were carried out using 20, 15, 10, and 5 wt % NaCl solutions, respectively. Examination of the cores with the SEM showed that the sandstones core grains are cemented by partial grain coating of clays. Kaolinite which is a dominant clay mineral in the cores develops as pseudohexagonal, platy crystals scattered through the pore system in a random arrangement. It affects rock petrophysical properties by reducing intergranular pore volume and by migrating with the flow in the pore system rather than changing the crystal lattice structure by swelling when contacted by injected water. SEM examination of Saudi sandstones after the flow test with NaCl solutions showed that the clay coating on the sand grains had become detached and had migrated into pore throats. They observed that formation damage represented by partial blocking of openings due to dispersed clays reduced permeability ratio. Variation temperature had a clear effect on the permeability ratio, the higher permeability ratio was obtained at higher temperatures for all sandstone core

used. Overall, they concluded that a drastic permeability reduction to water can be attributed to the dispersion and migration of pore-lining clays.

Mohan et al. (1993) performed an experiments on water sensitivity of sandstone containing swelling and non- swelling clays, to describe the ongoing studies on the mechanisms of permeability reduction. The experiments in this investigation were conducted on sandstone cores containing swelling and non- swelling clays. These cores were actual field samples supplied by the USA Department of energy and Chevron Company. These cores are from the Stevens in EIK Hills Field, CA, the samples from the depth of 7039 ft. They observed that these cores substantially damaged by water shocking when saturated with sodium chloride and the effluent of pH reached maximum of approximately 10.6 in all experiments. Thus, for swelling and non- swelling clays, potassium is less sensitizing than sodium. Hence, water shocking a Steven sandstone following saturation with potassium chloride should not result in as high damage as with sodium. Overall, they noticed that Stevens sandstone cores were sensitive to water shock experiments. These cores exhibit permeability reduction due to water shock flowing saturation with sodium chloride, potassium chloride, and calcium chloride solutions. The water shock of sodium chloride saturated cores causes the most damage. In some cases, the water shock of calcium chloride saturated cores causes more damage than potassium chloride saturated cores. Finally, their results of water shock experiments suggest that swelling clays contribute significantly to the total damage.

Xinghui (1996) declared that formation damage is a common problem encountered in almost every phase of reservoir development. Fine particles are always present in petroleum bearing formation and they contribute a great deal to the formation damage. During drilling and completion, fluids containing particle suspensions enter the formation. Chemical reactions can also generate particles within the formation. Sedimentary rocks usually contain fines loosely attached to pore surfaces. When injection fluids are incompatible with these minerals, they can be released from pore surfaces. These particles migrate through the porous media, deposit on the surfaces, and become trapped at pore constrictions to reduce the rock porosity and permeability.

Hayatdavoudi et al. (1996) performed experiments on controlling formation damage due to kaolinite migration; series of core plugs were prepared from Tuscaloosa sand and conducted several experiments under the same conditions. The test was run under room temperature, pH= 12 with caustic soda, 500 psi differential pressure and 1000 psi overburden pressure,

11.1 cc/ min flow rate, and 45 minutes of contact. Overall, they found that the kaolinite clay minerals undergoing a highly oxidative process by Sodium Peroxide could partially be altered. Formation damage is caused by dissolution process resulting in the disintegration of kaolinite booklets and the appearance of many other mineral fragments within the same pore space.

Zhou at al. (1997) applied a novel method called clay swelling diagrams to quantify the effects of solution composition, clay composition on clay swelling by using an X-ray diffraction method for clay swelling. This method requires a small number of samples. The swelling clays used in their study a montmorillonite (SWy -1, Crook County, Wyoming) and a saponite (SapCa-1, Ballarat, California); both were obtained from the Source Clay Project, the Clay Minerals Society. They observed that in 1.0 M (or 5.8 wt %) NaCl solution, the (001) peak is sharp, nearly symmetrical, and d-spacing is at 16 Å, a (001) peak of a Na-saturated saponite in the air would be 12.5 Å. When saponite soaked in a relatively concentrated NaCl solution, it will experience < 30% swelling compared with its dry counterpart in air. In 0.15 M (or 0.87 wt %) NaCl solutions, the (001) peak of the saponite is at 45 Å. This is a 360% increase from its dry counterpart and a 300% increase from the 0.1 M NaCl solution sample. They noted that the ability of Ca^{2+} to inhibit saponite swelling depends on the Na concentration in the solution. At low Na concentrations, a small amount of Ca in the solution would effectively limit the saponite swelling. They observed that the composition of clay minerals is another factor affecting clay swelling, the two most common swelling clays, montmorillonite and saponite, montmorillonite swelling more than saponite.

Ehrenberg and Nadeau (1998) studied the effects of diagenetic minerals on reservoir sands experimentally. They used synthetic sandstones (quartz 2.65g, kaolinite 2.62 g, dolomite 2.87 g). The reaction was typically performed in 250mL stainless steel hydrothermal reaction vessels at 200 ^{0}C for period 19 – 45 days. They showed that a large reduction in sand permeability is associated with the growth of not more than 5 wt% smectite clay.

Al- Bazzaz and Engler (2001) studied the impact of clay migration on impairing reservoir permeability; they studied clay mineralogy and pore geometry to a better understanding of clay mineral migration damage. To investigate such parameters, they applied electron microprobe together with XRD analysis. They showed that the clay mineral amount and type are not the only cut- off parameters in characterizing formation damage, but other physical

parameters such as clay composition, size, location, and distribution must be taken into account, these parameters will give a better understanding of formation damage.

Abbasi et al. (2011) experimentally investigated clay mineral's effect on permeability reduction of three core samples at different wells and depths on the Iranian southern field which is named (A- 1, 2, 3). The type and amount of clay minerals measured using XRD tests, the results core samples A1 and A3 contained kaolinite and illite, A2 only illite existed. The core samples fully saturated with formation water after cleaning, dried, and measured their petrophysical properties, then they placed inside the core holder to start the injection process. First formation water was injected at 4cc/hr to calculate initial permeability, and then the injection rate increased to 4; 9 and 7cc/hr under reservoir conditions (T= 80 ^{0}C, P= 2500 psi). Their experiment showed that the detected clay within them (illite and kaolinite) no impact on the permeability of the samples.

Wilson et al. (2014) studied the type and distribution of clay minerals in sandstone reservoir rocks and potential formation damage, they observed that both detrital and authigenic clay minerals commonly harm the reservoir quality of sandstone reservoir rock. Finally, he concluded that the most common clays that cause clay problems and formation damage are kaolinite, smectite, illite, and chlorite.

Xie (2014) tested the sandstone reservoir, he revealed in their analysis that the scale sorting, particle concentration and fluid flow velocity in rock tunnels are calculated in the loose sandstone from the sum of mobile particles and ranges of the disrupted region due to solid motion and reduction of in-situ permeability. The final stable permeability of the blockage zone depends on the minimum size of bridging particles as superimposed bridging and clogging in tunnels.

Al- Laboun et al. (2014) studied the effect of authigenic clay minerals on reservoir characterization of the Burqan formation sandstone from the Median basin in northwestern Saudi Arabia. They took 81 samples from 6 sandstone outcrops that were investigated, using different analytical techniques, such as thin- section microscopic observations, XRD and SEM. They concluded that an abundance of authigenic clay minerals (kaolinite and smectite) played an important role in controlling reservoir properties (permeability and porosity) in Burqan formation, thereby damaging the formation. Also, they found that calcite cementation as one of the main factors controlling the porosity and heterogeneity in Burqan sandstones.

Aksu at al. (2015) used 3D quantification of clay swelling by X-ray micro-computed tomography (μ- CT) to elucidate the effect of clay swelling on the permeability of porous media. They prepared simplified analog samples with soda lime beads and quartz grains, various amounts of swelling and non-swelling clay were used to coat soda-lime beads and quartz grains. They concluded that clay-coated samples, in general, had lower permeability than uncoated samples, high kaolinite content caused larger permeability reduction, while low kaolinite content did not affect permeability. Also, they observed no significant changes in permeability for montmorillonite- coated samples with time, after initial swelling damage. In- addition, they showed that the effect of swelling clay on permeability reduction depends on the matrix size, in high porosity/ permeability samples, the reduction in porosity due to clay swelling is insufficient to cause a meaningful reduction in permeability. Experimental results show a more significant permeability reduction in samples with smaller quartz grains (0.105- 0.210 mm) compared to the larger (0.707- 0.841mm) soda lime beads. Then they noticed as pore space decreases, the effect of clay swelling on the permeability reduction becomes more profound, the data from modelled natural rock sample confirmed the assumption that smaller porosity and higher clay content are favourable to more severe problems of formation damage due to clay swelling. Overall, they confirmed that fine migration is a primary reason for permeability reduction in a high amount of kaolinite-coated samples, growth of swelling clays such as montmorillonite was found to have a minimal impact on permeability in samples with high porosity (36 – 40%).

2.4 Formation damage in sandstone reservoirs

The identification and characterization of clay minerals is an important part of reservoir sandstone description as these minerals significantly affect petrophysical characteristics by introducing considerable microscopy to the pore system. Formation damage is not an easy issue to control. Because commonly formation damage is irreversible, it is better to avoid it than to deal with it after its occurrence using complex procedures and reaching little benefit. Unfortunately, today's formation damage is still serious problem facing the petroleum industry. Formation damage stills the active subject to discuss and research in our industry (Hurst 1995).

Formation damage within oil and gas reservoirs has been a topic of research for more than four decades, and many papers and studies have been published on the subject. The history

of formation damage study has been outlined in a paper by Porter (1989). The reason for such intense interest is because of the great financial gains to be obtained from increasing reservoir productivity. The obvious way to increase productivity is to minimize damage, and thus a comprehensive understanding of the modes of formation damage is needed. Formation damage due to particulate migration can be divided into two groups; migration of natural in-situ fines; and the introduction of foreign particles from drilling muds or other areas of the reservoir. In-situ fines can consist of varying quantities of clays, feldspars, small quartz crystals, etc.

Most workers have concentrated on the role of clays in formation damage. Clays can be a problem component of reservoir sandstones because of their large aspect ratios and charged surfaces. Most clay minerals have a negative charge due to isomorphous substitution in the clay lattice.

One of the main features of clay-water interaction is the formation of electric double layer (EDL), consisting of Stem layer, related to the electrical charge of the particles, and a diffuse layer, extending into the bulk liquid. The degree of compression of the diffuse layer depends on the concentration and valence of the ions in solution. In concentrated brine, the diffuse layer is compressed. When clay particle approaches another clay particle the diffuse layers interact and repulsion occurs. However, this repulsion is not the only force operating because, at a small distance between clay particles Van der Waals attractive forces predominate and flocculation results. Van der Waals attractions between single atom pairs are small and not very far-reaching, but they are additive and the total van der Waals attractions between particles or between pore walls lined with clay are large enough and far-reaching enough to compete with the repulsion between the diffuse layers. Thus, in concentrated brines in a porous system the diffuse double electrical layers associated with clay-lined pores may be compressed, leaving more space for fluid flow within the pores.

These theoretical explanations have been supported by research into the water-sensitivity of various sandstones. Clays were released from the pore walls when the brine dropped below a critical salt concentration (CSC). Below this CSC clays moved within the pore space, blocking pore restrictions and causing a drastic permeability drop. Lever (1984) found similar results with different brine compositions and concentrations.

Water sensitivity or loss of the permeability of sandstones in response to water salinity changes is well-documented, but still incompletely understood phenomena. Johnston and

Beeson (1945) was among the first to investigate and report significant reductions in the permeability of clay-containing sandstones with decreasing salinity of pore water. Several studies have revealed that have subsequently been carried out to pinpoint the cause and nature of permeability reduction in clay-containing sandstones. Moore (1960) gives a comprehensive summary and introduction to the literature on the subject. The consensus is that water sensitivity or loss of the permeability of sandstones can be attributed to either clay swelling in the rock pores, clay particle migration, or a combination of these effects.

Water sensitivity attributable to clay swelling is probably the best-documented damage mechanism. Studies by Foster (1955), Dodd et al. (1955), Monagham et al. (1959) and White et al. (1962) correlated water sensitivities directly to the presence of swelling clays in sandstone. The degree of damage is believed to be a function of the amount of swelling montmorillonite and mixed-layer clay present. Formation damage triggered by swelling of montmorillonite is now a widely recognized phenomenon by the oil industry and is routinely considered in evaluating "problem" wells by some oil companies.

Water sensitivity attributable to clay particle migration, on the other hand, is not so well understood. There is no obvious correlation between pore water salinity and clay migration as there is between clay swelling and salinity. As a result, there has been a tendency to discount the possibility of severe permeability reduction in sandstones, which contain negligible amounts of swelling or mixed layer clays. Hewitt (1964) has recognized the possibility of damage from migrating clays and has presented a scheme of analysis for recognizing sandstones that are susceptible to this type of permeability damage. Water sensitivity of sandstones, a problem in colloid chemistry, is a situation where the permeability of sandstones containing clay minerals decreases significantly and rapidly when freshwater replaces saltwater originally present in the sandstone formation (Khilar 1984).

Clay migration may be, in fact, a more prevalent formation damage mechanism than hitherto suspected. Distinguishing clay swelling damage from clay migration damage is always an interpretive problem. A steady, usually rapid decrease in permeability with decreasing salinity of the flowing liquids is considered a consequence of clay swelling; however, water sensitivity caused by particle migration will also be manifest in this fashion, but sometimes more irregularly. Damage caused by particle plugging was detected by noting a temporary change in permeability when the fluid flow direction was reversed. The Berea and the

Entrada sandstones produced dispersed clays before permeability decline occurred. This is considered be the best available evidence for clay migration damage as opposed to clay swelling- damage.

2.5 Formation damage and clay stability

Formation damage is a common problem in petroleum reservoirs and occurs in different stages of reservoir development from drilling to production. The causes of formation damage include particle invasion, the formation of fines migration, chemical precipitation, pore deformation, or collapse. The extent of formation damage depends on the fluid properties, rock properties, and rock- fluid interaction. It impairs the permeability of reservoir rocks, thereby reducing the natural productivity of reservoirs.

In sandstone reservoir rocks, there are some minerals (clay and non- clay) that are sensitive to some factors for instance invading fluids (pH and salinity), flow rate, temperature, and so on, and thus reduce reservoir permeability. This phenomenon is called a formation damage. According to Civan (2007), formation damage is a generic term referring to the impairment of the permeability of petroleum-bearing formations by various adverse processes. It may be caused by several factors, including physicochemical, chemical, biological, hydrodynamic, and thermal interactions of porous formations, particles and fluids, and the mechanical deformation of formation under stress and fluid shear. These processes are triggered during drilling, production, workover, and hydraulic operations. Generally, fine particles loosely attached to the pore surface are at equilibrium with the pore fluids. Any variation in chemical, thermodynamic, and stress states may break the equilibrium conditions, inducing particle detachment, and precipitation formation. Once ions and particles are introduced into the fluid phases, they become mobile and can then interact freely with other components of rocks and fluids in many intricate ways to create severe reservoir formation damage problems. Table 2.1 shows the description and typical problems caused by authigenic clay minerals.

Among other factors, the interactions of the clay minerals with aqueous solutions are the primary culprit for the damage of petroleum-bearing formations. Amaefule (1988) reports the rock-fluid interactions can be divided into two categories in the sedimentary formations:

1- Reactions stemming from rock salts reacting with incompatible compounds, and

2- External factors arising from high flow rates and gradients of friction.

Table 2.3 Description and typical problems caused by authigenic clay minerals Amaefule (1988); Civan (2000) and Ezzat (1990).

Mineral	Chemical Elements	Morphology	Surface area (m^2/gm)	Major reservoir Problems
Kaolinite	$Al_4[Si_4O_{10}](OH)_8$	Stacked plate or sheets	20	Breaks apart, migrates and concentrates at the pore throat causing severe plugging and loss of permeability.
Chlorite	$(Mg, Al., Fe)_{12}[(Si, Al)_8O_{20}](OH)_{16}$	Plates, honeycomb, cabbage-head rosette or fan	100	Extremely sensitive to acid and oxygenated waters. Will precipitate gelatinous $Fe(OH)_3$ which will not pass through pore throats.
Illite	$(K_{1-1,5}Al_4[Si_{7-6,5}Al_{1-1,5}O_{20}](OH)_4)$	Irregular with elongated spines or granules	100	Plugs pore throats with other migrating fines. Leaching of potassium ions will change it to expandable clay.
Smectite (or montmorillonite)	$(1/2Ca, Na)_{0,7}(Al, Mg, Fe)_4[(Si, Al)_8O_{20}]\bullet nH_2O$	Irregular, wavy, wrinkled sheets, webby or honeycomb	700	Water sensitive, 100% expandable. Causes loss of microporosity and permeability.
Mixed-Layer	Illite-Smectite and Chlorite-Smectite	Ribbons substantiated by filamentous morphology	100-700	Breaks apart in clumps and bridges across pores reducing permeability.

It should be remembered that five major elements mentioned in the table above influence the mineralogical performance of the sedimentary formations:

1- Specific mineralogy and chemical composition

A- Deposits disbanding,

B- Minerals burst, and

C – Current mineral precipitation.

Mineral abundance is a dominating factor where sensitive f sensitive minerals occur.

1- Mineral size plays an important role because,
   a- Mineral sensitivity is proportional to the surface area of minerals, and
   b- Mineral's size determines the surface area to volume ratio of particles.
2- Mineral morphology is important, because

a- Mineral morphology determines the grain shapes, and therefore the surface area to volume ratio, and
b- Minerals with platy, foliated, a circular, filiform, or bladed shape, such as clay minerals, have a high surface area to volume ratio.

3- The location of minerals is important from the point of their role in formation damage. The authigenic minerals are especially susceptible to alteration because they are present in the pore space as pore-lining, pore-filling, and pore-bridging deposits and they can be exposed directly to the fluids injected into the near-wellbore formation.

Mungan (1989) states that clay damage depends on (1) the type and amount of the exchangeable cations, such as K^+, Na^+, Ca^{2+}, and (2) the layered structure existing in the clay minerals.

Mohan and Fogler (1997) discuss three mechanisms that contributing to a decrease in permeability of clayey sedimentary formations:

1- Within desirable colloidal conditions, non-swelling clays, such as kaolinites and illite, may be released from the surface of the pores and then these fragments can migrate by porous formation with the fluid.
2- Whereas swelling clays, such as smectite and mixed-layer clays, first expand under favorable ionic conditions and then disintegrate and migrate.
3- Also, fines attached to swelling clays can be dislodged and liberated during clay swelling, the phenomenon of which is referred to as fine generation by discontinuous jumps or microquakes.

Amaefule (1988) concentrated on experimental findings that enhanced understanding of some of the various agents that produce formation damage. Civan (2007) lists them as follows:

- Invasion of foreign fluids, such as water and chemicals used to improve recovery, drilling mud invasion, and workover fluids;
- Invasion of foreign particles and mobilization of indigenous particles such as sand, mud fines, bacteria, and debris;
- Operation conditions such as well flow rates and wellbore pressures and temperatures;

- Properties of the formation fluids and porous matrix.

According to Adel and Ahmed (2008) formation damage is caused by (1) the contact of completion fluids, workover or simulation fluids with the producing formation. (2) This damage is caused by the precipitation of suspended solids in treating fluids, thus, plugging the pore channels. (3) This damage can be reduced by filtering the training fluids through a 2-micron filter at the surface. (4) Also, clay particles which exist in sandstone producing formations will swell and cause formation damage.

X-ray diffraction tests should be conducted to determine the type and amount of clay in the sandstone cores to choose the suitable treating fluid. Also, clays are capable of migration when contacted by foreign water. The formation damage due to employing brines with different densities was determined. Formation damage by high density brines increases at high temperatures. Adel and Ahmed (2008) the study revealed that low-density disruption induced by 3% $CaCl_2$ workover fluid due to swelling inhibition resulted in ion transfers with clay particles and high-density $CaCl_2$ / $CaBr_2$ work over fluids due to the presence of a large percentage of solids.

Bishop (1997) identified seven formation damage mechanisms described by Bennion D. B. (1994). They are concise at this time as keeping an eye on:

1. Fluid- fluid incompatibilities, for example, emulsions generated between invading oil-based mud filtrate and formation water.
2. Rock- fluid incompatibilities, for example, contact of potentially swelling smectite clay or flocculated kaolinite clay by non-equilibrium water-based fluids with the potential to severely reduce near wellbore permeability.
3. Solid invasion, for example, the invasion of weighting agents or drilled solids.
4. Phase trapping/blocking, for example, the invasion and entrapment of water-based fluids in the near-wellbore region of a gas well.
5. Chemical adsorption/ wettability alteration, for example, emulsifier adsorption changing the wettability and fluid flow characteristics of a formation.
6. Fines migration, for example, the internal movement of fine particles within a rock's pore structure resulting in bridging and plugging of pore throats.
7. The biological activity, for example, the introduction of bacterial agents into the formation during drilling and the subsequent generation of polysaccharide polymer slimes which reduce permeability.

Petroleum bearing formations are made up of various minerals which can be expressed as oxides such as SiO_2, Al_2O_3, FeO, Fe_2O_3, MgO, K_2O, CaO, P_2O_5, MnO, TiO_2, Na_2O, with other elements and ions such as S and Cl. These minerals form the porous matrix and may contain various swelling and non-swelling clays, some of which exist as tightly packed aggregates within the rock matrix, while others are located inside the pore space loosely attached to the pore surfaces (Bucke and Mankin, 1971). The latter has a greater chemical and physicochemical formation damage potential because of their direct exposure to the pore fluids. Fines migration and the interactions of clay minerals with aqueous solutions are primarily responsible for formation damage measured as permeability impairment (Chen and Civan, 1993) If swellable clays are lining the pore throats, a small amount of expansion can also cause a severe reduction in permeability (Bennion, 2002) In particular, smectite has a large surface area up to 700 m^2/g, which makes it highly water-sensitive, thereby causing loss of microporosity and permeability. Moreover, swelling effects are not the only mechanism for formation damage due to clays. The dispersion of clay aggregates may lead to the production of fine particles that may migrate to and plug pore throats.

Bailey (1984) stated that the clay formation in unconsolidated sandstone reservoirs poses a threat to the economic recovery of hydrocarbon reserves and is a result of the two factors; (1) migration of fine particles through the porous reservoir matrix and (2) swelling of indigenous clay particles.

Fines migration occurs predominantly in clastic formations because they have a high content of transportable materials within the rock. Common chemical mechanisms are clay swelling, in which hydrophilic materials in the formation, such as reactive smectite and mixed-layer clays, are hydrated and expand when interacting with fresh or low salinity water. This swelling can severely reduce permeability when clay lines the pore throats of a formation. Clay deflocculation, another common chemical change mechanism, results from rapid changes in pH or Salinity, (Faergestad, 2016). Fine particles are present in unconsolidated sandstone reservoirs and are not held in the overall cement matrix that binds the larger sand grains but is loosely attached to the outer surface of the grains. These particles include clays and other minerals and are classified as those passing through a #300 British mesh screen ($<53\mu m$).

Kaolinite is a non-swelling clay but will easily disperse and migrate. Montmorillonite/ smectite has a large exchange capacity of 90 to 150 meq/100 g, and will readily adsorb Na^+, all leading to a high degree of swelling and dispersion.

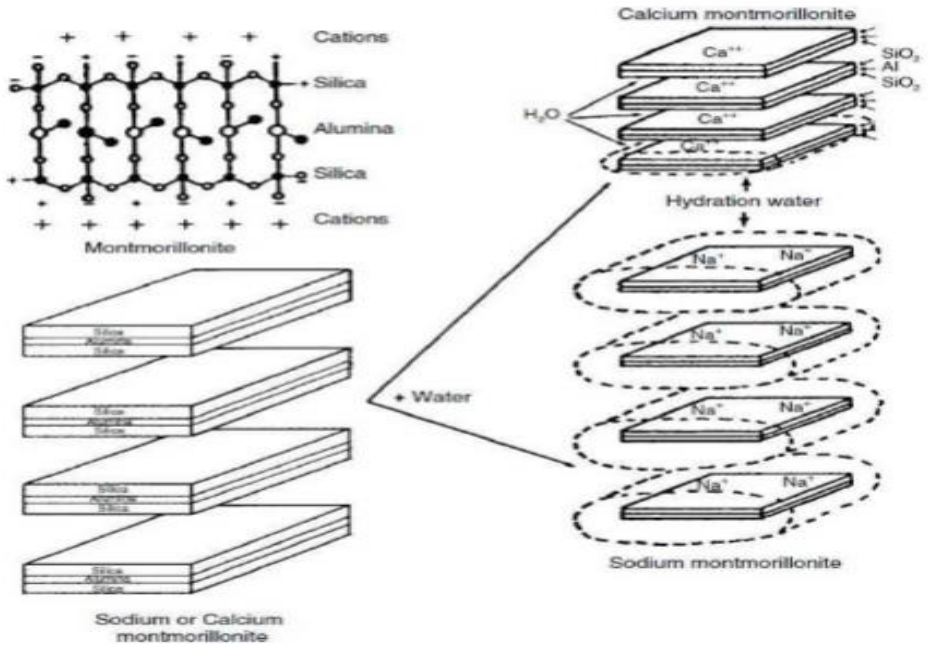

Fig. 2.12: Swelling effect of the Na- and Ca- montmorillonite (Civan, 2007)

It is accepted that Na-montmorillonite swells more than Ca-montmorillonite because the Ca^{+2} cation is more strongly attached to the clay surfaces compared to the Na^+ cation. Accordingly, under contact with water, Ca-montmorillonite platelets remain intact and close to each other, whereas the Na-montmorillonite aggregates readily swell and the platelets and form thicker water envelopes around the Na-montmorillonite platelets than the Ca-montmorillonite platelets, as shown in (Figure 1.12) However, recent studies using molecular dynamics simulations show that Na-montmorillonite and Ca-montmorillonite basal spacing are similar if water content is less than 0.05g H_2O/g clay or higher than 0.15 g H_2O/g clay, whereas, for water content ranging between 0.05 and 0.15 g H_2O/g clay, Ca-montmorillonite exhibits stronger swelling than Na-montmorillonite. These new results using molecular dynamics simulations demonstrate that the underlying mechanisms of clay swelling are still open to discussion.

Reed (1977) observed that neutral salt solutions dissolved significant amounts of carbonate in natural carbonate cement, even though naturally occurring carbonate minerals have low

solubility. This phenomenon, along with mica alteration, frees mineral particles that migrate with the flowing fluid, and ultimately can plug flow channels, reducing permeability.

2.6 Damage mechanism of clay minerals

Most sandstone formations typically contain original clays in their mineral composition. These clay can be present as part of the matrix, as coatings on pore walls, or within the pores themselves. Clay particles are often found at the junction of the sand grains, and in particular, are concentrated in shale lenses. The sandstone containing between 1.0 and 5.0% clay is considered 'clean' sand. Dirty sand would be containing 5.0 and 20.0% clay. Clay particle migration is the most important mechanism of permeability reduction in sandstones containing little or no swelling clays with a considerable amount of migratory or dispersible clays, such as kaolinite and illite (Khilar and Fogler, 1983).

From the chemical or physicochemical perspective, the temperature is an important factor for rock-fluid interactions. In water-sensitive sandstone formations, the effect of temperature is significant. Schembre et al. (2006) concluded that permeability reduction is observed with increasing temperature and that fines mobilization repeatedly occurs at a particular temperature that varies with solution pH and ionic strength. They experimentally found that fines released from the pore walls occur under conditions of elevated temperature, high pH, and moderate aqueous-phase salinity.

Khilar and Fogler (1983) studied the effect of temperature on permeability impairment in water-sensitive Berea sandstones, and found that permeability impairment becomes less severe at temperature decrease.

Permeability is a function of pore size and arrangement, the larger the pores, the larger the permeability. Different clay mineral cements affect permeability in different ways because they occupy different pore throats within the reservoirs. Pore filling clay cement has more effects on permeability than the pore-lining clay minerals (Pallatt et al., 1984).

2.7 Effect of salinity and pH

In petroleum reservoirs when the salinity of formation water is changed by injecting fluids, some changes will occur in some clay and clay minerals in the reservoir. These changes cause plenty of fines occurring in pores. The fines then migrate with fluids

flowing on pores and plug narrow pore throats, thereby the reservoir permeability might be notably decreased causing formation damage.

Latest studies have focused on fines migration in a porous media for various chemical parameters. Awadh (2014) conducted an experiment to investigate the influence of different pH on clay minerals migration, they observed that the strongest alkali has a greater impact on permeability due to the dispersion of native clay minerals (kaolinite, illite, and chlorite) and it reduced by 64%. They also showed that an increase in the alkalinity of the solution contributes to an increase in the formation damage, the degree of damage is assumed to be a function of the size, and the forms of clay minerals have been transferred. The high pH of the fluid promoted the dispersion of clay particles through repulsive forces exerted by negative charges in the system. Moreover, precipitations may produce from the reaction of the high pH fluid with silica. Berea Sandstone contain kaolinite, it is dispersed easily and behave as migrating fines through rock pores (Abdulah et al., 2017).

Khilar (1987) found that the permeability of the originally brine-saturated Berea sandstone decreased rapidly and dramatically when the brine flow through the cores was suddenly switched to freshwater or low salinity water. The rapid decrease in salinity that leads to this drastic decrease in permeability is called a “water shock” and the phenomenon is called” water sensitivity”. In the presence of brine, fine particles are undisturbed and a line the pore walls of the sandstone surface. When brought in contact with low-salinity water, the particles detach from the surface. The released fines migrate with flowing fluid and subsequently captured at pore throats, causing formation damage. An abrupt change from high saline to freshwater could also cause clay blocking which could be inhibited if the water salinity is lowered gradually. Earlier studies showed that permeability reduction can be minimized by gradually decreasing the salinity of the injection fluids. Gradually decreasing salinity from 30.000 ppm to 1.0 ppm resulted in no permeability reduction, but after suddenly switching brine to 1.0 ppm a drastic permeability reduction was observed (Valdya and Fogler, 1992).

According to Mungan (1989) damage from clay minerals depends on the type and amount of the exchangeable cations and the layer structure. Clays having adequately absorbed calcium or magnesium restricted dispersion by water and prevented permeability decline. Small concentrations of calcium or magnesium in the formation and invading waters could effectively restrain clay blocking. This behavior depends on the cation exchange properties of the clays.

The evidence of the flow of low salinity (fresh) water causing the release of clay particles strongly indicates that the release phenomenon is dependent on salt concentration. This detachment is governed by the balance of Van der Waal's force of attraction and electrostatic force of repulsion between the surface and clay particles. Hemeida (2008) set up an experimental work to investigate the effect of employing different workover brines on the permeability of some sandstone samples. It was shown that the damage caused by employing low-density brine of 3% $CaCl_2$ solution. He considered that when the calcium chloride was brought into contact with clay particles, some sodium ions were replaced resulting in clay particle shrinkage and hence less reduction in permeability. The damage resulting from high-density brine of 3% $CaCl_2$ solution and 97% CaBr2 was high due to insoluble salts formed during contact of calcium ions with rock matrix and low mobility of heavy brines.

The critical salt concentration value of sodium chloride and potassium chloride needed to prevent loss of permeability in the Stevens sandstones. The rate of salinity decrease and the low pH had only a marginal effect for controlling the permeability reduction, suggesting that pH control does not affect the mechanism that causes permeability loss.

Previous studies showed that the dispersion of clay minerals is minimized at low pH and therefore that the damage during a water shock can be prevented with acidic solutions (below pH 2.6). Furthermore, it was observed that, during a water shock, the effluent pH increased greatly beyond the initial value while permeability drastically decreased. Thus, the sudden decrease in salinity from brine to freshwater not only caused formation damage but also modified the pH of the permeability fluid, probably through an ion exchange process involving surface cations (Na^+) and the protons in water.

It, therefore, became apparent that, in a system containing exchangeable cations, the salinity and the pH of the medium can be expected to have correlative effects. Thus, it is critical to study the combined effects of salinity and pH and to address them in tandem, not separately as done previously. Little change in permeability was observed when fluids with increasing pH were injected until an injection pH of 9.0 was reached. A rapid and drastic decrease in permeability resembling a water shock was observed at a pH > 11.0 as researched by (Vaidya and Fogler, 1990). This means that the high-pH fluid interaction and the lack of salts in the solution caused considerable harm. The factors causing serious damage to Berea Sandstone are low salinity and high pH. They also observed that the decrease in permeability is in step with pH increase, and that the decrease in salinity induces an increase in pH which amplifies

the release of fines and drastically reduces the permeability. Abdulah et al. (2017) conducted a core flood experiments in Berea sandstone they observed that the permeability of the core decreased as fluid injection repeated. The main problem caused the damage was identified to be the high pH of the fluids. Also, they found that the damage was eliminated when the pH of the completion fluid was decreased from 11.5 to nearly 7 using dilute HCl solution. The damage to the core was mainly because of fine migrations and/ or precipitation results from clay sand/ clay minerals dissolutions and ion exchange processes.

Studies by Mohan and Vaidya (199.) show that when the salt concentration is reduced, a pH transient is set up in the core. Speedy reduction in salinity causes a transient to resemble a sharp wave with peak- attaining values of pH of 10.5. This increase in pH incites clay particles to develop high negative potentials, causing them to detach from the surface and migrate with the flow where they plug the pore throats (Gdanski, 2002). These studies show that the dispersion of clay particles is minimised at low pH, also leading to the prevention of damage during water shock, in acidic solutions. In sandstone reservoirs with acid fluid in the porous medium, the internal clays should be more stable relative to alkaline conditions if the pore walls (example quartz) remain negatively charged.

Moreover, extreme pH conditions (both alkaline and acid) can cause clay disintegration or their transformation to other mineralogical forms and consequent formation damage (Hayatdavoudi and Ghalambor, 1996). The charges of double-layer repulsion on clay particles are increasing with a pH rise and a decrease in salt, according to El-Monier and Nasr-El-Din (2011).

2.8 Effect of Temperature

Rock / fluid interactions to regulate the stabilisation of colloidal suspension for clay particles, temperature is a significant factor. Schembre et al . (2006) showed that permeability reductions are seen with increased temperature, and fines are continuously transported at a certain temperature, different pH and ionic force. It has been noted, under conditions of higher temperatures , high pH and lower salinity, that fines are emitted from port walls.

Zhou et al . (1997) studied the effect on clay swelling with XRD versus temperature and fluid pressure and overburden pressure. They concluded, that the differences between the overburden and fluid pressure has a major influence on the clay swelling, which has a slight effect on swelling between 20– 100^0C.

2.9 Effect of flow rate

The faster the fluid speed, the fine particles will fall off the stones and flow in the rivers with the fluids. Thus, migration fine parts can obstruct the pore throat and, eventually, cause severe permeability reduction. At an increased fluid flow rate, fine particles can allow the fluids in reservoirs to leak through fine particles. Through moving fine particulates, the poric throats may obstruct and ultimately contribute to a possible reduction in petroleum reservoir permeability. Yousef et al. (2008) conducted a labortaory study of the Messla field from Libya and used a sereies of flow rates ranges from 1.0 to 32 ml/min after each period of elevated flow rate, the rate was reduced to the baseline of 0.5 ml/min for comaprison. They obsreved that significant pereambility reduction is evident in that test (permeability was reduced to 18 mD from initial peremability of 42 mD, which is equivalent to >5% decraese of initail permeability following the highest flow rate), indicating possible damage due to fines migration.

2.10 Petrophysical Properties

Basic petrophysical properties are very important for the oil industry because they determine the economic viability of hydrocarbon- bearing reservoirs. A reservoir is subsurface layer or a sequence of layers of porous rock that contain hydrocarbons. These pores constitute pore system that stores the hydrocarbon and act as a pathway for hydrocarbons to flow out of the rock into the borehole. The parameters that determine the behavior of the pore system are known as petrophysical properties and are porosity and permeability. Porosity determines the storage capacity, while permeability indicates the flow capacity of the rock for fluids. Petrophysical measurements are made in the borehole and on cores in the laboratory to determine the major reservoir properties.

2.10.1 Porosity (ϕ)

The two major characteristics of the reservoir rock are porosity and permeability in terms of petroleum engineering. Porosity is one of the most critical elements of performance appraisal and reserve estimation. Porosity is the reservoir's measuring holding capacity. The percentage or fraction of void in the bulk amount of the rock is defined according to definition as stated by Xie (2014). It can be expressed as a fraction, only the interconnected porosity known as the effective porosity is of interest since this is the only capacity that can contribute to flow. Porosity is a critical rock property and is defined as that fraction of the bulk volume of the reservoir that is not occupied by the solid framework of the reservoir. It is an important reservoir parameters in the study of petroleum reservoir engineering. As

shown in Fig, 2.13, the total volume of rock ($\boldsymbol{V_b}$), also known as bulk volume, is composed of pore volume (*Vp*) and the solid volume (matrix volume) of rock particles (*Vs)*. The total porosity is the ratio of the pore volume (V_p) to the bulk volume (V_b). This can be expressed in mathematical form as:

$$\phi = \frac{Vp}{Vb} = \frac{Vb - Vs}{Vb} = \frac{Vb - (\frac{w}{\rho\, s})}{Vb}$$

Where ϕ is the porosity of a rock; V_p: volume of pores; V_s: volume of rock/solid; V_b: bulk volume; *w*: weight and ρ: specific density of the rock/solid. Porosity is conventionally given the symbol ϕ and is expressed either as a percentage varying between 1 and 100% or as a fraction varying between zero to one.

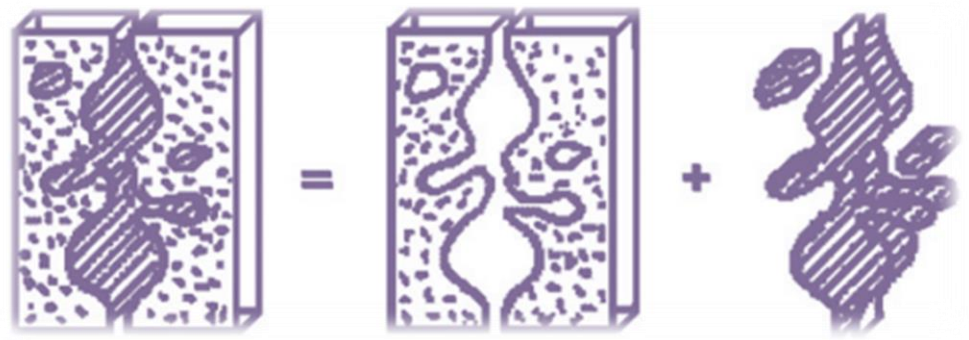

Total volume of reservoir rock**, $\mathbf{V_b}$** Matrix volume**, $\mathbf{V_s}$** Pore volume**, $\mathbf{V_p}$**

Fig. 2. 13: Total volume, matrix volume and pore volume of reservoir rock

The porosity of porous material can have a small range, according to the above description, but the porosity of most sedimentary rocks is usually from almost null to less than 50%. Although petroleum reservoir porosities vary from 5% to 40%, they are mostly 15% to 35% in reservoir sandstones as described by Paul et al. (2012). The extent of porosity in sedimentary rocks, such as grain uniformity, cementation degree or consolidation, compaction during and after deposition, packing methods are governed by several factors. Porosity can be calculated using different techniques. Porosity can be categorised in two different groups from an engineering point of view: total or absolute and effective porosity, whether related or separated from pores. Effective porosity can be defined as the ratio of the pore volume to the rock total volume. Efficient pores mean pores that can transfer fluids under conventional conditions in the reservoir. Generally, a rock has less effective porosity than its total porosity. Table 2.4 shows porosity ratios for typical reservoir rocks.

Table 2. 4: Degrees of reservoir clastic rock porosity

The Type of reservoir porosity	Porosity, ϕ (%)
Extremely high porosity	$\phi \geq 30$
High porosity	$25 \leq \phi < 30$
Moderate porosity	$15 \leq \phi < 25$
Low porosity	$10 \leq \phi < 15$
Extremely low porosity	$5 \leq \phi < 10$
Ultra- low porosity	$\phi < 5$

Porosity may be Primary or secondary. The primary is intergranular and relies on form, size and composition of the solids, the typical one of the clastic rocks. Secondary porosity is typical in carbonate rocks, usually as a result of the breakdown of mechanical forces caused by fissures or cracks in the matrix. The porosity of a given rock depends on several variables, including, individual grain structure, and matrix. The cementation by silica, calcite or material transmitted by outer source or groundwater and the compaction caused by overburdening of rocks are two important reasons for the loss of porosity, so the porosity decreases with increasing depth as stated in Lionel (1992), Ehrenberg and Nadeau (2005).

Total and efficient porosity can be measured by various techniques. All of these include calculating the volume of the sample, typically by measuring the amount of mercury displacing the sample. Under atmospheric pressure, mercury does not penetrate the pores. The most popular way of calculating effective porosity is to fill the pores space with gas or liquid. A reference volume V1 is shown for pressure P1 and a matrix cup with unknown volume V2 and original pressure P2, in Fig . 2.14. The ideal gas law (PV = nRT) based on Stoke 's laws is used in a procedure known as the gas expansion process.

The system consists of two chambers called the reference chamber, with a tubing connexion and a valve separation. At the beginning A is at a known pressure and B is evacuated if the tap is opened. The volume of chamber A and the resulting pressure can be determined by measuring chamber B volume. The solid volume can be determined by repeated the cooperation in chamber B with the porous sample. The gas-expansion technique for successful calculation of porosity needs to be continuously recalibrated with solid blocks of a specified volume and is vulnerable to significant experimental errors.

Thus the pressure-volume products are equal before and after opening the core holder valve:

$$p1V1 + p2V2 = p\ (V1 + V2)$$

$$\text{So, } V2 = \frac{(p-p1)V1}{p2-p}$$

Since all pressures in the equation above must be absolute and it is customary to set p1= 100 psi and p2 = 0 psi, the equation above can be simplified as follows:

$$V2 = \frac{V1(100-p)}{p}$$

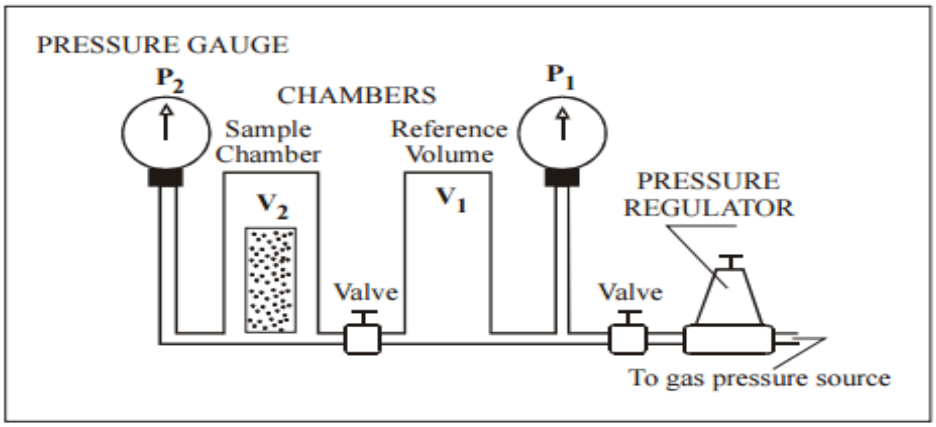

Fig. 2. 14: Schematic of helium porosimeter apparatus (Torsaeter and Abtahi, 2000)

2.10.2 Permeability

In addition to porosity, permeability is also a main petrophysical rock property depending on the pore space of rocks. However, permeability can be defined as a measurement of the ability of a rock to transmit fluid or gas through the porous medium in the rock, is a measure of how easily a fluid can flow through the rock and it defines the flow capacity of rock while porosity only characterizes the ability of the rock- holding fluids.

It is a function of the degree of interconnection among the pores. Based on the rock samples, accurate measurement of rock permeability might be difficult since it may be influenced by flow regimes and rock fluid interaction. Permeability is one of the most valuable petrophysical characteristics that the reservoir engineer seeks to determine in petroleum reservoirs. This originated from Darcy's basic work in 1856. Darcy's law was limited to homogeneous single-phase incompressible fluids and presented by the following equation which is called Darcy's law. So, Darcy's law was derived for one- dimensional and laminar flow. In the petroleum industry, Darcy's law is formulated in terms of pressure gradient and generalized for oil and gas flow, which leads to the concept of multiphase flow. The

permeability estimated in petroleum- reservoir rocks is commonly expressed in units known as Darcy (D) or millidarcy (mD) can be computed using Darcy's law.

$$Q = k\frac{A\Delta p}{\mu L}$$

Where Q: volumetric flow rate (cc/ min), A: cross- sectional area (cm^2), μ: dynamic viscosity of the fluid (mPa s; 1cP= 1 mPa s), Δp: pressure drop across the porous media (psi), L: length (cm), k: permeability (mD).

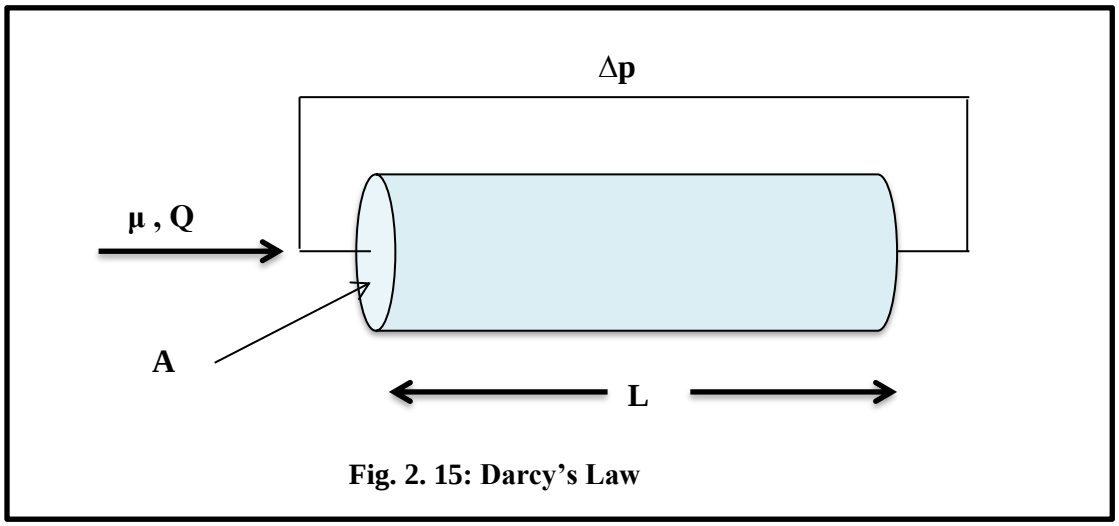

Fig. 2. 15: Darcy's Law

When Darcy's law is used for describing the flowing fluids in reservoir rocks, the proportionality constant k is called the *absolute permeability* of the rock in the case of single-phase flow in the rock. The absolute permeability of a rock is a measure of its ability to transmit fluid where the fluid completely saturated the porous medium. The permeability of the rock is measured on cores in the laboratory by the application of Darcy's law under steady-state conditions. During the measurement, the following conditions must be satisfied:

- Laminar flow of fluid in the rock;
- No reaction between fluid and the rock;
- Only one and incompressible fluid present at 100% pore space.

Several techniques can be used for permeability measurements of cores in the laboratory, depending on sample dimensions, shapes, fluid-applied (oil, water, or gas), ranges of confining pressure, and the purpose of the study. When oil and gas are used for the test, the result may deviate from the real value of rock permeability due to the physical adsorption of oil on the surface of the rock particles or clay swelling and fines migration caused by

passing water in the rock. Consequently, this measurement is performed on clean and dried samples; and dry gases (air, N_2, or He) are often used as measure fluid. The reasons include:

- The state of steady flow can be reached rapidly.
- Dried gas does not change the surface structure of minerals in the rock;
- Easy to build 100% fluid saturation rock pores for one fluid;
- Gas availability

The only problem is the gas expansion in rock pores, which results in an obvious slippage effect in the measurement.

2.11 Coreflooding Test

Fluid movement in pore rocks was generally researched experimentally by core flood studies. Ses tests in oil fields are commonly used to analyse and clarify sub-flows to optimise petroleum production, and to reach a sustainable economic cost of petroleum products. The consistency and precision of core tests determined by laboratory calculation procedures and conditions according to Al-Muthana (2008). The central flood experiment is planned to inject a fluid that has a varying degree of alkalinity to explore the effect of fine particle movement, a proportion of clay minerals and flow rates on the key petrophysical properties of the chosen sandstone reservoir. This measurements are typically done under laboratory conditions. In order to research the implications of alkalinities for the permeability of selected sandstone rock samples rock flood tests is carried out with a different pH. On the other hand, few core flood tests are normally being performed at the same pH values and flow rates to study the effect of clay minerals on formation damage.

The most critical rock quality is a single-phase permeability, which is also called absolute permeability. Permeability In order to analyse the impact of flow rates, alkalinity and tonal quality, core flood experiments were also carried out with various flow rates and alkalinity. The difference between the initial permeability of the sample and its permeability of the core flood is called formation damage.

Chapter Three

Laboratory and Experimental Work

3-1 Introduction

The different approaches and techniques used in this analysis and the role of main samples used are illustrated in this chapter. The flow map (Fig. 3.1) shows how the outcomes of multiple studies carried out for the analysis are obtained through step-by - step methods. This research would also aim to describe the mineralogy of clay and other characteristics such as scale, distribution and position in the reservoir mud pore geometry. The mineralogy of clay and the pores provides a deeper understanding of the damage caused by the oxidation of the clay and fine clay. The chosen sandstone core plugs measure the impact on reservoir characteristics of clay minerals (types and properties). In addition, the effect on the resilience of clay minerals and their effects on permeability reduction in sandstone storage rocks shall be measured by salinity, pH and flow rate. In order to determine the effects of clay minerals on the damage to formation, the clay mineralogy and its impact on petrophysical properties on the sandstone reservoir have to be investigated

3-2 Core Analysis

The set of routine core analyses performed on selected core samples. These include bulk and clay mineralogy, porosity, permeability. Measurements were made at room temperature and atmospheric pressure. Some special core analyses were conducted to investigate the influence of pH, salinity and flow rate on the stability of clay minerals in the sandstone reservoir, and their impact on permeability impairment.

3-3 Description of Laboratory Experiment

The purpose of the experiment was to analyse the pH and salinity (brine concentration), flow rate, temperature and times for petrophysical properties, and the mineralogy and the clay form of selected sandstone core plugs. The research examined the actual pH and salinities. The selected core compositions of samples are analysed by bulk sample process for X-ray diffraction (XRD). In order to determine the location of deposition of clay minerals in pores at the Institute of Mineralogy and Geology at the University of Miskolc, Hungary, the samples collected are analysed by an electron microscope and an energy dispersion spectroscope.

Petrophysical analyses such as (porosity and permeability) and core flooding were prepared at the *Research Institute of Applied Earth Science, University of Miskolc, Hungary* based on the standard procedures. Finally, flooded core samples were analysed using XRD and SEM-EDS to determine the effect on the stability of clay minerals such as fines migration as well as distribution and connectedness of the pores.

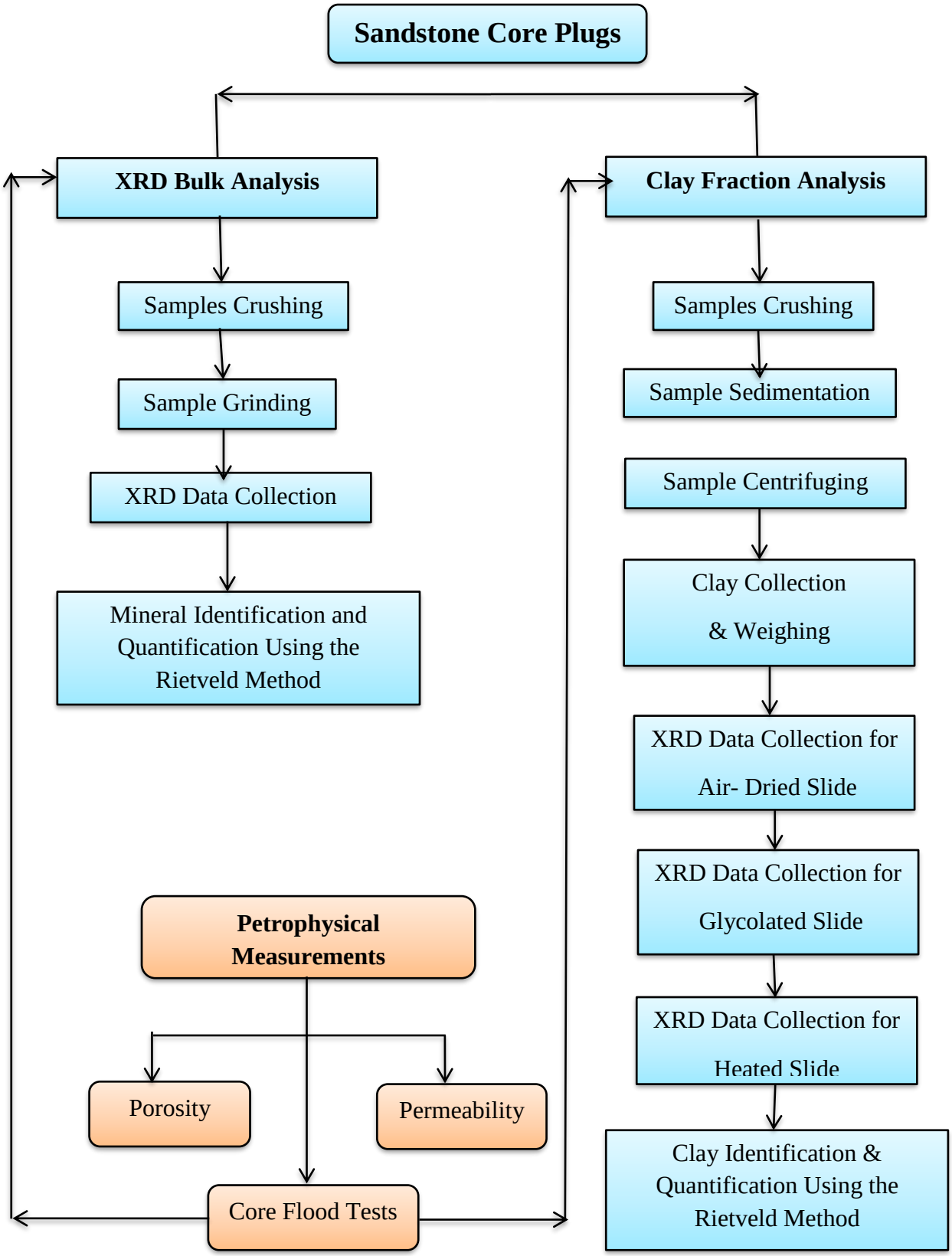

Fig. 3-1: XRD procedure of bulk, clay fraction analysis and Petrophysical Measurements

3-4 Methodology of the Experiment

3-4-1 Materials

In the Hosszúpályi gas field situated in the East part of the Greater Hungarian Plain, seven (7) sub-area sandstone core plugs were obtained (Fig. 3. 2 core picture plugs Appendix C) from four wells. The period in question is the Upper Miocene (Pannonian Formation). Sedimentary facies, mainly braided channels. They were colletced at the MOL Group-Hungary Szolnok Laboratory. The wells are D-2, D-3, D-4 and D-5, from the depth interval of 1868.9m to 2145.1m (Table 1.1) respectively

3-4-2 Core Preparation

Initially, the sandstone core plugs cut a section for XRD and SEM analysis. Then, the cores were placed in the oven for 2 days at 60 ^{o}C to remove the humidity and dry out to the constant weight. The dried core was weighted before test (W_d) and the selected cores were saturated with 5% NaCl brine in a vacuum saturated for two or three hours then the saturated weight (W_s) was measured using analytical weighing balance with a precision of 0.0001 g as shown in Appendix C. Technical method for subsampling procedure is shown in. Fig.3-3.

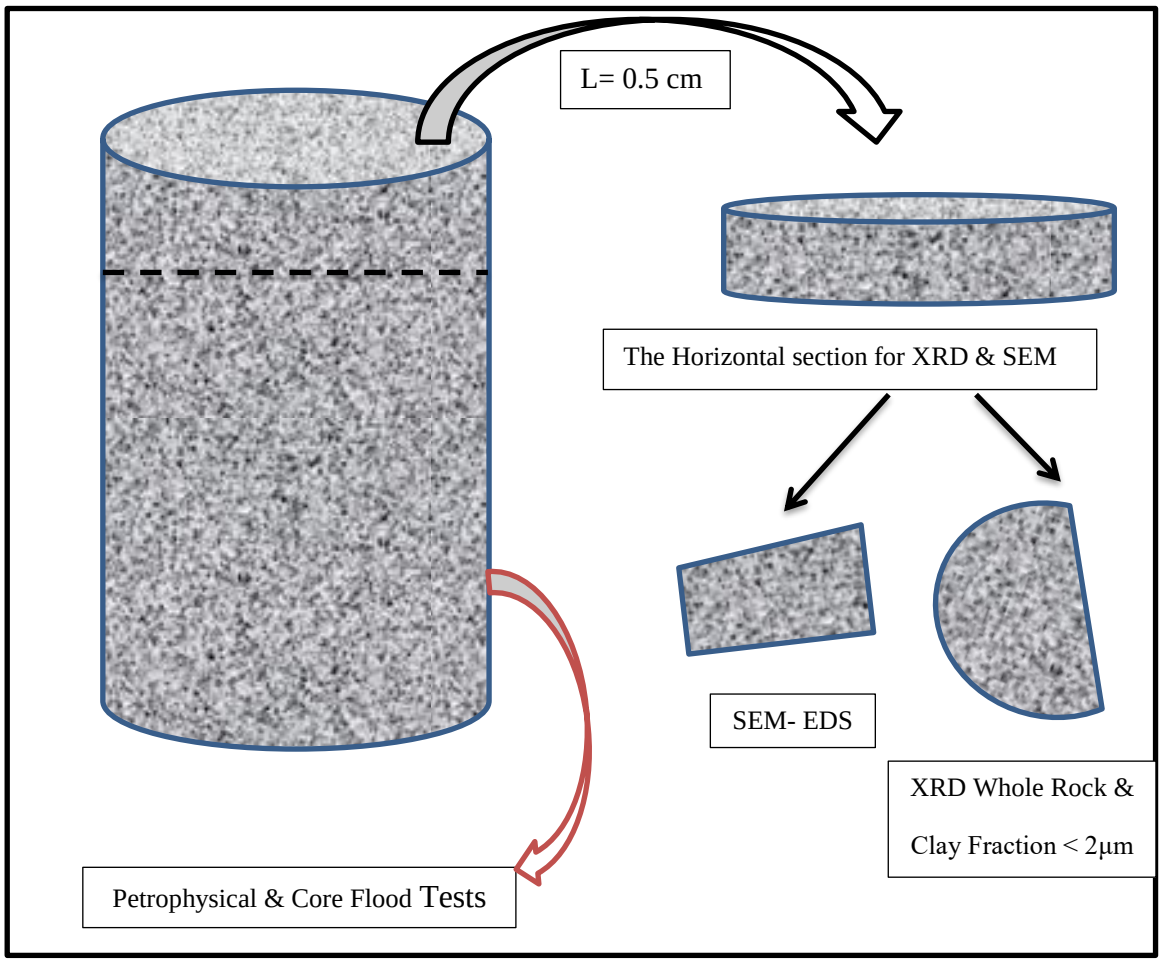

Fig. 3. 3: Illustrates the subsamples for each analytical method used in the study

3-4-3 Properties of Sandstone Core Plugs

The collection of the sample is dependent on sample location. Every sample was prepared at the scale of approximately 5.918 cm and diameter between 3.788 cm and 3.797 cm (5.918 to 6.185) cm. A bulk analysis was conducted for each sample chosen for XRD analysis. For XRD analysis of their clay percentage, chosen samples underwent mass analyses. XRD study findings reveals an overall clay content of 5-10% for illite, whereas 0.5%-2.7% chlorite and 0.1%-2% kaolinite, as shown in Table 3.1. The petrophysical property such as porosity (16,44-27,72%) and permeability for gas of (4-1363 mD) were calculated, and petrophysical evidence was given for absolute permeability between (0,33)mD (Table 4. 4 to 4.6- Appendix A).

3-4-4- X-Ray Diffraction (XRD):

X-ray diffraction (XRD) is one of the most powerful methods for analysing and defining the sandstone mineralogy. It is a method of analysing the phase of a crystalline material and can provide a cell unit measurement. It is the most common method for the detection of unknown crystalline materials. The intensities of the reflected region and the effect produced in a small zone are determined by X-ray diffraction; the atomic-level spacing of the crystal can be estimated that enable the material understand its crystal structure.

Advantages of XRD:

- A rapid and powerful technique for the identification of unknown mineral
- In most cases, it provides unambiguous mineral determination
- Sample preparation required is minimal
- XRD units are widely available
- Data interpretation is relatively straight forward

Limitation of XRD

- Homogeneous and single-phase material is best for identification of an unknown
- Access to a standard reference file of inorganic compounds required
- The detection limit is approximately 2- 5% of the sample (mixed material)
- The identification of all phases may be difficult and time consuming for mixed samples.

Requirements for an Ideal XRD

One of the chief considerations of the sample preparation is the reduction of sample size. The number of diffracted particles is inversely related to their size. The sample size should be small enough so that it fits in the sample holder and the surface of the sample must be smooth.

The applications of XRD given by Brady et al. (1995)

- Used for the identification of unknown crystalline materials
- Characterization of crystalline materials
- Identification of fine-grained minerals such as clays and interstratified clay layers.
- Unit- cell dimensions determination
- Measuring of sample purity

The sample size should be small enough so that it fits in the sample holder (silicon sample holder) and the surface of the sample must be smooth enough (should not be rough and irregular). Using a glass to smooth the surface of the sample so that we may get better results.

Each crystalline material has its own set of peaks "fingerprint". This prints X-ray diffraction can be used for mineral "phase" identification. The phase identification can be done by comparison of the experimental pattern with a database of known patterns. The Powder Diffraction File of the *International Centre for Diffraction Data (ICDD- PDF)* contains either or both the experimentally measured and calculated digitized patterns for hundreds of thousands of compounds. Phase identification can perform either visually or by using automatic searches but generally, a combination of both is used.

3-4-4-1 Preparation for XRD

Special care was taken to sample from the core, avoiding the outer core margins are necessary, in most instances a subsample section was cut from the core (Fig 3. 3). All XRD samples preparation was undertaken at the *Institute of Mineralogy and Geology at Miskolc University*.

Each XRD sample was cut by a machine with a few millimetres. A small piece was separated from the cut section by gently crushed in a ceramic mortar. The materials were then further crushed by hand, and continue grinding with a pestle to produce the material suitable for XRD measurement.

XRPD analysis for a bulk sample relies on the preparation of random powder samples to obtain a diffraction pattern with the correct relative intensities of all peaks; the identification of the bulk mineralogy of the samples was prepared with gently crushed and degraded a small amount of original core plugs in a Porcelain Mortar and continue further grinding in agate Mortar. The difficulty lies in the fact that many minerals for instance clay minerals, feldspars, carbonates have a habit of forming a preferred orientation. To determine the amount and type of bulk and clay minerals, a grinding technique was used to produce powders free of grains coarser with a mean particle diameter of 5- 10 μm. XRPD analysis relies on the preparation of random powder samples to obtain a diffraction pattern with the correct relative intensities of the peaks. The XRD measurements were done on the Bruker D8 Advance X-ray diffractometer (Cu- Kα source). The instrument is equipped with a vertical theta/theta goniometer and Göbel mirror for parallel beam geometry.

The components were identified by Search/Match in the Diffract *Plus* Eva software of Bruker, from the ICDD PDF2 database. The quantitative evaluation of the results was done using TOPAS4 software, with Rietveld profile fitting. It is a widely used method of identification and quantification of clay minerals in sandstones or other rock types. The *amorphous hump* method by, combining Rietveld refinement and single peak fitting, was applied to model the amorphous humps a broad peak was used to determine the percentage of amorphous content.

3-4-4-2 Preparation for Oriented Clay Mineral Fraction

The remaining hand-crushed sample, approximately 15- 20g, is placed within along with a 200ml vial filled with distilled water and subjected to ultrasonic disaggregation using an ultrasonic probe for minute, it was then transferred into 800ml cylinder filled with distilled water. The sample is then left to settle for 24hr (Fig 3. 4). The next step in the procedure was the separation of the clay- size fraction (< 2μm). This was done by settling under gravity based on Stock's Law. The centrifugation of clay mineral sample of higher purity may therefore to be done to obtain adequate quantity of suspension and placed in an overall oven for drying out Brindley (1980).

Fig. 3.4: Settling cylinders containing suspended sediment

After that, a (0.004 g) of this fraction was taken and added 0.2 ml distilled water (D.W.). The sample then subjected to a 5-second cycle of ultrasonic vibration using a (Real Sonic Cleaner). was prevent the flocculation of clay particles in suspension, each prepared sample was shaken vigorously by hand and machine shaker for at least 30min and then smeared on a glass slide using a plastic pipette and allowed to air dry until all traces of water had evaporated.

There are various methods available for producing such samples, such as glass slide method or smear mount (Adam, 1965), but the chosen method for this study is the glass slide method (Fig 3. 5). As with random powders, the oriented sample glass slides were run in Bruker D8 Advance X-ray diffractometer (Cu- Kα source), the type of clay minerals were identified from measurements in air-dried (AD) state after ethylene glycolate (EG) and heating up to 350 and 550^0 C, according to Thorez (1976), Grim (1968) and Moore and Reynolds (1989). The ethylene glycolate samples are obtained by applying solvation over 12 h at 60°C to the oriented air-dried samples. Heated samples were obtained by heating samples up to 350 °C and 550°C at 10°C/min linear heating in air, according to the standard procedure of Grim (1968) and Thorez (1976).

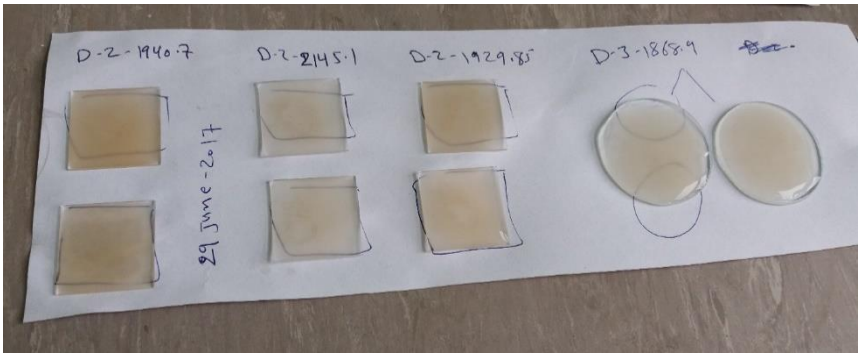

Fig. 3. 5: Glass slide and air drying

Several treatments have been undertaken to verify the clay minerals by using X-ray diffraction:

- **Ethylene glycol treatment**

  Ethylene- glycol solvated specimens were conducted to characterize the phyllosilicate/ clay mineralogy of the bulk samples. Based on these results, the selected samples for examination of the <2.0μm clay were separated. These were obtained from ultrasonic bath- dispersed specimens, followed by sedimentation of the dispersed <2.0 μm fraction directly onto glass slides by evaporation. The specimens were air-dried and ethylene-glycol solvated, and heated up to 550˚C and scan with Bruker D8 Advance X-ray diffractometer (Cu- Kα source). They were dried in the oven at 60˚C and then re-analyzed to determine the presence of swelling clay minerals such as smectite. It is easy to identify by comparing patterns of air-dried and ethylene glycol- solvated preparation. The glycol- treated give a very strong (001) reflection approximately 5.2° 2Θ (16.9Å), which in the air-dried condition, shifted about 6° (15Å) Moore (1989). While the patterns of kaolinite, chlorite, and illite are remaining unchanged during ethylene glycol- solvated.

- **Heating to 350 and 550°C treatment**

  The slides were heated in the furnace at temperature 350 and 550° C for 30 min to verify the kaolinite and chlorite peaks. Heating kaolinite up to 550° C for 30 min, causing the diffraction pattern to disappear. While, at the same temperature, the diffraction peaks of chlorite and illite remain unchanged. Heating smectite to 550° C for 30 min causes dehydrated and the intensity of the (001) reflection decreases to 10 Å.

3-4-4-3 Qualitative analysis:

The clay minerals were identified using the X-ray diffraction patterns which by the peak's position, intensity, shape, and breadth. The peak position is determined using Bragg's law ($n\lambda = 2d\sin\Theta$) where (λ: wavelength; d: lattice spacing; diffraction angle and n: the order of the diffraction peak). The peak positions on the XRD patterns are identified in terms of °2Θ and converted to lattice spacing (d) in angstroms (Å). Generally, clay peaks are at the 2Θ values of 40° or less; therefore, Θ is 20° or less. The precise identification of clay minerals was based on careful consideration of peak positions and intensities. The position of the peak is taken as the point of greatest intensity.

All minerals possess a unique XRD pattern so that the comparison of the diffraction patterns of unknown minerals against stets of standard patterns leads to their identification. The procedure of quantitative identification started by searching for a mineral that explains the strongest peak or peaks, then confirming the choice by finding the position of weaker peaks for the same minerals. Once a set of peaks was confirmed as belonging to a mineral, these peaks were eliminated from consideration. From the remaining peaks, a mineral that will explain the strongest remaining peak or peaks was searched and ten confirmed by looking for its peaks of leaser intensity. This method was repeated until all peaks were identified.

To distinguish between the different clay minerals in a separated clay fraction, samples undergo various treatments that affect the basal spacing such as ethylene glycosylation and heating up to 350 and 550°C. Illite peaks are unaffected by ethylene glycol solvation and heating to 550°C has a reflection of 10Å. Chlorite has a basal series of diffraction peaks based on the first-order reflection of 14.2Å. Kaolinite has reflections based on a 7.1Å structure. Chlorite and kaolinite can be differentiated by chemical or heat treatment and then re-examined. Smectite is easily identified by comparing the diffraction patterns of air-dried and ethylene glycol- solvated affects the basal spacing by expanding it to approximately 17Å (Moore, 1989).

Table 3- 1: An identification of clay minerals based on observation after various treatments. (GeoEnviromental Research Group Laboratory Manual 2008)

Minerals	**Air-dried**	**Ethylene Glycosylation**	**Heated 550° C**	**Acidic**
Montmorillonite/ Smectite	15.0 Å	16.9 Å	10.0 Å	Unchanged
Illite	10.0 Å	Unchanged	Unchanged	Unchanged
Chlorite	14.2 Å	Unchanged	Unchanged	Peak disappeared
Kaolinite	7.1 Å	Un changed	Peak disappeared	Unchanged

3-4-5 Scanning Electron Microscopy and Energy Dispersive Spectroscopy (SEM-EDS):

Scanning electron microscopy (SEM) allowed images to be taken of features within fine-grained rocks that are too small to be seen in this section using a standard optical binocular microscope (Fig. 3. 6). This type of image is especially helpful in providing a better understanding of different types of clay minerals and how they are distributed within the pores and affect the degree of pore connectivity and hence permeability. SEM may help determine microporosity within the clay minerals, which is not distinguished by petrography analysis (Fig.3.7 SEM Instrument Appendix C).

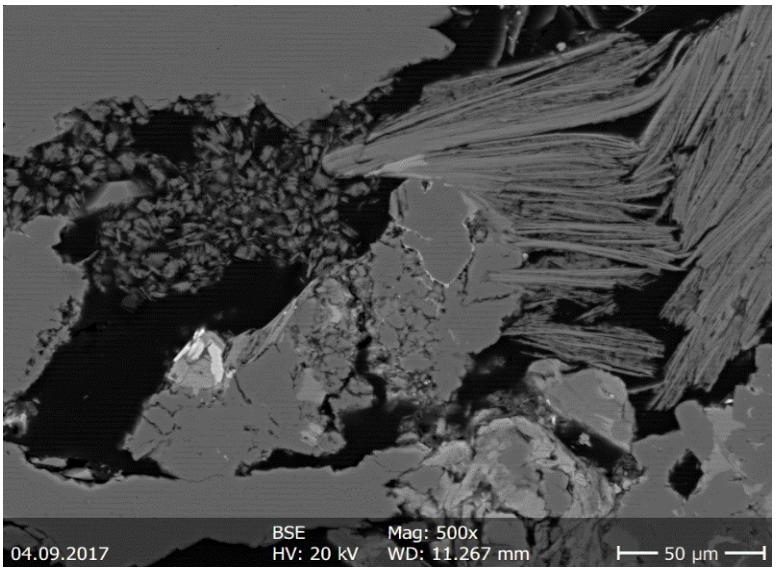

Fig. 3. 6: Sample D-3- 2 (1868.9m), with quartz and pore-filling kaolinite booklets and exfoliated micaceous flakes.

3-4-5-1 SEM and EDS Preparation

Scanning Electron microscopy (SEM) can better explain the mineralogy of clay and its effect on the porosity, permeability, and other features of the reservoir (Jiang, 2012). The SEM samples were prepared by grinding on a plate followed by polishing with emery paper using Struers RotoPol- 35 and Struers PdM- Force- 20. (See Fig. 3.8 Grinding paper the appendix C)**.** SEM/EDS was conducted under vacuum conditions on polished parts obtained from the core plugs after epoxy resin cementation so that empty pore spaces will be filled and clay cement immobilized, enabling us to detect the original texture in polished parts. The mineralogical identification was done by Search/ Match in the DiffractPlus Eva software of Bruker D8, from the ICDD PDF4 database.

The quantitative evaluation was done by using TOPAS4 software, with Rietveld profile fitting. Also, the Amorphous humps method, by combing Rietveld refinement and single peak fitting, was applied to model the amorphous humps as an abroad peak was used to determine the percentage of amorous content. Images were captured with scan speed (80/ 100s)/ (50/60 Hz) for micrograph. SEM+ EDS was conducted under vacuum conditions on polished parts obtained from the core plugs after epoxy resin cementation, such that empty pore spaces can be filled and clay cement immobilized, allowing it to detect the original texture in polished pieces. Backscattered electron (BSE) images were obtained on a Jeol JXA 8600 Superprobe instrument (W filament, 20 kV acceleration voltage, and 20 nA prob current, carbon coating) shown in (Fig. 17 in Appendix C). EDS spectra were the record of standardless mode (RemiX Si- drift detector, C- U detection range) with 60 secs collecting time (15% dead time), quantified by PAP correction at the *Institute of Mineralogy and Geology at the University of Miskolc, Hungary.*

3-5 Preparation of Solutions

Saline solutions of Sodium Chloride and Potassium Hydroxide are prepared at the *Institute of Mineralogy and Geology* with different pH (pH3 and pH11, strong acid to strong alkaline respectively) as shown in (Table 3-2) to inject into the core plugs for investigate the influence of clay mineral stability, their effects on permeability reduction and calculating their damage as well.

Table 3.2 Solution properties

Type of Solution	HCl 10% (ml)	KOH 1M (ml)	NaCl (g)	Distilled water (Liters)	pH
Acidic	**0.2**	**.....**	**0.4**	**3.2**	**3**
Basic	**.....**	**0.6**	**0.4**	**3.2**	**9**
Basic	……..	**0.6**	**0.4**	**3.2**	**11**

3-6 Petrophysical Characterization of Sandstone Core Plugs

This section presents properties sandstone core plugs by evaluation of the porosity and permeability. Petrophysical analysis and core flooding are prepared based on standard procedures. The selected sandstone core plugs have been saturated with brine solution 5% NaCl before starting the permeability measurement at room temperature and atmospheric pressure. The petrophysical analyses included measuring the porosity; air (gas) permeability and liquid permeability. Many laboratory experiments of core flood were conducted where the cores have been injected with a brine solution of NaCl.

Porosity and permeability parameters are critical for the oil and gas industry because they determine the economic feasibility of hydrocarbon-bearing reservoirs. Porosity is the basic feature of a reservoir rock; it defines the holding space. The pores must be interconnected to permit the passage of oil, gas, and water through the rock. In other words, the rock must be permeable; permeability indicates the flow capacity of the rock fluids. Therefore, the porosity and pore structure of reservoir rocks are the key factors that affect the quality of reservoirs and control the off-take potential of oil and gas wells (Rui, 2017).

3-6-1 Method of Porosity Determination (φ)- Helium Porosimeter (Multi- Pycnometer)

The porosity was measured through Helium (He) gas Porosimeter method using the Porosimeter apparatus, as shown in (Fig. 3. 9. Helium Porosimeter instrument Appendix C). This method relies on ideal gas law, or rather Boyle's law. The core sample is sealed in a container of known volume V_1 at atmospheric pressure P_1 (Fig 3-10). This container is attached by a valve to another container of known volume, V_2, containing gas at a known pressure, P_2. When the valve that connects the two volumes is opened slowly so that the system remains isothermal, the gas pressure in the two volumes equalizes to P_3. The volume of the equilibrium pressure can be used to calculate the volume of grains in the rock V_s.

Boyle's Law states that the pressure times the volume for a system is constant. Thus we can write the PV for the system before the valve is opened (left-hand side of the equation) and set it equal to the PV for the equilibrated system (right-hand side of the equation)

$$P1(V1 - Vs) + P2V2 = P3\ (V1 + V2 - Vs), So,$$

$$Vs = P1V1 + P2V2 - P3(\ V1 - V2)/\ (p1 - p2)$$

The porosity of the selected core plugs was calculated using the equation below. The results of the measurements and the effective porosity calculations are presented in (Table 4-1) in the next chapter.

$$\phi = \frac{Vp}{Vb}$$

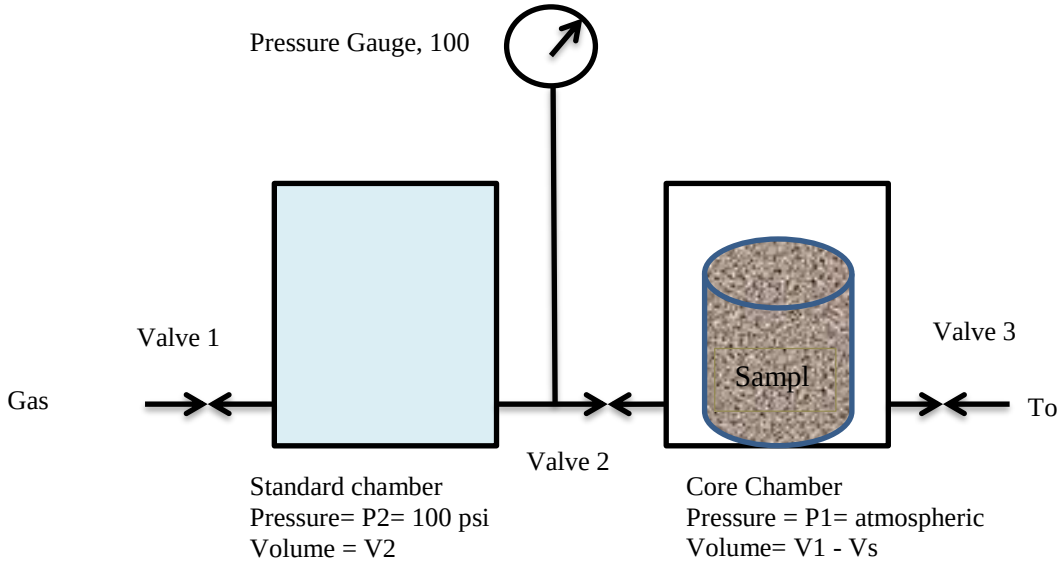

Figure 3-10 Principle diagram of He- Porosimetry (Rui, 2017), (modified by author)

The commonest gas was used to measure porosity is Helium (He) because the molecules so small can enter almost all pores. This method is fast, more precise, not sensitive to mineralogy, and the sample can be used for further petrophysical analyses.

3-6-2 Method of Water- Initial Permeability Determination

Permeability is a property of the porous medium and it is a measure of the capacity of the medium to transmit fluids. The core permeability was measured with a brine solution after

porosity measurement. The measurement of permeability was based upon the law of Darcy. Darcy (1856) studied vertical movement across columns of sand filled with water and found that the volumetric flow rate depends on the cross-sectional area of the column, the pressure gradient across the column, and the properties of the sand column. The flow rate also depends on the fluid viscosity; thus, for a general fluid, flow can be expressed by the equation below, which is known as Darcy's Law for laminar incompressible flow.

$$\frac{q}{\mu A} = \frac{k\Delta p}{L}$$

Where q is the flow rate, A is the area of the core, Δp is the pressure drop, the μ viscosity of the fluid, L, length of the core and k is the permeability.

The air and water permeability was measured by constant head permeameter apparatus as shown in (Fig.3.11 Hassler Core Holder Instrument Appendix C) using the Hassler cell method. The method consists of a pressure regulated by the upstream and downstream values on the side of the Hassler cell and measurement of the airflow in the flow meter. The experiments were conducted at room temperature conditions and backpressure sleeve (BPS) was kept to (number) bars in the Nitrogen (N_2) cylinder. The 7 core plugs were introduced and moved into the core holder using a vacuum. To start the measurements, the pressure gradient (Δp) was fixed at 3bars because the airflow at the core sample must be laminar. Specific permeability can be measured using conventional steady-state methods such as constant flow, constant head.

To measure the absolute permeability, the core must be fully saturated with a single-phase and have a known area and length. A fluid with known viscosity is passed through while maintaining a laminar flow and both the flow rate and differential pressure are measured.

Dry gas is preferably used for measurements to reduce reactions between the formation core and fluid, dry gas is readily available and convenient. According to Klinkenberg (1941), they show different results from those using liquids. Gases have a higher flow rate due to its slippage effect. When measuring permeability, fluid is flown carefully to prevent bypassing displaced fluid (Lionel, 1992).

Gas Permeability and Klinkenberg Effect

Air and nitrogen are usually used as a fluid for measuring the permeability of rock cores using permeameter in the laboratory, as shown in Fig 3.12. When the gas flows through the core at a constant temperature, the volumetric flow rate Q of the gas will vary with pressure because of the great compressibility of the gas. Therefore, the values of Q at each cross-sectional area are different, which results in no validity of Darcy's law in this flow. Suppose the flow of gas through the core is steady (no change with time), the mass flow of gas is then the same at each cross-section.

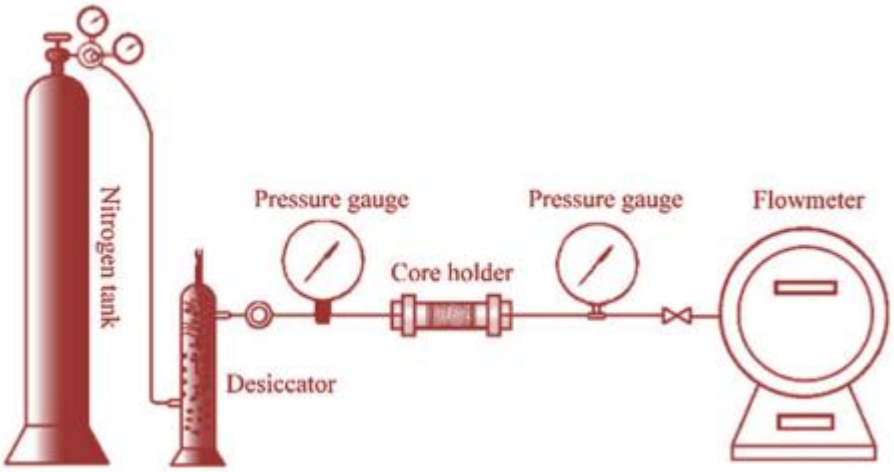

Figure 3.12: Flow chart for a permeameter (Rui, 2017)

The formula of gas permeability can be expressed by the following equation:

$$Ka = (2Q_0 p_0 \mu L / A({p_1}^2 - {p_2}^2)) \ * \ 10^{-}1$$

Where K_a gas permeability of the rock (mD); p_1 and p_2 upstream pressure (MPa); p_o may be downstream or upstream pressure (MPa); Q_o volumetric flow rate of the gas at pressure p_o (cm^3/ s). So, based on the equation above, it can be seen that the gas permeability is a function of the square difference in pressure, but not a function of pressure difference. Gas molecules flowing in a tube seem to slip from the surfaces of pores. Thus, whenever the mean free path of gas molecules approaches the dimensions of pores, gas molecules are always in motion on the pore surfaces and contribute an additional flux that increases the permeability of the rock. This phenomenon is called the *slippage phenomenon* or *Klinkenberg effect*. Based on the experimental results, Klinkenberg related the apparent permeability K_a measured for gas

at an average pressure Ṗ to the true permeability k∞ or Klinkenberg permeability by an equation with the form Klinkenberg (1941) and Rui (2017).

$$ka = k\infty\ (1 + \frac{b}{\dot{P}})$$

Where k_a is gas permeability (mD); k∞ is equivalent liquid permeability, Klinkenberg permeability or absolute permeability (mD); Ṗ is the average pressure (Mpa) = (p_1+ p_2/ 2); b is the slip coefficient, constant for a given gas in a given medium.

Slip coefficient depends upon the mean free path of gas molecules, the average pressure Ṗ and the pore size of a porous medium, can be expressed as:

$$b = \frac{4C\lambda\dot{P}}{r}$$

Where C: 1; r average pore radius of the porous medium; λ mean free path of gas molecules at average pressure Ṗ; λ related to the size of the gas molecules and the density of gas molecules by the following expression:

$$\lambda = \frac{1}{\sqrt{2}\pi d^2 n}$$

Where d is the diameter of the gas molecules; n density of gas molecules at average pressure Ṗ.

The above equations indicated that gas permeability is directly dependent on the size of the gas molecules. The pore size of the rock, and the average pressure for measurement. The smaller the size of gas molecules and pore radius, the lower the average pressure, and the larger the gas permeability K_a, and the slippage effect is more remarkable (Rui, 2017).

The initial permeability of the selected samples range can be divided into three group's lower permeability, intermediate and high. The deepest samples from D- 2 well was recorded 252.6mD, and high permeability ranges from above 552.4mD While the lowest permeability was record with sample D- 3- 1 was only 21.5 mD. From D- 4 group lowest permeability (absolute) was 343.2mD as presented in the table **(Appendix A- Tables 4.5 to 4.7).**

3-7 Core Flood procedure

Core flooding is the main component of oil field development, providing data that can be used to predict petrophysical characteristics and evaluation during production. To minimize the physical variables during laboratory core flooding test, it is imperative that on core plugs be obtained under conditions which reproduce those of the in-situ reservoir conditions such as temperature, pressure, and fluid chemistry (Ngwenya, 1994). Apart from formation damage, water floods are traditionally designed without considering the composition of injected brine. The single-phase core flooding resulted in an increase in pH from 7.7 to 8.8 during low salinity water flooding, and fines migration production was observed during some of the flooding (Bayat, 2016).

The petrophysical measurements and core flood tests were conducted at the *Research Institute of Applied Earth Sciences, University of Miskolc*. Petrophysical tests included porosity measurements of He- Porosimeter, and liquid initial permeability measurement, where the cores have been vacuum- dried and then vacuum- saturated using 5% NaCl brine (pH 7). The reason to choose 5wt% NaCl as formation brine during the test because at the Institute of Applied Science and Research, Miskolc University is used as formation water, which is close to the salinity of formation water (reservoir water salinity) in Hungary. The porosity of the score calculated by the help of He- Porosimeter "MultiPycnometer"

The permeability of cores was measured using Hassler type core holder and low salinity formation brine to, avoid any damage to clay minerals during the measurement. A sleeve (confining) pressured was kept until 25 bar/cm^2 in the Helium cylinder was applied. No back pressure was required during the testing conducted at ambient conditions. Core samples were obtained from the sandstone section of a gas reservoir in Hungary. The permeability and porosity ranges were 14-19vol% and 32- 731mD. Series of experiments were performed injection NaCl brine with different pH (Table 4.5- to Table 4.7- Appendix A).

After that, a series of core flood experiments were run by using the Hassler- type core holder (Fig. 4- 41 Appendix B). Then the core plugs were flooded with formation of brine NaCl 5wt% and different pH values 9 and 11 with different flow rates (50, 150 and 200ml/ h) at ambient conditions. Besides, 2 core plugs were flooded with formation brine and pH 3 with different flow rate at room temperature. To investigate the influence of pH, salinity and flow rate on the stability of clay minerals.

Ngwenya (1994) experimented on the Clashach sandstone at 80^0C using artificial brine solutions with an initial pH of 7.2 over durations ranging from 2 to 5 weeks with a volumetric flow rate of 0.3cc/m was chosen for all tests. They found that the online permeability dropped to 87% of the initial value in the first 24hr. This was followed by a more gradual decline throughout the experiment, although the permeability stabilized at approximately 70% of the initial value in the second half of the experiments.

Clay migration damage reduces reservoir permeability. The process of clay migration damage involves the movement of clay minerals within the low-permeability reservoir pore structure, as a result of migration damage is depends on the sizes of both clay minerals and restrictions.

Chapter Four

Results and Discussions

4-1 Introduction

This chapter presents the results and discussions of the measurements and calculations of different parameters referred to previous chapters. The results are discussed according to different values obtained and are also compared with the results achieved on the other references reviewed. In the scope of this thesis, reduction in permeability was analyzed from micro-scale to macro scale. The micro-scale deals with what is happening to the reservoir pore space. Thus, the analysis scheme was studied as follows:

- Pore throat plugging and bridging.
- Absolute permeability (by water) and water flooding experiments.
- XRD and SEM analyses of the core samples for permeability reduction analyses.

A series of core flooding tests were conducted on selected sandstone core plugs (***Reservoir sandstone- Hosszúpályi gas field- East- Hungary*)** to investigate the mechanism of fines migration due to changing in pH values and its contribution on petrophysical characteristics. Also, this chapter includes the of study of the mineralogy of bulk samples and clay minerals by the help of XRD analysis, determines the distribution, location, size, and geometry of the pore and minerals within the pore throats before and after flooding by using scanning electron microscopy (SEM). Through these experiments, the tendency and severity of fine particle migration in this field were investigated and the influence of reservoir depletion on permeability was observed. An essential aspect of this study understand the mechanism of fines mobilization within the pore throats and its influence on petrophysical characteristics of selected sandstone core plugs.

4-2- Mineralogical Composition of Core Samples

As discussed earlier, clay minerals have an important role in controlling sandstone reservoir characteristics. The presence of clay minerals in reservoir rocks has an important impact on reservoir properties such as porosity and permeability. The XRD and SEM proved, measured, and localized the fines migration in the damaged cores. The influence of migration in fine particles (clay and non- clay minerals) movement towards the porous media on the core flooding to test success in terms of formation damage. Based on SEM and core flooding

tests, damaged core plugs yielded different type of pore- size distribution and permeability compared to undamaged cores.

The following results were obtained by XRD and SEM was used to identify the clay minerals and non- clay minerals present in the sandstone core plugs. The resulted from diffractograms of air-dried (AD), ethylene glycolate (EG), and heated at 350 and 550° C, which shows the major basal reflections of the clay minerals in the studied samples. The type and amount of minerals of bulk sample and clay minerals are measured by the XRD test. The different reflection angle for different minerals could be used to identify the type and amount of the minerals. The results of XRD analysis show that the selected sandstone core plugs have variable contents of non- phyllosilicates such as quartz, calcite, dolomite, Microcline, Muscovite and albite as well as, phyllosilicates including clay minerals such as illite, chlorite, kaolinite and interstratified illite- chlorite. The percentage of quartz ranges between 69.4 to 83.3% while the percentage of carbonates varies between 0.5 to 7.2%, D-2-6 contain minimum percentage of carbonates was only 0.5% in contract D-3-1 recorded highest percentage more than 7%. Oligoclase recorded the second highest mineral composition in all samples its ranges between 5.7 to 9.5%. The other non-clay minerals such biotite, microcline recorded the lowest percentage of non-clay minerals. On the other hand, the results show that selected cores contain kaolinite, chlorite, illite and interstratified illite/chlorite. We can approximate amount of clay nearly 5% except D-3-1 recorded highest clay content more than 9.0%. However, the clay mineralogy in somewhat variable depends upon sample location within the reservoir, as shown in (Table 4. 1 to 4. 3 in Appendix A). Existing clay minerals have the capability to migrate and disperse, experiments show that would have considerable impact on the permeability. The existence of clays such as kaolinite, illite and chlorite shows no important swelling induced impaired permeability. The experiments conducted on the samples showed that the detected clays (kaolinite, illite, chlorite and inter-stratified illite/chlorite) have severe impact on the permeability of the samples.

Pore-throat size distribution is a key factor to control petrophysical properties of sandstone reservoir. According to SEM analysis samples have different pore-throat size distribution, samples have large pore-throat distribution have high permeability and samples have low permeability have small pore-throat distribution.

Allogenic clays “detrital” are mechanically transported particles, which form before deposition of sediment are mixed with the sand and silt size fraction during deposition, while authigenic clays are formed into the rock, of which they are a part, during or soon after, its deposition, and as a part of the diagenetic processes. They are located between and often blocked or occlude pores, or as replacements of pre-existing grains such as feldspar, biotite and so on which are less stable than grains such as quartz. Lejar (2012) stated that both types of clay minerals “detrital and authigenic” commonly harm the reservoir quality of sandstone reservoir rock.

The occurrence of these authigenic minerals affected the reservoir properties of the studied area by decrease porosity and permeability. Chlorite and illite which mostly occur as pore-filling material on the detrital grains control the properties of the sandstone reservoir. As a result, the pore throats between the sand grains reduce, initial porosity and as well as permeability declines. A similar observation had been observed by Das (2006) and Mehdi (2015). Clay minerals have a precise role in controlling the properties of sandstone reservoirs. In sandstone, the types, relative amounts, distribution, and origin of clay minerals can be identified in the laboratory by the application of X-ray diffraction (XRD) and scanning electronic microscope (SEM) as shown in Appendix A and Appendix B.

4- 2- 1 XRD interpretation of the Selected Samples:

X-ray diffractometric plots of the rock sample presented in (Fig. 4. 1 to Fig 4.7 - Appendix B). These plots show several peaks the height of which is a function of the amount of clay mineral present Weaver (1958). A comparison of the diffraction pattern of unknown mineral phases with a set of standard patterns lead to their identification. The results from the XRD analysis shown that the selected samples were composed of variable mixture of clay and non-clay minerals. The major clay minerals in most of these rock samples were mainly composed of illite, chlorite, kaolinite, and interstratified illite- chlorite. Non-clay minerals in the study area were composed of quartz, carbonates, microcline, muscovite, albite, and biotite less than 0.1%.

Sample ***D- 2- 6***, it was the shallowest sample (1943.0 m). X-ray diffraction analysis on a sample revealed that the percentage of non- clay minerals more than 95%, the dominant non-clay mineral was quartz and it’s characterized by spacing 4.27Å and 3.34Å in the selected sample and the rest as well. Oligoclase was a second abundant non- phyllosilicates characterized by a reflection of 3.19Å in this sample and the other selected core plugs.

Carbonates both calcite and dolomite were the next abundant non-clay minerals with a few percentage, characterized by reflections 3.03 Å and 2.88 Å respectively. Microcline existed with a 1.0 wt% in the selected sample. Biotite and phyllosilicates were recorded in all selected sandstone core plugs with a different percentage ranges from trace amount to 1.0%. XRD patterns of oriented specimen show that the sample was composed of kaolinite, chlorite, illite, and interstratified illite- chlorite with a few percentages (Fig 4- 11). The percentage of total clay minerals was 4.04%. The amount of illite was 2.5%, chlorite 1.0 and kaolinite 0.5%. XRD patterns of oriented specimen show that the sample was composed of kaolinite, chlorite, illite, and interstratified illite- chlorite with a few percentages (Fig 4- 11). The X-ray diffraction peaks of illite 10Å and chlorite 14Å remain unchanged after ethylene glycol solvation and heating to 350- 550°C which were indicated that there chlorite and illite occurred on the sample. The diffraction peaks of 7.2 and 3.57Å were the characteristics of diffraction peak of kaolinite and remain unchanged with ethylene glycol and disappeared at 550°C. This was proof that there was kaolinite in the sample, the presence of 11.5Å was the characteristic of interstratified clay minerals and the peak did not alter during ethylene glycol and heating to 350 and 550°C. This is indicating that the interstratified layer clay was illite-chlorite. Illite- chlorite is present less than 0.01 wt% of a bulk sample and about 1-2wt% of clay fraction (Fig. 4.8 to 4.14 Appendix B). The illite is the most widespread authigenic clay mineral in the sandstone sample, kaolinite and chlorite are the second abundant clay minerals in the this sample and the rest of selected core samples. Hong (2012) proved that diffraction peaks 10 ≈14°A was indicating diffraction peaks of interstratified layer illite- vermiculite. Lee et al. (1984) reported that the mixed layering of illite/chlorite is random at an individual layer level and that it separates into discrete packets of illite and chlorite layers as burial metamorphism proceeds. An ordered 24 Anstroms, 1:1 randomly interstratified illite/chlorite was reported and from the Martinsburg Formation at Lehigh Gap, Pennsylvania (Lee and Peacor, 1985). These clay minerals and non- quartz minerals occur both as granular detrital, authigenic material, and cement. In addition to clay mineralogy on stability of formation damage there are a number of interacting factors to take into account, other than the nature of clay minerals themselves. Most importantly these include the overall texture, structure, as well as size distribution and connectivity of the pores, because it is these factors which determine the extent to which the flooding fluid can interact with the clay minerals.

D- 2- 5 and **D- 2- 4** samples with a depth (2140.3m and 2145.1m) characterized by lower quartz content about 78% respectively if compare to D- 2- 6 core sample, the percentage of

carbonate is more than 5.5% while in D- 2- 6 only 0.5%, both samples has the same amount of oligoclase (Table 4.1). The percentage of other non-clay minerals such as microcline and biotite is less than one percent. Generally, both samples are composed of the same clay minerals as a previous sample of a different ratio, D- 2- 4 sample contains more kaolinite than D- 2- 5 and D- 2- 6 samples almost triple. While, it has less illite than the other, and the amount of chlorite in D- 2- 5 samples is higher than other samples. Generally, all samples have the same composition of minerals (clay and non- clay minerals see (Table 4.1 Appendix A) with different ratios and characterized with the same diffraction peaks (Fig. 4.1- 4.3). XRD of oriented clay fraction shows clay minerals composed of kaolinite, illite, chlorite, and interstratifies illite/chlorite (Fig. Clay fraction).

The XRD pattern of **D-4- 2 and D- 4- 1** with a depth **(1872.6m and 1874m) respectively,** X-ray analysis shows that those samples composed of around 80.0% of quartz, the percentage of carbonates almost the same for both samples. Other non- clay minerals such as microcline and oligoclase composed nearly 7% of total minerals. Both core samples have the same amount of clay minerals with few variations (Table 4- 2 Appendix A). Based on the XRD pattern of oriented fraction illite is a dominant clay mineral in both samples of 3.0% and characterized as a basal spacing 10.02Å shows no change after various treatments. Kaolinite is characterized by a diffraction peak of 7.2Å which disappeared at 550°C, which indicates for the presence of kaolinite in both samples and its percentage less than 1.0%. The diffraction peak of 14.2Å is the characteristics of chlorite with a different ratio in both samples, in D- 4- 1 sample has twice amount than the latter one. Their peaks remain unchanged after various treatments which indicate the presence of chlorite. The diffraction peaks of 11.5Å is the characteristics of the interstratified layer of clay and stay unchanged after ethylene glycolate and heating to 350 and 550°C. This proved that there is illite- chlorite presence in the sample and its percentage of0.1% (Fig 4- 26).

The sample ***D- 3- 2*** with a depth **(1868.9m),** based on the XRD analysis this sample characterized by around 94% of non- clay minerals, generally composed of quartz, carbonates, oligoclase and microcline (Table- 4.3). (Fig 4-19). Based on the XRD analysis of oriented specimen the total clay content is 5.47%, kaolinite 7.2 Å less dominated and its percentage less than 1.0% and its peak collapsed at 550°C, while the XRD pattern after various treatments of the sample shows the clay fraction is dominated by illite 10.02Å and its percentage 3.3% and the diffraction peaks to remain unchanged after various treatment methods that discussed earlier. The broad 10Å reflection that is often characteristic of

authigenic illites in sandstones, as representing mixtures of illites of different thicknesses and particle sizes in various stages of development. Authigenic kaolinite in sandstone reservoirs typically occurs in form where there is an almost total dominance of face to face contacts, so that it is disruption of these contacts which will control the dispersion of the clay minerals (Wilson et al., 2014). Chlorite is characterized by the diffraction peaks of 14.2, 7.1, and 3.55Å and remains unchanged after ethylene glycolation and heating up to 550°C. This is indicating the presence of chlorite in the sample, its percentage just 1.4%. Authigenic chlorite is often observed to be coating detrital grains of quartz, thus acting as a pore-lining clay in reservoir sandstones (Wilson et al., 2014). The 11.5 Å was the diffraction of interstratified illite- chlorite and remain unchanged after ethylene glycol and heating to 350 and 550°C. This proved that there is illite- chlorite in the sample. Its percentage of less than 0.1% of the bulk sample (Fig 4- 20).

The XRD pattern of *(D- 3- 1)* with a depth (1872.10m), this sample was taken from a deeper location than the previous one. Based on the XRD analysis of powder specimens contain the lowest percentage of quartz < 70%. While the shallowest one, it's the percentage > 70%. The percentage of carbonates is also higher than D- 3- 2 samples and is more than 7.0 %. The amoount of oligoclase and microcline higher than the other samples around 12% (Fig 4- 17). Based on the XRD analysis the percentage of clay minerals almost nearly two times higher than the previous one. The XRD patterns of the sample show that the clay fraction is dominated by illite 4.8% with a peak position 10.02Å and remain unchanged after various treatments which are a good proof of existing illite in the sample. The diffraction peak of 14.2 was the characteristics of diffraction peak of chlorite and did not alter after ethylene glycosylation and heating treatments and its percentage just 2.2% almost around twice than the other sample. The 7.2Å was the diffraction peak of kaolinite and remain unchanged after ethylene glycosylation and disappeared at 550°C. This proved to the presence of kaolinite in the sample, and its percentage 2.0% which represents the highest kaolinite content among the rest of the samples. The diffraction peak of 11.5Å was the characteristics of interstratified layer clay, and the peak position dose does not collapse after ethylene glycosylation and heating to 350 and 550°C. This indicated of interstratified illite-chlorite, its percentage only 0.1% (Fig. 4- 18).

4.2.2 Summary of XRD Interpretation

We can conclude that the mineralogy of all samples was mostly dominated by quartz with the percentage of 70 – 80% and its placement in formation rocks, percentage of non- clay

minerals such as carbonates, mica flakes, biotite, and oligoclase vary depending on type and location of the samples. But the clay fraction is mainly represented by kaolinite, illite, chlorite with a minor amount of interstratified illite/ chlorite depending on the sample location within the depth. These types of clay minerals are widespread in most sandstone reservoirs. Based on their textural position, their thin lamellar particles are prone to particle mobilization and migration. To establish textural relations, a microscopy analysis of polished specimens was performed. Also, the percentage of non- clay minerals such as oligoclase, microcline, and carbonates are different. XRD figures Fig. 4.1 to Fig 4. 7 and clay fraction XRD plots are From Fig 4.8 to Fig 4. 14.

4.3 Morphological and textural analysis of the selected core samples using SEM/EDS

SEM analysis is undertaken in support of XRD at higher magnification ranging from as low as 50 to 10.000 times magnification. This study helps better understand the different types of clay minerals, their distribution within pores, and the degree of pore connectivity. SEM observations confirm that the textures are typical of clay-rich rocks although there is a significant proportion of large detrital grains, these are included within continuous fine-grained matrix. Pore space must therefore be at the scale of sub-micrometer grains, and permeability defined by interconnection of nanometer-scale pores occurring primarily between clay mineral grains. SEM has been used as a tool for the study of reservoir rocks in terms of pore geometry, pore size distribution, and the presence of dispersed clays (Neasham, 1977). The SEM images of the selected sandstone core samples before flooding and after flooding are presented from Fig. 4. 15- to Fig. 4. 21 and Fig. 4. 34- 4.40 respectively. EDS of the matrix confirm relative homogeneity at the micrometer scale, but have an average composition as consistent with approximately 4.5 to 9% proportion of clay minerals.

The selected cores consist of quartz ranging between (78- 83% in D-2 well; 80% in D-4 well and 69- 75% in D-3 well recorded the lowest quartz content. The clay fraction is represented mainly by illite with ranging between (2- 4.8%), Chlorite (0.8- 2.2%) and kaolinite is between (0.1- 2%) recorded the lowest clay continent. The SEM image (Fig. 4.15- Appendix B) show the selected core generally before flooding. The sandstone core plug is comprised of variety of non-clay and clay minerals. The non-clay minerals are represented by quartz, Ca, and Mg carbonates, dolomite, oligoclase, biotite, microcline and amorphous with different sizes (Tables 4-1- Appendix A and Tables- Appendix G). Quartz grains (Q) of medium grey colour, are irregularly shapes, with signs of dissolution and coatings and different sizes ranging between (100- 200µm) with some fine grains of quartz which may

contribute fines migration. A clinochlore grain (1) is totally filling the pore between the quartz grains ranging between (100-200µm) generally in all core plugs. Carbonate (2), namely (calcite and dolomite or Fe and Mg carbonates) pore filling existed between micaceous flakes ranging between (<5- 50µm) which might be contributing fines migration. Micaceous flakes (3) are represented in various sizes ranging from (50-150µm) with intergrowths of Fe and Ca- carbonates (arrowed), which could contribute fines migration during core flooding.

Clay minerals are represented by chlorite, illite and kaolinite ranging around 10 to 50µm and partially filling up the pores, which could contribute to fines migration even before core flooding test. Kaolinite can easily be identified by the hexagonal shape of the individual particles and "booklet" like aggregates, ranging between (<0.2- 10 µm) in size with individual particles of <1.0 µm, that may well contribute to fines migration. The textures of the various clay minerals identified have clearly formed post-sedimentation. Pores are shown in black and clearly lack connectedness even before core flooding, presumably because of enhance oil recovery (EOR) attempts. Illite and chlorite ranging between (<10- 50µm) are partially filling up the pores, which could contribute to fines migration during core flooding.

The SEM image (Fig. 4.16- Appendix B) show the selected core generally before flooding. The sandstone core plug is comprised of variety of non-clay and clay minerals. The non-clay minerals are represented by quartz, Ca, and Mg carbonates, dolomite, oligoclase, biotite, microcline and amorphous with different sizes (Tables 4-1 to 4-3- Appendix A and Tables- Appendix G). Quartz grains (Q) of medium grey colour, are irregularly shapes, with signs of dissolution and coatings and different sizes ranging between (50- 300µm) with some fine grains of quartz which may contribute fines migration. A clinochlore grain is totally filling the pore between the quartz grains ranging between (50-150µm) generally in all core plugs. Carbonate (calcite and dolomite or Fe and Mg carbonates) pore filling existed between micaceous flakes ranging between (<5- 100µm) which might be contributing fines migration. Micaceous flakes are represented in various sizes ranging from (50-150µm) with intergrowths of Fe and Ca- carbonates (arrowed), which could contribute fines migration during core flooding.

Clay minerals are represented by illite, chlorite and kaolinite ranging between (<5 to 50µm) and partially filling up the pores, which could contribute to fines migration even before core flooding test. Kaolinite (2) can easily be identified by the hexagonal shape of the individual

particles and "booklet" like aggregates, ranging between <0.2- 10 μm) in size with individual particles of <1.0 μm, that may well contribute to fines migration. The textures of the various clay minerals identified have clearly formed post-sedimentation. Pores are shown in black and clearly lack connectedness even before core flooding, presumably because of enhance oil recovery (EOR) attempts. Flaky muscovite (Fig. 4.16B) (1) ranging between (50- 150 μm) could not contribute permeability reduction due to large grains.

Shows the BSE images of the selected core (D- 2- 4) Befor flooding. In (Fig 4.17a). Black colour represents the pore space filled by embedding resin. Pore sizes based on area values are set in two ranges, the larger one is between 50- 200μm, while on the border of adjacent grains pores of ~ 10 μm are observed. Some pores are filled by fine particles and cemented by calcite, while the majority is not filled up. Quartz grains (Q) medium to dark grey) are of different sizes and ranging between (100-400 μm) are usually cemented by illite. Albite (Ab) ranges between (50- 150 μm) and is present as intersticial grains. Pore filling/cementing calcite (Cc) is observed between quartz gains (> 50 μm), based on its textural emplacement it is not expected to be involving fines migration. Detrital chlorite (Chl) presents with flaky structure in quartz grains, ranging between (40- 50 μm), while authigenic and diagenetic chlorite is developed in the pore spaces. Few grains of epidote (Ep) are observed with a diameter < 50 μm as detrital material. Some of the intergranular pores are almost filling (Fig. 4.17-3b) flaky muscovite (1) and illite aggregates (2) cemented by silica (< 5 μm). Fe-Mg-rich carbonates (3) graining ranging between (5- 20 μm) existing between the chlorite lamella. (4) Chlorite particles have typically lamellar structure with less than 10 μm, as a pore filling. Special carbonates often with Fe and Ca-Mg mixing developed between chlorite flakes are frequent, generating microporosity and increasing overall porosity. Detrital chlorite or interstratified illite/chlorite (5) is associated with quartz grains, although sometimes as a pore -filling ranging (< 10μm). Albite (Ab) appears as large (> 100μm) and small intersticial grains (10 -80μm) too. At higher magnifications (Fig. 4.17- 3c) (1) kaolinite booklets ranging <10 μm filling the interconnected pores between the quartz grains. Illite (2) and illite particles cemented by silica (3) generally are < 5 μm as pore filling, but flake sizes are too small to be distinguished. Muscovite flakes (4) with a length of approximately 50 μm and thickness 10 μm are located between quartz grains, thus at higher fluid flow rates, they could be mobilized.

Shows the BSE images of the selected core (D-4-2) Befor flooding. (Fig.4.18-a) black colours represnet the pore spaces (porosity) with various shapes and sizes ranging from (50-200μm), the pore spaces filling by a mixture of fine partciles, which comaposed of clay minerals such as kaolinite, illite , and chlorite and non-clay minerals (calcite, Fe and Ca carbonates, mica flakes). The grey colours represent quratz grains (Q) with different shapes from irregular to regular and different sizes ranging between (20- 100μm). (1) composed of

muscovite flakes ranging less than (50μm) which could not be contributting fines migaration. (2) represents chlorite minerals as a pore filling between quartz grains which could contribute to fines migartion during core flooding. The rest of the pore filling minerals are kaolinite booklets ranging below (<5 μm) which contribute fines migration. (Fig.4.18- b) represents a mixture pore filling minerals, (1; 2; 3) exfoliated muscovite with interlayer mixture of minerals such as Fe and Mg- carbonates, chlinochlore flakes and kaolinite, these fine partices easily contribute to fines migaration during flooding. (4) represents of chlorite flakes ranging less than 10 μm). (5) shows illite flakes between chlorite minerals which could be contributing to fines migration. (6) composed of individual of fine kaolinite particles ranging is (<5 μm), that may well contribute to fine migration.

Shows the BSE images of the selected core (D-4-1) Befor flooding. (Fig. 4.19- a) black colours represnet the pore spaces (porosity) with various shapes and sizes ranging between (100- 300μm), some of the pores filled by fine partciles, which might be clay minerals such as kaolinite, illite , and chlorite or non- clay minerals (calcite, Fe and Ca carbonates, mica flakes). The grey colour represents quratz grains (Q) with different shapes from irregular to regular aare different sizes ranging between (50- >400μm). (1) composed of clinochlore with light grey color pore- filling chlorite with interstratified illite.(2) composed of clay minerals. (3) composed of interstartified clay with high silica content. (4) almost the same composition as no.2. (Fig. 4.19- b); (1) it is a typical kaolinite content, (2) interstratified with pyrite; (3) muscovite altered to illite, the presence of Fe, Mg and Ti indicated for this alteration. (Fig. 4.19- c), shows exfoliated chlinochlore + siderite with interstratified carbonates.

Shows the BSE images of the selected core (D- 3- 2) Befor flooding. (Fig. 4.20- a), black colours represnet the pore spaces (porosity) with variousshapes and sizes ranging from (100- 200μm), some of pores are filled by fine grain partciles, which might be clay minerals such as kaolinite, illite , and chlorite or non- clay minerals (calcite, Fe- Ca carbonates, mica flakes). The dark grey colours represents quratz grains (Q) with different shapes from irregular to regular and different sizes ranging between (50- >400 μm). K-feldspare and albite (K-fp + Ab) and grain particles ranging between (100 - 200 μm). The micaeous flakes associated with illite, chlorite, fine grains of quartz ranging between (300- 400 μm) and Fe and Ca carbonates developping microporosity and might contribute fines migration. (Fig. 4.20- b) Pore filling kaolinite booklets ranging less than 5 μm) that may well involve fines migration. (1) composed of dolomite, flaky muscovite with inter- filling kaolinite and some fine particles of illite (2), (3) represnets of clinochlore, (4) composed of interstratified illite/chlorite ranges below (5μm), (5) kaolinite mineral presence between muscovite lamella. (Fig. 4-20- c) show a clear evidence of kaolinite- booklets filling the pore spaces ranging <5μm, (1) micaceous flakes ranging

from (20- >30μm) could not contribute permeability reduction due to large grains, (2) Fe- Mg carbonates between micaceous flakes might be contributing fines migaration because their sizes below 5μm, (3) inter- stratified pore filling clay minerals generally is illite/ chlorite with below 5 μm, those fine particles that may contribute fines migration. (4) it represents pore filling chlorite could not contribute to fine migration.

Shows the BSE images of the selected core (D- 3- 1) Befor flooding. (Fig.4.21- a.) black colour represnets pore spaces (porosity) with various shapes and sizes ranging between (50- 300 μm), most of the pores are filling by fine partciles of clay minerals such as kaolinite, illite , and chlorite or non-clay minerals (calcite, Fe- Ca carbonates, mica flakes, pyrite). The grey colour represent quratz grains (Q) with different shapes from irregular to regular and different size ranging between (50- 400 μm). This sample contains more carbonates than D- 3- 2 sample that it appears between micaceous flakes and might be contributing fines migartion. (1) composed of Fe- Mg calcite as fine grains, (2) represents illite flakes filling the pore spaces with some fine grains of quartz. (3) composed of muscovite and it might not contribute to fine movement. (4; 5; 6) chlorite particles filling pore spaces. (7) represents diagentic albite. (Fig. 4.21- b) most of the pores between quratz grains filled by clay minerals such kaoliten easily dispersed during the flooding and mixture of fine grains of quartz with illite might be contribute with fines migration during the folloding. (Fig.c) pore between the sandstone grains filled up by a mixture of clay minerals such as illite and kaolinite with fine grains of quartz that may well contribute to fimes migration.

SEM image after flooding- D- 2- 6. (Fig.4.34- a) Generally, We observed that most of the matrix composed of clay minerals such as kaolinite, illite, chlorite with fine grains of quartz these fines cemented by silica and calcite. Some of the pore- filliping minerals are well developed and cemented; those minerals could not be able to contribute with fines migration during the flooding test and preserved on their places. While, other pore filling minerals, which are not cementing very well, influenced by flooding fluid leads to a significant reduction on permeability due to migrate those fines. (Fig.4.34- b) easily we can observe that most of the pore- filling minerals subjected by flooding and detached from their original places then migrated with flooding fluid and plugged or blocked smaller pore throats from downstream section. (Fig.4.34- c) shows that exfoliated micaceous with interlayer Fe- Mg-carbonated which a clear evidence for flushing out those carbonate minerals between flakes then might be blocking smaller pore channels and reduce permeability. Initial permeability of the selected core samples recorded with 5%NaCl brine and neutral pH (7), its initial permeability was 552mD and the selected core was flooded with pH9 at different flow rates. The percentage of permeability reduction increases with increasing flowrates.

SEM image after flooding- D- 2- 5. (Fig. 4.35- a) shows SEM images of core samples after flooding and proved that some pore filling materials were flushed out with flooding solution such clay minerals and fine grains of quartz with Fe- Mg carbonates. While, other pore- filling materirial, which they are very well developped and cemented within the pores remain as it was and did not contributed fines migration. (Fig. 4.35-b) shows a disturbed pore filling clay minerals with a mixture of fine grains of quartz and TiO_2 , those fine particles such clay and non clay minerals migarted within the pore channels during the flooding and causing a redcution on permeability. (Fig. 4.35- c) This SEM image can be used as a clear evidence to prove the fine migration within the pore**.** The SEM images have also proved that some fines mobilized and transported from their original places such Fe- Mg carbonates associated with chlorite flakes before the flooding while after the flooding partially mobilized and exist with a mixture of illite and silica. D-2-5 sample flooded with pH11 and highest value of formation damage was recorded at highest flow rate which are more than 55%.

SEM image after flooding- D- 2- 4. (Fig. 4.36- a) Generally, We observed the matrix composed of clay minerals such as kaolinite, illite, chlorite with fine grains of non- clay minerals. Most of the pore- filliping minerals are well developed and cemented; those minerals could not be able to contribute with fine migration during the flooding test and preserved on their places. While, other pore filling minerals, which are not cemented very well, influenced by flooding fluid leads to a significant reduction on permeability due migrated those fine particles. Quartz grains very well developed and connected to each compare to D- 2- 6 sample. (Fig.4.36- b) The SEM images have also proved that some fines have been mobilized and transported from their original places such Fe- Mg carbonates (1) which were observed between chlorite flakes before flooding was partially mobilized and detached from their original places, as a pore filling this is a good evidence for migration fine particles during the flooding test because at the SEM images before flooding always Fe- Mg carbonate exist between chlorite flakes never seen before flooding have been mobilized. The migrated fine particles (clay minerals such as kaolinite, illite and chlorite (2)) mobilized and detached from their original location, some fines passing through the pores with the flooding fluid because their sizes smaller than the pore throats enhance permeability. While others due their sizes blocking or plugging the pore throats and leads to reduction on permeability. The selected core flooded with acidic solution (pH3) and enhance in permeability was observed more than 55% at 200ml/hr.

Fig. 4. 37: SEM image after flooding- D- 4- 2. (Fig. 437- a) The quartz (Q) grains have a various shapes and sizes with many pore spaces most of them filled up by fine particles. We observed that some of the matrix within the pores mobilized and disturbed such as (pores surrounded by a red rectangle) while, well developed and cemented pore filling materials preserved own position and do not influence by the flooding solution such as (pores surrounded by red square d). Large grains such as detrital dolomite, k- feldspar, albite and

muscovite due to their big sizes remain as it was. (Fig.4.37- b) composed of a pore- filling chlorite flakes with interlayer of carbonates, most of the carbonated particles subjected by flooding fluid and migrated from their original position, then deposited somewhere else at downstream section which are the pore throats smaller than migrated particles. (Fig. 4.37- c) a mixture of pore filling fine particles composed of clay minerals such as illite, chlorite and kaolinite booklet and non- clay minerals such as carbonate and fine grain of quartz, those fine particles influenced by flooding solution and moved or shifted from original position, which are caused reduction on permeability. Initial permeability D-4-2 was 205.9mD and flooded with pH9 and different flow rates more than 51% in reduction on permeability was recorded.

SEM image after flooding- D- 4- 1. (Fig.4.38- a) We observed that some of the matrix filling the pores are well cemented and developed and do not mobiles during the flooding (pores surrounded with c and d red rectangle). While other pores surrounded by (a and b red rectangle) subjected by flooding fluid and mobiles from their original position. (Fig. 4.38- b) is a mixture of pore- filling clay and non- clay minerals migrated during the flooding. This SEM image has also proved that some fines have been mobilized and transported from their original places such Fe- Mg carbonates associated with chlorite flakes before the flooding while after the flooding partially mobilized and exist with a mixture of illite and kaolinite. (Fig. 4.38- c) is a clear evidence a mixture of pore- filling minerals which are subjected by flooding and mobiles from their original position such clay minerals and non- clay minerals with few grains of quartz. D-4-1 recorded highest value of initial permeability more 731mD, the core flooded with pH9 and different flow rates. Easily observed that the value of formation damage increases with increasing flow rate more than 56% of formation damage recorded.

SEM image after flooding- D- 3- 2. (Fig.4.39- a) SEM images proved that some pores are very clean. Alternatively, the fine particles were flushed and detached after the flooding test (rectangle a). While some pore- filling minerals developed and cemented very well remain as it was. (Fig.4.39- b)The migrated fine particles (clay minerals such as kaolinite, illite and chlorite) mobilized from their original places might be plugged or bridge some pore throats due to their sizes larger than pore throats then could reduce permeability. While, non- clay minerals such as muscovite, medium grains of quartz (silica) almost stay in their position and not been mobilized during the flooding because the sized are big and well cemented. (Fig.4.39- c) Fe- Mg carbonates, which were observed between chlorite flakes before flooding. Those carbonates were partially or completely mobilized and found with illite, as a pore filling this is good evidence for migration fine particles during the flooding test because at the SEM images before flooding always Fe- Mg carbonate exists between chlorite flakes never seen with illite. Easily we observed that the chlorite flakes totally flushed out

with carbonate during the flooding. The direction of the fine particles as pore filling between the quartz grains indicated the direction of flooding. Another prove of fine migration presence of kaolinite with illite as a pore- filling materials, such as mixture never seen before flooding. Before the flooding always illite, exist with silica and fine grains of quartz as a mixture. In addition, albite (Ab) particles have been mobilized and detached from their original grains and exist with illite and silica mixture.

SEM image after flooding- D- 3- 1. (Fig4.40- a)The quartz (Q) grains are compacted with smaller sizes compared to other D-3-2 samples that might be due to the sample taken from deeper locations. We observed that most of the pores filled up by the Authigenic and diagenetic minerals such as clay and non- clay minerals. Most of the pore- filliping minerals are well developed and cemented; those minerals could not be able to contribute with fine migration during the flooding test and preserved on their places. While, other pore filling minerals, which are not cemented very well, influenced by flooding fluid leads to a significant reduction on permeability due migrated those fine particles. (Fig.4.40- b) The SEM images have also proved that some pores were flushed during the flooding test. Fe- Mg carbonates which was observed between chlorite flakes before flooding was partially mobilized and detached from their original places, as a pore filling this is a good evidence for migration fine particles during the flooding test because at the SEM images before flooding always Fe- Mg carbonate exist between chlorite flakes never seen before flooding have been mobilized. Easily we observed that the chlorite flakes partially flushed out with carbonate during the flooding. (Fig.4.40- c) The migrated fine particles (clay minerals such as kaolinite, illite and chlorite) mobilized from their original places and plugged or bridged somewhere else, while and non- clay minerals such as muscovite, fine grains of quartz (silica). Also, there is few particles of albite and TiO_2 might migrate during the flooding.

D-3 well were flooded with the same pH9 and different flow rates 50ml/hr; 100ml/hr and 200ml/hr, we observed the percentage of formation damage increases with increasing flow rate at the same pH value. While the higher reduction on permeability recorded with D-3-1 because it contains highest percentage of clay minerals >9%.

4.3.1 Interpretation of core samples composition and morphology before flood

SEM analysis conducted as a part of this study. Before and after flooding experiments show that the sandstone is moderately to well sorted with varying grain shapes from angular to sub-angular. As observed by the SEM images the contact between grains is formed as a result of pore pressure of quartz overgrowth. SEM photographs show that individual clay minerals are dispersed matrix and in the pore spaces and permeable channels of the sandstones. Sometimes intergranular pore spaces are partially blocked by clays which are mostly chlorite, illite, and interstratified illite- chlorite. The samples are composed mainly of quartz with a variety of shapes, from angular to sub-angular, and sizes range from 50 to 400μms (Fig. 4.16 to Fig. 4.21 before flooding and Fig. 4.34 to Fig. 4.40 Appendix B). The SEM study displays that the common clay minerals observed are kaolinite, illite, chlorite, and interstratified layer of illite/ chlorite as pore-filling particles of the interconnected pores, some of them in the pore throats. A low percentage of non- clay minerals are also observed such as calcite, mica, feldspar, and pyrite. Booklets and vermicular kaolinite, fine particles of illite and exfoliated chlorite are also observed in the intergranular pores, leading to pore throat narrowing and permeability variation. Fine clay particles occur to quartz grains and because they are diagenetically generated from feldspar transformation, they were easily detached from their original places to other places and accumulated in large quantities of the pores and lead to pore blockage resulting in permeability variation (Fig. 4.24 to Fig. 4.30 in Appendix B).

Kaolinite is widely as booklets in the intergranular pores which leads to pore narrowing of the inter-granular pore, these causes to narrowing these pores. Authigenic growths of kaolinites decrease the permeability/ porosity. Also, kaolinite occurs on quartz grain because it is diagenetically generated from feldspar transformation. This is called fine clay migration and invasion. Based on observation from SEM and EDS images (Fig. 4.15 to Fig. 4.21-before flooding test). Which have taken before flooding for D-2; D-3 and D-4groups a part of clay minerals filling the pores between quartz gains and the carbonates exist between

exfoliated mica, those fine particles loosely attached to the grain surface of the grains which are easily detached from their original position and mobilised during the flooding. According to the XRD analysis the percentage of clay minerals varies from D-2; D-3 and D-4 wells, in cores the percentage is between 4-5% except D-3-1 contains >9%. Also based on the SEM images took from core samples shown that the samples composed of clay and non-clay minerals with a variety of shapes and sizes. According SEM images black colour represent empty pore spaces most of them filled up by clay and non-clay minerals and other are empty, their ranges were between less than 100 to >10µm. the dark grey colours represent quartz grain with different shapes and sizes, from rounded to sub-angular and their sizes between 20 to > 250 µm, with few amount of fine grain quartz exist between quartz grain within the pores associated with fine grain particles. The presence of those fine particles of quartz are varied from one core to another and might be involved fines migration. Some of the pores were filled up with carbonates such as calcite and dolomite ranges more than 50µm and do not contributing fines migration. The rest of the pores filled up with clay minerals such as kaolinite, illite, chlorite with intergranular fines particles of sand, also Fe-Mg carbonates found between exfoliated micaceous minerals with different sizes as shown in (Appendix G) which are easily detached from their original places, moving with the direction of injected fluid and particles might be transported to a pore constriction that is smaller than the particle size, where they are retaining by straining. SEM images a after flooding experiments showed that some of the fine grain particles of clay and non- clay minerals subjected by flooding fluid and mobilsed form their original position and redeposit somewhere have smaller pore throats that consequently causing a significant reduction on permeability with alkaline solution and enhance permeability with acidic one (Fig. 4.34 to 4.40 after flooding) and (Table 4.4 to 4.6 Appendix A).

4.3.2 Interpretation of core samples composition and morphology after flood test

The variation of reservoir rock characteristics depends not only on the framework mineralogy but also on the authigenic minerals and the composition, texture, and structure of the rocks. As mentioned earlier, clay minerals are in control of reservoir petrophysical characteristics. Clay minerals were identified and studied with the help of the XRD analysis and SEM. Major clay minerals in most of these rock samples are found to be mainly, illite, chlorite, and kaolinite. Apart from these, interstratified illite/ chlorite, quartz, feldspar, plagioclase, are also found to be present in the rock matrix of the study area (selected sandstone cores). Reservoir characteristics such as porosity and permeability of the reservoir

sandstone rocks have been found to depend on the framework mineralogy, composition, texture, and structure of the rocks. Most of the clay minerals occur as coating into the detrital grains and sometimes as a dispersed matrix in the pore spaces and permeable channels of the reservoir rock. The presence of clay minerals as a scattered matrix in the pore spaces and the reservoir sandstone's permeable channels influence the reservoir characteristics of the study region by reducing permeability. Both authigenic and detrital clay minerals are present and they play a definite role in modifying the reservoir characteristics of the study area.

Based on SEM analysis after flooding the following are the main observations for produced fines:

- Generally, produced fines are mainly composed of fine grains of quartz, silts, and fine particles of clay minerals (Appendix A and B)
- All selected samples showed increased fines production at higher flow rates (Appendix B)
- In general, Fe – Mg carbonates were detached from exfoliated micaceous mineral and deposited at smaller pore channels (SEM images after flooding Appendix B Fig. 4.34 to 4.40).

4-4 Petrophysical Properties of core samples:

Sandstone reservoirs are commonly composed of the same types of minerals composition, and percentages of these minerals, as well as the petrophysical properties might vary widely. Variation in compositional properties and petrophysical properties of reservoir sandstones can influence the severity of fines migration and the performance of the core flooding test. Petrophysical properties of reservoir rocks have been shown to depend not only on the framework mineralogy but also depend on the composition, the texture of the rocks, and authigenic minerals. The presence of authigenic clay minerals is strongly influenced by sandstone reservoirs characteristics (Hol et al., 2015).

Most oil and gas production formation contain clay minerals that were originally deposited during sedimentation which is called "Detrital Clay" or precipitated from fluids flowing through the matrix known as "Authigenic Clay: both types of clays can cause a substantial reduction of permeability and negative impact on reservoir quality of sandstone reservoir rock (Lejar, 2012). It is important to understand the types, origins, and distribution of the various clay minerals in sandstone reservoirs.

4-4-1- Analysis of initial permeability of core samples of varying mineralogical composition: the role of clay minerals under fluid flow

The initial permeability of the selected core plugs was calculated by the usage of the core holder of Hassler type, first the selected cores were saturated with 5% NaCl brine saturation with pH 7. After that, the selected cores were placed in a Hassler- type core holder to start measuring the initial permeability of the selected cores (Fig. 20 in Appendix C). Initial permeability of the selected cores varies from one well to another due to changing the mineralogical composition of each well, also the mineralogical composition could be varied from one core to another at the same well. Initial permeability 552.4mD; 328.2mD and 252.6mD recorded for the D-2- 6; D-2- 5 and D-2-4 respectively, from the obtained result easily observed initial permeability of the selected cores decreases with increasing depth. After measuring the initial permeability, the cores prepared for flooding with the selected fluid (pH 11, 9 and 3). D-2- group flooded with different pH values to investigate the influence of changing pH on formation damage. Among them, D-2-6 recorded highest level of permeability more than twice of D-2-4 with the value of 552.4mD and 252.6mD respectively. The D-2-6 core flooded with pH 9 and the percentage of formation damage increases with increasing flow rate, the highest reduction of permeability was recorded in D-2- with pH 11. While, D-2-4 enhancing permeability was observed and increase with increasing flow rate. (Table 4.4 Appendix A).

D-2-6 flooded at pH 9 with different flow rates (50ml/h; 100ml/hr and 200ml/hr), the percentage of formation damage increases with increasing flow rates the highest value of permeability reduction recorded >41%, permeability changed from 552.4mD to 334.1mD. In addition D-2-5 core flooded with pH 11 with different flow rates, the value of permeability significantly reduced from 207.1mD to 144.3mD at 200ml/hr and recorded highest percentage of formation damage more than 55%. While D-2-4 core flooded with acidic solution (pH3) with the for mentioned flow rate, enhance in permeability recorded and increased with increasing flow rate from 252.6mD to 391.7mD at 200ml/hr. The resulted of initial permeability and core flooding are presented in the tables in (Appendix A from Table 4. 4 to Table 4. 6).

The initial permeability of D-4-1 recorded more double of D-4.2, D-4 group flooded with the same pH (pH9) value and different flow rates such as 50ml/hr; 100ml/hr and 200ml/hr to investigate the influence of flow on permeability variation. The percentage of formation damage increases with increasing flow rate for instance initial permeability D-4-2 was

205.9mD significantly decreased to 167.4mD at 200ml/hr with more than 50% formation damage was recorded. Highest value of initial permeability was recorded with D-4-1 core sample and dramatically dropped to 405.2mD at 200ml/hr as shown in (Table 4.5 Appendix A). Also, we observed that the percentage of formation damage increases with increasing flow rate at the same pH value.

D-3 group recorded the lowest initial permeability 103.3mD and 32.4mD with D-3-2 and D-3-1 respectively. The selected cores flooded with the same value of alkaline (pH9) and different flow rates 50ml/hr; 100ml/he and 200ml/hr to investigate the impacts of clay content on formation damage and permeability reduction. We could easily observed that the percentage of formation damage increases the percentage of clay minerals content for instance the initial permeability D-3-1 was 32.4 mD and up rapidly reduced to 7.3mD with the percentage of formation damage more than 77% at 200ml/hr as shown in (Table 4.6 Appendix A). The highest degree of formation damage > 77% observed with D-3-1 because contain highest clay content more 9% (Table 4.3 Appendix A).

4.5 Core Flood test interpretation

In this study, we are interested in investigating how the degree of alkalinity, flow rates and percentage of clay content influencing basic petrophysical properties of selected sandstones core plugs. Seven sandstone core plugs were selected to perform core flood of constant pressure and temperature (ambient condition) and different degree of alkalinity. This study aims to investigate the extent and the impact of online particle mobilization in selected sandstone cores. Moreover, this work will study the petrophysical properties and core flooding process of damaged cores to quantify the effect of fines migration on the success of the core flooding test in terms of permeability variation. During the core flooding experiments three different pH values have been used, namely pH9, pH11 and pH3.

The mineralogy of the samples investigated was analysed by a combination of XRD and SEM/EDS, both before and after core flooding, thereby highlighting the mineralogical changes consequent on core flooding and their effect upon poro-perm properties. With regard to the latter, the graphs shown in the appendices plotting permeability against core flooding data for the various core samples illustrate three different scenarios namely (a) a decline in initial permeability from about 552 mD to 334 mD (D-2-6), (b) little or no change in permeability remaining at about 330 mD (D-2-5) and (c) an increase in permeability from about 220 mD to 260 mD (D-2-4). These changes occurred during initial permeability

measurements using 5% NaCl at pH7. The decrease of 34% for the D-2-6 sample (a) in the brine solution would have been caused by mobilisation id detached particles which are present in the core prior to permeability measurements.

4-5.1 Influence of clay minerals on fines detachment and migration

A series of laboratory core flood experiments on core plugs were conducted to investigate the reduction of permeability due to fine particle mobilization, at ambient conditions. Both sandstone core plugs (D-3-2 and D-3-1) were selected from the same well from Hungarian oilfield to investigate the impact on clay mineralogy and their percentages on the degree of formation damage. The type and amount of bulk and clay mineralogy are measured and identified by the help of XRD analysis. The different reflection angles for different clays could be used to identify the type of clay minerals. The results show that D- 3- 1 contains more clay minerals than D- 3- 2 almost double, 9.07%, and 5.47% respectively. D- 3 -1 has more kaolinite, illite, and chlorite content than the other one its percentage is 2.0; 4.8 and 2.2% respectively. While, D- 3- 2 has lower percentages of clay content 0.8; 3.3 and 0.8% respectively (Table 4.3- Appendix A). Gupta et al. (2011) showed that kaolinite occurring in booklets and vermicules will tend to disperse at pH value > 8 due to the repulsive effects between face-to-face contacts, and especially when these basal faces are exposed in the opposing surfaces of silt-and edge-shape micro- and mesopores, the kaolinite particles will tend to migrate from their point of origin within the sandstone until physically trapped in pore throats of smaller dimensions than the particle size of the dispersed clay. The dispersion properties of fine-grained <0.1µm and coarse grained 1-2 µm illites were investigated by Emerson and Chi (1977) from the dried state and wet remoulded state. Complete dispersion from both the dried and remoulded states was achieved for the fine-grained illite when only a small percentage (4-8%) of the exchange sites was occupied by Na, whereas the coarse-grained illite dispersed less readily.

The variation in clay minerals content has a considerable influence on permeability reduction. The occurrence of these clay minerals creates a possibility of their migration and have a considerable impact on the permeability. As stated by Wilson et al. (2014) there is not much evidence that migration of fine particles of chlorite is a significant factor in causing formation damage in reservoir sandstone. Although chlorite itself may be considered to be resistance to dispersion and migration compared with other authigenic clay minerals. X-ray

diffraction examination of what appears to be chlorite may reveal not presence of swelling layers when solvated with ethylene glycol, thus indicating not a mixed-layer chlorite/ smectite structure. The occurrence of these clay minerals creates a possibility of their migration.

Rock mineralogy, especially type of clay mineral content, position, and distribution within the rock matrix have a significant influence on fines migration. Generally, most sandstone reservoirs contain a certain percentage of clay minerals in their composition, prior to migrate they dispersed and detached from their original position and subsequently migrate with the flow which might cause drastic permeability impairment, due to their tendency to migrate and hence, plug, bridge or block the interconnecting pore throats because their diameter are smaller than migrated particles. The presence of clay minerals in reservoir sandstones is so important as cement types and authigenic minerals may influence the increase and decrease of sandstone porosity (Astuti et al., 2014). One of the main formation damage mechanisms in natural sandstone reservoir during water flooding and enhance oil recovery, is induced by migrating fine particles which are initially attached to the surface of the grain.

One of the main aims of this set of experiments is to understand the influence of clay minerals content of permeability reduction. Therefore, the experiments were started by conducting a series of core flooding experiments with the same solution (pH 9) and different flow rates. The reason for selection of this pH value is that the majority most of the drilling mud have been used for drilling has the same pH. The selected solution was injected into core plugs (D- 3- 2 and D- 3- 1) with initial permeability 103.33mD and 32.37mD respectively, the pressure differential between inlet and outlet versus time was recorded to identify any damaging behaviour. Liquid permeability was measured at 50 ml/hr then switched to 100 ml/hr, where formation damage was witnessed. Moreover, an additional one more cycle of the experiment with the same pH value was implemented at 200ml/hr flooding, which confirmed favourable results concerning permeability change. Core plug D- 3- 1 shown a significant reduction of formation damage and permeability around 77% at 200 ml/hr compared to D-3-2 with permeability decrease of about 25%. Sample D-3-2 contains smaller amount of clay minerals and therefore is not subjected to such a severe formation damage as D-3-1 which contained fewer clay minerals and exhibit plugging phenomenon for core plug that have more clay minerals (Table 4.6- Appendix A) and (Fig. 4.29 and Fig. 4.30 Appendix B).

For instance, at 50 ml/h flow rates the percentage of formation is around 10% in D- 3- 2 core plug. While, in D- 3- 1 core the percentage formation damage increased to around 68%, the porosity of the selected sample is less than D- 3- 2 (21.5 and 27%) respectively. Also observed that the percentage of the total clay content in D-3-1 sample is around twice than D-3-2 that was main reason for severe damage than D-3-2. D-3-2 contains smaller amount of clay minerals (5.4%) and therefore is not subjected to such a severe formation damage compare to D-3-1contains large amount of clay minerals more than 9.0%. For instance D-3-1 contain large amount of illite (4.8%) compare to D-3-2 contains smaller amount of illite only 3.3%. At this low flow rate (50ml/hr) the formation damage was most likely caused by thick bound water shells formation around the illite particles that have solid-like behaviour (Wilson and Wilson, 2014). These clays were more susceptible for detachment and mobilizing during the core flooding. After the illite particles hydrated at low fluid flow, the next was their detachment at higher flow, also involving other clay particles dispersion and migration. Most of the migrated fine particles are kaolinite, illite, and chlorite, furthermore Fe- Mg carbonates contributed (Fig. 4.39 and Fig. 4.40 Appendix B). Extreme reduction of permeability observed on D- 3- 1 core plug because it has more migrated clay minerals for instance contains twice as much kaolinite than D-3-2 sample which might cause a significant reduction in permeability due to blocking and bridging of interconnected pore throats. Chorom and Rengasamy (1995) founded that the dispersibility of illite, as with smectite and kaolinite, is also affected by pH, in the Na- form, illite tends not to disperse at pH< 4 in deionized water, in contrast to smectite which was 86% dispersible at pH 3.5. At pH>7, however, 85-97% of Na-illite became dispersible and it was concluded that this behaviour was due primarily to changes in the net negative charge on the clay with change of pH and electrolyte concentration also, thick layers of bound water around its particles. Kaolinite that occurs in sandstones is of mostly well crystalized variety, often occurring in booklets and vermicules, the euhedral nature of these forms of kaolinite and their textural relationships with other sandstone components indicate that they are authigenic (Wilson et al., 2014). Migration of fine clay vary depending upon clay mineralogy, morphology, abundance, and distribution. Where kaolinite is present there is certainly potential for damaging fines migration (Byrne, 2009).

Hayatdavoudi and Ghalambor (1996) used a Tuscaloosa sand core form central Louisiana. Several experiments at ambient condition, with pH 12 and caustic soda at 11.1 ccs/ min for 45 minutes were conducted to investigate the influence of kaolinite clay minerals on

controlling formation damage. The initial permeability of Core #1 is 163.30 mD, the final permeability was 71.78mD, loss of 55.99%, and Core #2 with initial permeability is 7.90 mD and after flooding reduced to 2.67mD with 66.2% reduction on permeability was observed.

In Berea sandstone cores the migrated fine particles mostly composed of kaolinite; illite and chlorite as the rock matrix not attached well by mechanical forces and easily detached from their original position, the detached fine clay particles flow in the pore space until the particles plug or blocked the pore connections that are smaller diameter than the particles, the extend of fines migration depends on pore size and fine particles distribution. The plugging of the pores results in permeability reduction. Further reduction of permeability was observed when flow rate stepwise increased as shown in (Table 4.7- Appendix A).

The presence of clay minerals such as kaolinite, illite, and chlorite that do not have a swelling capacity proves the fact that these clays dispersion and migration may induce a significant permeability reduction. Fine migration is the only significant point in these kinds of the sandstone formation. Since there is the possibility of fine particles detachment and movement along the flow paths as a result of high flow rate within the pores and loose structures in some cases. It can cause pore plugging, blocking, and bridging far within the reservoir (Russell et al., 2019). Usually, clay minerals or silica particles coat the rock surface, so their detachments yield an insignificant increase in rock permeability, while pore plugging by the migrating fine particles alters the flow trajectory, increases its tortuosity, leading to significant permeability decline (Khilar and Fogler, 1987). Fine clay particles are present in most sandstone rocks; they are capable to migrate when contacted with fresh or low salinity water. Fine particle migration proved by earlier studies, Mohan et al., (1983) proved that non- swelling clay minerals such as kaolinite and illite tend to detach from the rock surfaces and migrate with the injection water of low salinity. Migrating fine particles may trap into pore throats leading substantial reduction of permeability. Wilson et al. (2014) stated that the dispersion and migration of illite particles in sandstones will evidently depend to a large extent on their mode of occurrence. It is also clear from the arrangement of individual particles that the illitic clay is already dispersed to a high degree. Where such illite has grown within the pores and is not attached to the pore walls, then such fine particles could very easily be swept through the sandstone by fluid movement, especially if the fluid pH is above the 3.5 and 8.5 respectively (PZNC- Point of zero net charge). The PZNC values for illites studied by Du et al. (1997) and Lackovic et al. (2003) were at pH 3.5 and 8.5 respectively,

whereas according to studied by Gu and Evans (2007) the PZNC of Fithian illite ranges between pH 6.0 and 7.5. As illite is a non-swelling clay, than the bound water around its particles will not enter the interlamellar spaces but will cause an interparticle swelling by repulsing water covered particles from each other. This will create a high enough pressure to disperse the illite particles and enable them to get mobilised under fluid flow (Wilson and Wilson, 2014).

The process of clay migration damages involves migrating of clay minerals within the reservoir rocks; migration damage may depend on the sizes of both clay minerals and pore restrictions. So, fine clay migration can cause a severe permeability reduction. This type of damage can reduce permeability and porosity of the sandstone reservoir. Vinati et al. (2015) conducted a laboratory study of clay minerals and its importance of hydrocarbon production potential for a part of Geleki oilfield of Upper Assam Basin, they found that both allogenic and authigenic clay minerals play a definite role in modifying the reservoir characteristics of the study area.

Also, clay mineralogy and their percentage has a great impact on permeability variation, the location of the sample might be another factor that affects permeability changes. Muecke (1979) performed an experimental study to investigate the influence of fine migration phenomenon and observed that unconsolidated sandstone formation has very fine grain particles of different sizes and shapes which is unstable in porous media. Feng et al. (2018) conducted a series of core flood of tight sandstone of Yanchang Formation, Eastern Gansu, Ordos Basin, based on their analysis, the pore throat size distribution is a key factor to control the physical characteristic of this formation. Fine clay and non- clay particles are free to migrate through the pores along with any fluids that flow in the reservoir. If these fine particles migrate but are not carried through the formation by produced fluids, they might be concentrated on pore restrictions, causing to plug the pore throats and severe reduction in permeability.

4.5.2 The effect of pH on petrophysical properties

Three natural sandstone reservoir core plugs (East of Hungary) as shown in (Table 4.4 Appendix A) used for core flooding with different degree of alkali (Table 3.2 in Chapter Three). During core flooding tests at three pH values, namely pH9, pH11 and pH3. The decline in permeability at pH is evidently due to clay dispersion thus providing material for

fines migration and leading to the blockage of pores in the sandstones. This is illustrated by SEM images of the sandstone cores before and after flooding showing a clear change in pore connectedness. The dispersed material is made up of both clay and non-clay minerals, the former comprising kaolinite and micaceous materials and the latter of fine grained quartz, feldspars and carbonate minerals. The overall texture and pore structure of these materials suggest an initial post-sedimentation formation on which is superimposed changes relating to particle dispersion and pore blockage.

Several experiments were conducted to investigate the influences of pH on stability of fine grain particles and their effect on formation damage. In sandstone reservoirs of acidic fluid in the porous medium, the internal clays should be more stable relative to alkaline conditions. This study on fine mobilization due to changing from pH and flow rate and consequent permeability variation were carried out using permeability apparatus (more details in chapter three). Changes in fluid properties were assumed to have an immediate effect on the detachment criteria for attached particles. In this study, we are interested in investigating how the degree of alkalinity and depths influencing the percentage of formation damage and permeability variation concerning different flow rates. Generally, permeability reduction has been attributed to clay minerals which disperse or expand upon contact with water that has salinity less than connate water Mungan and Moor (1968). When low salinity or freshwater contacts with swelling clay minerals, causes swelling with clay minerals and thereby partially blocks the pores throats and reducing the permeability of sandstone reservoirs.

The specific clay minerals involved are kaolinite, which occurs in book-like aggregated made up of a polyphaser mixture of fine-grained micas (both dioctahedral mica and trioctahedral biotite), true illite and sericite (fine-grained dioctahedral mica formed by high temperature alteration of feldspars). Chlorite is also a clay minerals which ours widely in sandstones and whose texture clearly shows it to be of post sedimentation origin. Thus, chlorite typically occurs in aggregates of intersecting bladed crystals, sometimes showing a rosette formation, and considered to help preserve the porosity of sandstones by inhabiting silica cementation.

Among the most noticeable of the factors affecting the dispersion and migration of clay minerals are the ways in which they occur in sandstones, partially their spatial arrangement in relation to the fabric and structural features of the rock, their micro-aggregate structure, morphology, surface area, porosity and particle size distribution Wilson et al. (2014).

4.5.2.1 The influence of pH range and flow rate on mineralogical, morphological and petrophysical properties of core samples in D-2 well

To evaluate and study the reduction of permeability in selected sandstone core plugs, brine solutions prepared for chemical specifications similar to the formation of water in terms of the salinity and pH has been prepared. The samples were mounted on the core holder and subsequently injected with different pH values. The first set of experiments used KOH as an alkaline fluid with pH 9. The second set of the test a KOH solution to pH11 was used. The third set of experiments used acidic fluid with pH3. The experiments performed at different injection rates (50 ml/hr; 100ml/ hr and 200 ml/hr) to investigate the effects the degree of alkalinity on petrophysical properties. Once pH value increases dramatically, it dissolved silica cements exist between the grains and causes more fines and the result was fines migration. Lab experiments show that generally high pH value tends to cause fines migration while less disturbance has been observed with low pH value. The obtained result and the ratio of permeability variation and formation damage have been calculated according to the equations presented in (Table 4.4 Appendix A).

The graphs showing little or no change in permeability after core flooding may be explained by scenario where the sandstone contains little easily dispersible clay, which would be true if the clay minerals were mainly of post sedimentation and diagenetic origin, and core flooding was at pH9. At pH 11, however, the effect could be to dissolve the kaolinite aggregates and increase their mobility, so adding the kaolinite fines migration to the rest of clay and non-clay particles migration. The increase in permeability after core flooding at pH- could well be explained by dissolution effects of both clay minerals (chlorite) and non-clay minerals (carbonates). With regard to the dissolution of chlorite, the increase in permeability could well be a temporary feature as such treatment might result in the precipitation of an insoluble hydroxyl-ferriferous gel, causing further problems in hydrocarbon exploitation.

The alkaline solution at pH9 was injected into the core D-2-6, to investigate its influences on the degree of formation damage and fines migration. The experiments started by injecting pH 9 with 50ml/hr and switched to 100/ml/hr then 200ml/hr was injected. The initial permeability of the selected sample is 552mD/hr. The degree of permeability changes increase with increasing flow rate. At the starting point, the selected solution was injected at a rate of 50 ml/hr, permeability declines rapidly from (552mD to 349mD). The main reason for this variation in permeability is the detachment of fine grain particles and redeposition in

the interconnected pore throats which are smaller in size at the downstream section (Appendix A- Table 4.5 and Fig.4.15 Appendix B: Shows the BSE images of the selected core (D-2-6) before flooding. (Fig. 15A) includes (1) clinoclore grain totally filled up the pore between the quartz grain ranging between (100 to 200 μm); (2) represnet carbonte pore filling such as calcite and dolomite and ranging around (50 to 100 μm); (3) represents micaceous flakes with intergrowth of Fe, Ca- carbonates with various sizes between (50 to 150 μm); (4) represents clay minerals such as chlorite, illite, and kaolinite ranges around (10 to 50 μm) partially filled up the pores, which could contribute fines migartion during the core flooding. Apatite exists as a pore- filling material with less than 50 μm size . (Fig. 15B) is composed of (Q) quartz grains with different sizes and shapes. It is clear evidence of kaolinite booklets ranging between (10 to 20 μm) and some individual particles of kaolinite exist < 10 μm, that could be contributed fine migrations.

At the next step, the flow rate switched to 100 ml/hr, causing further reduction of permeability to 341.5mDs, this is due to further detachment of fine particles that are loosely attached to the grains then redeposited at downstream section. Finally, the flow rates switched to 200 ml/hr and permeability decreases sharply from 552mD to 334mD. The variation in permeability from initial to post core flooding of core flooding might be due to moving towards fine grain particles (clay and non- clay minerals) and deposited at the downstream of the core plug then partially plugging or blocking the interconnected pore throats. It can be observed that significantly permeability reduction was observed at each flow rate increase (permeability were reduced to 349mD; 341.5mD and 334mD at each flow rates mentioned above from initial permeability 552 mD, which are equivalent to 36.7%; 38.2% and 41.3% reduces of initial permeability respectively, indicating possible damage due to fines mobilization (Table 4. 4 appendix A) and (Fig. 4.24- and Fig. 4.31 Appendix B). Abdullah (2017) conducted an experimental study to investigate the impact on pH on permeability impairment, they selected Berea sandstone core plug and injected high pH fluid. They observed permeability decline from12- 31%, high pH fluid may interact rapidly with clay particles and cause clay instability. They concluded that with low pH, the surface potential is low and thus damage is eliminated while at high pH the potential is higher, promoting dispersion of fine particles and thus core permeability is reduced.

Besides alkaline solution to pH 9, high pH value (11) was used for the second portion of core flood experiment with different flow rates, D-2-5 core plug selected for during this experiment. Delta P was measured versus to time-based on injection profile further decline

on permeability was observed (Fig 4.25- Appendix B). High pH fluid leads to permeability damage due to the mobilization of fine clay particles, while low pH fluid produces no potential permeability reduction. The results presented in (Table 4.4- Appendix A) show a significant reduction in permeability when the injected solution is strongly alkaline, the initial permeability was recorded 328.2mD and dramatically decreased to 207.1, 159.96 and 144.34mD at 50ml/hr, 100ml/hr and 200ml/hr respectively and the highest damage ratio was reported around 60%. Based on the observations, it was seen that increasing to pH index results in a higher level of formation damage. This finding can be explained by the fact that a higher degree of alkalinity can have a damaging influence on permeability due to fine particle migration. At pH 11 kaolinite undergoes partial dissolution. This can cause detachment, booklets dispersion and the following migration under the flow rate. This is a very important as it is an additional cause of formation damage at this pH condition. Kaolinitic shales in South America were highly unstable and the use of K-based drilling fluids increased that instability (Carpacho et al., 2004). They suggested that the failure mechanism involved was through fluid invasion through micro-pores and micro—fractures, combined with mineralogical transformation of kaolinite to highly dispersible illite. A complete dissolution of kaolinite under highly alkaline conditions pH> 11was observed by Bauer et al. (1998).

The higher pH fluids cause considerably greater disturbance of material formation. Highly kaolinitic sandstone from Tuscaloosa, Louisiana had been subjected to sodium hydroxide treatment at pH 10- 12. This treatment lead to a significant decrease in permeability which was attributed to the in-situ conversion of kaolinite booklets to dickite and hallosite, resulting in disintegration, fragmentation and volume increase of the kaolinite mineral within the same pore space. Fines migration was ruled out as a cause of formation damage (Hayatdavoudi and Ghalambor 1996, 1998).

Detachment fine particles start migrating with the fluid flow, which might cause a drastic drop on permeability. Higher pH valued fluids would lead to a drastic permeability decline, plugged pores, and result in formation damaged (Suat et al., 2001). They conducted an experimental study to investigate entrainment and redeposition of naturally occurring fine particles in a porous media, they used high pH alkaline fluids (NaOH, Na_3SiO4), they used unconsolidated limestone packed mixture they have shown that fine particles detachment and redeposition are the main mechanisms that can lead to a significant reduction on permeability and resulted in formation damage. Fluids with low pH result in lower

permeability changes and the release of fine particles of the pore throats. For instance, at a higher flow rate of pH11 core D- 2- 5 was damaged yielding around 60% permeability dropping because kaolinite undergone partial dissolution that would have caused its detachment, booklets dispersion and following migration under the flow rate. Kaolinite that occurs in sandstones is nearly always of the well crystallized variety, often occurring in booklets and vermicules, and as discrete aggregates rather than as pore-lining or pore-bridging clays. The euhedral nature of these forms of kaolinite and their textural relationship with other sandstone components indicate that they are authigenic (Wilson et al., 2014). While, with core D- 2- 6 reductions in permeability about 41% was recorded. This result shows the plugging phenomenon of pores by suspended fine particles causing significant injection decline. Molenaar (1983) stated that higher pH fluids resulted in significant permeability impairment due to fines migration similar to lower salinity, they used Upper Cretaceous Rocky Mountain sandstone. This injection "permeability" decline can be restored by low pH fluid "acidic treatment". These observations are following literature data (Musharova, 2012) and may be assumed as dependent on the deflocculation of non-swelling clay minerals. The percentage of damage rises with increasing the flow rate of 50 ml/hr to 100 ml/hr and 200 ml/h (Table 4.4 Appendix A). Similarly, a stepwise increase in the flow rate of 10 l/hr to 30 l/hr causes consequent permeability reduction in the sandstone reservoir.

High alkaline fluid can lead to permeability reduction and consequently, the pores were plugged and accumulate at pore throats and constriction, thereby formation damaged was observed (Fig. 4.25- Appendix B). As a result, a higher flow rate has more impact on formation damage, because fine particles are more likely to be mobilized not only by the action of pH but also fluid circulation. Despite changing into pH values, depth in which the sample was taken also influences the degree of formation damage.

Most of the clay minerals identified by XRD were observed in the intergranular pore space, weakly attached to grain surfaces. Also, the intergranular pores are interconnected, forming a flow path, and controlling permeability. Small particles (<10 μm) of clay and non-clay minerals within the intergranular pores might be involved in fines migration. Larger grains (>50 μm) such as large flakes of micaceous particles, grains of K-feldspar, and carbonates are presumably not mobilized since the pore channels have a smaller throat cross-section. The composition and texture of both core plugs are similar, thus we expect that the measured damage parameters are the result of fluid pH and flow rate, allowing a direct comparison between acidic and alkaline damage evolution.

Consequently, the third core (D- 2- 4) was flushed with an acidic solution (pH3) at four different flow rates to measure initial and then damaged by injecting the acidic solution, the initial permeability of 252mD. At the starting point the core flooding experiment started at 50 ml/h flow rates for two hours, this process resulted in permeability increased from (252 mD to 255 mD). The reason for these slight changes of permeability is the dissolution of carbonates present in this samples in significantly larger amount of fine particles of the interconnected pores (Fig. 4.26- Appendix B). In the second step, the flow rate was switched to 100 ml/hr, causing recovery of permeability, to 352mD gradually. Finally, the flow rate was switched to 200 ml/hr, by which permeability increased gradually to 391mDs. Substantial increase in permeability was caused by dissolution of carbonate phases and possibly chlorite clay and subsequent removal of these phases at the flow rate of 200ml/hr. however, this treatment should be carried out with a great care, this might result in Fe-oxide. This might result in Fe- oxide gel like precipitate formation that can potentially block pore throats. The susceptibility of the chlorite minerals in general to acid dissolution, leading to the formation of gelatinous masses, could also lead to damage following acid treatment of the reservoir rock (Wilson et al., 2014).

The overall increase in permeability might be contributed to the high dissolution rate of the Fe- Mg carbonate that occurs between exfoliated mica (Fig. 4.17 before flooding and Fig. 4.36 after flooding- Appendix B). It can be easily observed that carbonate particles were detached from their original position and enhanced permeability with a different ratio as shown in (Fig. 4.26- Appendix B) and (Table. 4.4- Appendix A). This permeability rise can be attributed to the dissolution of Fe-Mg carbonates after the reaction with HCl, which freed the pore throats that were previously blocked by these minerals. At the higher flow rate, permeability started to build up, due to the clearing effect of fluid volume and pressure on the pore throats. Then a higher flow rate might be washing out those particles rising open porosity and fluid throughput. The permeability was restored by 55% (Table 4.4 Appendix A). Previous experiments show that a high degree of alkalinity of injected fluids generally pH more than 7 tends to cause fines migration.

Permeability increases to all samples could be explained by the mobilization of particles and their passage through core/ fragments. According to Musharova (2012) in sandstone reservoirs (Berea Sandstone) with acidic pore fluid, the clay minerals are more stable relative to alkaline conditions. High pH conditions, such as pH 11 lead to permeability damage due to the migration of fine clay particles as a result of deflocculation. Changing the degree of pH (acidity) from acidic to alkaline can cause fine clay particles to release and plug the pore

throats. At extreme pH conditions (both acidic and basic) fine clay particles disintegration may occur, or modification in interlayer composition (e.g. dehydration) can lead to particle detachment and mobilization. The SEM images of the samples showed that many of the pore throats are susceptible to be blocked by mobilized fine particles and interstitial fine particles were also identified, e.g. the carbonate hosting chlorite and kaolinite booklets. However, it is important to be cautious about a potential problem from the chlorite clay present in the formation. Solubility analyses indicated that chlorite is more susceptible to acidic attack than illite, kaolinite, or feldspar minerals (Musharova, 2012).

The influence of the flow rate, the fine particles release depends on the interstitial velocity, which is controlled by the size of both fine particles and the pore channels. It is also important for the oil and gas industry to bear in mind a hazardous nature of highly concentrated acids that are harmful for personnel and corrosive for instruments and tools. Mobilization potential for mineral particles is dependent on the bond strength between clay-clay and clay-rock matrix. Baudracco (1988) observed the decrease in permeability in time, even at a constant flow rate. Similarly, in our experiment for each stage of the flow rate test, the continuous decrease of permeability was recorded. This indicates the disaggregation of pore-filling clay mineral complexes (SEM Fig. 4.18 before flooding and Fig 4.36. after flooding Appendix B), under the action of fluid velocity, releasing more and more particles. Musharova (2012) conducted a series of core flood experiments on Berea sandstone (composed of 86 wt% quartz, 2 wt% calcite, 1wt% dolomite, 3wt% feldspar, 5wt% kaolinite, wt1% illite,2 wt% chlorite) with 2% cc NaOH at pH 13.3 at the different flow rate, observing flow rate effects on permeability reduction. She noted that the flow rate of 30 ml/hr caused more severe permeability decreased than the flow rate of 120 ml/hr. Our results show the same process even at pH11 but its inverse for pH3. The increase and almost linear stagnating of permeability with pH3 fluid are due to the early evacuation of pores (Fig 4.36-5a and 5b Appendix B) and the lower effect of fluid on clay particle deflocculation. According to Tchistiakov (2000) changing in physicochemical conditions, for instance, fluid ionic strength and pH may mobilize clay particles and lead to formation damage even at a relatively low flow rate.

In other experiments, the core flood showed significant permeability reduction due to clay migration and when increasing fluid velocity, a slight decrease in permeability was noticed (Al- Bazzaz and Engler, 2001). This shows that higher fluid velocity can evacuate plugged pore throats, however, this is not the case in our experiments.

The obtained results prove that the percentage of formation damage increases in increasing alkalinity (pH) and the flow rate of the solution (Fig. 4.24, 4.25, and 4.26 Appendix B). This indicates that the selected cores undergo a dispersion and migration of fine clay particles during core flood tests, and thus the reduction in permeability occurs. Elevated percentage of damage is formed even into the absence of swelling clay minerals and mixed pore-filling clay mineral complexes. Wilson et al. (2014) stated that dispersion and fine particle migration therefore seems to be a more commonly applicable mechanism, particularly at alkaline pH values and low salt concentrations, although formation damage problems are also encountered following invasion of high salinity brines into smectitic sandstones.

The initial and final permeability for solutions to different stages is presented in (Table 4. 4 Appendix A). The degree of permeability declined when the solution goes toward alkalinity. This means that the cores of the sandstone reservoir produce a dispersion of native clay minerals for instance kaolinite during core flood tests, so the permeability decline was observed in all flooded samples. Mobilization of a dispersed kaolinite booklets may lead to blocking of a large pore throat, which implies severe permeability reduction caused by a small number of kaolinite particles.

High pH condition, such as pH 11 might dissolve the silica, releasing fine particles, which may then block the pores and then reduce permeability. Mungan and Moore (1968) studied the influence of pH and salinity on permeability reduction in Berea sandstone, he observed that the primary cause of permeability reduction is blocking of the pore throats by dispersed fine particles. Migration of fine clay particles influenced by pH, Salah et al. (2014) studied the effect of different pH (from strong acidic pH 3 to strong alkaline pH 11) on the stability of non- swelling clay minerals. They used a natural sandstone core plugs with different pH solution, they observed that a permeability declined due to dispersion of native clay minerals such as (kaolinite, illite, and so on). They showed that the increase of alkalinity of the solution leads to an increase in the formation damage, and permeability reduced about 68%. Clay minerals are subjected to the dispersion phenomenon and partially fill the pores. They showed that the sudden increase in pH more influential than the gradual increase. So, the degree of damage to permeability is believed to be a function of the amount and type of clay minerals has been migrated.

4.5.2.2 The influence of pH and flow rate on mineralogical, morphological and petrophysical properties of core samples in D-4 and D-3 wells

In Petroleum Engineering, clay minerals have been considered one of the most important factors that cause formation damage (Ohen and Civan, 1993). Fine particles migration and interaction of clay minerals with aqueous solutions are primarily responsible for formation damage measured as permeability reduction (Ohen and Civan, 1993). If the swelling clay minerals lining pore throats, a small amount of expansion can also cause severe permeability impairment (Bennion, 2002). Moreover, swelling clay mineral's effects is not the only mechanism for permeability impairment due to clay minerals. Alteration of their structure due to instability may cause fines generation due to the breaking of the structure.

A series of core tests for natural sandstone cores were performed to investigate permeability decline due to fine particle movement at high flow rates, the experiments were conducted at ambient conditions. As mentioned previously, clay minerals have a significant role in controlling the reservoir properties. Both core samples (D-4-2 and D-4-1) are selected from the same well from the Hungarian sandstone reservoir. The type and amount of bulk mineralogy and clay minerals are measured and identified with using XRD analysis. The different reflection angles for different clays could be used to identify the type of clay minerals. The results show that (D-4-2 and D-4-1) samples contain illite, chlorite, kaolinite, and few percentages of interstratified illite/ chlorite non- clay minerals are also found to be quartz, mica, oligoclase, and carbonates. These existing clay minerals have the capability of migrating and have a considerable impact on the permeability. Krueger (1986) observed that, a number of reasons for the decline in permeability, in most instances the transport of particles, usually clay minerals, and the chemical reactions of these particles with formation fluids are most often involved.

The main petrophysical properties of sandstone reservoir such as porosity and permeability have been found to depend not only on the framework mineralogy but also on the authigenic minerals and the composition, texture, and structure of the rocks. The presence of authigenic minerals strongly effects and controls the sandstone reservoir characteristics.

This study focused on the influence of flow rate on mobilization fine particles and a subsequently considerable permeability reduction due to movement of fine particles, the selected fluid for both core has the same degree of alkalinity (pH9), two sandstone core plugs (D- 4- 2 and D- 4- 1) were selected which have a small difference of clay mineral content

(4.04% and 5.49 %) respectively. Both samples have the same percentage of kaolinite and illite and almost double of chlorite (Table 4. 2 Appendix A). Pore space and solids are distinguished based on BSE intensity threshold. Different minerals are identified based on EDS spectra. Based on SEM images took after flooding of the core (D-4-2, Fig 4.37 Appendix B) easily observed that the core composed of clay and clay minerals with different amount, also it can be used to study the morphology of the grains. Quartz grains represented as a dark grey colour have a various shape and sizes, their sizes ranges between 50 to >300µm and their shapes from rounded to sub-angular with a few percentage of fine grains quartz less than 10µm, their fine particles might be contributing fines migration and produce formation damage. While, clay minerals filled up the pore spaces between coarser grain of quartz have a variety of sizes and shapes, for example kaolinite booklet exit a pore filling with the size between <1 to <5µm easily mobilized from their original places and deposited within the pores which has smaller pore throat sizes. Also, easily observed that the Fe-Mg carbonates were mobilized from their original position (between the exfoliated micaceous mineral before flooding) and redeposited within the pores (Fig. 4.37b Appendix B). Kaolinite mobilization and also Fe-Mg carbonate mobilization would affect permeability during fluid injection in this core sample. Also, observed a mixture of clay minerals such as illite; chlorite and kaolinite booklets in intergranular pores mobilized from their original position and transported to a pore constriction that is smaller than the particle size, where they are retained by straining as shown in (Fig. 4.37-c). Wilson et al. (2014) stated that clay minerals and potential fines mobilisation kaolinite and also illite particles might reduce permeability by fines migration.

In contract D-4-1 core contain more clay minerals than D-4-2, based on the SEM images as shown in (Fig. 4.38 Appendix B) some of the pore spaces filled up with fine particles of clay and non-clay minerals. Kaolinite particles observed with a range of sizes, and they present both as kaolinite booklets and individual platelets. Redistribution of kaolinite, chlorite, illite and Fe-Mg carbonates within the pores shown in (Fig. 4.38b and 4.38c) observed was a good evidence of fine mobilisation, because fine grains of Fe-Mg carbonates which observed between exfoliated micaceous flakes before flooding and they did not exist with clay minerals within the pores (Fig. 4.19 Appendix B).

From the petrophysical point of view D- 4- 2 has a lower porosity than D- 4- 1, their porosity is (25.6% and 27.7% respectively. Both clay mineralogy and petrophysical characteristics have a significant influence on permeability reduction as observed at (Fig. 4.37 and 4.38

Appendix B). Most of the fine particles of clay and non-clay minerals have been detached from their original position and mobilised under the fluid flow leading to the deposition at the downstream section as a result blocking the interconnecting pore channels and reduce permeability and damage the formation.

In addition to mineralogy and porosity, the velocity of injected fluid has a great effect on the permeability of the core plugs. Stepwise increasing to flow rate causes a huge effect on permeability impairment, the percentage of permeability impairment increases with the increase in flow rate. For instance at a low flow rate 50 ml/h the percentage of formation damage is 40% in D- 4- 2 sample when flow rate raised to 100 ml/hr, it is observed that the ratio of damage on permeability increased by 7%, this percentage increased to around 51% when the rate of injection switched to 200ml/hr. The permeability of core plug D-4-1 at low flow rate reduced from 732mD to 419 mD, when the flow rate is stepwise increased to 100 ml/hr the percentage of formation damage increase up to more than 51%, a noticeable permeability reduction is raised at higher injection rate 200ml/hr, the ratio of formation damage increased to around 57% (Table 4.5 Appendix A) and (Fig. 4.27; 4. 28; 4. 32).

Two main causes of fines migration are high fluid velocity and low fluid salinity. According to petrophysical measurements D-4-1 has a higher initial porosity and permeability and initial permeability than D- 4- 2 core plug, Also according to the XRD analysis both selected core plugs have few percentages of clay minerals as mentioned above, these variations might have has a great influence on permeability variation after the flooding. The selected samples prepared for SEM analysis before and after flooding, based on the SEM images clay minerals such as kaolinite, chlorite, and illite filling the interconnected pore channels and slightly attached to the grain surfaces. According to the XRD analysis and for mentioned statement D-4-1 contain more amount of clay minerals than D-4-2. SEM examination of the D-4-1 core (Fig. 4.38 Appendix B) showed clay minerals and non-clay minerals filled up pores between quartz grain could be easily observed that kaolinite booklets, platy kaolinite, illite filled up the pores and Fe-Mg carbonates associated with chlorite and kaolinite within the pores in (Fig.4.38b) was a good proof for migrating fine particles from their original places and deposited somewhere which has smaller pore throat sizes, those fines before the flooding was observed between exfoliated micaceous plates as a result a significant reduction on permeability observed.

While, (Fig. 3.37) shows SEM image of D-4-2 core, quartz grains have a various shapes and sizes with a large number pore spaces often filled up by fine particles. We observed that some of the matrix within the pores mobilized and disturbed such as (pores surrounded by a red rectangle) while, well developed and cemented pore filling materials preserved own position and do not influence by the flooding solution such as (pores surrounded by red square d). Large grains such as detrital dolomite, k- feldspar, albite and muscovite due to their big sizes remain form their original position and did not influenced by injected fluid. (**Fig. b**) composed of a pore- filling chlorite flakes with interlayer of carbonates, most of the carbonated particles subjected by flooding fluid and migrated from their original position, then deposited at downstream section which are the pore throats smaller than migrated particles. (**Fig. c**) a mixture of pore filling fine particles composed of clay minerals such as illite, chlorite and kaolinite booklet and non- clay minerals such as carbonate and fine grain of quartz, those fine particles influenced by flooding solution and moved or shifted from original position, which are caused reduction on permeability. From the SEM images easily observed the D-4-2 was less influenced by injected fluids than D-4-1 because it contains less fine particles than the other core.

Also Fe- Mg carbonates occurring on the flakes of exfoliated chlorite when subjected to fluid flow moved down to the downstream section of the core plugs. These fine particles were moving as suspended particles fine particles as suspended particles within the pore channels with the injected fluid and redeposited at lower pore channels and downstream thus causing a substantial reduction on permeability (Fig. 4. 18; Fig. 4.19; Fig. 4.32; Fig. 4.37 and Fig. 4.38- After flooding Appendix B). According to the SEM analysis took after the flooding of the selected cores, D-4-1 contain more amount of kaolinite as pore filling particles and disturbed after flooding (Fig. 38.4a Appendix B). Clay and non-clay minerals such as Fe, Mg carbonates existed between exfoliated chlorite detached from their original position and might be deposited somewhere have smaller pore throats. While D-4-2 contain less amount of clay minerals, Fig 4.37 easily we can observed that a mixture of clay and non-clay minerals exited as a pore filling and susceptible to fines migration and permeability impairment.

Stepwise increase to flow rate and consequent permeability variation is accompanied by a sharp increase in-situ particles that were mobilised at the increased rate the rate of injectivity and transported with the flow. Throughout the test, we observed that the percentage of permeability reduction on the sample (D- 4- 1) significantly higher than the sample (D-4- 2).

This phenomenon may be related to the less number of released particles was captured in sample D-4-1 than the other sample; this is due to migrated fine particles larger than the pore throats. D-4-2 contains small amount of clay minerals compared to D-4-1 (4.04% and 5.49%) respectively which are directly influence on main petrophysical properties. The degree of formation damage is more severe in sample D-4-1 than D-4-2 with the same flow rate and pH value (9). For instance the percentage of formation damage in D-4-2 at 50ml/hr is only 40% while in D-4-1 is more than 42%, the degree of formation damage increase with increasing flow rates at 200ml/hr the percentage of damage raise to >56% in D-4-1 and around 50% in D-4-2. The reason for this variation in permeability might be due to migration loosely attached fine particles or between grains would be easily detached from their original position and migrated, as a result causing a drastic permeability reduction.

Hussain (2019) conducted a laboratory experiment to investigate the influence of fines migration on relative permeability by injecting into very low salinity/ high pH water in a dry core; they observed that significant permeability damage indicated the occurrence of fines mobilization and consequent permeability damage.

Earlier studies have shown that clay minerals had a significant influence on petrophysical properties of sandstone reservoir. According to the previous studies (laboratory and mathematical modelling) the reduction in productivity due to fines migration can be reliably predicted. Studies show that reduction in permeability during the core flooding with piecewise increasing velocity (Khilar and Fogler, 1998). Low-velocity fine migration in porous media explains the long permeability- stabilization periods. The higher flow velocity, the smaller the mobiles particles.

The pore throats could thus be blocked by migrating fine particles, and finally causes a severe reduction in permeability (Rui et al., 2017). At a higher flow rate of fluids, fine particles might flow with the fluids in reservoirs. The pore throats could thus be blocked by fine particles and finally cause fine particles, and finally causes a potential reduction in permeability in petroleum reservoirs (Russell, 2018), conducted a laboratory studies on an artificially prepared sand- kaolinite core (10%kaolinite and 90% sand) to stimulate the reduction of permeability due to fines migration at the high flow rate, the core flooded with sodium chloride solution with the ionic strength of 0.01M with the injection rate 40 ml/ min. Increasing the injection rate to 50ml/mins, the result of changing the flow rate was a reduction in permeability from 235mDs to 219mDs.

Kaolinite, that exists almost in all selected samples occurs as vermicular and booklet structure and might be originated as authigenic structure and similarly flaky habits of other clay minerals such as illite, chlorite could also have a significant role in determining reservoir quality. We observed a substantial reduction of permeability which may be due to blocking, bridging some of the existing pore throats by the migrating fine particles. Migrated clay minerals such as illite and kaolinite will first disperse at alkaline pH and then get detached and migrate. These migrating fine particles may get trapped in pore channels leading to a significant reduction in reservoir permeability. Ochi and Vernoux (1998) observed a threshold flow rate, below which permeability does not depend on flow rate and above which permeability is reduced. Mungan and Moore (1968) observed that pH changes can result in fines migration. The above result showed how modelling migration at the high flow rates (velocities) can be used to predict the in-flow performance of a production well. The existence of clay minerals like kaolinite, illite, chlorite and interstratifies illite/ chlorite shows induced impaired permeability. Fines migration is the only important point in these kinds of formations. Migration and dislodgement along the flow paths as a result of high flow rate within the pores and loose structures in some cases. It can cause a pore plugging far within the reservoir.

4.5.3 Influence of Temperature on fine mobilization and permeability impairment

From the physicochemical point of view, the temperature is an important factor for rock- fluid interactions. The effect of temperature is more significant, in water-sensitive sandstone formations. Schembre et al. (2006) conducted an experimental work and they observed that permeability reduces with increasing temperature and fine mobilization occurs repeatedly to a particular temperature that varies from solution pH and ionic strength. They experimentally found that fines released from pore walls take place under conditions of elevated temperature, high pH, and moderate aqueous- phase salinity. The greatest reduction in permeability occurs when the fines are produced in the effluent.

Nevertheless, Tchistiakov (2000) experimentally found that the effect of temperature on the stability of clay suspensions is much less evident than the effect of other physicochemical factors. At elevated temperature, the permeability remained approximately constant as the ionic strength was reduced from 2.0M to 0.00 M NaCl. They observed that particles had been mobilized at 20°C by the reduction of ionic strength and at 80°C they had been mobilized by heating. Also, they found that increasing ionic strength to 0.2M or 2.0M at 20°C did not improve the permeability. Similar influence on permeability variation observed

during changing in the temperature of core flooding experiments, permeability declined by heating the sample when saturated with 2.0M NaCl solution. At 20°C, mobilized kaolinite is perceived to form aggregates that plug the pore throats (Khilar, 1984). The mobilised of kaolinite particles may flocculate and form an aggregate that is too large to pass.

Due to several reasons, we have not been able to conduct a series of experiments to investigate the influence of temperature on fine migration and permeability variation, one of the main reasons is lacking time and cost which directly impacts us during the flooding. Another reason is that there is not enough equipment at the institute to experiment.

The composition, type, amount, size, and location of clay minerals are the cut- off parameters in characterizing permeability reduction. These parameters can give a better understanding of formation damage. Mineralogical characterization at the pore level reveals the existence of different types of clay minerals that might harm permeability. non- swelling clay minerals such as kaolinite, illite, chlorite, and interstratified illite- chlorite layers of clay can migrate their site filling the blanks, which they harm the petrophysical properties of oil and gas reservoirs.

Sandstones are important oil and gas reservoir rocks that may be deposited in many different dipositive environments and vary considerably from texture and composition. Most reservoirs contain clays, which play a certain role greatly affected the reservoir characteristics. Sandstone is a mixture of detrital grains, matrix, cement, replacements, and pores, in varying proportion. The clay minerals are present in the form of a detrital matrix and as a part of rock fragments (allogenic clays) and as replacements/cement (authigenic clays). The types, proportions, and distribution patterns of clay minerals in sandstones have a significant impact on porosity, permeability, density, and overall reservoir qualities. The presence of both detrital and authigenic clays minerals commonly harm the reservoir quality of sandstone reservoir rock Lejar (2012).

Authigenic clay minerals occur as pore linings, pore fillings, pseudomorphous replacements, and fracture fillings, the origin of which can be established based on clay composition, structure, morphology, distribution, and sandstone textural properties. The existence of genuine clay minerals greatly affecting the characteristics of the sandstone reservoir at different stages in the diagenetic past. It is important to understand the types, origins, and distribution of various clays in the sandstone reservoir. Different clay mineral cement can have different effects on permeability because they occupy different positions on the pore

network. Authigenic kaolinite and illite in sandstones could be easily susceptible to dispersion and migration where the pore fluids are at alkaline value, while, there is not much evidence that authigenic chlorite is susceptible to dispersion and migration within reservoir sandstones in same way as the other clay minerals just described. This could be due to its aggregate morphology which consists of an interlocking arrangement of comparatively large and thick crystals and in some instances a greater degree of face- to face contacts similar to kaolinite Wilson et al. (2014).

Xiao et al. (2017) stated that fines migration will occur as far as the flow rate is above critical velocity, especially for the particles of kaolinite, illite, or non-clay fines. Kaolinite is more easily to be mobilized because of its booklet morphology. The presence of clay minerals as a dispersed matrix in the pore spaces and permeability channel of the reservoir rock affect the reservoir characteristics of the selected sandstone core plugs by reducing porosity and permeability.

Clay minerals that are arranged perpendicular or sit within the pores and pore throats have more effect on permeability than clay minerals that are arranged tangentially to the grain surfaces. Formation damage causes a decline in the productivity of reservoir. Formation damage is monitored by conducting laboratory tests that can predict to assess formation damage.

Chapter Five

Conclusions and Recommendations

5-1 Conclusion:

This thesis is addressing the problems of formation damage in three wells covering a wide range of petrophysical properties change in the Pannonian sandstone reservoir during drilling, production and injection operations. The petroliferous sandstones from the three wells studied are characterised by diverse mineral compositions of non-clay and clay minerals that have been studied by XRD and SEM/EDS procedures, and also by poro-perm properties which were studied using porosimetry and permeability measurement techniques. These experiments yielded the following results:

1. The XRD and SEM/EDS analysis has indicated the presence of the following non-clay minerals, namely: quartz, feldspars, carbonates and micas, which are of both detrital and authigenic origin;

2. The analytical methods have also indicated the presence of the following clay minerals, namely: illite, chlorite, kaolinite and mixed-layer illite/chlorite.

3. Petrophysical properties were found to be within the following ranges: porosity from 21.5 to 27.3% and permeability from 32 to 732mD.

The presence of both non-clay and clay minerals affect porosity and permeability of the studied formations.

The flooding experiments showed that the poro-perm properties were affected by physical and chemical factors, namely: by the fluid flow rate and by the alkalinity of the fluids under study.

4. The increase of the flow rate resulted in a decline of permeability in alkaline media (pH9). It was concluded that this was due to the dispersion of pore-lining and pore-filling clay material that migrated under the fluid flow and blocked the pore throats. The formation damage variation was estimated within a range of 10 to 77% in different samples studied.

5. The highest permeability variation was observed in the sample with the lowest initial permeability (D-3-1). This sample was characterised by the highest clay fraction content 9.07%, compared to the other core samples of between 4.04 and 5.49%.

6. The fluid flow experiments conducted at pH11 resulted in permeability decline up to 55% that was caused by a partial dissolution of kaolinite and siliceous materials, followed by the detachment and migration under the fluid flow.

7. The fluid flow experiments conducted at pH3 showed the increase of permeability by 55% that was caused by dissolution of carbonate material and chlorite clay. The beneficial result of this study should be taken with the caution that the chlorite dissolution can also cause gel-like and insoluble iron oxides precipitation, if used with the purpose of improving permeability in high Fe-containing chlorite. This process can lead to deleterious blockage of pore throats during injection operations.

This study of the petroliferous sandstone formations in the Pannonian basin (Upper Miocene, Eastern Hungary) has emphasized the importance of both clay and non-clay materials in influencing poro-perm properties. Further studies would be required to clarify the long-term effects on the formation damage in the course of drilling, completion and injection operations.

5-2 Recommendation:

The author recommends for, future work:

- This study can be extended by performing additional lab core flood experiments in pH range closer to the practically reasonable: pH5 to pH8. These values are most widely used for the drilling, completion and injection operations.
- Also, it can be extended by applying different salinity and alkaline solutions such as brine combination, for example: KCl+NaCl, NaCl followed by substitution with $CaCl_2$, or from environmental point of view, when K_2SO_4 or K_2CO_3 are used to replace the shortage of KCl brine. Combined brine $CaCl_2/CaBr_2$ is often used as a heavy weight brine for deep drilling, so this brine can also be a subject of further study.
- Further, investigate fine particle migration and core flooding by using an X-ray computerized tomography (CT) scanning instrument is a non- destructive analytical technique proving 3D reconstructed images local porosity change as a result of before and after flooding.
- Investigate the influence of time (duration of flooding) on fines particle migration and permeability reduction:
- To study the effect of temperature
- To study the formation damage in over pressured formations.

Chapter Six

New Scientific Achievements

In this investigation, it is intended to study the clay mineralogy of several Hungarian Siliciclastic Rocks of potential interest as hydrocarbon reservoirs and contrasting in their fabric and texture. In brief, the study aims to: Investigate the influence of mineralogy on the permeability and addressing the problems of formation damage in three wells covering a wide range of petrophysical properties and their changes in typical sandstone of the Pannonian Basin, Eastern Hungary during drilling, production and injection operations.

New scientific results found through the research are presented in this chapter, these are listed as the following:

6-1 Thesis #1:
The XRD and SEM/EDS analyses has indicated the presence of the following non-clay minerals, namely: quartz, feldspars, carbonates and micas, which are of both detrital and authigenic origin.

6-2 Thesis #2
The analytical methods have also indicated the presence of the following clay minerals, namely: illite, chlorite, kaolinite and mixed-layer illite/chlorite.

6-3 Thesis #3:
Petrophysical properties were found to be within the following ranges: porosity from 21.5 to 27.3% and permeability from 32 to 732mD. The presence of both non-clay and clay minerals affect porosity and permeability of the studied formations. The flooding experiments showed that the poro-perm properties were affected by both physical and chemical factors, namely: by the fluid flow rate and by the alkalinity of the fluids under study.

6-4 Thesis #4:
The increase of the flow rate resulted in a decline of permeability in alkaline media (pH9) in the samples of D-4 well. It was concluded that this was due to the dispersion of pore-lining and pore-filling clay material that migrated under the fluid flow and blocked the pore throats. The formation damage variation was estimated within the range of 40 to 56% in different samples studied.

6-5 Thesis #5:
The highest permeability variation was observed in the sample with the lowest initial permeability (D-3-1). This sample was characterised by the highest clay fraction content 9.07%, compared to the other core samples of between 4.04 and 5.49% with the formation damage more than 77%.

6-6 Thesis #6:

The fluid flow experiments conducted at pH11 resulted in permeability decline up to 55% that was caused by a partial dissolution of kaolinite and siliceous materials, followed by the detachment and migration under the fluid flow.

6-7 Thesis #7:

The fluid flow experiments conducted at pH3 showed the increase of permeability by 55% that was caused by dissolution of carbonate material and chlorite clay. The beneficial result of this study should be taken with the caution that the chlorite dissolution can also cause gel-like and insoluble iron oxides precipitation, if used with the purpose of improving permeability in high Fe-containing chlorite. This process can lead to deleterious blockage of pore throats during injection operations.

The presence of clay and non-clay minerals affect porosity and permeability of the studied formation. The flooding experiments showed that the poro-perm properties were affected by physical and chemical factors. The increase of the flow rate resulted in a decline of permeability in alkaline media (pH9).

The highest permeability variation was observed in the sample with the lowest initial permeability, this sample is characterized by highest clay content. Up to 55% decline in permeability was observed at pH11 that was caused by partial dissolution of kaolinite and siliceous materials.

References:

Abbasi, S., Shahrabadi, A., and Golghanddashti. (2011). "Experimental investigation of clay minerals' effects on the permeability reduction in water injection process in the Oil Fields". *Journalof Society Petroleum Engineers (SPE 144248)*, 1- 10.

Abbasi, Z. H. (2001). Synthesis and physicochemical characterization of nanostructured Pt/CeO2 catalyst used for total oxidation of toluene. *International Journal of Chemical Reactor Engineering, 9(1)*.

Adam, G. & Gibbs J. H. (1965). On the temperature dependence of cooperative relaxation properties in glass-forming liquids. *The journal of chemical physics, 43(1)*, 139-146.

Abdulah Al Moajil, Mohammed Khaldi, Bilel Hamzaoui, Abdulah Al Rustum, and Hameed Al- Badairy, (2017). Formation Damage Assessment of High p and Salinity Completion Fluids in Gas Wells, SPE- 188266- MS.

Abdus S, Ghulam MI and James LB (2007). Practical enhanced reservoir engineering: assisted with simulation software. Penn Well Books, Tulsa

Adel M. Hemeida, Ahmed A. Gawish. (2008). Formation damage tests of some completion fluids. . *Journal of Oil and Gas Business, http://www.ogbus.ru/eng*, 1 - 6.

Ahmad, A.-G. M.-D. (2009). Mechanisms and chemistry of dye adsorption on manganese oxides-modified diatomite. *Journal of environmental management, 90(11)*, 3520-3527.

Ahmed Hanafy, Abdulla Ali, and Hisham A. Nasr-ElDin, (2015). Evaluating the effects of Acidic Stimulation Treatment Before and After Fines Migration on Petrophysical Properties in Sandstone Reservoirs. IPTC- 18596- MS.

Ahmed S. Al- Muthana and Taha Okasha (2008). Best Practices in Conventional Core Analysis- A Laboratory Investigation. SPE- 120814, Saudi Arabia Section Technical Symposium held in Alkhobar, Saudi Arabia, 10- 12 May 2008.

Ahmed, T. (2009). Working guide to Reservoir rock properties and fluid flow. Gulf Professional Publishing.

Ahmed, Tarek (2001). Reservoir Engineering Handbook. Texas: Gulf Professional Publishing.

Aksu I., Bazilevskaya E., and Karpyn, Z.T. (2015). Swelling of clay minerals in unconsolidated porous media and its impact on permeability. *GeoResJ 7, 30 March*, 1- 13.

Al- Bazzaz, W. H., & Kisr Engler, T. W. (2001). Impact of Clay Mineral Attributes in Estimating Damage in Carbonate Rock. *SCA, 38*, 1- 4.

Al- Quraishi A., Zaman H., and Benaafi M. (2014). Reservoir characterization of the Burqan sandstone from Midyan Basin, northern Saudi Arabia. Turkish Journal of Earth Sciences, *http:--journals.tubitika.gov.tr./earth/* 204- 214.

Alabi Olusegun Olalekan and Adeleke Ademola Ezra, (2014). The Effect of Water Salinity on Permeability of Oil Reservoir, 2nd International Conference on Research in Science, Engineering and Technology (ICRSET2014), March 21- 22, Dubai, UAE, pp. 78- 80.

Alexander Badalyan, Themis Carageorgos, Zhenjiang You, Ulrike Schacht, Pavel Bedrikovetsky, Martin Hand, Chris Mathews, (2015). Laboratory study on Formation Damage in Geothermal Reservoirs Due to Fines Migration, Proceedings World Geothermal Congress, Melbourne, Australia, 19- 25 April 2015.

Alexander Badalyan, Themis Carageorgos, Zhenjiang You, Ulrike Schacht, Pavel Bedrikovetsky, Martin Hand, (2014). A New Experimental Procedure for Formation Damage Assessment in Geothermal Wells, Proceedings, Thirty* Nine Workshop on Geothermal Reservoir Engineering, Stanford University, Stanford, California, Feb. 24- 26- 2014.

Ali S. A., Clark W. J., Moore W. R. and Dribus J. R., (2010). Diagenesis and reservoir quality. *Oilfield Rev Summer, 2010, 22, no. 2.*

Al-Muthana, A. S. (2008). Best Practices in Conventional Core Analysis-A Laboratory Investigation. In SPE Saudi Arabia Section Technical Symposium. *Society of Petroleum Engineers.*

Amaefule, J. O. (1994). "A hydraulic flow unit based approach for predicting formation damage profiles in uncored intervals / wells using core/ log data". *(SPE - 27365), Lafayette, La, Feb. 7-10*.

Amaefule, J., D. Kersey, D. Norman, and P. Shannon. (1988). Advances information damage assessment and control strategies. *In Annual Technical Meeting, Petroleum Society of Canada, Calgary, Alberta*.

Amaefule, J. O., Ajufo, Peterson, E. and Durst, K. (1987). "Understanding formation damage processes: An essential ingredient for improved measurment and interpretation of relatively permeability data". *Oklahoma City, OK, March 8-10*.

Amorim C.L.G., Lopes R.T., Barroso R.C., Queiroz J.C., Alves D.B., Perez C.A., Schelin H.R. (2007). Effect of clay-water interactions on clay swelling by X-ray diffraction. Nud Instrum Methods Phys Res A, 580*:* pp. 768- 770.

Anderson R.L., Ratcliffe I., Greenwell H.C., Williams P.A., Cliffe S., Coveney P.V. (2010). Clay swelling: a challenge in the oil-field . *Earth Sci Rev 98:*, pp. 201- 216.

Armin A., Mohammad S. Z., Laura R.-Z., and Bruce J. B. (2017), Magnetic- Resonance Imaging of Fine Migration in Berea Sandstone, SPE- 186089, pp. 1385- 1392

Armin A.; Mohammad S. Z.' Laura R. - Z; and Bruce J. B. (2012). Magnetic- Resonance Imaging of Fines Migration in Berea Sandstone. J. SPE.

Astuti T. R. P. S., Surjono, S. S., Warmada, I. W. and Kusuma, D. K. (2014). The Relationship between Smectite/ Illite Ratios and Diagenetic History of Sandstone Reservoir, Batu Ayau Formation, Upper Kutai Basen, East Kalimantan, Indonesia, IPTC-17895-MS, pp. 1- 12.

Awadh, S. M., Al -Yaseri, A.A. and Hussein, A.R. (2014). The influence of Kaolinite and pH on permeability in the Zubair reservoir in the North Rumaila Oilfield, Southern Iraq. *Iraqi Journal of Science, 2014, Vol 55, No. 2B,* pp. 780-789.

Azari, M. and Leimkuhler, J.M. (1990). "Formation Permeability Damage Induced by Completion Brines.". *Journal of Petroleum Technology 42(4):* , 486- 492.

B. Karpinski, B. and Szkodo, M. (2015). CLAY MINERALS – MINERALOGY AND PHENOMENON OF CLAY SWELLING IN OIL & GAS INDUSTRY. *Journal Advances in Materials Science, Vol. 15, No. 1 (43), March 2015*, pp. 37- 55.

Badalyan, Y. Z. (2015). Particle mobilization in porous media: temperature effects on competing electrostatic and drag forces. *Geophysical Research Letters, 42(8),* pp. 2852-2860.

Bailey, S. W. (1980). Structures of layer silicates. Crystal Structures of Clay Minerals and their X-ray Identification (Ed. by G. W. Brindley and G.Brown),. *Mineralogical Society of London*.

Bailey, S. W. (1984). *Micas. Reviews in Mineralogy* . Washington, DC, 13:584: Mineralogical Society of America.

Balogh, Z. J. (2009). WORLD SOCIETY OF ABDOMINAL COMPARTMENT SYNDROME. *Acta Clinica Belgica, 64*, 3.

Baptis, O.C. and Sweeney, S.A. (1954). The effect of clays on the permeability of reservoir sands to waters at different saline contents. *In: Pacific Coast Regional Conference on Clays and Clay Technology, June 25- 26 1954,*, (p. 505). Berkeley, California; .

Barshad, I. (1952). Factors affecting the interlayer expansion of vermiculite and montmorillonite with organic substances. *Soil Science Society of America Journal 16 (2)*, pp. 176- 182.

Baudracco, J. and Tardy Y. (1988). Dispersion and flocculation of clays in unconsolidated sandstone reservoirs subjected to percolation with NaCl and CaCl2 solutions at different temperatures. Journal *Applied Clay Science, 3(4),* pp. 347-360.

Bauer, A., Velde, B. and Berger, G. (1998) Kaolinite transformation in high molar KOH solutions. Applied Geochemistry, Vol.**13**, Issue 5, July 1998, pp. 619- 629.

Bayat, M. L. (2016). Investigation of gas injection flooding performance as an enhanced oil recovery method. *Journal of Natural Gas Science and Engineering, 29*, 37-45.

Bayliss, P. (1975). Nomenclature of the trioctahedral chlorites. *The Canadian Mineralogist, 13(2)*, 178-180.

Beaufort, D., Cassagnabere, A., Petit, S., Lanson, B., Berger, G., Lasharpagne, J.C. and Johansen H. (1998). Kaolinite-to-dickite reaction in sandstone reservoirs. *Clay minerals, Vol. 33(2)*, pp. 297-316.

Beard, D.C., and Weyl, P.K., (1973). Influence of Texture on Porosity and Permeability of Unconsolidated Sand AAPG Bulletin, February 1973, v. 57, pp 349-369

Bennion. D. B. (2002). An oeverview of formation damage mechanisms causing a reduction in productivity and injectivity of oil and gas producing formations. *Journal of Canadian Petroleum Technology 41 (11),* pp. 29-36, DOI: 10.2118/02-11-DAS.

Bennion, D. B. (1999). Formation damage-the the impairment of the invisible, by the inevitable and uncontrollable, resulting in an indeterminate reduction of the unquantifiable!. *Journal of Canadian Petroleum Technology, 38(02)*.

Bennion, D. B. (1994). Reductions in the productivity of oil and low permeability gas reservoirs due to aqueous phase trapping. *Journal of Canadian Petroleum Technology, 33(09)*.

Berg, R. R. (1986). *Reservoir Sandstone.* Englewood Cliffs, New Jersey, USA. : Prentice-Hall, Inc.

Berger, A. G. (2009). Porosity-preserving chlorite cements in shallow-marine volcaniclastic sandstones: Evidence from Cretaceous sandstones of the Sawan gas field,. *Pakistan AAPG Bulletin Volume 93, Issue 5*, pp. 595- 615.

Berry, S. L., Boles, J. L., Brannon, H. D., Brian B. B. (2008). Performance Evaluation of Ionic Liquids as a Clay Stabilizer and Shale Inhibitor. *SPE International Symposium and Exhibition on Formation Damage Control.* SPE Inetrnation Symposium and Exhibition on Formation Damage Control, 13- 15 Feb. 2008, Lafayette, Louisiana, USA: SPE- 112540- MS.

Bishop, S. R. (1997). The Experimental Investigation of Formation Damage Due to the induced flocculation of Clays within a Sandstone pore structure by a high salinity brine . *SPE European Formation Damage Conference. The Hague, Netherlands, Society of Pteroleum Engineers, Inc*.

Blachier C., Michot L., Bihannic I., Barres O., Jacquet M. and Mosquet M. (2009). Adsorption of polyamine on clay minerals. . *Journal of Colloid Interface Science, Vol. 336, Issue (2)*, pp. 599- 606.

Bloch, S. L. (2002). Anomalously high porosity and permeability in deeply buried sandstone reservoirs: Origin and predictability. *AAPG Bulletin. 2002. 86(2):*, 301- 328.

Blyth, F. G. H., de Freitas, M. H. (2005). *A Geology for Engineers, Seventh Edition.* . Butterworth-Heinemann, UK: Pubished by Elsevier Ltd., ISBN- 9780415502917.

Boles J.R. and Franks S. G. (1979). Clay diagenesis in Wilcox sandstones of Southwest Texas: Implications of Smectite diagenesis on sandstone cementation. *Journal of Sedimentary Petrology (1979), Vol.49- No. 1, pp.00*55- 0070.

Bradford, S. A., Yates, S.R., Bettahar, M., Simunek, J. (2002). Physical factors affecting the transport and rate of colloids in saturated porous Water Resour. Res. Vol. 38, (12), 1327.

Brindley G. W. and Brown G. (1980). Quantitative X-ray mineral analysis of clays. *Crystal structures of clay minerals and their X-ray identification, 5*, pp. 411-438. Mineralogical Soceity, London, England, UK.

Bucke D. P and Mankin C. J. (1971). Clay-mineral diagensis within interlaminated shales and sandstones. *Journal of Sediemntary Petrology, Vol. 41, No. 4*, pp. 971- 981.

Byrne, M. T. and Waggoner M. (2009). Fine migration in a High Temperature Gas Reservoir- Laboratory Simulation for completion Design. *SPE 8th European Formation Damage Conference. Scheveningen, The Netherland, Society of Petroleum Engineers*. SPE- 121897- MS.

Byrne, M. and Patey, I. (2003). Formation damage laboratory testing- A discussion of key parameters and pitfalls and potential, SPE 82250.

Caenn R., Darley HCH and Gray G. R. (2011). *Composition and Properties of Drilling and Completion Fluids.* Gulf Professional Publishing; Sixth Edition, August 29.

Carpacho C., Ramirez M., Osorio J. and Kenny P. (2004) Replacing potassium with aluminium complex over comes wellbore instability problems in kaolinitic shales in South America. AADE-04-DF-HO-17, American Association of Drilling Engineers2004, Drilling Fluids Conference, Houston, Texas, April 6-7-, 2004.

Cerda, C. M. (1987). Mobilization of kaolinite fines in porous media. *Colloids and Surfaces 27 (4)*, 219 - 241.

Chalk, P., Hutten S. J., You Z., Bedrikovesky P. G. (2011). Laboratory and Theoretical investigation of size exclusion suspension flow in rocks. *SPE European Formation Damage Conference. Noordwijk, The Netherlands, Society of Engineers*. SPE-144219-MS.

Chamley, H. (1989). Clay Sedimentology. Berlin (Springer- Verlag).

Chang, F. F. and Civan F. (1991). Modeling of formation damage due to physical and chemical interaction between fluids and reservoir rocks . *SPE Annual Technical Conference and Exhibition Dallas, Texas, Society of Petroleum Engineers*, SPE-22856-MS.

Chang, F. F. and Civan F. (1992). Modeling of formation damage due to physical and chemical interaction between fluid and reservoir rocks. *SPE Annual Technical Conference and Exhibition.* Dallas, Texas,: Copyright 1991, Society of Petroleum Engineers, Inc., SPE-23793-MS.

Chen, D., Zhou B. and Liu Z. (1986). Sand Control Techniques In Shengli Oilfield. . *International Meeting on Petroleum Engineering.* . Beijing, China: Society of Petroleum Engineers.SPE-14840-MS.

Christanti, Y., Ritz T., Busby B., Jeanpert J., Abad C. and Gadiyar B. R. (2011). A New Technique to Control Fines Migration in Poorly Consolidated Sandstones - Laboratory Development and Case Histories. *SPE European Formation Damage Conference.* Noordwijk, The Netherlands: Society of Petroleum Engineers. SPE-143947-MS.

Chorom M. and Rengasamy P. (1995) Dispersion and zeta potential of pure clays as related to net particle charge under varying pH, electrolyte concentration and cation type. European Journal of Soil Science, 46, 657- 665.

Civan, F. (2014). Reservoir Formation Damage, 3rd ed. Gulf Professional Publishing: Burlington, MA. USA

Civan F. (2007). *Reservoir formation damage: fundamentals, modeling, assessment, and mitigation, 2nd.* Gulf Professional Publishing.

Civan F. (2011). Reservoir formation damage: fundamentals, modeling, assessment and mitigation. *Elsevier, Burlington de Souza CEC, Lina AS, Nascimento RSV (2010) Hydrophobically modified poly (ethylene glycol) as reactive clays inhibitor aditive in water-based drilling fluids. J Appl Polym Sci 117,* 857- 864.

Civan F. (2000). *Mechanism of Clay Swelling from Reservoir Formation Damage - Fundamentals, Modeling, Assessment, and Mitigation;*. Elsevier.

Civan, F. (1996). "A multiple purpose formation damage model", Lafayette, La, Feb 14- 16. *(SPE 31101)*.

Civan, F. (1989). Alteration of permeability by fine particle processes. *Journal of petroleum science and engineering, 3(1/2)*, 65-79.

Crocker, M. E., Donaldson E. C., Marchin L. M. (1983). Comparison and Analysis of Reservoir Rocks and Related Clays. *SPE Annual Technical Conference and*

Exhibition. San Francisco, California,: Not subject to copyright. This document was prepared by government employees or with government funding that places it in the public domain.SPE-11973-MS.

Crowe, C. W. (1990). Laboratory Study Provides Guidelines For Selecting Clay Stabilizers. *CIM/SPE International Technical Meeting.* Calgary, Alberta, Canada: Copyright 1990 Society of Petroleum Engineers.

Dahab, A. S., Omar, A., Sayyouh, M. H. and Hemeida, A. (1993). Effects of Clay Content on Permeability Damage, Capillary Pressure and Wettability Characteristics of Saudi Reservoir Rocks. *Journal of The Japan Petroleum Institute, Vol. 36, No.3, May, 1993,* 196- 203.

Dake, L. P. (1978). Fundamentals of reservoir engineering, Developments in Petroleum Science 8, Elsevier, The Netherlands, 1978.

Darya Alexandrovna Musharova, (2012). The effect of physico-chemical factors on the stability and transport of clay particles, MSc. Thesis, Texas A & M University.

Das, M. and Medhi N. (2015). Clay Minerals and its importance on Hydrocarbon Production Potential in a part of Geleki oilfield of Upper Assam Basin . *International Journal of Research in Engineering and Applied Sciences, Volume 5, Issue 11, ISSN 2249-3905,* 25- 33.

Das, M. (2006). A study on the clay minerals and their influence on hydrocarbon production potential of Tipam Rersvoir Sands in Jorajan Oil Fied, Assam Basin, India. *Journal of Applied Geochemistry, 8 (2A),* 266- 276.

Deer. W. A., Howie, R. A., and Zussman, J. (1988). *An Introductionthe Rock-FormingMinerals.* London: Longman.

Devine, C. S. (2005). Approaches to Fracturing Fluid Selection Based on Laboratory Generated Data. *Canadian International Petroleum Conference.* Canadian International Petroleum Conference.: Petroleum Society of Canada.

Djebbar T. and Erle C. D. (2004). Petrophysics: Theory and Practice of Measuring Reservoir Rock and Fluid Transport Properties. (2nd Ed.). Gulf Professional Publishing, Burlington, USA, (P. 926).

Dodd C. G., Conley F. R. and Barnes P. M. (1955). Clay minerals in petroleum reservoir sands and water sensitivity effects:. *Clays and Clay Minerals, Prec. 3rd Conf.,* (pp. 221- 238). Natl. Acad. Sci.--Natl. Res. Council Pub.

Dullien, F. (1992). Porous Media (Fluid Transport and Pore Structure) 2nd Edition. United States: Academic Press

Du X., Sun Z., Forsling W. and Tang H. (1997) Acid-base properties of aqueous illite surfaces. Journal of Colloid and Interface Science, 187, 221-231.

Ehrenberg, S. N. (1993). Preservation of anomalously high porosity in deeply buried sandstones by grain-coating chlorite: examples from the Norwegian continental shelf. *AAPG Bull., 77*, 1260- 1286.

Ekerette E. and Joseph O. (2015). The effects of formation damage on Niger Delta wells. *International Advanced Research Journal in Science, Engineering and Technology Vol. 2, Issue 7*, 6 - 10.

Eleri, O. O. and Ursin J. R. (1992). Physical aspects of formation damage in linear flooding experiments. In the SPE Formation Damage Control Symposium. *Society of Petroleum Engineers*, pp. 179- 189, SPE-23784-MS.

El-Monier, I. A. and Nasr-El-Din H. A. (2013). "An Al/Zr-Based Clay Stabilizer for High pH Applications.". *Journal of Energy Resources Technology 135(2):022903-022903*.

El-Monier, E. A. and Nasr-El-Din H. A. (2011). Mitigation of fines migration using a new clay stabilizer: A Mechanistic study. *SPE European Formation Damage Conference. Noordwijk, The Netherlands, Society of Petroleum Engineers*.

Emerson W.W. and Chi C.L. (1997) Exchangeable calcium, magnesium and sodium and the dispersion of illites in water. II. Dispersion of illites in waster. Australian Journal of Soil Research , 15, 255-262.

Eslinger, E. and Pevear, D. (1988). Clay Minerals for Petroleum Geologists and Engineers. *SEPM Short Course Notes No. 22, Society of Economic Paleontologists and Mineralogists, Tulsa*.

Ezzat, A. M. (1990). “Completion Fluids Design Criteria and Current Technology Weaknesses,” . *SPE 19434 paper, the SPE Formation Damage Control Symposium held in Lafayette, Louisiana, February 22–23,*, 255- 266.

Faergestad, Irene (2016). The Defining Series: Foramtion Damage . Publication *OilField Review* 2016, Schlumberger. available online at: https://www.slb.com/resource-library/oilfield-review/defining-series/defining-formation-damage

Feng, H. K. (2018). Experimental study on a fine emulsion flooding system to enhance oil recovery for low permeability reservoirs. *Journal of Petroleum Science and Engineering, 171*, 974-981.

Foster, M. D. (1955). Relation between composition and swelling in clays: . *Clays and Clay Minerals, Prec. 3rd Conf.,* (pp. 205- 220). Natl. Acad. Sci.--Natl. Res. Council Pub.

Gauup, R. M. (1993). Diagenesis and fluid evolution of deeply buried Permain (Rotliegende) gas reservoir, northwest Germany. *AAPG Bull. 77.:* , 1111- 1128.

Gaupp, R., Matter, A., Platt, J., Ramseyer, K. and Walzebuck, J. (n.d.). Diagenesis and fluid evolution of deeply buried Permain (Rotliegende) gas reservoir, northwest Germany. *AAPG Bull. 77:*, 1111- 1128.

Gdanski, R. (2002). High-pH clay instability rating. *International Symposium and Exhibition on Formation Damage Control. Lafayette, Louisiana, Society of Petroleum Engineers Inc.* .

Gray, D. H. (1996). Formation Damage in Sandstones caused by Clay Dispersion and Migration. *Clays, Clay Minerals 14 (1) 355*.

Gray, D. H. and Rex, R. W. (1966). Formation damage in Sandstone caused by clay dispersion and migration . *Clay and Clay Min.*

Grigsby J. D. (2001). Origin and growth mechanism of authigenic chlorite in sandstones of the lower Vicksburg Formation, South Texas. *Journal of Sedimentary Research. Vol. 71(1):*, 27-36.

Grim, R. E. (1953). *"Clay mineralogy "*. New York: McGraw.

Grim, R. E. (1968). *Clay mineralogy 2 nd ed.* McGraw-hill Book Company.

Gu X. and Evans L.J (2007) Modelling the adsorption of Cd (II), Cu (II), Ni(II), Pb(II) onto Fithian ILLITE. Journal of Colloid and interface science, 307, 317-325/

Gunter, W. D. (1994). Modeling formation damage caused by Kaolinite from 25- 300 C in the oil sand~Reservoirs of Alberta. *SPE Advanced Technology Series, Apr. (SPE 23786)* .

Gupta V., Hampton M.A., Stokes J.R., Nguyen A.V. and Miller J.V. (2011) Particle interactions in kaolinite suspension and corresponding aggregate structures. Journal of Colloid and Interface Science, 359, 95- 103.

Gupta, A. (1987). A model for estimating formation damage in hydrocarbon reservoirs containing swelling clays. *Master's Thesis, The University of Texas at Austin*.

Guven, N. (1988). Smectites. In: Bailey W (ed) Hydrous phyllosilicates (exclusive of mica). *Rev Mineral19: ,* 497- 559.

Hayatdavoudi A. and Ghalambor A. (1998). Controlling formation damage caused by kaolinite clay minerals. Part II. *Society of Petroleum Engineers,* SPE 39464, 421- 430.

Hayatdavoudi A. and Ghalambor A. (1996). Controlling Formation Damage Caused by Kaolinite Clay Minerals: Part I. *SPE 31118, International Symposium on Formation Damage Control, , Lafayette, Louisiana,*.

Howard P. R., Hinkel J. J. and Moniaga N. (2012). Assessing formation damage from migratory clays in moderate permeability formations. *SPE International Symposium and Exhbition on Formation Damage Control, SPE- 151818-MS* (pp. 1- 12). Lafayette, Louisiana USA : Society Petroleum Engineers.

Hemeida, A. M. (2008). Formation Damage Tests of Some Completion Fluids. . *Сетевое издание «Нефтегазовое дело», (2)*.

Hewitt C. H. (1963). Analytical techniques for recognizing water sensitive reservoir rocks. *Journal of Petroleum Technology, 15 (8):813-8,* SPE-594-PA.

Hensen E. J. M. and Smit B . (2002). Why Clay Swell. *J Phys Chem B. 106,* 49, 12664-12667, copyright@ 2002 American Chemical Society.

Hill D. G., Liatard O. M., Piot B. M. and King G. E. (2000). *Formation damage: origin, diagnosis and treatment strategy, chap 14, Reservoir Stimulation.* Wiley, Chichester.

Hillier, S. (2003). Quantitative analysis of clay and other minerals in sandstones by X- ray powder diffraction (XRPD) In: Worden R. H., Morad S., editors, . *Clay mineral*

cements in sandtsones. International Association of Sedimentologists (pp. 213- 251). International Association of Sedimentologists special publication 34, .

Hol, S. M. ((2015, November).). Long-term compaction behavior of Permian sandstones-An investigation into the mechanisms of subsidence in the Dutch Wadden Sea. In 49th US Rock Mechanics/Geomechanics Symposium. *American Rock Mechanics Association.*

Hong, H. C. (2012). Kaolinite–smectite mixed-layer clays in the Jiujiang red soils and their climate significance. *Geoderma, 173*, 75-83.

Houseknecht D. W, Pittman E. D. (1992). Origin, diagenesis, and petrophysics of clay minerals in sandtsones. *SEPM Special Publictaion, vol. 47;*.

Hu, X.; Hu, S.; Jin, F.; Huang, S. (Eds), (2017). Physics of Petroleum Reservoirs, http://www.springer.com, 506 P. ISBN: 978-3-662- 53282-9.

Huerta, M. and D. McQuarrie. (1994). Ioinic size and the ability of electrolytes as clay stabilizers. *SPE Advance Technology Series 2 (1)*, 49 - 57.

Huerta, M. and D. McQuarrie. (1994). Ionic size and the ability of elctrolytes as clay stabilizer. *SPE Advanced Technology Series 2 (1)*, 49- 57.

Hurst, A. and Nadeau, P. H. . (1995). Clay Microporosity in Reservoir Sandstones: An Application of Quantitative Electron Microscopy in Petrophysical Evaluation1. *AAPG Bulletin, Vol. 79, No. 4*, 563- 573.

Hurst A., and Archer S., (1986). Some applications of Clay Mineralogy to Reservoir Description, The Mineralogical Society, Clay Minerals (1986) 21, pp 811-826. 15

Hussain F., Zeinijahromi A., Bedrikovetsky P., Badalyan A., Carageorgos T., , Cinar Y. (2013). An experimental study of improved oil recovery through fines- assisted waterflooding, J Petrol Sci Eng 2013; 109: 187- 197.

Hussain, Y. M. (2019). Journal of Petroleum Science and Engineering, 175. *Effects of fines migration on oil displacement by low-salinity water.*, 665-680.

Jiang, S. (2012). *Clay minerals from the perspective of oil and gas exploration. Clay Minerals in Nature-Their Characterization, Modification, and Application.* Croatia: Rijeka.

Jalel O. and Jean F. V. (1996). Permeability Decrease in sandstone reservoirs by fluid injection Hydrodynamic effects, Journal of Hydrology, 208 (1998) 237- 248.

Jie X., Jianghong W. and Xin S., (2017). Fines Migration: Problems and Treatments, Oil Gas Res, an open access journal, ISSN: 2472- 0518, Vol. 3, Issue1. 1000123, pp. 2-4.

Johnston, N., and Beeson, C. M. (1945). Water permeability of reservoir sands. *Trans. A.I.M.E. 160, 43*.

Jost S., Kuhnen M. and Gunther H. (2000). Transport of Iron Oxide Colloids in Packed Quartz Sand Media: Monolayer and Multilayer Deposition. *Journal of Colloid and Interface Science, Vol. 231*, 32- 14.

Karathanasis, A. D. and Barton CD. (2002). Clay Minerals. *Encyclopedia of Soil Science*, 188- 192.

Karazincir, O., Williams W., and Rijken, P. (2017). Prediction of Fines Migration through Core Testing, SPE- 187157- MS, PP. 1- 34.

Kaufman, P. B. (2008). Critical evaluation of additives used in Shale Slickwater Fracs. . *Paper presented at the SPE Shale Gas Production Confrenece, For Worth, Texas, USA. SPE-119900-MS. DOI:10.2118/119900-MS*.

Kaufman, P. B., Penny, G. S., and Paktinat, J. (2008). Critical evaluation of additives used in shale Slickwater Fracs. *Paper presneted at the SPE Shale Gas Production Conference,*. Fort Worth, Texas, USA: Society of Petroleum Engineers SPE-1199900-MS. DOL:10.2118/1199900-MS.

Khilar, K. C. and Fogler, H. S. (1998). *Migrations of Fines in Porous Media.* Dordrecht/ London/ Boston:: Kluwer Academic Publishers.

Khilar, K. C. and Fogler H. S. (1984). The existence of a critical salt concentration for particle release. *Journal of Colloid and Interface Science* , 214- 224..

Khilar, K. C. and Fogler H. S. (1983). "Water Sensitivity of Sandstones." . *Journal of Colloid and Interface Science **(1)***, 55- 64.

Khilar, K. C. (1987). Colloidally induced fines migration in porous media. *Reviews in chemical engineering,* ***4(1-2),*** 41-108.

Khilar, K. C., Vadya R. N. and Fogler H. S. (1990). Colloidal-induced fines release in porous media. *Journal of Petroleum Scince and Engineering* ***4 (3)***, 213-221.

Kia, S. F., Fogler H. S. and Reed M. G. (1987). Effect of salt composition on clay release in Berea Sandstone. *SPE Production Engineering* ***2 (4),*** 277 - 283.

Klinkenberg L. J. (1941). The permeability of porous media to liquids and gases. Drilling and production practice. American Petroleum Inst, Pp. 200- 2013

Knipe, R. J. (1981) The interaction of deformation and metamorphism in slates. Tectonophysics **78,** 249- 272.

Krueger, R. F. (1988). An overview of formation damage and well productivity in oilfield operations: An update. *SPE Clifornia Regional Meeting. Long Beach.* California: Society of Petroleum Engineers, Inc.

Kumar T. and Todd A. C. (1988). A new approach for mathematical modeling of formation damage due to invasion of solid suspensions. In SPE Annual Technical Conference and Exhibition. *Society of Petroleum Engineers, SPE-18203-MS.*

Lackovic K., Angove M.J., Wells J.D. and Johnson B.B. (2003) Modelling the adsorption of citric acid onto Muloorina illite and related clay minerals. Journal of Colloid and Interface Science, **267**, 49- 59.

Lee, J. H. and Peacor, D. R. (1985) Ordered 1:1 Interstratification of Illite and Chlorite: A Transmission and Analytical Electron Microscopy Study. Journal of Clay and Clay Minerals, Vol. 33, No. 5, 463- 467.

Lee, J. H., Peacor, D. R., Lewis, D. D., and Wintsch, R. P. (1984) Chlorite-illite/muscovite interlayered and interstratified crystals: a TEM-AEM study: Contrib. Mineral. Petrol. **88,** 372-385.

Lejar, Y. (2012). CLAY MINERALS IN SANDSTONE RESERVOIR ROCKS DISTRIBUTION, DIAGENETIC EVOLUTION & POTENTIAL FORMATION DAMAGE . *Jurnal Ilmiah MTG, Vol. 5, No. 2, Juli 2012* .

Lever, A. and Dawe, R. A. . (1984). *J. Pet. Geol.(1984), 7*, 97- 108.

Lionel, C. X. (1992). An experimental study of secondary oil migration. *AAPG Bulletin,* ***76(5)***, 638-650.

Liu S., Mo X, Zhang C., Sun D. and Mu C. (2004). Swelling inhibition by polyglycols in montmorillonite dispersions. *J Dispers Sci Technol **25 (1)***, 63- 66.

Liu X-D. and Lu X-C. (2006). Athermodynamic understanding of clay-swelling inhibition by potasium ions. . *Angew Chem Int Ed **45***, 6300- 6303.

Liu, X. and Civan F. (1996). "Formation damage and filter cake build up in laboratory core test: Modeling and model assisted analysis". *SPEFE, Mar, (SPE 25215-P)*.

Lloyd, G. E., (1985). Atomic number and crystallographic contrast images with the SEM; a review of backscattered electron techniques, Mineral magazine volume 51, page 3 – 19, 1985.

Luckham P. F. and Rossi S. (1999). The colloidal and rheological properties of bentonite suspensions. *Adv Colloid Interface Sci **82:***, 43- 92.

MaCabe, R. (1996). *Clay chemistry. In D. Bruce and D. O'Hare (Eds.), Inorganic Materials (Second ed.)., Cahpter 5.* New York: John Wiley and Sons.

MacCarthy, J. F., and Zachara J. M. . (1989). Subsurface transport of contaminants. *Journal Environmental Scince Technology, Vol. 23*, 496-502.

MacEwan, D. M. M. and Wilson, M. J. . (1980). "Interlayer and Intercalation Complexes of Clay Minerals" in Brindley, G. W., and Brown, G., editors, Crystal Structures of Clay Minerals and Their X-Ray Identification, Monograph No. 5, Mineralogical Society, London. 197- 248.

Mahmoud M. A., Nasr-EL-Din H. A. and DeWolf C. A. (2011). Removing Formation Damage and Sstimulation of Deep Illitic-Sandstone Reservoirs using Green Fluids. *Journal of Society Petroleum Engineers, SPE- 147395*, 1- 16.

Mathews, T., Matthews G. P., Moss A. K. and Powell G. (1993). Measurement and Simulation of Colloidal Flow Formation Damage in Sandstone. *Society of Petroleum Engineers.*

Max, C. and Rahman, S. S. (1987). "Evaluation of formation damage caused by drilling fluids, Specially in pressure reduced formations". *JPT, Nov. (SPE12494)*.

Mays, D. C. and Hunt, J. R. (2005). Hydrodynamic Aspects of Particle Clogging in Porous Media. *Environmental Science and Technology 39 (2)*, 577- 584.

Mehdi, D. (2015). Clay swelling — A challenge in the oilfield. *Earth-Science Reviews 98(3)*, 201-216.

Medhi, N., and Das, M. (2014). "Astudy on the interaction between the injection water and reservoir minerals and their effects on reservoir characteristics in Tipam reservoir sand and Geleki oilfield of Upper Assam Basin,. *Journal of Applied Geochemistry ISSN: 0972- 1967*, 321- 329.

Mohan, K. K., and Fogler, H. S., . (1997). “Colloidally Induced Smecticic Fines Migration: Existance of Microquakes,”. *AIChE Journal, 43(3), March* , 565- 576.

Mohan K. K., Fogler H. S., Vaidya R. N. and Reed M. G. (1993). Water sensitivity of sndstones containing swelling and non-swelling clays. *Journal of Colloids and Surfaces A: Physicochemical and Engineering Aspects, 73* , 237 - 254.

Moll Jr, W. F. ((2001)). Baseline studies of the clay minerals society source clays: Geological origin. *Clays and Clay Minerals, 49(5)*, 374-380.

Monagham P. H., Salathiel R. A., Morgan A. D. and Kaiser Jr. (1959). Laboratory studies of formation damage in sands containing clays. *Journal Petroleum Technology 11*,, 209- 2015.

Moore, D.N., and Reynolds R.C. Jr. (1997). X-Ray Diffraction and the Identification and Analysis of Clay Minerals, 2nd ed.: Oxford University, New York. P. 378.

Moore D.N, Renyolds R.C Jr. (1989). *X-ray diffraction and the identification of clay minerals.* Oxford: Oxford University Press.

Moore, J. E. (1960). Clay mineralogy problems in oil recovery. *Petroleum Engineer* , 78-101.

Muecke, T. W. (1979). Formation Fines and Factors Controlling Their Movement in Porous Media. *Journal of Petroleum Technology 31(2):*, pp. 144- 150.

Mungan, N. (1989). Discussion of An overview of formation damage. *Journal of Petroleum Technology 41 (11)*, 124.

Mungan, N. and Moor E. J. (1968). Certain wettability effects on electrical resistivity in porous media. *Journal of Canadian Petroleum Technology, 7(01),* pp. 20-25.

Mungan, N. (1965). Permeability Reduction through Changes in pH and Salinity. *Journal of Pteroleum Technology 17 (12),* 1449- 1453.

Musharova, D., Mohamed,I. M. and Nasr-El-Din H. A. (2012). Detrimental Effect of Temperature on Fines Migration in Sandstone Formations . *SPE International Symposium and Exhibition of Formation Damage Control. Lafayette, USA, Society of Petroleum Engineers*.

Nadeau, P. H. (1998). An experimental study of the effects of diagenetic clay minerals on reservoir sands. *Clays and Clay Minerals, 46(1),* 18-26.

Neasham, J. W. ((1977, January).). The morphology of dispersed clay in sandstone reservoirs and its effect on sandstone shakiness, pore space, and fluid flow properties. In SPE Annual Fall Technical Conference and Exhibition. *Society of Petroleum Engineers.*

Ngwenya, B. T. (1994). Hydrothermal rare earth mineralization in carbonatites of the Tundulu complex, Malawi: processes at the fluid/rock interface. *Geochimica et Cosmochimica Acta, 58(9),* 2061-2072.

Norrish, K. (1954). The swelling of montmorillonite. *Discussions of Faraday Soc 18:,* 120-134.

Ochi, J. and Vernoux J. F. (1998). Permeability decrease in sandstone reservoirs by fluid injection: hydrodynamic and chemical effects. *Journal of hydrology, 208(3-4),* 237-248.

Ochi J. and Vernoux J. F. (1993). "Experimental Percolation in Argillaceous Sandstones and Survey of Permeability and Porosity Changes: Application to the Reinjection of Cooled Brines into Geothermal Reserviors,". *presented at GEOFLUIDS, May 4-7.* Torquay,.

Ohen, H. A. and Civan F. (1989). Formation Damage in Petroleum Reservoirs - II. Case Studies and Parameter Estimation. *Society of Petroleum Engineers*.

Ohen, H. and Civan F. (1993). Simulation of formation damage in petroleum reservoirs. *SPE Advances Technology Series 1 (1),* 27- 35.

Ohen, H. and Civan, F. (1989). Formation damage in petroleum reservoirs{: modeling", Unsolicited Manuscritp, July,. *(SPE 19380).*

Oyenenin, M. B. (1995). Factors to consider in the effective management and control of fine migration in high permeability sands. *SPE 30112, The Hague, Netherlands, May 15-16.*

Oluwagbenga, O. O. (2015). Evaluation of formation damage and assessment of good productivity of the order field, Edo State, Nigeria. *American Journal of Engineering Research (AJER), 4(3),* 1-11.

Oyenenin, M. B. (1995). Factors to consider in the effective management and control of fine migration in high permeability sands. *SPE 30112, The Hague, Netherlands, May 15- 16.*

Page, R. and Wenk, H. R. (1979) Phyllosilicate alteration of plagioclase studied by transmission microscopy: Geology **7**, 393- 397.

Pallatt, N., Wilson, J., and McHardy, B., (1984): The relationship between permeability and the morphology of diagenetic illitie in reservoir rock, J. Pet. Technol, 36, 2225- 2227, 1984

Paul G. (2001). Petrophysics MSc course notes. http://www.2.ggl.ulaval.ca/personnel/paglover/CD%20Contents/GGL-66565%20Petrophysics%20English/Chapter%202.PDF;http://www.2.ggl.ulaval.ca/personnel/paglover/CD%20Contents/GGL 66565%20Petrophysics%20English/Chapter%203.PDF

Perdrial J. N. and Warr L. N. (2011). Hydration Behavior of MX80 bentonite in confined-volume system: implications for backfill design . *Journal of Clays and Clay Miner; 59 (6),* , 640- 653.

Pham H. and Nguyen O. P. (2014). Effect of silica nanoparticles on clay swelling and aqueous stability of nanoparticle dispersions. *J. Nanopart Res (2014) 16: 2137*, 1-11.

Pittman, E. D. (1970). *J. Sed. Petrol., 40, 1153.*

Porter, K. E. (1989). An overview of foramtion damage. *JPT*, 780- 786.

Priishalm, S. N. (1987). "Fine migration blocking and clay swelling of potential geothermal sandtsone reservoirs, Denmark". *Journal OF SPE - 15199.*

Priishalm, S., Neilson, B. L., and Haslund, O. (1987). "Finemigration blcoking and clay swelling of potential geothermal sandstone reservoirs, Denmark". *SPEFE - (SPE-15199).*

Qiu K., Gherryo Y., Shatwan M., Fuller J. and Martin W. (2008), "Fines Migration Evaluation in A Mature Field in Libya", pp. (1- 10), SPE 116063-MS, SPE Asia Pacific Oil and Gas Conference and Exhibition, Perth, Australia, 20-22 Oct. 2008.

Rahman, S. R. (1995). Response of low-permeability, illitic sandstone to drilling and completion "fluids. *J. Pet. Sci. Eng. 12 (4),*, 309- 322.

Reed, M. (1977). Formation permeability damage by mica alteration and carbonate dissolution. *Journal of Petroleum Technology 29 (9),* 1056- 1060.

Reinoso W., Aldana M., Campo P., Alvarez E. and Tovar E. (2016). Removing Formation Damage From Fines Migration in the Putumayo in Colombia: Challenges, Results, Lessons Learned, and New Opportunities after More than 100 Sandstone Acidizing Treatments, PPE- 178996- MS, pp. 1- 17.

Rept. Invest. 1Vo. 6093, U.S. Bureau of Mines, Washington, D.C. . (1959). Laboratory studies of formation damage in sands containing clays. *Journal Petroleum Technology 11, ,* 209- 2015.

Rita M. F. Fonseca, Femando J. A. S. Barriga, Patricia I. S. T. Conceicao (2009). Clay minerals in sediments of Portuguese reservoirs and their significance as weathering products from over- eroded soils: a comparative study of the Maranhao, Monte Novo and Divor Reservoirs (South Portugal. Int J Earth Sci (Geol Rundsch), DOI 10.1007/00531- 009- 0488- 3.

Rosenbrand, E., Kjoller, C., Riis, J. F., Kets, F. and Fabricius, I. L. (2015). Different Effects of Temperature and Salinity on Permeability Reduction by Fines Migration in Berea Sandstone, Geothermics

Rui, Z. L. (2017). A quantitative oil and gas reservoir evaluation system for development. *Journal of Natural Gas Science and Engineering*, *42*, 31-39.

Russel T., Chequer L., Borazjani S., You Z., Zeinijahromi A. and Bedrikovetsky, P. (2018). Formation Damage by Fines Migration, Chapter Three. Field Cases, January 2018,

DOI: 101016/B978-0-12-813782-6-00003-8, https://www.researchgate.net/publication/325663170.

Ruth, D, Pohjoisrimne, T., (1991). The precision of grain Volume Porosimeters, Paper SCA 9129, presented at the 5th annual technical Conference of the SCA, San Antonio, CA, USA.

Salah, T. A. A. (2014). Development of nano-hydroxyapatite/chitosan composite for cadmium ions removal in wastewater treatment. *Journal of the Taiwan Institute of Chemical Engineers, 45(4),* pp. 1571-1577.

Sanaei A., Shakiba M., Varavei A. and Sepehrnoori K. (2016). Modeling clay swelling induced conductivity damage in hydraulic fractures. *Journal Society of Petroleum Engineers*, pp. 1- 14, SPE-180211-MS.

Schechter, R. S. (1992). *Oil Well Stimulation.* Englewood Cliffs, New Jersey.: Printice Hall.

Schembre , J. M., Tnag, G.Q. and Kovscek, A.R. (2006). Interrelationship of Tmperature and Wettability on the relative Permeability of Heavy Oil in Diatomaceous Rocks. *SPE Reservoir Evaluation and Engineering 9 (3)*, 239- 250.

Schoonheydt, R. and Johnston C. (2013). *Surface and Interface Chemistry of Clay Minerals. In F. Bergaya and G. Lagaly *Eds.), Handbook of Clay Science, Developments in Clay Science, Vol 5, Chapter 5, Elsevier.* 139- 172.

Schulze, D. G. (2005). Clay Minerals. *Clay Minerals* , 246- 254.

Seemann, U. (1979). Diagenetically formed interstitial clay minerals as a factor in Rotliegend sandstone reservoir quality in the Dutch sector of the North Sea. *Journal of Petroleum Geology, 1(3),* 55-62.

Seetahal P. and Bruce P. N. (1984). Formation damage in a simulated Lower Cruse Formation. *West Indian Journal of Engineering, Vol. 9, No. 1* , pp. 22 - 28.

Shapiro A. A., Bedrikovetski P. G. Santos A., Medvedev O. O. (2007). A Stochastic Model for Filtration of Partculate Suspensions with Incomplete Pore Plugging. *Journal of Transport in Porous Media, Vol. 67 (1),* 135- 164.

Sharma M. M. and Yortsos, Y.C. (1987). Fines Migration in Porous Media. Reprinted from AIChE Journal, Vol. 33, No. 10, October, 1987, pp. 1654- 1662.

Shepperd, K. A. Morris and C. M. (1982). THE ROLE OF CLAY MINERALS IN INFLUENCING POROSITY AND PERMEABILITY CHARACTERISTICS IN THE BRIDPORT SANDS OF WYTCH FARM, DORSET. *Journal Clay Minerals (17)*, 41- 54.

Shaw H. F. (1972). The preparation of oriented clay mineral specimens for X-ray diffraction analysis by a suction onto ceramic tile method. Clay Miner. 9, pp. 345- 349.

Srodon, J. (1999). Use of clay minerals in construcing geological processes: recent advances and some perspectives. *Journal of Clays and Clay Minerals 34*, pp. 27- 37.

Suat B., Kok M. V. and Turksoy U. (2001). Effect of Brine Composition and Alkaline Fluid on the Permeability Damage of Limestone Reservoir, SPE- 65394, pp. 1- 11.

Sun, L., J. Tanskanen, J. Hirvi, S. Kasa, T. Schatz, and T. Pakkanen. (2015). Molecular dynamics study of montmorillonite crystalline swelling: roles of interlayer cation species and water content. *Chemical Physics 455,*, 23- 31.

Simon, D.E., McDaniel, B.W. and Coon, R.M. (1976). Evaluation of fluid pH effects on Low Permeability Sandstones, prepare for the 51st Annual Fall Technical Conference and Exhibition of the SPE of AIME, held in New Orleans 3- 6. , October 3 , pp. 1- 15.

Stalder, P. (1973) Influence of crystallographic habit and aggregate structure of authigenic clay minerals on sandstone permeability. Geologie en miljnbouw vol. 52 (4), Pp. 217- 220

Tchistiakov, A. A. (2000). Colloid Chemistry of In-Situ Clay-Induced Formation Damage. *SPE International Symposium on Formation Damage Control. Lafayette, Louisiana, Society of Petroleum Engineers*, SPE 58747. pp. 1- 9, presented at the 2000 SPE International Symposium on Formation Damage Control held in Lafayette, Louisiana, 23- 24 Feb. 2000.

Tchistiakov, A. A. (2000). PHYSICO-CHEMICAL ASPECTS OF CLAY MIGRATION AND INJECTIVITY DECREASE OF GEOTHERMAL CLASTIC RESERVOIRS. *Proceedings World Geothermal Congress*, (pp. 3087- 3095). Kyushu- Tohoku, Japan, May 28 - June 10, 2000.

Tchistiakov, A. A., (1999). Effect of flow rate and salinity on sandstone permeability. European Geothermal Conference Basel 99, Switzerland, September 28- 30, 1999, Proceeding, Vol.2, p.p. 189- 197.

Thair Al- Ani and Olli Sarapää, (2008). Clay and Clay Mineralogy, Physical- Chemical Properties and Industrial uses, Geologian Tutkimuskeskus. Pp. 95.

Thorez, J., (1976). Practical Identification of Clay Minerals in: Lellote G (ed) A laboratory handbook for teachers and students in clay mineralogy, Dison Belgium, 70p.

Torsaeter O. and Abtahi M. (2000). *Experimental Reservoir Engineering Laboratory Work Bok.* Norway: Norwegian University of Science and Technology.

Uddin, F. (2008). Clays, nanoclays, and montmorillonite minerals. *Metallurgical and Materials Transactions A 39A,* , 2804- 2814.

Vaidya, R.N. and Fogler, H.S. (1990). "Formation Damage Due to Colloidally induced fine migration,". *Colloids and Surface, 50,* 215- 227.

Valdya, R. N. and Fogler, H. S. (1992). Fine migration and formationdamage: influence of pH and Ion exchange. *SPE Production Engineering*, 325- 330.

Van Olphen, H. (1963). Clay Colloid Chemistry for Clay Technologists,. *Geologists and Soil Scientists, J., Willey and Sons., London*.

Velde, B. B. (2008). The origin of clay minerals in soils and weathered rocks. *Springer Science & Business Media.*

Vernoux J. F. and Ochi J. (1994). Aspects relative to the release and deposition of fines and their influence on the injectivity decrease of a clastic reservoir. Int. Symposium Geothermics 94 in Europe, Orleans, France, pp. 291- 302

Vinchon C. (1993). Textural and Mineralogical Changes in Argillaceous Sandstones, Induced by Experimental Ruid Percolation". *presented at GEOFLUIDS, May 4-7.* Torquay.

Wang, S. (2005). Modeling formation damage by asphaltene deposition during primary oil recovery. pp. 310-317.

Weaver, C. E. (1958). Geologic interpretation of argillaceous sediments: Part I. Origin and significance of clay minerals in sedimentary rocks. *AAPG Bulletin, 42(2),* 254-271

W~ITE, E. J., BAPTIST, O. C., and LAND, C. S. . (1962). Physical properties and clay mineral contents affecting susceptibility of oil sands to water damage, Powder River Basin, Wyoming. *Rept. Invest. 1Vo. 6093, U.S. Bureau of Mines, Washington, D.C.*

White E. J., Baptist O. C. and Land C. S.(1962). Physical properties and clay mineral contents affecting susceptibility of oil sands to water damage, Powder River Basin, Wyoming. *Rept. Invest. 1Vo. 6093, U.S. Bureau of Mines, Washington, D.C.*

Wilson M. J.; Wilson L.; Patey I. (2014). The influence of individual clay minerals on formation damage of reservoir sandstones: Acritical review with some new insights, Journal of Clay Minerals, **49**, pp. 147- 164.

Wilson, M. J.and Wislon, L. (2014). Clay mineralogy and shale instability: an alternative conceptual analysis. *Clay Minerals. **49**.* , 127- 145.

Wilson MD, Pittman ED. (1977). Authigenic clays in sandstones: recognition and influence on reservoir properties and paleoenvironmental analysis. *J Sediment Petrol **;47 (1),*** 3- 31.

Worden, R. H. and Morad, S. . (ed. 2003.). *Clay mineral cements in sandstones.* Oxford: Blackwell Publishing.

Wu H., Zhang C., Ji Y., Liu R., Cao S., Chen S., Zhang Y., Wang Y., Du W. and Liu G. (2018). Pore throat characteristics of tight sandstone of Yanchang Formation in eastern Gansu, Ordos Basin, Petroleum Research xxx (2018) 1- 11, KeAi Advancing Research Evolving Science, pp. 1- 12.

Xie, Q. L. (2014). Ions tuning water flooding experiments and interpretation by the thermodynamics of wettability. *Journal of Petroleum Science and Engineering, **124,*** 350-358.

Xiao, L.; Mao, Z.Q; Sun, Z.C., and Luo, X.P., 2011. “Comparison of Porosity Estimated from Conventional Logs in Complex Lithological Reservoirs”. SPE 140796 Paper was prepared for the Presentation at the EUROPEC/EAGE Annual Conference held in Vienna, Austria, May 23 - 26.

Xie Y., Chen Z. and Sun F. (2014). Particles migrating and plugging mechanism in loosen sandstone heavy oil reservoir and the strategy of production with moderate sanding .

5th International Conference on Porous Media and thier Application in Science, Engineering and Industry, 1 - 6.

Xinghui, C. (1996). "A multiple purpose formation damage model", Lafayette, La, Feb 14-16. *(SPE 31101)*.

You, Z.; Bedrikovetsky, P.; Badalyan, A. and Hand, M. (2015). Particle mobilization in porous media: temperature effects on competing electrostatic and drag forces. Geophys. Research Let, 42, 2852- 2860.

Young, B. M., McLaughlin H. C. and Borchardt J. K. (1980). Clay Stabilization Agents-Their Effectiveness in High-Temperature Steam. *Journal of Petroleum Technology Vol. **32, Issue, (12)**:* , pp. 2121-2131.SPE-7895-PA.

Zaltoun, A. and N. Berton. (1992). Stabilization of Montmorillonite Caly in porous media by High-Molecular-Weight polymers. *SPE Production Engineering **7 (2)***, 160 - 166.

Zeinijahromi, A., F. A. Machado et al. . (2011). Modified mathematical model for fines migration in oil fields. Brasil Offshore. *Macae, Brazil, Society of Petroleum Engineers.*

Zhihong (John) Zhou, Shauna Cameron, Bernice Kadatz, and William D. Gunter. (1997). Clay Swelling Diagrams: Their applications in Formation damage control. *SPE Journal, Volume 2 - SPE 31123*, 99- 106.

Zhao, J. J. (2017). Mineral types and organic matters of the Ordovician-Silurian Wufeng and Longmaxi Shale in the Sichuan Basin, China: Implications for pore systems, diagenetic pathways, and reservoir quality in fine-grained sedimentary rocks. *Marine and Petroleum Geology, **86,*** 655-674.

Zhou, Z., Cameron, S., Kadatz, B. et al. (1997). Clay Swelling Diagrams: Their Applications in Formation Damage Control. *SPE Journal 2 (2):*, 99- 106. DOI: 10.2118/31123-pa.

Zhou, Z., Gunter, W. D., Kadaty, B., and Cameron, S. (1996). "Effect of clay swelling on reservoir quality". *Journal of Canadian Petroleum Technology, 35, paper No. 95-54*, 18- 23.

Zhou, Z. (1995). Construction and application of clay swelling diagrams by use of XRD methods. *Journal of Petroleum Technology ; 306*.

Zhou, Z. J., Gunter, W. O. and Jonasson R. G. (1995). Controlling Formation Damage Using Clay Stabilizers. *A Review. Annual Technical Meeting. Calgary, Alberta, Petroleum Society of Canad*, PETSOC- 95-71.

Weaver C.E., (1958). Geologic Interpretation of argillaceous sediments, Part 1; Origin and significant of clay minerals in Sedimentary rocks, Bull. AAPG, , 42 (2), pp. 254- 27

Bulk and Clay XRD data

Table 4. 1: Quantitative XRD data by Rietveld refinement

Bulk and Clay XRD data											
Core ID	wt % of Non- Clay Minerals							wt % Clay Minerals			
	Q	**Cc. Mg**	**Dol.**	**Olig**	**Bio.**	**Mic.**	**Amor.**	**Chl.**	**Ill.**	**Kao**	**Total Clay**
D-2- 6	83.3	0.2	0.3	6.7	0.0	1.0	4.0	1.0	2.5	0.5	4.04
D-2- 5	78.3	4.6	1.4	6.4	0.1	0.8	4.0	2.0	2.3	0.1	4.45
D-2- 4	78.2	4.8	0.9	6.4	0.2	0.7	4.0	1.6	2.0	1.2	4.85
Q: Quartz; Cc. Mg: Calcite Mg; Olig: Oligocene; Bio: Biotite; Mic: Microcline; Amor: Amorphous; Chl: Chlorite; Ill: Illite; Kao: Kaolinite; wt% Weight percentage.											

Table 4. 2: Quantitative XRD data by Rietveld refinement

Bulk and Clay XRD data											
Core ID	wt % of Non- Clay Minerals							wt % Clay Minerals			
	Q	**Cc. Mg**	**Dol.**	**Olig**	**Bio.**	**Mic.**	**Amor.**	**Chl.**	**Ill.**	**Kao**	**Total Clay**
D-4- 2	80.0	3.2	0.9	6.0	0.0	1.0	4.0	0.8	3.3	0.9	4.04
D-4- 1	80.7	2.8	0.5	5.7	0.1	0.8	4.0	1.5	3.0	1.0	5.49

Q: Quartz; Cc. Mg: Calcite Mg; Olig: Oligocene; Bio: Biotite; Mic: Microcline; Amor: Amorphous; Chl: Chlorite; Ill: Illite; Kao: Kaolinite; wt% Weight percentage.

Table 4. 3: Quantitative XRD data by Rietveld refinement

Bulk and Clay XRD data											
Core ID	wt % of Non- Clay Minerals							wt % Clay Minerals			
	Q	**Cc. Mg**	**Dol.**	**Olig**	**Bio.**	**Mic.**	**Amor.**	**Chl.**	**Ill.**	**Kao**	**Total Clay**
D-3- 2	75.0	3.4	1.6	7.5	0.1	2.0	5.0	1.4	3.3	0.8	5.47
D-3- 1	69.4	4.9	2.3	9.5	0.1	1.8	3.0	2.2	4.8	2.0	9.07
Q: Quartz; Cc. Mg: Calcite Mg; Olig: Oligocene; Bio: Biotite; Mic: Microcline; Amor: Amorphous; Chl: Chlorite; Ill: Illite; Kao: Kaolinite; wt% Weight percentage.											

Table 4. 4: Petrophysical and core flooding data of core samples D- 2- 6; D- 2- 5 and D- 2- 4

Core ID	Depth (m)	L (cm)	D (cm)	ϕ (%)	k_i (mD)	k_{f1} (mD)	k_{f2} (mD)	k_{f3} (mD)	pH
D-2- 6	1943.0	6.2	3.8	27.3	552.4	349.59	341.52	334.1	**9**
Formation Damage %: 100- k_f *100/ k_i						**36.71**	**38.17**	**41.34**	
Permeability variation: k_i/ k_f						**-1.58**	**-1.62**	**-1.65**	
D-2- 5	2140.3	6.1	3.8	22.5	328.2	207.10	159.96	144.34	**11**
Formation Damage %: 100- k_f *100/ k_i						**36.92**	**51.26**	**55.99**	
Permeability variation: k_i/ k_f						**-1.58**	**-2.05**	**-2.27**	
D-2- 4	2145.1	6.2	3.8	22.8	252.6	255.33	352.72	391.71	**3**
Formation Damage %: 100- k_f *100/ k_i						**+1.08**	**+39.64**	**+55.07**	
Permeability variation: k_i/ k_f						**+0.99**	**+0.72**	**+0.64**	

L: Length; D: Diameter; φ: porosity; ki: initial permeability; k_{f1}: permeability at 50 ml/ h; k_{f2}: permeability at 100 ml/ h; k_{f3}: permeability at 200 ml/ h.

Table 4. 5: Petrophysical and core flooding data core samples D- 4- 2 and D- 4- 1

Core ID	Depth (m)	L (cm)	D (cm)	ϕ (%)	k_i (mD)	k_{f1} (mD)	k_{f2} (mD)	k_{f3} (mD)	pH
D-4- 2	1872.6	6.2	3.8	25.6	343.20	205.95	180.8	167.41	**9**
Damage Ratio: k_i/ k_f Formation Damage %: 100- k_f *100/ k_i						**40.0**	**47.33**	**51.23**	
Permeability variation: k_i/ k_f						**1.67**	**1.90**	**2.05**	
D-4- 1	1874.0	6.1	3.8	27.7	731.97	419.04	354.64	405.25	**9**
Formation Damage %: 100- k_f *100/ k_i						**42.75**	**51.55**	**56.64**	
Permeability variation: k_i/ k_f						**1.75**	**2.06**	**2.31**	

L: Length; D: Diameter; φ: porosity; ki: initial permeability; k_{f1}: permeability at 50 ml/ h; k_{f2}: permeability at 100 ml/ h; k_{f3}: permeability at 200 ml/ h.

Table 4. 6: Petrophysical and core flooding data core samples D- 3- 2 and D- 3- 1

Core ID	Depth (m)	L (cm)	D (cm)	ϕ (%)	k_i (mD)	k_{f1} (mD)	k_{f2} (mD)	k_{f3} (mD)	pH
D-3- 2	1868.9	6.2	3.8	27	103.33	92.92	85.49	77.51	**9**
Formation Damage %: 100- k_f *100/ k_i						**10.07**	**17.27**	**24.99**	
Permeability variation: k_i/ k_f						**1.11**	**1.21**	**1.33**	
D-3- 1	1872.1	6.1	3.8	21.5	32.37	10.11	7.83	7.38	**9**
Formation Damage %: 100- k_f *100/ k_i						**68.77**	**75.81**	**77.2**	
Permeability variation: k_i/ k_f						**3.20**	**4.13**	**4.39**	

L: Length; D: Diameter; φ: porosity; ki: initial permeability; k_{f1}: permeability at 50 ml/ h; k_{f2}: permeability at 100 ml/ h; k_{f3}: permeability at 200 ml/ h; D: damage ratio

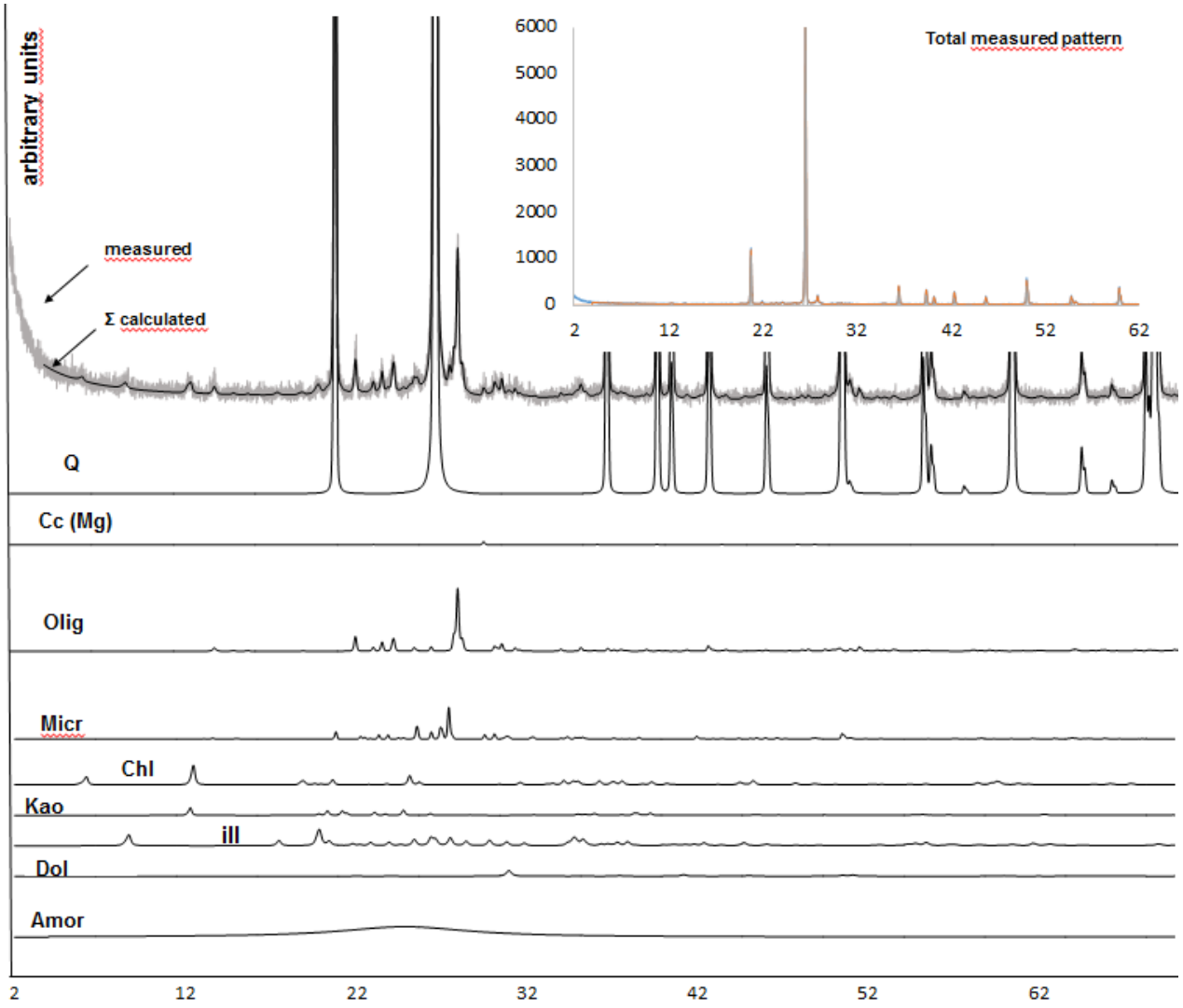

Fig. 4. 1: XRD pattern of the selected sample (D- 2- 6)

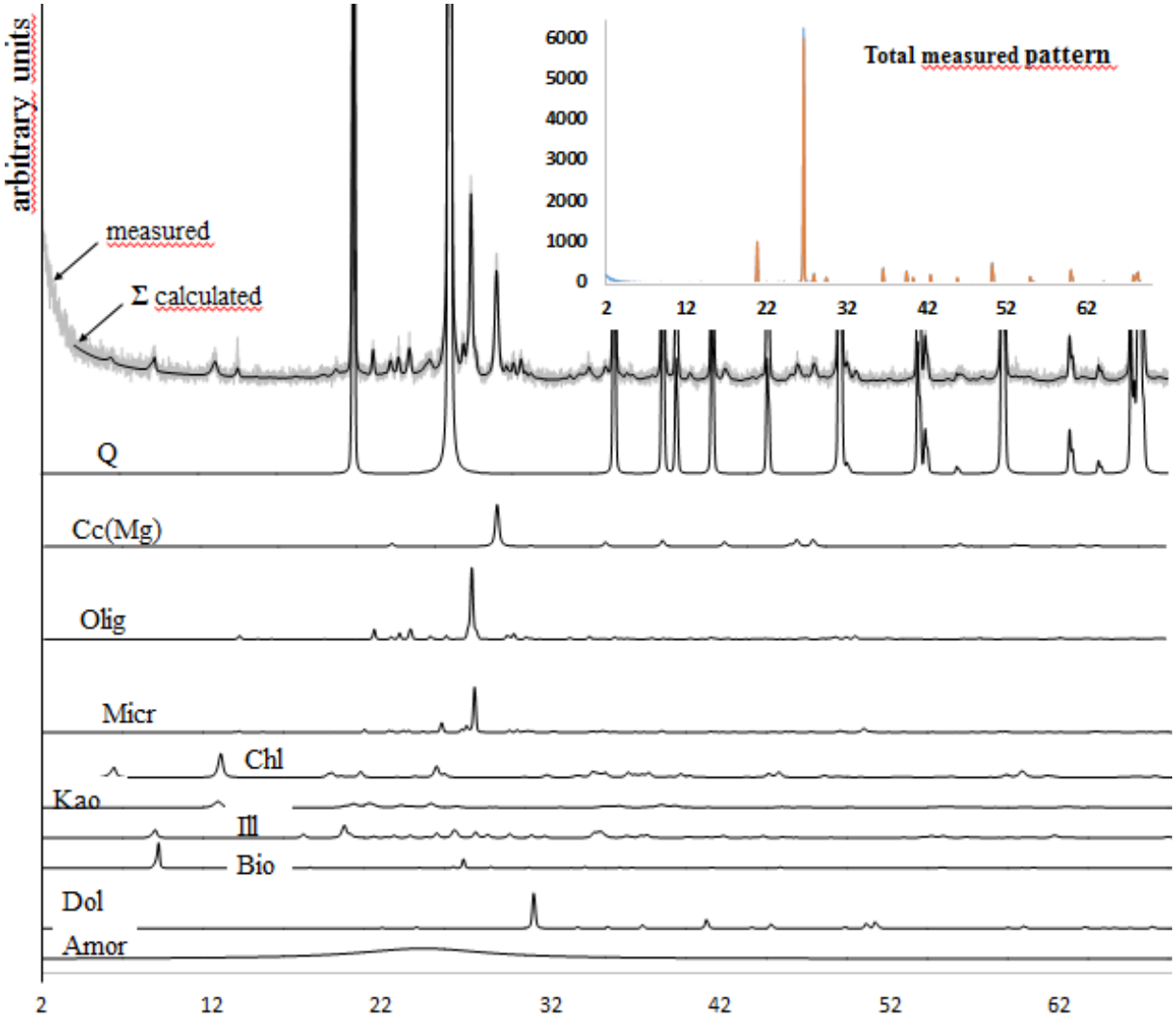

Fig. 4. 2: XRD analysis for the core D- 2- 5

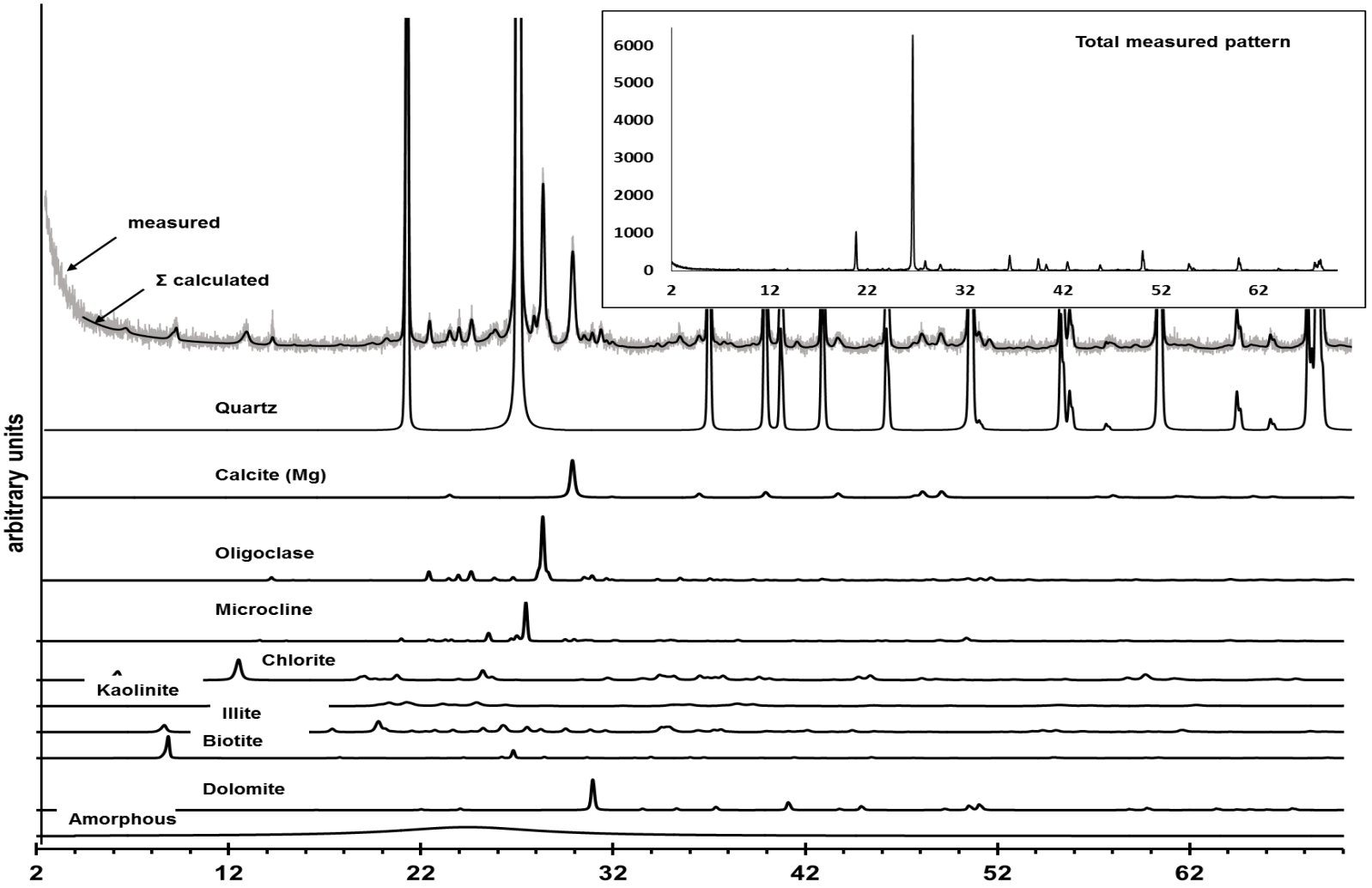

Fig. 4. 3: XRD analysis for the core D- 2- 4

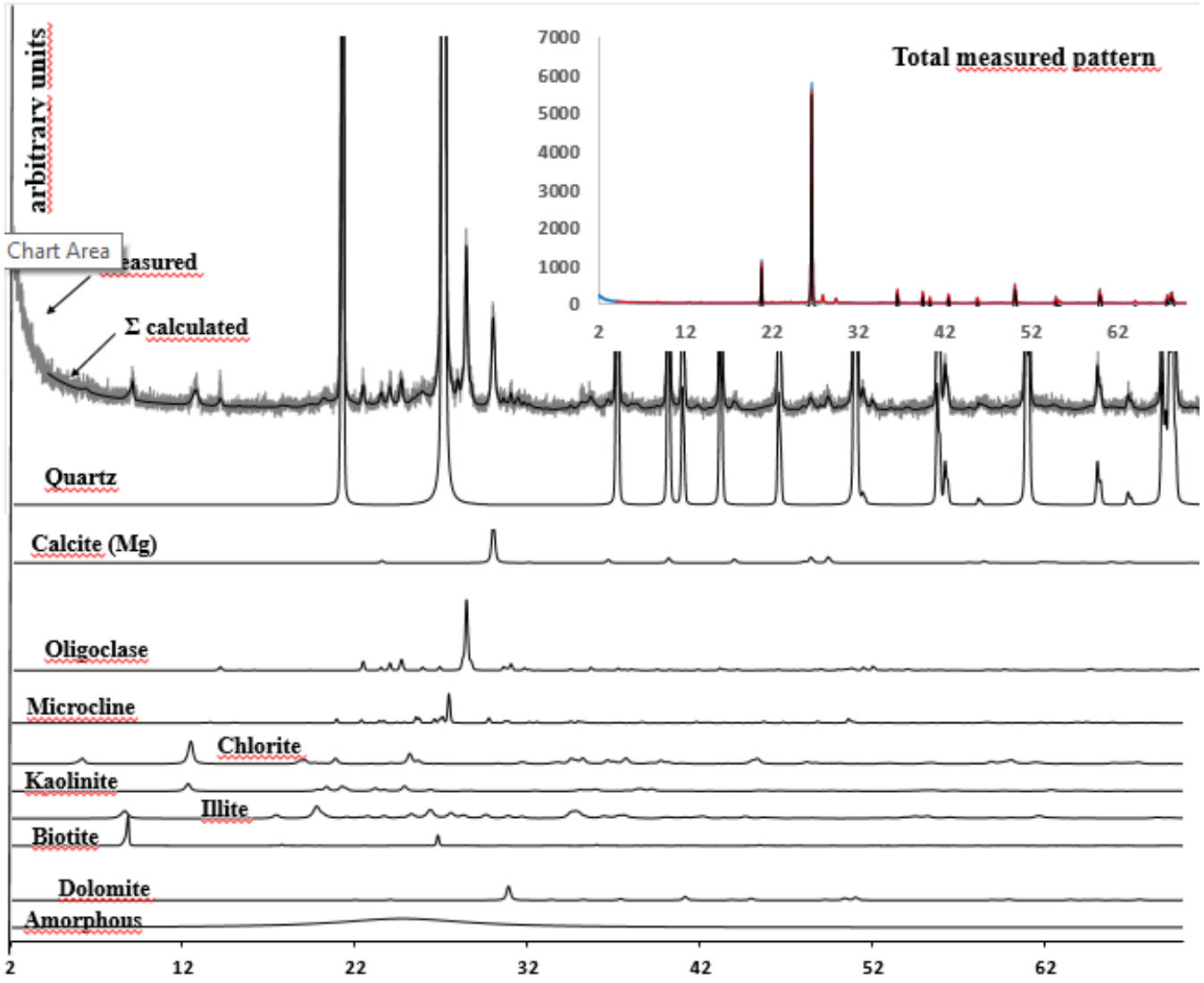

Fig. 4. 4: XRD analysis for the core D- 4- 2

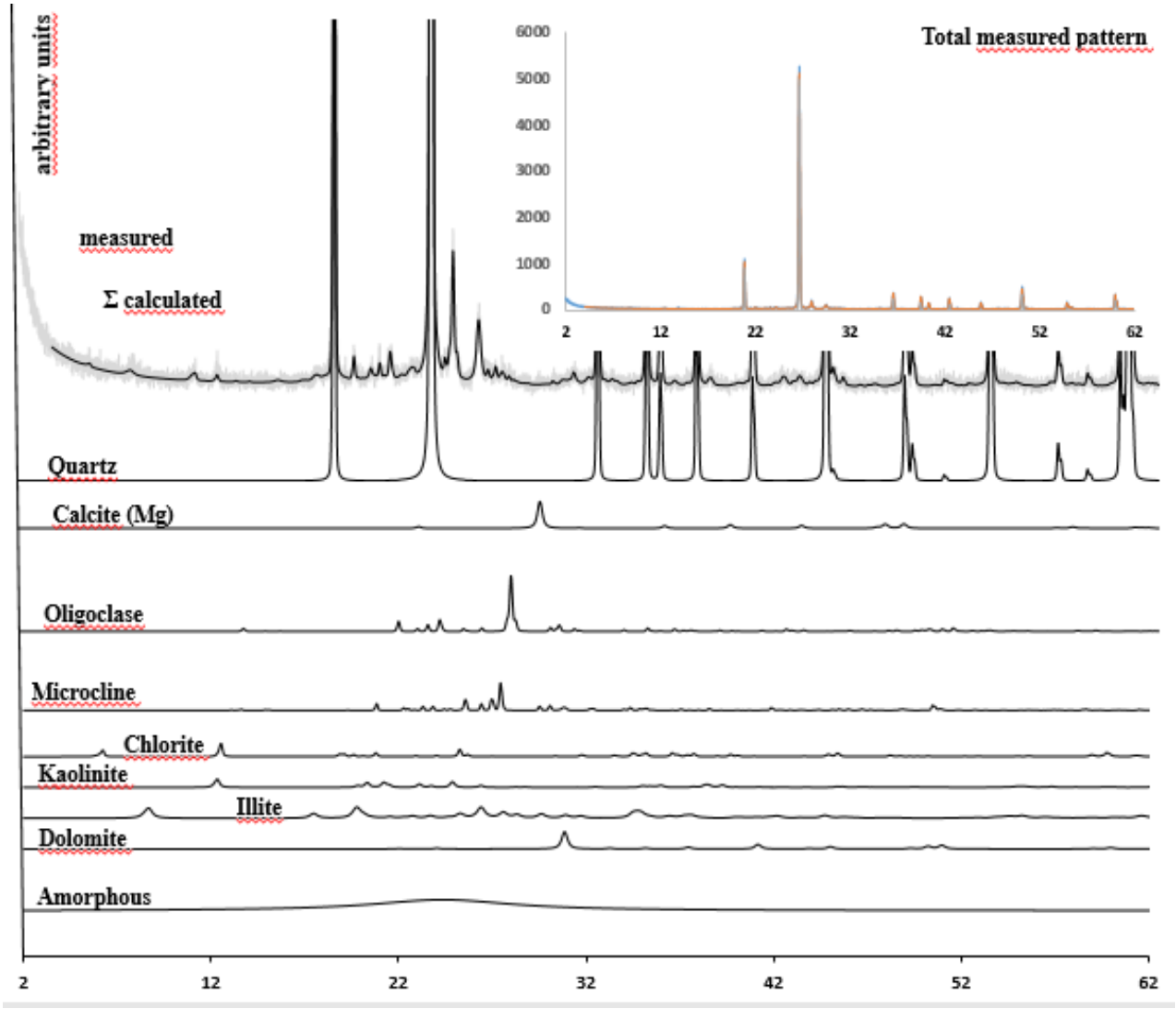

Fig. 4. 5: XRD analysis for the core D- 4- 1

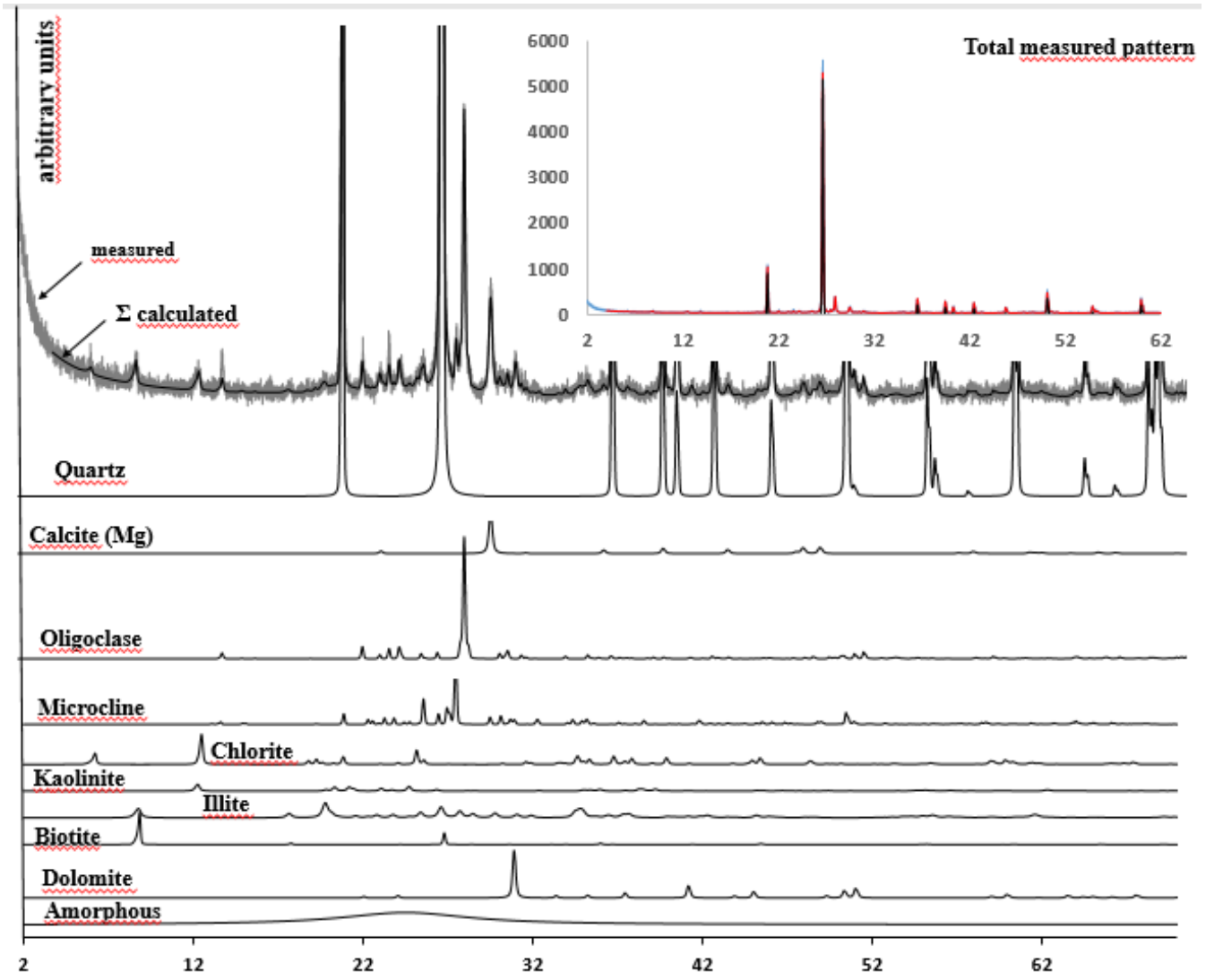

Fig. 4. 6: XRD analysis for the core D- 3- 2

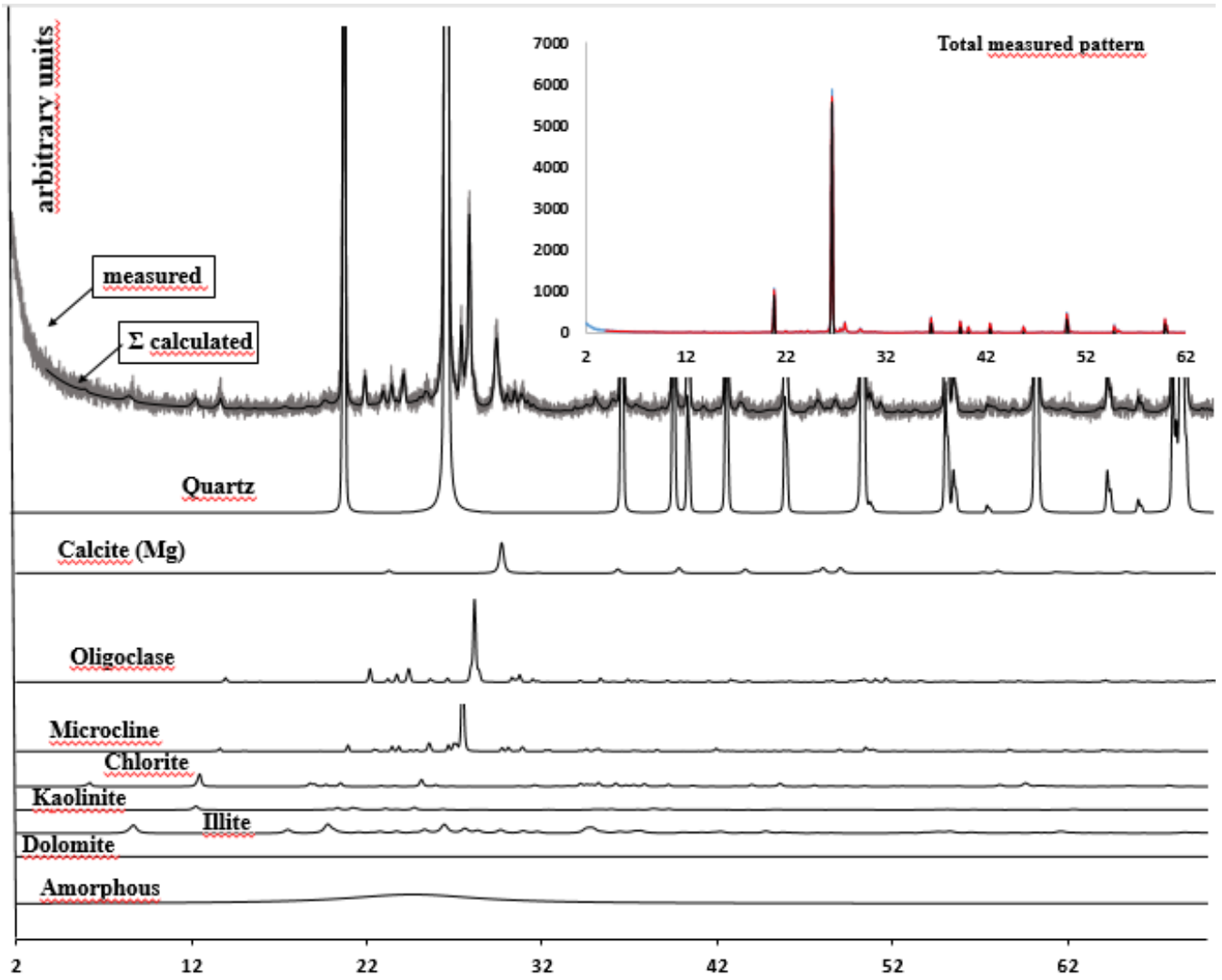

Fig. 4. 7: XRD analysis for the core D- 3- 1

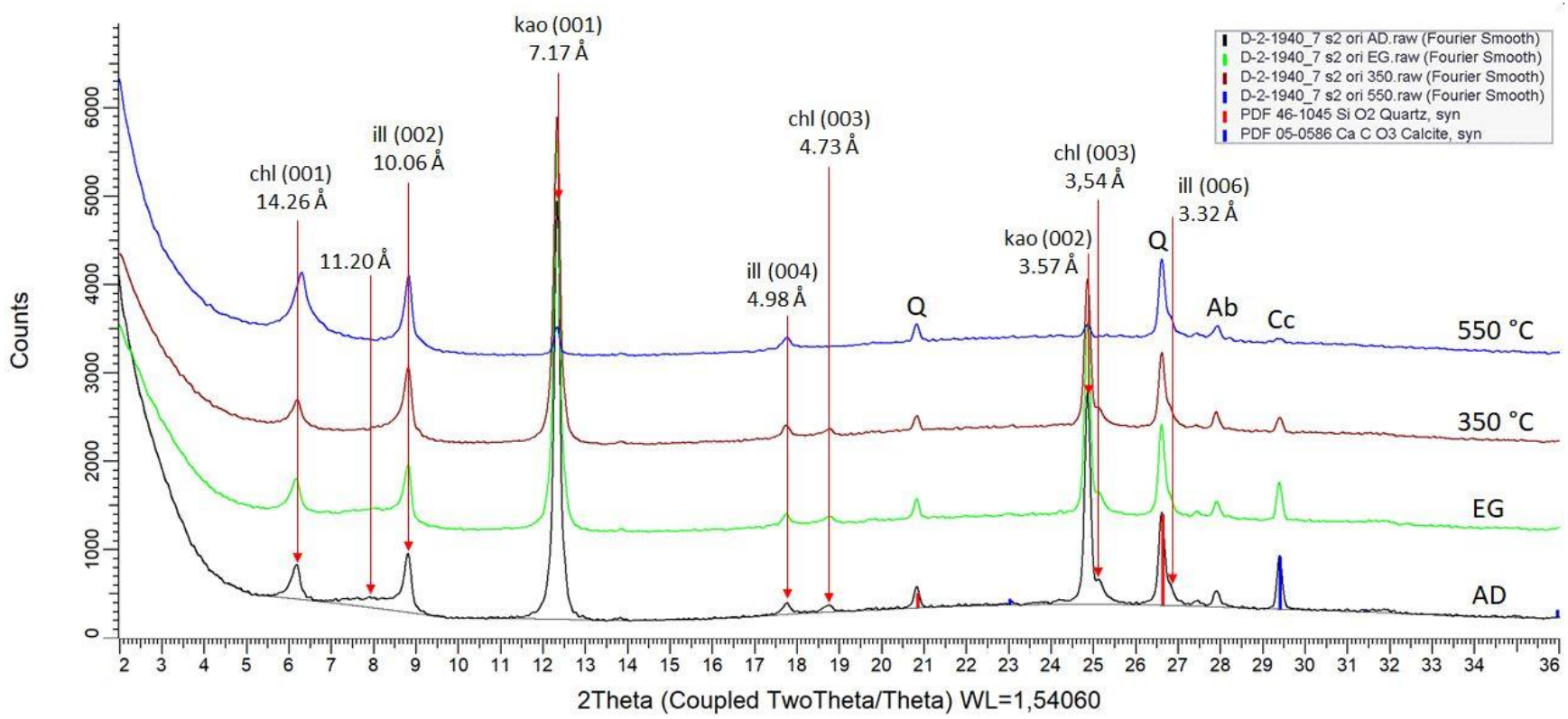

Fig. 4. 8: XRD pattern of the selected sample (D- 2- 6)

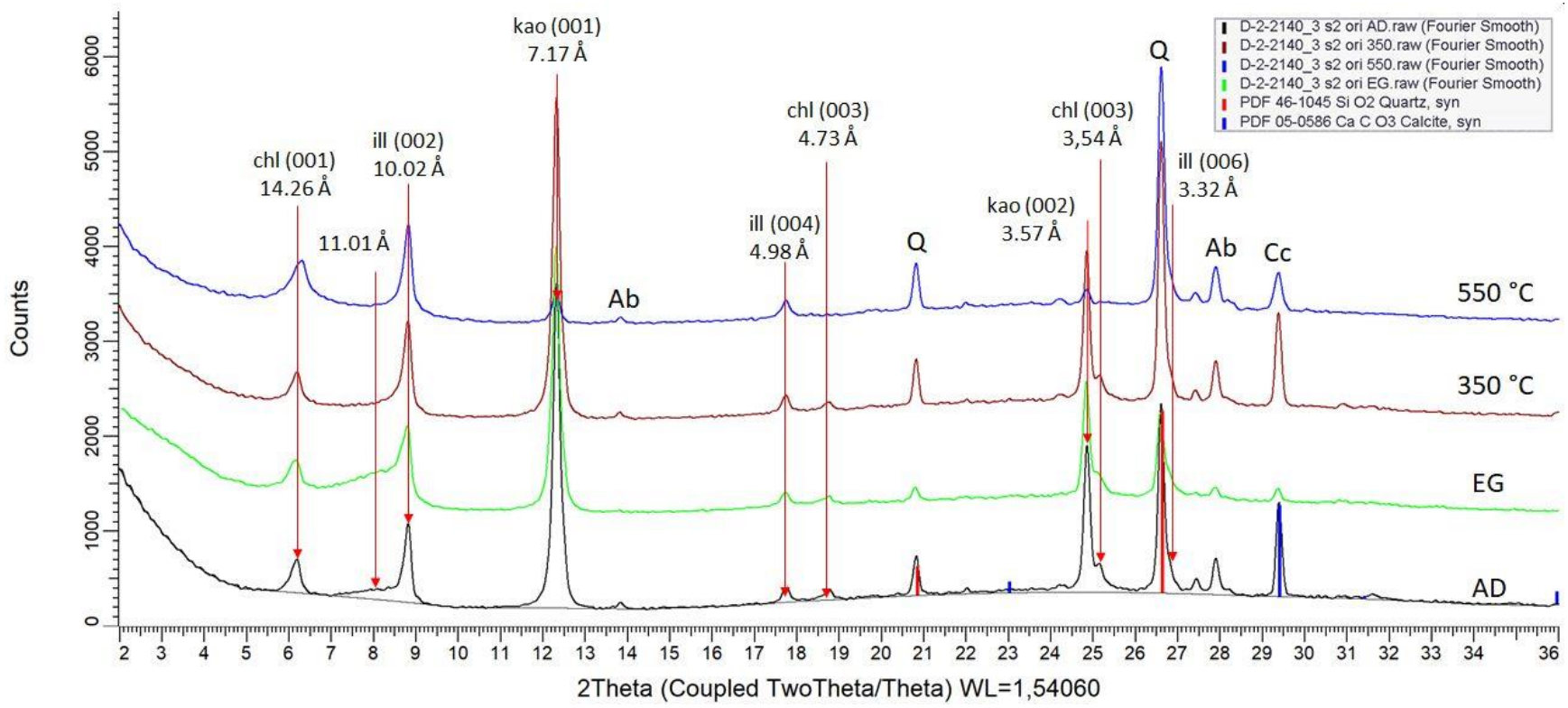

Fig. 4. 9: XRD pattern of the selected sample (D- 2- 5)

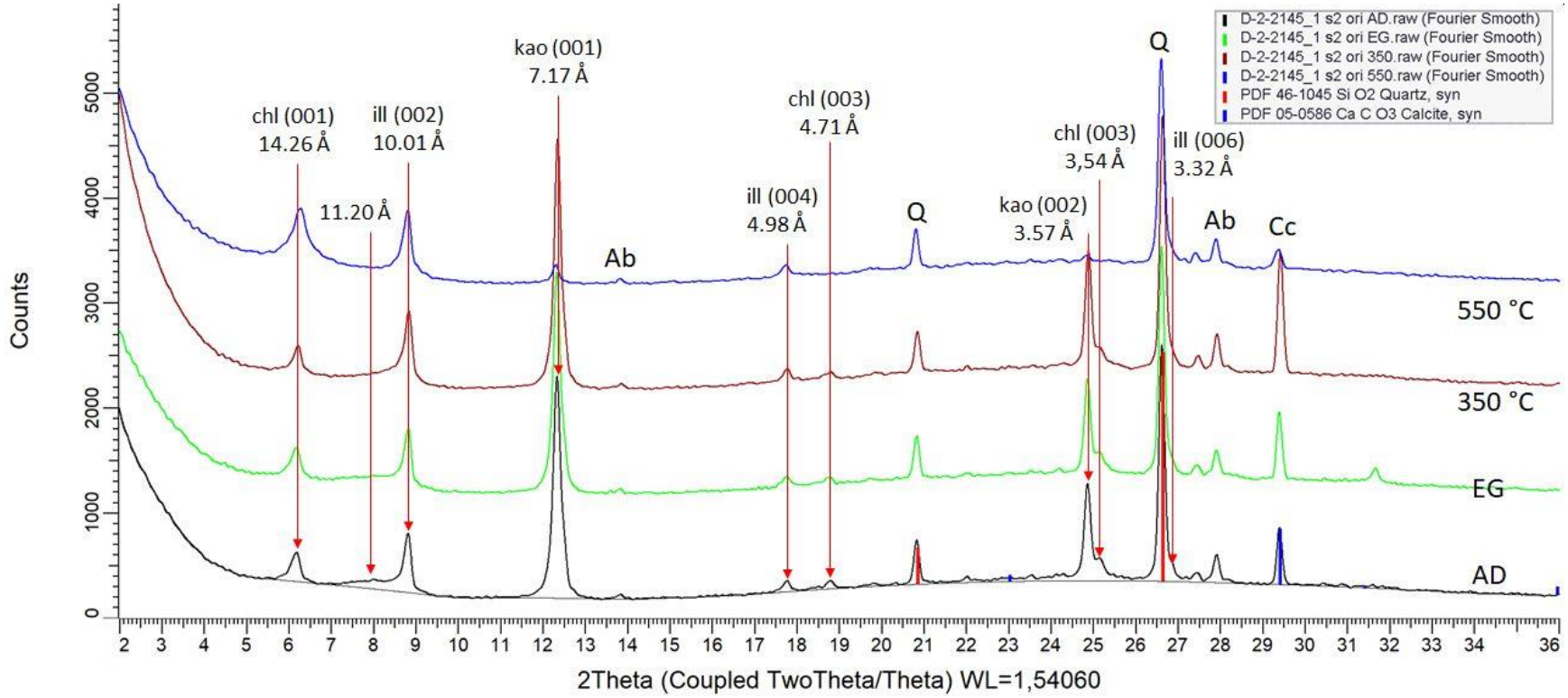

Fig. 4. 10: XRD pattern of the selected sample (D- 2- 4)

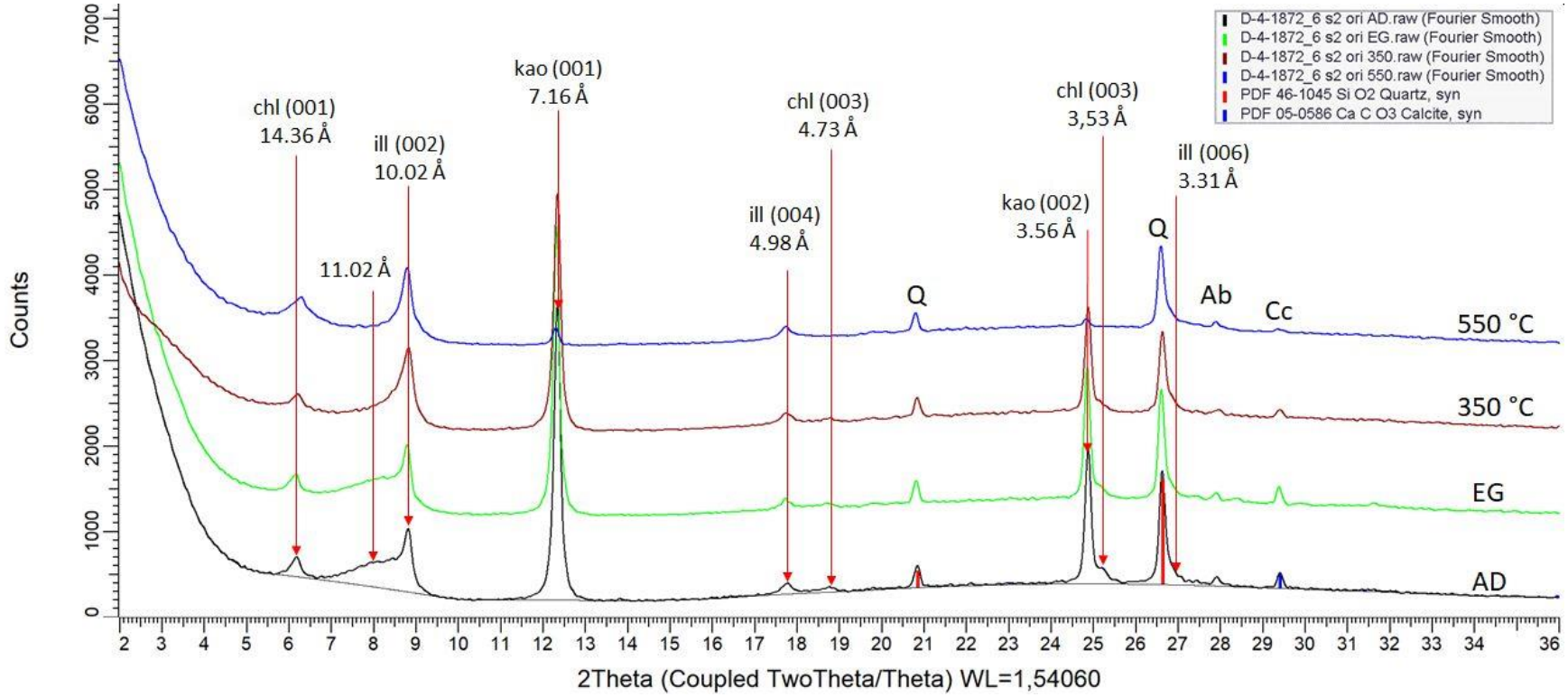

Fig. 4. 11: XRD pattern of the selected sample (D- 4- 2)

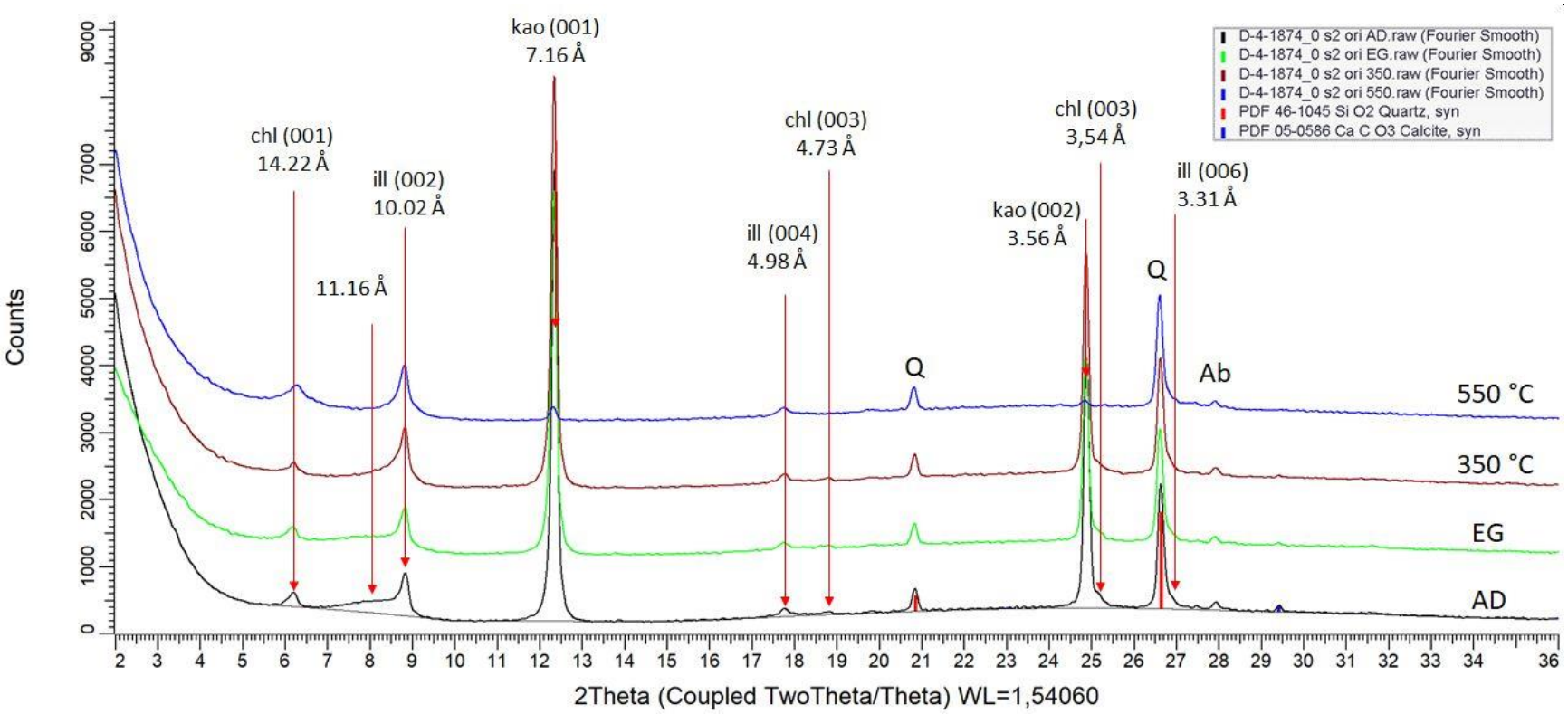

Fig. 4. 12: XRD pattern of the selected sample (D- 4- 1)

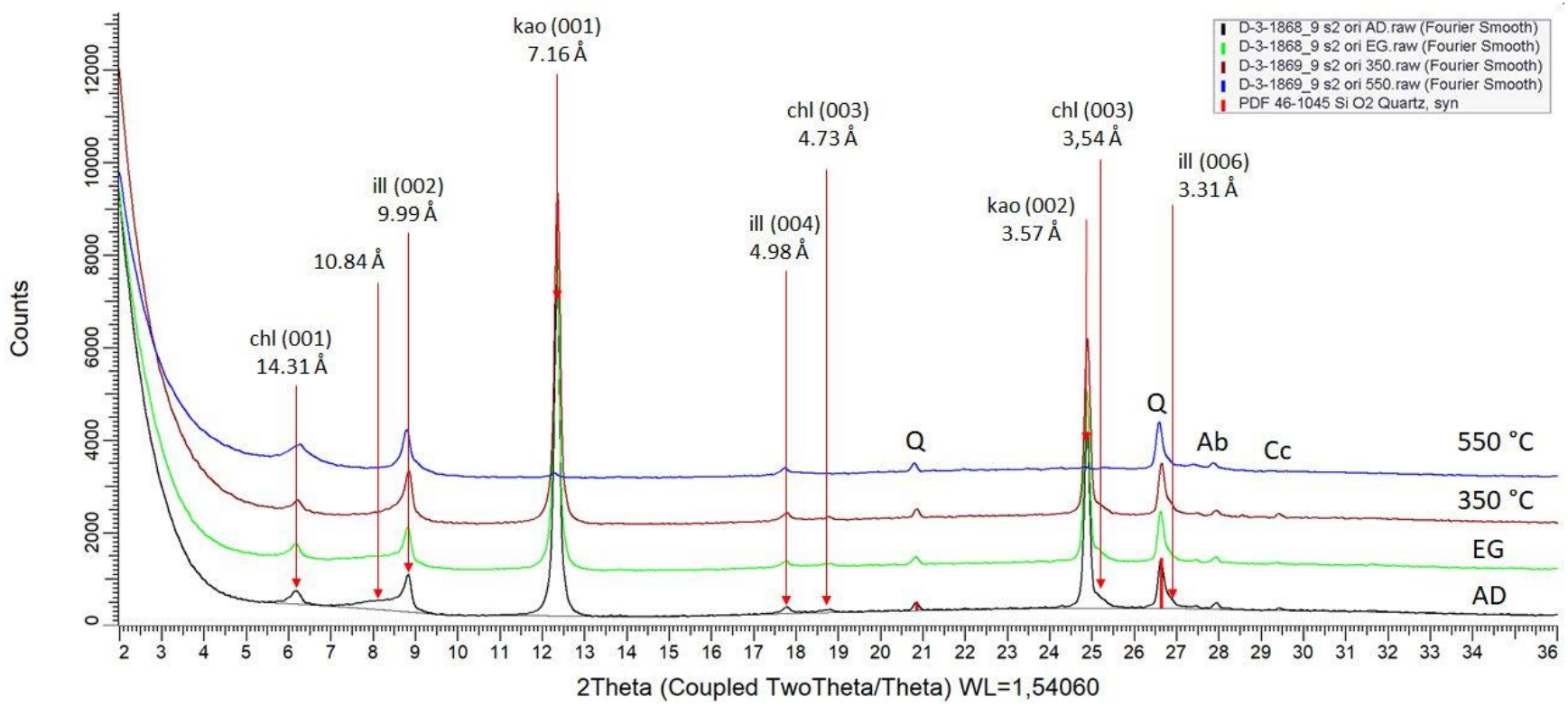

Fig. 4. 13: XRD pattern of the selected sample (D- 3- 2)

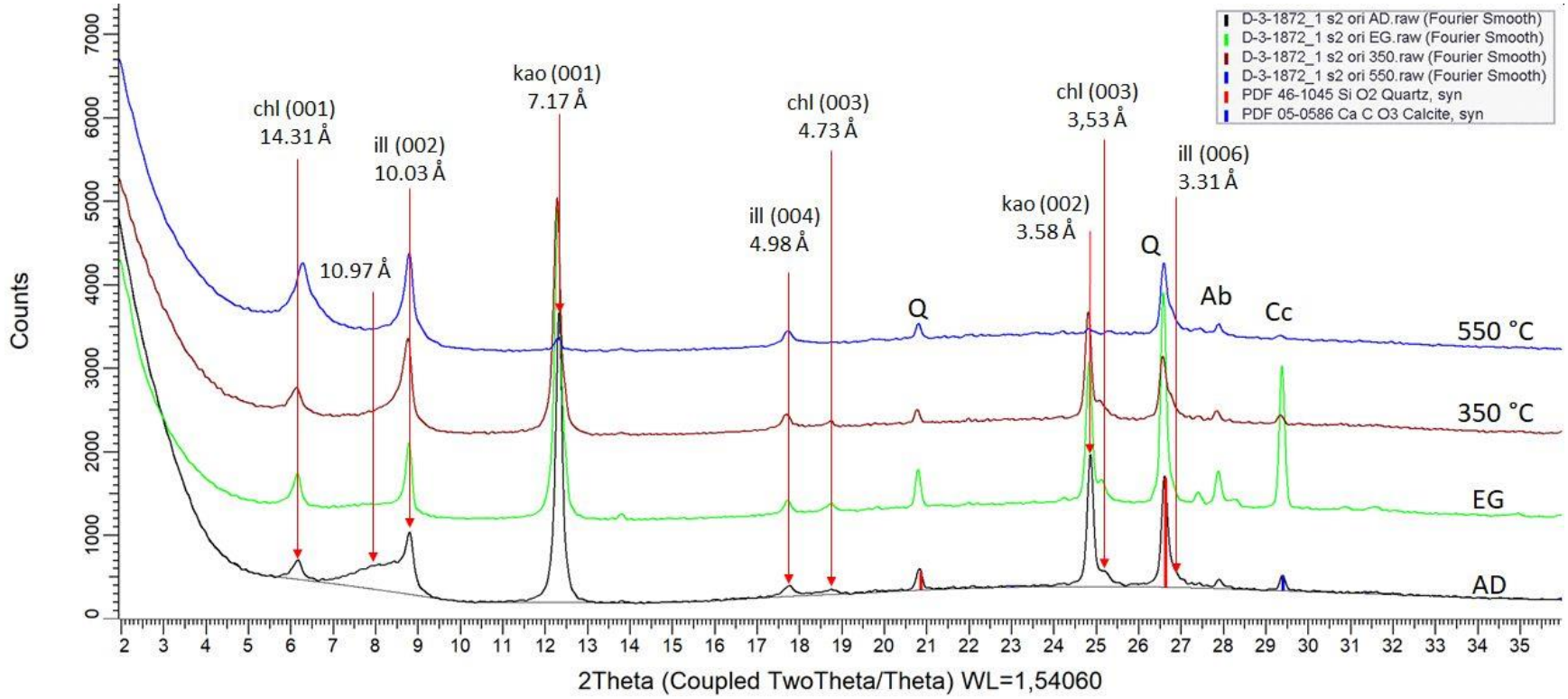

Fig. 4. 14: XRD pattern of the selected sample (D- 3- 1)

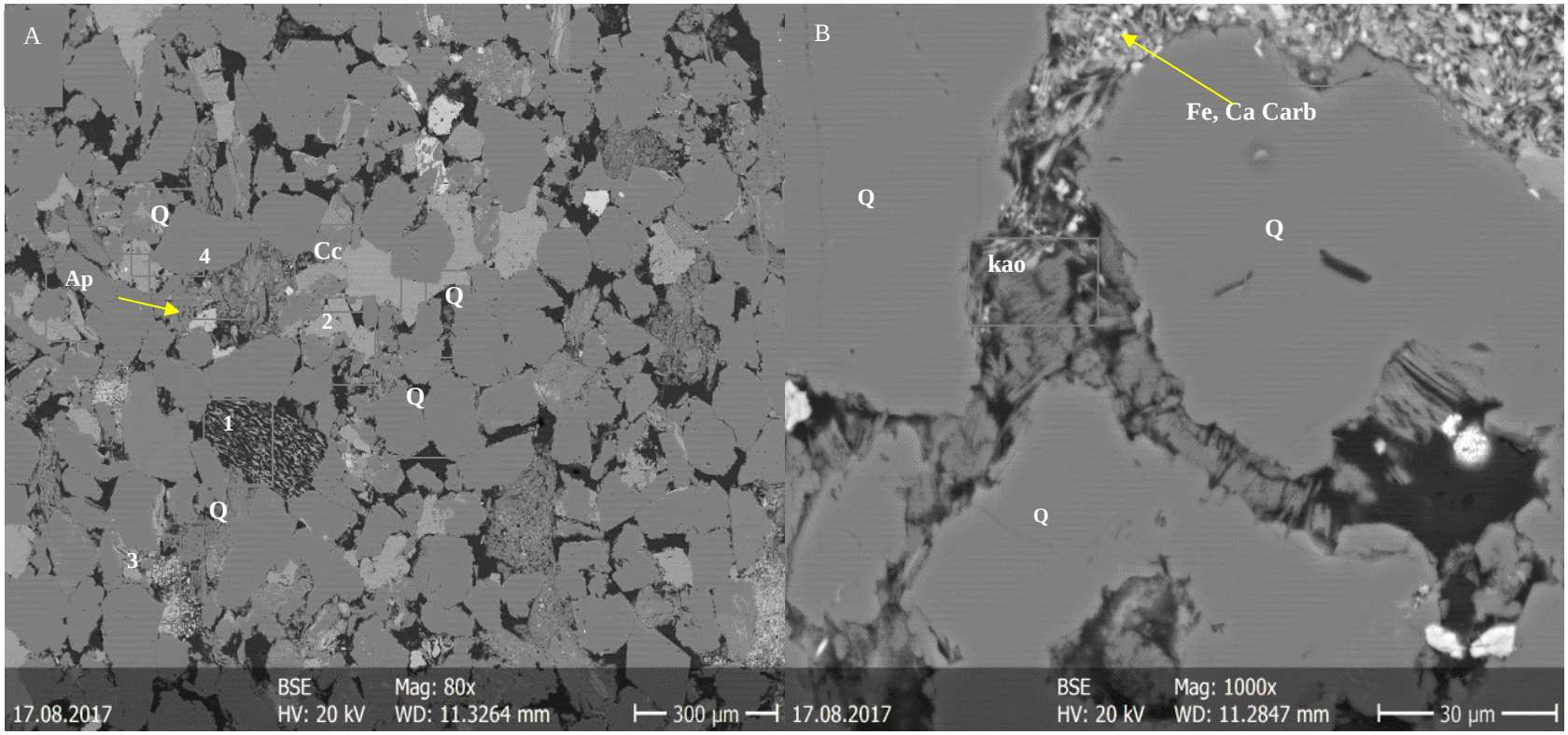

Fig. 4.15: Shows the BSE images of the selected core (D-2-6) before flooding. (Fig. 4.15A) (1) clinoclore grain totally filled up the pore between the quartz grain ranging between (100 to 200 µm); (2) represnets carbonate pore filling, namely calcite and dolomite (light grey) ranging between (50 to 100 µm); (3) represents micaceous flakes with intergrowths of Fe and Ca- carbonates in various sizes ranging between (50 to 150 µm); (4) represents clay minerals such as chlorite, illite, and kaolinite ranging around (10 to 50 µm) and partially filling up the pores, which could contribute to fines migration even before the core flooding. Apatite exists as a pore- filling material with less than 50 µm in size . (Fig. 5B) Quartz grains (Q) of medium grey colour are of different sizes and shapes. There is clear evidence of kaolinite booklets ranging between (10 to 20 µm) in size with individual particles of kaolinite exist < 10 µm, that may well contribute to fines migrations.

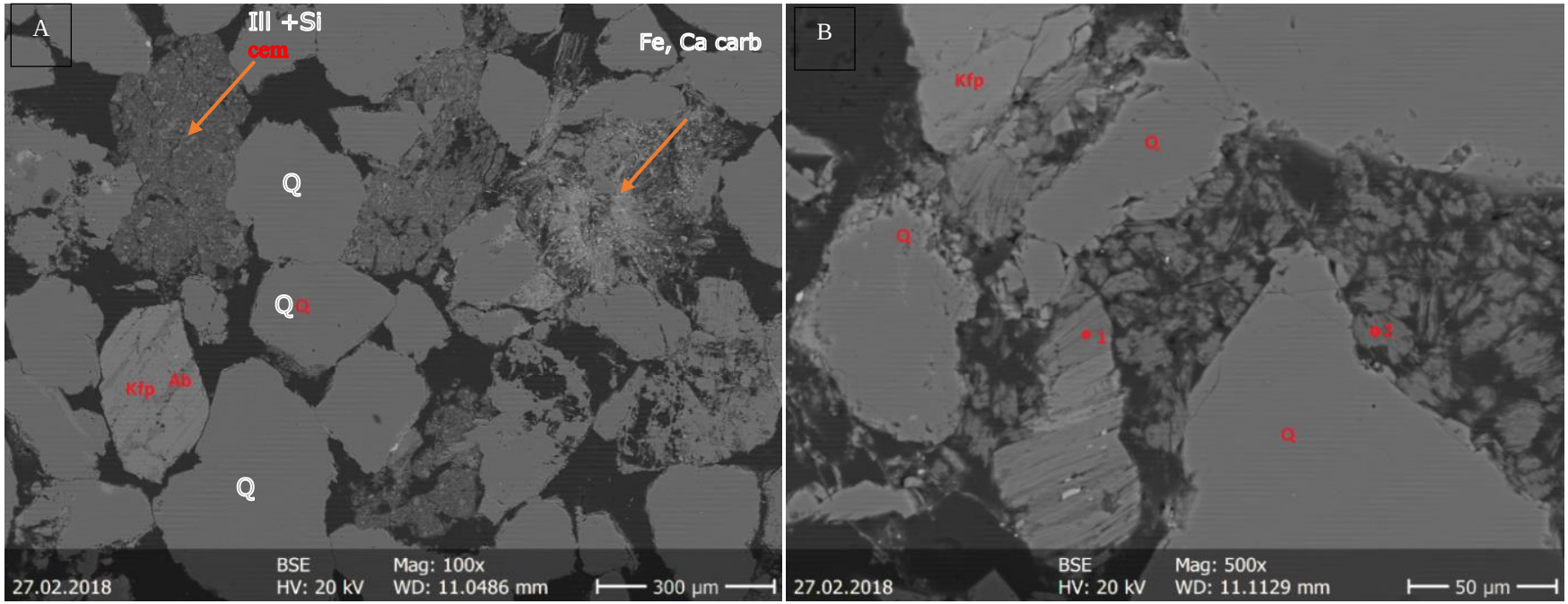

Fig. 4. 16: Shows the BSE images of the selected core (D-2-5) Befor flooding, Black colours represnet the pore spaces (porosity) with various shape and size ranging between (100- 200µm), some pores are filled by fine partciles which might be clay minerals such as kaolinite, illite , and chlorite or non- clay minerals (calcite, Fe- Ca carbonates, mica flakes). Quartz grains (Q) of medium grey colour are of different shapes from irregular to regular and in various sizes ranging from (50- 400µm). K-feldspare and albite (K-fp + Ab) and grain particles ranging between (100- 200µm). The micaeous flakes associated with illite, chlorite, fine grains of quartz ranging between (300- 400 µm) and Fe, Ca carbonates developed microporosity and might contribute to fine migrations. There is a clear evidence of kaolinite booklets (Fig. 4.16B) (2) ranging between (1-10µm) in size with individual particles of kaolinite of <2µm that may well contribute to fines migartion. Flaky muscovite (Fig. 4.16B) (1) ranging between (50- 150 µm) could not contribute permeability reduction due to large grains.

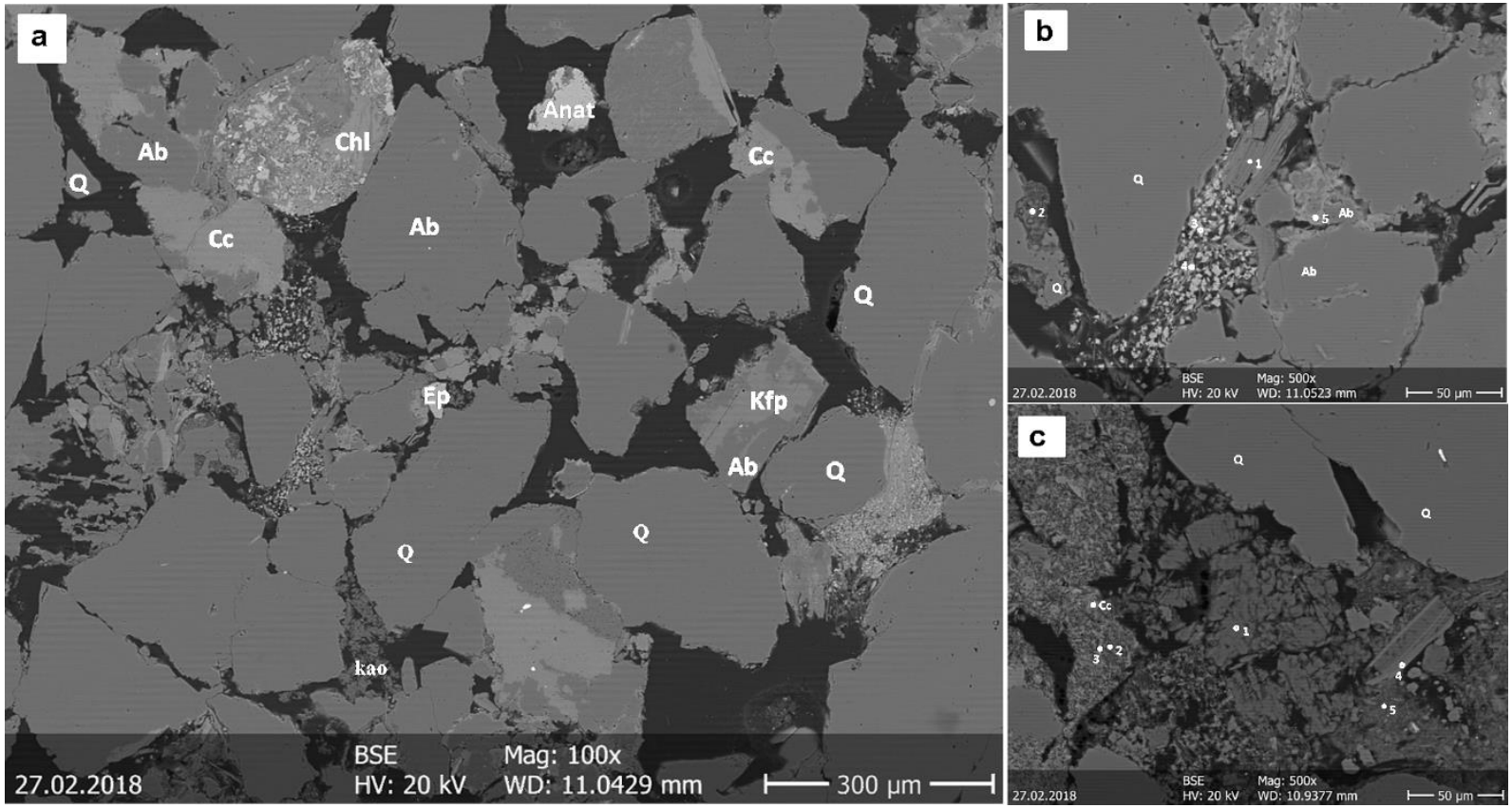

Fig. 4.17: Shows the BSE images of the selected core (D- 2- 4) Befor flooding. In (Fig 4.17a). Black colour represents the pore space filled by embedding resin. Pore sizes based on area values are set in two ranges, the larger one is between 50- 200µm, while on the border of adjacent grains pores of ~ 10 µm are observed. Some pores are filled by fine particles and cemented by calcite, while the majority is not filled up. Quartz grains (Q) medium to dark grey) are of different sizes and ranging between (100- 400 µm) are usually cemented by illite. Albite (Ab) ranges between (50- 150

μm) and is present as intersticial grains. Pore filling/cementing calcite (Cc) is observed between quartz gains (> 50 μm), based on its textural emplacement it is not expected to be involving fines migration. Detrital chlorite (Chl) presents with flaky structure in quartz grains, ranging between (40- 50 μm), while authigenic and diagenetic chlorite is developed in the pore spaces. Few grains of epidote (Ep) are observed with a diameter < 50 μm as detrital material. Some of the intergranular pores are almost filling (Fig. 4.17- 3b) flaky muscovite (1) and illite aggregates (2) cemented by silica (< 5 μm). Fe-Mg-rich carbonates (3) graining ranging between (5- 20 μm) existing between the chlorite lamella. (4) Chlorite particles have typically lamellar structure with less than 10 μm, as a pore filling. Special carbonates often with Fe and Ca-Mg mixing developed between chlorite flakes are frequent, generating microporosity and increasing overall porosity. Detrital chlorite or interstratified illite/chlorite (5) is associated with quartz grains, although sometimes as a pore -filling ranging (< 10μm). Albite (Ab) appears as large (> 100μm) and small intersticial grains (10 - 80μm) too. At higher magnifications (Fig. 4.17- 3c) (1) kaolinite booklets ranging <10 μm filling the interconnected pores between the quartz grains. Illite (2) and illite particles cemented by silica (3) generally are < 5 μm as pore filling, but flake sizes are too small to be distinguished. Muscovite flakes (4) with a length of approximately 50 μm and thickness 10 μm are located between quartz grains, thus at higher fluid flow rates, they could be mobilized.

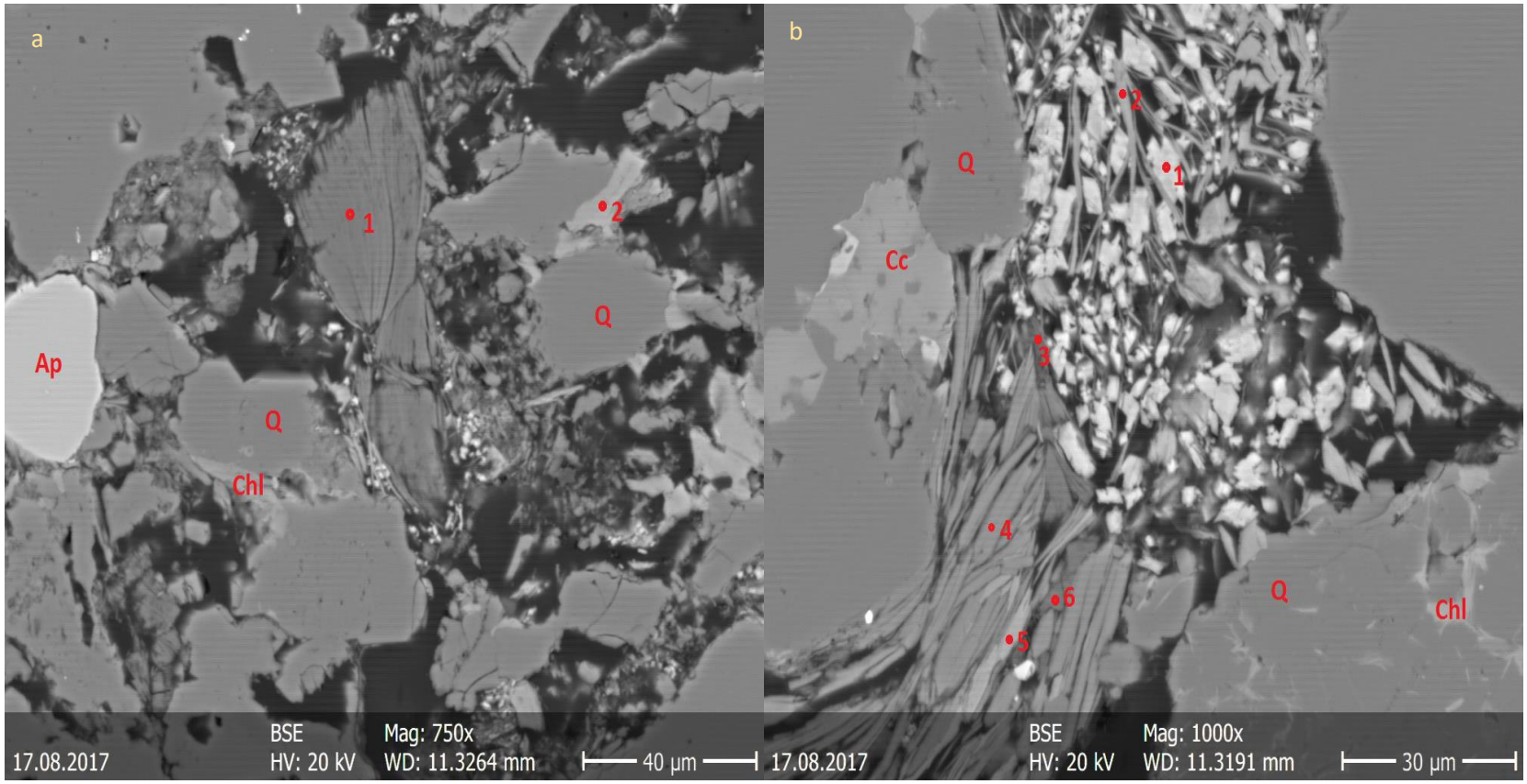

Fig. 4. 18: Shows the BSE images of the selected core (D-4-2) Befor flooding. (Fig.4.18-a) black colours represnet the pore spaces (porosity) with various shapes and sizes ranging from (50- 200µm), the pore spaces filling by a mixture of fine partciles, which comaposed of clay minerals such as kaolinite, illite , and chlorite and non-clay minerals (calcite, Fe and Ca carbonates, mica flakes). The grey colours represent quratz grains (Q) with different shapes from irregular to regular and different sizes ranging between (20-

100µm). (1) composed of muscovite flakes ranging less than (50µm) which could not be contributting fines migaration. (2) represents chlorite minerals as a pore filling between quartz grains which could contribute to fines migartion during core flooding. The rest of the pore filling minerals are kaolinite booklets ranging below (<5 µm) which contribute fines migration. (Fig.4.18- b) represents a mixture pore filling minerals, (1; 2; 3) exfoliated muscovite with interlayer mixture of minerals such as Fe and Mg- carbonates, chlinochlore flakes and kaolinite, these fine partices easily contribute to fines migaration during flooding. (4) represents of chlorite flakes ranging less than 10 µm). (5) shows illite flakes between chlorite minerals which could be contributing to fines migration. (6) composed of individual of fine kaolinite particles ranging is (<5 µm), that may well contribute to fine migration.

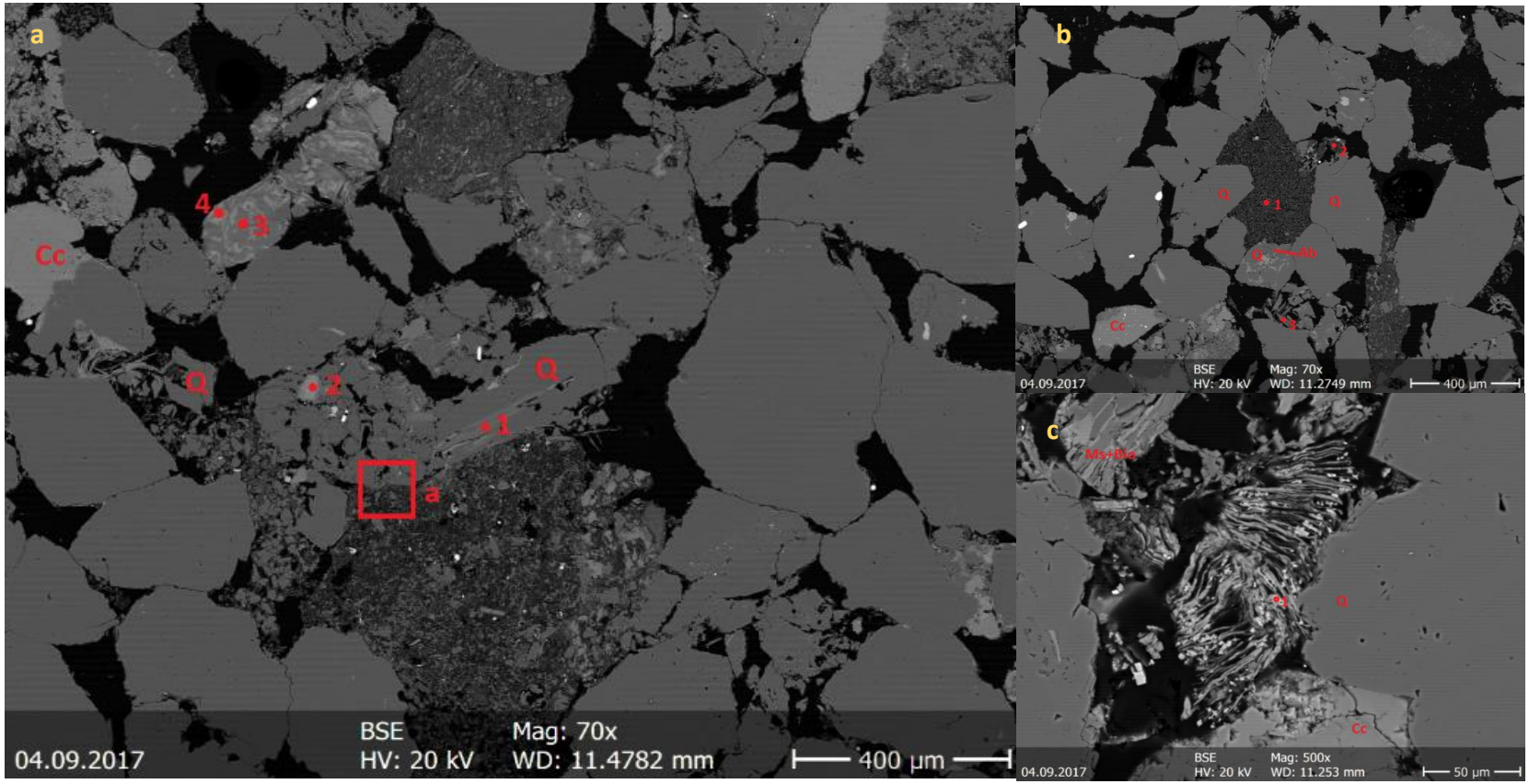

Fig. 4. 19: Shows the BSE images of the selected core (D-4-1) Befor flooding. (Fig. 4.19- a) black colours represnet the pore spaces (porosity) with various shapes and sizes ranging between (100- 300µm), some of the pores filled by fine partciles, which might be clay minerals such as kaolinite, illite , and chlorite or non- clay minerals (calcite, Fe and Ca carbonates, mica flakes). The grey colour represents quratz grains (Q) with different shapes from irregular to regular aare different sizes ranging between (50- >400µm). (1) composed of clinochlore with light grey color pore- filling chlorite with interstratified illite.(2) composed of clay minerals. (3) composed of interstartified clay with high silica content. (4) almost the same composition as no.2. (Fig. 4.19- b); (1) it is a typical kaolinite content, (2) interstratified with pyrite; (3) muscovite altered to illite, the presence of Fe, Mg and Ti indicated for this alteration. (Fig. 4.19- c), shows exfoliated chlinochlore + siderite with interstratified carbonates.

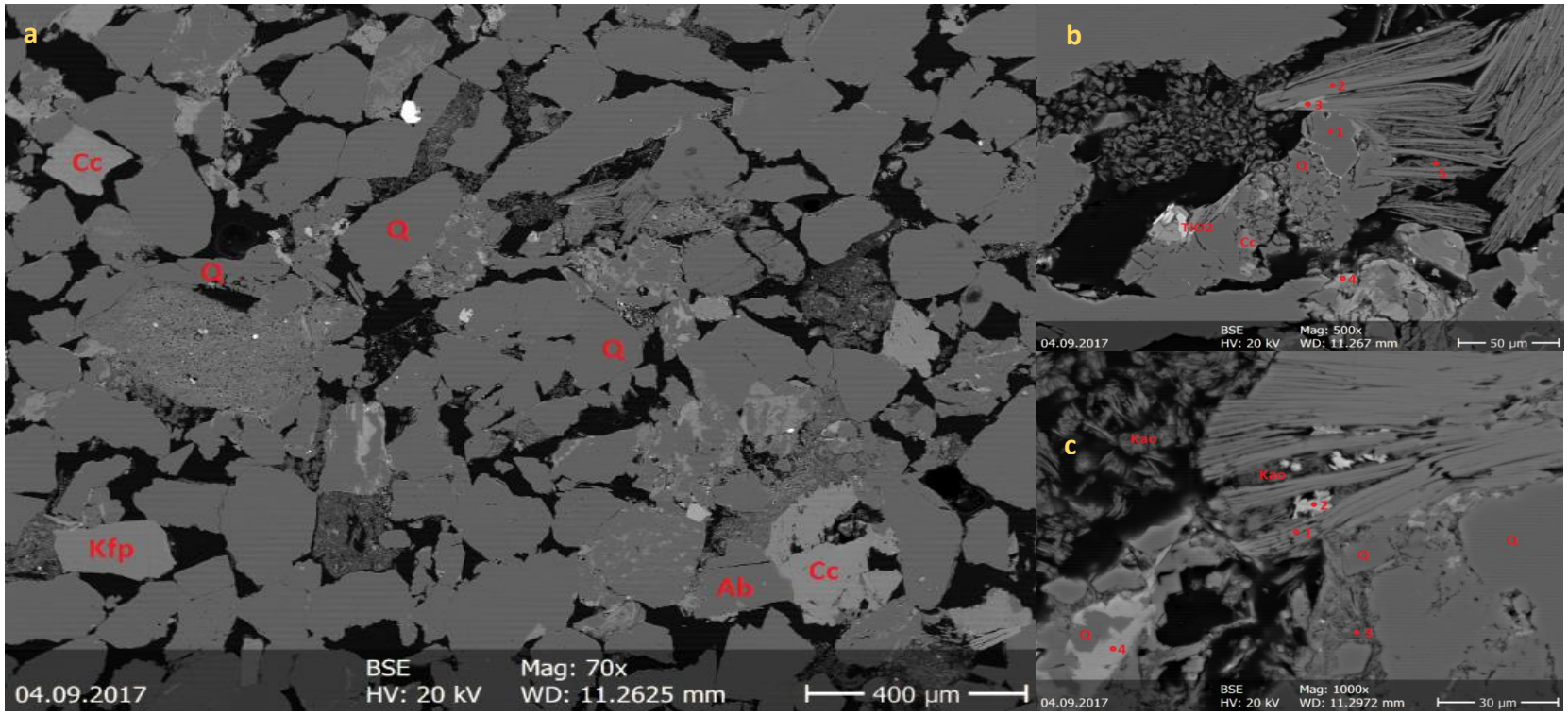

Fig. 4. 20: Shows the BSE images of the selected core (D- 3- 2) Befor flooding. (Fig. 4.20- a), black colours represnet the pore spaces (porosity) with variousshapes and sizes ranging from (100- 200μm), some of pores are filled by fine grain partciles, which might be clay minerals such as kaolinite, illite , and chlorite or non- clay minerals (calcite, Fe- Ca carbonates, mica flakes). The dark grey colours represents quratz grains (Q) with different shapes from irregular to regular and different sizes ranging between (50- >400 μm). K-feldspare and albite (K-fp + Ab) and grain particles ranging between (100 - 200 μm). The micaeous flakes associated with illite, chlorite, fine grains of quartz ranging between (300- 400 μm) and Fe and Ca carbonates developping microporosity and might contribute fines migration. (Fig. 4.20- b) Pore filling kaolinite booklets ranging less than 5 μm) that may well involve fines migration. (1) composed of dolomite, flaky muscovite with inter- filling kaolinite and some fine particles of illite (2), (3) represnets of clinochlore, (4) composed of interstratified illite/chlorite ranges below (5μm), (5) kaolinite mineral presence between muscovite lamella. (Fig. 4-20- c) show a clear evidence of kaolinite- booklets filling the pore spaces ranging <5μm, (1) micaceous flakes ranging from (20- >30μm) could not contribute permeability reduction due to large grains, (2) Fe- Mg carbonates between micaceous flakes might be contributing fines migaration because their sizes below 5μm, (3) inter- stratified pore filling clay minerals generally is illite/ chlorite with below 5 μm, those fine particles that may contribute fines migration. (4) it represents pore filling chlorite could not contribute to fine migration.

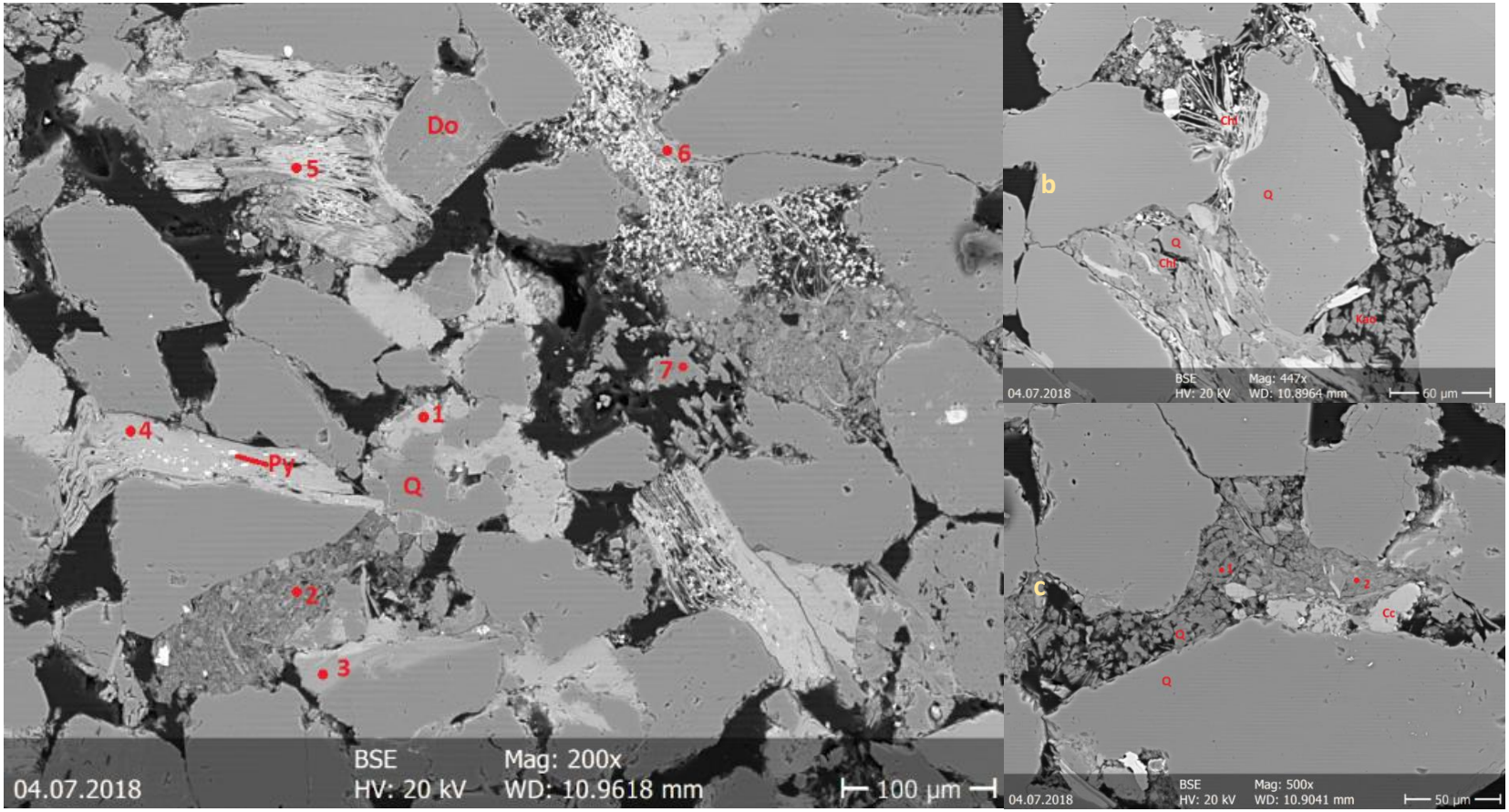

Fig. 4. 21: Shows the BSE images of the selected core (D- 3- 1) Befor flooding. (Fig.4.21- a.) black colour represnets pore spaces (porosity) with various shapes and sizes ranging between (50- 300 µm), most of the pores are filling by fine partciles of clay minerals such as kaolinite, illite , and chlorite or non- clay minerals (calcite, Fe- Ca carbonates, mica flakes, pyrite). The grey colour represent quratz grains (Q) with different shapes

from irregular to regular and different size ranging between (50- 400 μm). This sample contains more carbonates than D- 3- 2 sample that it appears between micaceous flakes and might be contributing fines migartion. (1) composed of Fe- Mg calcite as fine grains, (2) represents illite flakes filling the pore spaces with some fine grains of quartz. (3) composed of muscovite and it might not contribute to fine movement. (4; 5; 6) chlorite particles filling pore spaces. (7) represents diagentic albite. (Fig. 4.21- b) most of the pores between quratz grains filled by clay minerals such kaoliten easily dispersed during the flooding and mixture of fine grains of quartz with illite might be contribute with fines migration during the folloding. (Fig.c) pore between the sandstone grains filled up by a mixture of clay minerals such as illite and kaolinite with fine grains of quartz that may well contribute to fimes migration.

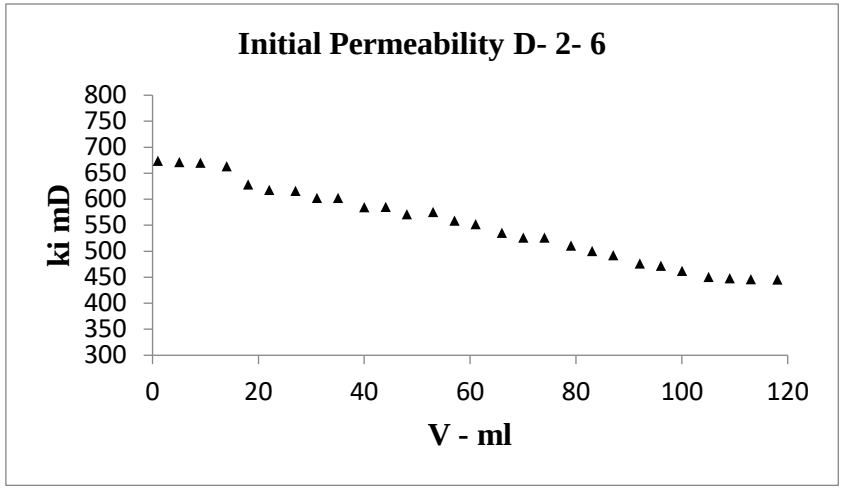

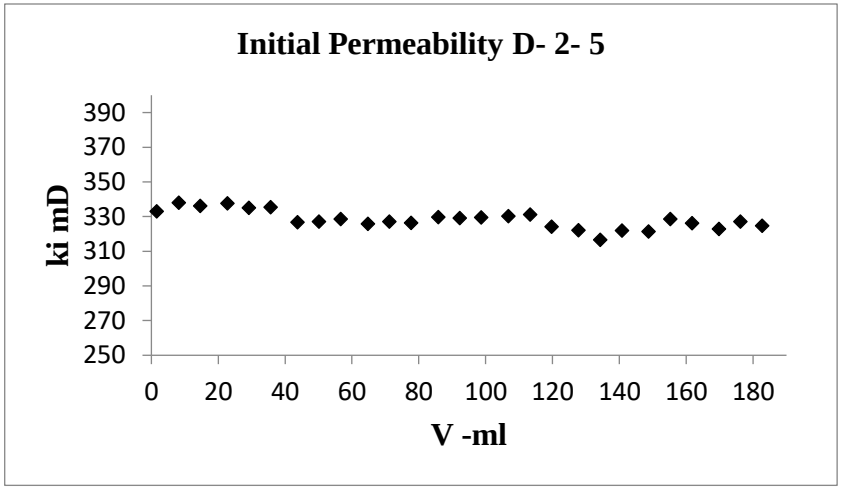

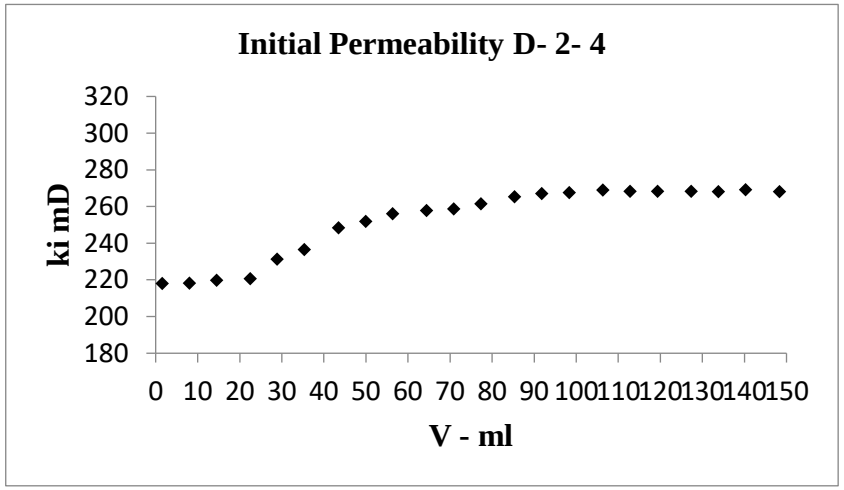

V: is volumetric flow rate 50ml/hr and use a NaCl 5% and brine solution ; ki: intial permeability mD.

Fig. 4. 22: Initial permeability of selected sandstone cores D- 2- 6; D- 2- 5 and D- 2- 4

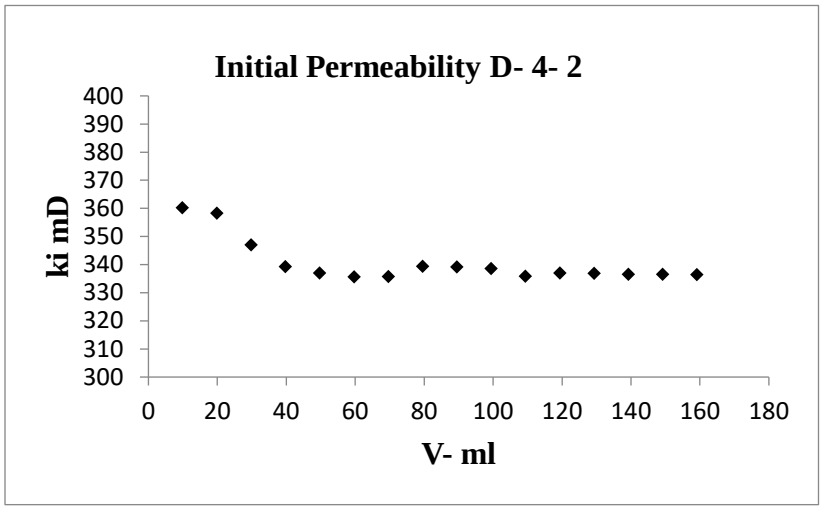

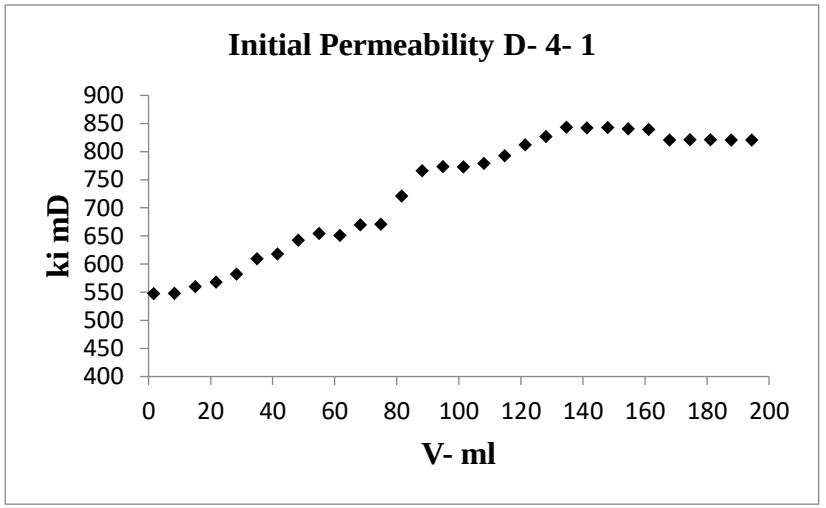

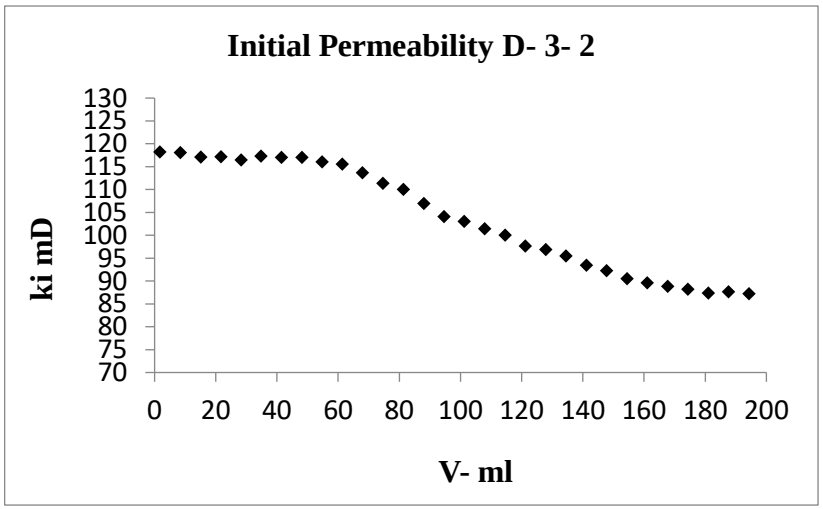

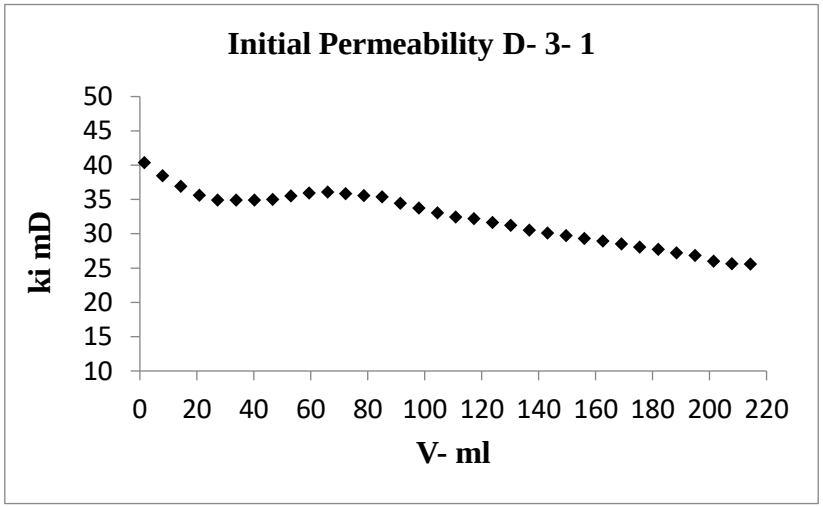

Fig. 4. 23: Initial permeability of selected sandstone cores D- 4- 2; D- 4- 1; D- 3- 2 and D- 3- 1

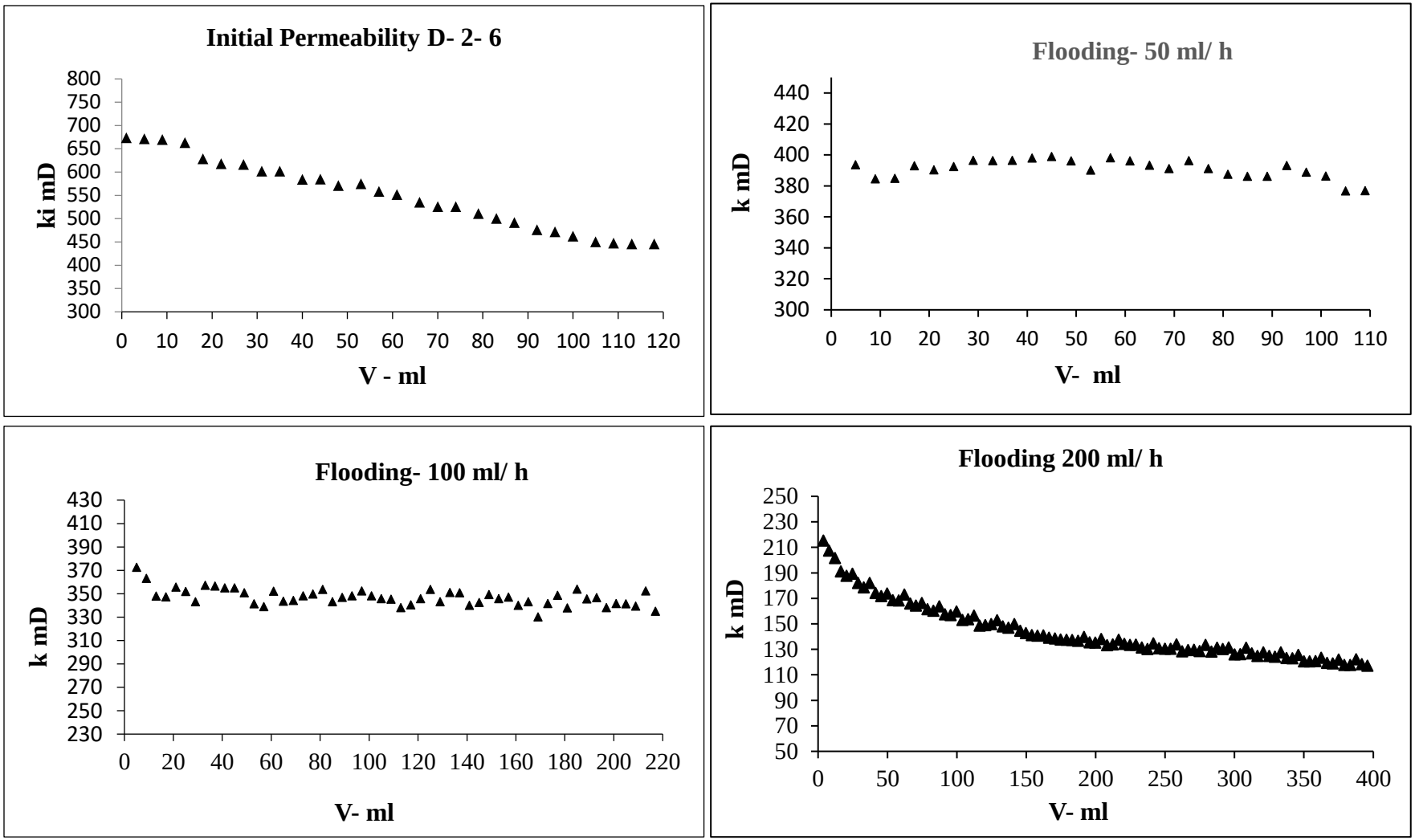

Fig. 4. 24: Core flooding drawing at different flow rate of sample D- 2- 6 / pH9

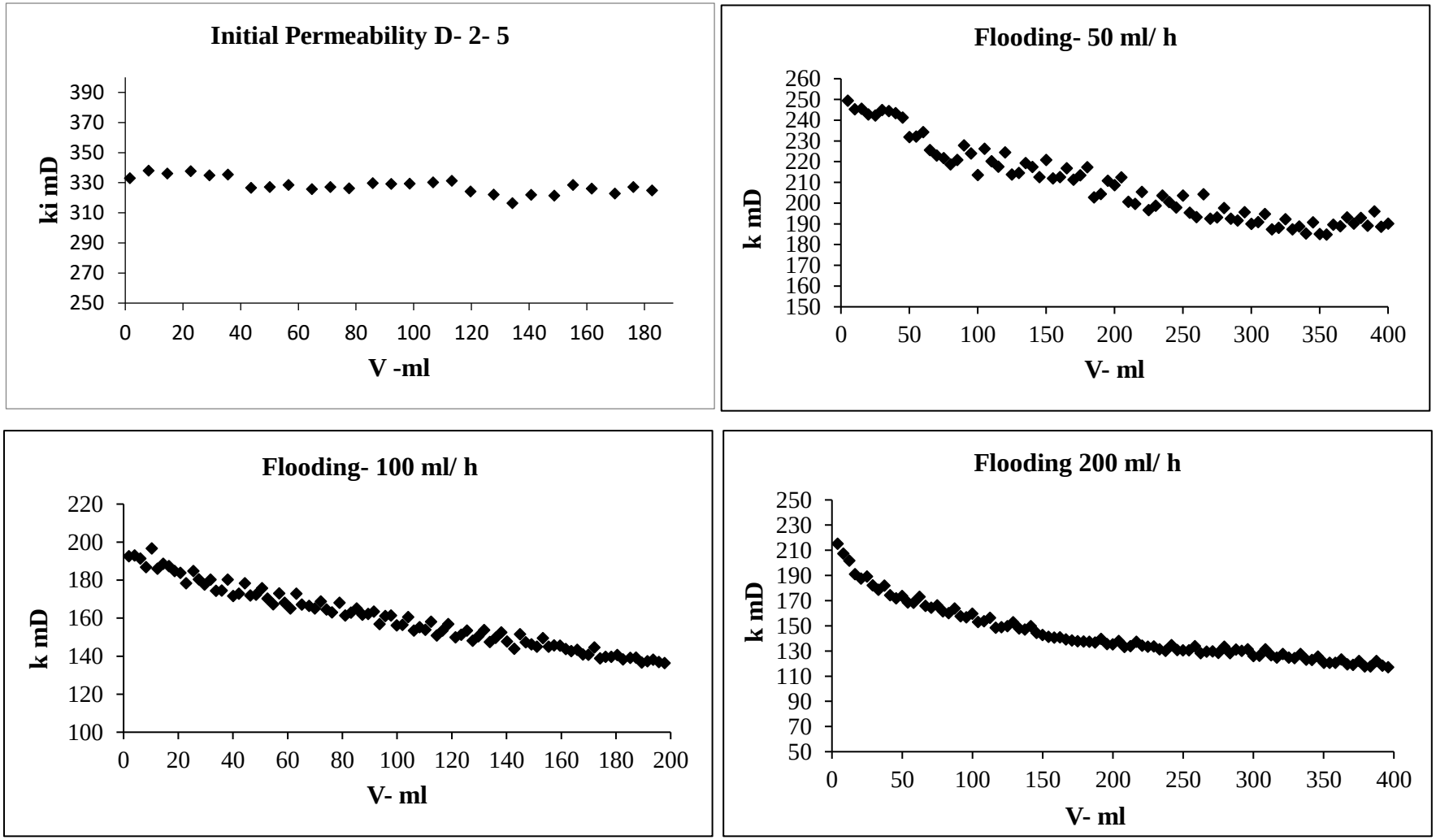

Fig. 4. 25: Core flooding drawing at different flow rate of sample D- 2- 5 / pH 11

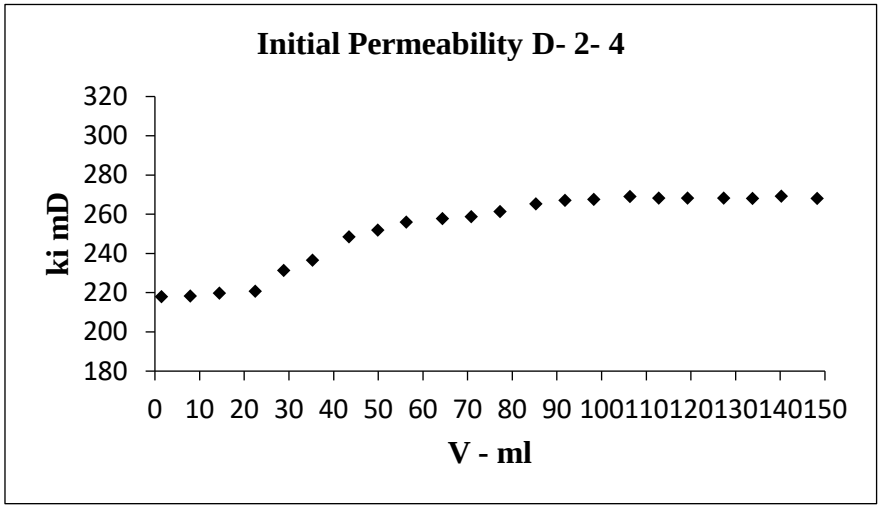

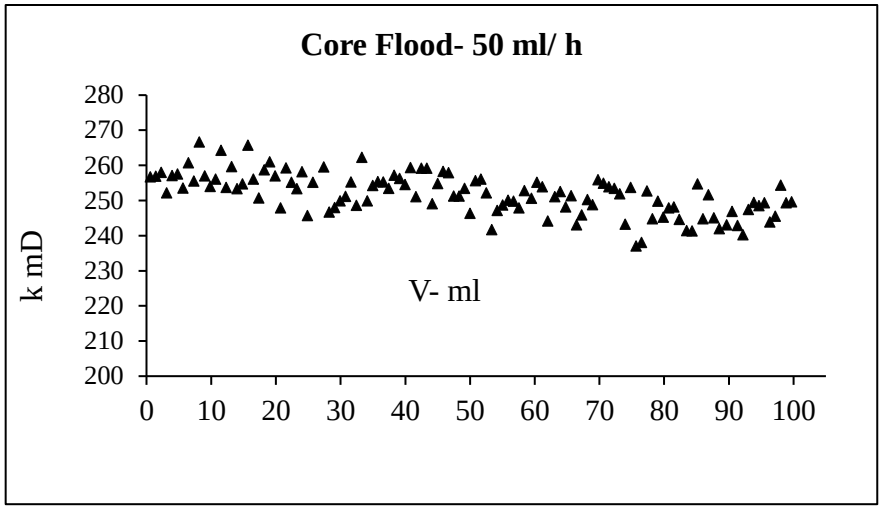

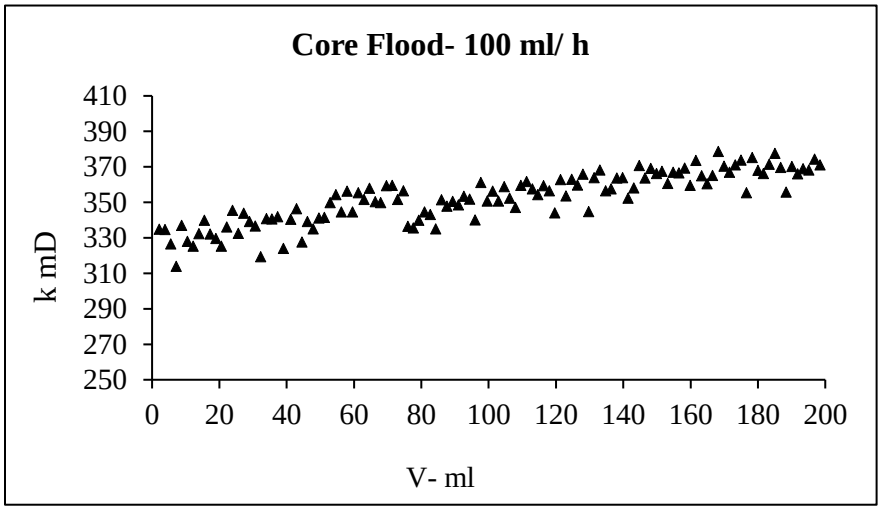

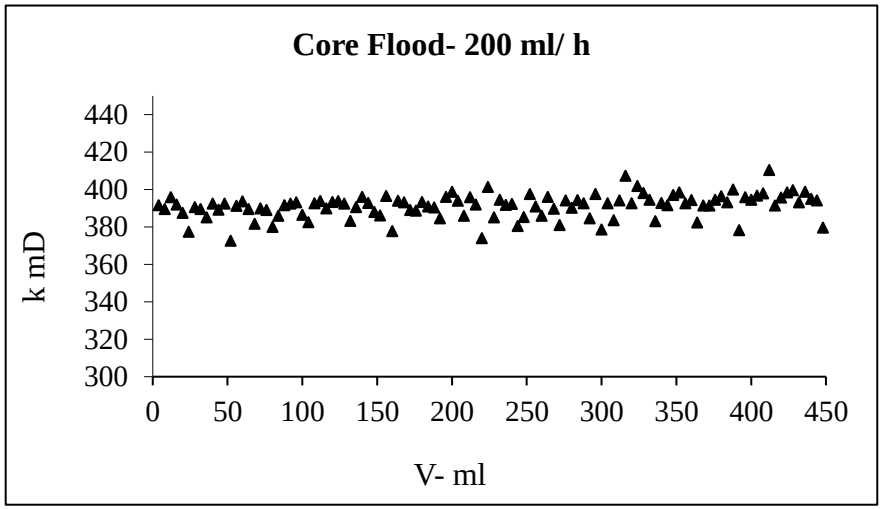

Fig. 4. 26: Core flooding drawing at different flow rate of sample D- 2- 4/ pH 3

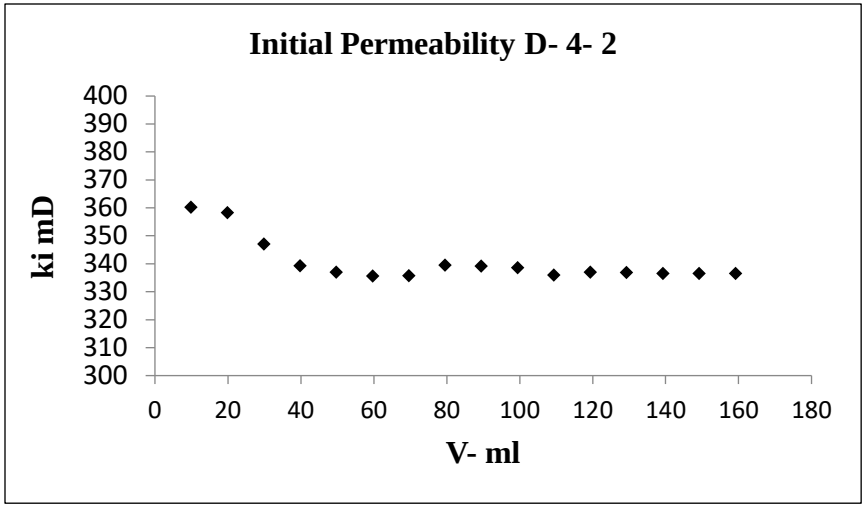

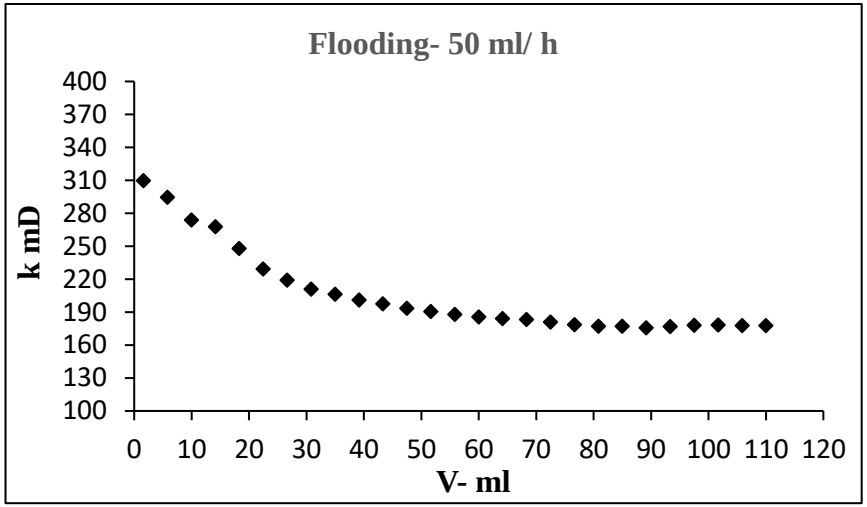

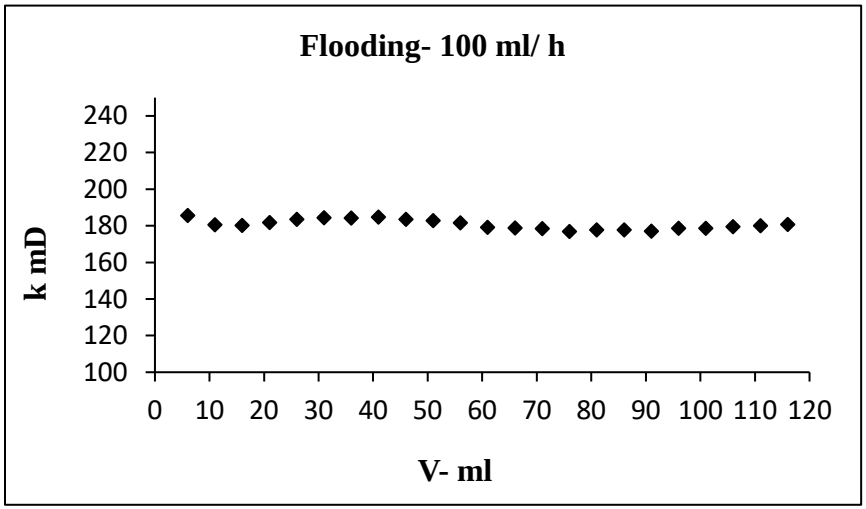

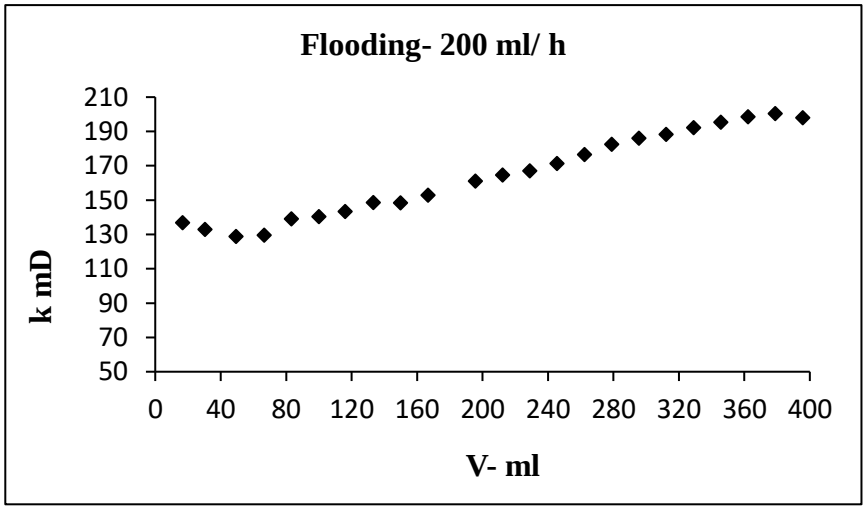

Fig. 4- 27: Core flooding drawing at different flow rate of sample D- 4- 2/ pH 9

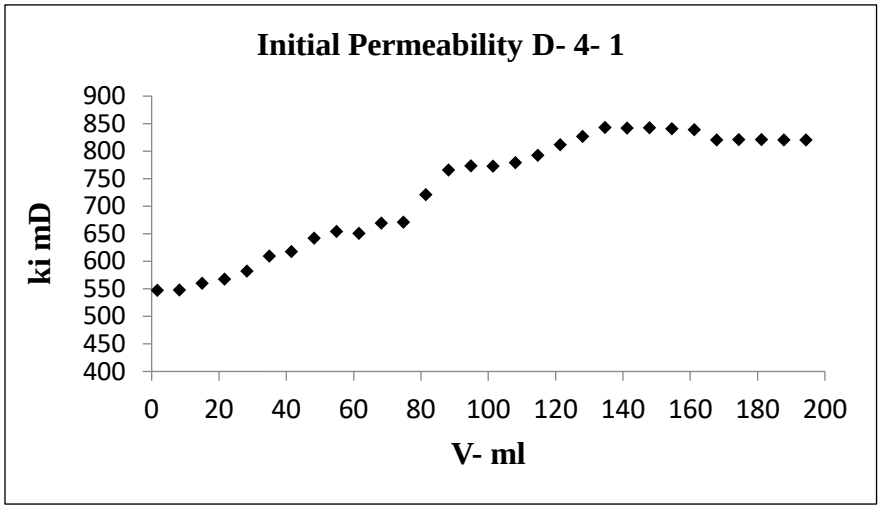

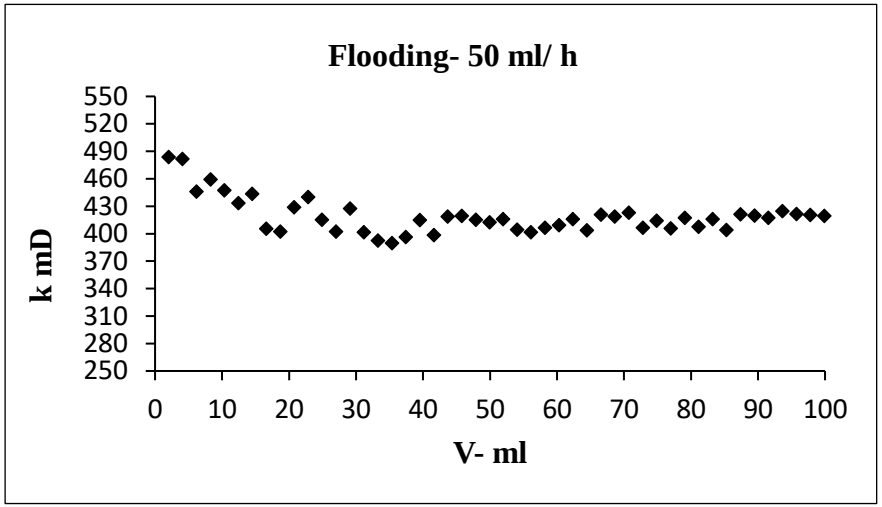

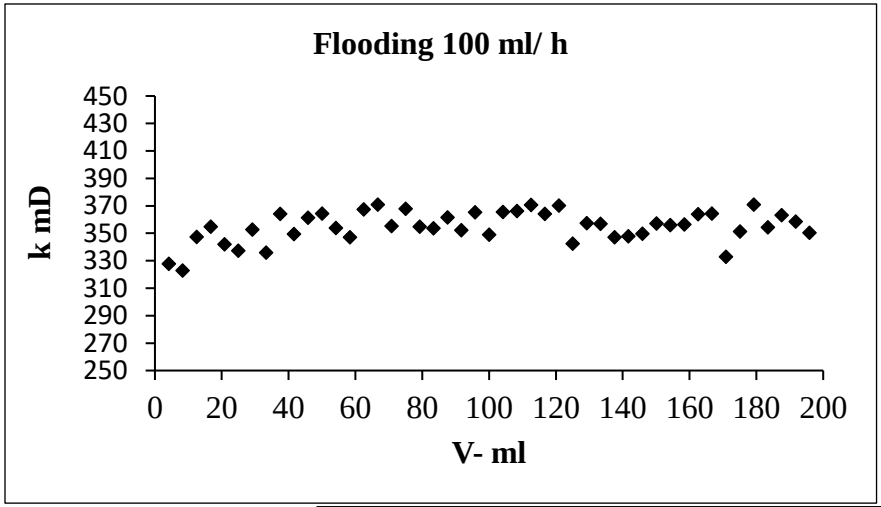

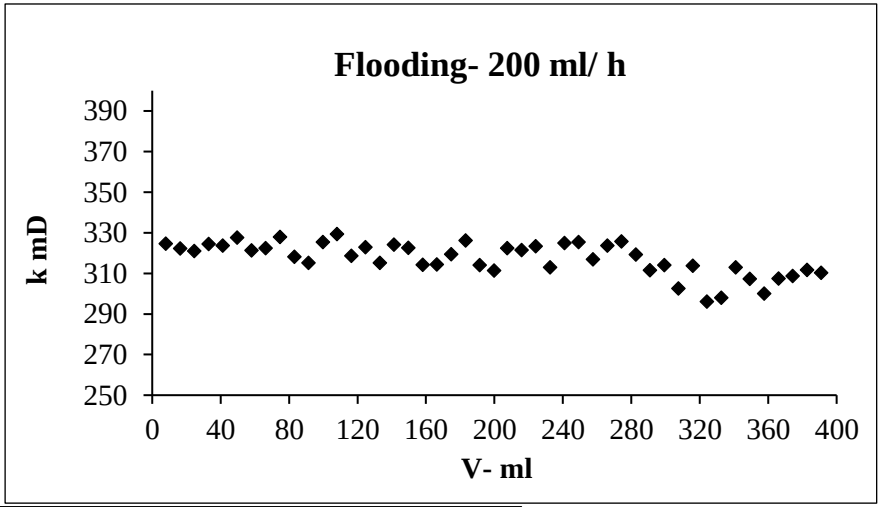

Fig. 4. 28: Core flooding drawing at different flow rate of sample D- 4- 1/ pH 9

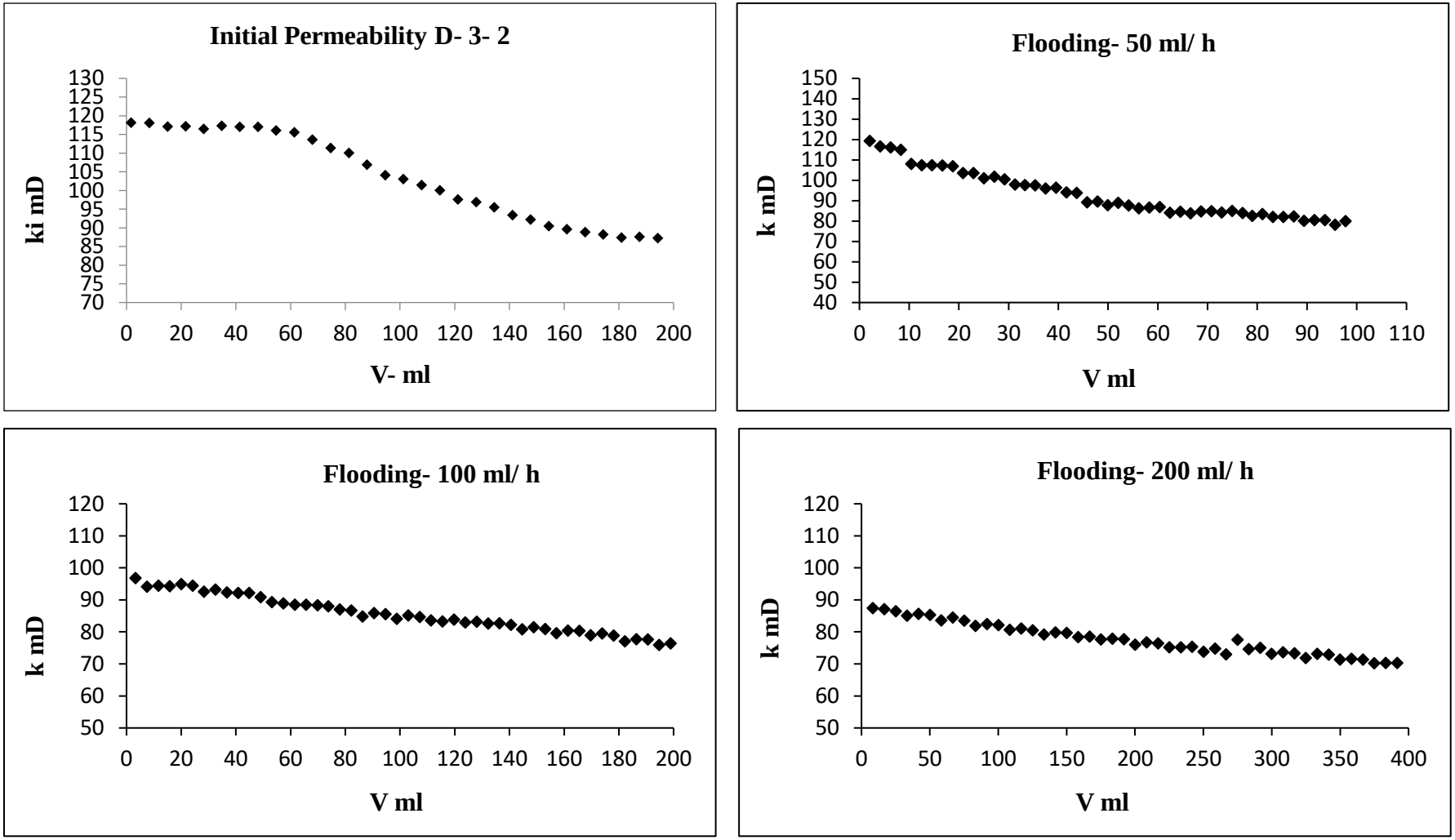

Fig. 4. 29: Core flooding drawing at different flow rate of sample D- 3- 2/ pH 9

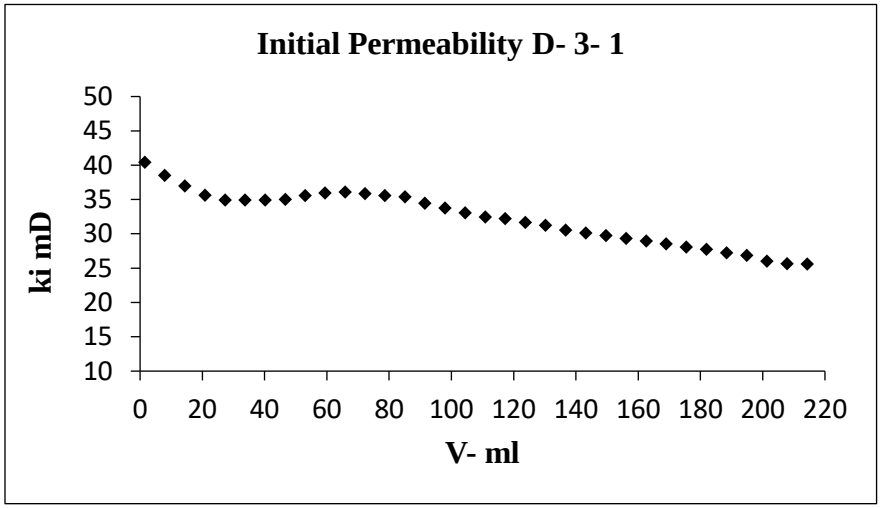

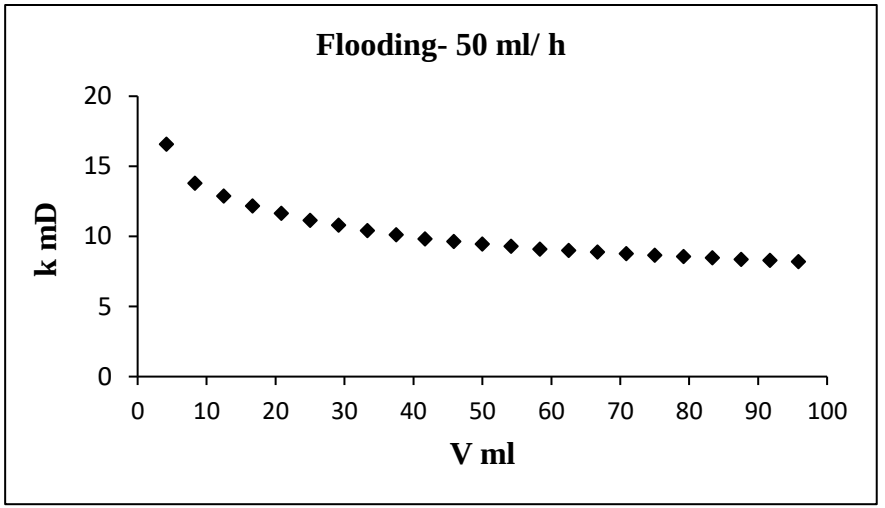

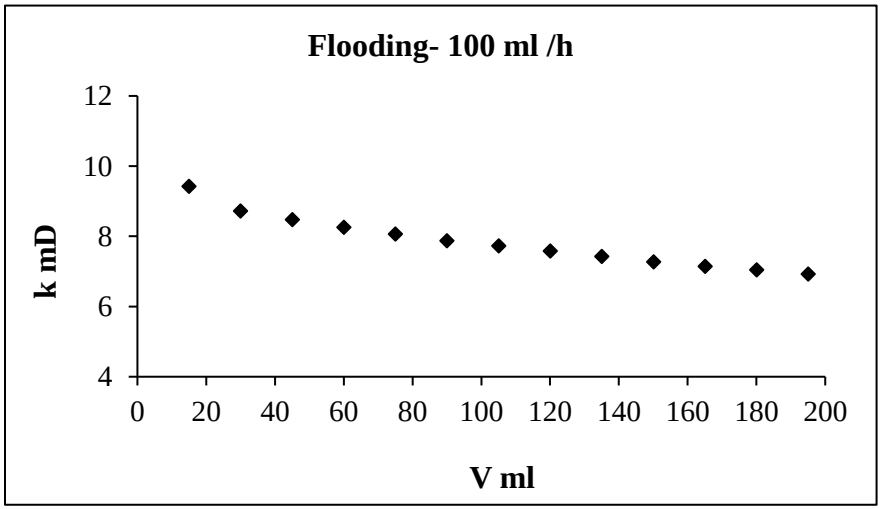

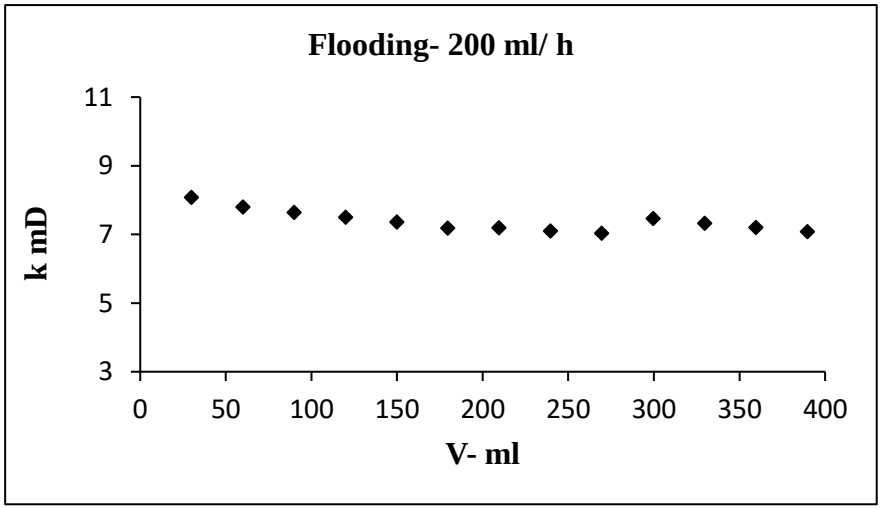

Fig. 4. 30: Core flooding drawing at different flow rate of sample D- 3- 1/ pH 9

D- 2- 6 / pH 9

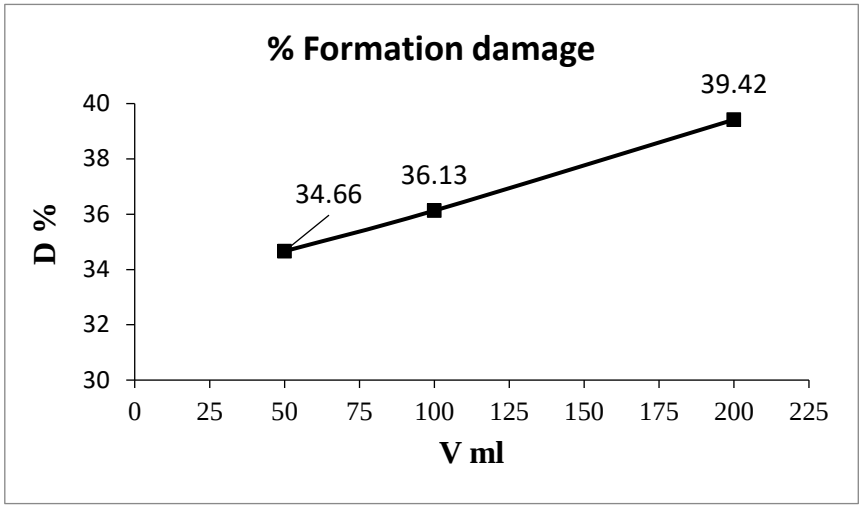

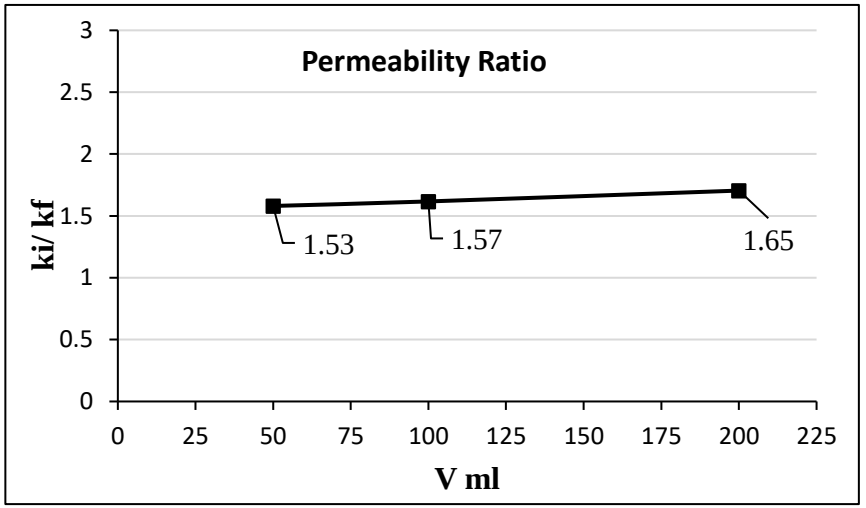

D- 2- 5 / pH 11

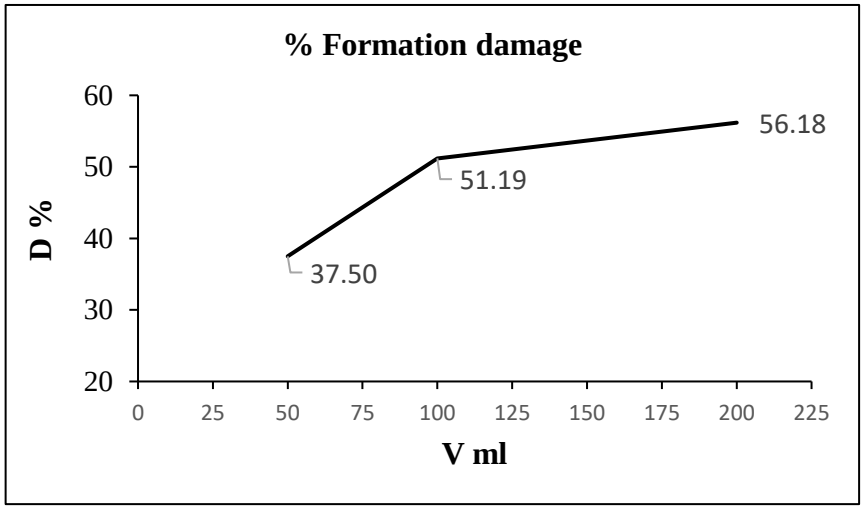

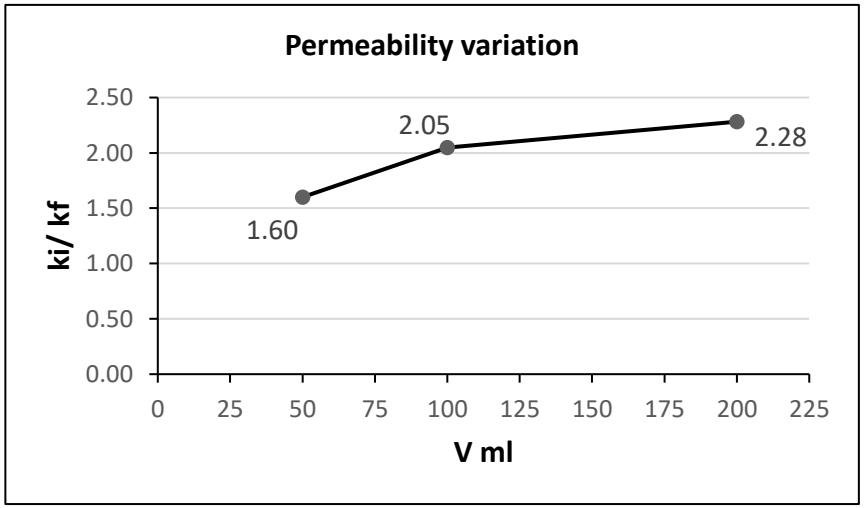

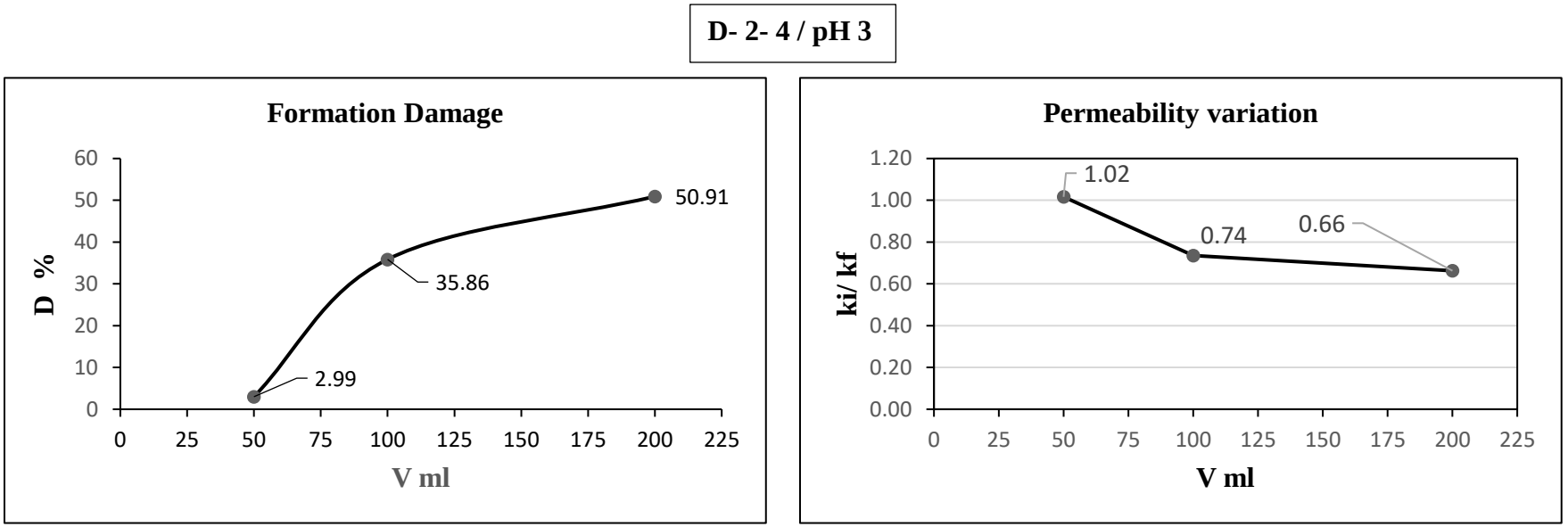

Fig. 4. 31: Formation damage and permeability variation plots D- 2- 6; D- 2- 5 and D- 2- 4

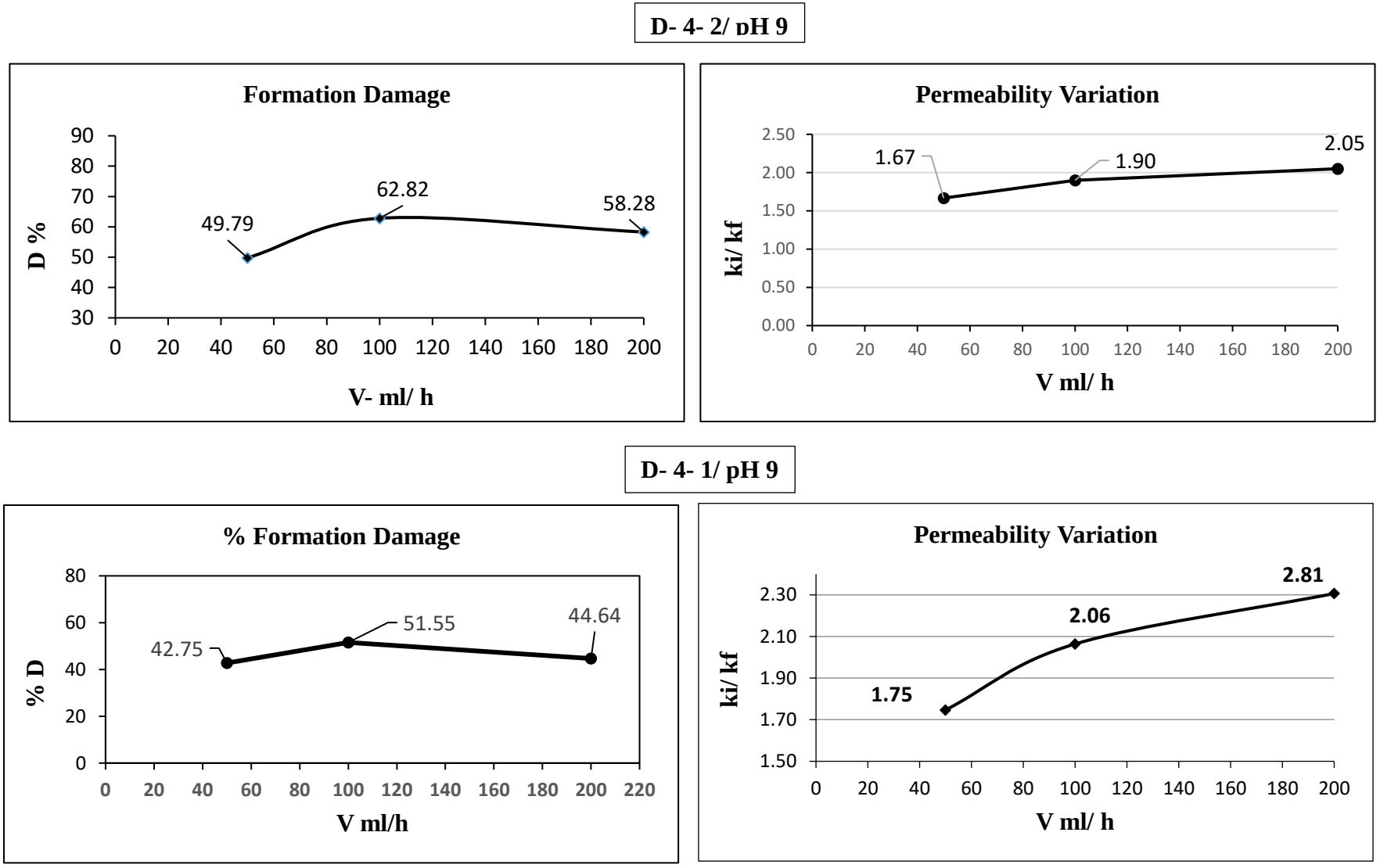

Fig. 4. 32: Formation damage and permeability variation plots D- 4- 2 and D- 4- 1

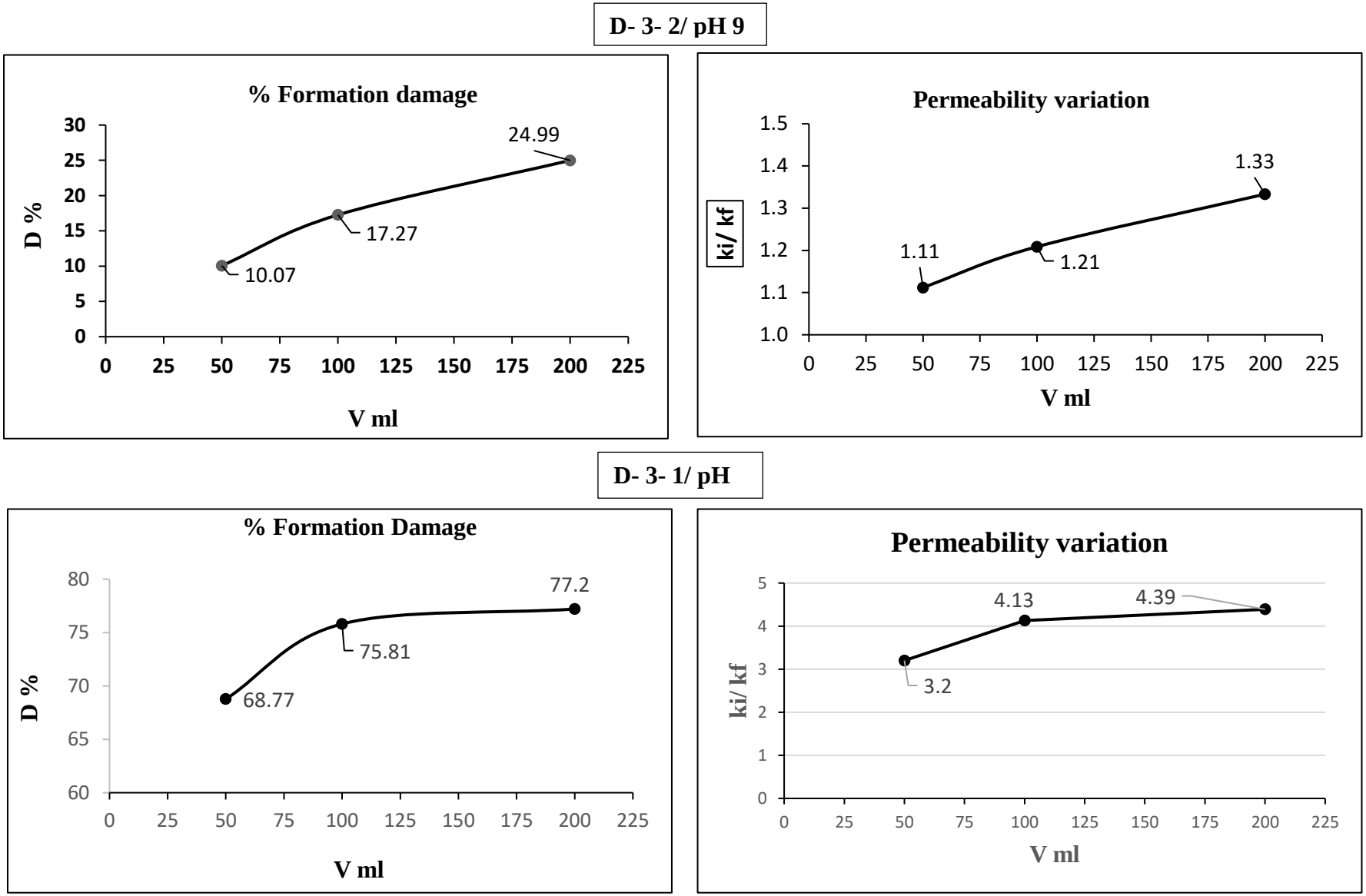

Fig. 4. 33: Formation damage and permeability variation D- 3- 2 and D- 3- 1

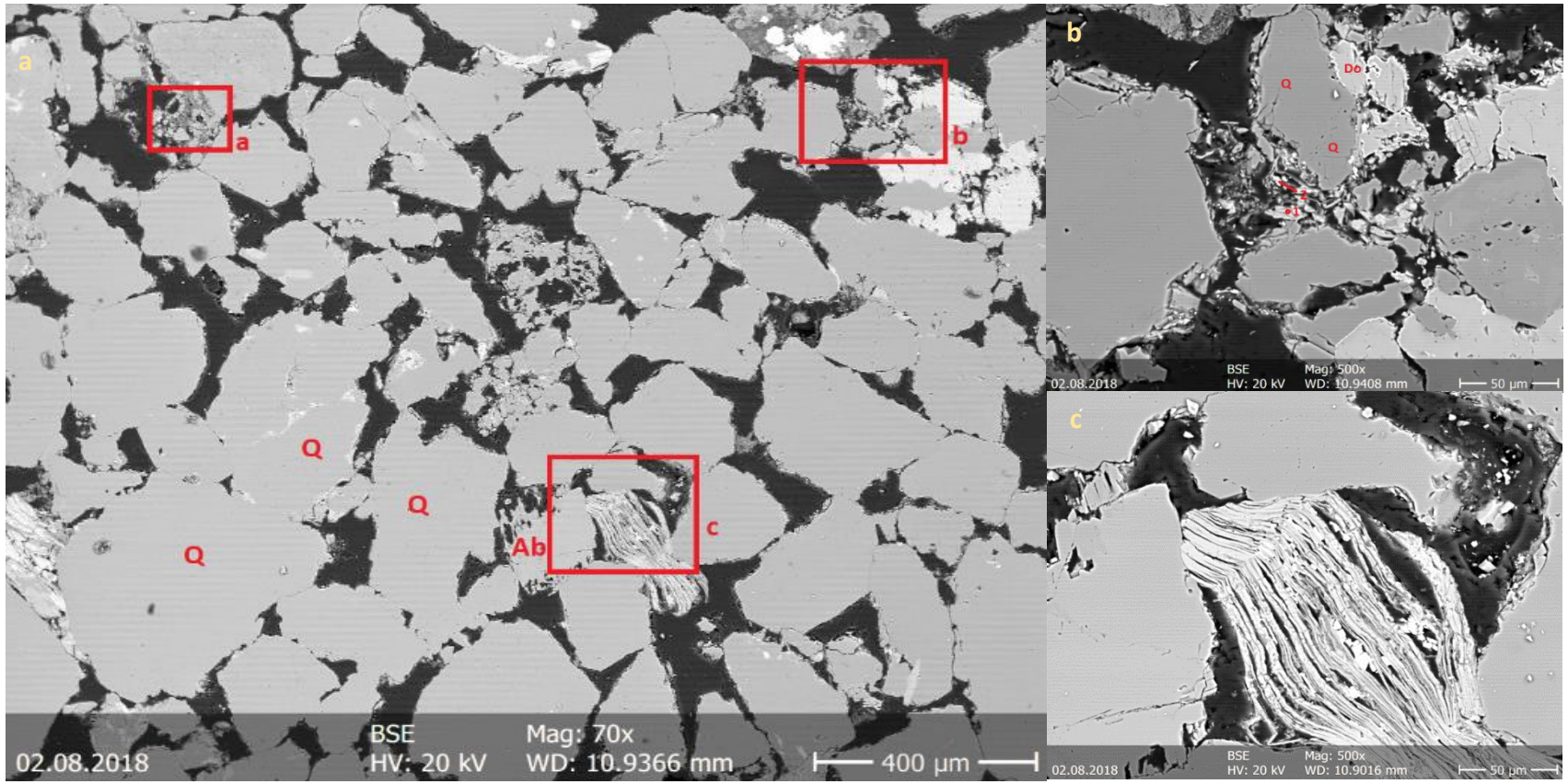

Fig. 4. 34: SEM image after flooding- D- 2- 6. (Fig.4.34- a) Generally, We observed that most of the matrix composed of clay minerals such as kaolinite, illite, chlorite with fine grains of quartz these fines cemented by silica and calcite. Some of the pore- filliping minerals are well developed and cemented; those minerals could not be able to contribute with fines migration during the flooding test and preserved on their places. While, other pore filling minerals, which are not cementing very well, influenced by flooding fluid leads to a significant reduction on permeability due to migrate those fines. (**Fig.4.34- b**) easily we can observe that most of the pore- filling

minerals subjected by flooding and detached from their original places then migrated with flooding fluid and plugged or blocked smaller pore throats from downstream section. (**Fig.4.34- c**) shows that exfoliated micaceous with interlayer Fe- Mg- carbonated which a clear evidence for flushing out those carbonate minerals between flakes then might be blocking smaller pore channels and reduce permeability.

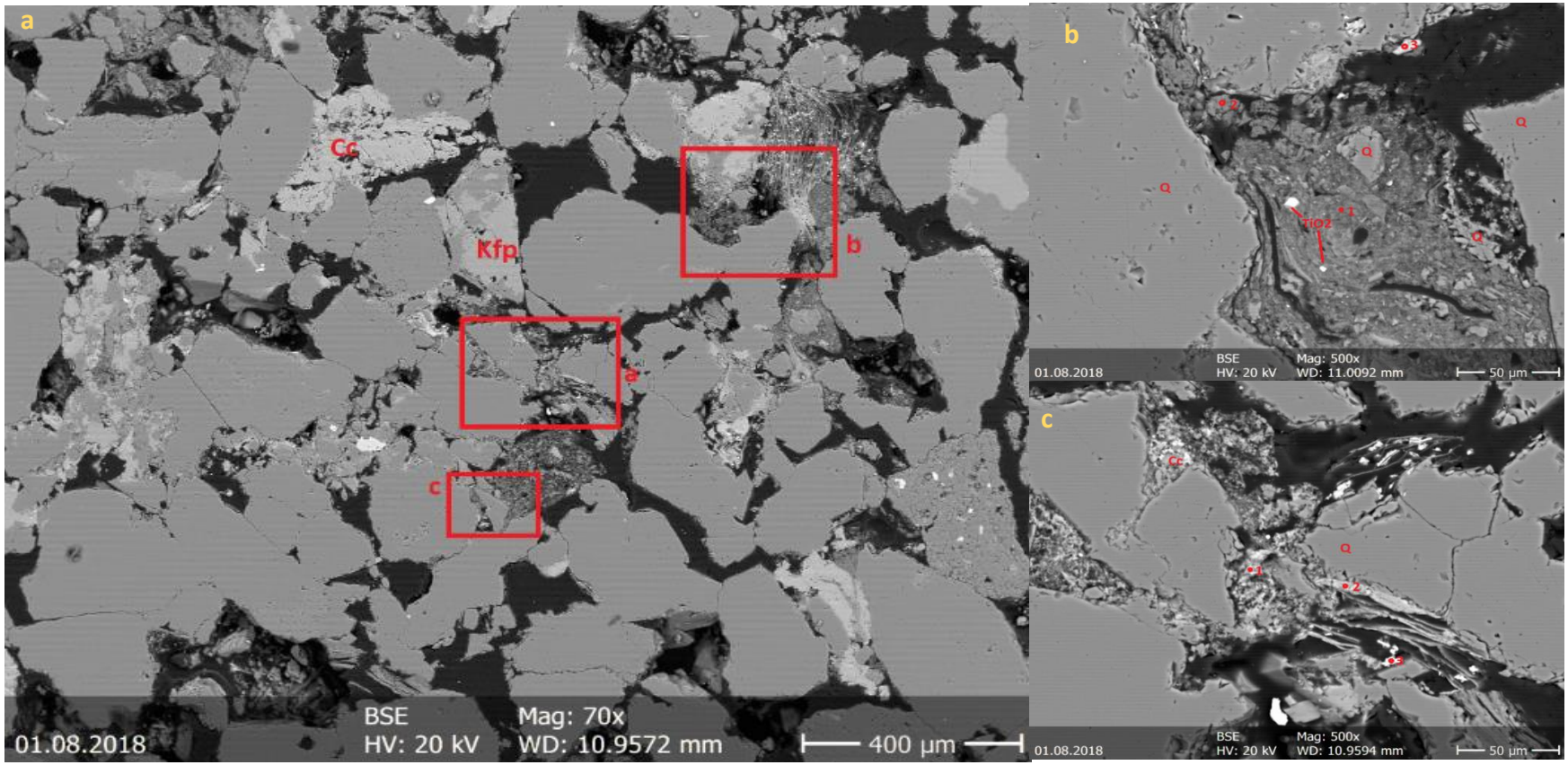

Fig. 4. 35: SEM image after flooding- D- 2- 5. (**Fig. 4.35- a**) shows SEM images of core samples after flooding and proved that some pore filling materials were flushed out with flooding solution such clay minerals and fine grains of quartz with Fe- Mg carbonates. While, other pore- filling materirial, which they are very well developped and cemented within the pores remain as it was and did not contributed fines migration. (**Fig. 4.35- b**) shows a disturbed pore filling clay minerals with a mixture of fine grains of quartz and TiO_2, those fine particles such clay and non clay minerals migarted within the pore channels during the flooding and causing a redcution on permeability. (**Fig. 4.35- c**) This SEM image can be used as a clear evidence to prove the fine migration within the pore**.** The SEM images have also proved that some fines mobilized and transported from their original places such Fe- Mg carbonates associated with chlorite flakes before the flooding while after the flooding partially mobilized and exist with a mixture of illite and silica.

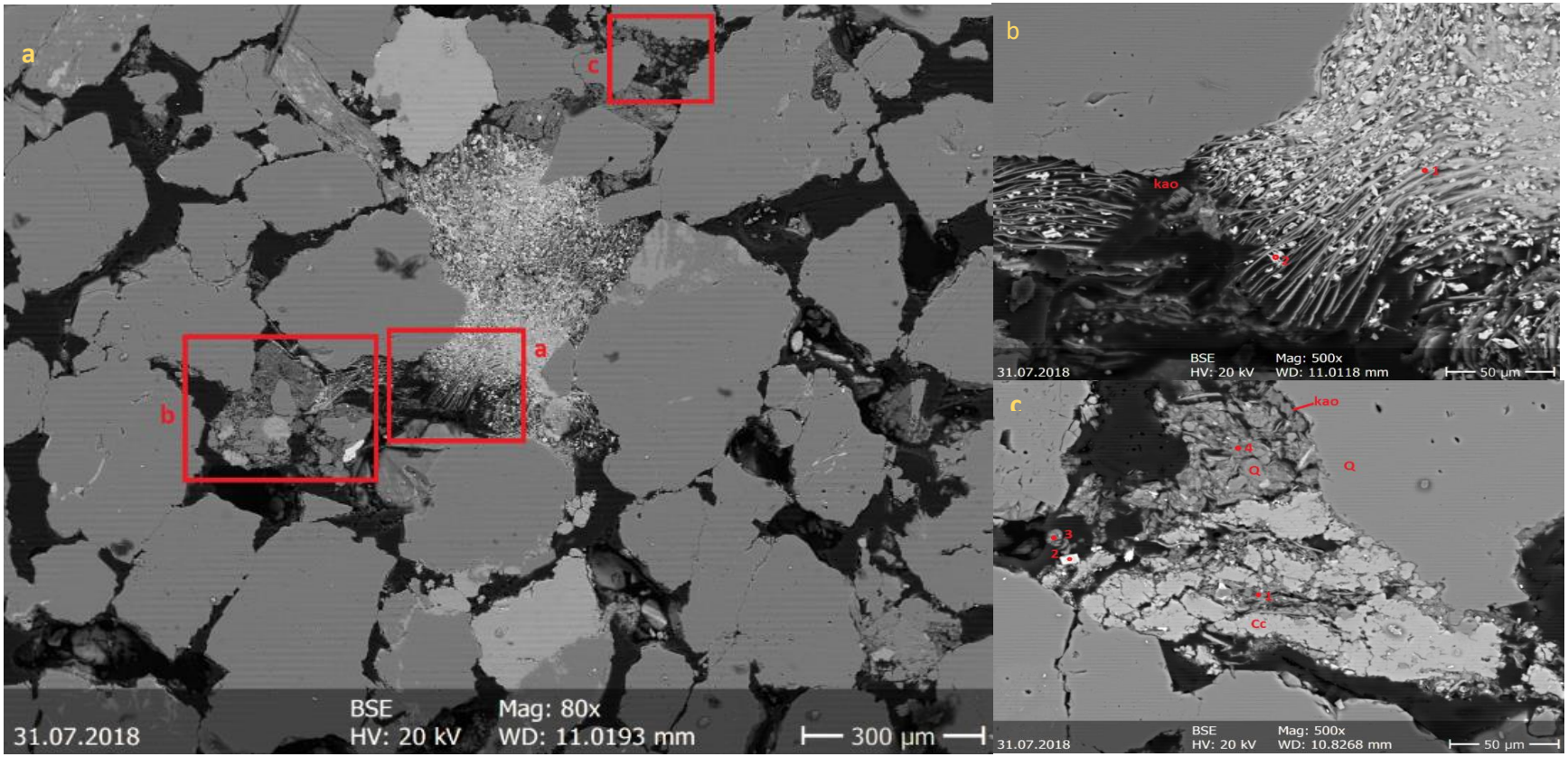

Fig. 4. 36: SEM image after flooding- D- 2- 4. (Fig. 4.36- a) Generally, We observed the matrix composed of clay minerals such as kaolinite, illite, chlorite with fine grains of non- clay minerals. Most of the pore- filliping minerals are well developed and cemented; those minerals could not be able to contribute with fine migration during the flooding test and preserved on their places. While, other pore filling minerals, which are not cemented very well, influenced by flooding fluid leads to a significant reduction on permeability due migrated those fine particles. Quartz grains very well developed and connected to each compare to D- 2- 6 sample. (**Fig.4.36- b**) The SEM images have also proved that some fines have been mobilized and transported from their original places such Fe- Mg carbonates (1) which were observed between chlorite flakes before flooding was partially mobilized and detached from their original places, as a pore filling this is a good evidence for migration fine particles during the flooding test because at the SEM images before flooding always Fe- Mg carbonate exist between chlorite flakes never seen before flooding have been mobilized. The migrated fine particles (clay minerals such as kaolinite, illite and chlorite (2)) mobilized and detached from their original location, some fines passing through the pores with the flooding fluid because their sizes smaller than the pore throats enhance permeability. While others due their sizes blocking or plugging the pore throats and leads to reduction on permeability.

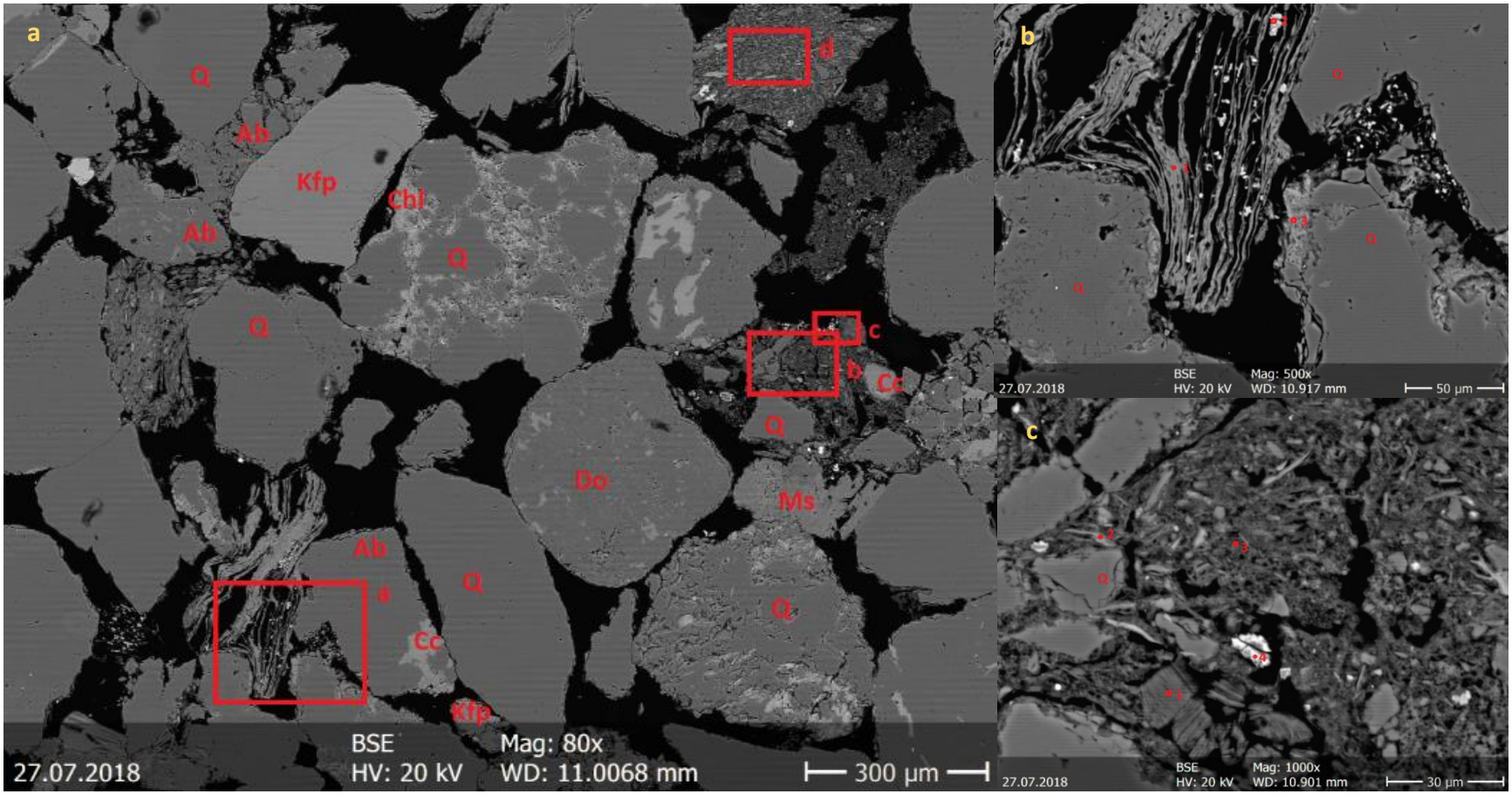

Fig. 4. 37: SEM image after flooding- D- 4- 2. (Fig. 437- a) The quartz (Q) grains have a various shapes and sizes with many pore spaces most of them filled up by fine particles. We observed that some of the matrix within the pores mobilized and disturbed such as (pores surrounded by a red rectangle) while, well developed and cemented pore filling materials preserved own position and do not influence by the flooding solution such as (pores surrounded by red square d). Large grains such as detrital dolomite, k- feldspar, albite

and muscovite due to their big sizes remain as it was. (**Fig.4.37- b**) composed of a pore- filling chlorite flakes with interlayer of carbonates, most of the carbonated particles subjected by flooding fluid and migrated from their original position, then deposited somewhere else at downstream section which are the pore throats smaller than migrated particles. (**Fig. 4.37- c**) a mixture of pore filling fine particles composed of clay minerals such as illite, chlorite and kaolinite booklet and non- clay minerals such as carbonate and fine grain of quartz, those fine particles influenced by flooding solution and moved or shifted from original position, which are caused reduction on permeability.

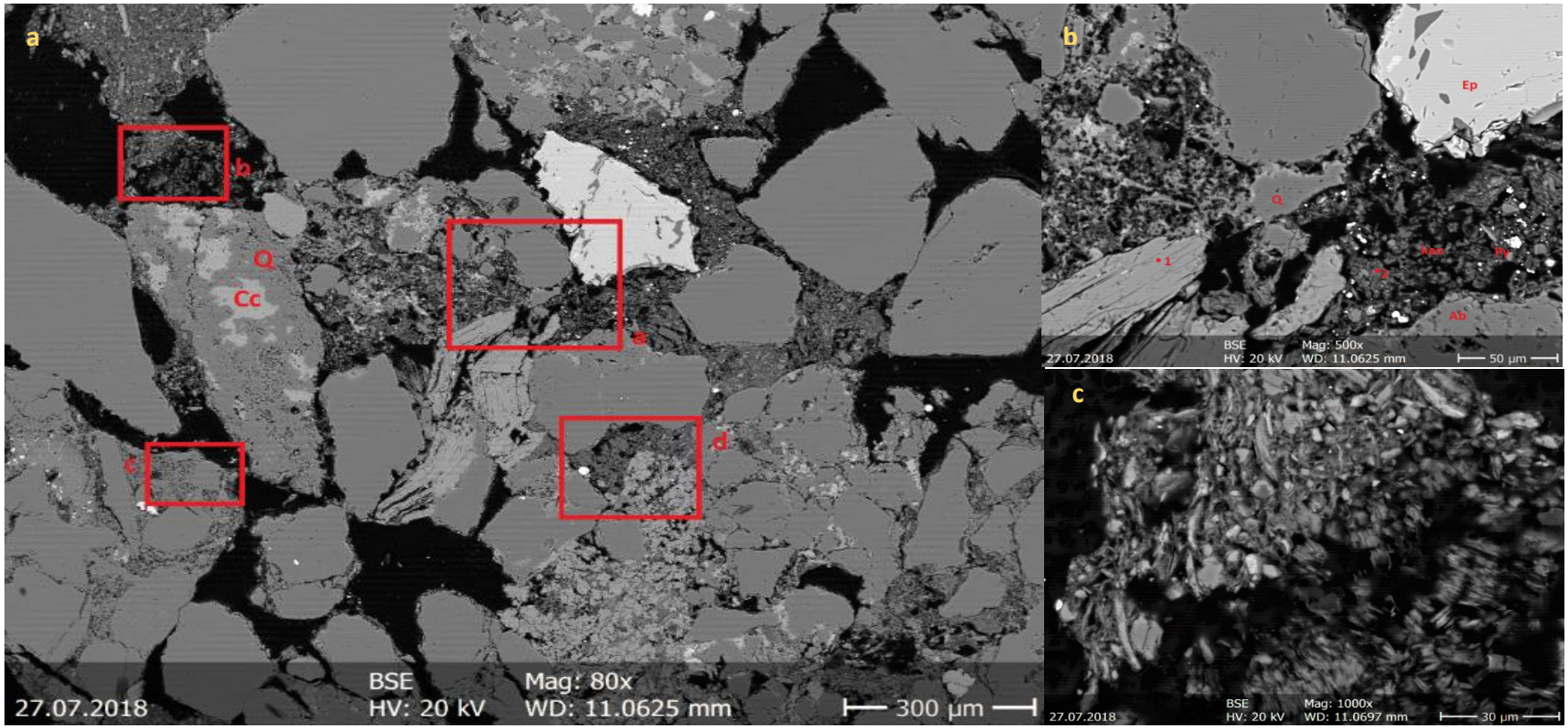

Fig. 4. 38: SEM image after flooding- D- 4- 1. (Fig.4.38- a) We observed that some of the matrix filling the pores are well cemented and developed and do not mobiles during the flooding (pores surrounded with c and d red rectangle). While other pores surrounded by (a and b red rectangle) subjected by flooding fluid and mobiles from their original position. (**Fig. 4.38- b**) is a mixture of pore- filling clay and non- clay minerals migrated during the flooding. This SEM image has also proved that some fines have been mobilized and transported from their original places such Fe- Mg carbonates associated with chlorite flakes before the flooding while after the flooding partially mobilized and exist with a mixture of illite and kaolinite. (**Fig. 4.38- c**) is a clear evidence a mixture of pore- filling minerals which are subjected by flooding and mobiles from their original position such clay minerals and non- clay minerals with few grains of quartz.

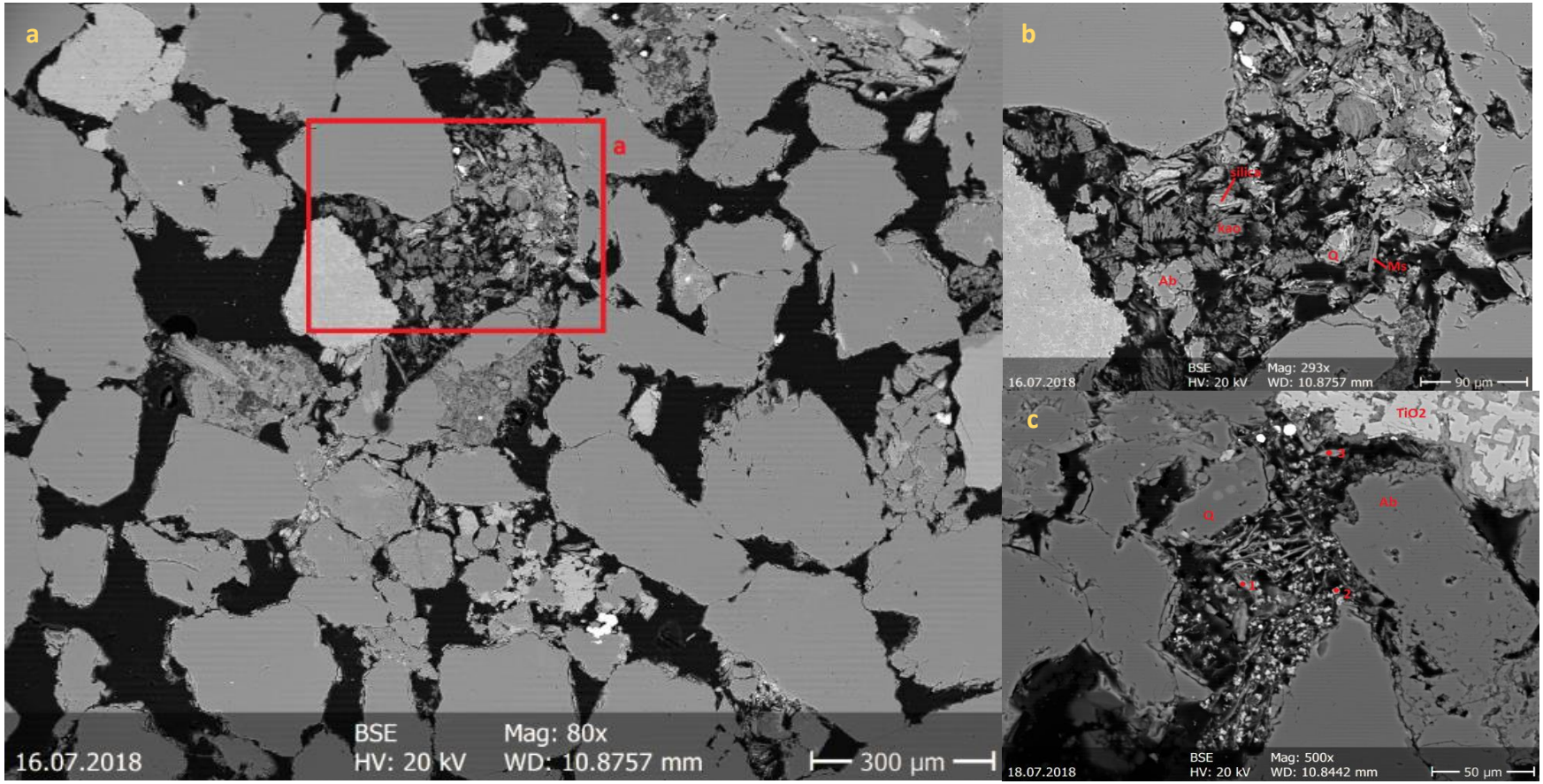

Fig. 4. 39: SEM image after flooding- D- 3- 2. (Fig.4.39- a) SEM images proved that some pores are very clean. Alternatively, the fine particles were flushed and detached after the flooding test (rectangle a). While some pore- filling minerals developed and cemented very well remain as it was. (**Fig.4.39- b**)The migrated fine particles (clay minerals such as kaolinite, illite and chlorite) mobilized from their original places might be plugged or bridge some pore throats due to their sizes larger than pore throats then could reduce permeability. While, non- clay minerals such as muscovite, medium grains of quartz (silica) almost stay in their position and not been mobilized during the flooding because the sized are big and well cemented. (**Fig.4.39- c**) Fe- Mg carbonates, which were observed between chlorite flakes before flooding. Those carbonates were partially or completely mobilized and found with illite, as a pore filling this is good evidence for migration fine particles during the flooding test because at the SEM images before flooding always Fe- Mg carbonate exists between chlorite flakes never seen with illite. Easily we observed that the chlorite flakes totally flushed out with carbonate during the flooding. The direction of the fine particles as pore filling between the quartz grains indicated the direction of flooding. Another prove of fine migration presence of kaolinite with illite as a pore- filling materials, such as mixture never seen before flooding. Before the flooding always illite, exist with silica and fine grains of quartz as a mixture. In addition, albite (Ab) particles have been mobilized and detached from their original grains and exist with illite and silica mixture.

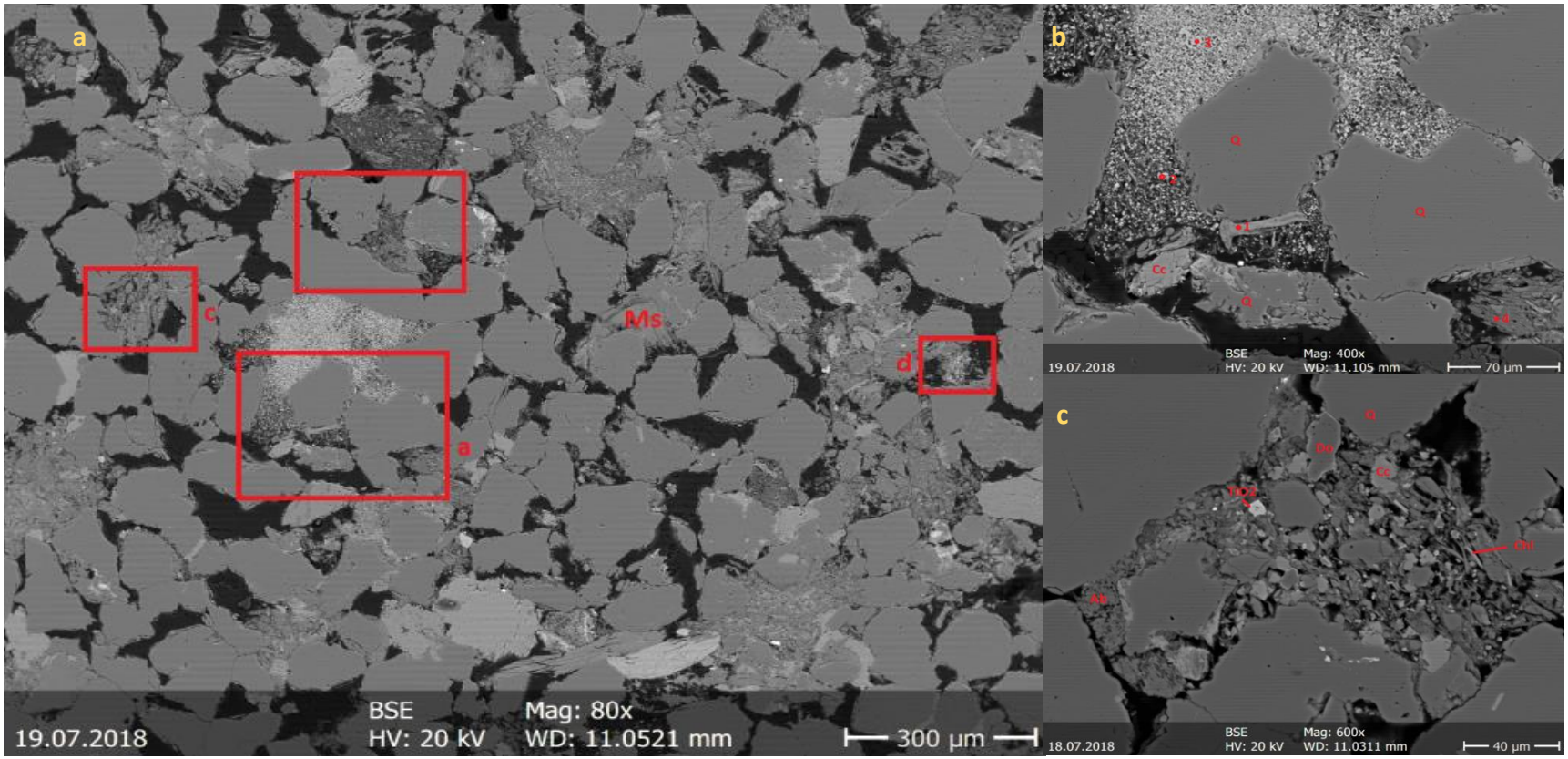

Fig. 4. 40: SEM image after flooding- D- 3- 1. (Fig4.40- a) The quartz (Q) grains are compacted with smaller sizes compared to other D-3-2 samples that might be due to the sample taken from deeper locations. We observed that most of the pores filled up by the Authigenic and diagenetic minerals such as clay and non- clay minerals. Most of the pore- filliping minerals are well developed and cemented; those minerals could not be able to contribute with fine migration during the flooding test and preserved on their places. While, other pore filling minerals, which

are not cemented very well, influenced by flooding fluid leads to a significant reduction on permeability due migrated those fine particles. (**Fig.4.40- b**) The SEM images have also proved that some pores were flushed during the flooding test. Fe- Mg carbonates which was observed between chlorite flakes before flooding was partially mobilized and detached from their original places, as a pore filling this is a good evidence for migration fine particles during the flooding test because at the SEM images before flooding always Fe- Mg carbonate exist between chlorite flakes never seen before flooding have been mobilized. Easily we observed that the chlorite flakes partially flushed out with carbonate during the flooding. **(Fig.4.40- c)** The migrated fine particles (clay minerals such as kaolinite, illite and chlorite) mobilized from their original places and plugged or bridged somewhere else, while and non- clay minerals such as muscovite, fine grains of quartz (silica). Also, there is few particles of albite and TiO_2 might migrate during the flooding.

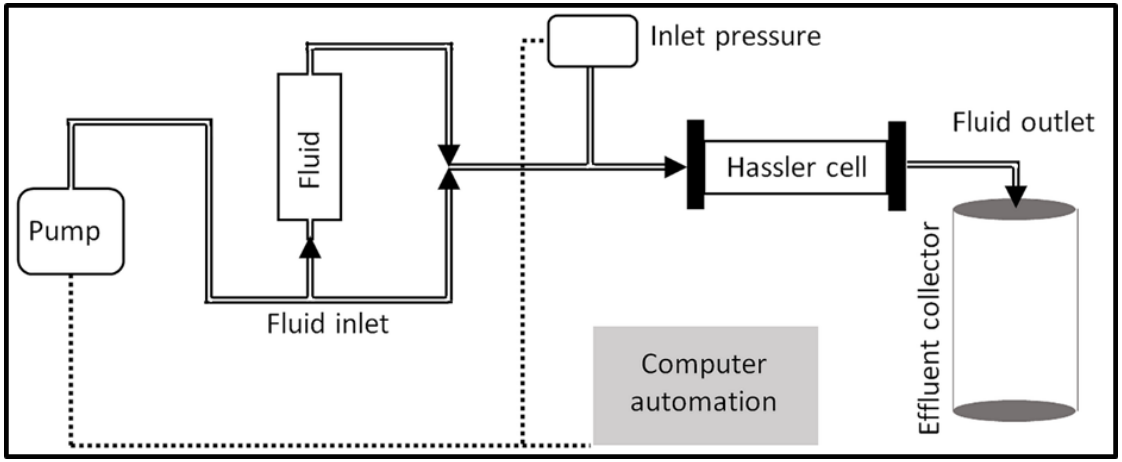

Fig.1: Experimental core- flooding testing set up

Appendix C

Appendix A includes all photos of selected core plugs and instruments that have been used during the study.

Fig. 1: Selected Sandstone Core plugs.

Fig.2: Scientific Balance for measuring weight of selected core plugs

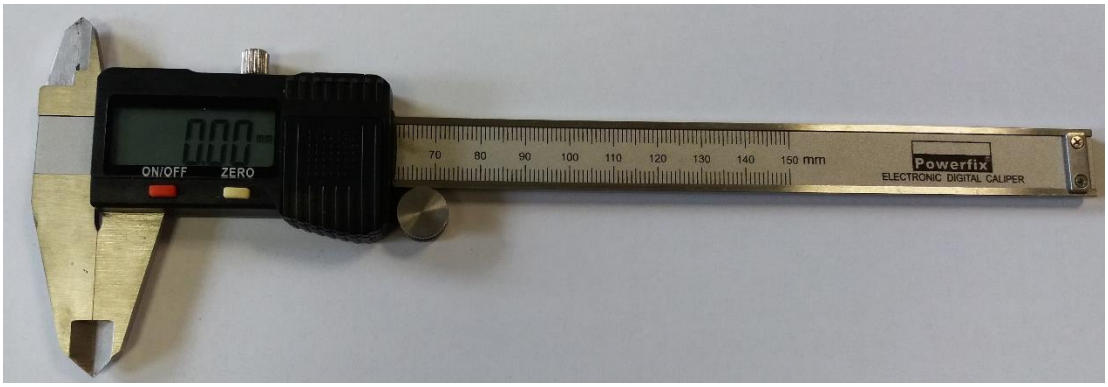

Fig. 3: Vernier to measure geometrical of core samples

Fig. 4: Porcelain and agate Mortar

Fig. 5: XRD sample holder

Fig. 6: Clay fraction preparation “suspension”

Fig. 6: Clay fraction separation

Fig. 7: Scientific balance to measure clay fraction

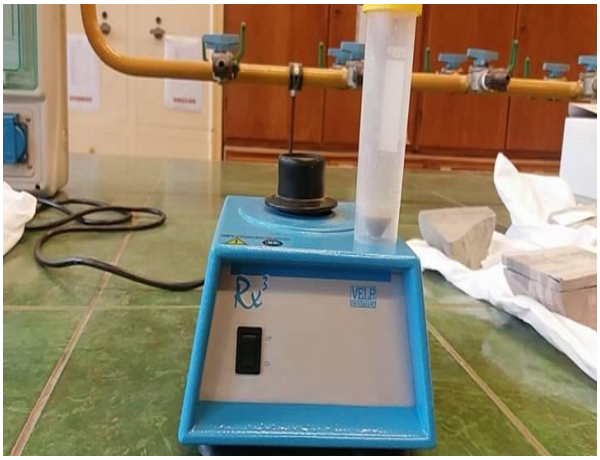

Fig. 8: Rotatory machine

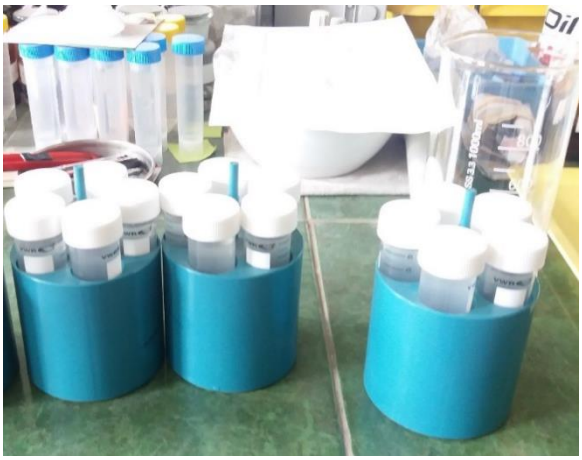

Fig. 9: Centrifugal sample holder

Fig. 10: Centrifuging ROTINA 420

Fig. 11: Ultra sonic bath machine and clay fraction

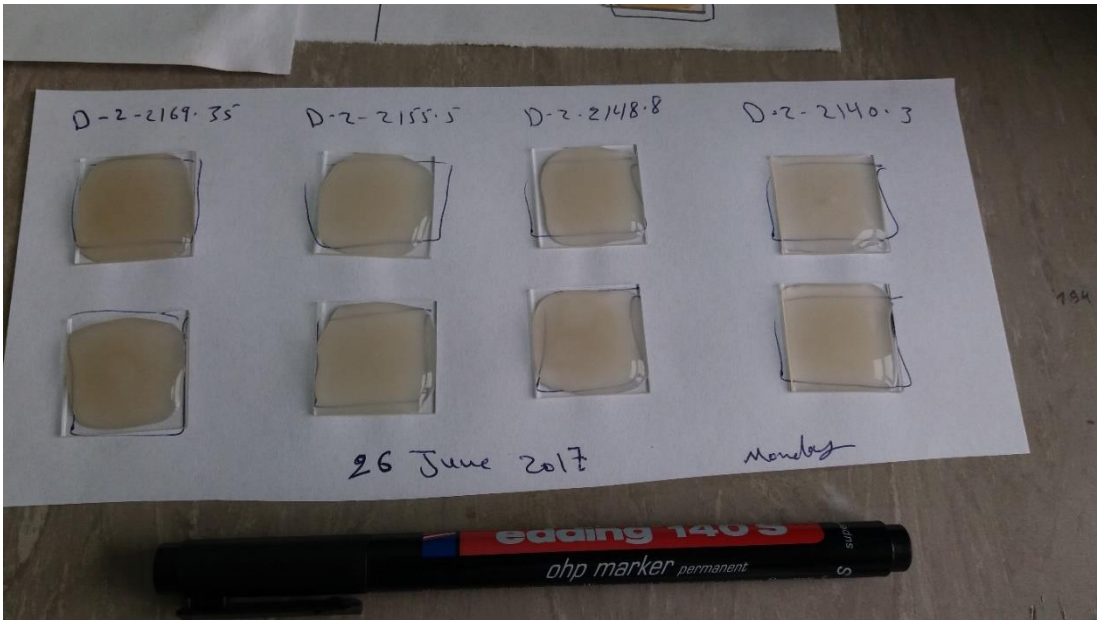

Fig. 12: Clay fraction

Fig. 13: XRD Machine- D8 Bruker

Fig. 14: SEM Samples preparation before polishing

Fig. 15: SEM samples after polishing

Fig. 16: SEM sample preparation

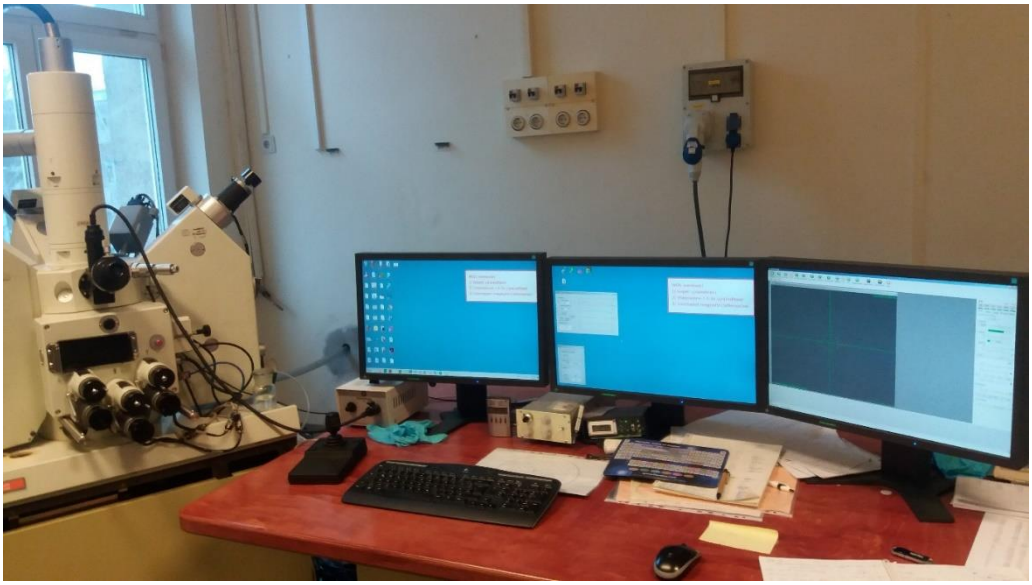

Fig. 17: SEM machine

Fig. 18: Vacuum Machine to evacuate the core samples and dried out.

Fig. 19: Helium Porosimeter

Fig. 20: Hassler Core holder Machine for measuring permeability

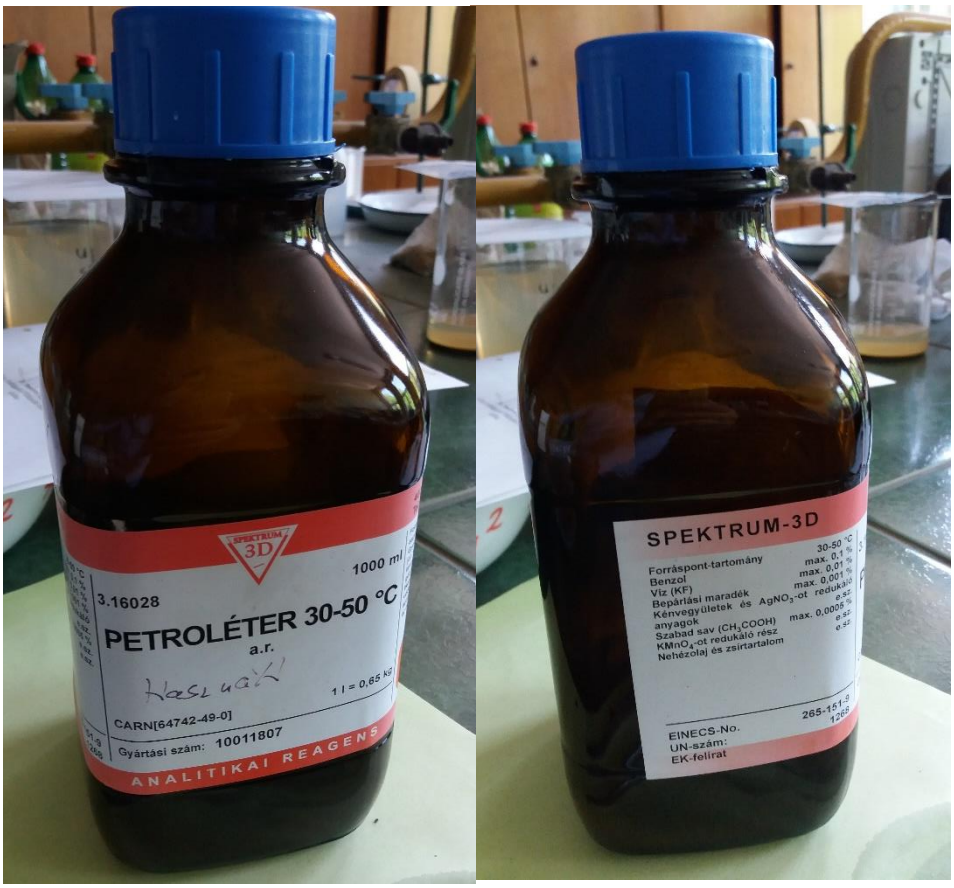

Fig. 21: Petroleter solution for cleaning SEM samples before runing the machine

Fig. 22: Selected core samples after the flooding to study XRD and SEM.

Core ID	D-2- 1943.0

Porosity	27%

Core geometry	
d [cm]	3.797
l [cm]	6.181
A [cm^2]	11.3232
Vtotal [cm^3]	69.9890
m(dry) [g]	134.85

	P1	P2	Vs	ρ	ϕ	ρ SD
	[psi]	[psi]	[cm3]	[g/cm3]	[-]	[g/cm3]
1	17.500	8.374	50.943	2.647	0.272	0.003
2	17.452	8.349	50.898	2.649	0.273	
3	17.445	8.343	50.840	2.652	0.274	
		Average ->	50.894	2.650	0.273	

Lab. Properties	
Ta [°C]	22.5
Pa [bar]	1.0090

Average Volume	50.8938
Average Density	2.6496
Standard Deviation	0.0030

He-porosimeter	
Vc	146.5
VR micro	5.621
VR small	11.014
VR large	87.710

69.9890	
50.8938	19.0952
19.0952	

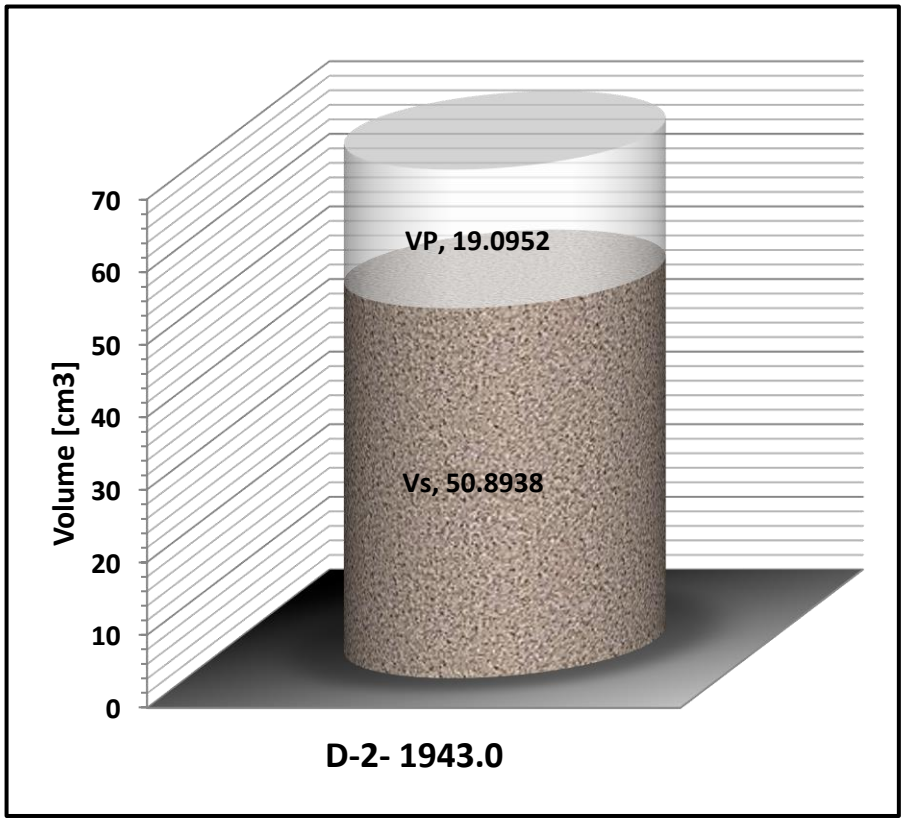

Core ID	D-2- 2140.3

Porosity	22%

Core geometry	
d [cm]	3.79
l [cm]	6.183
A [cm^2]	11.282
Vtotal [cm^3]	69.754
m(dry) [g]	144.15

	P1	P2	Vs	ρ	ϕ	ρ SD
	[psi]	[psi]	[cm3]	[g/cm3]	[-]	[g/cm3]
1	17.350	8.446	54.063	2.666	0.225	0.0003
2	17.368	8.455	54.068	2.666	0.225	
3	17.534	8.536	54.072	2.666	0.225	
		Average ->	54.068	2.666	0.225	

Lab. Properties	
Ta [°C]	22.5
Pa [bar]	1.009

Average Volume	54.068
Average Density	2.666
Standard Deviation	0.0003

He-porosimeter	
Vc	146.5
VR micro	5.621
VR small	11.014
VR large	87.710

69.7537	
54.0679	15.6858
15.6858	

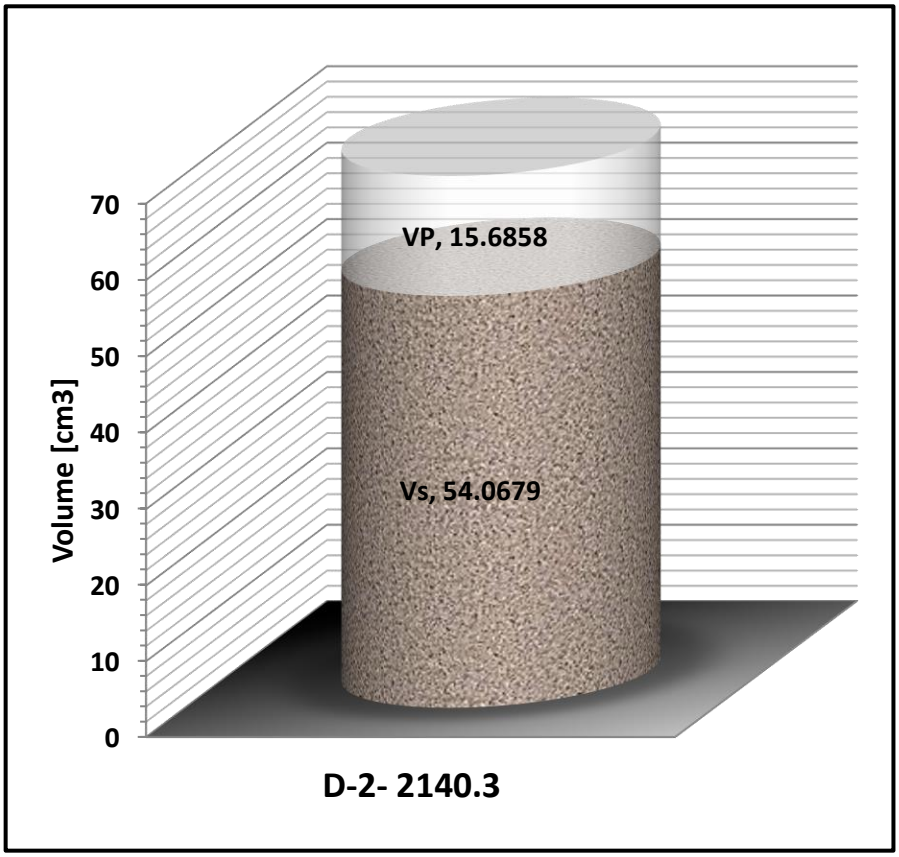

Core ID	D-2- 2145.1

Porosity	23%

Core geometry	
d [cm]	3.79
l [cm]	6.125
A [cm^2]	11.282
Vtotal [cm^3]	69.099
m(dry) [g]	142.21

	P1 [psi]	P2 [psi]	Vs [cm3]	ρ [g/cm3]	ϕ [-]	ρ SD [g/cm3]
1	17.461	8.464	53.296	2.668	0.229	0.002
2	17.290	8.383	53.337	2.666	0.228	
3	17.558	8.514	53.359	2.665	0.228	
		Average ->	53.331	2.667	0.228	

Lab. Properties	
Ta [°C]	22.5
Pa [bar]	1.0090

Average Volume	53.3309
Average Density	2.6666
Standard Deviation	0.0019

He-porosimeter	
Vc	146.5
VR micro	5.621
VR small	11.014
VR large	87.710

69.0994	
53.3309	15.7686
15.7686	

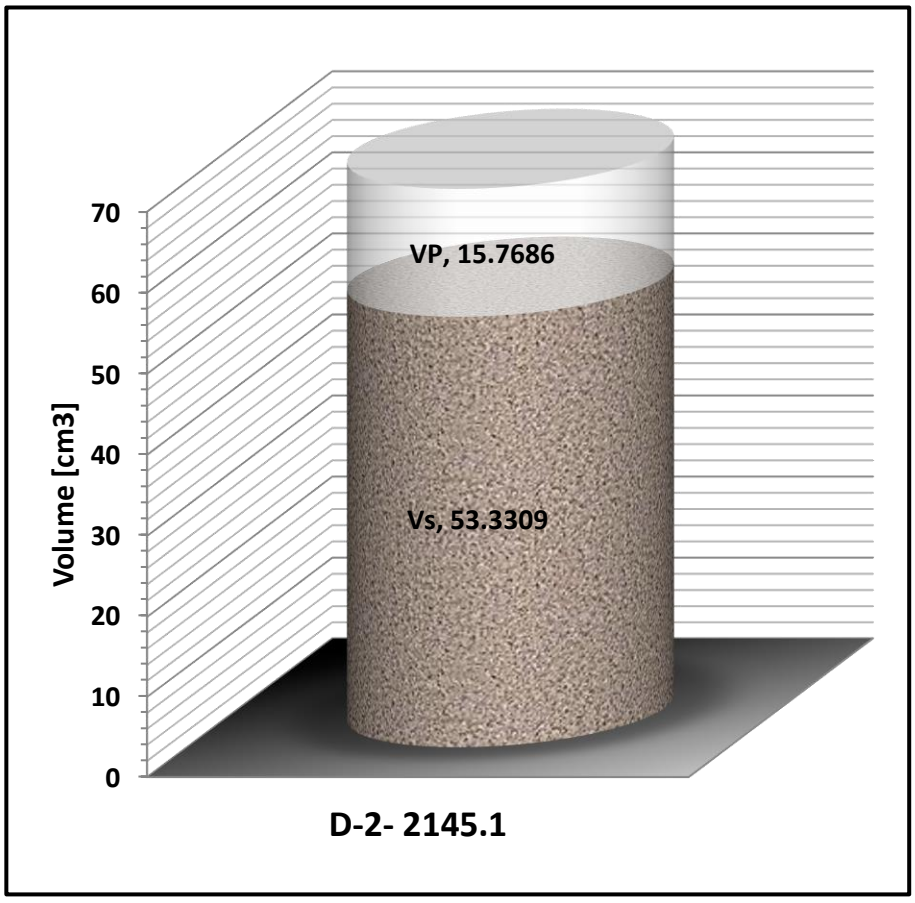

Core ID	D-4- 1872.6

Porosity	26%

Core geometry	
d [cm]	3.792
l [cm]	6.174
A [cm^2]	11.293
Vtotal [cm^3]	69.726
m(dry) [g]	137.77

	P1	P2	Vs	ρ	ϕ	ρ SD
	[psi]	[psi]	[cm3]	[g/cm3]	[-]	[g/cm3]
1	17.758	8.541	51.877	2.656	0.256	0.002
2	17.180	8.261	51.833	2.658	0.257	
3	17.736	8.530	51.868	2.656	0.256	
		Average ->	51.860	2.657	0.256	

Lab. Properties	
Ta [°C]	22.5
Pa [bar]	1.009

Average Volume	51.860
Average Density	2.657
Standard Deviation	0.0017

He-porosimeter	
Vc	146.5
VR micro	5.621
VR small	11.014
VR large	87.710

69.7257	
51.8597	17.8660
17.8660	

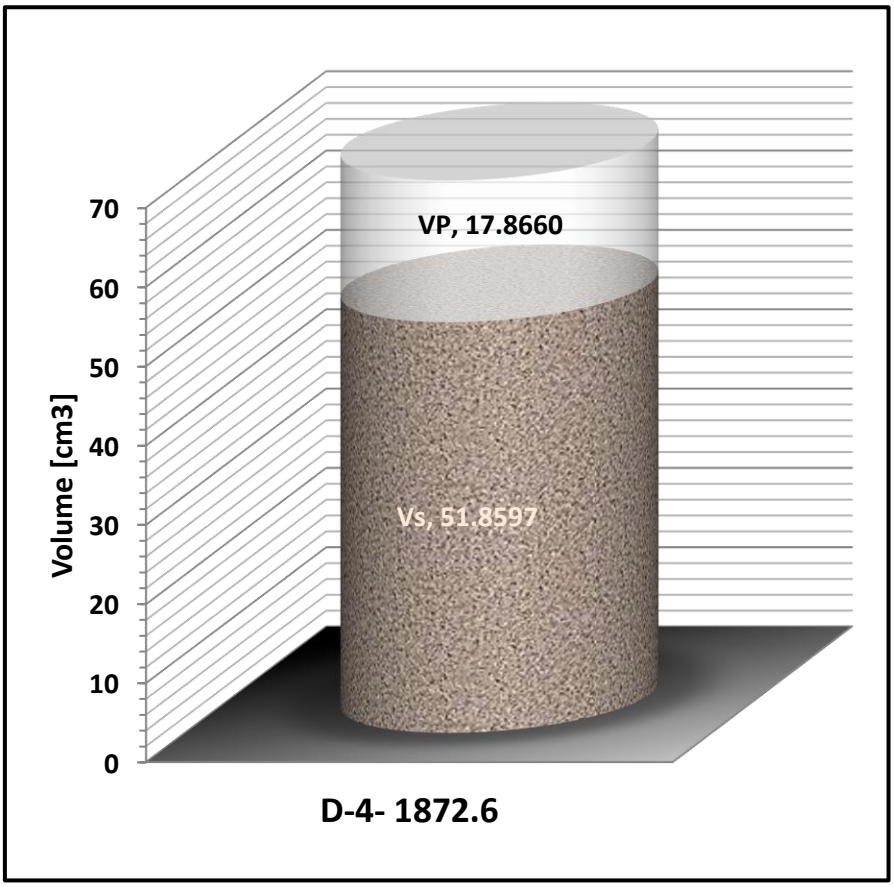

Core ID	D-4- 1874.0

Porosity	28%

Core geometry	
d [cm]	3.79
l [cm]	6.145
A [cm^2]	11.2815
Vtotal [cm^3]	69.3250
m(dry) [g]	132.57

	P1 [psi]	P2 [psi]	Vs [cm3]	ρ [g/cm3]	ϕ [-]	ρ SD [g/cm3]
1	17.464	8.320	50.133	2.644	0.277	0.002
2	17.301	8.241	50.103	2.646	0.277	
3	17.488	8.329	50.079	2.647	0.278	
		Average ->	50.105	2.646	0.277	

Lab. Properties	
Ta [°C]	23.5
Pa [bar]	1.0090

Average Volume	50.1048
Average Density	2.6459
Standard Deviation	0.0017

He-porosimeter	
Vc	146.5
VR micro	5.6212
VR small	11.0142
VR large	87.7104

69.325	
50.105	19.220
19.220	

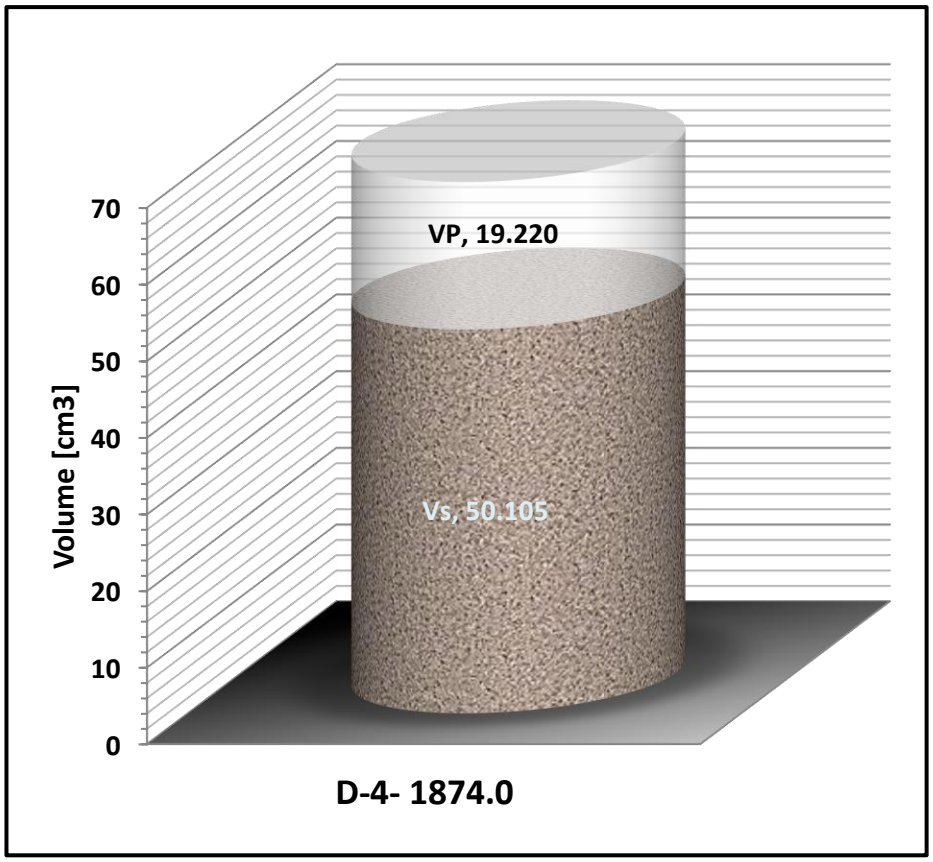

Core ID	D-3- 1868.9

Porosity	24%

Core geometry	
d [cm]	3.79
l [cm]	6.182
A [cm^2]	11.282
Vtotal [cm^3]	69.742
m(dry) [g]	142.07

	P1	P2	Vs	ρ	ϕ	ρ SD
	[psi]	[psi]	[cm3]	[g/cm3]	[-]	[g/cm3]
1	17.420	8.441	53.229	2.669	0.237	0.001
2	17.214	8.340	53.204	2.670	0.237	
3	17.507	8.482	53.204	2.670	0.237	
		Average ->	53.212	2.670	0.237	

Lab. Properties	
Ta [°C]	22.5
Pa [bar]	1.009

Average Volume	53.212
Average Density	2.670
Standard Deviation	0.001

He-porosimeter	
Vc	146.5
VR micro	5.621
VR small	11.014
VR large	87.710

69.7425	
53.2124	16.5301
16.5301	

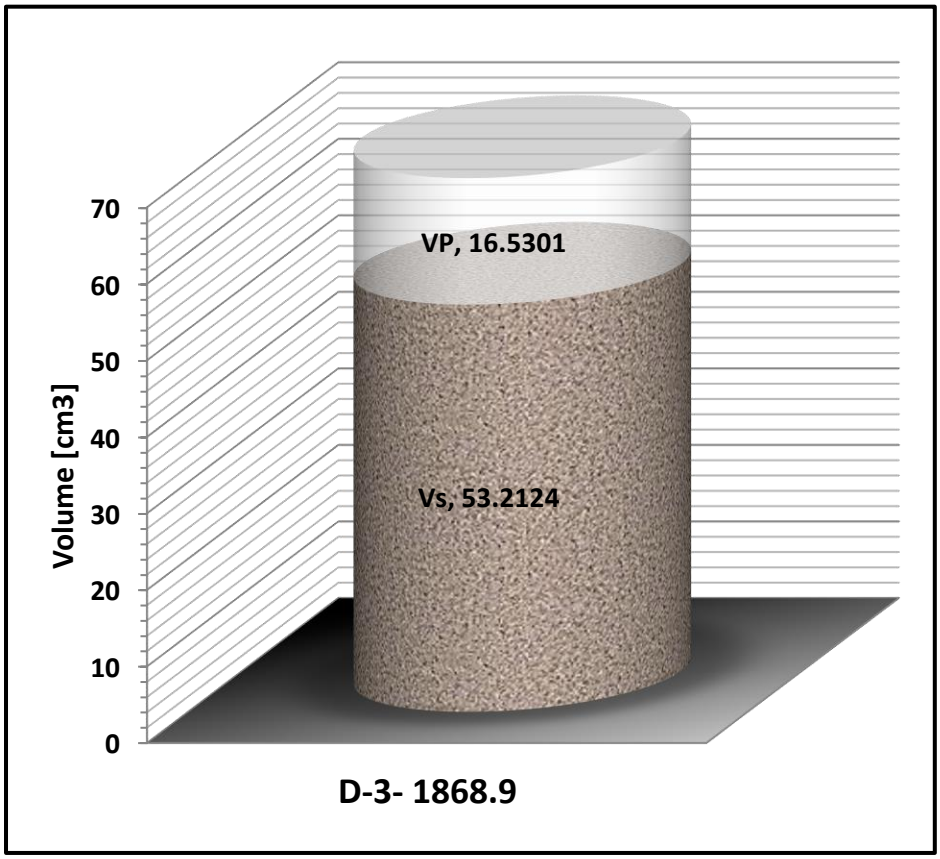

Core ID	D-3-1872.1

Porosity	22%

Core geometry	
d [cm]	3.79
l [cm]	6.185
A [cm^2]	11.282
Vtotal [cm^3]	69.776
m(dry) [g]	146.3

	P1	P2	Vs	ρ	ϕ	ρ SD
	[psi]	[psi]	[cm3]	[g/cm3]	[-]	[g/cm3]
1	17.802	8.703	54.829	2.668	0.214	0.003
2	17.543	8.573	54.758	2.672	0.215	
3	17.351	8.478	54.733	2.673	0.216	
		Average ->	54.773	2.671	0.215	

Lab. Properties	
Ta [°C]	22.5
Pa [bar]	1.0090

Average Volume	54.7731
Average Density	2.6710
Standard Deviation	0.0030

He-porosimeter	
Vc	146.5
VR micro	5.6212
VR small	11.0142
VR large	87.7104

69.776	
54.773	15.003
15.003	

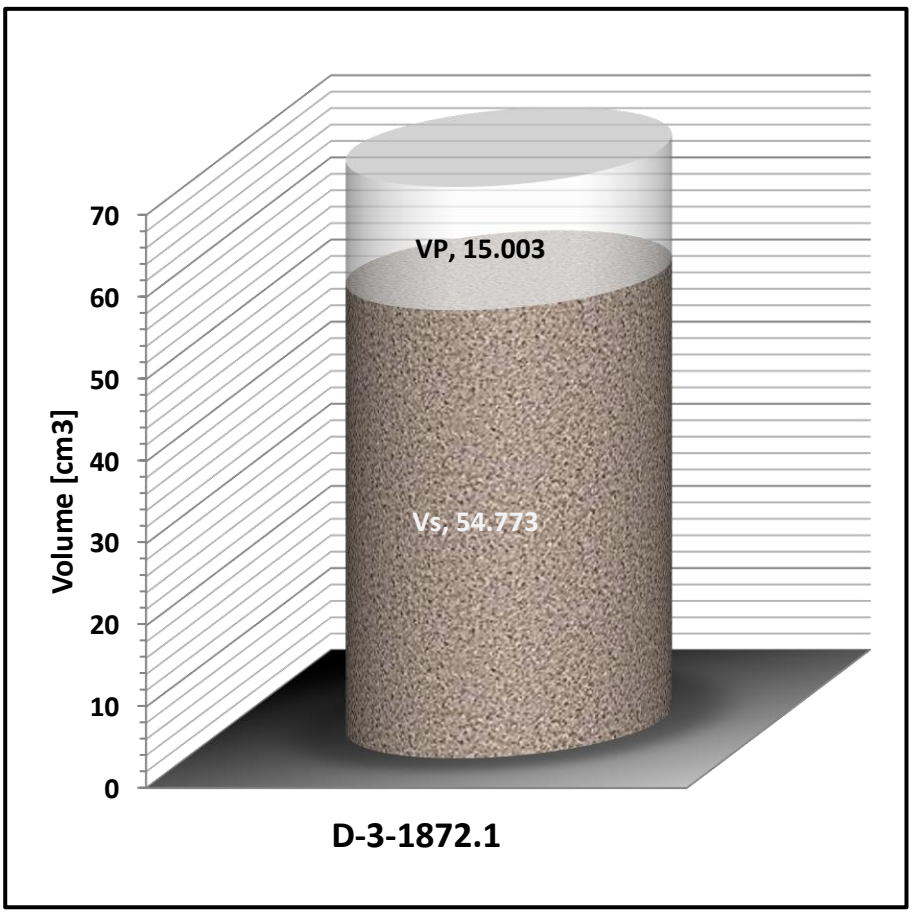

Initail Permeability

D2_ 4				D2_ 5				D2_ 6			
Time [hh:mm:ss]	Volume [cm3]	Permeability [mD]	Av. k [mD]	Time [hh:mm:ss]	Volume [cm3]	Permeability [mD]	Av. k [mD]	Time [hh:mm:ss]	Volume [cm3]	Permeability [mD]	Av. k [mD]
0:01:00	1.51	219.21	217.90	0:01:00	1.58	322.11	333.05	0:01:00	1.82	676.11	673.85
0:02:00	3.15	215.89		0:02:00	3.23	341.65		0:02:00	3.43	673.41	
0:03:00	4.8	220.85		0:03:00	4.83	332.41		0:03:00	4.99	671.18	
0:04:00	6.37	215.66		0:04:00	6.48	336.01		0:04:00	6.65	674.69	
0:05:00	7.97	215.58	218.20	0:05:00	8.12	342.26	337.93	0:05:00	8.3	671.39	671.70
0:06:00	9.63	221.71		0:06:00	9.7	334.90		0:06:00	9.88	671.04	
0:07:00	11.22	218.40		0:07:00	11.3	339.27		0:07:00	11.52	674.09	
0:08:00	12.79	217.12		0:08:00	12.99	335.30		0:08:00	13.19	670.28	
0:09:00	14.46	221.88	219.70	0:09:00	14.59	340.44	336.11	0:09:00	14.78	668.59	670.21
0:10:00	16.06	218.46		0:10:00	16.18	337.50		0:10:00	16.35	670.05	
0:11:00	17.61	218.88		0:11:00	17.82	332.60		0:11:00	18.03	671.39	
0:12:00	19.24	219.57		0:12:00	19.47	333.91		0:12:00	19.66	670.82	
0:13:00	20.9	218.66		0:13:00	21.02	342.39		0:13:00	21.23	659.37	
0:14:00	22.48	225.53	220.63	0:14:00	22.67	341.08	337.58	0:14:00	22.88	662.77	663.54
0:15:00	24.03	222.23		0:15:00	24.32	339.07		0:15:00	24.53	664.22	
0:16:00	25.72	221.08		0:16:00	25.89	334.75		0:16:00	26.12	678.59	
0:17:00	27.32	213.69		0:17:00	27.49	335.43		0:17:00	27.71	648.56	
0:18:00	28.87	223.98	231.31	0:18:00	29.17	342.50	334.95	0:18:00	29.4	650.50	628.60
0:19:00	30.5	234.80		0:19:00	30.76	332.95		0:19:00	31.02	623.55	
0:20:00	32.18	232.00		0:20:00	32.32	326.30		0:20:00	32.55	602.75	
0:21:00	33.75	234.45		0:21:00	33.98	338.05		0:21:00	34.21	637.62	
0:22:00	35.31	232.39	236.47	0:22:00	35.64	339.17	335.32	0:22:00	35.86	620.84	617.98
0:23:00	36.97	235.24		0:23:00	37.22	337.73		0:23:00	37.43	617.19	
0:24:00	38.6	234.65		0:24:00	38.79	327.28		0:24:00	39.02	610.73	
0:25:00	40.14	243.58		0:25:00	40.48	337.11		0:25:00	40.71	623.17	
0:26:00	41.78	247.17		0:26:00	42.11	334.52		0:26:00	42.33	623.55	
0:27:00	43.44	242.62	248.36	0:27:00	43.66	323.84	326.68	0:27:00	43.87	606.69	616.35
0:28:00	45.03	252.22		0:28:00	45.34	333.68		0:28:00	45.51	614.57	
0:29:00	46.62	248.14		0:29:00	46.97	321.68		0:29:00	47.19	629.56	
0:30:00	48.27	250.47		0:30:00	48.55	327.52		0:30:00	48.75	614.57	
0:31:00	49.9	253.31	251.80	0:31:00	50.14	321.32	327.17	0:31:00	50.35	615.85	602.47
0:32:00	51.45	247.59		0:32:00	51.82	330.49		0:32:00	52.02	606.10	
0:33:00	53.1	249.05		0:33:00	53.42	330.19		0:33:00	53.62	594.75	
0:34:00	54.73	257.23		0:34:00	54.98	326.67		0:34:00	55.19	593.16	
0:35:00	56.32	255.99	255.97	0:35:00	56.65	337.86	328.54	0:35:00	56.84	608.43	602.43
0:36:00	57.9	248.91		0:36:00	58.31	334.37		0:36:00	58.49	608.43	
0:37:00	59.56	259.29		0:37:00	59.84	314.69		0:37:00	60.05	588.18	
0:38:00	61.18	259.68		0:38:00	61.47	327.26		0:38:00	61.68	604.68	
0:39:00	62.74	250.06		0:39:00	63.13	324.49		0:39:00	63.34	590.84	
0:40:00	64.38	255.95	257.69	0:40:00	64.75	327.74	325.76	0:40:00	64.91	580.09	584.69
0:41:00	66.04	261.97		0:41:00	66.31	317.69		0:41:00	66.46	575.00	
0:42:00	67.61	255.46		0:42:00	67.99	330.49		0:42:00	68.13	594.40	
0:43:00	69.21	257.37		0:43:00	69.63	327.14		0:43:00	69.76	589.27	
0:44:00	70.86	260.39	258.70	0:44:00	71.16	322.61	327.04	0:44:00	71.29	576.87	585.35
0:45:00	72.47	258.98		0:45:00	72.79	333.75		0:45:00	72.92	604.68	
0:46:00	74.04	252.54		0:46:00	74.47	325.98		0:46:00	74.58	590.84	
0:47:00	75.69	262.88		0:47:00	76.06	325.80		0:47:00	76.12	569.00	
0:48:00	77.32	264.05	261.39	0:48:00	77.64	321.81	326.31	0:48:00	77.69	567.57	571.46
0:49:00	78.89	256.83		0:49:00	79.29	329.91		0:49:00	79.34	572.91	
0:50:00	80.5	261.97		0:50:00	80.92	326.28		0:50:00	80.95	580.90	
0:51:00	82.14	262.73		0:51:00	82.5	327.22		0:51:00	82.49	564.48	
0:52:00	83.74	263.38		0:52:00	84.13	322.71		0:52:00	84.13	590.56	
0:53:00	85.34	264.67	265.20	0:53:00	85.79	330.42	329.70	0:53:00	85.75	585.65	575.29
0:54:00	86.98	264.04		0:54:00	87.37	330.48		0:54:00	87.32	578.93	
0:55:00	88.6	265.45		0:55:00	88.98	332.62		0:55:00	88.92	571.69	
0:56:00	90.16	266.65		0:56:00	90.63	325.28		0:56:00	90.55	564.90	
0:57:00	91.81	265.61	267.05	0:57:00	92.25	327.38	329.14	0:57:00	92.15	571.69	558.67
0:58:00	93.44	266.67		0:58:00	93.81	323.74		0:58:00	93.73	559.13	
0:59:00	95.04	267.82		0:59:00	95.47	335.10		0:59:00	95.36	557.56	
1:00:00	96.65	268.11		1:00:00	97.11	330.34		1:00:00	96.96	546.29	
1:01:00	98.31	266.75	267.53	1:01:00	98.67	323.02	329.44	1:01:00	98.53	537.04	552.28
1:02:00	99.91	268.93		1:02:00	100.3	334.52		1:02:00	100.16	559.64	
1:03:00	101.49	266.30		1:03:00	101.95	331.28		1:03:00	101.78	557.24	
1:04:00	103.13	268.15		1:04:00	103.56	328.95		1:04:00	103.37	555.21	
1:05:00	104.77	267.95		1:05:00	105.13	320.43		1:05:00	104.97	548.32	
1:06:00	106.35	269.80	269.02	1:06:00	106.78	329.84	330.17	1:06:00	106.61	547.77	535.69
1:07:00	107.98	269.25		1:07:00	108.41	329.76		1:07:00	108.22	537.75	
1:08:00	109.6	269.54		1:08:00	109.98	325.45		1:08:00	109.79	524.39	
1:09:00	111.21	267.48		1:09:00	111.61	335.63		1:09:00	111.42	532.85	
1:10:00	112.81	269.70	268.25	1:10:00	113.25	333.98	331.18	1:10:00	113.05	523.56	526.21
1:11:00	114.45	267.18		1:11:00	114.85	335.05		1:11:00	114.65	524.90	
1:12:00	116.05	269.06		1:12:00	116.45	330.56		1:12:00	116.26	528.18	
1:13:00	117.65	267.06		1:13:00	118.08	325.14		1:13:00	117.87	528.18	
1:14:01	119.29	264.66	268.16	1:14:00	119.71	331.94	324.18	1:14:00	119.48	540.69	526.02
1:15:01	120.9	270.13		1:15:01	121.29	316.48		1:15:01	121.08	519.07	
1:16:01	122.48	268.59		1:16:01	122.91	323.15		1:16:01	122.7	522.17	
1:17:01	124.11	269.25		1:17:01	124.54	325.14		1:17:01	124.32	522.17	
1:18:01	125.74	267.25		1:18:01	126.13	320.62		1:18:01	125.91	512.50	
1:19:01	127.34	266.81	268.26	1:19:01	127.76	324.10	322.11	1:19:01	127.53	514.97	511.04
1:20:01	128.94	269.35		1:20:01	129.39	320.65		1:20:01	129.15	510.57	
1:21:01	130.58	268.69		1:21:01	131	327.15		1:21:01	130.74	507.18	
1:22:01	132.19	268.18		1:22:01	132.58	316.53		1:22:01	132.36	511.44	
1:23:01	133.78	269.54	268.06	1:23:01	134.23	320.16	316.49	1:23:01	133.99	504.24	500.51
1:24:01	135.41	267.18		1:24:01	135.85	314.34		1:24:01	135.59	494.96	
1:25:01	137.03	268.26		1:25:01	137.42	308.85		1:25:01	137.18	494.35	
1:26:01	138.63	267.27		1:26:01	139.06	322.62		1:26:01	138.81	508.50	
1:27:01	140.24	269.43	269.09	1:27:01	140.71	324.59	322.01	1:27:01	140.43	502.83	492.13
1:28:01	141.88	268.34		1:28:01	142.3	321.67		1:28:01	142.02	487.77	
1:29:01	143.46	268.85		1:29:01	143.9	319.16		1:29:01	143.64	486.45	
1:30:01	145.07	269.73		1:30:01	145.54	322.62		1:30:01	145.29	491.46	
1:31:01	146.7	268.80		1:31:01	147.16	327.03		1:31:01	146.89	484.39	
1:32:01	148.31	267.32	268.00	1:32:01	148.74	318.95	321.36	1:32:01	148.49	482.02	476.48
1:33:01	149.91	268.37		1:33:01	150.38	322.62		1:33:01	150.11	477.13	
1:34:01	151.53	267.26		1:34:01	152	323.15		1:34:01	151.74	477.02	
1:35:01	153.15	269.07		1:35:01	153.58	320.70		1:35:01	153.34	469.74	
		252.74	**252.58**	1:36:01	155.22	328.20	328.51	1:36:01	154.96	469.62	472.25
				1:37:01	156.85	329.76		1:37:01	156.6	472.45	
				1:38:01	158.44	326.31		1:38:01	158.2	473.51	
				1:39:01	160.07	329.76		1:39:01	159.81	473.43	
				1:40:01	161.7	329.76	326.12	1:40:01	161.44	466.65	462.52
				1:41:01	163.31	329.68		1:41:01	163.06	463.79	
				1:42:01	164.89	318.95		1:42:01	164.65	455.20	
				1:43:01	166.53	326.08		1:43:01	166.3	464.45	
				1:44:01	168.16	324.10		1:44:01	167.92	448.47	
				1:45:01	169.75	317.17	322.78	1:45:01	169.52	449.00	450.34
				1:46:01	171.37	323.15		1:46:01	171.14	448.47	
				1:47:01	173.02	329.13		1:47:01	172.79	450.69	
				1:48:01	174.61	321.67		1:48:01	174.4	453.19	
				1:49:01	176.21	325.83	327.09	1:49:01	176.01	453.19	447.86
				1:50:01	177.84	330.49		1:50:01	177.64	444.56	
				1:51:01	179.45	326.07		1:51:01	179.29	450.02	

D- 2- 4	D- 2- 5	D- 2- 6
252.58	328.2	552.44

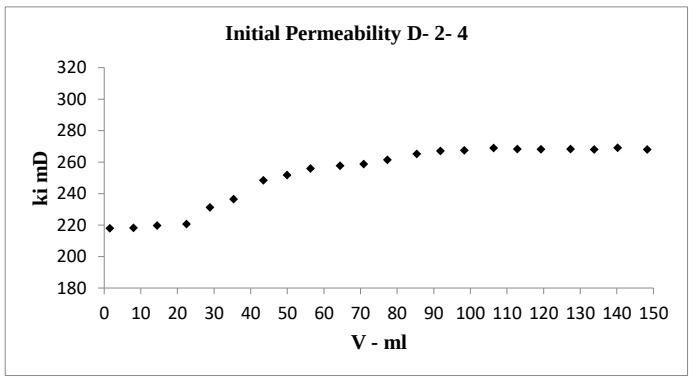

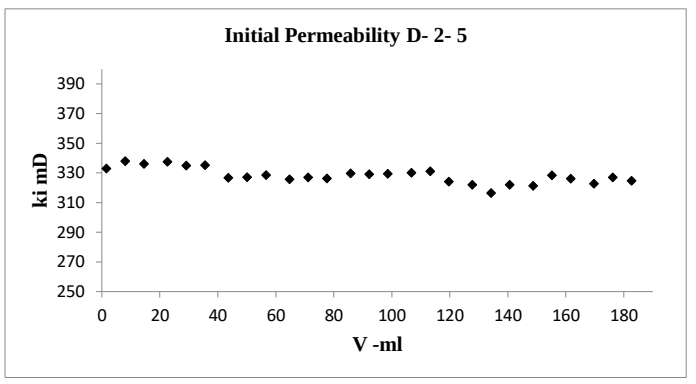

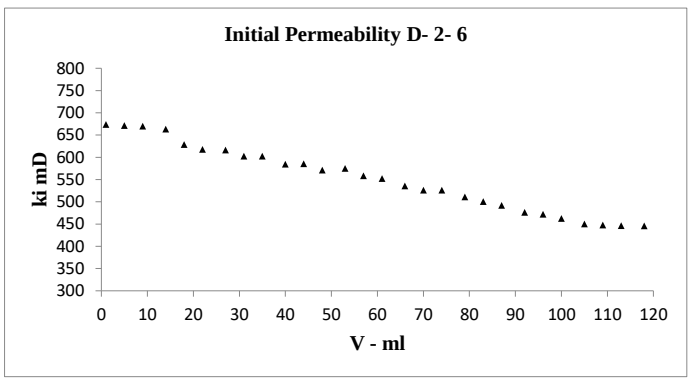

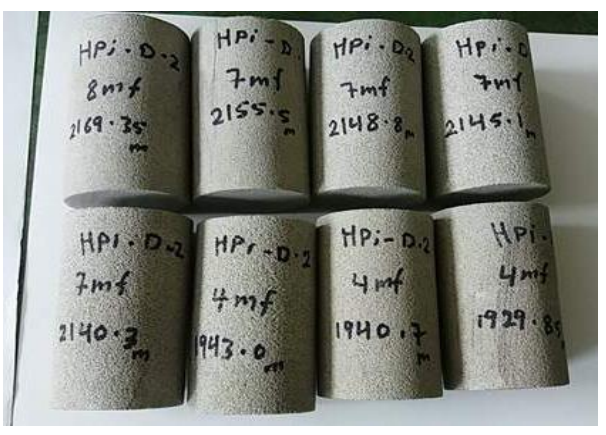

				1:52:01	181.07	325.96		1:52:01	180.88	443.65	
				1:53:01	182.69	324.20	324.79	1:53:01	182.5	444.38	446.38
				1:54:01	184.31	323.15		1:54:01	184.14	447.72	
				1:55:01	185.91	323.69		1:55:01	185.78	445.69	
						328.12	**328.20**	1:56:01	187.39	447.72	
								1:57:01	189.03	441.96	
								1:58:01	190.63	443.23	445.95
								1:59:01	192.25	447.30	**552.44**
								2:00:01	193.89	445.87	
								2:01:01	195.52	447.40	
										551.84	

\

Initial Permeability

D3_ 1				D3_ 2			
Time [hh:mm:ss]	Volume [cm3]	Permeability [mD]	Av k [mD]	Time [hh:mm:ss]	Volume [cm3]	Permeability [mD]	Av k [mD]
0:01:00	1.51	42.34	42.93	0:01:00	1.66	119.81	118.18
0:02:00	3.12	44.11		0:02:00	3.38	119.66	
0:03:00	4.77	43.57		0:03:00	5.05	117.73	
0:04:00	6.35	41.69		0:04:00	6.64	115.50	
0:05:00	7.94	41.40	40.40	0:05:00	8.36	118.61	118.08
0:06:00	9.58	40.85		0:06:00	10.06	118.16	
0:07:00	11.2	40.30		0:07:00	11.69	116.87	
0:08:00	12.77	39.05		0:08:00	13.34	118.68	
0:09:00	14.42	39.59	38.49	0:09:00	15.04	117.65	117.08
0:10:00	16.05	38.92		0:10:00	16.67	116.16	
0:11:00	17.61	37.66		0:11:00	18.3	117.08	
0:12:00	19.22	37.77		0:12:00	20	117.42	
0:13:00	20.87	37.73	36.95	0:13:00	21.65	117.77	117.14
0:14:00	22.47	36.92		0:14:00	23.21	117.90	
0:15:00	24.06	36.36		0:15:00	24.91	116.23	
0:16:00	25.71	36.78		0:16:00	26.6	116.67	
0:17:00	27.31	35.63	35.63	0:17:00	28.21	115.36	116.48
0:18:00	28.89	35.48		0:18:00	29.84	115.10	
0:19:00	30.51	35.56		0:19:00	31.55	117.70	
0:20:00	32.17	35.86		0:20:00	33.19	117.74	
0:21:00	33.75	34.70	34.92	0:21:00	34.79	118.41	117.29
0:22:00	35.34	34.36		0:22:00	36.48	115.37	
0:23:00	37.02	35.53		0:23:00	38.18	120.29	
0:24:00	38.65	35.11		0:24:00	39.78	115.11	
0:25:00	40.2	34.05	34.94	0:25:00	41.44	117.01	117.04
0:26:00	41.82	35.03		0:26:00	43.14	120.07	
0:27:00	43.47	35.62		0:27:00	44.74	115.69	
0:28:00	45.04	35.04		0:28:00	46.39	115.37	
0:29:00	46.61	34.61	34.93	0:29:00	48.09	114.61	117.01
0:30:00	48.23	34.93		0:30:00	49.73	115.11	
0:31:00	49.83	35.25		0:31:00	51.34	119.05	
0:32:00	51.4	34.92		0:32:00	53.05	119.29	
0:33:00	53.03	35.31	35.01	0:33:00	54.72	115.80	116.05
0:34:00	54.65	34.97		0:34:00	56.32	117.17	
0:35:00	56.2	34.39		0:35:00	58	115.33	
0:36:00	57.81	35.37		0:36:00	59.7	115.91	
0:37:00	59.45	35.34	35.55	0:37:00	61.32	115.65	115.57
0:38:00	61.03	35.01		0:38:00	62.98	115.45	
0:39:00	62.6	35.29		0:39:00	64.66	115.07	
0:40:00	64.26	36.54		0:40:00	66.31	116.12	
0:41:00	65.88	35.91	35.93	0:41:00	67.95	114.03	113.64
0:42:00	67.44	35.50		0:42:00	69.65	115.00	
0:43:00	69.03	35.87		0:43:00	71.31	113.12	
0:44:00	70.67	36.44		0:44:00	72.95	112.42	
0:45:00	72.25	35.89	36.10	0:45:00	74.63	113.23	111.36
0:46:00	73.82	35.65		0:46:00	76.31	111.65	
0:47:00	75.46	36.37		0:47:00	77.93	108.67	
0:48:00	77.09	36.51		0:48:00	79.61	111.89	
0:49:00	78.65	35.54	35.85	0:49:00	81.3	111.04	110.02
0:50:00	80.25	35.88		0:50:00	82.95	110.73	
0:51:00	81.88	36.05		0:51:00	84.59	108.83	
0:52:00	83.47	35.93		0:52:00	86.29	109.48	
0:53:00	85.06	35.87	35.57	0:53:00	87.95	108.60	106.92
0:54:00	86.69	35.86		0:54:00	89.57	105.58	
0:55:00	88.28	35.28		0:55:00	91.25	106.71	
0:56:00	89.86	35.25		0:56:00	92.93	106.78	
0:57:00	91.48	35.53	35.40	0:57:00	94.56	103.74	104.08
0:58:00	93.12	35.83		0:58:00	96.24	105.51	
0:59:00	94.7	34.81		0:59:00	97.91	104.00	
1:00:00	96.33	35.42		1:00:00	99.55	103.07	
1:01:00	97.96	34.68	34.46	1:01:00	101.22	103.24	103.02
1:02:00	99.57	34.62		1:02:00	102.9	103.03	
1:03:00	101.15	33.97		1:03:00	104.55	103.00	
1:04:00	102.79	34.56		1:04:00	106.21	102.82	
1:05:00	104.42	34.23	33.75	1:05:00	107.89	102.76	101.44
1:06:00	106.01	33.49		1:06:00	109.55	101.87	
1:07:00	107.63	33.69		1:07:00	111.18	99.50	
1:08:00	109.27	33.61		1:08:00	112.87	101.62	
1:09:00	110.87	33.22	33.05	1:09:00	114.53	100.34	100.04
1:10:00	112.46	32.90		1:10:00	116.18	100.49	
1:11:00	114.09	33.12		1:11:00	117.84	99.49	
1:12:00	115.7	32.98		1:12:00	119.52	99.85	
1:13:00	117.31	32.83	32.43	1:13:00	121.15	97.29	97.61
1:14:00	118.95	32.89		1:14:00	122.81	97.97	
1:15:01	120.57	31.97		1:15:01	124.49	96.72	
1:16:01	122.15	32.02		1:16:01	126.15	98.44	
1:17:01	123.77	32.58	32.22	1:17:01	127.8	97.88	96.90
1:18:01	125.4	32.41		1:18:01	129.48	97.75	
1:19:01	127	32.05		1:19:01	131.15	96.95	
1:20:01	128.6	31.85		1:20:01	132.78	95.02	
1:21:01	130.24	32.21	31.66	1:21:01	134.45	95.81	95.48
1:22:01	131.84	31.51		1:22:01	136.13	96.00	
1:23:01	133.44	31.49		1:23:01	137.77	94.83	
1:24:01	135.06	31.42		1:24:01	139.43	95.27	
1:25:01	136.71	31.80	31.22	1:25:01	141.11	95.35	93.42
1:26:01	138.31	31.10		1:26:01	142.75	93.40	

k D- 3- 1	k D- 3- 2	
32.37	103.33	

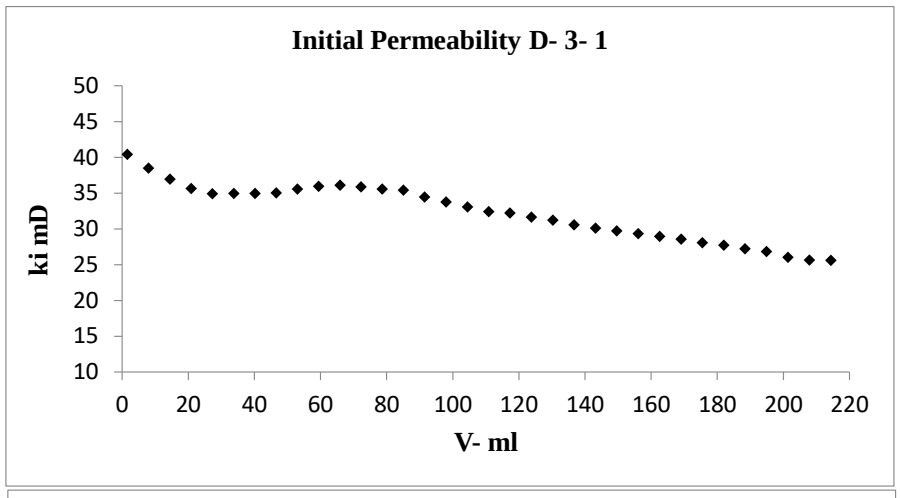

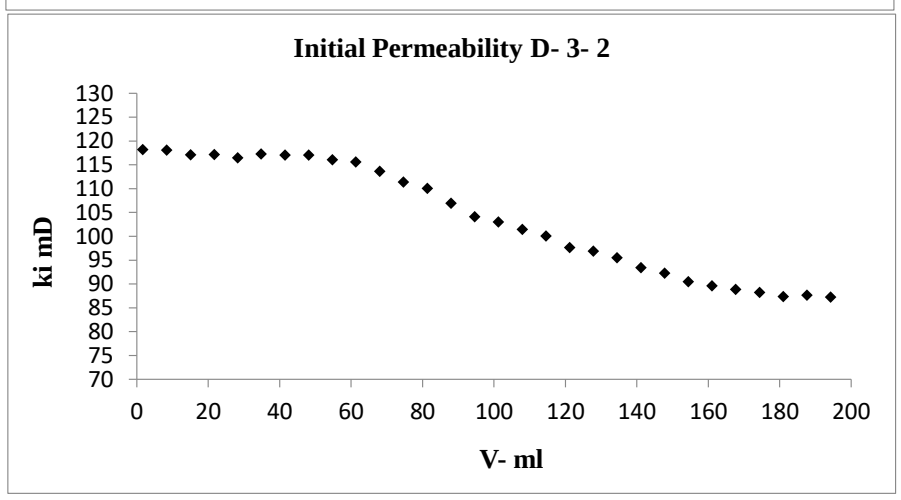

1:27:01	139.92	30.96		1:27:01	144.38	91.81	
1:28:01	141.55	31.01		1:28:01	146.06	93.12	
1:29:01	143.15	30.70	30.55	1:29:01	147.74	93.12	92.24
1:30:01	144.76	30.66		1:30:01	149.39	91.82	
1:31:01	146.39	30.59		1:31:01	151.05	91.71	
1:32:01	148	30.26		1:32:01	152.73	92.29	
1:33:01	149.61	30.28	30.10	1:33:01	154.37	89.91	90.48
1:34:01	151.24	30.27		1:34:01	156.02	89.27	
1:35:01	152.87	30.19		1:35:01	157.71	91.41	
1:36:01	154.46	29.66		1:36:01	159.37	91.33	
1:37:01	156.08	29.94	29.72	1:37:01	161.03	91.33	89.60
1:38:01	157.71	29.76		1:38:01	162.7	90.32	
1:39:01	159.32	29.58		1:39:01	164.34	88.37	
1:40:01	160.93	29.61		1:40:01	165.98	88.37	
1:41:01	162.57	29.82	29.34	1:41:01	167.66	89.32	88.83
1:42:01	164.17	29.09		1:42:01	169.33	88.39	
1:43:01	165.77	29.19		1:43:01	170.99	89.73	
1:44:01	167.39	29.27		1:44:01	172.62	87.88	
1:45:01	169.03	29.40	28.93	1:45:01	174.31	89.73	88.22
1:46:01	170.64	28.97		1:46:01	175.97	88.44	
1:47:01	172.24	28.67		1:47:01	177.61	86.87	
1:48:01	173.86	28.67		1:48:01	179.29	87.84	
1:49:01	175.49	28.86	28.55	1:49:01	180.96	86.99	87.36
1:50:01	177.09	28.41		1:50:01	182.6	87.19	
1:51:01	178.71	28.44		1:51:01	184.26	88.85	
1:52:01	180.34	28.48		1:52:01	185.94	86.42	
1:53:01	181.95	28.24	28.06	1:53:01	187.59	89.27	87.62
1:54:01	183.57	28.20		1:54:01	189.25	85.70	
1:55:01	185.19	27.94		1:55:01	190.93	87.80	
1:56:01	186.8	27.86		1:56:01	192.58	87.70	
1:57:01	188.4	27.70	27.72	1:57:01	194.23	85.76	87.25
1:58:01	190.03	27.86		1:58:01	195.93	87.45	
1:59:01	191.67	27.91		1:59:01	197.58	86.94	
2:00:01	193.27	27.39		2:00:01	199.24	88.84	
2:01:01	194.88	27.26	27.22	2:01:01	200.91	87.84	87.70
2:02:01	196.51	27.25		2:02:01	202.6	86.62	
2:03:01	198.13	27.25		2:03:01	204.24	88.67	
2:04:01	199.74	27.11		2:04:01	205.9	87.66	
2:05:01	201.37	27.15	26.84			**103.33**	
2:06:01	203	27.11					
2:07:01	204.59	26.53					
2:08:01	206.2	26.56					
2:09:01	207.83	25.66	26.01				
2:10:01	209.46	26.75					
2:11:01	211.07	25.25					
2:12:01	212.7	26.38					
2:13:01	214.31	25.19	25.64				
2:14:01	215.93	25.41					
2:15:01	217.54	25.96					
2:16:01	219.16	25.99					
2:17:01	220.77	24.92	25.59				
2:18:01	222.39	25.87					
2:19:01	224.04	26.15					
2:20:01	225.64	25.43					
2:21:01	227.24	25.38	25.51				
2:22:01	228.88	25.80					
2:23:01	230.51	25.63					
2:24:01	232.11	25.24					
2:25:01	233.73	25.32					
		32.37					

Initiality Permeability

D4_1				D4_2			
Time [hh:mm:ss]	Volume [cm3]	Permeability [mD]	Av.k [mD]	Time [hh:mm:ss]	Volume [cm3]	Permeability [mD]	Av.k [mD]
0:01:00	1.63	570.27	547.24	0:01:00	1.6	365.55	
0:02:00	3.29	556.13		0:02:00	3.26	363.26	
0:03:00	5	546.21		0:03:00	4.9	365.80	
0:04:00	6.67	516.37		0:04:00	6.6	363.92	
0:05:00	8.28	525.18	547.58	0:05:00	8.25	365.14	
0:06:00	10	556.13		0:06:00	9.85	363.95	364.60
0:07:00	11.7	561.50		0:07:00	11.54	361.56	
0:08:00	13.31	547.50		0:08:00	13.24	363.57	
0:09:00	15.01	546.78	559.77	0:09:00	14.85	364.32	
0:10:00	16.7	535.14		0:10:00	16.5	364.00	
0:11:00	18.32	565.54		0:11:00	18.22	365.16	
0:12:00	19.96	591.61		0:12:00	19.85	363.60	363.70
0:13:00	21.67	579.37	567.73	0:13:00	21.45	361.17	
0:14:00	23.32	564.24		0:14:00	23.17	361.46	
0:15:00	24.95	557.40		0:15:00	24.84	360.24	
0:16:00	26.66	569.92		0:16:00	26.44	359.41	
0:17:00	28.33	576.43	581.80	0:17:00	28.12	359.30	
0:18:00	29.92	565.80		0:18:00	29.82	360.17	360.29
0:19:00	31.64	590.37		0:19:00	31.46	358.06	
0:20:00	33.34	594.60		0:20:00	33.08	359.96	
0:21:00	34.95	603.26	609.44	0:21:00	34.81	363.83	
0:22:00	36.59	602.23		0:22:00	36.47	353.95	
0:23:00	38.33	627.68		0:23:00	38.05	356.89	
0:24:00	39.96	604.60		0:24:00	39.76	357.18	358.31
0:25:00	41.55	601.89	617.49	0:25:00	41.44	350.92	
0:26:00	43.29	644.10		0:26:00	43.03	348.58	
0:27:00	44.98	613.25		0:27:00	44.7	348.54	
0:28:00	46.58	610.71		0:28:00	46.42	347.50	
0:29:00	48.26	630.77	642.21	0:29:00	48.06	342.12	
0:30:00	49.97	639.43		0:30:00	49.67	344.88	347.09
0:31:00	51.6	659.08		0:31:00	51.4	342.27	
0:32:00	53.22	639.57		0:32:00	53.07	348.83	
0:33:00	54.95	657.60	653.89	0:33:00	54.65	333.80	
0:34:00	56.59	651.66		0:34:00	56.34	332.68	
0:35:00	58.21	653.60		0:35:00	58.06	337.51	
0:36:00	59.92	652.69		0:36:00	59.66	340.76	339.31
0:37:00	61.6	638.59	650.93	0:37:00	61.29	339.32	
0:38:00	63.2	642.71		0:38:00	63.01	341.13	
0:39:00	64.88	660.42		0:39:00	64.65	332.77	
0:40:00	66.6	662.00		0:40:00	66.25	330.43	
0:41:00	68.24	674.99	669.49	0:41:00	67.95	334.65	
0:42:00	69.85	661.16		0:42:00	69.6	343.70	337.00
0:43:00	71.54	662.94		0:43:00	71.22	339.44	
0:44:00	73.23	678.86		0:44:00	72.88	328.88	
0:45:00	74.81	671.75	670.89	0:45:00	74.57	332.68	
0:46:00	76.49	680.79		0:46:00	76.17	337.54	
0:47:00	78.2	670.83		0:47:00	77.83	332.09	
0:48:00	79.82	660.18		0:48:00	79.54	343.07	335.62
0:49:00	81.48	737.10	720.85	0:49:00	81.19	338.22	
0:50:00	83.17	678.52		0:50:00	82.78	338.63	
0:51:00	84.8	731.58		0:51:00	84.49	341.22	
0:52:00	86.44	736.19		0:52:00	86.16	329.74	
0:53:00	88.15	752.63	765.67	0:53:00	87.77	327.93	
0:54:00	89.82	765.78		0:54:00	89.45	338.86	335.77
0:55:00	91.41	768.46		0:55:00	91.15	341.22	
0:56:00	93.12	775.82		0:56:00	92.77	337.81	
0:57:00	94.8	780.50	773.14	0:57:00	94.4	339.59	
0:58:00	96.42	784.32		0:58:00	96.09	333.00	
0:59:00	98.07	768.36		0:59:00	97.77	338.62	
1:00:00	99.79	759.40		1:00:00	99.39	346.62	339.48
1:01:00	101.42	772.89	772.68	1:01:00	101.08	345.58	
1:02:00	103.05	757.27		1:02:00	102.75	336.86	
1:03:00	104.73	761.28		1:03:00	104.35	343.53	
1:04:00	106.42	799.28		1:04:00	106.05	333.10	
1:05:00	108.03	746.10	778.97	1:05:00	107.74	336.99	
1:06:00	109.71	761.28		1:06:00	109.35	339.22	339.21
1:07:00	111.39	792.51		1:07:00	111.02	347.65	
1:08:00	113.04	816.02		1:08:00	112.71	331.02	
1:09:00	114.69	794.66	792.22	1:09:00	114.35	337.27	
1:10:00	116.39	797.85		1:10:00	115.98	341.63	
1:11:00	118.03	794.00		1:11:00	117.68	340.73	
1:12:00	119.68	782.37		1:12:00	119.35	333.22	338.59
1:13:00	121.35	775.85	811.63	1:13:00	120.96	336.29	
1:14:01	123.03	844.48		1:14:00	122.65	340.30	
1:15:01	124.64	822.78		1:15:01	124.32	330.40	
1:16:01	126.33	803.41		1:16:01	125.94	333.48	
1:17:01	128.01	819.84	826.53	1:17:01	127.61	341.87	
1:18:01	129.63	827.89		1:18:01	129.29	333.20	335.92
1:19:01	131.31	835.35		1:19:01	130.94	335.54	
1:20:01	133.01	823.05		1:20:01	132.59	337.77	

ki D- 4- 1	ki D- 4- 2
731.97	343.20

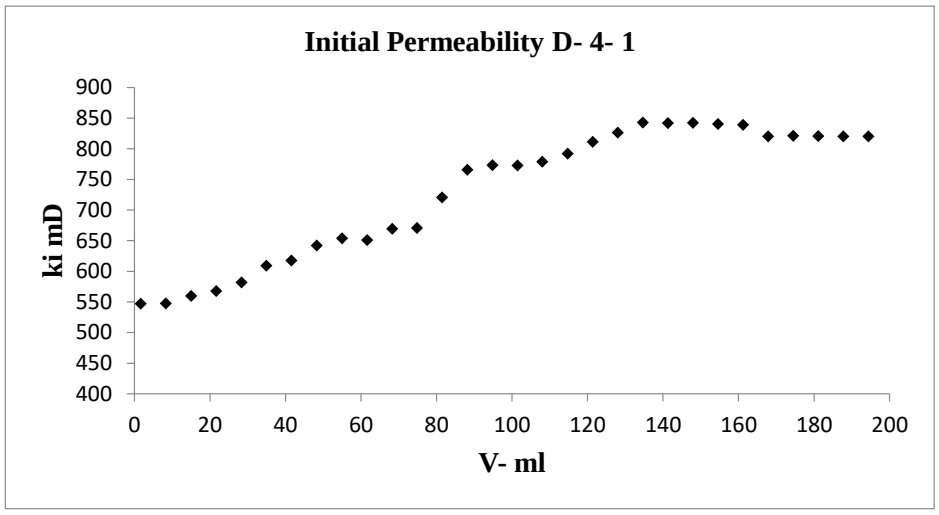

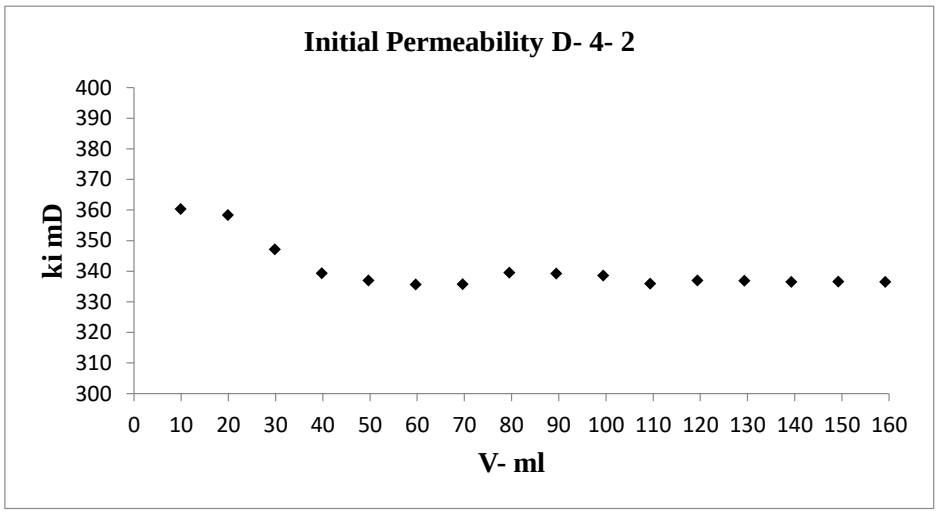

1:21:01	134.65	852.31	843.02	1:21:01	134.29	341.57	
1:22:01	136.28	849.52		1:22:01	135.93	334.61	
1:23:01	137.96	837.61		1:23:01	137.56	332.20	
1:24:01	139.63	832.62		1:24:01	139.25	340.30	337.00
1:25:01	141.26	810.49	842.09	1:25:01	140.92	331.49	
1:26:01	142.95	844.89		1:26:01	142.55	340.86	
1:27:01	144.62	855.82		1:27:01	144.22	335.48	
1:28:01	146.26	857.16		1:28:01	145.91	341.81	
1:29:01	147.93	847.91	842.40	1:29:01	147.53	332.74	
1:30:01	149.58	842.38		1:30:01	149.19	339.07	336.91
1:31:01	151.23	837.34		1:31:01	150.87	334.68	
1:32:01	152.9	841.97		1:32:01	152.52	334.26	
1:33:01	154.58	838.06	840.40	1:33:01	154.17	338.15	
1:34:01	156.23	847.51		1:34:01	155.85	339.77	
1:35:01	157.86	839.52		1:35:01	157.48	333.68	
1:36:01	159.55	836.52		1:36:01	159.14	338.69	336.54
1:37:01	161.21	839.01	838.94	1:37:01	160.82	338.66	
1:38:01	162.84	837.12		1:38:01	162.48	331.73	
1:39:01	164.52	843.81		1:39:01	164.12	339.51	
1:40:01	166.19	835.82		1:40:01	165.8	336.45	
1:41:01	167.83	859.60	820.47	1:41:01	167.48	334.64	
1:42:01	169.48	820.43		1:42:01	169.1	338.35	336.56
1:43:01	171.15	808.52		1:43:01	170.74	338.80	
1:44:01	172.78	793.33		1:44:01	172.45	337.72	
1:45:01	174.45	814.96	821.10	1:45:01	174.1	336.18	
1:46:01	176.13	835.35		1:46:01	175.74	338.56	
1:47:01	177.79	815.98		1:47:01	177.41	336.26	
1:48:01	179.41	818.10		1:48:01	179.09	331.55	336.51
1:49:01	181.11	829.60	820.84	1:49:01	180.72	338.34	
1:50:01	182.77	820.96				**343.20**	**343.24**
1:51:01	184.4	822.68					
1:52:01	186.07	810.10					
1:53:01	187.77	818.36	820.44				
1:54:01	189.39	819.89					
1:55:01	191.04	820.43					
1:56:01	192.72	823.10					
1:57:01	194.38	815.98	820.56				
1:58:01	196.02	819.91					
1:59:01	197.7	826.79					
2:00:01	199.36	819.57					
2:01:01	201	818.07	820.65				
2:02:01	202.66	817.39					
2:03:01	204.34	820.21					
2:04:01	205.99	826.94					
		731.97	**731.97**				

50 ml/ h				100 ml/ h				200 ml/ h			
time, [hh:mm:ss]	V, [cm^3]	k, [mD]		time, [hh:mm:ss]	V, [cm^3]	k, [mD]		time, [hh:mm:ss]	V, [cm^3]	k, [mD]	
0:00:15	0.02	265.09		0:00:15	0.36	339.36		0:00:30	0.68	359.40	
0:00:30	0.22	258.71		0:00:49	1.33	335.65		0:00:45	1.57	418.47	
0:00:45	0.44	248.03		0:01:04	1.72	305.11		0:01:00	2.35	367.22	
0:01:00	0.64	234.48	256.71	0:01:19	2.17	359.50	334.90	0:01:15	3.24	421.65	391.69
0:01:15	0.86	277.24		0:01:34	2.56	318.67		0:01:30	4.02	367.69	
0:01:30	1.05	247.87		0:01:49	3.01	351.77		0:01:45	4.91	416.28	
0:01:45	1.28	277.24		0:02:04	3.40	304.33		0:02:00	5.70	363.04	
0:02:00	1.47	238.39	256.88	0:02:19	3.84	364.31	334.77	0:02:15	6.59	411.50	389.63
0:02:15	1.70	278.48		0:02:34	4.25	326.82		0:02:30	7.37	372.47	
0:02:30	1.89	242.43		0:02:49	4.69	348.81		0:02:45	8.26	428.12	
0:02:45	2.09	243.67		0:03:05	5.08	285.31		0:03:00	9.04	365.35	
0:03:00	2.31	282.02	258.06	0:03:20	5.53	345.13	326.52	0:03:15	9.94	417.68	395.90
0:03:15	2.51	243.67		0:03:35	5.92	305.89		0:03:30	10.72	364.88	
0:03:30	2.73	278.48		0:03:50	6.37	348.02		0:03:45	11.62	416.89	
0:03:45	2.93	242.43		0:04:05	6.76	299.51		0:04:00	12.40	365.35	
0:04:01	3.15	256.73	252.18	0:04:20	7.15	302.67	314.02	0:04:15	13.29	420.83	391.99
0:04:16	3.35	239.61		0:04:35	7.60	364.31		0:04:30	14.08	368.63	
0:04:31	3.57	273.84		0:04:50	7.99	318.67		0:04:46	14.97	394.08	
0:04:46	3.77	239.61		0:05:05	8.44	352.56		0:05:01	15.76	368.63	
0:05:01	3.99	273.84	257.07	0:05:20	8.83	312.54	337.02	0:05:16	16.65	418.61	387.49
0:05:16	4.19	242.90		0:05:35	9.28	354.13		0:05:31	17.44	361.68	
0:05:31	4.41	272.62		0:05:50	9.67	305.89		0:05:46	18.22	364.90	
0:05:46	4.61	239.61		0:06:05	10.12	349.59		0:06:01	19.12	419.08	
0:06:01	4.84	270.56	257.53	0:06:20	10.51	302.67	328.07	0:06:16	19.90	363.97	377.41
0:06:17	5.03	228.44		0:06:35	10.96	351.15		0:06:31	20.80	415.50	
0:06:32	5.26	278.48		0:06:51	11.35	289.85		0:06:46	21.58	367.22	
0:06:47	5.45	239.61		0:07:06	11.80	350.37		0:07:01	22.48	418.14	
0:07:02	5.68	270.56	253.57	0:07:21	12.19	309.97	325.33	0:07:16	23.26	361.68	390.64
0:07:17	5.87	239.61		0:07:36	12.64	353.34		0:07:31	24.16	411.22	
0:07:32	6.07	239.61		0:07:51	13.04	310.75		0:07:46	24.95	364.43	
0:07:47	6.29	270.56		0:08:06	13.48	348.81		0:08:01	25.84	418.61	
0:08:02	6.49	239.61	260.74	0:08:21	13.88	316.78	332.42	0:08:16	26.63	363.97	389.56
0:08:17	6.71	278.48		0:08:36	14.27	323.90		0:08:31	27.52	413.81	
0:08:32	6.91	247.87		0:08:51	14.72	357.19		0:08:47	28.,31	340.80	
0:08:47	7.13	278.48		0:09:06	15.11	313.33		0:09:02	29.10	367.22	
0:09:02	7.33	244.92	255.59	0:09:21	15.56	365.12	339.88	0:09:17	29.99	418.61	385.11
0:09:17	7.56	284.55		0:09:36	15.95	319.48		0:09:32	30.78	367.22	
0:09:32	7.75	247.87		0:09:51	16.40	353.34		0:09:47	31.67	418.61	
0:09:47	7.98	284.55		0:10:06	16.79	306.67		0:10:02	32.46	367.22	
0:10:02	8.17	247.87	266.67	0:10:21	17.24	348.81	332.07	0:10:17	33.36	416.89	392.49
0:10:18	8.40	262.24		0:10:36	17.63	306.67		0:10:32	34.14	359.42	
0:10:33	8.59	239.61		0:10:52	18.08	338.54		0:10:47	35.04	416.89	
0:10:48	8.79	243.67		0:11:07	18.47	320.30		0:11:02	35.83	366.75	
0:11:03	9.01	279.73	256.98	0:11:22	18.92	353.34	329.71	0:11:17	36.72	413.81	389.22
0:11:18	9.21	239.61		0:11:37	19.31	306.67		0:11:51	38.56	377.27	
0:11:33	9.43	282.02		0:11:52	19.70	315.97		0:12:06	39.46	417.68	
0:11:48	9.63	253.51		0:12:07	20.15	365.12		0:12:21	40.24	360.76	
0:12:03	9.85	278.48	254.00	0:12:22	20.55	313.33	325.27	0:12:36	41.13	414.11	392.45
0:12:18	10.05	243.67		0:12:37	20.99	353.34		0:12:51	41.92	370.02	
0:12:33	10.27	278.48		0:12:52	21.39	309.18		0:13:07	42.71	341.65	
0:12:48	10.47	239.61		0:13:07	21.83	365.12		0:13:22	43.61	416.89	
0:13:03	10.69	269.35	256.10	0:13:22	22.23	316.78	336.11	0:13:37	44.39	361.68	372.56
0:13:18	10.89	235.68		0:13:37	22.67	353.34		0:13:52	45.29	414.27	
0:13:33	11.12	275.06		0:13:52	23.07	323.90		0:14:07	46.07	366.29	
0:13:48	11.31	243.67		0:14:07	23.52	377.71		0:14:22	46.97	419.55	
0:14:03	11.54	283.29	264.28	0:14:22	23.91	326.74	345.42	0:14:37	47.76	364.90	391.25
0:14:19	11.73	229.61		0:14:37	24.36	365.94		0:14:52	48.65	417.68	
0:14:34	11.93	239.61		0:14:53	24.75	289.85		0:15:07	49.44	371.49	
0:14:49	12.15	273.84		0:15:08	25.20	361.11		0:15:22	50.33	421.77	
0:15:04	12.35	239.61	253.70	0:15:23	25.59	313.33	332.56	0:15:37	51.12	363.50	393.61
0:15:19	12.57	275.06		0:15:38	25.98	313.33		0:15:52	52.01	415.96	
0:15:34	12.77	243.67		0:15:53	26.43	373.42		0:16:07	52.80	364.90	
0:15:49	12.99	278.48		0:16:08	26.82	328.41		0:16:22	53.58	364.43	
0:16:04	13.19	243.67	259.64	0:16:23	27.27	360.30	343.87	0:16:37	54.48	412.89	389.54
0:16:19	13.41	289.54		0:16:38	27.66	309.97		0:16:52	55.27	363.52	
0:16:34	13.61	252.22		0:16:53	28.11	357.98		0:17:08	56.16	389.53	
0:16:49	13.83	278.48		0:17:08	28.51	323.90		0:17:23	56.95	363.06	
0:17:04	14.03	236.89	253.33	0:17:23	28.95	365.12	339.24	0:17:38	57.84	410.76	381.72
0:17:19	14.26	275.06		0:17:38	29.35	315.97		0:17:53	58.63	360.33	
0:17:34	14.45	247.87		0:17:53	29.79	365.12		0:18:08	59.53	416.43	
0:17:50	14.68	261.08		0:18:08	30.19	312.54		0:18:23	60.31	366.29	
0:18:05	14.87	240.83	254.73	0:18:23	30.63	353.34	336.74	0:18:38	61.21	416.43	389.87
0:18:20	15.07	243.67		0:18:38	31.03	309.18		0:18:53	62.00	365.82	
0:18:35	15.29	278.48		0:18:54	31.47	334.86		0:19:08	62.89	415.96	
0:18:50	15.49	235.68		0:19:09	31.87	313.33		0:19:23	63.68	362.14	
0:19:05	15.71	270.56	265.80	0:19:24	32.26	320.30	319.42	0:19:38	64.57	412.42	389.09
0:19:20	15.91	239.61		0:19:39	32.71	364.31		0:19:53	65.36	367.69	
0:19:35	16.13	273.84		0:19:54	33.10	314.13		0:20:08	66.14	369.10	
0:19:50	16.33	239.61		0:20:09	33.55	365.12		0:20:23	67.04	418.61	
0:20:05	16.55	273.84	256.10	0:20:24	33.94	319.48	340.76	0:20:38	67.82	364.43	379.96
0:20:20	16.75	235.68		0:20:39	34.39	357.19		0:20:53	68.72	415.96	
0:20:35	16.97	273.84		0:20:54	34.78	323.07		0:21:09	69.51	339.94	
0:20:50	17.17	243.67		0:21:09	35.23	370.05		0:21:24	70.40	415.50	
0:21:05	17.39	269.35	250.70	0:21:24	35.62	312.54	340.71	0:21:39	71.19	372.43	385.96
0:21:20	17.59	240.83		0:21:39	36.07	357.98		0:21:54	72.09	422.71	
0:21:35	17.81	282.02		0:21:54	36.46	319.48		0:22:09	72.87	364.43	
0:21:51	18.01	233.57		0:22:09	36.91	373.42		0:22:24	73.77	415.96	
0:22:06	18.21	247.87	258.74	0:22:24	37.30	316.78	341.92	0:22:39	74.56	363.52	391.66
0:22:21	18.43	283.29		0:22:40	37.75	327.74		0:22:54	75.45	412.89	
0:22:36	18.63	247.87		0:22:55	38.15	309.97		0:23:09	76.24	367.22	
0:22:51	18.85	278.48		0:23:10	38.54	309.97		0:23:24	77.02	367.69	
0:23:06	19.05	239.61	260.99	0:23:25	38.99	348.81	324.12	0:23:39	77.92	422.24	392.51
0:23:21	19.27	279.73		0:23:40	39.38	307.45		0:23:54	78.71	371.49	
0:23:36	19.47	243.67		0:23:55	39.83	364.31		0:24:09	79.60	418.61	
0:23:51	19.69	273.84		0:24:29	40.74	333.42		0:24:24	80.39	364.90	
0:24:06	19.89	240.83	257.01	0:24:44	41.19	356.39	340.39	0:24:39	81.28	417.68	393.17
0:24:21	20.11	278.48		0:24:59	41.58	318.67		0:24:55	82.07	344.27	
0:24:36	20.31	243.67		0:25:14	42.03	363.49		0:25:10	82.96	418.14	
0:24:51	20.53	278.48		0:25:29	42.42	322.25		0:25:25	83.75	367.22	
0:25:06	20.73	240.83	247.92	0:25:44	42.87	381.09	346.37	0:25:40	84.65	415.96	386.40
0:25:21	20.93	235.68		0:25:59	43.26	319.48		0:25:55	85.43	369.57	
0:25:36	21.15	273.84		0:26:14	43.71	365.94		0:26:10	86.33	421.30	
0:25:52	21.35	224.64		0:26:29	44.10	315.97		0:26:25	87.12	367.69	
0:26:07	21.57	269.35	259.33	0:26:44	44.50	309.18	327.64	0:26:40	87.90	371.49	382.51
0:26:22	21.77	236.89		0:26:59	44.94	365.12		0:26:55	88.96	424.01	
0:26:37	21.99	269.35		0:27:14	45.34	320.30		0:27:10	89.58	363.97	
0:26:52	22.19	239.61		0:27:29	45.79	357.98		0:27:25	90.48	415.50	
0:27:07	22.41	278.48	255.18	0:27:44	46.18	313.33	339.18	0:27:40	91.26	367.22	392.67
0:27:22	22.61	239.61		0:28:00	46.63	331.26		0:27:55	92.16	418.14	
0:27:37	22.83	278.48		0:28:15	47.02	319.48		0:28:10	92.94	369.57	
0:27:52	23.03	244.92		0:28:30	47.47	370.05		0:28:25	93.84	421.30	
0:28:07	23.25	283.29	253.34	0:28:45	47.86	319.48	335.07	0:28:40	94.62	366.29	393.82
0:28:22	23.45	258.66		0:29:00	48.31	365.12		0:28:55	95.52	426.77	
0:28:37	23.65	239.61		0:29:15	48.70	313.33		0:29:11	96.30	350.98	
0:28:52	23.87	269.35		0:29:30	49.15	365.94		0:29:26	97.20	415.03	
0:29:07	24.07	243.67	258.21	0:29:45	49.54	320.30	341.17	0:29:41	97.98	366.75	389.88
0:29:22	24.29	283.29		0:30:00	49.99	357.19		0:29:56	98.77	369.57	
0:29:37	24.49	249.14		0:30:15	50.38	319.48		0:30:11	99.66	418.14	
0:29:53	24.71	256.73		0:30:30	50.78	320.30		0:30:26	100.45	367.22	
0:30:08	24.91	233.07	245.72	0:30:45	51.22	369.23	341.55	0:30:41	101.35	418.14	393.27
0:30:23	25.14	265.01		0:31:00	51.62	335.19		0:30:56	102.13	361.68	
0:30:38	25.33	235.68		0:31:15	52.06	382.11		0:31:11	103.03	419.08	
0:30:53	25.53	249.14		0:31:30	52.46	331.34		0:31:26	103.81	373.42	
0:31:08	25.75	282.02	255.15	0:31:46	52.91	350.86	349.88	0:31:41	104.71	421.30	393.87
0:31:23	25.95	239.61		0:32:01	53.30	326.74		0:31:56	105.49	363.97	
0:31:38	26.17	269.35		0:32:16	53.75	373.42		0:32:11	106.39	415.96	
0:31:53	26.37	233.07		0:32:31	54.14	330.50		0:32:26	107.17	366.29	
0:32:08	265.91	272.62	248.85	0:32:46	54.59	386.60	354.32	0:32:41	108.07	423.54	392.44
0:32:23	26.79	244.92		0:33:01	54.98	335.19		0:32:56	108.85	368.63	
0:32:38	27.01	272.62		0:33:16	55.43	374.25		0:33:11	109.74	418.14	
0:32:53	27.21	240.83		0:33:31	55.82	330.50		0:33:26	110.53	371.49	
0:33:08	27.43	273.84	259.53	0:33:46	56.21	338.28	344.56	0:33:41	111.32	374.37	383.16
0:33:23	27.63	243.67		0:34:01	56.66	382.96		0:33:57	112.21	399.65	
0:33:38	27.85	273.84		0:34:16	57.05	331.34		0:34:12	113.00	373.90	
0:33:53	28.05	245.72		0:34:31	57.50	377.71		0:34:27	113.89	421.77	
0:34:08	28.25	243.67	246.76	0:34:46	57.90	333.03	356.26	0:34:42	114.68	367.22	390.63
0:34:23	28.47	273.84		0:35:01	58.35	369.23		0:34:57	115.57	423.54	
0:34:39	28.67	229.61		0:35:16	58.74	323.90		0:35:12	116.36	371.96	
0:34:54	28.89	272.62		0:35:32	59.19	354.11		0:35:27	117.26	422.24	
0:35:09	29.09	236.89	248.03	0:35:47	59.58	331.34	344.64	0:35:42	118.04	366.29	396.00
0:35:24	29.31	269.35		0:36:02	60.03	382.11		0:35:57	118.94	422.71	
0:35:39	29.51	231.88		0:36:17	60.42	335.19		0:36:12	119.72	368.63	
0:35:54	29.73	265.01		0:36:32	60.87	377.71		0:36:27	120.62	415.03	
0:36:09	29.93	235.68	249.95	0:36:47	61.26	326.74	355.44	0:36:42	121.40	364.90	392.82
0:36:24	30.15	272.62		0:37:02	61.71	374.25		0:37:16	123.35	401.31	
0:36:39	30.35	239.61		0:37:17	62.10	327.58		0:37:31	124.13	364.88	
0:36:55	30.57	256.73		0:37:32	62.49	326.74		0:37:46	124.92	365.82	
0:37:10	30.77	239.61	251.16	0:37:47	62.94	377.71	351.57	0:38:01	125.81	419.88	387.97
0:37:25	30.99	279.73		0:38:02	63.34	339.14		0:38:16	126.60	370.98	
0:37:40	31.19	239.61		0:38:17	63.78	382.96		0:38:31	127.49	419.08	
0:37:55	31.41	269.35		0:38:32	64.18	331.34		0:38:46	128.28	364.43	

Total Clay; 4.85

Core ID: D- 2- 4

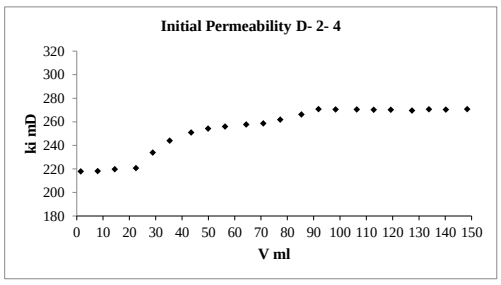

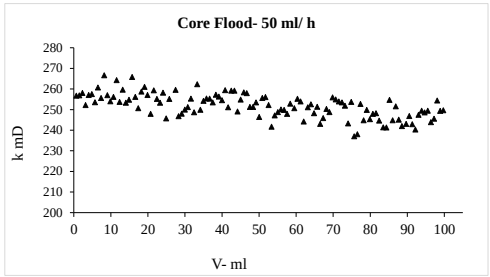

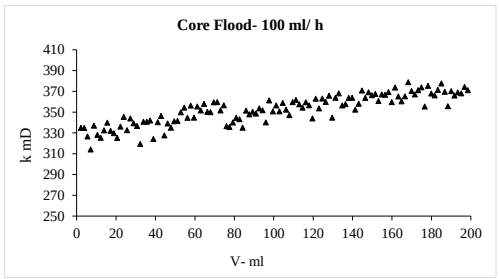

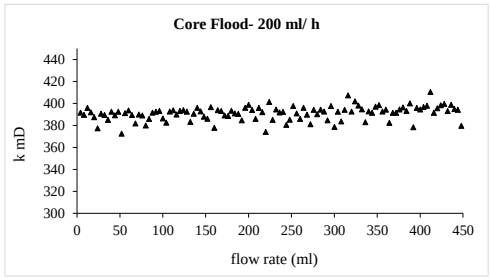

Group	Sample ID	Quartz	Calcite Mg	Oligoclase	Microcline	Chl. IIb	Kao.	Illite 2M1	Biotite 1M	Dol.	amorph.	Total Cla	Φ_{He} (%)	kwi (mD)
D- 2	D- 2- 2145.10	78.2	4.8	6.4	0.7	1.6	1.2	2.0	0.2	0.9	4.0	4.85	22.82	297.16

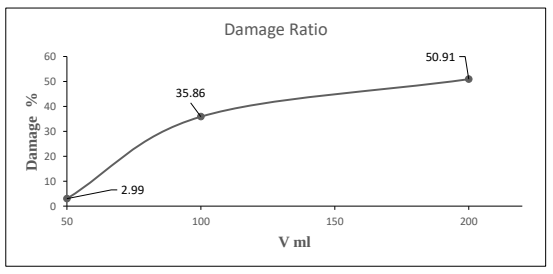

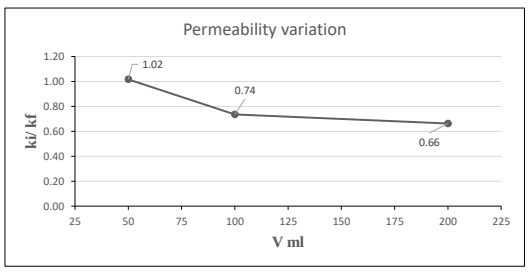

Initial k (mD)	k (50ml/ h (mD)	k (100ml/ h (mD)	k (200ml/ h (mD)	50 ml/h	100 ml/ h	200 ml/ h
259.56	251.8	352.65	391.71	255.33	352.72	391.71
	2.989674834	24.51	35.28	1.63	-35.89	-50.91

D= 100- kf *100/ ki		100	100
2.989674834	-35.86454	-50.9131	

flow rate ml/ h	D %	ki/kf
50	2.99	1.02
100	35.86	0.74
200	50.91	0.66

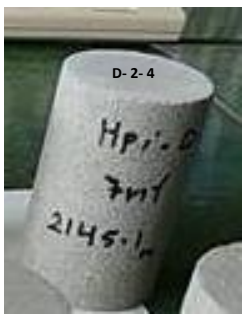

0:38:10	31.61	239.61	255.32	0:38:47	64.63	378.56	358.00	0:39:02	129.18	389.96	386.12
0:38:25	31.83	269.35		0:39:02	65.02	326.74		0:39:17	129.96	369.10	
0:38:40	32.03	231.88		0:39:17	65.47	377.71		0:39:32	130.86	424.01	
0:38:55	32.23	235.68		0:39:32	65.86	335.19		0:39:47	131.64	371.96	
0:39:10	32.45	269.35	248.65	0:39:48	66.31	361.63	350.32	0:40:02	132.54	421.30	396.59
0:39:25	32.65	231.88		0:40:03	66.70	334.34		0:40:17	133.32	362.14	
0:39:40	32.87	265.01		0:40:18	67.15	382.96		0:40:32	134.22	415.50	
0:39:55	33.07	233.07		0:40:33	67.54	343.18		0:40:47	135.00	366.75	
0:40:10	33.29	265.01	262.28	0:40:48	67.93	339.14	349.90	0:41:02	135.79	366.75	377.79
0:40:25	33.49	231.88		0:41:03	68.38	387.46		0:41:17	136.69	419.08	
0:40:40	33.71	269.35		0:41:18	68.77	334.34		0:41:32	137.47	363.97	
0:40:55	33.91	240.83		0:41:33	69.22	377.71		0:41:47	138.36	420.83	
0:41:10	34.13	263.83	249.93	0:41:48	69.61	338.28	359.45	0:42:02	139.15	371.96	393.96
0:41:26	34.33	218.50		0:42:03	70.06	386.60		0:42:17	140.05	420.83	
0:41:41	34.55	265.01		0:42:18	70.45	338.28		0:42:32	140.83	368.63	
0:41:56	34.75	231.88		0:42:33	70.90	382.11		0:42:47	141.73	419.08	
0:42:11	34.97	270.56	254.27	0:42:48	71.30	331.34	359.58	0:43:02	142.51	363.97	393.13
0:42:26	35.17	228.20		0:43:03	71.74	377.71		0:43:18	143.41	392.89	
0:42:41	35.37	235.68		0:43:18	72.14	331.34		0:43:33	144.19	371.96	
0:42:56	35.59	278.48		0:43:34	72.59	359.82		0:43:48	145.09	424.96	
0:43:11	35.79	239.61	255.39	0:43:49	72.98	337.41	351.57	0:44:03	145.88	366.29	389.02
0:43:26	36.01	273.84		0:44:04	73.43	382.11		0:44:18	146.77	416.43	
0:43:41	36.21	243.67		0:44:19	73.82	331.34		0:44:33	147.56	366.29	
0:43:56	36.43	278.48		0:44:34	74.21	335.19		0:44:48	148.34	367.22	
0:44:11	36.63	244.92	255.29	0:44:49	74.66	377.71	356.59	0:45:24	150.42	404.71	388.66
0:44:26	36.85	272.62		0:45:04	75.05	331.34		0:45:39	151.20	370.07	
0:44:41	37.05	236.89		0:45:19	75.50	370.05		0:45:54	152.10	422.59	
0:44:56	37.27	265.01		0:45:34	75.89	323.07		0:46:09	152.88	363.04	
0:45:11	37.47	231.88	253.47	0:45:49	76.04	321.42	336.47	0:46:24	153.78	417.82	393.38
0:45:26	37.69	273.84		0:46:04	76.34	325.72		0:46:40	154.56	343.83	
0:45:42	37.89	224.64		0:46:19	76.73	323.07		0:46:55	155.46	421.77	
0:45:57	38.08	247.87		0:46:34	77.18	365.94		0:47:10	156.24	373.42	
0:46:12	38.31	283.29	257.22	0:46:49	77.57	327.58	335.58	0:47:25	157.14	424.49	390.88
0:46:27	38.50	240.83		0:47:04	78.02	365.12		0:47:40	157.93	366.29	
0:46:42	38.73	272.62		0:47:20	78.41	301.81		0:47:55	158.82	415.96	
0:46:57	38.92	240.83		0:47:35	78.86	373.42		0:48:10	159.61	364.43	
0:47:12	39.15	273.84	256.28	0:47:50	79.25	319.48	339.96	0:48:25	160.50	415.03	390.43
0:47:27	39.34	238.39		0:48:05	79.65	313.33		0:48:40	161.29	367.22	
0:47:42	39.57	269.35		0:48:20	80.10	368.38		0:48:55	162.07	368.63	
0:47:57	39.76	235.68		0:48:35	80.49	326.74		0:49:10	162.97	424.49	
0:48:12	39.99	270.56	254.52	0:48:50	80.94	370.01	344.62	0:49:25	163.75	378.33	384.67
0:48:27	40.18	235.69		0:49:05	81.34	320.30		0:49:40	164.65	426.77	
0:48:42	40.41	279.73		0:49:20	81.79	373.42		0:49:55	165.43	366.75	
0:48:57	40.60	243.67		0:49:35	82.18	320.30		0:50:11	166.36	417.99	
0:49:12	40.83	278.48	259.39	0:49:50	82.63	358.78	343.20	0:50:28	167.24	372.57	396.02
0:49:27	41.02	243.67		0:50:05	83.02	320.30		0:50:44	168.19	421.03	
0:49:43	41.22	225.78		0:50:20	83.41	330.50		0:50:59	168.98	372.87	
0:49:58	41.44	272.62		0:50:36	83.86	359.02		0:51:15	169.95	426.26	
0:50:13	41.64	236.89	251.08	0:50:51	84.25	330.50	335.08	0:51:30	170.75	375.16	398.83
0:50:28	41.87	265.01		0:51:06	84.70	373.42		0:51:46	171.66	396.93	
0:50:43	42.06	233.07		0:51:21	85.10	327.58		0:52:04	172.64	382.72	
0:50:58	42.29	269.35		0:51:36	85.54	373.42		0:52:21	173.53	368.70	
0:51:13	42.48	239.61	259.21	0:51:51	85.94	331.34	351.44	0:52:36	174.43	427.72	394.02
0:51:28	42.71	278.48		0:52:06	86.39	370.05		0:52:51	175.21	369.57	
0:51:43	42.90	244.92		0:52:21	86.78	319.48		0:53:06	176.11	413.35	
0:51:58	43.13	273.84		0:52:36	87.23	374.25		0:53:22	176.89	339.94	
0:52:13	43.32	239.61	259.21	0:52:51	87.62	327.58	347.84	0:53:37	177.80	421.07	385.98
0:52:28	43.55	273.84		0:53:06	88.07	376.87		0:53:52	178.59	369.10	
0:52:43	43.74	240.83		0:53:21	88.46	332.19		0:54:07	179.48	424.01	
0:52:58	43.97	268.15		0:53:36	88.91	372.59		0:54:22	180.27	369.10	
0:53:13	44.16	239.61	249.06	0:53:51	89.30	320.30	350.49	0:54:37	181.16	421.30	395.88
0:53:28	44.36	244.92		0:54:06	89.69	323.07		0:54:52	181.95	366.75	
0:53:43	44.58	283.28		0:54:21	90.14	378.56		0:55:07	182.84	418.61	
0:53:59	44.78	228.44		0:54:36	90.53	329.66		0:55:22	183.63	366.75	
0:54:14	45.00	269.35	254.83	0:54:52	90.98	363.25	348.63	0:55:37	184.52	415.96	392.02
0:54:29	45.20	235.68		0:55:07	91.37	334.34		0:55:52	185.31	365.82	
0:54:44	45.42	269.35		0:55:22	91.82	378.56		0:56:07	186.10	364.90	
0:54:59	45.62	244.92		0:55:37	92.21	323.07		0:56:22	186.99	415.96	
0:55:14	45.85	283.28	258.31	0:55:52	92.68	378.16	353.53	0:56:38	187.79	349.56	374.06
0:55:29	46.04	243.67		0:56:08	93.08	310.23		0:56:53	188.69	427.72	
0:55:44	46.27	273.84		0:56:23	93.53	379.40		0:57:08	189.47	374.85	
0:55:59	46.46	235.68		0:56:38	93.92	335.19		0:57:23	190.37	426.77	
0:56:14	46.69	270.56	257.94	0:56:53	94.37	382.11	351.73	0:57:39	191.23	375.80	401.29
0:56:29	46.88	243.67		0:57:08	94.76	330.50		0:57:54	192.12	413.81	
0:56:44	47.08	243.67		0:57:23	95.16	335.08		0:58:09	192.91	366.29	
0:56:59	47.30	273.84		0:57:39	95.62	359.64		0:58:25	193.81	393.32	
0:57:14	47.50	240.83	251.25	0:57:54	96.01	335.19	340.10	0:58:40	194.60	366.75	385.04
0:57:29	47.72	273.84		0:58:09	96.46	377.71		0:58:55	195.49	418.14	
0:57:45	47.92	220.95		0:58:24	96.86	345.43		0:59:10	196.28	372.90	
0:58:00	48.14	269.35		0:58:39	97.31	386.60		0:59:25	197.06	369.10	
0:58:15	48.34	240.83	251.25	0:58:54	97.70	335.19	361.23	0:59:40	197.96	417.68	394.46
0:58:30	48.56	272.62		0:59:09	98.15	382.96		0:59:55	198.74	366.75	
0:58:45	48.76	240.83		0:59:25	98.55	315.04		1:00:11	199.68	409.53	
0:59:00	48.98	273.84		0:59:44	99.13	393.24		1:00:26	200.46	370.04	
0:59:15	49.18	235.68	253.50	1:00:01	99.55	311.70	350.74	1:00:41	201.36	420.83	391.79
0:59:30	49.40	269.35		1:00:16	100.00	382.11		1:00:56	202.15	367.69	
0:59:45	49.60	239.61		1:00:31	100.39	339.14		1:01:11	203.04	415.96	
1:00:00	49.82	269.35		1:00:46	100.84	381.25		1:01:26	203.83	366.75	
1:00:15	50.02	235.68	246.37	1:01:01	101.23	323.07	356.39	1:01:41	204.72	419.08	392.37
1:00:30	50.22	239.61		1:01:16	101.62	323.07		1:01:56	205.51	369.10	
1:00:45	50.44	269.35		1:01:31	102.07	378.56		1:02:11	206.41	421.77	
1:01:00	50.64	240.83		1:01:46	102.46	326.74		1:02:26	207.19	363.97	
1:01:15	50.86	272.62	255.60	1:02:01	102.91	374.25	350.66	1:02:41	207.98	367.22	380.51
1:01:30	51.06	236.89		1:02:16	103.30	331.34		1:02:56	208.87	419.08	
1:01:45	51.28	278.48		1:02:31	103.75	378.56		1:03:11	209.66	366.29	
1:02:01	51.48	232.38		1:02:46	104.15	335.19		1:03:26	210.55	416.43	
1:02:16	51.70	278.48	256.09	1:03:01	104.59	390.33	358.86	1:03:42	211.34	339.07	385.22
1:02:31	51.90	240.83		1:03:16	104.98	338.28		1:03:57	212.23	418.14	
1:02:46	52.12	269.35		1:03:31	105.43	382.96		1:04:12	213.04	381.33	
1:03:01	52.32	235.68		1:03:46	105.83	335.19		1:04:27	213.94	421.30	
1:03:16	52.54	273.84	252.20	1:04:02	106.27	353.32	352.44	1:04:42	214.73	369.57	397.59
1:03:31	52.74	236.89		1:04:17	106.67	331.34		1:04:58	215.66	408.24	
1:03:46	52.96	265.01		1:04:32	107.06	339.14		1:05:13	216.45	363.97	
1:04:01	53.16	233.07		1:04:47	107.51	386.60		1:05:28	217.35	422.24	
1:04:16	53.36	231.88	241.71	1:05:02	107.90	331.34	347.11	1:05:43	218.13	369.10	390.89
1:04:31	53.58	269.35		1:05:17	108.35	377.71		1:05:58	219.03	419.08	
1:04:46	53.78	235.68		1:05:32	108.74	335.19		1:06:13	219.82	368.15	
1:05:01	54.00	269.35		1:05:47	109.19	387.46		1:06:28	220.60	367.22	
1:05:16	54.20	235.68	247.14	1:06:02	109.58	338.28	359.66	1:06:44	221.50	389.53	386.00
1:05:31	54.42	265.01		1:06:17	110.03	382.11		1:06:59	222.28	367.22	
1:05:47	54.62	218.50		1:06:32	110.42	338.28		1:07:14	223.18	421.77	
1:06:02	54.84	269.35		1:06:47	110.87	391.20		1:07:29	223.98	376.63	
1:06:17	55.04	235.68	248.77	1:07:02	111.26	335.19	361.69	1:07:44	224.88	418.61	396.06
1:06:32	55.26	265.01		1:07:17	111.71	382.96		1:07:59	225.67	370.49	
1:06:47	55.46	229.37		1:07:32	112.10	338.28		1:08:14	226.57	421.30	
1:07:02	55.68	265.01		1:07:47	112.55	377.71		1:08:29	227.35	367.22	
1:07:17	55.88	240.83	250.05	1:08:02	112.95	331.34	357.57	1:08:45	228.26	400.25	389.81
1:07:32	56.10	273.84		1:08:18	113.34	313.45		1:09:00	229.05	373.85	
1:07:47	56.30	239.61		1:08:33	113.79	382.11		1:09:15	229.84	366.75	
1:08:02	56.50	239.61		1:08:48	114.18	334.34		1:09:30	230.73	416.43	
1:08:17	56.72	269.35	249.83	1:09:03	114.63	387.46	354.34	1:09:45	231.52	367.22	381.06
1:08:32	56.92	231.88		1:09:18	115.02	339.14		1:10:00	232.41	423.54	
1:08:47	57.14	266.19		1:09:33	115.47	381.25		1:10:15	233.20	369.57	
1:09:02	57.34	231.88		1:09:48	115.86	334.34		1:10:30	234.10	416.89	
1:09:18	57.56	249.55	247.90	1:10:03	116.31	382.96	359.42	1:10:45	234.88	366.75	394.19
1:09:33	57.76	231.88		1:10:18	116.70	335.19		1:11:01	235.82	412.60	
1:09:48	57.98	270.56		1:10:33	117.15	382.11		1:11:18	236.69	361.12	
1:10:03	58.18	239.61		1:10:48	117.54	331.34		1:11:33	237.59	416.43	
1:10:18	58.40	269.35	252.85	1:11:03	117.99	377.71	356.59	1:11:48	238.39	370.96	390.28
1:10:33	58.60	233.07		1:11:18	118.38	335.19		1:12:03	239.28	422.24	
1:10:48	58.82	269.35		1:11:34	118.78	317.75		1:12:18	240.07	368.63	
1:11:24	59.32	246.51		1:11:49	119.25	388.67		1:12:33	240.97	419.55	
1:11:39	59.51	234.48	250.67	1:12:04	119.64	334.34	343.99	1:12:48	241.75	367.22	394.41
1:11:54	59.73	269.35		1:12:19	120.09	386.60		1:13:03	242.54	366.75	
1:12:09	59.93	230.70		1:12:34	120.48	343.18		1:13:18	243.43	415.96	
1:12:24	60.15	268.15		1:12:49	120.93	386.60		1:13:33	244.22	366.75	
1:12:39	60.35	242.06	255.24	1:13:04	121.32	335.19	362.89	1:13:48	245.11	421.30	392.69
1:12:55	60.57	256.73		1:13:20	121.77	358.22		1:14:04	245.90	343.83	
1:13:10	60.77	243.67		1:13:35	122.16	336.05		1:14:19	246.80	416.43	
1:13:25	60.99	278.48		1:13:50	122.61	382.11		1:14:34	247.58	363.97	
1:13:40	61.19	236.89	253.94	1:14:05	123.00	338.28	353.66	1:14:52	248.64	414.16	384.60
1:13:55	61.42	269.35		1:14:20	123.45	386.60		1:15:07	249.42	373.90	
1:14:10	61.61	235.68		1:14:35	123.84	339.14		1:15:22	250.33	425.06	
1:14:25	61.84	273.84		1:14:50	124.24	340.00		1:15:37	251.11	370.04	
1:14:40	62.03	240.83	244.19	1:15:05	124.68	386.60	363.09	1:15:52	252.01	421.30	397.57
1:14:55	62.26	265.01		1:15:20	125.08	335.19		1:16:07	252.79	366.75	
1:15:29	62.71	239.05		1:15:35	125.53	377.71		1:16:22	253.58	367.22	
1:15:44	62.91	231.88		1:15:50	125.92	335.19		1:16:37	254.47	415.50	
1:15:59	63.13	268.15	251.13	1:16:05	126.37	391.20	359.83	1:16:52	255.26	364.90	378.59
1:16:14	63.33	234.48		1:16:20	126.76	347.31		1:17:07	256.16	418.61	
1:16:29	63.55	266.19		1:16:35	127.21	390.33		1:17:22	256.94	366.75	
1:16:44	63.75	235.68		1:16:50	127.60	339.14		1:17:37	257.84	418.14	
1:16:59	63.97	273.84	252.55	1:17:05	128.05	386.60	365.84	1:17:52	258.62	366.75	392.57
1:17:14	64.17	240.83		1:17:20	128.44	342.30		1:18:07	259.52	415.96	
1:17:29	64.39	273.84		1:17:36	128.89	362.44		1:18:22	260.30	361.68	
1:17:44	64.59	235.68		1:17:51	129.28	335.19		1:18:38	261.20	389.96	
1:17:59	64.81	265.01	248.21	1:18:06	129.67	339.14	344.77	1:18:53	261.98	366.75	383.59
1:18:15	65.01	224.64		1:18:21	130.12	386.60		1:19:08	262.88	418.14	
1:18:30	65.23	273.84		1:18:36	130.51	334.34		1:19:23	263.66	367.22	
1:18:45	65.43	229.37		1:18:51	130.96	387.46		1:19:38	264.45	366.75	
1:19:00	65.66	265.01	251.33	1:19:06	131.36	347.31	363.93	1:19:53	265.35	424.49	394.15

1:19:15	65.85	239.61		1:19:21	131.80	395.92		1:20:08	266.13	368.63	
1:19:30	66.05	235.68		1:19:36	132.20	342.30		1:20:23	267.12	458.09	
1:19:45	66.27	265.01		1:19:51	132.64	391.20		1:20:38	268.02	423.54	
1:20:00	66.47	231.88	243.05	1:20:06	133.04	343.18	368.15	1:20:53	268.80	379.30	407.39
1:20:15	66.69	270.56		1:20:21	133.48	386.60		1:21:08	269.70	424.49	
1:20:30	66.89	245.72		1:20:36	133.88	330.50		1:21:23	270.49	367.22	
1:20:45	67.12	249.35		1:20:51	134.33	378.56		1:21:38	271.38	413.35	
1:21:00	67.28	247.57	245.90	1:21:06	134.72	330.50	356.54	1:21:53	272.17	365.36	392.60
1:21:15	67.52	252.58		1:21:21	135.17	382.11		1:22:08	272.96	369.57	
1:21:30	67.74	243.84		1:21:37	135.56	320.91		1:22:23	273.85	424.01	
1:21:45	67.94	239.61		1:21:52	135.95	340.00		1:22:38	274.64	380.84	
1:22:01	68.16	246.73	250.25	1:22:07	136.40	387.46	357.62	1:22:53	275.53	433.35	401.94
1:22:16	68.36	240.83		1:22:22	136.79	338.28		1:23:08	276.32	371.49	
1:22:31	68.58	273.84		1:22:37	137.24	382.96		1:23:23	277.21	420.83	
1:22:46	68.78	239.61		1:22:52	137.63	337.41		1:23:38	278.00	367.22	
1:23:01	68.98	240.83	248.78	1:23:07	138.08	395.92	363.64	1:23:53	278.90	432.87	398.10
1:23:16	69.20	269.35		1:23:22	138.47	344.05		1:24:08	279.68	379.30	
1:23:31	69.40	235.68		1:23:37	138.92	391.20		1:24:23	280.58	418.61	
1:23:46	69.62	278.48		1:23:52	139.31	338.28		1:24:38	281.36	363.97	
1:24:01	69.82	240.83	255.91	1:24:07	139.76	382.11	363.91	1:24:53	282.26	416.43	394.58
1:24:16	70.04	269.35		1:24:22	140.16	340.00		1:25:08	283.04	368.63	
1:24:31	70.24	239.61		1:24:37	140.60	391.20		1:25:23	283.83	374.85	
1:24:46	70.46	273.84		1:24:52	141.00	343.18		1:25:38	284.73	421.77	
1:25:01	70.66	243.67	254.93	1:25:07	141.39	335.20	352.39	1:25:53	285.51	366.75	383.00
1:25:16	70.88	278.48		1:25:23	141.84	362.44		1:26:08	286.41	424.01	
1:25:31	71.08	240.83		1:25:38	142.23	339.14		1:26:23	287.19	367.22	
1:25:47	71.30	256.73		1:25:53	142.68	387.46		1:26:38	288.09	412.89	
1:26:02	71.50	239.61	253.91	1:26:08	143.07	343.18	358.05	1:26:53	288.88	367.22	392.83
1:26:17	71.72	273.84		1:26:23	143.52	395.03		1:27:08	289.77	418.61	
1:26:32	71.92	239.61		1:26:38	143.91	348.19		1:27:23	290.56	363.97	
1:26:47	72.12	236.89		1:26:53	144.36	396.80		1:27:38	291.45	416.43	
1:27:02	72.34	269.35	253.50	1:27:08	144.76	343.18	370.80	1:27:53	292.24	367.22	391.56
1:27:17	72.54	236.89		1:27:23	145.20	386.60		1:28:08	293.13	424.01	
1:27:32	72.76	268.15		1:27:38	145.60	339.14		1:28:23	293.92	369.57	
1:27:47	72.96	239.61		1:27:53	146.05	386.60		1:28:38	294.82	418.61	
1:28:02	73.18	269.35	251.87	1:28:08	146.44	342.30	363.66	1:28:53	295.60	376.34	397.14
1:28:17	73.38	231.88		1:28:23	146.89	395.92		1:29:08	296.39	379.30	
1:28:32	73.60	269.35		1:28:38	147.28	343.18		1:29:23	297.28	424.01	
1:28:47	73.80	236.89		1:28:53	147.67	342.30		1:29:38	298.07	369.57	
1:29:02	74.02	235.01	243.28	1:29:08	148.12	395.03	369.11	1:29:53	298.96	420.83	398.43
1:29:17	74.22	231.88		1:29:24	148.51	324.78		1:30:08	299.75	369.57	
1:29:32	74.44	239.35		1:29:39	148.98	418.64		1:30:23	300.65	418.15	
1:29:47	74.64	235.68		1:29:54	149.37	346.43		1:30:38	301.43	364.90	
1:30:03	74.86	252.52	253.73	1:30:10	149.82	375.31	366.29	1:30:53	302.33	418.15	392.69
1:30:18	75.06	243.67		1:30:25	150.23	364.96		1:31:08	303.11	369.10	
1:30:33	75.25	243.67		1:30:40	150.68	396.80		1:31:23	304.01	421.30	
1:30:48	75.48	275.06		1:30:55	151.07	340.00		1:31:38	304.79	369.10	
1:31:03	75.67	239.61	237.03	1:31:11	151.52	368.39	367.54	1:31:53	305.69	418.15	394.41
1:31:18	75.90	235.06		1:31:26	151.92	355.89		1:32:08	306.47	364.43	
1:31:33	76.10	239.61		1:31:41	152.36	399.85		1:32:23	307.37	416.43	
1:31:48	76.32	233.84		1:31:56	152.76	344.05		1:32:38	308.16	374.37	
1:32:03	76.52	243.67	238.05	1:32:11	153.15	343.18	360.74	1:32:53	308.94	374.37	382.40
1:32:18	76.74	278.48		1:32:26	153.60	395.03		1:33:08	309.84	419.55	
1:32:33	76.94	239.61		1:32:41	153.99	347.31		1:33:23	310.62	365.82	
1:32:48	77.16	269.35		1:32:56	154.44	386.60		1:33:38	311.52	416.89	
1:33:03	77.36	235.68	252.69	1:33:11	154.83	339.14	367.02	1:33:53	312.30	363.50	391.44
1:33:18	77.58	269.35		1:33:26	155.28	390.33		1:34:08	313.20	416.43	
1:33:33	77.78	231.88		1:33:41	155.67	339.14		1:34:23	313.99	364.43	
1:33:48	78.00	273.84		1:33:56	156.12	385.74		1:34:38	314.88	418.61	
1:34:03	78.20	244.92	244.77	1:34:11	156.51	351.55	366.69	1:34:53	315.67	366.29	391.44
1:34:19	78.39	224.64		1:34:26	156.96	399.85		1:35:08	316.56	416.43	
1:34:34	78.62	273.84		1:34:41	157.35	343.18		1:35:23	317.35	366.29	
1:34:49	78.81	235.68		1:34:56	157.80	391.20		1:35:38	318.25	423.65	
1:35:04	79.04	265.01	249.79	1:35:11	158.19	343.18	369.35	1:35:53	319.03	371.49	394.46
1:35:19	79.23	235.68		1:35:26	158.64	390.33		1:36:08	319.82	369.10	
1:35:34	79.46	273.84		1:35:42	159.03	317.94		1:36:23	320.71	421.77	
1:35:49	79.65	239.61		1:35:57	159.42	338.28		1:36:38	321.50	371.01	
1:36:04	79.88	270.56	245.30	1:36:12	159.87	392.08	359.66	1:36:53	322.39	423.54	396.36
1:36:19	80.07	235.68		1:36:27	160.27	351.55		1:37:08	323.18	370.04	
1:36:34	80.30	235.35		1:36:42	160.71	400.74		1:37:23	324.08	416.43	
1:36:49	80.49	239.61		1:36:57	161.11	346.43		1:37:38	324.86	366.75	
1:37:04	80.72	238.48	247.92	1:37:12	161.55	395.92	373.66	1:37:53	325.76	419.55	393.19
1:37:19	80.91	235.68		1:37:27	161.95	339.14		1:38:08	326.55	366.75	
1:37:34	81.14	273.84		1:37:42	162.40	387.46		1:38:23	327.44	424.49	
1:37:49	81.33	243.67		1:37:57	162.79	341.43		1:38:38	328.23	378.82	
1:38:04	81.53	239.61	248.20	1:38:12	163.24	392.08	365.03	1:38:53	329.12	430.04	400.02
1:38:19	81.75	273.84		1:38:27	163.63	347.31		1:39:08	329.91	366.29	
1:38:35	81.95	229.61		1:38:42	164.08	399.85		1:39:23	330.81	416.43	
1:38:50	82.17	278.48		1:38:57	164.47	347.31		1:39:38	332.64	362.34	
1:39:05	82.37	239.61	244.62	1:39:12	164.86	347.31	360.44	1:39:53	333.42	368.16	378.30
1:39:20	82.59	269.35		1:39:27	165.31	391.20		1:40:08	334.32	420.36	
1:39:35	82.79	235.68		1:39:42	165.70	339.14		1:40:23	335.10	369.59	
1:39:50	83.01	233.84		1:39:58	166.15	375.70		1:40:38	336.00	424.59	
1:40:26	83.51	246.51	241.39	1:40:13	166.54	354.98	365.25	1:40:53	336.79	369.10	395.91
1:40:41	83.73	238.15		1:40:28	166.99	400.74		1:41:08	337.68	420.36	
1:40:56	83.93	243.67		1:40:43	167.39	348.19		1:41:23	338.46	371.01	
1:41:11	84.15	237.24		1:40:58	167.83	406.60		1:41:38	339.36	421.77	
1:41:26	84.35	246.16	241.31	1:41:13	168.23	359.42	378.74	1:41:53	340.15	364.90	394.51
1:41:41	84.57	248.48		1:41:28	168.67	400.74		1:42:08	341.04	422.24	
1:41:57	84.77	220.95		1:41:43	169.07	343.18		1:42:23	341.83	371.01	
1:42:12	84.96	236.89		1:41:58	169.51	390.33		1:42:38	342.73	421.77	
1:42:27	85.19	238.48	254.70	1:42:13	169.91	347.31	370.39	1:42:53	343.51	371.96	396.74
1:42:42	85.38	247.87		1:42:28	170.36	391.20		1:43:08	344.30	373.42	
1:42:57	85.61	283.29		1:42:43	170.75	342.30		1:43:23	345.19	427.72	
1:43:12	85.80	249.14		1:42:58	171.14	343.18		1:43:38	345.98	368.63	
1:43:27	86.03	243.29	244.78	1:43:13	171.59	391.20	366.97	1:43:53	346.87	421.77	397.88
1:43:42	86.22	243.67		1:43:28	171.98	354.98		1:44:08	347.66	373.90	
1:43:57	86.45	248.48		1:43:43	172.43	410.76		1:44:23	348.55	423.54	
1:44:12	86.64	243.67		1:43:59	172.82	326.43		1:44:38	350.53	427.23	
1:44:27	86.87	270.56	251.60	1:44:14	173.27	392.08	371.06	1:44:53	351.42	417.21	410.47
1:44:42	87.07	239.61		1:44:29	173.66	346.43		1:45:08	352.20	360.76	
1:44:57	87.29	283.29		1:44:44	174.11	401.64		1:45:23	353.09	411.50	
1:45:12	87.49	244.92		1:44:59	174.50	350.65		1:45:38	353.88	370.04	
1:45:27	87.68	239.61	245.12	1:45:14	174.95	396.80	373.88	1:45:53	354.78	423.54	391.46
1:45:43	87.91	244.08		1:45:29	175.35	350.16		1:46:08	355.45	380.08	
1:45:58	88.10	253.51		1:45:44	175.81	394.70		1:46:23	355.75	392.30	
1:46:13	88.33	243.29		1:45:59	176.20	346.43		1:46:38	356.65	441.09	
1:46:28	88.52	239.61	242.02	1:46:15	176.59	330.41	355.42	1:46:53	357.43	369.10	395.64
1:47:04	89.04	234.88		1:46:30	177.04	399.45		1:47:08	358.33	419.55	
1:47:19	89.24	246.61		1:46:45	177.44	349.08		1:47:23	359.11	368.16	
1:47:34	89.46	246.97		1:47:00	177.89	406.11		1:47:38	360.01	429.56	
1:47:49	89.66	243.67	243.03	1:47:15	178.29	346.43	375.27	1:47:53	360.79	376.34	398.40
1:48:04	89.88	249.73		1:47:30	178.73	391.20		1:48:08	361.69	429.56	
1:48:19	90.08	243.67		1:47:45	179.13	346.43		1:48:23	362.48	379.78	
1:48:34	90.30	243.84		1:48:00	179.57	392.08		1:48:38	363.37	420.83	
1:48:49	90.50	244.92	246.88	1:48:15	179.97	342.30	368.00	1:48:53	364.15	368.63	399.70
1:49:05	90.72	245.58		1:48:30	180.41	400.74		1:49:08	365.05	422.24	
1:49:20	90.92	247.87		1:48:45	180.81	346.43		1:49:23	365.84	363.97	
1:49:35	91.12	249.14		1:49:01	181.26	372.00		1:49:38	366.73	419.55	
1:49:50	91.34	248.48	242.87	1:49:16	181.65	345.54	366.18	1:49:53	367.52	366.75	393.13
1:50:05	91.54	243.67		1:49:31	182.04	346.43		1:50:08	368.31	368.15	
1:50:20	91.76	238.48		1:49:46	182.49	396.80		1:50:23	369.20	421.77	
1:50:35	91.96	240.83		1:50:01	182.88	346.43		1:50:38	369.99	375.86	
1:50:50	92.18	238.15	240.29	1:50:16	183.33	395.92	371.39	1:50:53	370.88	429.56	398.83
1:51:05	92.38	240.83		1:50:31	183.72	351.55		1:51:08	371.67	368.63	
1:51:20	92.60	248.48		1:50:46	184.17	405.69		1:51:23	372.56	420.83	
1:51:35	92.80	239.61		1:51:01	184.56	350.65		1:51:38	373.35	368.63	
1:51:50	93.02	248.48	247.44	1:51:16	185.01	402.53	377.61	1:51:53	374.24	421.77	394.96
1:52:05	93.22	243.67		1:51:32	185.43	349.63		1:52:08	375.03	369.10	
1:52:20	93.44	248.48		1:51:47	185.88	396.80		1:52:23	375.93	421.30	
1:52:35	93.64	249.14		1:52:04	186.32	339.20		1:52:38	376.71	367.69	
1:52:50	93.86	247.24	249.46	1:52:19	186.77	392.95	369.64	1:52:53	377.61	418.61	394.17
1:53:05	94.06	244.92		1:52:34	187.16	342.30		1:53:08	378.39	366.29	
1:53:21	94.25	228.44		1:52:49	187.55	342.30		1:53:23	379.18	368.15	
1:53:36	94.48	277.24		1:53:04	188.00	391.20		1:53:38	380.08	419.55	
1:53:51	94.67	243.67	248.57	1:53:19	188.39	347.31	355.78	1:53:53	380.86	364.43	379.60
1:54:06	94.90	249.73		1:53:34	188.84	396.80		1:54:08	381.76	418.61	
1:54:21	95.09	243.67		1:53:49	189.23	346.43		1:54:23	382.54	389.10	
1:54:36	95.32	248.48		1:54:04	189.68	395.03		1:54:38	383.44	418.61	
1:54:51	95.52	253.51	249.40	1:54:19	190.07	342.30	370.14	1:54:53	384.23	394.90	405.31
1:55:06	95.74	243.40		1:54:34	190.52	391.20		1:55:08	385.12	413.35	
1:55:21	95.94	252.22		1:54:50	190.91	325.60		1:55:23	385.91	382.14	
1:55:36	96.16	248.48		1:55:05	191.36	400.74		1:55:38	386.80	415.50	
1:55:51	96.36	240.83	243.92	1:55:20	191.75	346.43	365.99	1:55:53	387.59	366.29	394.32
1:56:06	96.58	243.29		1:55:35	192.20	395.92		1:56:08	388.49	420.01	
1:56:21	96.78	247.87		1:55:50	192.59	346.43		1:56:23	389.27	383.97	
1:56:36	96.97	243.67		1:56:05	193.04	391.20		1:56:38	390.17	419.08	
1:56:51	97.20	247.29	245.53	1:56:20	193.43	342.30	368.96	1:56:53	390.95	395.86	404.73
1:57:06	97.39	243.67		1:56:35	193.83	343.18		1:57:08	391.74	393.90	
1:57:21	97.62	247.29		1:56:50	194.27	391.20		1:57:23	392.63	419.08	
1:57:37	97.81	240.68		1:57:05	194.67	342.30		1:57:38	393.42	389.57	
1:57:52	98.04	243.40	254.41	1:57:20	195.11	395.92	368.15	1:57:53	394.31	420.83	405.84
1:58:07	98.23	247.87		1:57:35	195.51	352.44		1:58:08	395.10	388.63	
1:58:22	98.46	278.48		1:57:50	195.96	395.92		1:58:23	395.77	397.38	
1:58:37	98.65	247.87		1:58:05	196.35	347.31		1:58:38	396.68	427.41	
1:58:52	98.88	243.29	249.36	1:58:20	196.80	401.64	374.33	1:58:53	397.59	426.65	410.02
1:59:07	99.07	256.73		1:58:35	197.19	350.65		Av. K		**391.71**	**391.71**
1:59:22	99.30	249.54		1:58:51	197.64	376.54					
1:59:37	99.49	247.87		1:59:06	198.03	350.65					
1:59:52	99.72	244.55	249.67	1:59:21	198.48	406.60	371.11				
2:00:07	99.91	243.67		1:59:36	198.87	356.79					

2:00:22	100.11	252.22		1:59:51	199.27	351.55					
2:00:37	100.33	293.40		2:00:06	199.71	399.85					
2:00:52	100.53	253.51		2:00:21	200.11	342.30	362.62				
2:01:07	100.76	288.26		2:00:36	200.56	388.33					
Av. K		**252.50**	**251.82**	**Av. k**		**352.72**	**352.65**				

50 ml/ h				100 ml/ h				200 ml/ h			
time, [hh:mm:ss]	V, [cm3]	k, [mD]		time, [hh:mm:ss]	V, [cm3]	k, [mD]		time, [hh:mm:ss]	V, [cm3]	k, [mD]	
00:00:30	0.165	239.08		00:00:15	0.268	152.65		00:00:15	0.633	198.60	
00:00:45	0.387	249.45		00:00:30	0.658	200.54		00:00:30	1.411	221.35	
00:01:00	0.582	253.92		00:00:45	1.104	210.34		00:00:45	2.298	220.68	
00:01:15	0.804	260.50		00:01:00	1.494	186.31		00:01:00	3.075	216.29	
00:01:30	0.998	244.20	249.43	00:01:15	1.94	213.06	192.58	00:01:15	3.963	219.10	215.21
00:01:45	1.221	240.71		00:01:30	2.331	185.59		00:01:30	4.742	203.82	
00:02:00	1.416	238.38		00:01:45	2.777	209.01		00:01:45	5.631	227.77	
00:02:15	1.638	249.08		00:02:00	3.167	180.49		00:02:00	6.411	195.12	
00:02:30	1.833	243.92		00:02:15	3.613	207.70		00:02:15	7.3	219.42	
00:02:45	2.059	254.29	245.28	00:02:30	4.004	182.09	192.97	00:02:30	8.079	191.00	207.43
00:03:00	2.26	243.01		00:02:45	4.451	204.31		00:02:45	8.969	216.07	
00:03:15	2.484	247.34		00:03:00	4.843	176.99		00:03:00	9.749	187.52	
00:03:30	2.688	252.58		00:03:15	5.29	199.39		00:03:15	10.639	211.90	
00:03:45	2.885	243.91		00:03:30	5.681	174.41		00:03:30	11.418	184.88	
00:04:00	3.108	240.71	245.51	00:03:45	6.128	201.82	191.38	00:03:45	12.309	208.12	201.70
00:04:15	3.302	244.20		00:04:00	6.52	178.07		00:04:00	13.089	181.05	
00:04:30	3.526	241.96		00:04:15	6.966	203.85		00:04:15	13.98	207.47	
00:04:45	3.721	245.46		00:04:30	7.358	179.17		00:04:30	14.76	179.92	
00:05:00	3.944	240.71		00:04:46	7.805	192.73		00:04:45	15.54	181.05	
00:05:15	4.139	241.44	242.75	00:05:01	8.197	180.28	186.82	00:05:00	16.431	206.17	191.13
00:05:30	4.334	237.54		00:05:16	8.644	205.16		00:05:15	17.212	178.49	
00:05:45	4.557	241.65		00:05:31	9.036	196.12		00:05:30	18.103	203.00	
00:06:00	4.752	241.44		00:05:46	9.483	204.31		00:05:45	18.885	178.16	
00:06:15	4.975	241.65		00:06:01	9.876	177.44		00:06:00	19.778	202.83	
00:06:30	5.171	248.79	242.21	00:06:16	10.323	200.60	196.72	00:06:15	20.559	175.77	187.65
00:06:45	5.394	252.34		00:06:31	10.716	174.25		00:06:30	21.451	200.15	
00:07:00	5.59	241.23		00:06:46	11.11	174.69		00:06:45	22.233	174.41	
00:07:15	5.813	247.22		00:07:01	11.557	200.60		00:07:00	23.126	198.57	
00:07:30	6.008	239.90		00:07:16	11.949	176.99		00:07:15	23.908	173.88	
00:07:45	6.232	243.66	244.87	00:07:31	12.397	203.51	186.01	00:07:30	24.801	199.16	189.23
00:08:00	6.427	245.64		00:07:46	12.789	178.07		00:07:45	25.582	174.18	
00:08:15	6.651	248.55		00:08:01	13.238	203.96		00:08:00	26.475	197.38	
00:08:30	6.846	244.30		00:08:16	13.63	180.28		00:08:15	27.257	172.85	
00:08:45	7.069	242.25		00:08:31	14.078	204.77		00:08:30	28.149	195.99	
00:09:00	7.265	241.23	244.40	00:08:46	14.47	175.91	188.60	00:08:45	28.932	170.02	182.08
00:09:15	7.46	255.64		00:09:02	14.919	186.64		00:09:00	29.715	170.02	
00:09:30	7.683	242.34		00:09:17	15.311	174.85		00:09:15	30.609	193.56	
00:09:45	7.879	246.95		00:09:32	15.759	201.04		00:09:30	31.391	168.81	
00:10:00	8.102	239.86		00:09:47	16.151	174.85		00:09:45	32.284	192.78	
00:10:15	8.298	232.21	243.40	00:10:02	16.599	199.83	187.44	00:10:00	33.067	168.05	178.64
00:10:30	8.521	248.67		00:10:17	16.993	175.75		00:10:15	33.96	191.10	
00:10:45	8.716	234.94		00:10:32	17.386	174.25		00:10:30	34.741	168.60	
00:11:00	8.94	235.38		00:10:47	17.835	197.89		00:10:45	35.634	193.34	
00:11:15	9.135	227.23		00:11:02	18.228	175.30		00:11:00	36.417	167.56	
00:11:30	9.358	259.86	241.22	00:11:17	18.676	201.04	184.85	00:11:15	37.31	189.46	182.01
00:11:45	9.554	228.40		00:11:32	19.067	174.41		00:11:30	38.092	166.39	
00:12:00	9.777	255.67		00:11:47	19.515	199.83		00:11:45	38.986	189.67	
00:12:15	9.973	224.72		00:12:02	19.908	174.25		00:12:00	39.767	163.82	
00:12:30	10.196	225.67		00:12:17	20.356	197.45		00:12:15	40.661	187.53	
00:12:45	10.392	224.72	231.83	00:12:32	20.749	173.21	183.83	00:12:30	41.442	163.82	174.25
00:13:00	10.587	227.23		00:12:47	21.196	195.85		00:12:45	42.225	163.32	
00:13:15	10.81	238.67		00:13:02	21.588	170.74		00:13:00	43.119	185.94	
00:13:30	11.006	232.21		00:13:18	22.036	182.94		00:13:15	43.901	162.65	
00:13:45	11.229	247.68		00:13:33	22.429	171.17		00:13:30	44.793	185.53	
00:14:00	11.425	214.34	232.03	00:13:48	22.82	171.31	178.40	00:13:45	45.576	161.50	171.79
00:14:15	11.648	247.68		00:14:03	23.269	196.72		00:14:00	46.468	182.45	
00:14:30	11.843	216.58		00:14:37	24.189	174.73		00:14:15	47.25	159.95	
00:14:45	12.067	248.79		00:14:52	24.635	193.12		00:14:30	48.144	183.37	
00:15:00	12.262	213.25		00:15:07	25.027	168.75		00:14:45	48.927	160.60	
00:15:15	12.486	244.96	234.25	00:15:22	25.473	190.89	184.84	00:15:00	49.819	182.45	173.77
00:15:30	12.681	240.65		00:15:37	25.868	172.05		00:15:15	50.6	160.19	
00:15:45	12.904	241.64		00:15:52	26.316	196.29		00:15:30	51.494	183.88	
00:16:00	13.1	204.89		00:16:07	26.708	172.77		00:15:45	52.276	159.95	
00:16:15	13.323	233.11		00:16:22	27.156	193.99		00:16:00	53.059	158.41	
00:16:30	13.519	207.33	225.52	00:16:37	27.548	166.81	180.38	00:16:15	53.951	180.46	168.58
00:16:45	13.714	208.75		00:16:52	27.995	190.22		00:16:30	54.733	159.07	
00:17:00	13.938	242.72		00:17:07	28.388	169.18		00:16:45	55.627	182.86	
00:17:15	14.133	213.91		00:17:22	28.836	195.13		00:17:00	56.408	159.75	
00:17:30	14.357	242.72		00:17:37	29.228	167.78		00:17:15	57.302	181.36	
00:17:45	14.552	206.27	222.88	00:17:52	29.62	165.86	177.63	00:17:30	58.083	158.87	168.38
00:18:00	14.775	233.11		00:18:07	30.068	192.86		00:17:45	58.976	181.65	
00:18:15	14.97	201.47		00:18:22	30.461	169.18		00:18:00	59.758	159.51	
00:18:30	15.194	234.16		00:18:38	30.909	180.81		00:18:15	60.65	183.47	
00:18:45	15.389	206.27		00:18:53	31.3	168.32		00:18:30	61.433	160.16	
00:19:00	15.612	233.11	221.62	00:19:08	31.75	190.40	180.32	00:18:45	62.326	180.17	172.99
00:19:15	15.808	207.33		00:19:23	32.142	163.99		00:19:00	63.109	156.27	
00:19:30	16.031	241.64		00:19:38	32.589	188.06		00:19:15	64.001	178.51	
00:19:45	16.227	204.89		00:19:53	32.982	166.28		00:19:30	64.783	157.77	
00:20:00	16.45	230.40		00:20:08	33.429	188.06		00:19:45	65.565	157.35	
00:20:15	16.645	208.75	218.60	00:20:23	33.822	165.34	174.35	00:20:00	66.458	179.19	165.82
00:20:30	16.841	209.82		00:20:38	34.271	187.83		00:20:15	67.239	157.57	
00:20:45	17.064	235.89		00:20:53	34.664	164.41		00:20:30	68.132	179.19	
00:21:00	17.26	209.82		00:21:08	35.056	164.92		00:20:45	68.913	154.62	
00:21:15	17.483	238.73		00:21:23	35.504	189.56		00:21:00	69.806	175.86	
00:21:30	17.679	209.82	220.82	00:21:38	35.896	165.86	174.51	00:21:15	70.589	154.61	164.37
00:21:45	17.902	241.64		00:21:53	36.344	188.48		00:21:30	71.482	176.80	
00:22:00	18.097	211.30		00:22:08	36.736	163.99		00:21:45	72.263	155.04	
00:22:15	18.321	239.80		00:22:23	37.184	188.48		00:22:00	73.157	175.59	
00:22:30	18.517	207.33		00:22:38	37.576	168.75		00:22:15	73.938	151.39	
00:22:45	18.74	238.73	227.76	00:22:53	38.024	191.75	180.29	00:22:30	74.831	173.10	166.38
00:23:00	18.935	211.30		00:23:08	38.417	164.41		00:22:45	75.614	152.17	
00:23:15	19.159	245.72		00:23:24	38.865	175.70		00:23:00	76.506	173.81	
00:23:30	19.354	213.91		00:23:39	39.258	166.28		00:23:15	77.289	153.38	
00:23:45	19.577	241.64		00:23:54	39.706	188.48		00:23:30	78.072	154.20	
00:24:00	19.773	207.33	223.98	00:24:09	40.099	163.48	171.67	00:23:45	78.964	174.27	161.57
00:24:15	19.968	201.47		00:24:24	40.492	163.48		00:24:00	79.747	152.17	
00:24:30	20.191	230.40		00:24:39	40.939	185.94		00:24:15	80.64	173.55	
00:24:45	20.387	202.50		00:24:54	41.331	163.07		00:24:30	81.422	150.79	
00:25:00	20.61	230.40		00:25:09	41.779	187.41		00:24:45	82.315	172.64	
00:25:15	20.806	202.50	213.46	00:25:24	42.172	164.41	172.86	00:25:00	83.098	151.77	160.19
00:25:30	21.029	233.11		00:25:39	42.62	187.41		00:25:15	83.99	172.45	
00:25:45	21.225	209.82		00:25:54	43.012	163.99		00:25:30	84.773	151.38	
00:26:00	21.448	238.73		00:26:09	43.46	187.41		00:25:45	85.668	171.68	
00:26:15	21.644	207.33		00:26:24	43.853	165.34		00:26:00	86.45	150.40	
00:26:30	21.867	241.64	226.13	00:26:39	44.301	187.41	178.31	00:26:15	87.343	172.64	163.71
00:26:45	22.063	209.82		00:26:54	44.694	167.24		00:26:30	88.124	149.82	
00:27:00	22.286	233.11		00:27:09	45.142	190.64		00:26:45	89.018	170.17	
00:27:15	22.482	207.33		00:27:24	45.534	163.07		00:27:00	89.801	149.04	
00:27:30	22.677	208.75		00:27:39	45.981	184.91		00:27:15	90.584	149.04	
00:27:45	22.9	241.64	220.13	00:27:55	46.376	154.04	171.98	00:27:30	91.477	169.54	157.52
00:28:00	23.096	209.82		00:28:10	46.768	165.86		00:27:45	92.259	148.47	
00:28:15	23.319	233.11		00:28:25	47.216	188.48		00:28:00	93.152	169.54	
00:28:30	23.515	204.89		00:28:40	47.607	161.74		00:28:15	93.933	148.66	
00:28:45	23.738	235.89		00:28:55	48.055	184.29		00:28:30	94.826	169.54	
00:29:00	23.933	203.84	217.51	00:29:10	48.448	161.67	172.41	00:28:45	95.609	147.90	156.82
00:29:15	24.157	234.16		00:29:25	48.896	185.32		00:29:00	96.501	168.49	
00:29:30	24.352	208.75		00:29:40	49.29	162.98		00:29:15	97.284	147.53	
00:29:45	24.576	239.80		00:29:55	49.738	184.29		00:29:30	98.176	167.21	
00:30:00	24.771	206.27		00:30:10	50.131	161.67		00:29:45	98.959	147.15	
00:30:15	24.994	233.11	224.42	00:30:25	50.578	184.91	175.83	00:30:00	99.853	167.59	159.59
00:30:30	25.19	204.89		00:30:40	50.971	163.48		00:30:15	100.636	144.94	
00:30:45	25.413	235.89		00:30:55	51.42	185.73		00:30:30	101.418	144.76	
00:31:00	25.609	202.50		00:31:10	51.812	160.36		00:30:45	102.311	165.31	
00:31:15	25.804	196.89		00:31:25	52.204	159.48		00:31:00	103.093	144.76	
00:31:30	26.028	228.77	213.79	00:31:40	52.652	182.26	170.26	00:31:15	103.987	165.49	153.05
00:31:45	26.223	203.84		00:31:55	53.044	159.48		00:31:30	104.768	144.94	
00:32:00	26.446	233.11		00:32:11	53.492	171.82		00:31:45	105.662	167.16	
00:32:15	26.642	202.50		00:32:26	53.884	160.36		00:32:00	106.444	145.85	
00:32:30	26.865	230.40		00:32:41	54.332	183.27		00:32:15	107.337	166.14	
00:32:45	27.061	202.50	214.47	00:32:56	54.724	161.25	167.24	00:32:30	108.119	144.04	153.62
00:33:00	27.285	234.16		00:33:11	55.172	184.29		00:32:45	109.012	163.26	
00:33:15	27.48	203.84		00:33:26	55.565	159.89		00:33:00	109.796	143.34	
00:33:30	27.703	230.40		00:33:41	56.014	181.67		00:33:15	110.69	165.08	
00:33:45	27.899	192.08		00:33:56	56.407	159.01		00:33:30	111.471	145.67	
00:34:00	28.122	235.89	219.27	00:34:11	56.855	180.28	173.03	00:33:45	112.365	164.67	156.40
00:34:15	28.318	204.89		00:34:26	57.248	160.77		00:34:00	113.146	142.44	
00:34:30	28.541	230.40		00:34:41	57.696	183.27		00:34:15	113.929	142.45	
00:34:45	28.736	206.27		00:34:56	58.089	158.15		00:34:30	114.823	162.64	
00:35:00	28.932	209.82		00:35:11	58.481	157.75		00:34:46	115.606	133.55	
00:35:15	29.155	235.89	217.45	00:35:26	58.929	180.28	168.05	00:35:01	116.5	161.85	148.59
00:35:30	29.35	203.84		00:35:41	59.322	157.30		00:35:16	117.281	140.70	
00:35:45	29.574	234.16		00:35:56	59.769	178.91		00:35:31	118.175	161.06	
00:36:00	29.769	203.84		00:36:11	60.162	159.01		00:35:46	118.957	141.23	
00:36:15	29.992	222.63		00:36:26	60.61	181.27		00:36:01	119.851	161.06	
00:36:30	30.188	197.90	212.48	00:36:42	61.003	149.08	165.11	00:36:16	120.633	140.88	148.99
00:36:45	30.411	233.11		00:36:57	61.452	183.68		00:36:31	121.528	161.64	
00:37:00	30.607	202.50		00:37:12	61.844	160.36		00:36:46	122.31	141.57	
00:37:15	30.83	227.75		00:37:27	62.292	181.27		00:37:01	123.203	162.06	
00:37:30	31.025	203.84		00:37:42	62.684	157.75		00:37:16	123.986	142.45	
00:37:45	31.249	236.94	220.83	00:37:57	63.132	181.27	172.87	00:37:31	124.768	141.23	149.79
00:38:00	31.444	199.16		00:38:12	63.525	159.89		00:37:46	125.661	160.10	
00:38:15	31.668	226.17		00:38:27	63.917	158.61		00:38:01	126.443	141.23	
00:38:30	31.863	201.47		00:38:42	64.366	179.71		00:38:16	127.337	161.45	
00:38:45	32.059	204.89		00:38:57	64.758	157.75		00:38:31	128.118	140.70	
00:39:00	32.282	227.75	211.89	00:39:12	65.205	179.88	167.17	00:38:46	129.012	160.67	152.83
00:39:15	32.477	199.16		00:39:46	66.125	161.58		00:39:01	129.794	140.20	
00:39:30	32.701	231.43		00:40:01	66.573	179.31		00:39:16	130.689	160.07	
00:39:45	32.896	199.16		00:40:16	66.963	157.80		00:39:31	131.471	139.53	

Total Clay: 4.46

Core ID: D- 2- 5

	ki	k @ 50 ml/ h		k @ 100 ml/ h		k @ 200 ml/ h			flow rate ml/ h	k %	pH 3	ki/ kf
	328.2	205.13		160.19		143.82			50	37.50	14.08	1.60
Damage Ration		37.50		51.19		56.18			100	51.19	18.7	2.05
D= 100- kf *100/ ki									200	56.18	31.82	2.28

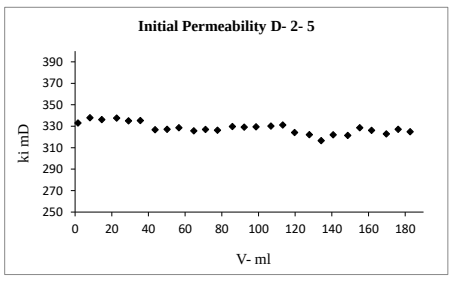

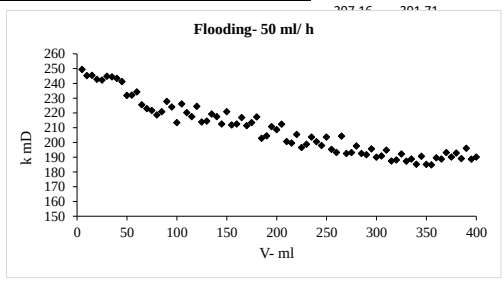

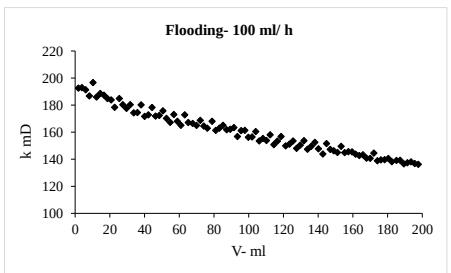

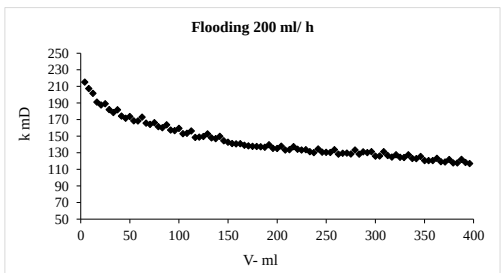

Group	Sample ID	Quartz	Calcite Mg	Oligoclase	Microcline	Chl. IIb	Kao.	Illite 2M1	Biotite 1M	Dol.	amorph.	Total Clay	Φ_{He} (%)	k_{wi} (mD)
D- 2- 5	D- 2- 2140.3	78.3	4.6	6.4	0.8	2.0	0.1	2.3	0.1	1.4	4.0	4.45	22.49	325.32

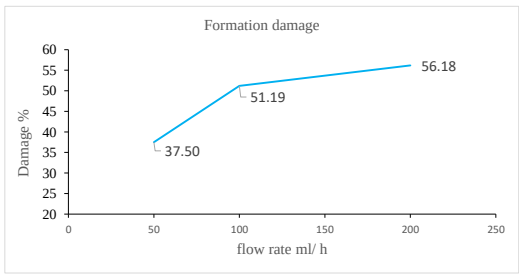

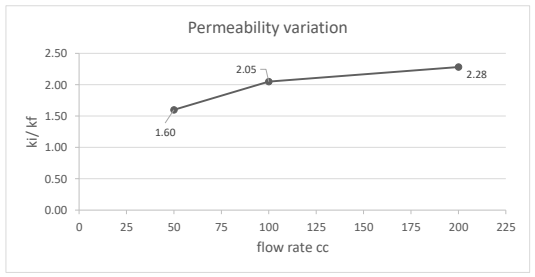

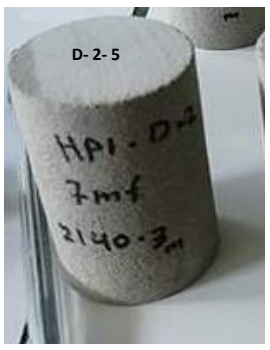

00:40:00	33.119	227.75		00:40:31	67.409	180.46		00:39:46	132.364	160.10	
00:40:15	33.315	204.89	212.48	00:40:47	67.815	153.17	166.46	00:40:01	133.145	140.02	147.99
00:40:30	33.538	233.11		00:41:03	68.301	183.35		00:40:16	134.039	159.89	
00:40:45	33.734	200.18		00:41:18	68.699	158.44		00:40:31	134.821	139.53	
00:41:00	33.957	225.16		00:41:34	69.164	172.62		00:40:46	135.604	139.03	
00:41:15	34.153	197.90		00:41:49	69.556	155.22		00:41:01	136.496	158.01	
00:41:30	34.376	227.75	216.82	00:42:04	69.949	155.61	165.05	00:41:16	137.279	138.70	147.03
00:41:45	34.572	202.50		00:42:19	70.399	179.14		00:41:31	138.171	158.01	
00:42:00	34.768	195.68		00:42:34	70.796	158.04		00:41:46	138.953	138.52	
00:42:15	34.991	222.63		00:42:50	71.244	168.10		00:42:01	139.846	157.43	
00:42:30	35.186	201.47		00:43:05	71.636	157.75		00:42:16	140.628	137.86	
00:42:45	35.41	234.16	211.29	00:43:20	72.083	180.86	168.78	00:42:31	141.521	157.43	149.85
00:43:00	35.605	201.47		00:43:35	72.475	158.61		00:42:46	142.302	136.71	
00:43:15	35.829	228.77		00:43:50	72.924	178.74		00:43:01	143.194	156.14	
00:43:30	36.024	201.47		00:44:05	73.317	154.79		00:43:16	143.978	137.24	
00:43:45	36.247	230.40		00:44:20	73.764	176.05		00:43:31	144.87	155.77	
00:44:00	36.443	204.89	213.40	00:44:35	74.157	154.79	164.60	00:43:46	145.653	136.42	144.46
00:44:15	36.666	233.11		00:44:50	74.604	175.12		00:44:01	146.547	155.03	
00:44:30	36.862	200.18		00:45:05	74.997	153.97		00:44:16	147.328	135.12	
00:44:45	37.085	225.16		00:45:20	75.445	175.51		00:44:31	148.111	135.15	
00:45:00	37.281	200.18		00:45:35	75.837	153.58		00:44:46	149.004	153.77	
00:45:15	37.504	227.75	217.28	00:45:50	76.231	156.85	163.01	00:45:01	149.785	134.80	142.77
00:45:30	37.7	200.18		00:46:05	76.681	178.18		00:45:16	150.678	133.77	
00:45:45	37.895	201.47		00:46:20	77.073	153.58		00:45:31	151.46	133.73	
00:46:00	38.118	222.63		00:46:35	77.521	177.39		00:45:46	152.353	152.71	
00:46:15	38.314	195.68		00:47:12	78.505	157.12		00:46:01	153.136	133.90	
00:46:30	38.482	193.86	202.77	00:47:27	78.952	174.20	168.09	00:46:16	154.028	151.84	141.19
00:46:45	38.633	176.54		00:47:42	79.343	152.38		00:46:31	154.811	132.98	
00:47:00	38.828	201.47		00:47:57	79.789	173.81		00:46:46	155.705	151.83	
00:47:15	39.052	221.15		00:48:12	80.184	153.13		00:47:01	156.488	133.28	
00:47:30	39.247	192.52		00:48:27	80.632	173.68		00:47:16	157.381	152.36	
00:47:45	39.47	230.40	204.42	00:48:42	81.025	153.97	161.39	00:47:31	158.164	133.28	140.74
00:48:00	39.666	204.89		00:48:57	81.473	178.35		00:47:46	159.056	151.84	
00:48:15	39.889	227.75		00:49:12	81.865	155.22		00:48:01	159.84	133.76	
00:48:30	40.085	197.90		00:49:27	82.257	152.77		00:48:16	160.623	134.21	
00:48:45	40.308	225.16		00:49:42	82.705	174.59		00:48:31	161.516	152.36	
00:49:00	40.504	197.90	210.72	00:49:57	83.098	153.97	162.98	00:48:46	162.299	132.67	140.97
00:49:15	40.7	197.90		00:50:12	83.546	176.45		00:49:01	163.192	131.66	
00:49:30	40.923	227.75		00:50:27	83.938	154.39		00:49:16	163.974	131.90	
00:49:45	41.118	201.47		00:50:43	84.387	166.68		00:49:31	164.869	149.59	
00:50:00	41.342	223.63		00:50:58	84.78	154.79		00:49:46	165.65	131.13	
00:50:15	41.537	192.52	208.66	00:51:13	85.227	173.29	165.12	00:50:01	166.544	151.48	139.15
00:50:30	41.761	221.15		00:51:28	85.619	153.58		00:50:16	167.326	131.90	
00:50:45	41.956	192.52		00:51:43	86.067	176.45		00:50:31	168.22	149.77	
00:51:00	42.179	225.16		00:51:58	86.459	152.77		00:50:46	169.002	131.00	
00:51:15	42.375	197.90		00:52:13	86.907	174.59		00:51:01	169.896	149.09	
00:51:30	42.598	225.16	212.38	00:52:28	87.299	151.97	161.87	00:51:16	170.678	130.41	138.43
00:51:45	42.794	191.38		00:52:43	87.692	152.35		00:51:31	171.46	130.71	
00:52:00	43.017	210.79		00:52:58	88.14	175.51		00:51:46	172.352	148.42	
00:52:15	43.212	184.33		00:53:13	88.533	154.79		00:52:01	173.135	130.58	
00:52:30	43.436	218.72		00:53:28	88.983	176.30		00:52:16	174.027	149.09	
00:52:45	43.632	197.90	200.62	00:53:43	89.375	151.97	162.18	00:52:31	174.809	130.12	137.78
00:53:00	43.827	190.40		00:53:58	89.823	172.77		00:52:46	175.702	138.59	
00:53:15	44.05	210.79		00:54:13	90.216	151.56		00:53:01	176.484	130.41	
00:53:30	44.246	185.27		00:54:28	90.663	172.39		00:53:16	177.377	139.26	
00:53:45	44.469	217.74		00:54:43	91.055	149.62		00:53:31	178.16	130.87	
00:54:00	44.665	193.50	199.54	00:54:58	91.503	170.99	163.47	00:53:46	179.052	148.76	137.58
00:54:15	44.888	213.06		00:55:13	91.895	151.18		00:54:01	179.833	130.25	
00:54:30	45.084	191.38		00:55:28	92.342	172.39		00:54:16	180.727	148.76	
00:54:45	45.307	220.16		00:55:43	92.735	150.00		00:54:31	181.511	130.16	
00:55:00	45.503	189.30		00:55:59	93.127	138.83		00:54:46	182.292	129.37	
00:55:15	45.726	213.06	205.39	00:56:14	93.575	171.88	156.85	00:55:01	183.185	148.26	137.36
00:55:30	45.921	186.31		00:56:29	93.967	152.77		00:55:16	183.967	130.12	
00:55:45	46.145	216.34		00:56:44	94.416	174.06		00:55:31	184.862	148.59	
00:56:00	46.34	186.31		00:56:59	94.817	155.46		00:55:46	185.643	128.80	
00:56:15	46.536	185.27		00:57:14	95.266	174.06		00:56:01	186.535	146.77	
00:56:30	46.759	208.57	196.56	00:57:29	95.657	149.24	161.12	00:56:16	187.318	129.13	136.68
00:56:45	46.955	183.32		00:57:44	96.105	169.25		00:56:31	188.211	146.94	
00:57:00	47.178	217.74		00:57:59	96.496	147.71		00:56:46	188.993	128.96	
00:57:15	47.373	190.40		00:58:14	96.944	169.25		00:57:01	189.886	147.27	
00:57:30	47.596	213.06		00:58:29	97.337	150.00		00:57:16	190.669	128.84	
00:57:45	47.792	189.30	198.76	00:58:44	97.785	170.99	161.44	00:57:31	191.561	146.45	139.69
00:58:00	48.015	215.37		00:58:59	98.178	150.00		00:57:46	192.344	128.27	
00:58:15	48.211	187.26		00:59:15	98.626	160.30		00:58:01	193.237	146.94	
00:58:30	48.434	213.06		00:59:30	99.019	150.00		00:58:16	194.018	128.22	
00:58:45	48.63	189.30		00:59:45	99.412	150.00		00:58:31	194.801	127.70	
00:59:00	48.853	213.06	203.61	01:00:00	99.86	170.99	156.26	00:58:46	195.695	146.13	135.45
00:59:15	49.048	186.31		01:00:15	100.252	149.62		00:59:01	196.476	128.22	
00:59:30	49.272	221.15		01:00:30	100.7	168.39		00:59:16	197.371	146.29	
00:59:45	49.467	192.52		01:00:45	101.093	147.71		00:59:31	198.152	127.38	
01:00:00	49.663	189.30		01:01:00	101.541	168.39		00:59:46	199.046	146.13	
01:00:15	49.886	213.06	200.47	01:01:15	101.932	148.47	156.52	01:00:01	199.829	127.99	135.20
01:00:30	50.081	184.33		01:01:30	102.38	169.25		01:00:16	200.722	145.97	
01:00:45	50.304	210.79		01:01:45	102.775	147.72		01:00:31	201.504	127.82	
01:01:00	50.5	191.38		01:02:00	103.222	168.87		01:00:46	202.398	145.81	
01:01:15	50.723	217.74		01:02:15	103.616	148.85		01:01:01	203.181	126.59	
01:01:30	50.919	185.27	197.90	01:02:30	104.063	168.01	160.54	01:01:16	204.075	143.91	138.02
01:01:45	51.142	213.06		01:02:45	104.456	146.97		01:01:31	204.857	125.88	
01:02:00	51.338	189.30		01:03:00	104.849	146.97		01:01:46	205.639	126.15	
01:02:15	51.561	215.37		01:03:15	105.297	168.39		01:02:01	206.532	144.06	
01:02:30	51.757	187.26		01:03:31	105.69	138.48		01:02:16	207.313	125.99	
01:02:45	51.98	213.06	203.61	01:03:46	106.138	166.69	153.50	01:02:31	208.207	144.53	133.32
01:03:00	52.176	187.26		01:04:01	106.53	146.59		01:02:46	208.99	126.59	
01:03:15	52.399	210.79		01:04:16	106.979	169.62		01:03:01	209.883	144.06	
01:03:30	52.594	184.33		01:04:31	107.371	147.34		01:03:16	210.663	126.10	
01:03:45	52.79	183.32		01:04:46	107.819	167.54		01:03:31	211.557	145.17	
01:04:00	53.013	210.79	195.30	01:05:01	108.212	145.50	155.32	01:03:46	212.339	126.98	133.78
01:04:15	53.209	185.27		01:05:16	108.661	164.59		01:04:01	213.232	144.69	
01:04:30	53.432	206.40		01:05:31	109.053	145.86		01:04:16	214.013	126.26	
01:04:45	53.628	181.41		01:05:46	109.501	166.69		01:04:31	214.907	144.53	
01:05:00	53.851	208.57		01:06:01	109.893	145.13		01:04:46	215.689	126.43	
01:05:15	54.046	184.33	193.20	01:06:16	110.286	146.97	153.85	01:05:01	216.581	145.16	137.41
01:05:30	54.27	211.74		01:06:31	110.734	166.69		01:05:16	217.364	128.27	
01:05:45	54.466	191.38		01:06:46	111.127	146.23		01:05:31	218.146	127.54	
01:06:00	54.689	217.74		01:07:01	111.575	166.69		01:05:46	219.038	144.84	
01:06:15	54.885	187.26		01:07:16	111.967	145.13		01:06:01	219.819	126.26	
01:06:30	55.108	213.06	204.24	01:07:31	112.415	165.86	158.12	01:06:16	220.712	144.37	134.26
01:06:45	55.303	184.33		01:07:46	112.807	145.13		01:06:31	221.495	126.59	
01:07:00	55.527	211.74		01:08:02	113.256	155.07		01:06:46	222.387	143.90	
01:07:15	55.722	186.31		01:08:17	113.649	144.06		01:07:01	223.169	126.15	
01:07:30	55.917	184.33		01:08:32	114.097	165.04		01:07:16	224.061	143.90	
01:07:45	56.14	195.54	192.45	01:08:47	114.489	145.13	150.88	01:07:31	224.844	126.31	133.37
01:08:00	56.336	185.27		01:09:02	114.937	165.04		01:07:46	225.736	142.65	
01:08:15	56.56	211.74		01:09:17	115.329	144.41		01:08:01	226.52	124.84	
01:08:30	56.755	182.38		01:09:32	115.721	145.86		01:08:16	227.414	142.66	
01:08:45	56.979	207.33		01:09:47	116.17	167.07		01:08:31	228.196	124.79	
01:09:00	57.174	178.62	193.07	01:10:02	116.563	144.77	153.43	01:08:47	229.089	133.60	133.71
01:09:15	57.398	207.33		01:10:17	117.01	164.67		01:09:02	229.871	124.79	
01:09:30	57.593	182.38		01:10:32	117.404	145.14		01:09:17	230.653	124.52	
01:09:45	57.816	206.40		01:10:47	117.852	164.22		01:09:32	231.546	141.59	
01:10:00	58.011	182.38		01:11:02	118.245	144.77		01:09:47	232.328	123.99	
01:10:15	58.235	209.51	197.60	01:11:17	118.694	165.40	156.84	01:10:02	233.223	141.91	131.36
01:10:30	58.431	181.41		01:11:32	119.086	144.41		01:10:17	234.005	123.72	
01:10:45	58.626	180.49		01:12:09	120.125	155.17		01:10:32	234.898	140.99	
01:11:00	58.85	209.51		01:12:24	120.517	143.69		01:10:47	235.679	122.78	
01:11:15	59.045	182.38		01:12:39	120.963	163.49		01:11:02	236.571	139.93	
01:11:30	59.268	208.57	192.47	01:12:54	121.354	142.62	149.87	01:11:17	237.353	123.46	130.18
01:11:45	59.463	184.33		01:13:09	121.806	164.87		01:11:32	238.246	141.29	
01:12:00	59.687	209.51		01:13:24	122.198	142.98		01:11:47	239.029	123.88	
01:12:15	59.882	178.62		01:13:39	122.591	143.35		01:12:02	239.922	141.89	
01:12:30	60.105	204.27		01:13:54	123.04	162.97		01:12:17	240.704	124.52	
01:12:45	60.301	181.41	191.63	01:14:09	123.433	141.95	151.22	01:12:32	241.596	141.73	134.66
01:13:00	60.524	206.40		01:14:24	123.881	162.61		01:12:47	242.378	123.99	
01:13:15	60.719	180.49		01:14:39	124.274	141.95		01:13:02	243.161	124.41	
01:13:30	60.942	204.27		01:14:54	124.722	160.25		01:13:17	244.053	141.43	
01:13:45	61.138	179.54		01:15:09	125.113	140.54		01:13:32	244.837	123.78	
01:14:00	61.362	207.33	195.61	01:15:24	125.562	162.18	153.51	01:13:47	245.729	140.53	130.83
01:14:15	61.557	180.49		01:15:39	125.954	140.90		01:14:02	246.512	123.36	
01:14:30	61.78	206.40		01:15:55	126.401	151.36		01:14:17	247.404	140.53	
01:14:45	61.976	181.41		01:16:10	126.794	142.65		01:14:32	248.186	123.46	
01:15:00	62.171	178.62		01:16:25	127.242	162.61		01:14:47	249.08	141.45	
01:15:15	62.395	203.10	190.00	01:16:40	127.634	142.98	148.10	01:15:02	249.863	123.88	130.53
01:15:30	62.591	179.54		01:16:55	128.027	143.35		01:15:17	250.757	141.75	
01:15:45	62.814	204.27		01:17:10	128.475	161.82		01:15:32	251.539	123.72	
01:16:00	63.009	178.62		01:17:25	128.867	141.59		01:15:47	252.432	140.39	
01:16:15	63.233	209.51		01:17:40	129.315	163.41		01:16:02	253.215	123.36	
01:16:30	63.428	182.38	190.87	01:17:55	129.707	142.28	150.49	01:16:17	253.996	123.04	130.45
01:16:45	63.651	206.40		01:18:10	130.155	161.03		01:16:32	254.89	140.84	
01:17:00	63.847	181.41		01:18:25	130.549	142.31		01:16:47	255.672	123.99	
01:17:15	64.07	204.27		01:18:40	130.997	161.82		01:17:02	256.564	140.83	
01:17:30	64.266	179.54		01:18:55	131.39	141.95		01:17:17	257.347	123.36	
01:17:45	64.489	202.19	194.76	01:19:10	131.838	161.82	153.78	01:17:32	258.24	140.09	133.82
01:18:00	64.685	175.91		01:19:25	132.231	141.26		01:17:47	259.022	121.65	
01:18:15	64.88	176.80		01:19:40	132.679	162.61		01:18:02	259.915	138.91	
01:18:30	65.103	202.19		01:19:55	133.071	142.28		01:18:17	260.698	121.29	
01:18:45	65.299	177.71		01:20:10	133.464	140.58		01:18:32	261.59	138.47	
01:19:00	65.522	204.27	187.38	01:20:26	133.912	150.24	147.39	01:18:47	262.372	121.39	128.34
01:19:15	65.718	179.54		01:20:41	134.304	141.59		01:19:02	263.264	137.60	
01:19:30	65.941	200.15		01:20:56	134.752	162.61		01:19:17	264.046	120.63	
01:19:45	66.137	177.71		01:21:11	135.144	140.90		01:19:32	264.94	137.34	
01:20:00	66.36	206.40		01:21:26	135.592	161.03		01:19:47	265.723	120.28	
01:20:15	66.555	176.80	188.12	01:21:41	135.985	141.95	149.62	01:20:02	266.643	131.72	129.51
01:20:30	66.779	203.10		01:21:56	136.432	159.89		01:20:17	267.537	127.61	
01:20:45	66.974	176.80		01:22:11	136.826	140.94		01:20:32	268.319	126.56	
01:21:00	67.198	199.03		01:22:26	137.274	161.03		01:20:47	269.211	134.32	

01:21:15	67.394	177.71		01:22:41	137.667	140.58		01:21:02	269.992	132.03	
01:21:30	67.617	204.27	192.18	01:22:56	138.115	160.25	152.54	01:21:17	270.887	127.60	129.62
01:21:45	67.812	178.62		01:23:11	138.508	141.26		01:21:32	271.668	128.51	
01:22:00	68.008	177.71		01:23:26	138.901	141.26		01:21:47	272.562	128.42	
01:22:15	68.231	202.19		01:23:41	139.349	160.25		01:22:02	273.345	130.58	
01:22:30	68.427	177.71		01:23:56	139.741	138.22		01:22:17	274.239	127.76	
01:22:45	68.65	200.15	187.28	01:24:11	140.19	157.57	147.71	01:22:32	275.02	127.66	128.59
01:23:00	68.846	179.54		01:24:26	140.583	139.23		01:22:47	275.914	144.22	
01:23:15	69.069	204.27		01:24:42	141.031	149.51		01:23:02	276.698	124.84	
01:23:30	69.265	177.71		01:24:57	141.424	139.23		01:23:17	277.479	125.17	
01:23:45	69.488	204.27		01:25:31	142.395	151.77		01:23:32	278.372	144.69	
01:24:00	69.684	177.71	188.70	01:25:46	142.787	139.55	143.86	01:23:47	279.155	128.27	133.44
01:24:15	69.907	200.15		01:26:01	143.233	159.54		01:24:02	280.048	126.29	
01:24:30	70.102	176.80		01:26:16	143.625	139.55		01:24:17	280.829	125.72	
01:24:45	70.326	201.04		01:26:31	144.075	159.43		01:24:32	281.722	123.12	
01:25:00	70.521	173.27		01:26:46	144.467	139.55		01:24:47	282.504	125.06	
01:25:15	70.716	175.02	185.25	01:27:01	144.916	159.84	151.58	01:25:02	283.398	141.45	128.33
01:25:30	70.94	203.10		01:27:16	145.308	140.22		01:25:17	284.18	124.52	
01:25:45	71.135	176.80		01:27:31	145.703	141.29		01:25:32	285.073	142.81	
01:26:00	71.358	200.15		01:27:46	146.15	158.36		01:25:47	285.854	123.57	
01:26:15	71.554	174.15		01:28:01	146.542	138.22		01:26:02	286.746	141.13	
01:26:30	71.778	199.03	190.65	01:28:16	146.991	158.32	147.28	01:26:17	287.529	124.15	131.24
01:26:45	71.973	175.02		01:28:31	147.383	138.22		01:26:32	288.312	123.62	
01:27:00	72.197	203.10		01:28:46	147.831	158.72		01:26:47	289.206	141.14	
01:27:15	72.392	175.02		01:29:01	148.225	139.59		01:27:02	289.989	123.62	
01:27:30	72.615	198.14		01:29:16	148.673	157.21		01:27:17	290.883	140.54	
01:27:45	72.811	174.15	185.09	01:29:31	149.065	137.56	146.26	01:27:32	291.664	122.00	130.19
01:28:00	73.034	198.14		01:29:46	149.513	158.72		01:27:47	292.557	138.62	
01:28:15	73.23	174.15		01:30:02	149.905	130.20		01:28:02	293.339	121.14	
01:28:30	73.453	198.14		01:30:17	150.353	158.72		01:28:17	294.232	138.33	
01:28:45	73.649	175.91		01:30:32	150.746	139.23		01:28:32	295.015	121.29	
01:29:00	73.845	177.71	184.81	01:30:47	151.138	138.22	145.02	01:28:47	295.907	137.89	131.45
01:29:15	74.068	200.15		01:31:02	151.586	157.21		01:29:02	296.69	120.28	
01:29:30	74.263	171.55		01:31:17	151.979	138.57		01:29:17	297.583	136.62	
01:29:45	74.487	197.06		01:31:32	152.428	158.32		01:29:32	298.366	119.05	
01:30:00	74.682	175.02		01:31:47	152.819	136.56		01:29:47	299.258	135.07	
01:30:15	74.905	204.27	189.61	01:32:02	153.269	157.17	149.57	01:30:02	300.041	119.05	126.01
01:30:30	75.101	189.30		01:32:17	153.661	135.63		01:30:17	300.822	118.50	
01:30:45	75.324	193.06		01:32:32	154.11	155.36		01:30:32	301.716	135.65	
01:31:00	75.52	183.32		01:32:47	154.502	136.91		01:30:47	302.498	120.13	
01:31:15	75.744	183.63		01:33:02	154.95	157.96		01:31:02	303.392	137.62	
01:31:30	75.939	194.68	188.80	01:33:17	155.342	138.88	144.95	01:31:17	304.173	119.24	126.23
01:31:45	76.163	214.01		01:33:32	155.79	159.48		01:31:32	305.066	136.90	
01:32:00	76.358	184.33		01:33:47	156.182	139.55		01:31:47	305.849	120.79	
01:32:15	76.554	183.32		01:34:02	156.574	136.27		01:32:02	306.741	138.18	
01:32:30	76.777	198.57		01:34:17	157.023	155.36		01:32:17	307.524	122.06	
01:32:45	76.973	185.27	193.10	01:34:32	157.415	137.56	145.64	01:32:32	308.417	138.62	131.31
01:33:00	77.196	188.57		01:34:48	157.863	146.00		01:32:47	309.198	120.98	
01:33:15	77.391	178.62		01:35:03	158.256	135.98		01:33:02	310.092	137.62	
01:33:30	77.614	186.40		01:35:18	158.704	156.47		01:33:17	310.874	119.14	
01:33:45	77.81	185.27		01:35:33	159.096	135.63		01:33:32	311.656	119.39	
01:34:00	78.034	211.74	190.12	01:35:48	159.544	153.58	145.53	01:33:47	312.55	136.49	126.72
01:34:15	78.229	184.33		01:36:03	159.936	135.63		01:34:02	313.332	118.65	
01:34:30	78.453	207.33		01:36:18	160.385	155.36		01:34:17	314.225	134.67	
01:34:45	78.648	180.49		01:36:33	160.777	135.63		01:34:32	315.007	117.93	
01:35:00	78.871	208.57		01:36:48	161.225	156.47		01:34:47	315.901	135.09	
01:35:15	79.067	183.32	192.81	01:37:03	161.618	135.98	143.82	01:35:02	316.682	117.78	124.83
01:35:30	79.262	180.49		01:37:18	162.01	134.38		01:35:17	317.577	134.42	
01:35:45	79.486	205.19		01:37:33	162.46	155.70		01:35:32	318.358	116.83	
01:36:00	79.682	179.54		01:37:48	162.852	135.63		01:35:47	319.252	133.46	
01:36:15	79.905	202.19		01:38:03	163.299	153.23		01:36:02	320.033	117.54	
01:36:30	80.101	177.71	189.02	01:38:18	163.692	134.72	142.73	01:36:17	320.925	135.90	127.63
01:36:45	80.324	204.27		01:38:33	164.14	152.87		01:36:32	321.708	119.54	
01:37:00	80.52	181.41		01:38:48	164.533	134.10		01:36:47	322.601	134.94	
01:37:15	80.744	205.19		01:39:03	164.98	153.23		01:37:02	323.382	117.30	
01:37:30	80.939	180.49		01:39:18	165.374	133.82		01:37:17	324.167	117.90	
01:37:45	81.162	208.57	195.99	01:39:34	165.822	142.66	143.34	01:37:32	325.059	133.97	124.73
01:38:00	81.358	181.41		01:39:49	166.214	133.76		01:37:47	325.842	118.08	
01:38:15	81.581	204.27		01:40:04	166.662	152.17		01:38:02	326.736	135.09	
01:38:30	81.777	179.54		01:40:19	167.055	134.10		01:38:17	327.518	117.93	
01:38:45	81.973	177.71		01:40:34	167.447	133.15		01:38:32	328.41	133.70	
01:39:00	82.196	200.15	188.62	01:40:49	167.896	151.12	140.86	01:38:47	329.191	116.59	124.28
01:39:15	82.391	176.80		01:41:04	168.288	132.54		01:39:02	330.085	133.73	
01:39:30	82.615	205.19		01:41:19	168.736	152.17		01:39:17	330.868	117.60	
01:39:45	82.81	180.49		01:41:34	169.129	132.88		01:39:32	331.761	134.67	
01:40:00	83.033	206.40		01:41:49	169.576	151.83		01:39:47	332.544	118.08	
01:40:15	83.229	181.41	190.06	01:42:04	169.971	134.16	140.71	01:40:02	333.436	133.97	127.61
01:40:30	83.452	204.27		01:42:19	170.419	150.78		01:40:17	334.219	116.65	
01:40:45	83.648	177.71		01:42:34	170.812	132.88		01:40:32	335.002	115.95	
01:41:00	83.871	204.27		01:42:49	171.26	152.17		01:40:47	335.894	132.89	
01:41:15	84.066	180.49		01:43:04	171.652	133.76		01:41:02	336.676	116.98	
01:41:30	84.289	204.27	194.20	01:43:19	172.101	153.21	144.56	01:41:17	337.569	133.58	123.21
01:41:45	84.485	177.71		01:43:35	172.493	124.82		01:41:32	338.351	116.98	
01:42:00	84.708	202.19		01:43:50	172.886	133.49		01:41:47	339.244	133.31	
01:42:15	84.904	166.60		01:44:05	173.333	151.13		01:42:02	340.027	116.42	
01:42:30	85.099	178.62		01:44:20	173.725	132.54		01:42:17	340.919	132.10	
01:42:45	85.323	207.33	186.49	01:44:35	174.174	152.51	138.90	01:42:32	341.702	115.95	122.95
01:43:00	85.518	180.49		01:44:50	174.566	132.54		01:42:47	342.595	132.78	
01:43:15	85.741	204.27		01:45:05	175.015	151.12		01:43:02	343.377	116.27	
01:43:30	85.937	175.91		01:45:20	175.407	131.93		01:43:17	344.271	132.39	
01:43:45	86.16	204.27		01:45:35	175.854	150.45		01:43:32	345.053	115.81	
01:44:00	86.356	181.41	189.27	01:45:50	176.248	132.01	139.61	01:43:47	345.945	131.05	125.66
01:44:15	86.579	200.15		01:46:05	176.696	150.10		01:44:02	346.727	113.98	
01:44:30	86.775	175.91		01:46:20	177.088	131.93		01:44:17	347.51	114.13	
01:44:45	86.998	200.15		01:46:35	177.535	151.13		01:44:32	348.404	130.31	
01:45:00	87.193	175.02		01:46:50	177.929	133.21		01:44:47	349.185	113.84	
01:45:15	87.417	201.04	190.45	01:47:05	178.321	131.93	139.66	01:45:02	350.081	130.60	120.57
01:45:30	87.613	172.43		01:47:20	178.769	150.10		01:45:17	350.863	114.21	
01:45:45	87.836	196.18		01:47:35	179.161	131.34		01:45:32	351.756	130.16	
01:46:00	88.031	175.02		01:47:50	179.609	150.10		01:45:47	352.538	113.98	
01:46:15	88.227	177.71		01:48:06	180.002	122.34		01:46:02	353.433	130.71	
01:46:30	88.45	202.19	184.71	01:48:21	180.45	149.42	140.66	01:46:17	354.215	114.21	120.65
01:46:45	88.646	179.54		01:48:36	180.842	130.75		01:46:32	355.108	130.94	
01:47:00	88.869	204.27		01:48:51	181.291	149.09		01:46:47	355.889	114.06	
01:47:15	89.064	175.02		01:49:06	181.683	130.75		01:47:02	356.783	130.56	
01:47:30	89.287	200.15		01:49:21	182.131	149.42		01:47:17	357.566	114.35	
01:47:45	89.483	177.71	187.34	01:49:36	182.523	131.34	138.27	01:47:32	358.347	113.61	120.71
01:48:00	89.706	202.19		01:49:51	182.971	149.42		01:47:47	359.242	130.45	
01:48:15	89.902	177.71		01:50:27	183.955	136.14		01:48:02	360.023	113.39	
01:48:30	90.125	202.19		01:50:42	184.402	148.42		01:48:17	360.917	129.80	
01:48:45	90.321	175.91		01:50:57	184.794	130.75		01:48:32	361.698	113.61	
01:49:00	90.544	198.14	191.23	01:51:12	185.185	131.00	139.15	01:48:47	362.592	129.29	123.31
01:49:15	90.74	174.15		01:51:27	185.635	149.42		01:49:02	363.373	112.95	
01:49:30	90.963	200.15		01:51:42	186.027	129.58		01:49:17	364.266	129.15	
01:49:45	91.159	175.91		01:51:58	186.475	138.83		01:49:32	365.049	113.02	
01:50:00	91.354	175.02		01:52:13	186.867	130.16		01:49:47	365.943	129.04	
01:50:15	91.577	196.18	184.28	01:52:28	187.316	148.42	139.28	01:50:02	366.724	112.51	119.33
01:50:30	91.773	170.74		01:52:43	187.708	128.43		01:50:17	367.618	128.79	
01:50:45	91.996	198.14		01:52:58	188.155	147.10		01:50:32	368.401	112.36	
01:51:00	92.192	174.15		01:53:13	188.548	129.91		01:50:47	369.294	128.14	
01:51:15	92.415	196.18		01:53:28	188.996	148.09		01:51:02	370.075	112.73	
01:51:30	92.611	170.74	181.99	01:53:43	189.389	129.91	136.69	01:51:17	370.857	112.87	118.98
01:51:45	92.834	196.18		01:53:58	189.837	147.43		01:51:32	371.749	128.50	
01:52:00	93.029	173.27		01:54:13	190.229	129.58		01:51:47	372.532	112.80	
01:52:15	93.253	199.03		01:54:28	190.631	132.88		01:52:02	373.425	128.39	
01:52:30	93.448	171.55		01:54:43	191.078	147.10		01:52:17	374.207	112.43	
01:52:45	93.671	196.18	187.24	01:54:58	191.471	129.91	137.38	01:52:32	375.1	127.90	122.00
01:53:00	93.867	175.91		01:55:14	191.919	138.22		01:52:47	375.883	111.93	
01:53:15	94.063	189.30		01:55:29	192.311	128.43		01:53:02	376.775	128.25	
01:53:30	94.192	174.59		01:55:44	192.758	146.45		01:53:17	377.557	112.00	
01:53:45	94.387	175.02		01:55:59	193.151	129.33		01:53:32	378.451	126.57	
01:54:00	94.61	198.14	182.59	01:56:14	193.599	148.09	138.10	01:53:47	379.232	110.15	117.78
01:54:15	94.806	175.91		01:56:29	193.992	129.91		01:54:02	380.125	125.95	
01:54:30	95.029	202.19		01:56:44	194.441	148.42		01:54:17	380.908	111.07	
01:54:45	95.225	175.91		01:56:59	194.834	129.33		01:54:32	381.8	127.75	
01:55:00	95.448	196.18		01:57:14	195.282	147.43		01:54:47	382.581	111.86	
01:55:15	95.643	171.55	184.35	01:57:29	195.675	129.33	136.89	01:55:02	383.364	112.36	117.80
01:55:30	95.838	173.27		01:57:44	196.122	147.10		01:55:17	384.257	128.89	
01:55:45	96.061	198.14		01:57:59	196.515	128.76		01:55:32	385.04	112.58	
01:56:00	96.257	172.43		01:58:14	196.908	129.33		01:55:47	385.933	128.14	
01:56:15	96.48	198.14		01:58:29	197.356	148.09		01:56:02	386.715	112.65	
01:56:30	96.676	174.15	183.23	01:58:44	197.748	128.43	136.34	01:56:17	387.61	128.43	122.14
01:56:45	96.9	195.13		01:58:59	198.196	146.78		01:56:32	388.39	111.28	
01:57:00	97.095	171.55		01:59:36	199.18	126.77		01:56:47	389.283	127.90	
01:57:15	97.318	196.18		01:59:51	199.626	137.60		01:57:02	390.066	112.58	
01:57:30	97.514	170.74		02:00:06	200.017	121.65		01:57:17	390.958	128.00	
01:57:45	97.737	192.37	185.20			**159.96**	**160.19**	01:57:32	391.741	112.14	118.38
01:58:00	97.933	167.46						01:57:47	392.634	127.90	
01:58:15	98.156	194.26						01:58:02	393.417	111.49	
01:58:30	98.351	169.87						01:58:17	394.2	110.64	
01:58:45	98.574	192.37						01:58:32	395.092	125.57	
01:59:00	98.77	169.08	178.61					01:58:47	395.875	110.01	117.12
01:59:15	98.965	168.22						01:59:02	396.767	125.09	
01:59:30	99.189	191.38						01:59:17	397.549	109.25	
01:59:45	99.384	165.01								**143.71**	**143.82**
02:00:00	99.607	188.71									
02:00:15	99.803	165.86	175.84								
02:00:30	100.026	190.52									
	Av	**205.10**	**205.13**								

50 ml/ h				100 ml/ h				200 ml/ h			
time, [hh:mm:ss]	V, [cm3]	k, [mD]	k, [mD]	time, [hh:mm:ss]	V, [cm3]	k, [mD]	k, [mD]	time, [hh:mm:ss]	V, [cm3]	k, [mD]	k, [mD]
0:00:15	0.13	390.38		0:00:15	0.23	383.03887		0:00:15	0.49	358.99	
0:00:30	0.35	396.13		0:00:30	0.67	375.60126		0:00:30	1.27	354.67	
0:00:45	0.54	397.42		0:00:45	1.06	351.57072		0:00:45	2.15	346.67	
0:01:00	0.76	390.85	393.70	0:01:00	1.50	379.99444	372.551	0:01:00	2.93	342.51	
0:01:15	0.96	388.74		0:01:15	1.89	334.82926		0:01:15	3.82	336.53	
0:01:30	1.18	399.32		0:01:30	2.34	383.0309		0:01:30	4.60	345.74	
0:01:45	1.38	357.68		0:01:45	2.73	345.80727		0:01:45	5.49	325.11	
0:02:00	1.60	392.79	384.63	0:02:00	3.17	389.20882	363.219	0:02:00	6.27	341.29	
0:02:15	1.79	359.52		0:02:15	3.56	324.52682		0:02:15	7.16	353.42	
0:02:30	2.02	369.30		0:02:30	4.01	371.24533		0:02:30	7.94	341.98	344.69
0:02:45	2.21	378.45		0:02:45	4.40	325.36108		0:02:45	8.83	325.81	
0:03:00	2.43	432.79	385.02	0:03:00	4.84	370.41107	347.886	0:03:00	9.60	345.74	
0:03:15	2.63	376.51		0:03:15	5.23	325.36108		0:03:15	10.05	342.45	
0:03:30	2.85	432.79		0:03:30	5.68	366.44202		0:03:30	10.83	335.69	
0:03:45	3.05	378.45		0:03:45	6.07	325.36108		0:03:45	11.72	314.11	
0:04:00	3.27	384.48	393.06	0:04:00	6.51	372.07959	347.311	0:04:00	12.50	338.30	
0:04:15	3.46	388.67		0:04:15	6.90	325.36108		0:04:15	13.39	325.81	
0:04:30	3.69	372.79		0:04:30	7.35	377.04604		0:04:30	14.18	354.53	
0:04:45	3.88	378.45		0:04:45	7.74	336.55074		0:04:45	15.07	339.39	
0:05:00	4.10	421.69	390.40	0:05:00	8.18	383.89164	355.712	0:05:00	15.85	354.58	337.64
0:05:15	4.30	368.74		0:05:15	8.58	331.29214		0:05:15	16.74	365.87	
0:05:30	4.50	380.39		0:05:30	9.02	377.89333		0:05:30	17.52	324.00	
0:05:45	4.72	432.79		0:05:45	9.41	326.19534		0:05:45	18.30	323.58	
0:06:00	4.91	388.67	392.65	0:06:00	9.86	372.07959	351.865	0:06:00	19.20	369.57	
0:06:15	5.14	432.79		0:06:15	10.25	326.19534		0:06:15	19.98	320.81	
0:06:30	5.33	370.63		0:06:30	10.70	361.78209		0:06:30	20.87	361.85	
0:06:45	5.56	421.69		0:06:45	11.09	327.78431		0:06:45	21.65	319.99	
0:07:00	5.75	361.37	396.62	0:07:00	11.48	356.44136	343.051	0:07:00	22.55	365.87	
0:07:15	5.98	423.58		0:07:15	11.92	372.07959		0:07:15	23.33	320.81	
0:07:30	6.17	380.67		0:07:30	12.32	336.55074		0:07:30	24.22	369.99	344.23
0:07:45	6.39	412.79		0:07:45	12.76	383.89164		0:07:45	25.00	319.99	
0:08:00	6.59	368.74	396.45	0:08:00	13.15	336.55074	357.268	0:08:00	25.90	361.85	
0:08:15	6.81	424.73		0:08:15	13.60	379.58792		0:08:15	26.68	317.28	
0:08:30	7.01	378.45		0:08:30	13.99	330.44484		0:08:30	27.57	362.26	
0:08:45	7.23	424.73		0:08:45	14.44	384.75239		0:08:45	28.36	316.88	
0:09:00	7.43	358.45	396.59	0:09:00	14.83	331.29214	356.519	0:09:00	29.25	369.57	
0:09:15	7.62	370.63		0:09:15	15.27	383.89164		0:09:15	30.03	324.41	
0:09:30	7.85	421.69		0:09:30	15.67	337.41149		0:09:30	30.81	316.88	
0:09:45	8.04	378.45		0:09:45	16.11	372.07959		0:09:45	31.71	357.92	
0:10:00	8.26	421.69	398.12	0:10:00	16.50	326.19534	354.895	0:10:00	32.49	313.43	336.05
0:10:15	8.46	361.37		0:10:15	16.95	384.75239		0:10:15	33.38	362.26	
0:10:30	8.68	421.69		0:10:30	17.34	331.29214		0:10:30	34.16	320.40	
0:10:45	8.88	380.39		0:10:45	17.73	326.19534		0:10:45	35.06	369.57	
0:11:00	9.10	432.79	399.06	0:11:00	18.18	377.89333	355.033	0:11:00	35.84	319.99	
0:11:15	9.30	378.45		0:11:15	18.57	337.41149		0:11:15	36.73	362.26	
0:11:30	9.52	421.69		0:11:30	19.02	372.07959		0:11:30	37.51	317.28	
0:11:45	9.72	361.37		0:11:45	19.41	321.25298		0:11:45	38.41	374.19	
0:12:00	9.94	423.58	396.27	0:12:00	19.85	372.91385	350.914	0:12:00	39.19	331.87	
0:12:15	10.13	378.45		0:12:15	20.25	322.0746		0:12:15	40.08	365.46	
0:12:30	10.36	423.58		0:12:30	20.69	345.90001		0:12:30	40.86	316.47	343.97
0:12:45	10.55	378.45		0:12:45	21.08	330.44677		0:12:45	41.64	316.88	
0:13:00	10.75	380.39	390.22	0:13:00	21.53	367.26364	341.421	0:13:00	42.54	358.32	
0:13:15	10.97	411.15		0:13:15	21.92	321.25298		0:13:15	43.32	316.47	
0:13:30	11.17	368.74		0:13:30	22.37	372.91385		0:13:30	44.21	365.87	
0:13:45	11.39	434.73		0:13:45	22.76	330.44484		0:13:45	45.00	324.41	
0:14:00	11.59	378.45	398.27	0:14:00	23.15	331.29214	338.976	0:14:00	45.89	373.77	
0:14:15	11.81	423.58		0:14:15	23.60	378.74063		0:14:15	46.67	316.88	
0:14:30	12.01	368.74		0:14:30	23.99	331.29214		0:14:30	47.56	357.52	
0:14:45	12.23	421.69		0:14:45	24.43	372.07959		0:14:45	48.34	309.66	
0:15:00	12.42	370.63	396.16	0:15:00	24.82	326.19534	352.077	0:15:00	49.24	354.87	339.46
0:15:15	12.65	421.69		0:15:15	25.27	373.74811		0:15:15	50.02	319.99	
0:15:30	12.84	361.37		0:15:30	25.66	321.25298		0:15:30	50.91	362.26	
0:15:45	13.07	421.69		0:15:45	26.11	362.59145		0:15:45	51.70	313.83	
0:16:00	13.26	368.74	393.37	0:16:00	26.50	316.45816	343.513	0:16:00	52.59	357.92	
0:16:15	13.49	423.58		0:16:15	26.95	372.91385		0:16:15	53.37	309.66	
0:16:30	13.68	368.74		0:16:30	27.34	321.25298		0:16:30	54.15	309.66	
0:16:45	13.88	361.37		0:16:45	27.79	361.78209		0:16:45	55.04	362.26	
0:17:00	14.10	411.15	391.21	0:17:00	28.18	321.25298	344.3	0:17:00	55.83	323.58	
0:17:15	14.30	361.37		0:17:15	28.57	321.25298		0:17:15	56.72	362.66	
0:17:30	14.52	411.15		0:17:30	29.02	367.26364		0:17:30	57.50	317.28	333.91
0:17:45	14.71	380.39		0:17:45	29.41	326.19534		0:17:45	58.40	365.46	
0:18:00	14.94	432.79	396.42	0:18:00	29.85	377.89333	348.151	0:18:00	59.18	320.81	
0:18:15	15.13	361.37		0:18:15	30.24	326.19534		0:18:15	60.07	365.87	
0:18:30	15.36	421.69		0:18:30	30.69	378.74063		0:18:30	60.85	316.88	
0:18:45	15.55	370.63		0:18:45	31.08	332.13943		0:18:45	61.75	358.32	
0:19:00	15.78	411.15	391.21	0:19:00	31.53	361.78209	349.714	0:19:00	62.53	313.43	
0:19:15	15.97	368.74		0:19:15	31.92	326.19534		0:19:15	63.42	361.85	
0:19:30	16.19	432.79		0:19:30	32.37	383.89164		0:19:30	64.21	313.83	
0:19:45	16.39	380.39		0:19:45	32.76	330.44484		0:19:45	65.10	357.92	
0:20:00	16.58	368.74	387.66	0:20:00	33.21	373.74811	353.57	0:20:00	65.88	316.88	339.13
0:20:15	16.81	412.99		0:20:15	33.60	325.36108		0:20:15	66.66	316.47	
0:20:30	17.00	359.52		0:20:30	34.04	384.75239		0:20:30	67.56	358.32	
0:20:45	17.23	412.99		0:20:45	34.43	336.55074		0:20:45	68.34	353.83	
0:21:00	17.42	359.52	386.26	0:21:00	34.82	326.19534	343.215	0:21:00	69.23	337.92	
0:21:15	17.65	411.15		0:21:15	35.27	367.26364		0:21:15	70.01	357.28	
0:21:30	17.84	361.37		0:21:30	35.66	320.43136		0:21:30	70.91	316.28	
0:21:45	18.06	411.15		0:21:45	36.11	373.74811		0:21:45	71.69	357.28	
0:22:00	18.26	361.37	386.26	0:22:00	36.50	326.19534	346.91	0:22:00	72.58	314.07	
0:22:15	18.48	421.69		0:22:15	36.95	367.26364		0:22:15	73.37	350.46	
0:22:30	18.68	380.39		0:22:30	37.34	326.19534		0:22:30	74.26	313.68	337.56
0:22:45	18.90	411.15		0:22:45	37.78	372.07959		0:22:45	75.04	303.92	
0:23:00	19.10	359.52	393.19	0:23:00	38.18	327.0296	348.142	0:23:00	75.94	310.31	
0:23:15	19.32	423.58		0:23:15	38.62	384.75239		0:23:15	76.72	313.43	
0:23:30	19.52	359.52		0:23:30	39.01	331.29214		0:23:30	77.50	313.43	
0:23:45	19.71	361.37		0:23:45	39.46	367.26364		0:23:45	78.39	354.47	
0:24:00	19.94	411.15	388.91	0:24:00	39.85	326.19534	352.376	0:24:00	79.17	309.66	
0:24:15	20.13	352.55		0:24:15	40.24	332.13943		0:24:15	80.07	358.32	
0:24:30	20.35	401.12		0:24:30	40.69	372.91385		0:24:30	80.85	319.99	
0:24:45	20.55	368.74		0:24:45	41.08	320.43136		0:24:45	81.74	366.69	
0:25:00	20.77	423.58	386.50	0:25:00	41.53	367.26364	348.187	0:25:00	82.53	320.40	327.06
0:25:15	20.97	350.76		0:25:15	41.92	321.25298		0:25:15	83.42	361.85	
0:25:30	21.19	382.46		0:25:30	42.37	361.78209		0:25:30	84.20	310.46	
0:25:45	21.39	352.55		0:25:45	42.76	321.25298		0:25:45	85.09	353.68	
0:26:00	21.61	421.69	376.87	0:26:00	43.20	378.74063	345.757	0:26:00	85.88	307.15	
0:26:15	21.81	352.55		0:26:15	43.60	326.19534		0:26:15	86.77	349.91	
0:26:30	22.03	391.57		0:26:30	44.04	366.44202		0:26:30	87.55	313.83	
0:26:45	22.23	352.55		0:26:45	44.43	321.25298		0:26:45	88.33	316.88	
0:27:00	22.45	411.15	376.96	0:27:00	44.88	367.26364	345.288	0:27:00	89.23	366.28	
0:27:15	22.64	352.55		0:27:15	45.27	322.0746		0:27:15	90.01	320.40	
0:27:30	22.84	350.76		0:27:30	45.66	326.19534		0:27:30	90.91	358.72	335.92
0:27:45	23.06	412.99		0:27:45	46.11	377.89333		0:27:45	91.69	310.06	
0:28:00	23.26	359.52	368.96	0:28:00	46.50	326.19534	338.09	0:28:00	92.58	354.87	
0:28:15	23.48	401.12		0:28:15	46.95	361.78209		0:28:15	93.36	313.03	
0:28:30	23.68	361.37		0:28:30	47.34	311.80437		0:28:30	94.26	358.32	
0:28:45	23.90	421.69		0:28:45	47.78	361.78209		0:28:45	95.04	309.66	
0:29:00	24.10	352.55	384.18	0:29:00	48.18	326.19534	340.391	0:29:00	95.93	358.72	
0:29:15	24.32	391.57		0:29:15	48.62	372.91385		0:29:15	96.72	310.06	
0:29:30	24.52	352.55		0:29:30	49.01	321.25298		0:29:30	97.61	354.07	
0:29:45	24.74	421.69		0:29:45	49.46	366.44202		0:29:45	98.39	319.99	
0:30:00	24.93	378.45	386.06	0:30:00	49.85	322.0746	345.671	0:30:00	99.28	370.40	335.92
0:30:15	25.16	423.58		0:30:15	50.30	377.89333		0:30:15	100.07	317.69	
0:30:30	25.35	352.55		0:30:30	50.69	336.55074		0:30:30	100.85	310.46	
0:30:45	25.55	350.76		0:30:45	51.14	378.74063		0:30:45	101.74	350.70	
0:31:00	25.77	412.99	384.97	0:31:00	51.53	321.25298	353.609	0:31:00	102.53	303.15	
0:31:15	25.97	359.52		0:31:15	51.92	316.45816		0:31:15	103.42	350.31	
0:31:30	26.19	411.15		0:31:30	52.36	361.78209		0:31:30	104.20	313.83	
0:31:45	26.39	370.63		0:31:45	52.76	321.25298		0:31:45	105.09	361.45	
0:32:00	26.61	421.69	390.75	0:32:00	53.20	372.91385	343.102	0:32:00	105.88	317.28	
0:32:15	26.81	352.55		0:32:15	53.59	322.0746		0:32:15	106.77	357.92	
0:32:30	27.03	391.57		0:32:30	54.04	372.07959		0:32:30	107.55	313.83	329.66
0:32:45	27.22	352.55		0:32:45	54.43	332.13943		0:32:45	108.44	361.45	
0:33:01	27.45	397.11	373.45	0:33:00	54.88	377.89333	351.047	0:33:00	109.23	313.83	
0:33:16	27.64	368.74		0:33:15	55.27	331.29214		0:33:15	110.12	354.07	
0:33:31	27.87	402.92		0:33:30	55.72	372.91385		0:33:30	110.90	313.43	
0:33:46	28.06	350.76		0:33:45	56.11	326.19534		0:33:45	111.69	313.83	
0:34:01	28.26	361.37	370.95	0:34:00	56.55	372.91385	350.829	0:34:00	112.58	350.31	
0:34:16	28.48	401.12		0:34:16	56.95	316.53247		0:34:15	113.36	299.20	
0:34:31	28.68	344.16		0:34:31	57.34	360.57581		0:34:30	114.25	332.61	
0:34:46	28.90	391.57		0:34:46	57.78	366.44202		0:34:46	115.04	343.07	
0:35:01	29.10	344.16	370.25	0:35:01	58.17	316.45816	340.002	0:35:01	115.93	341.23	332.30
0:35:16	29.32	391.57		0:35:16	58.62	360.97274		0:35:16	116.71	298.43	
0:35:31	29.51	342.40		0:35:31	59.01	326.01699		0:35:31	117.60	335.63	
0:35:46	29.74	401.12		0:35:46	59.46	361.78209		0:35:46	118.39	299.20	
0:36:01	29.93	370.63	376.43	0:36:01	59.85	321.25298	342.506	0:36:01	119.28	350.31	
0:36:16	30.16	401.12		0:36:16	60.29	366.44202		0:36:16	120.06	309.66	
0:36:31	30.35	328.52		0:36:31	60.69	322.0746		0:36:31	120.95	354.87	
0:36:46	30.58	382.46		0:36:46	61.13	362.85396		0:36:46	121.74	306.37	
0:37:01	30.77	361.37	368.37	0:37:01	61.52	346.04798	349.355	0:37:01	122.63	347.01	
0:37:16	30.99	401.12		0:37:16	61.97	361.78209		0:37:16	123.41	303.92	
0:37:31	31.19	342.40		0:37:31	62.36	322.0746		0:37:31	124.20	307.15	321.25
0:37:46	31.39	361.37		0:37:46	62.81	372.91385		0:37:46	125.09	349.91	

D- 2- 6

Total Clay: 4.04 %

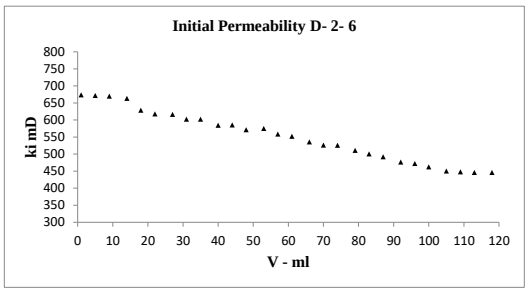

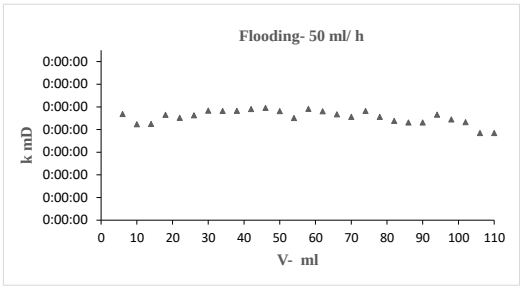

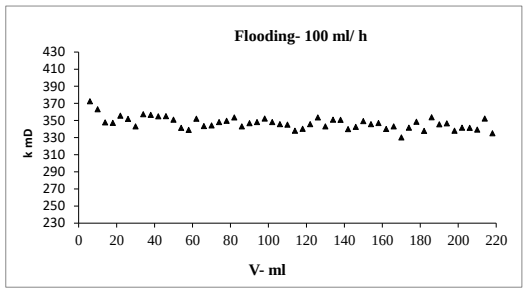

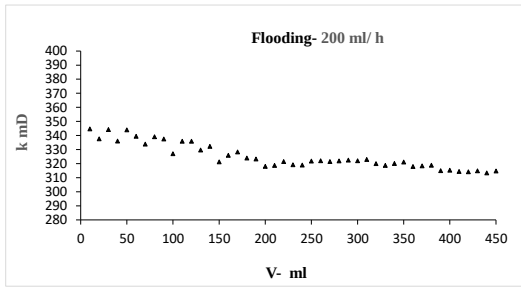

Group	Sample ID	Quartz	Calcite Mg	Oligoclase	Microcline	Chl. IIb	Kao.	Illite 2M1	Biotite 1M	Dol.	amorph.	Total Clay	Φ_{He} (%)	k_{wi} (mD)
D- 2 -6	D- 2- 1943.0	83.8	0.2	6.7	1.0	1.0	0.5	2.5	....	0.3	4.0	4.04	27.28	389.53

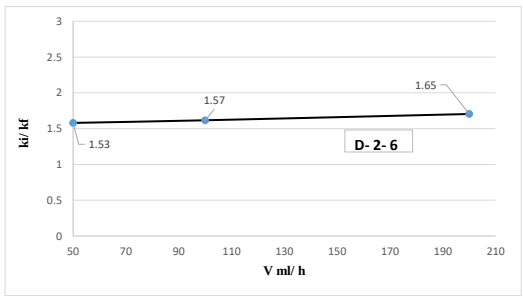

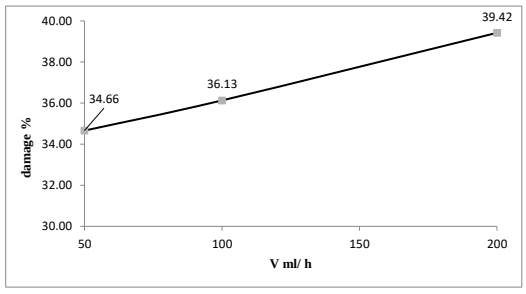

flow rate ml/	k %	ki/ kf		Damage Ratio		100			
50	34.66	10.5	1.57	36.72701	10.50	50			
100	36.13	12.33	2.03	38.15351	12.33	100			
200	39.42	14.23	2.25	41.33961	14.23	200			
552.4		349.52		341.64	324.04	1.580453	1.616907	1.704728	
						50	1.580453		
						100	1.616907		
						200	1.704728		

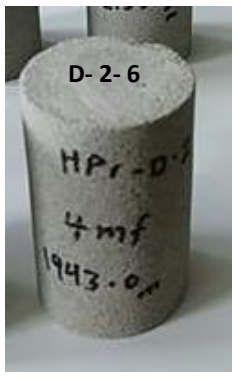

0:38:01	31.61	401.12	376.50	0:38:01	63.20	326.19534	345.741	0:38:01	125.87	300.76	
0:38:16	31.80	344.16		0:38:16	63.59	322.0746		0:38:16	126.76	342.62	
0:38:31	32.03	382.46		0:38:31	64.04	372.91385		0:38:31	127.54	310.06	
0:38:46	32.22	344.16		0:38:46	64.43	325.36108		0:38:46	128.44	354.07	
0:39:01	32.45	401.12	367.98	0:39:01	64.88	368.08526	347.109	0:39:01	129.22	300.76	
0:39:16	32.64	352.55		0:39:16	65.27	321.25298		0:39:16	130.11	339.47	
0:39:31	32.87	401.12		0:39:31	65.71	366.44202		0:39:31	130.90	300.76	
0:39:46	33.06	352.55		0:39:46	66.11	321.25298		0:39:46	131.79	350.70	
0:40:01	33.28	401.12	376.84	0:40:01	66.55	351.29566	340.061	0:40:01	132.57	309.66	325.88
0:40:16	33.48	342.40		0:40:16	66.94	311.00691		0:40:16	133.47	350.70	
0:40:31	33.70	375.45		0:40:31	67.39	379.58792		0:40:31	134.25	310.46	
0:40:46	33.90	319.58		0:40:46	67.78	321.25298		0:40:46	135.03	310.46	
0:41:01	34.12	373.77	352.80	0:41:01	68.23	360.97274	343.205	0:41:01	135.92	346.62	
0:41:16	34.32	328.52		0:41:16	68.62	321.25298		0:41:16	136.71	303.53	
0:41:31	34.51	342.40		0:41:31	69.01	316.45816		0:41:31	137.60	347.01	
0:41:46	34.74	384.18		0:41:46	69.46	360.97274		0:41:46	138.38	310.06	
0:42:01	34.93	319.58	343.67	0:42:01	69.85	322.0746	330.19	0:42:01	139.28	354.07	
0:42:16	35.16	375.45		0:42:16	70.29	372.07959		0:42:16	140.06	303.53	
0:42:31	35.35	326.84		0:42:31	70.68	321.25298		0:42:31	140.95	346.23	328.27
0:42:46	35.57	373.77		0:42:46	71.13	356.46177		0:42:46	141.73	307.15	
0:43:01	35.77	321.22	349.32	0:43:01	71.52	316.45816	341.563	0:43:01	142.63	350.70	
0:43:16	35.99	357.52		0:43:16	71.97	377.89333		0:43:16	143.41	300.76	
0:43:31	36.19	307.55		0:43:31	72.36	337.41149		0:43:31	144.30	343.01	
0:43:46	36.41	357.52		0:43:46	72.81	367.26364		0:43:46	145.08	303.53	
0:44:01	36.61	319.58	335.54	0:44:01	73.20	311.80437	348.593	0:44:01	145.87	310.06	
0:44:16	36.83	359.12		0:44:16	73.64	360.97274		0:44:16	146.76	353.68	
0:44:31	37.03	321.22		0:44:31	74.04	317.26752		0:44:31	147.54	303.53	
0:44:46	37.25	365.46		0:44:46	74.43	311.80437		0:44:46	148.43	354.07	
0:45:01	37.44	312.63	339.61	0:45:01	74.87	361.78209	337.957	0:45:01	149.21	313.03	323.95
0:45:16	37.64	314.23		0:45:16	75.27	331.29214		0:45:16	150.11	347.01	
0:45:31	37.86	349.91		0:45:31	75.71	384.75239		0:45:31	150.89	299.99	
0:45:46	38.06	307.55		0:45:46	76.10	326.19534		0:45:46	151.78	347.01	
0:46:01	38.28	359.12	332.70	0:46:01	76.55	372.91385	353.788	0:46:01	152.57	303.92	
0:46:16	38.48	305.98		0:46:16	76.94	326.19534		0:46:16	153.46	350.70	
0:46:31	38.70	342.62		0:46:31	77.39	367.26364		0:46:31	154.24	306.37	
0:46:46	38.90	314.23		0:46:46	77.78	321.25298		0:46:46	155.14	350.70	
0:47:01	39.12	365.46	332.07	0:47:01	78.23	367.26364	345.494	0:47:01	155.92	298.43	
0:47:16	39.32	305.98		0:47:16	78.62	326.19534		0:47:16	156.81	332.61	
0:47:31	39.54	344.16		0:47:31	79.06	372.91385		0:47:31	157.59	296.51	323.32
0:47:46	39.73	287.62		0:47:46	79.46	321.25298		0:47:46	158.37	295.37	
0:48:01	39.96	330.39	317.04	0:48:01	79.90	366.44202	346.701	0:48:01	159.27	338.11	
0:48:16	40.15	305.98		0:48:16	80.29	327.0296		0:48:16	160.05	296.89	
0:48:31	40.35	321.22		0:48:31	80.68	330.44484		0:48:31	160.94	339.85	
0:48:46	40.57	365.46		0:48:46	81.13	373.74811		0:48:46	161.73	295.75	
0:49:01	40.77	321.22	328.47	0:49:01	81.52	321.25298	338.119	0:49:01	162.62	337.73	
0:49:16	40.99	357.52		0:49:16	81.97	367.26364		0:49:16	163.40	300.76	
0:49:31	41.19	305.98		0:49:31	82.36	316.45816		0:49:31	164.30	343.39	
0:49:46	41.41	351.48		0:49:46	82.81	361.78209		0:49:46	165.08	296.13	
0:50:01	41.61	299.60	328.65	0:50:01	83.20	321.25298	341.689	0:50:01	165.97	336.38	318.04
0:50:16	41.83	342.62		0:50:16	83.64	366.44202		0:50:16	166.75	298.82	
0:50:31	42.02	307.55		0:50:31	84.04	321.25298		0:50:31	167.65	347.01	
0:50:46	42.25	365.46		0:50:46	84.48	361.78209		0:50:46	168.43	303.53	
0:51:01	42.44	321.22	334.21	0:51:01	84.87	316.45816	341.484	0:51:01	169.21	300.37	
0:51:16	42.67	349.91		0:51:16	85.32	360.97274		0:51:16	170.10	339.09	
0:51:31	42.86	301.14		0:51:31	85.71	311.80437		0:51:31	170.89	303.92	
0:51:46	43.09	349.91		0:51:46	86.10	312.60182		0:51:46	171.78	347.01	
0:52:01	43.28	314.23	328.80	0:52:01	86.55	372.07959	339.365	0:52:01	172.56	297.66	
0:52:16	43.48	312.63		0:52:16	86.94	336.55074		0:52:16	173.46	343.39	
0:52:31	43.70	349.91		0:52:31	87.39	383.89164		0:52:31	174.24	307.15	318.79
0:52:46	43.90	314.23		0:52:46	87.78	327.0296		0:52:46	175.13	344.42	
0:53:01	44.12	373.77	337.64	0:53:01	88.22	361.78209	352.314	0:53:01	175.91	293.87	
0:53:16	44.31	321.22		0:53:16	88.61	315.64881		0:53:16	176.81	341.99	
0:53:31	44.54	349.91		0:53:31	89.06	356.46177		0:53:31	177.59	303.53	
0:53:46	44.73	307.55		0:53:46	89.45	312.60182		0:53:46	178.49	343.39	
0:54:01	44.96	365.46	336.04	0:54:01	89.90	355.66432	335.094	0:54:01	179.27	303.15	
0:54:16	45.15	319.58		0:54:16	90.29	312.60182		0:54:16	180.16	346.62	
0:54:31	45.37	357.52		0:54:31	90.74	355.66432		0:54:31	180.94	297.66	
0:54:46	45.57	314.23		0:54:46	91.13	311.80437		0:54:46	181.73	298.04	
0:55:01	45.79	337.14	332.12	0:55:01	91.57	360.97274	335.261	0:55:01	182.62	342.62	321.53
0:55:16	45.99	293.49		0:55:16	91.97	316.45816		0:55:16	183.40	300.76	
0:55:31	46.19	307.55		0:55:31	92.36	312.60182		0:55:31	184.29	343.01	
0:55:46	46.41	349.91		0:55:46	92.80	361.78209		0:55:46	185.08	300.76	
0:56:01	46.60	312.63	315.89	0:56:01	93.19	325.36108	329.051	0:56:01	185.97	339.47	
0:56:16	46.83	349.91		0:56:16	93.64	368.08526		0:56:16	186.75	296.89	
0:56:31	47.02	301.14		0:56:31	94.03	315.64881		0:56:31	187.65	347.01	
0:56:46	47.25	342.62		0:56:46	94.48	367.26364		0:56:46	188.43	310.06	
0:57:01	47.44	307.55	325.31	0:57:01	94.87	326.19534	344.298	0:57:01	189.32	346.23	
0:57:16	47.66	349.91		0:57:16	95.32	366.44202		0:57:16	190.10	303.15	
0:57:31	47.86	312.63		0:57:31	95.71	317.26752		0:57:31	190.99	304.63	319.20
0:57:46	48.08	365.46		0:57:46	96.15	366.44202		0:57:46	191.78	308.47	
0:58:01	48.28	314.23	335.56	0:58:01	96.55	322.0746	343.057	0:58:01	192.56	306.89	
0:58:16	48.50	359.12		0:58:16	96.99	360.97274		0:58:16	193.45	343.39	
0:58:31	48.70	312.63		0:58:31	97.38	320.43136		0:58:31	194.23	300.37	
0:58:46	48.92	365.46		0:58:46	97.77	331.29214		0:58:46	195.13	339.47	
0:59:01	49.12	321.22	339.61	0:59:01	98.22	367.26364	344.99	0:59:01	195.91	300.37	
0:59:16	49.34	365.46		0:59:16	98.61	312.60182		0:59:16	196.80	347.01	
0:59:31	49.54	321.22		0:59:31	99.06	366.44202		0:59:31	197.59	300.76	
0:59:46	49.73	312.63		0:59:46	99.45	321.25298		0:59:46	198.48	343.01	
1:00:01	49.95	367.10	341.60	1:00:01	99.90	361.78209	340.52	1:00:01	199.26	300.37	319.01
1:00:16	50.15	319.58		1:00:16	100.29	321.25298		1:00:16	200.15	339.47	
1:00:31	50.37	359.12		1:00:31	100.73	361.78209		1:00:31	200.94	297.66	
1:00:46	50.57	312.63		1:00:46	101.13	316.45816		1:00:46	201.83	339.85	
1:01:01	50.79	357.52	337.21	1:01:01	101.57	366.44202	341.484	1:01:01	202.61	300.76	
1:01:16	50.99	307.55		1:01:16	101.96	316.45816		1:01:16	203.40	300.37	
1:01:31	51.21	342.62		1:01:31	102.41	355.66432		1:01:31	204.29	343.01	
1:01:46	51.41	307.55		1:01:46	102.80	311.80437		1:01:46	205.07	310.46	
1:02:01	51.63	357.52	328.81	1:02:01	103.25	346.27715	332.551	1:02:01	205.97	357.92	
1:02:16	51.83	314.23		1:02:16	103.64	302.89567		1:02:16	206.75	306.76	
1:02:31	52.05	357.52		1:02:31	104.03	316.45816		1:02:31	207.64	321.51	321.78
1:02:46	52.24	314.23		1:02:46	104.47	366.44202		1:02:46	208.53	319.20	
1:03:01	52.44	305.98	322.99	1:03:01	104.87	327.0296	328.206	1:03:01	209.42	318.23	
1:03:16	52.66	357.52		1:03:16	105.31	366.44202		1:03:16	210.31	316.41	
1:03:31	52.86	328.52		1:03:31	105.70	311.80437		1:03:31	211.20	325.36	
1:03:46	53.08	365.46		1:03:46	106.15	361.78209		1:03:46	212.09	320.60	
1:04:01	53.28	314.23	341.43	1:04:01	106.54	321.25298	340.32	1:04:01	212.98	326.99	
1:04:16	53.50	349.91		1:04:16	106.99	361.78209		1:04:16	213.87	325.25	
1:04:31	53.70	312.63		1:04:31	107.38	311.00691		1:04:31	214.76	323.51	
1:04:46	53.92	359.12		1:04:46	107.83	361.78209		1:04:46	215.65	320.71	
1:05:01	54.11	305.98	331.91	1:05:01	108.22	315.64881	337.555	1:05:01	216.54	324.69	322.09
1:05:16	54.34	365.46		1:05:16	108.66	356.46177		1:05:16	217.43	327.40	
1:05:31	54.53	321.22		1:05:31	109.05	317.26752		1:05:31	218.32	321.87	
1:05:46	54.76	365.46		1:05:46	109.50	366.44202		1:05:46	219.21	318.07	
1:06:01	54.95	321.22	343.34	1:06:01	109.89	307.28546	336.864	1:06:01	220.10	318.10	
1:06:16	55.18	349.91		1:06:16	110.28	308.07136		1:06:16	220.99	319.57	
1:06:31	55.37	307.55		1:06:31	110.73	367.26364		1:06:31	221.88	324.41	
1:06:46	55.57	319.58		1:06:46	111.12	321.25298		1:06:46	222.77	324.19	
1:07:01	55.79	365.46	335.63	1:07:01	111.57	366.44202	340.758	1:07:01	223.66	321.02	
1:07:16	55.98	312.63		1:07:16	111.96	316.45816		1:07:16	224.55	319.99	
1:07:31	56.21	359.12		1:07:31	112.41	362.59145		1:07:31	225.44	319.99	321.46
1:07:47	56.40	294.59		1:07:46	112.80	321.25298		1:07:46	226.33	319.57	
1:08:02	56.63	357.52	330.97	1:08:01	113.24	361.78209	340.521	1:08:01	227.22	324.00	
1:08:17	56.82	307.55		1:08:16	113.64	311.80437		1:08:16	228.11	324.19	
1:08:32	57.05	349.91		1:08:31	114.08	362.59145		1:08:31	229.00	321.44	
1:08:47	57.24	321.22		1:08:47	114.47	296.67953		1:08:47	229.89	311.13	
1:09:02	57.47	357.52	334.05	1:09:02	114.92	360.97274	333.012	1:09:02	230.78	322.89	
1:09:17	57.66	305.98		1:09:17	115.31	316.45816		1:09:17	231.67	321.87	
1:09:32	57.88	349.91		1:09:32	115.70	315.64881		1:09:32	232.56	330.40	
1:09:47	58.08	314.23		1:09:47	116.15	367.26364		1:09:47	233.45	323.58	
1:10:02	58.30	365.46	333.90	1:10:02	116.54	316.45816	328.957	1:10:02	234.34	320.40	321.95
1:10:17	58.50	314.23		1:10:17	116.99	356.46177		1:10:17	235.23	324.00	
1:10:32	58.69	314.23		1:10:32	117.38	316.45816		1:10:32	236.12	323.77	
1:10:47	58.92	349.91		1:10:47	117.82	367.26364		1:10:47	237.01	322.10	
1:11:02	59.11	307.55	321.48	1:11:02	118.22	326.19534	341.595	1:11:02	237.90	321.57	
1:11:17	59.34	349.91		1:11:17	118.66	372.91385		1:11:17	238.79	322.68	
1:11:32	59.53	301.14		1:11:32	119.05	322.0746		1:11:32	239.68	321.57	
1:11:47	59.76	349.91		1:11:47	119.50	360.97274		1:11:47	240.57	320.81	
1:12:02	59.95	314.23	328.80	1:12:02	119.89	302.89567	339.714	1:12:02	241.46	324.19	
1:12:17	60.17	349.91		1:12:17	120.34	351.29566		1:12:17	242.35	321.10	
1:12:32	60.37	307.55		1:12:32	120.73	326.19534		1:12:32	243.24	323.58	322.54
1:12:47	60.59	357.52		1:12:47	121.12	326.19534		1:12:47	244.13	321.99	
1:13:02	60.79	307.55	330.63	1:13:02	121.57	367.26364	342.737	1:13:02	245.02	321.87	
1:13:17	61.01	349.91		1:13:17	121.96	321.25298		1:13:17	245.91	328.07	
1:13:32	61.21	314.23		1:13:32	122.41	361.78209		1:13:32	246.80	320.81	
1:13:47	61.40	326.84		1:13:47	122.80	311.80437		1:13:47	247.69	320.87	
1:14:02	61.63	373.77	341.19	1:14:02	123.24	356.46177	337.825	1:14:02	248.58	324.41	
1:14:17	61.82	305.98		1:14:17	123.63	316.45816		1:14:17	249.47	319.57	
1:14:32	62.05	351.48		1:14:32	124.08	372.91385		1:14:32	250.36	320.81	
1:14:47	62.24	312.63		1:14:47	124.47	321.25298		1:14:47	251.25	319.99	
1:15:02	62.46	351.48	330.39	1:15:02	124.92	360.97274	342.899	1:15:02	252.14	321.87	322.02
1:15:17	62.66	305.98		1:15:17	125.31	317.26752		1:15:17	253.03	323.77	
1:15:32	62.88	357.52		1:15:32	125.76	360.97274		1:15:32	253.92	324.41	
1:15:47	63.08	314.23		1:15:47	126.15	321.25298		1:15:47	254.81	321.02	
1:16:02	63.30	349.91	331.91	1:16:02	126.59	366.44202	341.484	1:16:02	255.70	324.61	
1:16:17	63.50	307.55		1:16:17	126.98	321.25298		1:16:17	256.59	324.41	
1:16:32	63.72	357.52		1:16:32	127.38	331.29214		1:16:32	257.48	324.19	
1:16:47	63.92	314.23		1:16:47	127.82	378.74063		1:16:47	258.37	320.81	
1:17:02	64.14	357.52	334.20	1:17:02	128.21	317.26752	337.138	1:17:02	259.26	320.52	

1:17:17	64.33	293.49		1:17:17	128.66	355.66432		1:17:17	260.15	321.60	
1:17:32	64.53	294.99		1:17:32	129.05	322.0746		1:17:32	261.04	324.41	322.97
1:17:47	64.75	357.52		1:17:47	129.50	378.74063		1:17:47	261.93	320.40	
1:18:02	64.95	319.58	316.39	1:18:02	129.89	321.25298	344.433	1:18:02	262.82	317.28	
1:18:17	65.17	365.46		1:18:17	130.34	355.66432		1:18:17	263.71	321.45	
1:18:32	65.37	321.22		1:18:32	130.73	321.25298		1:18:32	264.60	320.81	
1:18:47	65.59	365.46		1:18:47	131.17	367.26364		1:18:47	265.49	322.26	
1:19:02	65.79	314.23	341.59	1:19:02	131.57	316.45816	340.16	1:19:02	266.38	317.28	
1:19:17	66.01	349.91		1:19:17	132.01	366.44202		1:19:17	267.27	323.58	
1:19:32	66.20	305.98		1:19:32	132.40	322.0746		1:19:32	268.16	319.99	
1:19:47	66.43	359.12		1:19:47	132.79	316.45816		1:19:47	269.05	320.40	
1:20:02	66.62	312.63	331.91	1:20:02	133.24	360.97274	341.487	1:20:02	269.94	316.69	320.01
1:20:17	66.85	351.48		1:20:17	133.63	322.0746		1:20:17	270.83	316.47	
1:20:32	67.04	305.98		1:20:32	134.08	351.29566		1:20:32	271.72	321.85	
1:20:47	67.27	359.12		1:20:47	134.47	306.49957		1:20:47	272.61	319.99	
1:21:02	67.46	312.63	332.30	1:21:02	134.92	368.08526	336.989	1:21:02	273.50	316.28	
1:21:17	67.66	307.55		1:21:17	135.31	315.64881		1:21:17	274.39	320.81	
1:21:32	67.88	357.52		1:21:32	135.75	356.46177		1:21:32	275.28	319.57	
1:21:47	68.08	319.58		1:21:47	136.15	312.60182		1:21:47	276.17	320.40	
1:22:02	68.30	359.12	335.94	1:22:02	136.59	360.97274	336.421	1:22:02	277.06	321.85	
1:22:17	68.49	312.63		1:22:17	136.98	326.19534		1:22:17	277.95	313.43	
1:22:32	68.72	365.46		1:22:32	137.43	372.91385		1:22:32	278.84	317.28	318.79
1:22:47	68.91	321.22		1:22:47	137.82	315.64881		1:22:47	279.73	325.87	
1:23:02	69.14	349.91	337.31	1:23:02	138.27	361.78209	344.135	1:23:02	280.62	316.47	
1:23:17	69.33	307.55		1:23:17	138.66	326.19534		1:23:17	281.51	321.85	
1:23:32	69.56	357.52		1:23:32	139.05	327.0296		1:23:32	282.40	313.83	
1:23:47	69.75	294.99		1:23:47	139.50	350.50976		1:23:47	283.29	313.68	
1:24:02	69.97	349.91	327.49	1:24:02	139.89	302.121	326.464	1:24:02	284.18	316.47	
1:24:17	70.17	328.52		1:24:17	140.33	361.78209		1:24:17	285.07	316.28	
1:24:32	70.39	357.52		1:24:32	140.72	316.45816		1:24:32	285.96	324.00	
1:24:47	70.59	321.22		1:24:47	141.17	355.66432		1:24:47	286.85	324.19	
1:25:02	70.78	319.58	331.71	1:25:02	141.56	311.80437	336.427	1:25:02	287.74	328.52	320.12
1:25:17	71.01	357.52		1:25:17	142.01	356.46177		1:25:17	288.63	319.57	
1:25:32	71.20	321.22		1:25:32	142.40	311.80437		1:25:32	289.52	317.28	
1:25:47	71.43	357.52		1:25:47	142.85	360.97274		1:25:47	290.41	321.85	
1:26:02	71.62	299.60	333.96	1:26:02	143.24	317.26752	336.627	1:26:02	291.30	320.81	
1:26:17	71.85	344.16		1:26:17	143.68	360.97274		1:26:17	292.19	319.99	
1:26:32	72.04	305.98		1:26:32	144.07	316.45816		1:26:32	293.08	325.46	
1:26:47	72.26	351.48		1:26:47	144.52	355.66432		1:26:47	293.97	320.81	
1:27:02	72.46	305.98	326.90	1:27:02	144.91	317.26752	337.591	1:27:02	294.86	321.45	
1:27:17	72.68	359.12		1:27:17	145.30	316.45816		1:27:17	295.75	324.00	
1:27:32	72.88	312.63		1:27:32	145.75	360.97274		1:27:32	296.64	320.40	321.16
1:27:47	73.10	357.52		1:27:47	146.14	316.45816		1:27:47	297.53	320.40	
1:28:02	73.30	307.55	334.20	1:28:02	146.59	362.59145	339.12	1:28:02	298.42	319.57	
1:28:17	73.49	301.14		1:28:17	146.98	315.64881		1:28:17	299.31	320.81	
1:28:32	73.72	349.91		1:28:32	147.43	356.46177		1:28:32	300.20	317.52	
1:28:47	73.91	305.98		1:28:47	147.82	311.00691		1:28:47	301.09	313.83	
1:29:02	74.13	342.62	324.91	1:29:02	148.26	357.25922	335.094	1:29:02	301.98	321.85	
1:29:17	74.33	301.14		1:29:17	148.65	311.00691		1:29:17	302.87	317.28	
1:29:32	74.55	349.91		1:29:32	149.10	366.44202		1:29:32	303.76	317.52	
1:29:47	74.75	307.55		1:29:47	149.49	327.0296		1:29:47	304.65	313.03	
1:30:02	74.97	349.91	327.13	1:30:02	149.94	366.44202	342.73	1:30:02	305.54	317.69	317.95
1:30:17	75.17	307.55		1:30:17	150.33	317.26752		1:30:17	306.43	311.45	
1:30:32	75.39	342.62		1:30:32	150.72	311.80437		1:30:32	307.32	317.28	
1:30:47	75.59	307.55		1:30:47	151.17	360.97274		1:30:47	308.21	315.87	
1:31:02	75.81	357.52	328.81	1:31:02	151.56	322.0746	328.03	1:31:02	309.10	323.58	
1:31:17	76.01	314.23		1:31:17	152.00	366.44202		1:31:17	309.99	326.28	
1:31:32	76.23	335.46		1:31:32	152.40	322.0746		1:31:32	310.88	319.99	
1:31:47	76.42	312.63		1:31:47	152.84	366.44202		1:31:47	311.77	316.28	
1:32:02	76.62	324.13	321.61	1:32:02	153.23	321.25298	344.053	1:32:02	312.66	320.81	
1:32:17	76.84	304.34		1:32:17	153.68	360.97274		1:32:17	313.55	315.87	
1:32:32	77.04	301.14		1:32:32	154.07	311.80437		1:32:32	314.44	316.88	318.43
1:32:47	77.26	357.52		1:32:47	154.52	360.97274		1:32:47	315.33	319.16	
1:33:02	77.46	319.58	320.64	1:33:02	154.91	317.26752	337.754	1:33:02	316.22	324.41	
1:33:17	77.68	337.14		1:33:17	155.35	345.50248		1:33:17	317.11	315.87	
1:33:32	77.88	293.49		1:33:32	155.75	307.28546		1:33:32	318.00	316.47	
1:33:47	78.10	359.12		1:33:47	156.19	361.78209		1:33:47	318.89	317.28	
1:34:02	78.30	312.63	325.59	1:34:02	156.58	311.80437	331.594	1:34:02	319.78	316.28	
1:34:17	78.52	349.91		1:34:17	156.97	311.80437		1:34:17	320.67	323.58	
1:34:32	78.71	307.55		1:34:32	157.42	361.78209		1:34:32	321.56	320.81	
1:34:47	78.94	357.52		1:34:47	157.81	320.43136		1:34:47	322.45	316.47	
1:35:02	79.13	307.55	330.63	1:35:02	158.26	367.26364	340.32	1:35:02	323.34	317.92	318.83
1:35:17	79.36	342.62		1:35:17	158.65	315.64881		1:35:17	324.23	316.47	
1:35:32	79.55	301.14		1:35:32	159.10	361.78209		1:35:32	325.12	312.26	
1:35:47	79.75	299.60		1:35:47	159.49	316.45816		1:35:47	326.01	313.83	
1:36:02	79.97	351.48	323.71	1:36:02	159.93	356.46177	337.588	1:36:02	326.90	311.45	
1:36:17	80.17	312.63		1:36:17	160.32	321.25298		1:36:17	327.79	317.28	
1:36:32	80.39	365.46		1:36:32	160.77	372.07959		1:36:32	328.68	311.85	
1:36:47	80.59	314.23		1:36:47	161.16	326.19534		1:36:47	329.57	316.88	
1:37:02	80.81	349.91	335.56	1:37:02	161.61	372.91385	348.11	1:37:02	330.46	320.81	
1:37:17	81.00	307.55		1:37:17	162.00	316.45816		1:37:17	331.35	315.87	
1:37:32	81.23	349.91		1:37:32	162.45	361.78209		1:37:32	332.24	313.03	314.97
1:37:47	81.42	314.23		1:37:47	162.84	321.25298		1:37:47	333.13	318.32	
1:38:02	81.65	349.91	330.40	1:38:02	163.23	321.25298	330.187	1:38:02	334.02	317.28	
1:38:17	81.84	307.55		1:38:17	163.68	367.26364		1:38:17	334.91	317.52	
1:38:32	82.07	357.52		1:38:32	164.07	316.45816		1:38:32	335.80	310.85	
1:38:47	82.26	314.23		1:38:47	164.51	360.97274		1:38:47	336.69	313.68	
1:39:02	82.46	312.63	322.98	1:39:02	164.90	307.28546	337.995	1:39:02	337.58	313.83	
1:39:17	82.68	357.52		1:39:17	165.35	350.50976		1:39:17	338.47	311.85	
1:39:32	82.88	307.55		1:39:32	165.74	321.25298		1:39:32	339.36	317.69	
1:39:47	83.10	342.62		1:39:47	166.19	361.78209		1:39:47	340.25	311.45	
1:40:02	83.29	289.09	324.20	1:40:02	166.58	316.45816	337.501	1:40:02	341.14	320.40	315.29
1:40:17	83.52	342.62		1:40:17	167.03	361.78209		1:40:17	342.03	311.45	
1:40:32	83.71	301.14		1:40:32	167.42	316.45816		1:40:32	342.92	310.46	
1:40:47	83.94	316.27		1:40:47	167.86	361.78209		1:40:47	343.81	316.47	
1:41:02	84.13	289.09	312.28	1:41:02	168.25	316.45816	339.12	1:41:02	344.70	316.28	
1:41:17	84.36	349.91		1:41:17	168.70	361.78209		1:41:17	345.59	316.88	
1:41:32	84.55	312.63		1:41:32	169.09	311.80437		1:41:32	346.48	311.85	
1:41:48	84.77	344.16		1:41:47	169.48	311.80437		1:41:47	347.37	317.28	
1:42:03	84.97	312.63	329.83	1:42:02	169.93	356.46177	335.463	1:42:02	348.26	317.92	
1:42:18	85.19	351.48		1:42:18	170.32	291.56898		1:42:17	349.15	313.43	
1:42:33	85.39	305.98		1:42:33	170.77	356.46177		1:42:32	350.04	312.26	314.43
1:42:48	85.58	312.63		1:42:48	171.16	311.80437		1:42:47	350.93	313.83	
1:43:03	85.81	357.52	331.90	1:43:03	171.60	355.66432	328.875	1:43:02	351.82	317.52	
1:43:18	86.00	301.14		1:43:18	172.00	312.60182		1:43:18	352.71	297.45	
1:43:33	86.23	351.48		1:43:33	172.44	355.66432		1:43:33	353.60	319.99	
1:43:48	86.42	319.58		1:43:48	172.83	321.25298		1:43:48	354.49	319.99	
1:44:03	86.64	365.46	334.42	1:44:03	173.28	366.44202	338.99	1:44:03	355.38	310.06	
1:44:18	86.84	307.55		1:44:18	173.67	317.26752		1:44:18	356.27	317.92	
1:44:33	87.06	342.62		1:44:33	174.12	366.44202		1:44:33	357.16	317.28	
1:44:48	87.26	289.09		1:44:48	174.51	316.45816		1:44:48	358.05	317.92	
1:45:03	87.48	335.63	318.72	1:45:03	174.95	355.66432	338.958	1:45:03	358.94	310.46	314.24
1:45:18	87.68	307.55		1:45:18	175.35	316.45816		1:45:18	359.83	313.68	
1:45:33	87.90	342.62		1:45:33	175.74	317.26752		1:45:33	360.72	310.85	
1:45:48	88.10	305.98		1:45:48	176.18	356.46177		1:45:48	361.61	313.68	
1:46:03	88.32	349.91	326.52	1:46:03	176.58	311.80437	325.498	1:46:03	362.50	317.28	
1:46:18	88.52	307.55		1:46:18	177.02	356.46177		1:46:18	363.39	319.99	
1:46:33	88.71	321.22		1:46:33	177.41	316.45816		1:46:33	364.28	317.28	
1:46:48	88.93	342.62		1:46:48	177.86	360.97274		1:46:48	365.17	317.52	
1:47:03	89.13	294.99	316.60	1:47:03	178.25	317.26752	337.79	1:47:03	366.06	317.28	
1:47:18	89.35	357.52		1:47:18	178.70	360.97274		1:47:18	366.95	311.85	
1:47:33	89.55	312.63		1:47:33	179.09	316.45816		1:47:33	367.84	309.66	314.91
1:47:48	89.77	359.12		1:47:48	179.54	367.26364		1:47:48	368.73	306.76	
1:48:03	89.97	312.63	335.48	1:48:03	179.93	317.26752	340.491	1:48:03	369.62	309.91	
1:48:18	90.19	357.52		1:48:18	180.37	360.97274		1:48:18	370.51	310.46	
1:48:33	90.39	314.23		1:48:33	180.76	321.25298		1:48:33	371.40	311.85	
1:48:48	90.61	351.48		1:48:48	181.16	322.0746		1:48:48	372.29	313.03	
1:49:03	90.81	299.60	330.71	1:49:03	181.60	372.07959	344.095	1:49:03	373.18	318.32	
1:49:18	91.03	365.46		1:49:18	181.99	327.0296		1:49:18	374.07	316.88	
1:49:33	91.22	328.52		1:49:33	182.44	362.59145		1:49:33	374.96	311.45	
1:49:48	91.42	314.23		1:49:48	182.83	320.43136		1:49:48	375.85	317.28	
1:50:03	91.64	349.91	339.53	1:50:03	183.28	377.89333	346.986	1:50:03	376.74	317.92	313.39
1:50:18	91.84	301.14		1:50:18	183.67	321.25298		1:50:18	377.63	313.43	
1:50:33	92.06	342.62		1:50:33	184.12	356.46177		1:50:33	378.52	317.92	
1:50:48	92.26	307.55		1:50:48	184.51	311.80437		1:50:48	379.41	310.46	
1:51:03	92.48	349.91	325.31	1:51:03	184.95	361.78209	337.825	1:51:03	380.30	312.26	
1:51:18	92.68	305.98		1:51:18	185.35	316.45816		1:51:18	381.19	316.47	
1:51:33	92.90	367.10		1:51:33	185.79	356.46177		1:51:33	382.08	313.03	
1:51:48	93.10	299.60		1:51:48	186.18	316.45816		1:51:48	382.97	318.32	
1:52:03	93.32	337.14	327.46	1:52:03	186.58	317.26752	326.661	1:52:03	383.86	314.63	
1:52:18	93.52	314.23		1:52:18	187.02	346.27715		1:52:18	384.75	317.52	
1:52:33	93.74	349.91		1:52:33	187.41	307.28546		1:52:33	385.64	313.83	314.79
1:52:48	93.93	307.55		1:52:48	187.86	366.44202		1:52:48	386.53	311.85	
1:53:03	94.13	314.23	321.48	1:53:03	188.25	322.0746	335.52	1:53:03	387.42	316.88	
1:53:18	94.35	357.52		1:53:18	188.70	367.26364		1:53:18	388.31	316.28	
1:53:33	94.55	312.63		1:53:33	189.09	315.64881		1:53:33	389.20	317.28	
1:53:48	94.77	359.12		1:53:48	189.54	356.46177		1:53:48	390.09	318.32	
1:54:03	94.97	312.63	335.48	1:54:03	189.93	316.45816	338.958	1:54:03	390.98	313.43	
1:54:18	95.19	357.52		1:54:18	190.37	350.50976		1:54:18	391.87	313.68	
1:54:33	95.39	314.23		1:54:33	190.76	312.60182		1:54:33	392.76	313.83	
1:54:48	95.61	349.91		1:54:48	191.21	367.26364		1:54:48	393.65	313.03	
1:55:03	95.81	301.14	330.70	1:55:03	191.60	316.45816	336.708	1:55:03	394.54	312.26	314.68
1:55:18	96.03	349.91		1:55:18	191.99	307.28546		1:55:18	395.43	317.28	
1:55:33	96.22	312.63		1:55:33	192.44	346.27715		1:55:33	396.32	314.07	
1:55:48	96.45	359.12		1:55:48	192.83	316.45816		1:55:48	397.21	310.46	
1:56:03	96.64	307.55	332.30	1:56:03	193.28	361.78209	332.951	1:56:03	398.10	313.68	
1:56:18	96.87	349.91		1:56:18	193.67	302.89567		1:56:18	398.99	307.15	

1:56:33	97.06	307.55		1:56:33	194.12	345.50248		1:56:33	399.88	310.70	
1:56:48	97.26	319.58		1:56:48	194.51	312.60182		1:56:48	400.77	309.66	
1:57:03	97.48	365.46	335.63	1:57:03	194.95	355.66432	329.166	1:57:03	401.66	310.31	
1:57:18	97.68	307.55		1:57:18	195.34	302.89567		1:57:18	402.55	303.92	
1:57:33	97.90	359.12		1:57:33	195.79	350.50976		1:57:33	403.44	314.07	311.13
1:57:48	98.10	319.58		1:57:48	196.18	316.45816		1:57:48	404.33	313.03	
1:58:03	98.32	367.10	338.34	1:58:03	196.63	356.46177	331.581	1:58:03	405.22	309.91	
1:58:18	98.51	293.49		1:58:18	197.02	316.45816		1:58:18	406.11	307.15	
1:58:33	98.74	337.14		1:58:33	197.47	351.29566		1:58:33	407.00	313.83	
1:58:48	98.93	312.63		1:58:48	197.86	307.28546		1:58:48	407.89	318.32	
1:59:03	99.16	359.12	325.59	1:59:03	198.25	316.45816	322.874	1:59:03	408.78	310.46	
1:59:18	99.35	319.58		1:59:18	198.70	356.46177		1:59:18	409.67	313.68	
1:59:33	99.58	367.10		1:59:33	199.09	311.00691		1:59:33	410.56	309.66	
1:59:48	99.77	312.63		1:59:48	199.53	357.25922		1:59:48	411.45	314.87	
2:00:03	99.97	307.55	326.71	2:00:03	199.92	316.45816	335.297	2:00:03	412.34	309.66	312.06
2:00:18	100.19	357.52		2:00:18	200.37	366.44202		2:00:18	413.23	314.07	
		349.55035	**349.5338**			**341.68746**	**341.636**	2:00:33	414.12	310.06	
								2:00:48	415.01	311.09	
								2:01:03	415.90	303.15	
								2:01:18	416.79	317.01	
								2:01:33	417.68	307.15	
								2:01:48	418.57	310.46	
								2:02:03	419.46	310.31	
								2:02:18	420.35	310.46	
								2:02:33	421.24	318.32	311.21
								2:02:48	422.13	310.46	
								2:03:03	423.02	314.07	
								2:03:18	423.91	307.15	
										323.96	**324.04**

50 ml/ h				100 ml/ h				200 ml/ h			
time, [hh:mm:ss]	V, [cm^3]	k, [mD]		time, [hh:mm:ss]	V., [cm^3]	k, [mD]		time, [hh:mm:ss]	V., [cm^3]	k, [mD]	
0:01:00	0.844	18.97		0:01:00	1.69	11.15		0:01:00	3.328	8.59	
0:02:00	1.677	17.49		0:02:00	3.35	10.19		0:02:00	6.657	8.41	
0:03:00	2.509	16.07		0:03:00	5.02	9.33		0:03:00	9.987	8.14	
0:04:00	3.341	15.45		0:04:00	6.68	9.15		0:04:00	13.317	8.03	
0:05:00	4.174	14.96	16.59	0:05:00	8.35	9.14		0:05:00	16.645	7.97	
0:06:00	5.006	14.47		0:06:00	10.10	9.05		0:06:00	19.975	7.93	
0:07:00	5.84	14.07		0:07:00	11.68	8.95		0:07:00	23.305	7.93	
0:08:00	6.672	13.67		0:08:00	13.35	8.95		0:08:00	26.635	7.90	
0:09:00	7.505	13.40		0:09:00	15.01	8.91	9.42	0:09:00	29.965	7.87	8.09
0:10:00	8.338	13.40	13.80	0:10:00	16.68	8.81		0:10:00	33.297	7.87	
0:11:00	9.171	13.29		0:11:00	18.34	8.80		0:11:00	36.627	7.83	
0:12:00	10.004	13.02		0:12:00	20.21	8.82		0:12:00	39.959	7.83	
0:13:00	10.837	12.91		0:13:00	21.67	8.76		0:13:00	43.291	7.82	
0:14:00	11.67	12.71		0:14:00	23.34	8.70		0:14:00	46.621	7.80	
0:15:00	12.503	12.51	12.89	0:15:00	25.01	8.67		0:15:00	49.955	7.81	
0:16:00	13.337	12.42		0:16:00	26.67	8.68		0:16:00	53.287	7.78	
0:17:00	14.17	12.36		0:17:00	28.34	8.65		0:17:00	56.62	7.74	
0:18:00	15.003	12.22		0:18:00	30.01	8.62	8.72	0:18:00	59.952	7.72	7.80
0:19:00	15.837	12.01		0:19:00	31.67	8.58		0:19:00	63.286	7.71	
0:20:00	16.67	11.87	12.18	0:20:00	33.34	8.55		0:20:00	66.619	7.70	
0:21:00	17.503	11.83		0:21:00	35.01	8.54		0:21:00	69.953	7.68	
0:22:00	18.337	11.75		0:22:00	36.68	8.50		0:22:00	73.286	7.66	
0:23:00	19.17	11.61		0:23:00	38.34	8.46		0:23:00	76.619	7.66	
0:24:00	20.004	11.58		0:24:00	40.01	8.45		0:24:00	79.953	7.64	
0:25:00	20.838	11.50	11.65	0:25:00	41.68	8.40		0:25:00	83.288	7.61	
0:26:00	21.672	11.34		0:26:00	43.34	8.39		0:26:00	86.622	7.58	
0:27:00	22.505	11.20		0:27:00	45.01	8.39	8.47	0:27:00	89.956	7.55	7.64
0:28:00	23.34	11.15		0:28:00	46.68	8.39		0:28:00	93.291	7.55	
0:29:00	24.174	11.06		0:29:00	48.35	8.34		0:29:00	96.625	7.55	
0:30:00	25.007	11.02	11.15	0:30:00	50.01	8.31		0:30:00	99.96	7.54	
0:31:00	25.841	10.95		0:31:00	51.68	8.28		0:31:00	103.294	7.51	
0:32:00	26.675	10.88		0:32:00	53.35	8.25		0:32:00	106.628	7.49	
0:33:00	27.509	10.80		0:33:00	55.02	8.25		0:33:00	109.963	7.50	
0:34:00	28.342	10.68		0:34:00	56.68	8.22		0:34:00	113.296	7.48	
0:35:00	29.176	10.67	10.80	0:35:00	58.34	8.18		0:35:00	116.631	7.47	
0:36:00	30.01	10.63		0:36:00	60.02	8.14	8.26	0:36:00	119.964	7.45	7.50
0:37:00	30.843	10.51		0:37:00	61.68	8.14		0:37:00	123.3	7.42	
0:38:00	31.677	10.39		0:38:00	63.35	8.15		0:38:00	126.634	7.41	
0:39:00	32.51	10.28		0:39:00	65.02	8.12		0:39:00	129.969	7.40	
0:40:00	33.344	10.25	10.41	0:40:00	66.69	8.10		0:40:00	133.303	7.39	
0:41:00	34.177	10.21		0:41:00	68.35	8.07		0:41:00	136.637	7.37	
0:42:00	35.011	10.15		0:42:00	70.01	8.02		0:42:00	139.971	7.34	
0:43:00	35.845	10.12		0:43:00	71.69	8.03		0:43:00	143.305	7.34	
0:44:00	36.679	10.09		0:44:00	73.36	8.03		0:44:00	146.641	7.32	
0:45:00	37.512	9.98	10.11	0:45:00	75.02	7.98	8.07	0:45:00	149.976	7.31	7.37
0:46:00	38.346	9.91		0:46:00	76.69	7.94		0:46:00	153.324	7.35	
0:47:00	39.18	9.87		0:47:00	78.36	7.96		0:47:00	156.715	7.42	
0:48:00	40.013	9.83		0:48:00	80.03	7.95		0:48:00	159.979	7.14	
0:49:00	40.847	9.78		0:49:00	81.69	7.91		0:49:00	163.314	7.30	
0:50:00	41.68	9.71	9.82	0:50:00	83.36	7.88		0:50:00	166.427	6.81	
0:51:00	42.514	9.70		0:51:00	85.03	7.86		0:51:00	169.585	6.89	
0:52:00	43.348	9.70		0:52:00	86.69	7.83		0:52:00	172.921	7.26	
0:53:00	44.182	9.67		0:53:00	88.36	7.80		0:53:00	176.255	7.25	
0:54:00	45.016	9.58		0:54:00	90.03	7.79	7.88	0:54:00	179.589	7.26	7.19
0:55:00	45.85	9.52	9.63	0:55:00	91.70	7.77		0:55:00	182.923	7.28	
0:56:00	46.683	9.51		0:56:00	93.36	7.77		0:56:00	186.257	7.24	
0:57:00	47.517	9.49		0:57:00	95.03	7.78		0:57:00	189.591	7.21	
0:58:00	48.351	9.43		0:58:00	96.70	7.76		0:58:00	192.925	7.21	
0:59:00	49.184	9.42		0:59:00	98.36	7.72		0:59:00	196.259	7.19	
1:00:00	50.018	9.43	9.46	1:00:00	100.03	7.70		1:00:00	199.594	7.19	
1:01:00	50.851	9.39		1:01:00	101.70	7.71		1:01:00	202.928	7.16	
1:02:00	51.685	9.33		1:02:00	103.37	7.67		1:02:00	206.262	7.15	
1:03:00	52.519	9.28		1:03:00	105.03	7.65	7.73	1:03:00	209.596	7.15	7.20
1:04:00	53.352	9.24		1:04:00	106.70	7.66		1:04:00	212.93	7.15	
1:05:00	54.186	9.22	9.29	1:05:00	108.37	7.62		1:05:00	216.264	7.14	
1:06:00	55.02	9.19		1:06:00	110.03	7.61		1:06:00	219.598	7.12	
1:07:01	55.853	8.98		1:07:00	111.70	7.60		1:07:00	222.934	7.11	
1:08:01	56.687	9.14		1:08:00	113.37	7.59		1:08:00	226.268	7.10	
1:09:01	57.521	9.09		1:09:00	115.04	7.58		1:09:00	229.601	7.10	
1:10:01	58.354	9.00	9.08	1:10:00	116.71	7.55		1:10:00	232.938	7.11	
1:11:01	59.188	8.99		1:11:00	118.37	7.52		1:11:00	236.271	7.06	
1:12:01	60.021	8.98		1:12:00	120.04	7.52	7.58	1:12:00	239.607	7.06	7.11
1:13:01	60.855	8.99		1:13:01	121.71	7.39		1:13:00	242.941	7.07	
1:14:01	61.689	9.02		1:14:01	123.38	7.51		1:14:01	246.275	6.94	
1:15:01	62.523	8.99	8.99	1:15:01	125.04	7.47		1:15:01	249.613	7.04	
1:16:01	63.356	8.90		1:16:01	126.71	7.45		1:16:01	252.948	7.01	
1:17:01	64.19	8.89		1:17:01	128.38	7.44		1:17:01	256.282	7.00	
1:18:01	65.024	8.87		1:18:01	130.05	7.42		1:18:01	259.617	7.00	
1:19:01	65.858	8.87		1:19:01	131.71	7.39		1:19:01	262.952	6.99	
1:20:01	66.692	8.87	8.88	1:20:01	133.38	7.40		1:20:01	266.286	6.99	
1:21:01	67.525	8.81		1:21:01	135.05	7.39	7.43	1:21:01	269.621	7.28	7.04
1:22:01	68.359	8.77		1:22:01	136.72	7.32		1:22:01	272.9557	7.58	
1:23:01	69.192	8.76		1:23:01	138.38	7.31		1:23:01	276.2904	7.56	
1:24:01	70.026	8.77		1:24:01	140.05	7.30		1:24:01	279.6251	7.51	
1:25:01	70.859	8.71	8.76	1:25:01	141.72	7.30		1:25:01	282.9598	7.48	
1:26:01	71.693	8.70		1:26:01	143.39	7.30		1:26:01	286.2945	7.45	
1:27:01	72.527	8.70		1:27:01	145.05	7.27		1:27:01	289.6292	7.44	
1:28:01	73.36	8.69		1:28:01	146.72	7.23		1:28:01	292.9639	7.42	
1:29:01	74.194	8.65		1:29:01	148.39	7.20		1:29:01	296.2986	7.38	
1:30:01	75.028	8.61	8.67	1:30:01	150.06	7.23	7.27	1:30:01	299.6333	7.39	7.47
1:31:01	75.862	8.61		1:31:01	151.72	7.20		1:31:01	302.968	7.40	
1:32:01	76.696	8.58		1:32:01	153.39	7.16		1:32:01	306.3027	7.39	
1:33:01	77.529	8.55		1:33:01	155.06	7.18		1:33:01	309.6374	7.36	
1:34:01	78.363	8.54		1:34:01	156.73	7.18		1:34:01	312.9721	7.33	
1:35:01	79.196	8.50	8.56	1:35:01	158.39	7.15		1:35:01	316.3068	7.33	
1:36:01	80.03	8.51		1:36:01	160.06	7.13		1:36:01	319.6415	7.30	
1:37:01	80.864	8.49		1:37:01	161.73	7.13		1:37:01	322.9762	7.28	
1:38:01	81.698	8.44		1:38:01	163.39	7.10		1:38:01	326.3109	7.26	
1:39:01	82.531	8.43		1:39:01	165.06	7.09	7.15	1:39:01	329.6456	7.26	7.32
1:40:01	83.365	8.47	8.47	1:40:01	166.73	7.11		1:40:01	332.9803	7.26	
1:41:01	84.198	8.43		1:41:01	168.04	7.10		1:41:01	336.315	7.23	
1:42:01	85.032	8.38		1:42:01	170.06	7.07		1:42:01	339.6497	7.23	
1:43:01	85.866	8.36		1:43:01	171.73	7.08		1:43:01	342.9844	7.22	
1:44:01	86.7	8.36		1:44:01	173.45	7.04		1:44:01	346.3191	7.20	
1:45:01	87.533	8.31	8.37	1:45:01	175.06	7.02		1:45:01	349.6538	7.18	
1:46:01	88.367	8.32		1:46:01	176.73	7.02		1:46:01	352.9885	7.18	
1:47:01	89.201	8.32		1:47:01	178.40	7.01		1:47:01	356.3232	7.17	
1:48:01	90.034	8.28		1:48:01	180.07	6.99	7.05	1:48:01	359.6579	7.15	7.20
1:49:01	90.868	8.27		1:49:01	181.73	6.98		1:49:01	362.9926	7.14	
1:50:01	91.702	8.23	8.28	1:50:01	183.40	6.96		1:50:01	366.3273	7.14	
1:51:01	92.536	8.21		1:51:01	185.07	6.95		1:51:01	369.662	7.10	
1:52:01	93.369	8.20		1:52:01	186.73	6.93		1:52:01	372.9967	7.09	
1:53:01	94.203	8.19		1:53:01	188.40	6.93		1:53:01	376.3314	7.09	
1:54:01	95.037	8.19		1:54:01	190.07	6.93		1:54:01	379.6661	7.07	
1:55:01	95.871	8.19	8.19	1:55:01	191.74	6.90		1:55:01	383.0008	7.05	
1:56:01	96.704	8.16		1:56:01	193.40	6.89		1:56:01	386.3355	7.04	
1:57:01	97.538	8.15		1:57:01	195.07	6.88	6.93	1:57:01	389.6702	7.03	7.08
1:58:01	98.372	8.11		1:58:01	196.74	6.87		1:58:01	393.0049	7.02	
1:59:01	99.205	8.08		1:59:01	198.41	6.87		1:59:01	396.3396	7.01	
		10.11	8.52			**7.83**		2:00:01	399.6743	7.01	
										7.38	

ki (mD)	k @ 50 ml/h (mD)	k @ 100 ml/ h (mD)	k @ 200 ml/ h
32.37	10.11	7.83	7.38
	68.77	75.81	77.20

Damage Ratio (D)		Total clay	9.07
3.2018	4.1341	4.38618	

Core ID: D- 3- 1

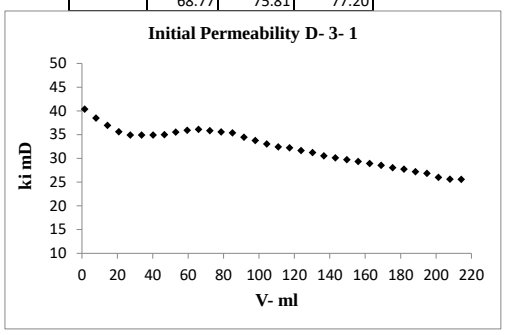

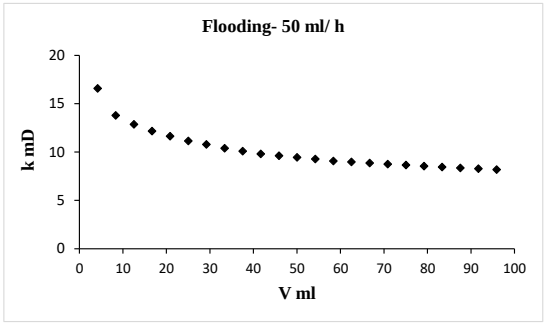

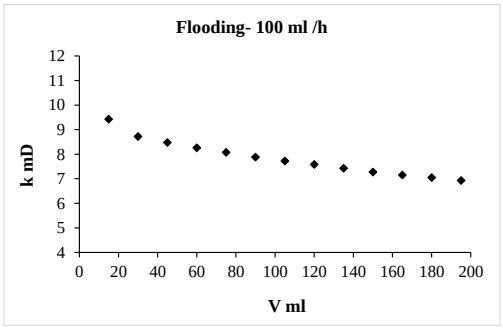

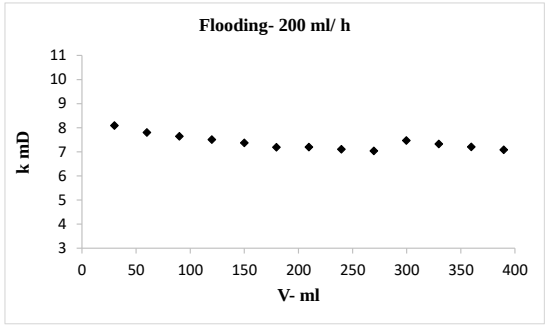

Group	Sample ID	Quartz	Calcite Mg	Oligoclase	Microcline	Chl. IIb	Kao.	Illite 2M1	Biotite 1M	Dol.	amorph.	Total Clay	Φ_{He} (%)	kwi (mD)
D-3	D- 3- 1- 1872.10	69.4	4.9	9.5	1.8	2.2	**2.0**	4.8	0.1	2.3	3.0	9.07	21.50	25.79
	D- 3- 2- 1868.90	75.0	3.4	7.5	2.0	1.4	0.8	3.3	0.1	1.6	5.0	5.47	23.70	84.99

V ml/ h	k (mD)		D: formation damage		
50	68.77	3.20			
100	75.81	4.13		50	3.2
200	77.2	4.39		100	4.13
				200	4.39

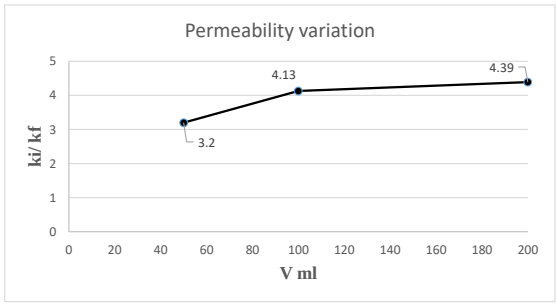

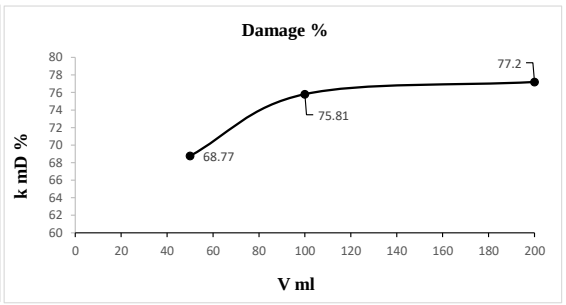

50 ml/ h				100 ml/ h				200 ml/ h			
time, [hh:mm:ss]	V, [cm^3]	k, [mD]		time, [hh:mm:ss]	V, [cm^3]	k, [mD]		time, [hh:mm:ss]	V, [cm^3]	k, [mD]	
0:00:15	0.223	121.17		0:00:15	0.444	102.64		0:00:15	0.889	92.66	
0:00:30	0.417	120.07		0:00:30	0.833	101.43		0:00:30	1.665	80.89	
0:00:45	0.639	119.31		0:00:45	1.277	102.12		0:00:45	2.553	93.74	
0:01:00	0.833	118.39		0:01:00	1.666	88.86		0:01:00	3.332	83.30	
0:01:15	1.056	119.96		0:01:15	2.11	101.42		0:01:15	4.221	94.72	
0:01:30	1.25	119.11		0:01:30	2.499	88.86		0:01:30	4.999	81.09	
0:01:45	1.472	120.01		0:01:45	2.943	102.57		0:01:45	5.889	91.12	
0:02:00	1.667	120.30		0:02:00	3.333	89.09		0:02:00	6.667	80.66	
0:02:15	1.889	116.74		0:02:15	3.777	101.42		0:02:15	7.555	93.23	
0:02:30	2.084	117.51	119.26	0:02:30	4.167	89.09	96.75	0:02:30	8.334	82.24	87.37
0:02:45	2.306	115.96		0:02:45	4.613	100.76		0:02:45	9.224	93.96	
0:03:00	2.501	120.30		0:03:00	5.003	87.46		0:03:00	10.004	81.89	
0:03:15	2.724	116.58		0:03:15	5.447	98.85		0:03:15	10.894	93.10	
0:03:30	2.919	117.51		0:03:30	5.838	87.05		0:03:30	11.674	81.30	
0:03:45	3.141	116.74		0:03:45	6.283	99.07		0:03:45	12.565	93.21	
0:04:00	3.336	117.51		0:04:00	6.673	86.83		0:04:00	13.347	81.81	
0:04:15	3.559	117.32		0:04:15	7.118	100.90		0:04:15	14.238	92.54	
0:04:30	3.755	112.86		0:04:30	7.509	90.32		0:04:30	15.018	80.29	
0:04:45	3.949	114.25		0:04:45	7.899	89.09		0:04:45	15.909	91.71	
0:05:00	4.172	117.32	116.63	0:05:00	8.345	100.02	94.04	0:05:00	16.69	80.82	87.06
0:05:15	4.368	118.11		0:05:15	8.736	88.66		0:05:15	17.581	91.71	
0:05:30	4.591	116.58		0:05:30	9.182	101.88		0:05:30	18.364	80.60	
0:05:45	4.786	117.51		0:05:45	9.572	89.09		0:05:45	19.146	81.51	
0:06:00	5.009	117.32		0:06:00	10.018	101.13		0:06:00	20.037	92.37	
0:06:15	5.205	115.42		0:06:15	10.409	87.69		0:06:15	20.82	80.17	
0:06:30	5.428	117.32		0:06:30	10.856	100.24		0:06:30	21.712	92.15	
0:06:45	5.624	115.42		0:06:45	11.246	86.83		0:06:45	22.495	81.32	
0:07:00	5.847	113.38		0:07:00	11.693	99.52		0:07:00	23.388	91.92	
0:07:15	6.042	115.40		0:07:15	12.083	87.46		0:07:15	24.17	80.49	
0:07:30	6.266	113.98	116.05	0:07:30	12.531	101.21	94.37	0:07:30	25.064	92.02	86.43
0:07:45	6.461	114.84		0:07:45	12.921	90.43		0:07:45	25.846	80.49	
0:08:00	6.685	117.91		0:08:00	13.368	103.65		0:08:00	26.739	92.75	
0:08:15	6.88	114.84		0:08:15	13.759	89.32		0:08:15	27.52	80.39	
0:08:30	7.075	114.84		0:08:30	14.205	103.03		0:08:30	28.414	91.70	
0:08:45	7.299	114.98		0:08:45	14.596	90.32		0:08:45	29.197	81.03	
0:09:00	7.494	112.28		0:09:00	14.987	89.32		0:09:00	29.98	81.03	
0:09:15	7.717	117.32		0:09:15	15.434	100.98		0:09:15	30.872	91.49	
0:09:30	7.913	115.42		0:09:30	15.824	87.46		0:09:30	31.655	79.89	
0:09:45	8.136	114.41		0:09:45	16.271	100.24		0:09:45	32.548	91.45	
0:10:00	8.331	112.28	114.91	0:10:00	16.662	87.69	94.24	0:10:00	33.329	79.68	84.99
0:10:15	8.555	114.98		0:10:15	17.108	100.02		0:10:15	34.223	90.89	
0:10:30	8.751	110.41		0:10:30	17.5	87.91		0:10:30	35.004	80.39	
0:10:45	8.974	108.94		0:10:45	17.946	100.02		0:10:45	35.898	92.02	
0:11:00	9.169	107.51		0:11:00	18.338	89.54		0:11:00	36.68	79.50	
0:11:15	9.393	109.49		0:11:15	18.784	103.81		0:11:15	37.573	90.79	
0:11:30	9.588	105.27		0:11:30	19.176	90.22		0:11:30	38.358	80.09	
0:11:45	9.812	106.92		0:11:45	19.622	100.76		0:11:45	39.25	91.33	
0:12:00	10.007	105.27		0:12:00	20.013	88.33		0:12:00	40.033	79.89	
0:12:15	10.203	105.81		0:12:15	20.459	100.76		0:12:15	40.926	90.79	
0:12:30	10.427	105.18	107.98	0:12:30	20.85	87.69	94.90	0:12:30	41.708	80.21	85.59
0:12:45	10.622	109.84		0:12:45	21.241	88.66		0:12:45	42.49	79.92	
0:13:00	10.845	117.92		0:13:00	21.688	101.35		0:13:00	43.384	91.37	
0:13:15	11.041	103.65		0:13:15	22.079	87.05		0:13:15	44.166	79.92	
0:13:30	11.264	106.38		0:13:30	22.525	101.13		0:13:30	45.058	90.37	
0:13:45	11.46	103.65		0:13:45	22.916	88.01		0:13:45	45.841	79.32	
0:14:00	11.683	106.38		0:14:00	23.363	98.80		0:14:00	46.735	90.25	
0:14:15	11.878	107.51		0:14:15	23.754	87.69		0:14:15	47.516	79.40	
0:14:30	12.102	106.92		0:14:30	24.201	100.98		0:14:30	48.41	91.21	
0:14:45	12.297	105.27		0:14:45	24.592	89.32		0:14:45	49.193	79.89	
0:15:00	12.52	106.38	107.39	0:15:00	25.039	101.35	94.43	0:15:00	50.086	91.11	85.28
0:15:15	12.716	103.65		0:15:15	25.429	86.83		0:15:15	50.867	79.12	
0:15:30	12.939	110.92		0:15:30	25.876	100.24		0:15:30	51.76	90.15	
0:15:45	13.135	105.81		0:15:45	26.268	87.91		0:15:45	52.542	78.95	
0:16:00	13.33	103.12		0:16:00	26.714	99.30		0:16:00	53.324	79.22	
0:16:15	13.554	109.08		0:16:15	27.105	87.05		0:16:15	54.216	91.01	
0:16:30	13.749	103.12		0:16:30	27.496	88.66		0:16:30	54.998	79.78	
0:16:45	13.973	118.45		0:16:45	27.943	102.11		0:16:45	55.89	90.37	
0:17:00	14.168	101.06		0:17:00	28.334	87.05		0:17:00	56.672	78.95	
0:17:15	14.391	115.57		0:17:15	28.78	98.58		0:17:15	57.564	89.58	
0:17:30	14.587	103.65	107.44	0:17:30	29.172	87.27	92.50	0:17:30	58.347	78.23	83.54
0:17:45	14.81	115.57		0:17:45	29.619	100.24		0:17:45	59.24	89.22	
0:18:00	15.006	99.58		0:18:00	30.01	88.33		0:18:00	60.021	78.43	
0:18:15	15.229	112.20		0:18:15	30.456	100.02		0:18:15	60.915	90.57	
0:18:30	15.425	98.62		0:18:30	30.847	86.42		0:18:30	61.696	78.71	
0:18:45	15.648	115.57		0:18:45	31.294	98.80		0:18:45	62.591	89.88	
0:19:00	15.844	101.57		0:19:00	31.685	87.05		0:19:00	63.372	79.12	
0:19:15	16.039	99.07		0:19:15	32.131	98.58		0:19:15	64.264	90.37	
0:19:30	16.262	113.30		0:19:30	32.522	87.05		0:19:30	65.046	78.95	
0:19:45	16.458	101.57		0:19:45	32.913	87.05		0:19:45	65.938	90.05	
0:20:00	16.681	115.57	107.26	0:20:00	33.36	98.10	93.17	0:20:00	66.721	79.05	84.43
0:20:15	16.877	101.57		0:20:15	33.751	86.42		0:20:15	67.503	78.26	
0:20:30	17.1	115.57		0:20:30	34.198	99.52		0:20:30	68.395	88.50	
0:20:45	17.296	101.57		0:20:45	34.589	85.50		0:20:45	69.177	76.93	
0:21:00	17.519	115.57		0:21:00	35.036	97.06		0:21:00	70.069	88.05	
0:21:15	17.714	101.06		0:21:15	35.427	86.42		0:21:15	70.852	77.96	
0:21:30	17.938	116.08		0:21:30	35.873	98.58		0:21:30	71.745	88.91	
0:21:45	18.133	99.07		0:21:45	36.264	85.81		0:21:45	72.526	78.43	
0:22:00	18.357	110.56		0:22:00	36.711	98.80		0:22:00	73.42	90.25	
0:22:15	18.552	96.24		0:22:15	37.101	86.20		0:22:15	74.201	78.43	
0:22:30	18.775	111.12	106.84	0:22:30	37.548	98.80	92.31	0:22:30	75.096	89.11	83.48
0:22:45	18.971	99.58		0:22:45	37.939	87.05		0:22:45	75.877	77.49	
0:23:00	19.166	99.07		0:23:00	38.386	98.80		0:23:00	76.771	89.01	
0:23:15	19.39	111.62		0:23:15	38.777	85.81		0:23:15	77.552	78.03	
0:23:30	19.585	97.17		0:23:30	39.168	85.81		0:23:30	78.445	88.91	
0:23:45	19.809	111.62		0:23:45	39.615	98.10		0:23:45	79.227	77.59	
0:24:00	20.004	97.17		0:24:00	40.006	84.90		0:24:00	80.009	77.32	
0:24:15	20.228	110.56		0:24:15	40.453	97.06		0:24:15	80.903	87.65	
0:24:30	20.423	98.11		0:24:30	40.845	86.03		0:24:30	81.685	76.67	
0:24:45	20.647	112.70		0:24:45	41.291	99.30		0:24:45	82.578	88.00	
0:25:00	20.842	98.11	103.57	0:25:00	41.479	98.14	92.10	0:25:00	83.36	77.59	81.83
0:25:15	21.066	112.70		0:25:15	41.926	94.97		0:25:15	84.253	88.60	
0:25:30	21.261	96.24		0:25:30	42.316	89.09		0:25:30	85.035	77.06	
0:25:45	21.484	111.12		0:25:45	42.763	98.80		0:25:45	85.929	88.10	
0:26:00	21.68	96.74		0:26:00	43.154	86.42		0:26:00	86.711	77.06	
0:26:15	21.876	96.74		0:26:15	43.601	99.52		0:26:15	87.603	87.45	
0:26:30	22.099	110.06		0:26:30	43.992	86.42		0:26:30	88.386	76.77	
0:26:45	22.295	95.82		0:26:45	44.438	96.84		0:26:45	89.278	87.90	
0:27:00	22.518	110.06		0:27:00	44.83	85.72		0:27:00	90.06	77.06	
0:27:15	22.713	96.24		0:27:15	45.221	85.50		0:27:15	90.842	76.67	
0:27:30	22.937	109.51	103.52	0:27:30	45.667	97.53	92.08	0:27:30	91.737	87.30	82.40
0:27:45	23.132	95.34		0:27:45	46.058	86.42		0:27:45	92.519	76.28	
0:28:00	23.356	107.49		0:28:00	46.505	98.10		0:28:00	93.412	87.11	
0:28:15	23.551	93.57		0:28:15	46.896	84.90		0:28:15	94.195	76.38	
0:28:30	23.774	110.06		0:28:30	47.343	96.04		0:28:30	95.087	87.45	
0:28:45	23.97	96.74		0:28:45	47.734	84.90		0:28:45	95.869	77.06	
0:29:00	24.193	110.06		0:29:00	48.181	97.06		0:29:00	96.762	87.55	
0:29:15	24.389	96.74		0:29:15	48.572	84.90		0:29:15	97.545	76.38	
0:29:30	24.612	109.02		0:29:30	49.019	97.06		0:29:30	98.44	87.30	
0:29:45	24.807	96.24		0:29:45	49.41	83.42		0:29:45	99.223	77.03	
0:30:00	25.003	94.93	101.02	0:30:00	49.857	95.37	90.82	0:30:00	100.115	88.20	82.07
0:30:15	25.226	107.01		0:30:15	50.248	84.01		0:30:15	100.896	76.57	
0:30:30	25.422	95.82		0:30:30	50.639	84.01		0:30:30	101.789	87.55	
0:30:45	25.645	109.02		0:30:45	51.085	95.82		0:30:45	102.57	76.31	
0:31:00	25.84	95.34		0:31:00	51.477	84.22		0:31:00	103.352	75.77	
0:31:15	26.064	109.51		0:31:15	51.923	95.82		0:31:15	104.246	86.62	
0:31:30	26.259	95.34		0:31:30	52.314	84.01		0:31:30	105.029	76.51	
0:31:45	26.483	109.51		0:31:45	52.761	97.06		0:31:45	105.922	87.55	
0:32:00	26.678	95.34		0:32:00	53.152	84.90		0:32:00	106.704	76.28	
0:32:15	26.901	107.01		0:32:15	53.598	97.53		0:32:15	107.596	86.72	
0:32:30	27.097	94.05	101.79	0:32:30	53.99	85.11	89.25	0:32:30	108.378	76.02	80.59
0:32:45	27.32	107.01		0:32:45	54.436	95.16		0:32:45	109.272	87.20	
0:33:00	27.516	92.34		0:33:00	54.828	83.64		0:33:00	110.053	76.57	
0:33:15	27.74	107.49		0:33:15	55.275	94.71		0:33:15	110.948	88.50	
0:33:30	27.935	95.34		0:33:30	55.665	83.21		0:33:30	111.73	76.67	
0:33:45	28.131	94.05		0:33:45	56.057	83.64		0:33:45	112.623	86.81	
0:34:00	28.354	105.06		0:34:00	56.504	95.37		0:34:00	113.404	75.67	
0:34:16	28.55	88.17		0:34:16	56.894	78.01		0:34:16	114.296	80.75	
0:34:31	28.773	110.06		0:34:31	57.342	95.59		0:34:31	115.079	75.86	
0:34:46	28.969	96.74		0:34:46	57.732	83.79		0:34:46	115.861	75.77	

		D %	V ml/ h	ki/ kf
ki	103.33		50	1.11
k 50	92.92	10.07	100	1.21
k 100	85.49	17.27	200	1.33
k 200	77.51	24.99		

Core ID: D- 3- 2

total clay	5.47

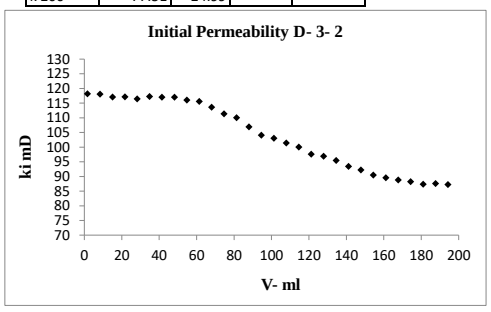

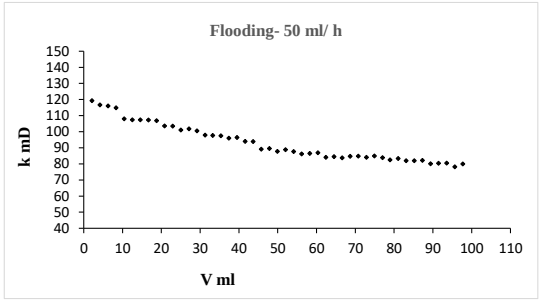

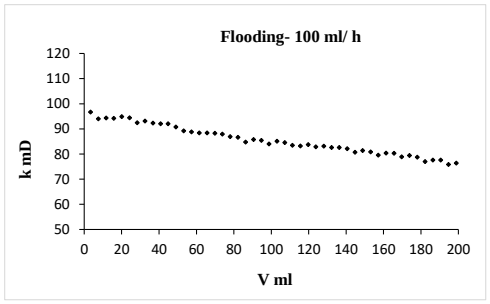

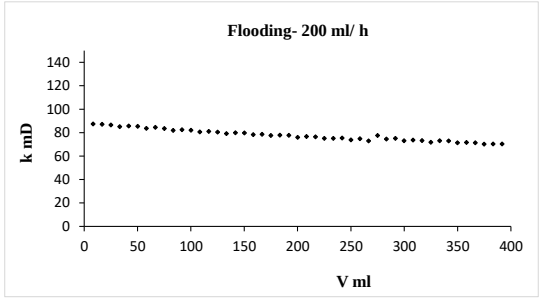

Group	Sample ID	Quartz	Calcite Mg	Oligoclase	Microcline	Chl. IIb	Kao.	Illite 2M1	Biotite 1M	Dol.	amorph.	Total Clay	Φ_{He} (%)	k_{wi} (mD)
D-3	D- 3- 1- 1872.10	69.4	4.9	9.5	1.8	2.2	**2.0**	4.8	0.1	2.3	3.0	9.07	21.50	25.79
	D- 3- 2- 1868.90	75.0	3.4	7.5	2.0	1.4	0.8	3.3	0.1	1.6	5.0	5.47	23.70	84.99

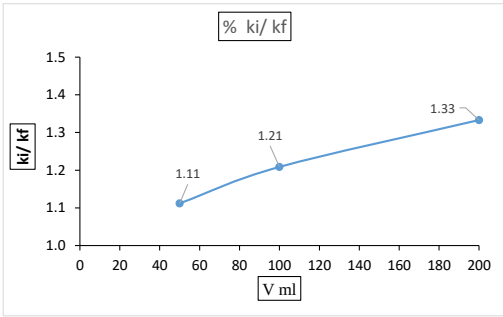

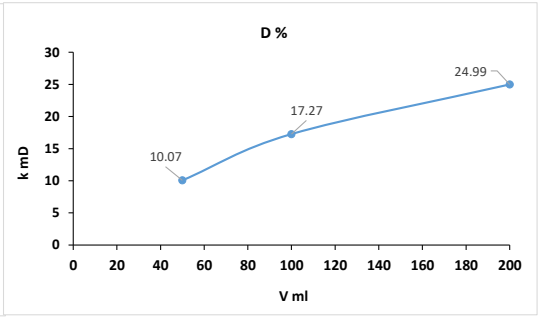

V ml/ h	Damage
50	10.07
100	17.27
200	24.99

0:35:01	29.192	109.02	100.53	0:35:01	58.179	95.37	88.85	0:35:01	116.754	86.52	81.03
0:35:16	29.387	93.57		0:35:16	58.569	83.21		0:35:16	117.535	75.42	
0:35:31	29.61	107.01		0:35:31	59.016	97.06		0:35:31	118.427	85.42	
0:35:46	29.806	94.05		0:35:46	59.407	84.90		0:35:46	119.209	74.52	
0:36:01	30.029	107.01		0:36:01	59.853	95.16		0:36:01	120.103	85.61	
0:36:16	30.225	94.05		0:36:16	60.245	83.06		0:36:16	120.886	75.36	
0:36:31	30.449	105.53		0:36:31	60.692	95.37		0:36:31	121.78	86.04	
0:36:46	30.644	91.87		0:36:46	61.083	84.01		0:36:46	122.562	75.51	
0:37:01	30.84	90.69		0:37:01	61.53	94.71		0:37:01	123.455	85.80	
0:37:16	31.063	103.18		0:37:16	61.92	82.64		0:37:16	124.238	74.98	
0:37:31	31.259	92.34	97.93	0:37:31	62.311	84.01	88.41	0:37:31	125.13	85.42	80.41
0:37:46	31.482	105.06		0:37:46	62.759	95.59		0:37:46	125.912	74.52	
0:38:01	31.678	94.05		0:38:01	63.149	82.64		0:38:01	126.694	74.89	
0:38:16	31.901	107.01		0:38:16	63.596	94.07		0:38:16	127.587	85.95	
0:38:31	32.097	92.34		0:38:31	63.986	82.07		0:38:31	128.369	75.26	
0:38:46	32.32	105.06		0:38:46	64.433	94.71		0:38:46	129.262	85.52	
0:39:01	32.488	82.92		0:39:01	64.824	82.85		0:39:01	130.044	74.52	
0:39:16	32.634	82.24		0:39:16	65.27	93.85		0:39:16	130.938	85.90	
0:39:31	32.829	107.51		0:39:31	65.662	82.49		0:39:31	131.719	74.79	
0:39:46	33.053	108.49		0:39:46	66.109	94.07		0:39:46	132.613	84.91	
0:40:01	33.248	91.87	97.65	0:40:01	66.499	82.07	88.44	0:40:01	133.395	75.14	79.14
0:40:16	33.444	92.34		0:40:16	66.947	94.93		0:40:16	134.289	85.61	
0:40:31	33.667	105.06		0:40:31	67.338	82.85		0:40:31	135.07	74.18	
0:40:46	33.863	92.34		0:40:46	67.784	93.85		0:40:46	135.964	85.19	
0:41:01	34.087	103.65		0:41:01	68.175	81.72		0:41:01	136.745	74.18	
0:41:16	34.282	88.64		0:41:16	68.567	82.49		0:41:16	137.638	85.52	
0:41:31	34.505	103.18		0:41:31	69.013	93.85		0:41:31	138.42	75.14	
0:41:46	34.701	92.34		0:41:46	69.405	82.49		0:41:46	139.202	74.27	
0:42:01	34.924	105.06		0:42:01	69.851	92.90		0:42:01	140.095	84.81	
0:42:16	35.12	90.69		0:42:16	70.242	81.44		0:42:16	140.878	74.12	
0:42:31	35.343	101.37	97.47	0:42:31	70.688	96.16	88.27	0:42:31	141.77	84.86	79.79
0:42:46	35.538	90.23		0:42:46	71.08	84.52		0:42:46	142.555	74.93	
0:43:01	35.762	105.53		0:43:01	71.526	94.50		0:43:01	143.447	85.42	
0:43:16	35.957	90.23		0:43:16	71.714	91.08		0:43:16	144.228	75.04	
0:43:31	36.18	101.37		0:43:31	72.16	89.15		0:43:31	145.121	84.81	
0:43:46	36.376	90.69		0:43:46	72.552	86.33		0:43:46	145.902	74.18	
0:44:01	36.571	91.87		0:44:01	72.998	94.50		0:44:01	146.795	84.81	
0:44:16	36.795	101.83		0:44:16	73.389	82.28		0:44:16	147.578	74.12	
0:44:31	36.99	87.12		0:44:31	73.78	82.28		0:44:31	148.47	84.44	
0:44:46	37.214	105.53		0:44:46	74.226	93.22		0:44:46	149.253	74.12	
0:45:01	37.409	95.34	95.97	0:45:01	74.618	81.93	87.98	0:45:01	150.146	84.54	79.64
0:45:16	37.632	107.01		0:45:16	75.064	92.27		0:45:16	150.927	73.93	
0:45:31	37.828	90.69		0:45:31	75.455	80.90		0:45:31	151.709	74.03	
0:45:46	38.051	101.37		0:45:46	75.902	92.48		0:45:46	152.602	84.81	
0:46:01	38.247	89.10		0:46:01	76.293	81.44		0:46:01	153.386	74.22	
0:46:16	38.47	101.37		0:46:16	76.741	94.93		0:46:16	154.278	84.86	
0:46:31	38.666	89.10		0:46:31	77.131	82.07		0:46:31	155.061	74.49	
0:46:46	38.889	101.37		0:46:46	77.577	91.66		0:46:46	155.953	84.17	
0:47:01	39.084	88.64		0:47:01	77.969	79.76		0:47:01	156.734	74.18	
0:47:16	39.308	103.65		0:47:16	78.415	92.27		0:47:16	157.627	84.81	
0:47:31	39.503	91.87	96.42	0:47:31	78.806	81.72	86.95	0:47:31	158.409	73.43	78.29
0:47:46	39.699	90.69		0:47:46	79.252	93.85		0:47:46	159.303	83.27	
0:48:01	39.922	99.63		0:48:01	79.643	81.44		0:48:01	160.084	72.74	
0:48:16	40.117	85.64		0:48:16	80.034	80.09		0:48:16	160.978	83.94	
0:48:31	40.341	100.07		0:48:31	80.481	91.56		0:48:31	161.76	73.79	
0:48:46	40.536	87.12		0:48:46	80.872	80.90		0:48:46	162.653	83.99	
0:49:01	40.759	99.63		0:49:01	81.318	92.27		0:49:01	163.436	73.28	
0:49:16	40.955	89.10		0:49:16	81.71	80.29		0:49:16	164.219	73.28	
0:49:31	41.178	99.63		0:49:31	82.156	91.35		0:49:31	165.112	83.99	
0:49:46	41.374	87.56		0:49:46	82.547	80.90		0:49:46	165.895	73.28	
0:50:01	41.597	101.37	94.04	0:50:01	82.993	93.85	86.65	0:50:01	166.787	83.48	78.50
0:50:16	41.793	89.10		0:50:16	83.385	81.65		0:50:16	167.57	73.28	
0:50:31	42.016	99.63		0:50:31	83.831	92.27		0:50:31	168.463	84.12	
0:50:46	42.212	87.56		0:50:46	84.222	80.90		0:50:46	169.244	73.57	
0:51:01	42.408	89.10		0:51:01	84.668	91.35		0:51:01	170.137	82.91	
0:51:16	42.631	103.18		0:51:16	85.059	80.09		0:51:16	170.919	73.19	
0:51:31	42.827	89.10		0:51:31	85.506	90.95		0:51:31	171.812	84.26	
0:51:46	43.05	99.63		0:51:46	85.898	79.23		0:51:46	172.595	73.64	
0:52:01	43.246	87.56		0:52:01	86.289	79.56		0:52:01	173.488	84.54	
0:52:16	43.469	99.63		0:52:16	86.736	90.95		0:52:16	174.27	73.43	
0:52:31	43.664	94.00	93.85	0:52:31	87.126	80.69	84.76	0:52:31	175.052	72.60	77.55
0:52:46	43.888	96.74		0:52:46	87.573	93.11		0:52:46	175.944	83.08	
0:53:01	44.084	84.64		0:53:01	87.964	79.56		0:53:01	176.727	72.93	
0:53:16	44.307	94.99		0:53:16	88.41	91.66		0:53:16	177.62	82.91	
0:53:31	44.503	83.49		0:53:31	88.802	81.10		0:53:31	178.403	72.46	
0:53:46	44.726	94.99		0:53:46	89.248	90.75		0:53:46	179.295	82.81	
0:54:01	44.921	81.94		0:54:01	89.639	79.56		0:54:01	180.077	72.83	
0:54:16	45.117	82.36		0:54:16	90.086	91.56		0:54:16	180.969	82.81	
0:54:31	45.34	93.70		0:54:31	90.477	80.09		0:54:31	181.751	72.60	
0:54:46	45.536	83.49		0:54:46	90.924	91.56		0:54:46	182.645	83.00	
0:55:01	45.759	94.99	89.13	0:55:01	91.314	79.35	85.83	0:55:01	183.428	72.69	77.81
0:55:16	45.954	83.06		0:55:16	91.761	91.86		0:55:16	184.32	82.81	
0:55:31	46.178	96.74		0:55:31	92.152	80.90		0:55:31	185.103	73.28	
0:55:46	46.373	84.21		0:55:46	92.543	80.09		0:55:46	185.996	83.58	
0:56:01	46.597	95.41		0:56:01	92.989	90.75		0:56:01	186.779	72.46	
0:56:16	46.792	81.94		0:56:16	93.38	79.56		0:56:16	187.56	71.93	
0:56:31	47.015	94.99		0:56:31	93.827	91.56		0:56:31	188.454	82.34	
0:56:46	47.211	84.64		0:56:46	94.219	80.29		0:56:46	189.237	73.05	
0:57:01	47.434	94.99		0:57:01	94.665	90.75		0:57:01	190.131	83.40	
0:57:16	47.63	83.49		0:57:16	95.056	79.03		0:57:16	190.912	71.93	
0:57:31	47.853	96.30	89.58	0:57:31	95.502	90.15	85.49	0:57:31	191.805	81.85	77.66
0:57:46	48.048	83.06		0:57:46	95.894	79.76		0:57:46	192.586	71.93	
0:58:01	48.244	82.36		0:58:01	96.34	90.75		0:58:01	193.48	82.34	
0:58:16	48.467	94.99		0:58:16	96.731	79.56		0:58:16	194.263	71.77	
0:58:31	48.663	84.64		0:58:31	97.177	90.75		0:58:31	195.156	81.85	
0:58:46	48.886	94.99		0:58:46	97.569	79.23		0:58:46	195.937	71.93	
0:59:01	49.082	82.36		0:59:01	97.96	79.56		0:59:01	196.83	82.64	
0:59:16	49.305	94.99		0:59:16	98.407	90.95		0:59:16	197.613	71.88	
0:59:31	49.5	83.06		0:59:31	98.798	79.03		0:59:31	198.505	82.15	
0:59:46	49.724	94.12		0:59:46	99.244	90.15		0:59:46	199.288	72.11	
1:00:01	49.919	83.06	87.76	1:00:01	99.636	80.56	84.03	1:00:01	200.069	71.13	75.97
1:00:16	50.143	95.41		1:00:16	100.082	93.22		1:00:16	200.962	81.98	
1:00:31	50.338	81.94		1:00:31	100.474	81.10		1:00:31	201.743	71.93	
1:00:46	50.561	93.70		1:00:46	100.919	90.54		1:00:46	202.637	81.94	
1:01:01	50.757	82.36		1:01:01	101.311	79.23		1:01:01	203.42	71.54	
1:01:16	50.98	94.99		1:01:16	101.758	90.35		1:01:16	204.313	81.98	
1:01:31	51.176	83.49		1:01:31	102.148	78.83		1:01:31	205.096	71.88	
1:01:46	51.372	82.36		1:01:46	102.596	89.96		1:01:46	205.99	81.43	
1:02:01	51.595	94.99		1:02:01	102.987	79.03		1:02:01	206.773	71.32	
1:02:16	51.791	84.64		1:02:16	103.434	90.35		1:02:16	207.665	81.24	
1:02:31	52.014	94.99	88.89	1:02:31	103.825	78.52	85.11	1:02:31	208.448	71.54	76.68
1:02:46	52.209	83.06		1:02:46	104.216	79.03		1:02:46	209.34	81.50	
1:03:01	52.433	93.49		1:03:01	104.663	90.35		1:03:01	210.123	71.32	
1:03:16	52.628	80.31		1:03:16	105.055	79.76		1:03:16	210.905	71.45	
1:03:31	52.851	93.70		1:03:31	105.501	90.15		1:03:31	211.799	81.68	
1:03:46	53.047	82.36		1:03:46	105.892	78.01		1:03:46	212.581	71.23	
1:04:01	53.27	93.70		1:04:01	106.338	89.56		1:04:01	213.474	81.08	
1:04:16	53.466	82.36		1:04:16	106.73	79.23		1:04:16	214.257	71.32	
1:04:31	53.689	93.70		1:04:31	107.177	90.95		1:04:31	215.151	81.68	
1:04:46	53.885	82.36		1:04:46	107.568	79.56		1:04:46	215.932	71.13	
1:05:01	54.108	91.84	87.69	1:05:01	108.014	89.56	84.62	1:05:01	216.825	81.59	76.40
1:05:16	54.304	81.80		1:05:16	108.406	78.21		1:05:16	217.608	71.54	
1:05:31	54.499	83.06		1:05:31	108.852	89.56		1:05:31	218.502	81.43	
1:05:46	54.723	94.12		1:05:46	109.243	80.35		1:05:46	219.285	71.09	
1:06:01	54.918	81.94		1:06:01	109.634	80.35		1:06:01	220.177	80.99	
1:06:16	55.141	93.70		1:06:16	110.081	90.35		1:06:16	220.959	71.23	
1:06:32	55.337	77.21		1:06:31	110.473	79.76		1:06:31	221.851	80.99	
1:06:47	55.56	93.70		1:06:46	110.919	90.75		1:06:46	222.634	71.09	
1:07:02	55.756	82.36		1:07:01	111.311	78.72		1:07:01	223.417	71.32	
1:07:17	55.979	93.70		1:07:16	111.757	88.98		1:07:16	224.309	80.99	
1:07:32	56.174	80.31	86.19	1:07:31	112.148	78.01	83.50	1:07:31	225.092	70.54	75.12
1:07:47	56.397	90.05		1:07:46	112.595	89.76		1:07:46	225.985	80.07	
1:08:02	56.593	80.72		1:08:01	112.986	79.03		1:08:01	226.766	70.36	
1:08:17	56.816	94.99		1:08:16	113.433	89.76		1:08:17	227.66	75.50	
1:08:32	57.012	81.80		1:08:31	113.824	77.25		1:08:32	228.442	70.45	
1:08:47	57.235	90.05		1:08:47	114.271	83.33		1:08:47	229.336	81.17	
1:09:02	57.43	78.74		1:09:02	114.662	79.03		1:09:02	230.119	71.09	
1:09:17	57.626	81.80		1:09:17	115.053	77.75		1:09:17	231.013	80.92	
1:09:32	57.849	94.99		1:09:32	115.5	88.89		1:09:32	231.794	70.69	
1:09:47	58.045	80.72		1:09:47	115.891	78.52		1:09:47	232.687	80.45	
1:10:02	58.268	91.84	86.57	1:10:02	116.337	88.98	83.23	1:10:02	233.469	70.45	75.11
1:10:17	58.463	80.31		1:10:17	116.728	78.01		1:10:17	234.251	70.78	
1:10:32	58.686	91.84		1:10:32	117.175	90.35		1:10:32	235.145	80.54	
1:10:47	58.882	82.36		1:10:47	117.566	79.56		1:10:47	235.926	70.03	
1:11:02	59.105	93.70		1:11:02	118.013	89.76		1:11:02	236.82	80.79	
1:11:17	59.301	82.36		1:11:17	118.404	78.01		1:11:17	237.602	70.45	
1:11:32	59.524	93.70		1:11:32	118.85	89.56		1:11:32	238.496	79.91	
1:11:47	59.719	81.94		1:11:47	119.242	79.23		1:11:47	239.277	70.03	
1:12:02	59.942	91.84		1:12:02	119.688	88.69		1:12:02	240.17	80.45	

1:12:17	60.138	79.15		1:12:17	120.079	76.52		1:12:17	240.953	70.32	
1:12:32	60.361	91.84	86.90	1:12:32	120.526	88.32	83.80	1:12:32	241.845	79.74	75.30
1:12:47	60.557	80.72		1:12:47	120.917	78.01		1:12:47	242.628	70.21	
1:13:02	60.753	79.15		1:13:02	121.308	78.01		1:13:02	243.521	79.83	
1:13:17	60.976	90.05		1:13:17	121.755	89.18		1:13:17	244.305	69.87	
1:13:32	61.171	78.74		1:13:32	122.146	78.01		1:13:32	245.199	79.67	
1:13:47	61.394	90.05		1:13:47	122.592	88.98		1:13:47	245.98	69.81	
1:14:02	61.59	79.15		1:14:02	122.983	79.03		1:14:02	246.763	69.99	
1:14:17	61.814	90.46		1:14:17	123.43	90.95		1:14:17	247.656	79.58	
1:14:32	62.009	80.31		1:14:32	123.821	78.52		1:14:32	248.438	69.47	
1:14:47	62.233	92.25		1:14:47	124.268	89.76		1:14:47	249.331	79.33	
1:15:02	62.428	80.31	84.12	1:15:02	124.658	78.32	82.88	1:15:02	250.114	69.56	73.73
1:15:17	62.652	92.25		1:15:17	125.105	89.18		1:15:17	251.007	79.33	
1:15:32	62.847	77.73		1:15:32	125.496	77.25		1:15:32	251.79	69.99	
1:15:47	63.071	89.30		1:15:47	125.942	88.69		1:15:47	252.682	79.74	
1:16:02	63.266	78.74		1:16:02	126.334	78.72		1:16:02	253.465	69.99	
1:16:17	63.462	79.15		1:16:17	126.781	88.32		1:16:17	254.358	79.83	
1:16:32	63.685	88.90		1:16:32	127.173	76.71		1:16:32	255.14	69.90	
1:16:47	63.881	78.13		1:16:47	127.564	77.75		1:16:47	256.033	79.58	
1:17:02	64.104	91.84		1:17:02	128.01	89.56		1:17:02	256.816	69.56	
1:17:17	64.299	80.31		1:17:17	128.401	77.25		1:17:17	257.597	69.60	
1:17:32	64.523	89.30	84.56	1:17:32	128.847	88.12	83.16	1:17:32	258.491	79.91	74.74
1:17:47	64.718	77.73		1:17:47	129.238	78.01		1:17:47	259.273	69.69	
1:18:02	64.942	90.46		1:18:02	129.685	89.18		1:18:02	260.165	79.00	
1:18:17	65.137	78.74		1:18:17	130.077	78.21		1:18:17	260.948	69.56	
1:18:32	65.36	91.84		1:18:32	130.523	88.98		1:18:32	261.841	79.33	
1:18:47	65.556	80.72		1:18:47	130.914	78.01		1:18:47	262.622	69.17	
1:19:02	65.779	88.90		1:19:02	131.361	89.18		1:19:02	263.515	79.09	
1:19:17	65.975	78.13		1:19:17	131.752	78.01		1:19:17	264.186	70.07	
1:19:32	66.198	90.05		1:19:32	132.198	90.15		1:19:32	264.812	67.95	
1:19:47	66.393	80.31		1:19:47	132.588	78.83		1:19:47	265.595	71.66	
1:20:02	66.589	80.72	83.76	1:20:02	132.98	77.45	82.60	1:20:02	266.565	73.88	72.94
1:20:17	66.812	90.05		1:20:17	133.427	89.47		1:20:17	267.458	77.72	
1:20:32	67.007	78.74		1:20:32	133.818	79.03		1:20:32	268.29	78.12	
1:20:47	67.231	90.46		1:20:47	134.265	88.32		1:20:47	269.073	72.69	
1:21:02	67.426	80.31		1:21:02	134.656	77.25		1:21:02	269.965	82.81	
1:21:17	67.649	91.84		1:21:17	135.102	88.98		1:21:17	270.747	72.02	
1:21:32	67.845	79.15		1:21:32	135.494	77.45		1:21:32	271.64	81.85	
1:21:47	68.068	88.90		1:21:47	135.94	88.12		1:21:47	272.421	72.51	
1:22:02	68.264	78.13		1:22:02	136.331	76.76		1:22:02	273.316	83.76	
1:22:17	68.487	90.05		1:22:17	136.778	85.83		1:22:17	274.098	72.25	
1:22:32	68.683	79.15	84.68	1:22:32	137.168	75.36	82.66	1:22:32	274.992	81.68	77.54
1:22:47	68.906	90.05		1:22:47	137.615	87.47		1:22:47	275.773	71.13	
1:23:02	69.102	79.15		1:23:02	138.006	76.03		1:23:02	276.558	71.50	
1:23:17	69.325	90.05		1:23:17	138.453	86.37		1:23:17	277.451	81.08	
1:23:32	69.521	78.13		1:23:32	138.845	77.45		1:23:32	278.233	71.23	
1:23:47	69.716	79.26		1:23:47	139.235	77.56		1:23:47	279.128	81.13	
1:24:02	69.94	92.25		1:24:02	139.682	87.47		1:24:02	279.909	69.81	
1:24:17	70.135	80.31		1:24:17	140.073	76.52		1:24:17	280.803	79.91	
1:24:32	70.358	91.84		1:24:32	140.52	88.32		1:24:32	281.586	69.99	
1:24:47	70.554	78.13		1:24:47	140.91	77.06		1:24:47	282.479	79.58	
1:25:02	70.777	88.90	84.81	1:25:02	141.357	87.47	82.17	1:25:02	283.262	69.99	74.54
1:25:17	70.973	81.80		1:25:17	141.747	75.84		1:25:17	284.154	80.36	
1:25:32	71.196	94.99		1:25:32	142.194	88.32		1:25:32	284.937	70.87	
1:25:47	71.391	80.31		1:25:47	142.585	77.25		1:25:47	285.829	80.36	
1:26:02	71.615	90.46		1:26:02	143.031	86.73		1:26:02	286.612	69.99	
1:26:17	71.81	78.74		1:26:17	143.422	76.52		1:26:17	287.394	69.47	
1:26:32	72.033	90.05		1:26:32	143.869	86.92		1:26:32	288.287	79.33	
1:26:47	72.229	79.15		1:26:47	144.26	76.03		1:26:47	289.069	69.69	
1:27:02	72.452	90.05		1:27:02	144.706	87.28		1:27:02	289.963	79.91	
1:27:17	72.647	77.73		1:27:17	145.097	76.03		1:27:17	290.746	70.21	
1:27:32	72.843	78.13	84.14	1:27:32	145.488	76.76	80.77	1:27:32	291.64	79.67	74.99
1:27:47	73.066	90.05		1:27:47	145.934	88.12		1:27:47	292.421	69.38	
1:28:02	73.261	78.74		1:28:02	146.326	76.23		1:28:02	293.316	79.51	
1:28:17	73.485	92.25		1:28:17	146.772	86.73		1:28:17	294.097	69.17	
1:28:32	73.68	80.31		1:28:32	147.164	76.71		1:28:32	294.991	78.82	
1:28:47	73.904	90.46		1:28:47	147.61	86.73		1:28:47	295.772	68.54	
1:29:02	74.099	78.74		1:29:02	148.001	75.55		1:29:02	296.664	78.64	
1:29:17	74.323	90.46		1:29:17	148.448	86.37		1:29:17	297.447	69.35	
1:29:32	74.518	78.74		1:29:32	148.839	75.55		1:29:32	298.23	69.35	
1:29:47	74.741	90.05		1:29:47	149.285	86.18		1:29:47	299.123	78.73	
1:30:02	74.937	79.15	84.90	1:30:02	149.677	75.75	81.39	1:30:02	299.906	69.45	73.09
1:30:17	75.16	90.05		1:30:17	150.123	86.73		1:30:17	300.798	79.49	
1:30:32	75.355	78.74		1:30:32	150.515	76.23		1:30:32	301.581	69.35	
1:30:47	75.579	89.30		1:30:47	150.962	85.83		1:30:47	302.473	78.64	
1:31:02	75.774	77.73		1:31:02	151.353	75.55		1:31:02	303.255	68.94	
1:31:17	75.97	78.13		1:31:17	151.745	76.23		1:31:17	304.148	78.73	
1:31:32	76.193	87.77		1:31:32	152.191	86.18		1:31:32	304.93	68.63	
1:31:47	76.389	78.13		1:31:47	152.582	75.08		1:31:47	305.823	77.90	
1:32:02	76.612	90.05		1:32:02	153.029	85.83		1:32:02	306.606	68.09	
1:32:17	76.808	79.15		1:32:17	153.419	75.36		1:32:17	307.5	77.75	
1:32:32	77.031	90.05	83.91	1:32:32	153.866	85.83	80.89	1:32:32	308.281	68.13	73.56
1:32:47	77.227	79.15		1:32:47	154.258	75.75		1:32:47	309.174	78.37	
1:33:02	77.45	88.90		1:33:02	154.705	87.47		1:33:02	309.957	68.72	
1:33:17	77.645	76.75		1:33:17	155.095	75.36		1:33:17	310.738	68.33	
1:33:32	77.869	88.17		1:33:32	155.542	85.83		1:33:32	311.631	78.13	
1:33:47	78.064	77.73		1:33:47	155.932	74.89		1:33:47	312.412	68.33	
1:34:02	78.204	73.39		1:34:02	156.379	85.30		1:34:02	313.306	77.98	
1:34:17	78.34	72.91		1:34:17	156.77	75.08		1:34:17	314.089	68.30	
1:34:32	78.536	97.51		1:34:32	157.162	75.75		1:34:32	314.981	78.04	
1:34:47	78.759	93.07		1:34:47	157.608	85.64		1:34:47	315.764	68.30	
1:35:02	78.954	77.73	82.53	1:35:02	157.999	74.61	79.57	1:35:02	316.658	77.75	73.23
1:35:17	79.178	89.30		1:35:17	158.445	85.11		1:35:17	317.44	68.01	
1:35:32	79.374	79.15		1:35:32	158.836	75.08		1:35:32	318.334	77.51	
1:35:47	79.597	90.05		1:35:47	159.283	85.04		1:35:47	319.115	67.41	
1:36:02	79.792	77.73		1:36:02	159.674	74.38		1:36:02	320.009	77.63	
1:36:17	79.987	77.73		1:36:17	160.12	85.64		1:36:17	320.79	67.82	
1:36:32	80.211	89.30		1:36:32	160.512	75.27		1:36:32	321.683	77.31	
1:36:47	80.406	76.75		1:36:47	160.958	85.64		1:36:47	322.464	68.33	
1:37:02	80.63	88.17		1:37:02	161.349	75.08		1:37:02	323.247	68.30	
1:37:17	80.825	76.75		1:37:17	161.797	86.57		1:37:17	324.14	77.43	
1:37:32	81.048	88.90	83.38	1:37:32	162.188	76.03	80.39	1:37:32	324.923	68.09	71.79
1:37:47	81.244	78.13		1:37:47	162.634	87.28		1:37:47	325.815	77.81	
1:38:02	81.467	87.77		1:38:02	163.026	76.23		1:38:02	326.596	68.13	
1:38:17	81.663	78.13		1:38:17	163.418	75.27		1:38:17	327.489	77.66	
1:38:32	81.886	88.90		1:38:32	163.864	85.11		1:38:32	328.272	67.89	
1:38:47	82.082	78.13		1:38:47	164.255	74.61		1:38:47	329.165	77.66	
1:39:02	82.305	87.77		1:39:02	164.702	84.51		1:39:02	329.947	68.73	
1:39:17	82.5	76.75		1:39:17	165.094	74.12		1:39:17	330.84	78.49	
1:39:32	82.724	90.46		1:39:32	165.541	85.30		1:39:32	331.623	68.30	
1:39:47	82.919	77.73		1:39:47	165.933	74.81		1:39:47	332.517	77.98	
1:40:02	83.115	76.18	82.00	1:40:02	166.38	85.83	80.31	1:40:02	333.298	68.13	73.08
1:40:17	83.338	86.67		1:40:17	166.771	75.55		1:40:17	334.191	77.90	
1:40:32	83.534	78.13		1:40:32	167.217	85.64		1:40:32	334.972	67.92	
1:40:47	83.757	88.90		1:40:47	167.608	73.93		1:40:47	335.754	68.01	
1:41:02	83.952	76.75		1:41:02	167.999	73.25		1:41:02	336.646	77.81	
1:41:18	84.176	82.65		1:41:17	168.446	85.04		1:41:17	337.429	68.30	
1:41:33	84.372	77.14		1:41:32	168.837	75.08		1:41:32	338.322	77.66	
1:41:48	84.595	87.77		1:41:47	169.284	85.30		1:41:47	339.103	68.13	
1:42:03	84.79	76.75		1:42:02	169.674	74.89		1:42:02	339.996	77.90	
1:42:18	85.013	87.77		1:42:17	170.121	85.83		1:42:17	340.779	67.89	
1:42:33	85.209	77.14	81.97	1:42:32	170.511	74.42	78.89	1:42:32	341.672	76.85	72.84
1:42:48	85.432	86.67		1:42:48	170.958	79.97		1:42:47	342.454	67.30	
1:43:03	85.628	76.18		1:43:03	171.35	75.27		1:43:02	343.347	77.43	
1:43:18	85.851	86.67		1:43:18	171.796	85.64		1:43:17	344.128	67.92	
1:43:33	86.047	76.18		1:43:33	172.188	74.81		1:43:32	345.022	77.40	
1:43:48	86.242	77.73		1:43:48	172.634	85.11		1:43:47	345.804	67.20	
1:44:03	86.465	88.90		1:44:03	173.024	74.42		1:44:02	346.697	76.74	
1:44:18	86.661	77.14		1:44:18	173.471	85.30		1:44:17	347.48	67.28	
1:44:33	86.884	87.77		1:44:33	173.862	75.55		1:44:32	348.261	67.11	
1:44:48	87.08	77.14		1:44:48	174.253	74.85		1:44:47	349.154	77.31	
1:45:03	87.303	87.77	82.22	1:45:03	174.7	83.74	79.47	1:45:02	349.937	67.38	71.31
1:45:18	87.499	77.14		1:45:18	175.091	73.25		1:45:17	350.83	75.83	
1:45:33	87.722	87.77		1:45:33	175.537	83.55		1:45:32	351.612	66.41	
1:45:48	87.917	75.79		1:45:48	175.928	73.25		1:45:47	352.505	76.28	
1:46:03	88.141	87.06		1:46:03	176.375	83.74		1:46:02	353.286	67.11	
1:46:18	88.336	75.79		1:46:18	176.765	73.74		1:46:17	354.18	76.59	
1:46:33	88.559	85.60		1:46:33	177.212	84.51		1:46:32	354.961	66.91	
1:46:48	88.755	75.24		1:46:48	177.603	72.81		1:46:47	355.855	76.82	
1:47:03	88.978	85.60		1:47:03	178.049	83.81		1:47:02	356.638	66.89	
1:47:18	89.174	75.24		1:47:18	178.441	74.81		1:47:17	357.531	75.83	
1:47:33	89.37	75.24	80.05	1:47:33	178.887	84.32	78.78	1:47:32	358.314	66.49	71.52
1:47:48	89.593	85.60		1:47:48	179.279	73.44		1:47:47	359.095	66.72	
1:48:03	89.788	74.86		1:48:03	179.725	83.05		1:48:02	359.989	76.37	
1:48:18	90.011	85.60		1:48:18	180.116	72.37		1:48:17	360.77	66.72	
1:48:33	90.207	75.24		1:48:33	180.507	72.37		1:48:32	361.664	76.82	
1:48:48	90.43	85.60		1:48:48	180.953	81.81		1:48:47	362.446	66.80	
1:49:03	90.626	75.24		1:49:03	181.345	71.90		1:49:02	363.338	75.75	
1:49:18	90.849	85.60		1:49:18	181.791	82.55		1:49:17	364.121	66.01	

1:49:33	91.045	75.24		1:49:33	182.182	73.47		1:49:32	365.014	75.50	
1:49:48	91.268	85.60		1:49:48	182.629	85.30		1:49:47	365.797	66.69	
1:50:03	91.463	75.79	80.44	1:50:03	183.019	73.74	77.00	1:50:02	366.689	75.42	71.28
1:50:18	91.687	87.06		1:50:18	183.466	83.23		1:50:17	367.472	66.59	
1:50:33	91.882	75.79		1:50:33	183.857	72.37		1:50:32	368.364	76.20	
1:50:48	92.077	75.79		1:50:48	184.303	81.81		1:50:47	369.147	66.49	
1:51:03	92.301	85.99		1:51:03	184.694	72.15		1:51:02	370.04	75.83	
1:51:18	92.497	75.24		1:51:18	185.141	83.23		1:51:17	370.823	66.49	
1:51:33	92.72	85.60		1:51:33	185.532	72.37		1:51:32	371.604	66.32	
1:51:48	92.916	73.87		1:51:48	185.978	83.05		1:51:47	372.498	75.92	
1:52:03	93.139	84.05		1:52:03	186.37	72.99		1:52:02	373.28	66.12	
1:52:18	93.335	75.24		1:52:18	186.761	72.37		1:52:17	374.173	75.17	
1:52:33	93.558	86.67	80.53	1:52:33	187.207	83.05	77.66	1:52:32	374.955	66.12	70.13
1:52:48	93.753	74.40		1:52:48	187.598	72.81		1:52:47	375.847	75.42	
1:53:03	93.976	85.08		1:53:03	188.045	82.73		1:53:02	376.632	66.08	
1:53:18	94.172	74.78		1:53:18	188.436	72.81		1:53:17	377.524	74.87	
1:53:33	94.396	82.92		1:53:33	188.882	83.55		1:53:32	378.307	65.53	
1:53:48	94.591	73.49		1:53:48	189.274	72.99		1:53:47	379.201	74.49	
1:54:03	94.814	85.60		1:54:03	189.721	82.73		1:54:02	379.983	65.16	
1:54:18	95.01	75.24		1:54:18	190.112	72.37		1:54:17	380.875	74.87	
1:54:33	95.205	73.49		1:54:33	190.558	82.55		1:54:32	381.656	65.55	
1:54:48	95.428	82.55		1:54:48	190.95	71.90		1:54:47	382.551	74.90	
1:55:03	95.624	73.87	78.14	1:55:03	191.396	81.81	77.62	1:55:02	383.332	65.36	70.22
1:55:18	95.848	83.41		1:55:18	191.787	72.37		1:55:17	384.224	74.33	
1:55:33	96.043	73.49		1:55:33	192.233	82.55		1:55:32	385.007	65.25	
1:55:48	96.267	88.17		1:55:48	192.624	71.72		1:55:47	385.79	66.01	
1:56:03	96.462	75.79		1:56:03	193.015	71.72		1:56:02	386.683	75.50	
1:56:18	96.685	85.60		1:56:18	193.462	81.99		1:56:17	387.465	65.83	
1:56:33	96.881	75.24		1:56:33	193.853	71.72		1:56:32	388.358	75.50	
1:56:48	97.104	85.60		1:56:48	194.3	81.99		1:56:47	389.139	65.84	
1:57:03	97.299	74.86		1:57:03	194.692	71.26		1:57:02	390.032	74.41	
1:57:18	97.523	84.42		1:57:18	195.138	81.81		1:57:17	390.814	65.16	
1:57:33	97.718	73.49	80.01	1:57:33	195.529	71.72	75.88	1:57:32	391.707	74.41	70.22
1:57:48	97.942	85.99		1:57:48	195.976	81.99		1:57:47	392.49	65.25	
1:58:03	98.137	75.79		1:58:03	196.367	71.72		1:58:02	393.383	74.41	
1:58:18	98.333	74.78		1:58:18	196.813	81.08		1:58:17	394.164	64.80	
1:58:33	98.556	84.05		1:58:33	197.205	71.26		1:58:32	395.057	74.09	
1:58:48	98.751	75.79		1:58:48	197.652	81.26		1:58:47	395.84	64.96	
1:59:03	98.975	87.06		1:59:03	198.043	71.72		1:59:02	396.623	65.43	
1:59:18	99.17	74.86		1:59:18	198.433	71.54		1:59:17	397.515	74.87	
		92.92		1:59:33	198.879	80.60		1:59:32	398.296	65.08	
				1:59:48	199.271	71.48		1:59:47	399.189	74.41	
			81.40	2:00:03	199.717	81.32	76.40			**77.51**	70.08
				2:00:18	200.109	70.85					
				2:00:33	200.422	74.62					
						85.48					

50 ml/ h				100 ml/ h				200 ml/ h			
time, [hh:mm:ss]	V, [cm^3]	k, [mD]	k, [mD]	time, [hh:mm:ss]	V, [cm^3]	k, [mD]	k, [mD]	time, [hh:mm:ss]	V, [cm^3]	k, [mD]	k, [mD]
0:00:15	0.11	497.00		0:00:45	0.83	325.6337411		0:00:15	0.41	320.54847	
0:00:30	0.33	493.81		0:01:00	1.22	323.8286331		0:00:30	1.19	317.60988	
0:00:45	0.53	481.71		0:01:15	1.67	328.5873557		0:00:45	2.07	316.76842	
0:01:00	0.75	497.79		0:01:30	2.06	292.4935764		0:01:00	2.85	312.69087	
0:01:15	0.94	486.70		0:01:45	2.50	319.141277		0:01:15	3.74	356.4435	
0:01:30	1.16	510.53		0:02:00	2.89	323.4014939		0:01:30	4.52	322.46246	
0:01:45	1.36	448.44		0:02:15	3.33	331.8507549		0:01:45	5.41	356.4435	
0:02:00	1.58	494.88		0:02:30	3.72	364.3377109		0:02:00	6.19	313.09227	
0:02:15	1.78	465.54		0:02:45	4.17	332.7873557		0:02:15	7.08	317.59631	
0:02:30	2.00	460.13	483.65	0:03:00	4.56	334.8347857	327.69	0:02:30	7.86	313.09227	324.6748
0:02:45	2.19	512.50		0:03:15	5.00	362.760278		0:02:45	8.74	345.95987	
0:03:00	2.42	510.53		0:03:30	5.39	301.3513072		0:03:00	9.52	303.88367	
0:03:15	2.61	450.74		0:03:45	5.78	317.2119023		0:03:15	10.41	332.08811	
0:03:30	2.83	471.26		0:04:00	6.23	340.055076		0:03:30	11.19	299.47956	
0:03:45	3.03	413.94		0:04:15	6.62	294.0012753		0:03:45	12.08	332.41025	
0:04:00	3.25	511.09		0:04:30	7.06	319.8600637		0:04:00	12.86	323.29034	
0:04:15	3.45	512.50		0:04:45	7.45	302.1240028		0:04:15	13.76	322.04911	
0:04:30	3.67	473.38		0:05:00	7.90	344.6222641		0:04:30	14.54	313.49367	
0:04:45	3.87	450.74		0:05:15	8.29	302.1240028		0:04:45	15.43	358.04911	
0:05:00	4.09	510.53	481.72	0:05:30	8.74	344.6222641	322.873	0:05:00	16.21	291.41665	322.212
0:05:15	4.28	416.07		0:05:45	9.13	318.0252661		0:05:15	17.10	332.46125	
0:05:30	4.51	473.38		0:06:00	9.57	382.9136268		0:05:30	17.88	291.41665	
0:05:45	4.70	413.94		0:06:15	9.97	335.6933365		0:05:45	18.78	342.8657	
0:06:00	4.92	512.83		0:06:30	10.41	318.6738892		0:06:00	19.56	313.49367	
0:06:15	5.12	450.74		0:06:45	10.80	366.2109125		0:06:15	20.45	347.90784	
0:06:30	5.32	416.07		0:07:00	11.25	363.5736419		0:06:30	21.23	292.16291	
0:06:45	5.54	473.38		0:07:15	11.64	294.7551247		0:06:45	22.13	343.24965	
0:07:00	5.73	413.94		0:07:30	12.09	362.760278		0:07:00	22.91	334.14636	
0:07:15	5.96	473.38		0:07:45	12.48	366.2109125		0:07:15	23.80	297.65208	
0:07:30	6.15	416.07	445.98	0:08:00	12.92	363.5736419	347.239	0:07:30	24.58	313.89507	320.9251
0:07:45	6.38	473.38		0:08:15	13.32	345.2845747		0:07:45	25.37	313.89507	
0:08:00	6.57	448.44		0:08:30	13.71	360.8320038		0:08:00	26.26	324.07854	
0:08:15	6.80	515.13		0:08:45	14.15	376.6605573		0:08:15	27.04	300.24746	
0:08:30	6.99	416.07		0:09:00	14.54	318.0252661		0:08:30	27.93	333.65208	
0:08:45	7.21	512.83		0:09:15	14.99	344.6222641		0:08:45	28.72	305.05245	
0:09:00	7.41	448.44		0:09:30	15.38	302.8966985		0:09:00	29.61	347.90784	
0:09:15	7.63	475.51		0:09:45	15.83	393.8540161		0:09:15	30.39	314.29647	
0:09:30	7.83	413.94		0:10:00	16.22	345.2845747		0:09:30	31.28	333.23814	
0:09:45	8.05	473.38		0:10:15	16.67	394.7370969		0:09:45	32.07	313.89507	
0:10:00	8.25	416.07	459.32	0:10:30	17.06	365.2743117	354.747	0:10:00	32.96	358.85191	324.5115
0:10:15	8.44	450.74		0:10:45	17.50	363.5736419		0:10:15	33.74	324.11823	
0:10:30	8.67	559.45		0:11:00	17.89	302.1240028		0:10:30	34.64	333.23814	
0:10:45	8.86	448.44		0:11:15	18.34	345.3949598		0:10:45	35.42	324.11823	
0:11:00	9.08	473.38		0:11:30	18.73	318.0252661		0:11:00	36.20	334.57366	
0:11:15	9.28	386.35		0:11:45	19.12	335.6933365		0:11:15	37.09	308.45208	
0:11:30	9.50	439.57		0:12:00	19.57	383.7721775		0:11:30	37.88	304.66286	
0:11:45	9.70	386.35		0:12:15	19.96	366.2109125		0:11:45	38.77	358.45051	
0:12:00	9.92	439.57		0:12:30	20.41	375.7239565		0:12:00	39.55	324.11823	
0:12:15	10.12	416.07		0:12:45	20.80	318.0252661		0:12:15	40.45	312.05208	
0:12:30	10.34	473.38	447.33	0:13:00	21.24	309.8540161	341.84	0:12:30	41.23	313.49367	323.7278
0:12:45	10.54	416.07		0:13:15	21.64	318.8320038		0:12:45	42.12	348.29744	
0:13:00	10.76	473.38		0:13:30	22.08	352.7370969		0:13:00	42.90	323.29034	
0:13:15	10.96	384.38		0:13:45	22.47	318.0252661		0:13:15	43.80	316.06603	
0:13:30	11.18	439.57		0:14:00	22.92	328.3136268		0:13:30	44.58	305.05245	
0:13:45	11.37	416.07		0:14:15	23.31	318.83863		0:13:45	45.47	358.85191	
0:14:00	11.57	384.38		0:14:30	23.76	362.760278		0:14:00	46.26	351.58588	
0:14:15	11.79	441.54		0:14:45	24.15	335.6933365		0:14:15	47.15	315.83169	
0:14:30	11.99	448.44		0:15:00	24.59	322.8738892		0:14:30	47.93	304.27327	
0:14:45	12.21	515.13		0:15:15	24.99	348.8344497		0:14:45	48.71	304.27327	
0:15:00	12.41	413.94	433.29	0:15:30	25.38	365.2743117	337.218	0:15:00	49.60	348.29744	327.582
0:15:15	12.63	515.13		0:15:45	25.82	352.7370969		0:15:15	50.39	313.89507	
0:15:30	12.83	413.94		0:16:00	26.21	317.2119023		0:15:30	51.28	343.24965	
0:15:45	13.05	410.26		0:16:15	26.66	383.7721775		0:15:45	52.06	291.41665	
0:16:00	13.25	386.35		0:16:30	27.05	335.6933365		0:16:00	52.95	347.90784	
0:16:15	13.47	512.83		0:16:45	27.50	383.7721775		0:16:15	53.74	304.27327	
0:16:30	13.66	448.44		0:17:00	27.89	334.8347857		0:16:30	54.63	333.20751	
0:16:45	13.89	475.51		0:17:15	28.34	363.5736419		0:16:45	55.41	292.16291	
0:17:00	14.08	416.07		0:17:30	28.73	318.83863		0:17:00	56.30	347.51825	
0:17:15	14.31	473.38		0:17:45	29.17	376.6605573		0:17:15	57.09	304.66286	
0:17:30	14.50	384.38	443.63	0:18:00	29.56	359.8017429	352.69	0:17:30	57.98	334.06603	321.236
0:17:45	14.70	386.35		0:18:15	30.01	334.6605573		0:17:45	58.76	333.71907	
0:18:00	14.92	439.57		0:18:30	30.40	334.8347857		0:18:00	59.65	322.45051	
0:18:15	15.12	386.35		0:18:45	30.85	329.1721775		0:18:15	60.44	313.89507	
0:18:30	15.34	439.57		0:19:00	31.24	365.2743117		0:18:30	61.22	313.89507	
0:18:45	15.53	358.75		0:19:15	31.63	319.8622647		0:18:45	62.11	347.90784	
0:19:00	15.76	412.10		0:19:30	32.09	320.4509852		0:19:00	62.89	291.41665	
0:19:15	15.95	360.59		0:19:45	32.48	323.1240028		0:19:15	63.78	342.8657	
0:19:30	16.18	410.26		0:20:00	32.93	331.7370969		0:19:30	64.57	333.71907	
0:19:45	16.37	386.35		0:20:15	33.32	344.4014939		0:19:45	65.46	310.00364	
0:20:00	16.60	473.38	405.33	0:20:30	33.72	354.998463	335.852	0:20:00	66.24	313.49367	322.3366
0:20:15	16.79	384.38		0:20:45	34.17	376.6605573		0:20:15	67.13	347.90784	
0:20:30	17.01	410.26		0:21:00	34.56	366.2109125		0:20:30	67.92	305.05245	
0:20:45	17.21	386.35		0:21:15	35.00	393.8540161		0:20:45	68.81	358.45051	
0:21:00	17.43	439.57		0:21:30	35.39	345.2845747		0:21:00	69.59	313.49367	
0:21:15	17.63	360.59		0:21:45	35.84	394.7370969		0:21:15	70.48	348.29744	
0:21:30	17.82	358.75		0:22:00	36.23	302.1240028		0:21:30	71.27	313.49367	
0:21:45	18.05	410.26		0:22:15	36.68	394.7370969		0:21:45	72.16	343.24965	
0:22:00	18.24	386.35		0:22:30	37.07	365.2743117		0:22:00	72.94	291.78978	
0:22:15	18.47	473.38		0:22:45	37.52	383.7721775		0:22:15	73.72	314.29647	
0:22:30	18.66	413.94	402.38	0:23:00	37.91	317.2119023	363.987	0:22:30	74.62	342.48175	327.8513
0:22:45	18.89	441.54		0:23:15	38.35	394.7370969		0:22:45	75.40	292.16291	
0:23:00	19.08	384.38		0:23:30	38.74	344.4014939		0:23:00	76.29	347.90784	
0:23:15	19.30	475.51		0:23:45	39.13	318.83863		0:23:15	77.07	291.78978	
0:23:30	19.50	413.94		0:24:00	39.58	362.760278		0:23:30	77.97	328.57963	
0:23:45	19.72	473.38		0:24:15	39.97	318.0252661		0:23:45	78.75	300.6314	
0:24:00	19.92	416.07		0:24:30	40.42	383.7721775		0:24:00	79.64	333.20751	
0:24:15	20.14	473.38		0:24:45	40.81	335.6933365		0:24:15	80.42	299.86351	
0:24:30	20.34	384.38		0:25:00	41.26	336.216843		0:24:30	81.32	358.45051	
0:24:45	20.56	412.10		0:25:15	41.65	281.7643707		0:24:45	82.10	313.49367	
0:25:00	20.76	413.95	428.86	0:25:30	42.09	417.7239565	349.393	0:25:00	82.99	315.65208	318.1739
0:25:15	20.95	488.11		0:25:45	42.48	366.2109125		0:25:15	83.77	313.49367	
0:25:30	21.17	512.83		0:26:00	42.89	331.8524516		0:25:30	84.67	333.20751	
0:25:45	21.37	413.94		0:26:15	43.36	397.5089892		0:25:45	85.45	292.16291	
0:26:00	21.59	475.51		0:26:30	43.75	334.8347857		0:26:00	86.23	291.41665	
0:26:15	21.79	413.94		0:26:45	44.14	336.5518872		0:26:15	87.12	342.48175	
0:26:30	22.01	473.38		0:27:00	44.58	382.9136268		0:26:30	87.90	313.89507	
0:26:45	22.21	386.35		0:27:15	44.97	366.2109125		0:26:45	88.80	348.29744	
0:27:00	22.43	410.26		0:27:30	45.42	393.8540161		0:27:00	89.58	291.41665	
0:27:15	22.63	384.38		0:27:45	45.81	318.83863		0:27:15	90.47	333.20751	
0:27:30	22.85	441.54	440.03	0:28:00	46.26	383.7721775	361.255	0:27:30	91.25	292.16291	315.1742
0:27:45	23.04	358.75		0:28:15	46.65	335.6933365		0:27:45	92.15	342.8657	
0:28:00	23.27	441.54		0:28:30	47.10	382.9136268		0:28:00	92.93	333.71907	
0:28:15	23.46	384.38		0:28:45	47.49	336.5518872		0:28:15	93.82	333.23814	
0:28:30	23.69	475.51		0:29:00	47.93	382.9136268		0:28:30	94.60	305.05245	
0:28:45	23.88	448.44		0:29:15	48.33	335.6933365		0:28:45	95.50	348.29744	
0:29:00	24.08	386.35		0:29:30	48.77	417.7239565		0:29:00	96.28	305.05245	
0:29:15	24.30	410.26		0:29:45	49.16	366.2109125		0:29:15	97.17	347.90784	
0:29:30	24.50	413.94		0:30:00	49.61	382.9136268		0:29:30	97.95	304.27327	
0:29:45	24.72	475.51		0:30:15	50.00	336.5518872		0:29:45	98.74	324.11823	
0:30:00	24.92	358.75	415.34	0:30:30	50.39	366.2109125	364.338	0:30:00	99.63	309.57634	325.4101
0:30:15	25.14	410.26		0:30:45	50.84	393.8540161		0:30:15	100.41	313.49367	
0:30:30	25.33	358.75		0:31:00	51.23	302.8966985		0:30:30	101.30	347.90784	
0:30:45	25.56	412.10		0:31:15	51.68	362.760278		0:30:45	102.09	304.27327	
0:31:00	25.75	384.38		0:31:30	52.07	367.1475133		0:31:00	102.98	358.85191	
0:31:15	25.98	441.54		0:31:45	52.51	393.8540161		0:31:15	103.76	314.29647	
0:31:30	26.17	384.38		0:32:00	52.90	318.0252661		0:31:30	104.65	332.83438	
0:31:45	26.39	473.38		0:32:15	53.35	382.9136268		0:31:45	105.44	300.24746	
0:32:00	26.59	386.35		0:32:30	53.74	335.6933365		0:32:00	106.33	358.45051	
0:32:15	26.81	410.26		0:32:45	54.19	363.5736419		0:32:15	107.11	304.66286	
0:32:30	27.01	360.59	402.20	0:33:00	54.58	318.0252661	353.874	0:32:30	108.00	358.45051	329.3469
0:32:45	27.20	384.38		0:33:15	55.03	417.7239565		0:32:45	108.79	313.49367	
0:33:00	27.43	441.54		0:33:30	55.42	346.1676554		0:33:00	109.68	333.20751	

D- 4- 1

731.97 ml **419.04** k @ 100 n **354.64** k @ 200ml **317.37**

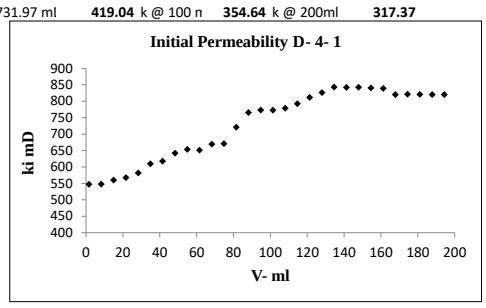

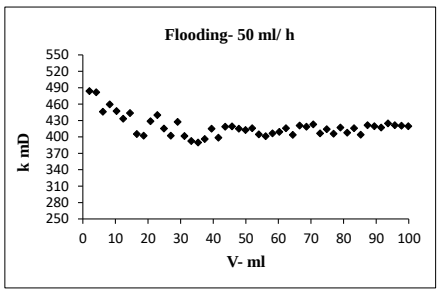

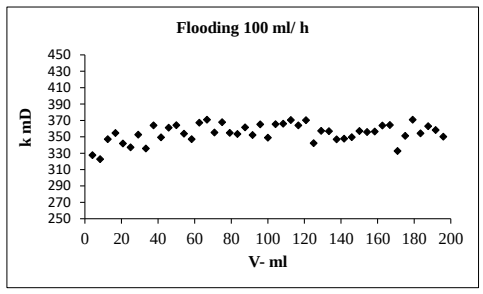

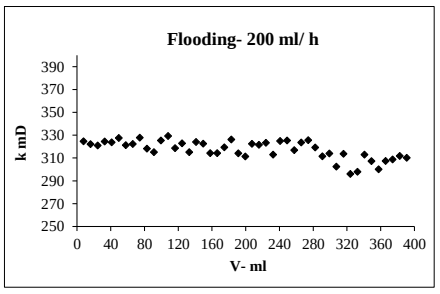

Group	Sample ID	Quartz	Calcite Mg	Oligoclase	Microcline	Chl. IIb	Kao.	Illite 2M1	Biotite 1M	Dol.	amorph.	Total Clay	Φ_{He} (%)	k_{wi} (mD)
D- 4	D- 4- 1874.00	80.7	2.8	5.7	0.8	1.5	1.0	3.0	0.1	0.5	4.0	5.49	27.72	830.34
	D- 4- 1872.60	80.0	3.2	6.0	1.0	0.8	0.9	3.3	....	0.9	4.0	4.95	25.62	338.92

ki	k@ 50 ml/h	k@ 100 ml/h	k@ 200 ml/h
731.97 mD	419.04 mD	354.64 mD	317.37 mD

Total Clay: 5.49%

	731.97	k ratio	
	50	1.75	42.75
	100	2.06	51.55
100	200	2.31	44.64

flow rate ml/ h

50	42.75	Damage Ration
100	51.55	
200	56.64	

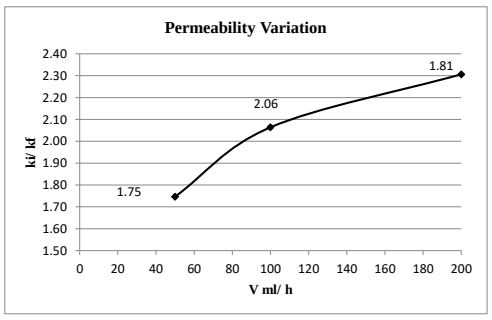

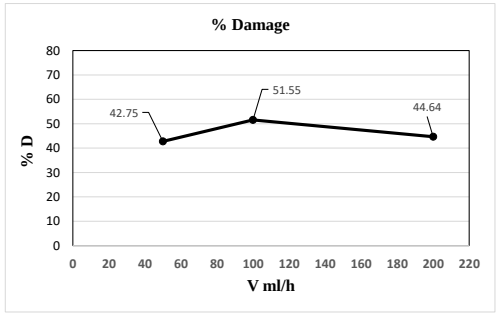

0:33:15	27.62	384.38		0:33:45	55.86	363.5736419		0:33:15	110.46	280.31847	
0:33:30	27.85	512.83		0:34:00	56.26	335.6933365		0:33:30	111.24	292.16291	
0:33:45	28.04	416.07		0:34:16	56.65	298.148687		0:33:45	112.14	332.83438	
0:34:00	28.27	410.26		0:34:31	57.09	345.3949598		0:34:00	112.92	292.16291	
0:34:16	28.46	362.20		0:34:46	57.48	318.0252661		0:34:15	113.81	347.90784	
0:34:31	28.68	473.38		0:35:01	57.93	383.7721775		0:34:30	114.59	323.29034	
0:34:46	28.88	416.07		0:35:16	58.32	318.0252661		0:34:46	115.49	357.72782	
0:35:01	29.10	473.38	427.45	0:35:31	58.77	344.6222641	347.115	0:35:01	116.27	313.49367	318.66
0:35:16	29.30	384.38		0:35:46	59.16	318.0252661		0:35:16	117.16	348.29744	
0:35:31	29.52	412.10		0:36:01	59.61	382.9136268		0:35:31	117.94	304.66286	
0:35:46	29.72	384.38		0:36:16	60.00	366.2109125		0:35:46	118.84	347.51825	
0:36:01	29.91	386.35		0:36:31	60.44	417.7239565		0:36:01	119.62	305.05245	
0:36:16	30.14	410.26		0:36:46	60.83	336.5518872		0:36:16	120.51	358.85191	
0:36:31	30.33	386.35		0:37:01	61.28	417.7239565		0:36:31	121.29	299.86351	
0:36:46	30.56	439.57		0:37:16	61.67	403.8622647		0:36:46	122.19	319.6991	
0:37:01	30.75	358.75		0:37:31	62.12	393.8540161		0:37:01	122.97	292.16291	
0:37:16	30.97	439.57		0:37:46	62.51	318.0252661		0:37:16	123.75	304.27327	
0:37:31	31.17	416.07	401.78	0:38:01	62.90	318.0252661	367.292	0:37:31	124.64	348.29744	322.8679
0:37:46	31.39	441.54		0:38:16	63.35	344.6222641		0:37:46	125.43	304.66286	
0:38:01	31.59	358.75		0:38:31	63.74	318.0252661		0:38:01	126.32	347.51825	
0:38:16	31.81	412.10		0:38:46	64.18	361.6709158		0:38:16	127.10	304.66286	
0:38:31	32.01	384.38		0:39:01	64.58	389.837423		0:38:31	127.99	332.83438	
0:38:46	32.23	439.57		0:39:16	65.02	364.9971581		0:38:46	128.78	309.60548	
0:39:01	32.43	386.35		0:39:31	65.41	365.2743117		0:39:01	129.67	297.65208	
0:39:16	32.65	439.57		0:39:46	65.86	418.6605573		0:39:16	130.45	283.43263	
0:39:31	32.84	326.14		0:40:01	66.25	365.2743117		0:39:31	131.34	311.63455	
0:39:46	33.04	327.81		0:40:16	66.70	418.6605573		0:39:46	132.13	300.6314	
0:40:01	33.26	410.26	392.65	0:40:31	67.09	361.8622647	370.889	0:40:01	133.02	358.45051	315.1085
0:40:16	33.46	327.81		0:40:46	67.54	368.126613		0:40:16	133.80	313.49367	
0:40:31	33.68	372.97		0:41:01	67.93	345.2845747		0:40:31	134.58	300.6314	
0:40:46	33.88	309.08		0:41:16	68.32	345.2845747		0:40:46	135.48	333.20751	
0:41:01	34.10	372.97		0:41:31	68.77	419.5971581		0:41:01	136.26	313.49367	
0:41:16	34.30	416.07		0:41:46	69.16	318.0252661		0:41:16	137.15	358.85191	
0:41:31	34.52	439.57		0:42:01	69.60	344.6222641		0:41:31	137.93	313.49367	
0:41:46	34.72	358.75		0:42:16	70.00	302.8966985		0:41:46	138.83	358.45051	
0:42:01	34.94	412.10		0:42:31	70.44	345.3949598		0:42:01	139.61	314.29647	
0:42:16	35.13	413.94		0:42:46	70.83	345.2845747		0:42:16	140.50	342.8657	
0:42:31	35.36	475.51	389.88	0:43:01	71.28	417.7239565	355.224	0:42:31	141.28	291.78978	324.0574
0:42:46	35.55	358.75		0:43:16	71.67	334.8347857		0:42:46	142.18	347.90784	
0:43:01	35.78	410.26		0:43:31	72.12	384.6307282		0:43:01	142.96	305.05245	
0:43:16	35.97	386.35		0:43:46	72.51	335.6933365		0:43:16	143.85	348.29744	
0:43:31	36.17	384.38		0:44:01	72.95	382.9136268		0:43:31	144.63	291.41665	
0:43:46	36.39	412.10		0:44:16	73.35	335.6933365		0:43:46	145.53	333.20751	
0:44:01	36.59	358.75		0:44:31	73.74	366.2109125		0:44:01	146.31	305.05245	
0:44:16	36.81	441.54		0:44:46	74.18	418.6605573		0:44:16	147.09	313.49367	
0:44:31	37.01	384.38		0:45:01	74.57	366.2109125		0:44:31	147.99	310.00364	
0:44:46	37.23	441.54		0:45:16	75.02	418.6605573		0:44:46	148.77	323.29034	
0:45:01	37.42	384.38	396.24	0:45:31	75.41	335.6933365	367.92	0:45:01	149.66	347.90784	322.563
0:45:16	37.65	412.10		0:45:46	75.86	363.5736419		0:45:16	150.44	304.66286	
0:45:31	37.84	384.38		0:46:01	76.25	302.1240028		0:45:31	151.33	347.90784	
0:45:46	38.07	439.57		0:46:16	76.70	362.760278		0:45:46	152.12	291.78978	
0:46:01	38.26	386.35		0:46:31	77.09	335.6933365		0:46:01	153.01	332.83438	
0:46:16	38.49	398.38		0:46:46	77.53	383.7721775		0:46:16	153.79	305.05245	
0:46:31	38.68	420.74		0:47:01	77.93	318.0252661		0:46:31	154.68	305.16345	
0:46:46	38.88	413.94		0:47:16	78.37	362.760278		0:46:46	155.47	298.28766	
0:47:01	39.10	439.57		0:47:31	78.76	335.6933365		0:47:01	156.36	343.24965	
0:47:16	39.30	416.07		0:47:46	79.21	418.6605573		0:47:16	157.14	279.96047	
0:47:31	39.52	439.57	415.07	0:48:01	79.60	365.2743117	354.834	0:47:31	158.04	333.58065	314.2489
0:47:46	39.71	358.75		0:48:16	79.99	336.5518872		0:47:46	158.82	291.41665	
0:48:01	39.94	412.10		0:48:31	80.44	382.9136268		0:48:01	159.60	300.6314	
0:48:16	40.13	358.75		0:48:46	80.83	318.0252661		0:48:16	160.49	358.45051	
0:48:31	40.36	410.26		0:49:01	81.28	363.5736419		0:48:31	161.27	304.27327	
0:48:46	40.55	360.59		0:49:16	81.67	365.2743117		0:48:46	162.17	358.85191	
0:49:01	40.77	410.26		0:49:31	82.11	348.5370969		0:49:01	162.95	291.78978	
0:49:16	40.97	386.35		0:49:46	82.50	318.0252661		0:49:16	163.84	310.93738	
0:49:31	41.19	437.83		0:50:01	82.95	382.9136268		0:49:31	164.62	280.31847	
0:49:46	41.39	413.24		0:50:16	83.34	336.5518872		0:49:46	165.52	333.20751	
0:50:01	41.61	437.83	398.60	0:50:31	83.79	382.9136268	353.528	0:50:01	166.30	313.49367	314.3371
0:50:16	41.81	428.24		0:50:46	84.18	367.1475133		0:50:16	167.19	358.45051	
0:50:31	42.00	384.38		0:51:01	84.63	366.3175201		0:50:31	167.97	304.66286	
0:50:46	42.23	439.57		0:51:16	85.02	368.6057183		0:50:46	168.87	348.29744	
0:51:01	42.42	431.99		0:51:31	85.46	353.6201776		0:51:01	169.65	291.78978	
0:51:16	42.65	398.38		0:51:46	85.85	344.4014939		0:51:16	170.54	320.05711	
0:51:31	42.84	360.59		0:52:01	86.25	361.8622647		0:51:31	171.32	299.86351	
0:51:46	43.06	439.57		0:52:16	86.69	376.6605573		0:51:46	172.11	300.24746	
0:52:01	43.26	416.07		0:52:31	87.08	366.2109125		0:52:01	173.00	332.83438	
0:52:16	43.48	473.38		0:52:46	87.53	375.7239565		0:52:16	173.78	304.66286	
0:52:31	43.68	413.94	418.61	0:53:01	87.92	335.6933365	361.624	0:52:31	174.67	332.83438	319.37
0:52:46	43.90	515.13		0:53:16	88.37	383.7721775		0:52:46	175.46	292.16291	
0:53:01	44.10	413.94		0:53:31	88.76	318.0252661		0:53:01	176.35	347.90784	
0:53:16	44.32	410.26		0:53:46	89.21	352.7370969		0:53:16	177.13	314.29647	
0:53:31	44.52	327.25		0:54:01	89.60	344.4014939		0:53:31	178.02	358.04911	
0:53:46	44.74	426.54		0:54:16	90.04	363.5736419		0:53:46	178.81	291.78978	
0:54:01	44.93	413.94		0:54:31	90.43	318.0252661		0:54:01	179.70	332.83438	
0:54:16	45.13	416.07		0:54:46	90.88	363.5736419		0:54:16	180.48	313.89507	
0:54:31	45.35	417.07		0:55:01	91.27	366.2109125		0:54:31	181.37	358.85191	
0:54:46	45.55	416.07		0:55:16	91.66	366.2109125		0:54:46	182.15	304.27327	
0:55:01	45.77	437.83	419.41	0:55:31	92.11	345.9721775	352.25	0:55:01	183.05	347.90784	326.1969
0:55:16	45.97	448.44		0:55:46	92.50	335.6933365		0:55:16	183.83	304.27327	
0:55:31	46.19	440.13		0:56:01	92.95	362.760278		0:55:31	184.61	314.29647	
0:55:46	46.39	413.94		0:56:16	93.34	318.0252661		0:55:46	185.50	358.45051	
0:56:01	46.61	398.38		0:56:31	93.78	382.9136268		0:56:01	186.29	284.15845	
0:56:16	46.81	405.74		0:56:46	94.18	336.5518872		0:56:16	187.18	323.71563	
0:56:31	47.03	405.88		0:57:01	94.62	375.7239565		0:56:31	187.96	304.27327	
0:56:46	47.22	386.35		0:57:16	95.01	366.2109125		0:56:46	188.85	348.29744	
0:57:01	47.45	398.38		0:57:31	95.46	376.6605573		0:57:01	189.64	292.16291	
0:57:16	47.64	413.94		0:57:46	95.85	402.8320038		0:57:16	190.53	319.6991	
0:57:31	47.87	439.57	415.08	0:58:01	96.30	394.7370969	365.211	0:57:31	191.31	291.41665	314.0744
0:57:46	48.06	386.35		0:58:16	96.69	301.3513072		0:57:46	192.20	333.20751	
0:58:01	48.26	416.07		0:58:31	97.14	394.7370969		0:58:01	192.99	280.31847	
0:58:16	48.48	439.57		0:58:46	97.53	360.8320038		0:58:16	193.88	332.46125	
0:58:31	48.68	384.38		0:59:01	97.92	366.2109125		0:58:31	194.66	292.16291	
0:58:46	48.90	441.54		0:59:16	98.36	363.5736419		0:58:46	195.55	332.83438	
0:59:01	49.09	384.38		0:59:31	98.75	317.2119023		0:59:01	196.34	291.78978	
0:59:16	49.32	437.83		0:59:46	99.20	384.6307282		0:59:16	197.12	280.31847	
0:59:31	49.51	420.74		1:00:01	99.59	334.8347857		0:59:31	198.01	332.83438	
0:59:46	49.74	398.38		1:00:16	100.04	364.3870057		0:59:46	198.79	304.66286	
1:00:01	49.93	416.07	412.53	1:00:31	100.43	301.3513072	348.912	1:00:01	199.68	332.83438	311.3424
1:00:16	50.16	437.83		1:00:46	100.88	321.297637		1:00:16	200.47	292.16291	
1:00:31	50.27	407.57		1:01:01	101.27	295.5089741		1:00:31	200.78	320.54455	
1:00:46	50.48	401.27		1:01:16	101.72	418.6605573		1:00:46	201.67	306.58317	
1:01:01	50.68	421.18		1:01:31	102.11	366.2109125		1:01:01	202.46	314.29647	
1:01:16	50.90	437.83		1:01:46	102.55	417.7239565		1:01:16	203.35	347.51825	
1:01:31	51.10	413.94		1:02:01	102.95	403.8622647		1:01:31	204.13	305.44205	
1:01:46	51.29	416.07		1:02:16	103.39	393.8540161		1:01:46	205.02	315.39739	
1:02:01	51.52	398.38		1:02:31	103.78	318.0252661		1:02:01	205.80	339.18987	
1:02:16	51.71	384.38		1:02:46	104.17	335.6933365		1:02:16	206.70	358.85191	
1:02:31	51.94	441.54	416.00	1:03:01	104.62	382.9136268	365.375	1:02:31	207.48	324.11823	322.4105
1:02:46	52.13	384.38		1:03:16	105.01	366.2109125		1:02:46	208.37	358.04911	
1:03:01	52.35	410.26		1:03:31	105.46	417.7239565		1:03:01	209.16	313.89507	
1:03:16	52.55	386.35		1:03:46	105.85	335.6933365		1:03:16	210.05	343.6336	
1:03:31	52.77	441.54		1:04:01	106.29	383.7721775		1:03:31	210.83	279.96047	
1:03:46	52.97	358.75		1:04:16	106.69	335.6933365		1:03:46	211.72	332.83438	
1:04:01	53.19	439.57		1:04:31	107.13	382.9136268		1:04:01	212.51	304.66286	
1:04:16	53.39	416.07		1:04:46	107.52	336.5518872		1:04:16	213.29	292.16291	
1:04:31	53.61	439.57		1:05:01	107.97	382.9136268		1:04:31	214.18	342.48175	
1:04:46	53.81	358.75		1:05:16	108.36	335.6933365		1:04:46	214.96	314.29647	
1:05:01	54.03	410.26	404.55	1:05:31	108.81	383.7721775	366.094	1:05:01	215.86	333.20751	321.5184
1:05:16	54.22	386.35		1:05:46	109.20	335.6933365		1:05:16	216.64	291.41665	
1:05:31	54.42	413.94		1:06:01	109.59	366.2109125		1:05:31	217.53	348.29744	
1:05:46	54.64	439.57		1:06:16	110.04	417.7239565		1:05:46	218.31	323.70429	
1:06:01	54.84	386.35		1:06:31	110.43	318.83863		1:06:01	219.21	369.65208	
1:06:16	55.06	398.38		1:06:46	110.87	362.760278		1:06:16	219.99	304.27327	
1:06:31	55.26	386.35		1:07:01	111.26	366.2109125		1:06:31	220.88	347.90784	
1:06:46	55.48	398.38		1:07:16	111.71	418.6605573		1:06:46	221.66	340.05847	
1:07:01	55.68	413.94		1:07:31	112.10	365.2743117		1:07:01	222.56	315.83169	
1:07:16	55.90	400.51		1:07:46	112.55	419.5971581		1:07:16	223.34	291.78978	
1:07:31	56.10	390.74	401.45	1:08:01	112.94	334.8347857	370.58	1:07:31	224.12	301.01535	323.3947
1:07:46	56.32	398.38		1:08:16	113.39	382.9136268		1:07:46	225.02	297.23814	
1:08:01	56.51	448.44		1:08:31	113.78	367.1475133		1:08:01	225.80	300.6314	
1:08:16	56.74	409.45		1:08:47	114.22	391.6162092		1:08:16	226.69	342.48175	
1:08:31	56.93	416.07		1:09:02	114.61	318.0252661		1:08:31	227.47	313.49367	
1:08:47	57.16	412.10		1:09:17	115.06	363.5736419		1:08:46	228.37	348.68703	

1:09:02	57.35	416.07		1:09:32	115.45	335.6933365		1:09:01	229.15	304.27327	
1:09:17	57.55	384.38		1:09:47	115.84	335.6933365		1:09:16	230.04	333.20751	
1:09:32	57.77	410.26		1:10:02	116.29	417.7239565		1:09:31	230.82	292.53605	
1:09:47	57.97	360.59		1:10:17	116.68	366.2109125		1:09:46	231.72	324.07854	
1:10:02	58.19	410.26	406.60	1:10:32	117.13	362.760278	364.136	1:10:01	232.50	272.59309	312.922
1:10:17	58.38	386.35		1:10:47	117.52	302.1240028		1:10:16	233.39	342.8657	
1:10:32	58.61	398.38		1:11:02	117.96	394.7370969		1:10:31	234.17	313.89507	
1:10:47	58.80	416.07		1:11:17	118.36	402.8320038		1:10:46	235.07	332.83438	
1:11:02	59.03	398.38		1:11:32	118.80	418.6605573		1:11:01	235.85	300.6314	
1:11:17	59.22	384.38		1:11:47	119.19	366.2109125		1:11:16	236.63	324.11823	
1:11:32	59.44	439.57		1:12:02	119.64	417.7239565		1:11:31	237.53	358.85191	
1:11:47	59.64	416.07		1:12:17	120.03	335.6933365		1:11:46	238.31	304.27327	
1:12:02	59.86	398.38		1:12:32	120.48	363.5736419		1:12:01	239.20	347.51825	
1:12:17	60.06	416.07		1:12:47	120.87	318.0252661		1:12:16	239.98	291.78978	
1:12:32	60.28	437.83	409.15	1:13:02	121.31	382.9136268	370.249	1:12:31	240.87	332.83438	324.9612
1:12:47	60.48	413.94		1:13:17	121.71	336.5518872		1:12:46	241.66	305.05245	
1:13:02	60.67	386.35		1:13:32	122.10	335.6933365		1:13:01	242.55	347.90784	
1:13:17	60.90	473.38		1:13:47	122.54	383.7721775		1:13:16	243.33	305.44205	
1:13:32	61.09	416.07		1:14:02	122.94	335.6933365		1:13:31	244.23	358.45051	
1:13:47	61.32	398.38		1:14:17	123.38	382.9136268		1:13:46	245.01	299.86351	
1:14:02	61.51	413.94		1:14:32	123.77	335.6933365		1:14:01	245.90	342.8657	
1:14:17	61.73	439.57		1:14:47	124.22	363.5736419		1:14:16	246.68	323.70429	
1:14:32	61.93	360.59		1:15:02	124.61	302.8966985		1:14:31	247.58	369.65208	
1:14:47	62.15	439.57		1:15:17	125.06	345.3949598		1:14:46	248.36	299.86351	
1:15:02	62.35	416.07	415.79	1:15:32	125.45	301.3513072	342.353	1:15:01	249.14	300.6314	325.3433
1:15:17	62.57	439.57		1:15:47	125.90	394.7370969		1:15:16	250.03	342.8657	
1:15:32	62.77	360.59		1:16:02	126.29	345.2845747		1:15:31	250.81	291.78978	
1:15:47	62.99	410.26		1:16:17	126.73	418.6605573		1:15:46	251.71	347.51825	
1:16:02	63.19	386.35		1:16:32	127.12	389.837423		1:16:01	252.49	292.16291	
1:16:17	63.41	398.38		1:16:47	127.57	363.5736419		1:16:16	253.38	333.20751	
1:16:32	63.61	416.07		1:17:02	127.96	317.2119023		1:16:31	254.16	291.41665	
1:16:47	63.80	413.94		1:17:17	128.35	318.0252661		1:16:46	255.06	320.05711	
1:17:02	64.02	400.51		1:17:32	128.80	344.6222641		1:17:01	255.84	299.86351	
1:17:17	64.22	413.94		1:17:47	129.19	318.83863		1:17:16	256.73	358.85191	
1:17:32	64.44	398.38	403.80	1:18:02	129.64	362.760278	357.355	1:17:31	257.51	291.41665	316.915
1:17:47	64.64	384.38		1:18:17	130.03	318.83863		1:17:46	258.41	333.20751	
1:18:02	64.86	441.54		1:18:32	130.47	382.9136268		1:18:01	259.19	305.05245	
1:18:17	65.06	413.94		1:18:47	130.87	318.0252661		1:18:16	260.08	347.90784	
1:18:32	65.28	440.13		1:19:02	131.31	345.3949598		1:18:31	260.86	291.41665	
1:18:47	65.48	448.44		1:19:17	131.70	317.2119023		1:18:46	261.64	299.86351	
1:19:02	65.70	398.38		1:19:32	132.15	383.7721775		1:19:01	262.54	342.8657	
1:19:17	65.89	386.35		1:19:47	132.54	335.6933365		1:19:16	263.32	291.41665	
1:19:32	66.12	439.57		1:20:02	132.99	383.7721775		1:19:31	264.21	348.29744	
1:19:47	66.31	413.94		1:20:17	133.38	365.2743117		1:19:46	264.99	323.70429	
1:20:02	66.54	441.54	420.82	1:20:32	133.82	418.6605573	356.956	1:20:01	265.89	352.70509	323.6437
1:20:17	66.73	416.07		1:20:47	134.22	335.6933365		1:20:16	266.67	292.16291	
1:20:32	66.93	413.94		1:21:02	134.61	335.6933365		1:20:31	267.56	358.45051	
1:20:47	67.15	439.57		1:21:17	135.05	336.9706925		1:20:46	268.34	300.24746	
1:21:02	67.35	416.07		1:21:32	135.44	318.0252661		1:21:01	269.24	342.8657	
1:21:17	67.57	398.38		1:21:47	135.89	375.4963521		1:21:16	270.02	314.29647	
1:21:32	67.77	416.07		1:22:02	136.28	366.2109125		1:21:31	270.91	358.04911	
1:21:47	67.99	437.83		1:22:17	136.73	383.7721775		1:21:46	271.70	314.29647	
1:22:02	68.18	448.44		1:22:32	137.12	335.6933365		1:22:01	272.59	358.45051	
1:22:17	68.41	439.57		1:22:47	137.57	364.3870057		1:22:16	273.37	313.89507	
1:22:32	68.60	360.59	418.65	1:23:02	137.96	318.0252661	346.997	1:22:31	274.15	304.27327	325.6987
1:22:47	68.83	439.57		1:23:17	138.41	418.6605573		1:22:46	275.05	359.25331	
1:23:02	69.02	416.07		1:23:32	138.80	345.2845747		1:23:01	275.83	299.86351	
1:23:17	69.24	398.38		1:23:47	139.24	345.3949598		1:23:16	276.72	344.01755	
1:23:32	69.44	416.07		1:24:02	139.63	301.3513072		1:23:31	277.50	313.49367	
1:23:47	69.66	398.38		1:24:17	140.03	302.8966985		1:23:46	278.40	332.83438	
1:24:02	69.86	448.44		1:24:32	140.47	362.760278		1:24:01	279.18	291.78978	
1:24:17	70.05	416.07		1:24:47	140.86	318.0252661		1:24:16	280.07	348.29744	
1:24:32	70.28	439.57		1:25:02	141.31	363.5736419		1:24:31	280.85	291.78978	
1:24:47	70.47	413.94		1:25:17	141.70	335.6933365		1:24:46	281.75	319.34109	
1:25:02	70.70	441.54	422.80	1:25:32	142.15	383.7721775	347.741	1:25:01	282.53	292.16291	319.2843
1:25:17	70.89	384.38		1:25:47	142.54	281.045584		1:25:16	283.42	347.51825	
1:25:32	71.11	398.38		1:26:02	142.99	321.297637		1:25:31	284.20	291.78978	
1:25:47	71.31	416.07		1:26:17	143.38	335.6933365		1:25:46	285.10	320.05711	
1:26:02	71.53	439.57		1:26:32	143.82	382.9136268		1:26:01	285.88	291.78978	
1:26:17	71.73	386.35		1:26:47	144.21	335.6933365		1:26:16	286.66	291.78978	
1:26:32	71.95	398.38		1:27:02	144.66	363.5736419		1:26:31	287.55	319.6991	
1:26:47	72.15	384.38		1:27:17	145.05	345.2845747		1:26:46	288.34	291.78978	
1:27:02	72.37	400.51		1:27:32	145.44	403.8622647		1:27:01	289.23	347.90784	
1:27:17	72.57	413.94		1:27:47	145.89	358.6963521		1:27:16	290.01	292.16291	
1:27:32	72.79	441.54	406.35	1:28:02	146.28	367.1475133	349.521	1:27:31	290.91	320.05711	311.4561
1:27:47	72.99	384.38		1:28:17	146.73	382.9136268		1:27:46	291.69	299.86351	
1:28:02	73.18	386.35		1:28:32	147.12	366.2109125		1:28:01	292.58	342.8657	
1:28:17	73.40	437.83		1:28:47	147.56	350.2963521		1:28:16	293.36	291.78978	
1:28:32	73.60	414.21		1:29:02	147.96	346.1676554		1:28:31	294.26	333.20751	
1:28:47	73.82	440.13		1:29:17	148.40	362.760278		1:28:46	295.04	300.24746	
1:29:02	74.02	416.07		1:29:32	148.79	335.6933365		1:29:01	295.93	358.04911	
1:29:17	74.24	398.38		1:29:47	149.24	382.9136268		1:29:16	296.71	313.89507	
1:29:32	74.44	413.94		1:30:02	149.63	336.5518872		1:29:31	297.49	299.86351	
1:29:47	74.66	441.54		1:30:17	150.08	362.760278		1:29:46	298.39	319.6991	
1:30:02	74.86	408.19	414.10	1:30:32	150.47	345.2845747	357.155	1:30:01	299.17	280.31847	313.9799
1:30:17	75.08	404.24		1:30:47	150.92	334.526613		1:30:16	300.06	319.34109	
1:30:32	75.28	405.74		1:31:02	151.31	366.2109125		1:30:31	300.84	280.31847	
1:30:47	75.50	398.38		1:31:17	151.70	318.83863		1:30:46	301.74	332.83438	
1:31:02	75.69	386.35		1:31:32	152.14	362.760278		1:31:01	302.52	292.16291	
1:31:17	75.92	439.57		1:31:47	152.54	366.2109125		1:31:16	303.41	319.6991	
1:31:32	76.11	358.75		1:32:02	152.98	417.7239565		1:31:31	304.19	291.41665	
1:31:47	76.31	360.59		1:32:17	153.37	337.4104379		1:31:46	305.09	333.20751	
1:32:02	76.53	439.57		1:32:32	153.82	382.9136268		1:32:01	305.87	279.60246	
1:32:17	76.73	428.24		1:32:47	154.21	335.6933365		1:32:16	306.76	311.28597	
1:32:32	76.95	437.83	405.93	1:33:02	154.66	336.216843	355.851	1:32:31	307.54	265.60352	302.5472
1:32:47	77.15	413.94		1:33:17	155.05	294.7551247		1:32:46	308.44	311.98313	
1:33:02	77.37	400.51		1:33:32	155.49	382.9136268		1:33:01	309.22	292.16291	
1:33:17	77.56	413.94		1:33:47	155.89	318.83863		1:33:16	310.00	304.66286	
1:33:32	77.79	400.51		1:34:02	156.33	393.8540161		1:33:31	310.89	347.51825	
1:33:47	77.98	413.94		1:34:17	156.72	402.8320038		1:33:46	311.68	292.53605	
1:34:02	78.21	398.38		1:34:32	157.17	418.6605573		1:34:01	312.57	332.83438	
1:34:17	78.40	437.50		1:34:47	157.56	294.7551247		1:34:16	313.35	292.16291	
1:34:32	78.63	438.72		1:35:02	157.95	294.7551247		1:34:31	314.25	343.24965	
1:34:47	78.82	413.94		1:35:17	158.40	417.7239565		1:34:46	315.03	300.24746	
1:35:02	79.04	441.54	417.29	1:35:32	158.79	345.2845747	356.437	1:35:01	315.92	319.6991	313.7057
1:35:17	79.24	413.94		1:35:47	159.24	345.3949598		1:35:16	316.70	279.96047	
1:35:32	79.44	413.24		1:36:02	159.63	318.0252661		1:35:31	317.60	320.05711	
1:35:47	79.66	439.57		1:36:17	160.07	418.6605573		1:35:46	318.38	279.96047	
1:36:02	79.85	384.38		1:36:32	160.46	365.2743117		1:36:01	319.27	319.6991	
1:36:17	80.08	398.38		1:36:47	160.91	363.5736419		1:36:16	320.06	272.94167	
1:36:32	80.27	416.07		1:37:02	161.30	302.1240028		1:36:31	320.95	310.93738	
1:36:47	80.50	439.57		1:37:17	161.75	417.7239565		1:36:46	321.73	300.6314	
1:37:02	80.69	386.35		1:37:32	162.14	389.837423		1:37:01	322.51	300.24746	
1:37:17	80.91	398.38		1:37:47	162.59	382.9136268		1:37:16	323.40	310.93738	
1:37:32	81.11	386.35	407.62	1:38:02	162.98	335.6933365	363.922	1:37:31	324.19	265.94317	296.1316
1:37:47	81.33	439.57		1:38:17	163.42	363.5736419		1:37:46	325.08	311.28597	
1:38:02	81.53	413.94		1:38:32	163.81	345.2845747		1:38:01	325.86	272.2445	
1:38:17	81.75	398.38		1:38:47	164.21	330.8057183		1:38:16	326.75	303.30427	
1:38:32	81.95	398.24		1:39:02	164.65	418.6605573		1:38:31	327.54	272.59309	
1:38:47	82.14	401.99		1:39:17	165.04	302.1240028		1:38:46	328.43	319.6991	
1:39:02	82.37	398.38		1:39:32	165.49	393.8540161		1:39:01	329.21	291.78978	
1:39:17	82.56	416.07		1:39:47	165.88	346.1676554		1:39:16	330.10	332.83438	
1:39:32	82.79	439.57		1:40:02	166.33	393.8540161		1:39:31	330.89	280.31847	
1:39:47	82.98	413.94		1:40:17	166.72	366.2109125		1:39:46	331.78	310.93738	
1:40:02	83.20	437.83	415.79	1:40:32	167.16	382.9136268	364.345	1:40:01	332.56	284.15845	297.9165
1:40:17	83.40	386.35		1:40:47	167.56	336.5518872		1:40:16	333.45	347.51825	
1:40:32	83.62	439.57		1:41:02	168.00	382.9136268		1:40:31	334.24	304.66286	
1:40:47	83.82	416.07		1:41:17	168.39	317.2119023		1:40:46	335.02	314.29647	
1:41:02	84.04	439.57		1:41:32	168.84	345.3949598		1:41:01	335.91	343.24965	
1:41:17	84.24	360.59		1:41:47	169.23	302.1240028		1:41:16	336.69	272.2445	
1:41:32	84.46	439.57		1:42:02	169.68	363.5736419		1:41:31	337.59	303.30427	
1:41:47	84.66	413.94		1:42:17	170.07	334.8347857		1:41:46	338.37	272.94167	
1:42:02	84.88	400.51		1:42:32	170.46	318.83863		1:42:01	339.26	332.83438	
1:42:17	85.07	384.38		1:42:48	170.91	323.0833726		1:42:16	340.04	305.05245	
1:42:32	85.27	360.59	404.11	1:43:03	171.30	302.8966985	332.742	1:42:31	340.94	333.20751	312.9312
1:42:48	85.49	443.80		1:43:18	171.74	345.3949598		1:42:46	341.72	272.94167	
1:43:03	85.69	413.94		1:43:33	172.13	317.2119023		1:43:01	342.61	332.83438	
1:43:18	85.91	400.51		1:43:48	172.58	418.6605573		1:43:16	343.39	313.49367	
1:43:33	86.11	414.21		1:44:03	172.97	365.2743117		1:43:31	344.29	348.68703	
1:43:48	86.33	422.79		1:44:18	173.42	383.7721775		1:43:46	345.07	291.41665	
1:44:03	86.53	440.13		1:44:33	173.81	335.6933365		1:44:01	345.85	299.86351	
1:44:18	86.75	436.09		1:44:48	174.26	362.760278		1:44:16	346.74	333.20751	
1:44:33	86.95	419.35		1:45:03	174.65	302.8966985		1:44:31	347.52	283.43263	

1:44:48	87.17	409.45		1:45:18	175.09	362.760278		1:44:46	348.42	324.80436	
1:45:03	87.36	413.24	421.35	1:45:33	175.49	318.83863	351.326	1:45:01	349.20	272.2445	307.2926
1:45:18	87.59	439.57		1:45:48	175.93	362.760278		1:45:16	350.09	319.34109	
1:45:33	87.78	416.07		1:46:03	176.32	318.0252661		1:45:31	350.87	272.2445	
1:45:48	88.01	440.13		1:46:18	176.71	346.1676554		1:45:46	351.77	311.28597	
1:46:03	88.20	416.07		1:46:33	177.16	417.7239565		1:46:01	352.55	280.31847	
1:46:18	88.40	413.94		1:46:48	177.55	366.2109125		1:46:16	353.44	333.58065	
1:46:33	88.62	415.33		1:47:03	178.00	418.6605573		1:46:31	354.23	284.15845	
1:46:48	88.82	413.24		1:47:18	178.39	335.6933365		1:46:46	355.12	303.30427	
1:47:03	89.04	417.07		1:47:33	178.84	383.7721775		1:47:01	355.90	283.79554	
1:47:18	89.24	386.35		1:47:48	179.23	366.2109125		1:47:16	356.79	333.20751	
1:47:33	89.46	439.57	419.73	1:48:03	179.67	393.8540161	370.908	1:47:31	357.58	279.60246	300.0839
1:47:48	89.65	384.38		1:48:18	180.07	318.83863		1:47:46	358.36	291.41665	
1:48:03	89.88	441.54		1:48:33	180.51	417.7239565		1:48:01	359.25	359.25331	
1:48:18	90.07	384.38		1:48:48	180.90	366.2109125		1:48:16	360.03	291.41665	
1:48:33	90.30	398.38		1:49:03	181.35	383.7721775		1:48:31	360.93	311.63455	
1:48:48	90.49	398.24		1:49:18	181.74	335.6933365		1:48:46	361.71	272.94167	
1:49:03	90.72	437.83		1:49:33	182.13	335.6933365		1:49:01	362.60	310.93738	
1:49:18	90.91	437.50		1:49:48	182.58	319.6709158		1:49:16	363.38	279.96047	
1:49:33	91.13	425.69		1:50:03	182.97	366.2109125		1:49:31	364.28	332.83438	
1:49:48	91.33	448.44		1:50:18	183.42	363.5736419		1:49:46	365.06	291.41665	
1:50:03	91.53	416.07	417.24	1:50:33	183.81	334.8347857	354.222	1:50:01	365.95	333.20751	307.5019
1:50:18	91.75	437.83		1:50:48	184.25	383.7721775		1:50:16	366.73	292.16291	
1:50:33	91.94	448.44		1:51:03	184.64	318.0252661		1:50:31	367.63	333.20751	
1:50:48	92.17	441.54		1:51:18	185.09	362.760278		1:50:46	368.41	305.05245	
1:51:03	92.36	413.94		1:51:33	185.48	389.837423		1:51:01	369.30	347.51825	
1:51:18	92.59	437.83		1:51:48	185.93	418.6605573		1:51:16	370.08	292.16291	
1:51:33	92.78	386.35		1:52:03	186.32	318.0252661		1:51:31	370.87	279.96047	
1:51:48	93.00	398.38		1:52:18	186.77	383.7721775		1:51:46	371.76	319.6991	
1:52:03	93.20	416.72		1:52:33	187.16	317.2119023		1:52:01	372.54	292.16291	
1:52:18	93.42	437.83		1:52:48	187.60	394.7370969		1:52:16	373.43	332.83438	
1:52:33	93.62	428.24	424.71	1:53:03	187.99	344.4014939	363.12	1:52:31	374.22	292.16291	308.6924
1:52:48	93.84	437.83		1:53:18	188.38	318.0252661		1:52:46	375.11	324.07854	
1:53:03	94.04	448.44		1:53:33	188.83	383.7721775		1:53:01	375.89	284.15845	
1:53:18	94.26	425.69		1:53:48	189.22	318.0252661		1:53:16	376.78	347.51825	
1:53:33	94.46	437.50		1:54:03	189.67	393.8540161		1:53:31	377.57	292.16291	
1:53:48	94.65	416.07		1:54:18	190.06	346.1676554		1:53:46	378.46	343.6336	
1:54:03	94.88	398.38		1:54:33	190.51	344.6222641		1:54:01	379.24	313.49367	
1:54:18	95.07	398.24		1:54:48	190.90	345.2845747		1:54:16	380.14	333.58065	
1:54:33	95.29	398.38		1:55:03	191.34	394.7370969		1:54:31	380.92	279.60246	
1:54:48	95.49	413.94		1:55:18	191.74	345.2845747		1:54:46	381.81	319.6991	
1:55:03	95.71	440.13	421.46	1:55:33	192.18	394.7370969	358.451	1:55:01	382.59	279.60246	311.753
1:55:18	95.91	413.94		1:55:48	192.57	302.1240028		1:55:16	383.37	291.78978	
1:55:33	96.13	407.83		1:56:03	193.02	344.6222641		1:55:31	384.27	347.51825	
1:55:48	96.33	420.74		1:56:18	193.41	318.83863		1:55:46	385.05	291.78978	
1:56:03	96.55	413.38		1:56:33	193.86	382.9136268		1:56:01	385.94	311.98313	
1:56:18	96.75	420.74		1:56:48	194.25	335.6933365		1:56:16	386.72	272.2445	
1:56:33	96.97	437.83		1:57:03	194.64	335.6933365		1:56:31	387.62	311.28597	
1:56:48	97.16	418.44		1:57:18	195.09	383.7721775		1:56:46	388.40	283.79554	
1:57:03	97.36	420.74		1:57:33	195.48	334.8347857		1:57:01	389.29	333.20751	
1:57:18	97.58	435.88		1:57:48	195.92	418.6605573		1:57:16	390.07	300.24746	
1:57:33	97.78	416.07	420.56	1:58:03	196.31	345.2845747	350.244	1:57:31	390.97	358.85191	310.2714
1:57:48	98.00	413.38		1:58:18	196.76	344.6222641		1:57:46	391.75	291.41665	
1:58:03	98.20	417.63		1:58:33	197.15	318.0252661		1:58:01	392.64	333.20751	
1:58:18	98.42	413.59		1:58:48	197.60	316.5721775		1:58:16	393.42	291.78978	
1:58:33	98.62	406.88		1:59:03	197.99	335.6933365		1:58:31	394.32	319.6991	
1:58:48	98.84	410.26		1:59:18	198.44	362.760278		1:58:46	395.10	280.31847	
1:59:03	99.04	416.35		1:59:33	198.83	345.2845747		1:59:01	395.88	279.96047	
1:59:18	99.26	458.38		1:59:48	199.27	418.6605573		1:59:16	396.78	319.6991	
1:59:33	99.45	416.07		2:00:03	199.66	335.6933365				317.14787	**317.37**
1:59:48	99.68	430.33		2:00:18	200.11						
2:00:03	99.87	413.24	419.61			**354.64**	**354.76**				
2:00:18	100.10	437.83									
		419.04									
		0.00									

50 ml/ h				100 ml/ h				200 ml/ h			
time, [hh:mm:ss]	V, [cm^3]	k, [mD]	k, [mD]	time, [hh:mm:ss]	V, [cm^3]	k, [mD]	k, [mD]	time, [hh:mm:ss]	V, [cm^3]	k, [mD]	k, [mD]
0:01:00	0.766	367.46		0:01:00	1.609	193.88		0:01:00	3.33	134.6845	
0:02:00	1.602	338.97		0:02:00	3.274	191.80		0:02:00	6.66	138.9164	
0:03:00	2.434	268.33		0:03:00	4.939	181.95		0:03:00	9.99	135.788	
0:04:00	3.267	290.06		0:04:00	6.604	180.22		0:04:00	13.32	137.7534	
0:05:00	4.1	283.95	309.75	0:05:00	8.269	180.22	185.62	0:05:00	16.65	137.7112	136.9707
0:06:00	4.932	289.24		0:06:00	9.934	179.76		0:06:00	19.97	137.2067	
0:07:00	5.765	305.85		0:07:00	11.599	178.68		0:07:00	23.31	138.8421	
0:08:00	6.598	305.85		0:08:00	13.264	179.14		0:08:00	26.64	130.3102	
0:09:00	7.431	307.54		0:09:00	14.93	179.87		0:09:00	29.97	125.4941	
0:10:00	8.266	264.30	294.56	0:10:00	16.651	185.01	180.49	0:10:00	30.33	133.1295	132.9965
0:11:00	9.103	294.77		0:11:00	18.316	179.45		0:11:00	36.63	129.8189	
0:12:00	9.937	244.99		0:12:00	19.982	180.33		0:12:00	39.96	127.2008	
0:13:00	10.77	317.25		0:13:00	21.648	179.87		0:13:00	43.29	125.2415	
0:14:00	11.604	264.78		0:14:00	23.314	180.18		0:14:00	46.63	129.0908	
0:15:00	12.437	246.93	273.74	0:15:00	24.98	181.27	180.22	0:15:00	49.40	132.8228	128.8349
0:16:00	13.271	225.16		0:16:00	26.646	181.27		0:16:00	53.30	124.1249	
0:17:00	14.105	295.92		0:17:00	28.312	181.27		0:17:00	56.63	132.1849	
0:18:00	14.938	281.75		0:18:00	29.978	181.90		0:18:00	59.96	125.9279	
0:19:00	15.772	272.41		0:19:00	31.645	182.01		0:19:00	63.29	130.6186	
0:20:00	16.605	263.99	267.85	0:20:00	33.311	182.38	181.76	0:20:00	66.63	135.5088	129.673
0:21:00	17.438	256.79		0:21:00	34.978	183.28		0:21:00	69.96	129.3915	
0:22:00	18.279	255.34		0:22:00	36.645	183.61		0:22:00	73.29	139.5709	
0:23:00	19.112	248.33		0:23:00	38.311	183.50		0:23:00	76.63	144.8468	
0:24:00	19.947	241.76		0:24:00	39.979	183.72		0:24:00	79.96	138.5687	
0:25:00	20.78	237.75	247.99	0:25:00	41.646	183.93	183.61	0:25:00	83.29	143.5318	139.182
0:26:00	21.615	235.72		0:26:00	43.314	184.36		0:26:00	86.63	143.3897	
0:27:00	22.449	231.11		0:27:00	44.982	184.69		0:27:00	89.96	137.4432	
0:28:00	23.283	226.94		0:28:00	46.648	184.47		0:28:00	93.30	137.9977	
0:29:00	24.119	226.80		0:29:00	48.316	184.36		0:29:00	96.63	138.744	
0:30:00	24.953	225.59	229.23	0:30:00	49.983	183.93	184.36	0:30:00	99.97	144.7009	140.4551
0:31:00	25.786	222.98		0:31:00	51.65	184.25		0:31:00	103.30	140.2951	
0:32:00	26.62	220.96		0:32:00	53.317	184.25		0:32:00	106.64	141.921	
0:33:00	27.454	219.36		0:33:00	54.985	184.36		0:33:00	109.97	143.1072	
0:34:00	28.287	216.89		0:34:00	56.652	184.25		0:34:00	113.30	144.9073	
0:35:00	29.121	214.98	219.03	0:35:00	58.319	183.93	184.21	0:35:00	116.04	147.2426	143.4946
0:36:00	29.955	214.37		0:36:00	59.986	184.25		0:36:00	119.97	149.1761	
0:37:00	30.789	211.66		0:37:00	61.653	184.58		0:37:00	123.31	146.0463	
0:38:00	31.623	210.19		0:38:00	63.321	184.69		0:38:00	126.64	148.5798	
0:39:00	32.457	209.61		0:39:00	64.988	185.07		0:39:00	129.89	150.9886	
0:40:00	33.29	208.78	210.92	0:40:00	66.655	184.74	184.66	0:40:00	133.31	148.3825	148.6347
0:41:00	34.125	208.70		0:41:00	68.323	184.36		0:41:00	136.64	151.4664	
0:42:00	34.958	207.05		0:42:00	69.99	183.93		0:42:00	139.98	148.8781	
0:43:00	35.792	206.45		0:43:00	71.657	183.61		0:43:00	143.31	146.1979	
0:44:00	36.625	204.80		0:44:00	73.325	183.23		0:44:00	146.65	149.2274	
0:45:00	37.46	204.19	206.24	0:45:00	74.993	182.91	183.61	0:45:00	149.98	146.1846	148.3909
0:46:00	38.293	202.33		0:46:00	76.66	183.28		0:46:00	153.32	148.8541	
0:47:00	39.127	201.76		0:47:00	78.328	183.39		0:47:00	156.65	151.3372	
0:48:00	39.961	201.76		0:48:00	79.995	183.28		0:48:00	159.98	153.2205	
0:49:00	40.794	200.45		0:49:00	81.662	182.80		0:49:00	163.32	154.8029	
0:50:00	41.628	198.84	201.03	0:50:00	83.329	181.69	182.89	0:50:00	166.65	156.4184	152.9266
0:51:00	42.462	198.84		0:51:00	84.997	181.17		0:51:00	169.99	157.4183	
0:52:00	43.295	198.08		0:52:00	86.665	181.49		0:52:00	173.32	159.1368	
0:53:00	44.129	196.76		0:53:00	88.335	182.81		0:53:00	188.91	162.4	
0:54:00	44.963	196.76		0:54:00	90.002	181.85		0:54:00	192.25	162.6161	
0:55:00	45.796	196.78	197.44	0:55:00	91.669	180.44	181.55	0:55:00	195.58	163.6971	161.0536
0:56:01	46.63	192.78		0:56:00	93.288	174.79		0:56:00	189.92	164.1851	
0:57:01	47.464	194.98		0:57:00	94.956	180.08		0:57:00	202.25	164.4781	
0:58:01	48.297	194.00		0:58:00	96.623	180.44		0:58:00	205.95	164.4781	
0:59:01	49.131	192.99		0:59:00	98.29	179.97		0:59:00	208.92	164.8714	
1:00:01	49.965	192.50	193.45	1:00:00	99.968	180.39	179.13	1:00:00	212.25	165.6337	164.7293
1:01:01	50.798	191.05		1:01:00	101.634	178.79		1:01:00	215.59	165.5841	
1:02:01	51.632	190.79		1:02:00	103.302	178.70		1:02:00	218.19	166.4331	
1:03:01	52.466	191.52		1:03:00	104.97	178.70		1:03:00	222.26	167.1091	
1:04:01	53.299	190.56		1:04:00	106.637	178.90		1:04:00	225.56	167.4337	
1:05:01	54.133	189.12	190.61	1:05:00	108.304	178.59	178.74	1:05:00	228.93	168.58	167.028
1:06:01	54.966	187.48		1:06:00	109.971	178.29		1:06:00	232.26	169.4084	
1:07:01	55.8	187.71		1:07:00	111.638	178.90		1:07:00	235.60	170.263	
1:08:01	56.634	188.18		1:08:00	113.305	178.14		1:08:00	238.94	171.345	
1:09:01	57.467	187.95		1:09:00	114.972	177.83		1:09:00	242.28	172.4938	
1:10:01	58.301	187.71	187.80	1:10:00	116.64	178.70	178.37	1:10:00	245.60	173.8153	171.4651
1:11:01	59.135	186.55		1:11:01	118.307	174.92		1:11:00	248.93	175.8908	
1:12:01	59.968	185.64		1:12:01	119.974	177.83		1:12:00	252.27	176.7022	
1:13:01	60.802	185.40		1:13:01	121.642	177.94		1:13:00	255.60	176.7022	
1:14:01	61.636	184.95		1:14:01	123.309	177.08		1:14:01	258.93	174.7533	
1:15:01	62.469	184.73	185.45	1:15:01	124.976	177.08	176.97	1:15:01	262.35	178.903	176.5903
1:16:01	63.303	185.40		1:16:01	126.643	178.44		1:16:01	265.60	180.2123	
1:17:01	64.136	185.18		1:17:01	128.31	178.44		1:17:01	268.98	181.6497	
1:18:01	64.97	183.82		1:18:01	129.977	177.08		1:18:01	272.27	182.944	
1:19:01	65.803	182.49		1:19:01	131.644	176.78		1:19:01	275.61	183.7114	
1:20:01	66.637	183.37	184.05	1:20:01	133.312	177.64	177.68	1:20:01	278.94	184.2697	182.5574
1:21:01	67.471	184.04		1:21:01	134.979	178.90		1:21:01	282.41	184.1592	
1:22:01	68.304	183.15		1:22:01	136.647	178.55		1:22:01	285.61	185.1483	
1:23:01	69.138	183.37		1:23:01	138.314	177.38		1:23:01	288.94	186.148	
1:24:01	69.972	184.04		1:24:01	139.981	177.08		1:24:01	292.28	186.5509	
1:25:01	70.805	182.27	183.38	1:25:01	141.649	176.89	177.76	1:25:01	295.61	188.4423	186.0897
1:26:01	71.639	181.39		1:26:01	143.316	177.08		1:26:01	298.25	188.3858	
1:27:01	72.473	181.39		1:27:01	144.985	177.29		1:27:01	302.03	188.4988	
1:28:01	73.306	181.17		1:28:01	146.652	176.78		1:28:01	305.68	189.8951	
1:29:01	74.14	180.74		1:29:01	148.321	176.99		1:29:01	608.65	189.8381	
1:30:01	74.974	179.66	180.87	1:30:01	149.988	177.53	177.14	1:30:01	312.29	185.2893	188.3814
1:31:01	75.807	179.45		1:31:01	151.656	179.00		1:31:01	315.62	186.3521	
1:32:01	76.641	179.24		1:32:01	153.322	179.10		1:32:01	318.95	192.3806	
1:33:01	77.475	178.39		1:33:01	154.989	178.59		1:33:01	322.32	192.811	
1:34:01	78.309	177.97		1:34:01	156.656	178.29		1:34:01	352.62	193.9536	
1:35:01	79.142	177.75	178.56	1:35:01	158.323	177.83	178.56	1:35:01	328.96	195.4929	192.198
1:36:01	79.976	177.97		1:36:01	159.991	177.94		1:36:01	332.29	194.8819	
1:37:01	80.81	177.97		1:37:01	161.658	178.59		1:37:01	335.65	194.5589	
1:38:01	81.644	177.55		1:38:01	163.326	178.70		1:38:01	338.96	195.0506	
1:39:01	82.477	176.30		1:39:01	164.993	178.29		1:39:01	342.30	195.3757	
1:40:01	83.311	176.51	177.26	1:40:01	166.66	179.67	178.64	1:40:01	345.65	197.5622	195.4858
1:41:01	84.145	177.55		1:41:01	168.327	180.28		1:41:01	348.96	197.5622	
1:42:01	84.978	177.34		1:42:01	169.994	179.51		1:42:01	352.30	197.5622	
1:43:01	85.812	177.13		1:43:01	171.661	179.51		1:43:01	355.32	199.2752	
1:44:01	86.646	177.13		1:44:01	173.328	179.20		1:44:01	358.97	199.2752	
1:45:01	87.479	176.30	177.09	1:45:01	174.996	179.31	179.56	1:45:01	362.20	199.2752	198.59
1:46:01	88.313	175.89		1:46:01	176.663	179.97		1:46:01	365.62	199.2752	
1:47:01	89.147	175.48		1:47:01	178.33	179.67		1:47:01	368.97	200.901	
1:48:01	89.981	175.48		1:48:01	179.997	179.20		1:48:01	372.30	201.3704	
1:49:01	90.814	175.68		1:49:01	181.664	179.97		1:49:01	375.64	199.8568	
1:50:01	91.648	175.89	175.69	1:50:01	183.331	181.06	179.98	1:50:01	378.98	200.901	200.4609
1:51:01	92.482	176.51		1:51:01	184.998	181.06		1:51:01	382.21	197.4307	
1:52:01	93.315	176.92		1:52:01	186.666	180.55		1:52:01	385.46	197.9711	
1:53:01	94.149	176.51		1:53:01	188.333	180.44		1:53:01	388.97	197.3698	
1:54:01	94.982	176.71		1:54:01	190	180.44		1:54:01	392.31	198.0914	
1:55:01	95.816	177.97	176.92	1:55:01	191.668	181.17	180.73	1:55:01	395.64	199.18	198.0086
1:56:01	96.65	177.55		1:56:01	193.335	182.48		1:56:01	398.98	198.0303	
1:57:01	97.484	177.55		1:57:01	195.002	183.28		1:57:01	402.31	198.6334	
1:58:01	98.318	178.39		1:58:01	196.669	183.28		1:58:01	405.68	200.8348	
1:59:01	99.151	178.17		1:59:01	198.336	182.80		1:59:01	408.98	200.8967	
2:00:01	99.985	177.97	177.93	2:00:01	200.004	182.91	182.95	2:00:01	412.22	199.6666	199.6124
2:01:01	100.818	177.75				180.80	180.7998	2:01:01	415.65	199.8514	
2:02:01	101.652	178.39						2:02:01	418.98	200.8348	
2:03:01	102.486	178.81						2:03:01	422.23	201.3304	
2:04:01	103.319	178.60						2:04:01	429.65	204.5057	
2:05:01	104.153	177.97	178.30							167.1417	201.6306
2:06:01	104.987	177.97									167.4176
2:07:02	105.821	175.46									
2:08:02	106.655	178.39									
2:09:02	107.488	178.60									
2:10:02	108.322	178.81	177.85								
2:11:02	109.155	178.60									
2:12:02	109.989	178.39									
2:13:02	110.822	177.75									
2:14:02	111.656	178.81									
2:15:02	112.469	174.72	177.65								
		205.95	205.95								

D- 4- 2

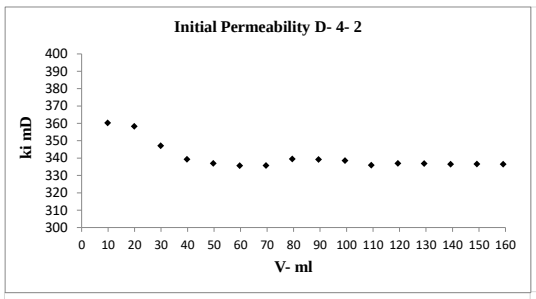

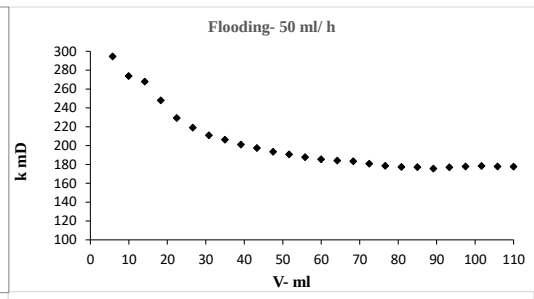

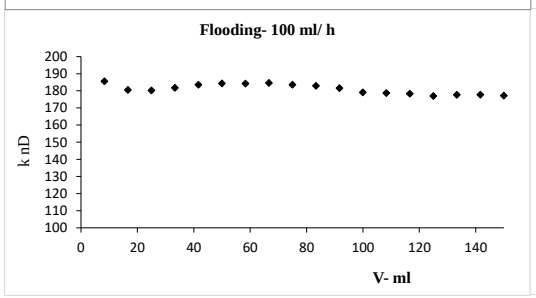

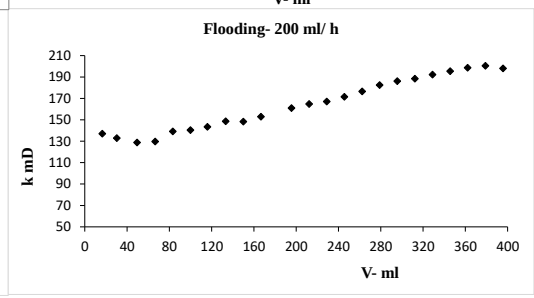

Total Clay 4.95

Group	Sample ID	Quartz	Calcite Mg	Oligoclase	Microcline	Chl. IIb	Kao.	Illite 2M1	Biotite 1M	Dol.	amorph.	Total Clay	Φ_{He} (%)	k_{wi} (mD)
D- 4	- 4- 1874.0	80.7	2.8	5.7	0.8	1.5	1.0	3.0	0.1	0.5	4.0	5.49	27.72	830.34
	- 4- 1872.6	80.0	3.2	6.0	1.0	0.8	0.9	3.3	....	0.9	4.0	4.95	25.62	338.92

ki	k1	k2	k3
343.24	205.95	180.8	167.41
100			
D :	40.00	47.33	51.23
		ki/kf	
50	49.79	1.67	50
100	62.82	1.90	100
200	58.28	2.05	200

Appendix G

SME images and Tables of core characteristics before Flooding

Sample D- 2- 6 (5%NaCl Brine)	Size µm	Textural pos.	Associated	micro p.
kaolinite booklets	20*150	pore filling	no	developed
kaolinite coating	<20		no	No developed
Chlorite and illite	10- 50	partially filling the pores	no	Developed
Micaceous flakes	100*150	pore filling	Fe, Ca carb	Developed
Clinochlore	100- 200	pore filling	no	Might be developed
carbonates	50- 100	Totally filling the pores	no	Developed
Quartz grains	10- 200	grains	no	Not developed
Aptite	<50	pore filling	no	Not developed
ill=illite, cc=calcite, si=silica, apatite, carbonate				

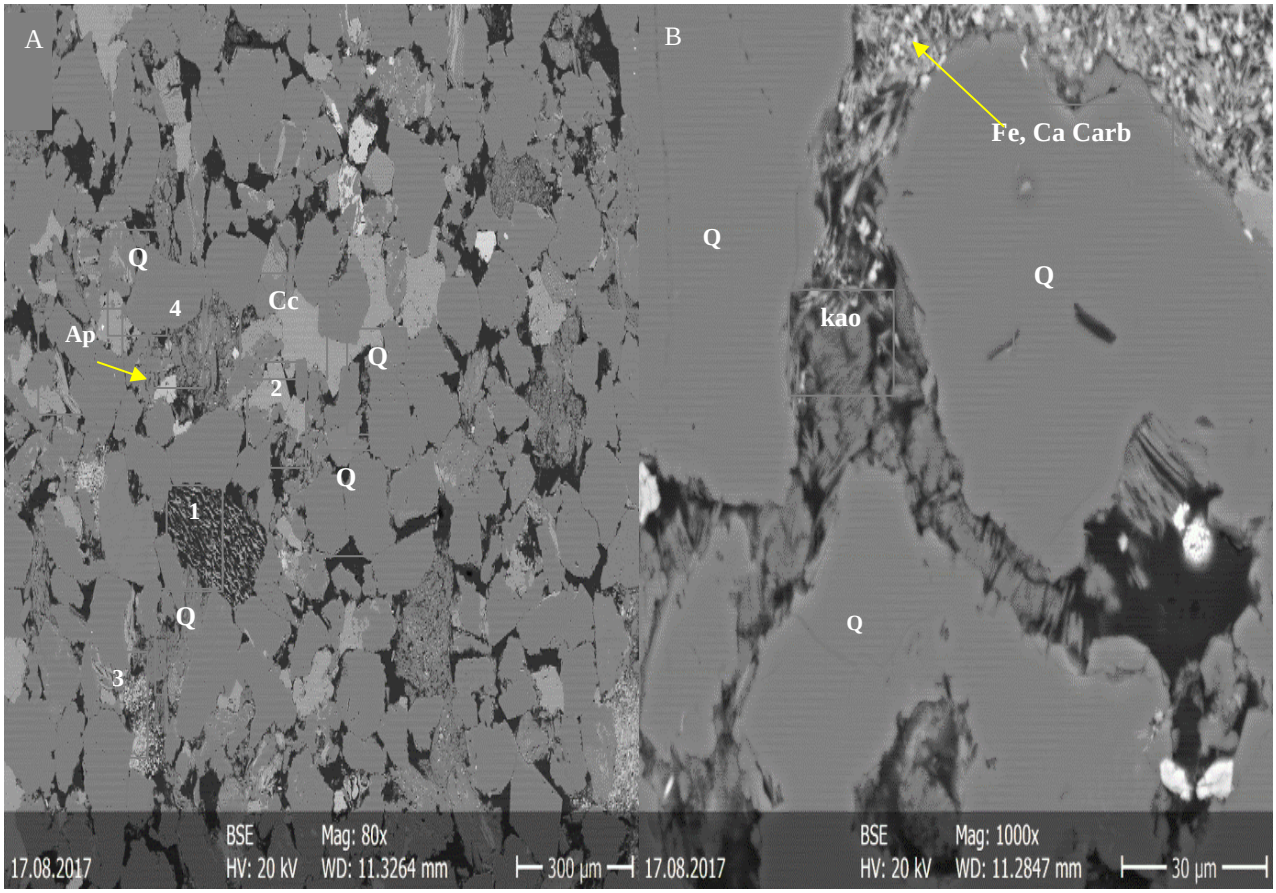

Appendix G

Sample D- 2- 5 (5%NaCl Brine)	Size µm	Textural pos.	Associated	micro p.
kaolinite booklets	20*100	pore filling	not	not
kaolinite platelets	< 10	Pore filling	With chl	Might be
exfoliated chlorite	100*150	pore filling	Fe, Ca carb	Not generated
Chlorite lamella	< 20	Pore filling	Ill + si	not
Kfp and Ab	100* 200	Between the quartz grains	not	Not developed
Flaky muscovite	20* 50	Filling the pores	not	Not generated
ill=illite, cc=calcite, si=silica, Ap= apatite, chl= chlorite, Kfp= K- feldspar, Ab= albite				

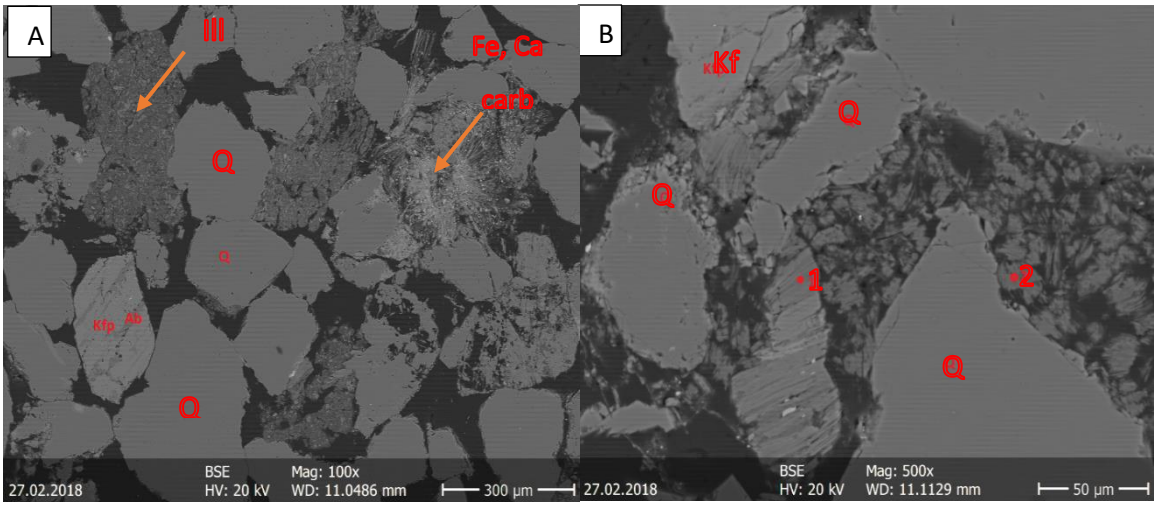

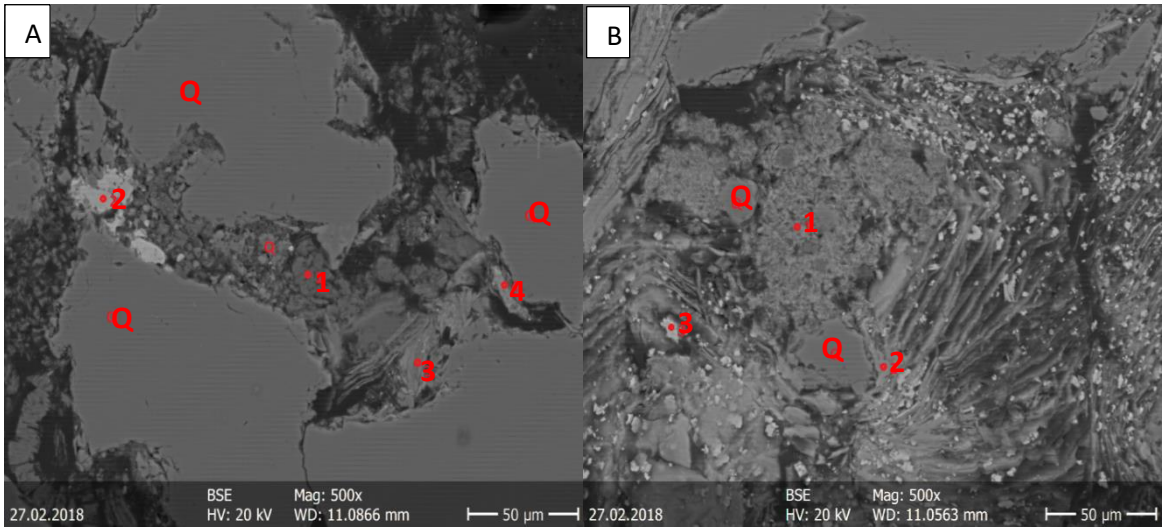

Appendix G

Sample D- 2- 4 (5%NaCl Brine)	Size µm	Textural pos.	Associated	micro p.
kaolinite booklets	20*200	pore filling	ill, cc, si	Not developed
kaolinite coating	< 20	Pore filling		Not developed
exfoliated chlorite	100*150	Bridging the interconnected pore channels	Fe, Ca carb	Developed
illite flakes	30* 100	Pore filling	With si and cc	Cemented by silica not generate micro porosity
Flaky muscovite	30* 50	Pore filling	As an individual grains	Not generate
Illite/ chlorite	<10	Pore filling	With Fe, Ca carb	developed
ill=illite, cc=calcite, si=silica, Ab= albite, kao= kaolinite, chl= chlorite, Ms= muscovite, cc= calcite, Kfp= k- feldspar, Ep, epidote				

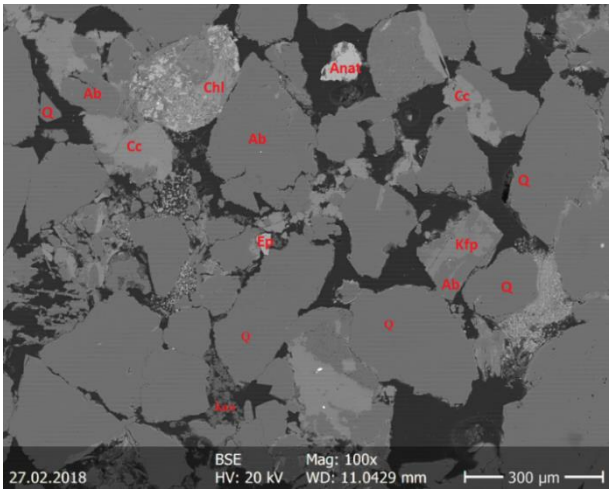

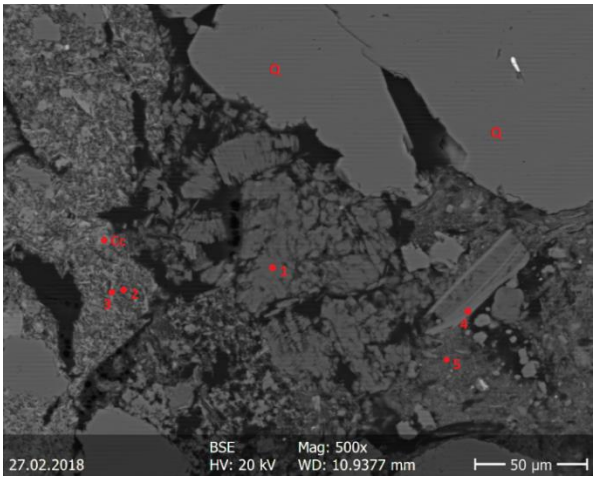

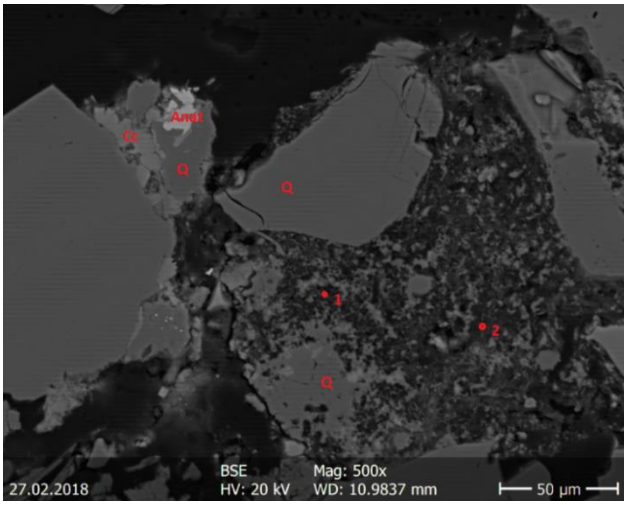

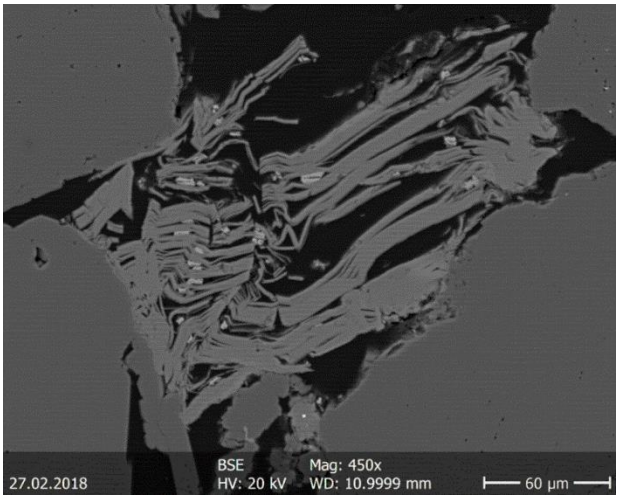

Appendix G

Sample D- 4- 2 (5%NaCl Brine)	size	Textural pos.	Associated	micro p.
kaolinite booklets	5-30	pore filling	ill, cc, si	developed
kaolinite coating	<40	Pore filling	no	developed
chlorite	<30	pore filling	no	developed
illite	<10	Pore filling	no	Might be developed
Exfoliated muscovite	5- 20	Pore filling	Fe,Ca carb	developed
Quartz	20- 120	Pore grains	no	Might be developed
carbonates	<8	Pore filling	Fe,Ca carb	developed
ill=illite, cc=calcite, si=silica				

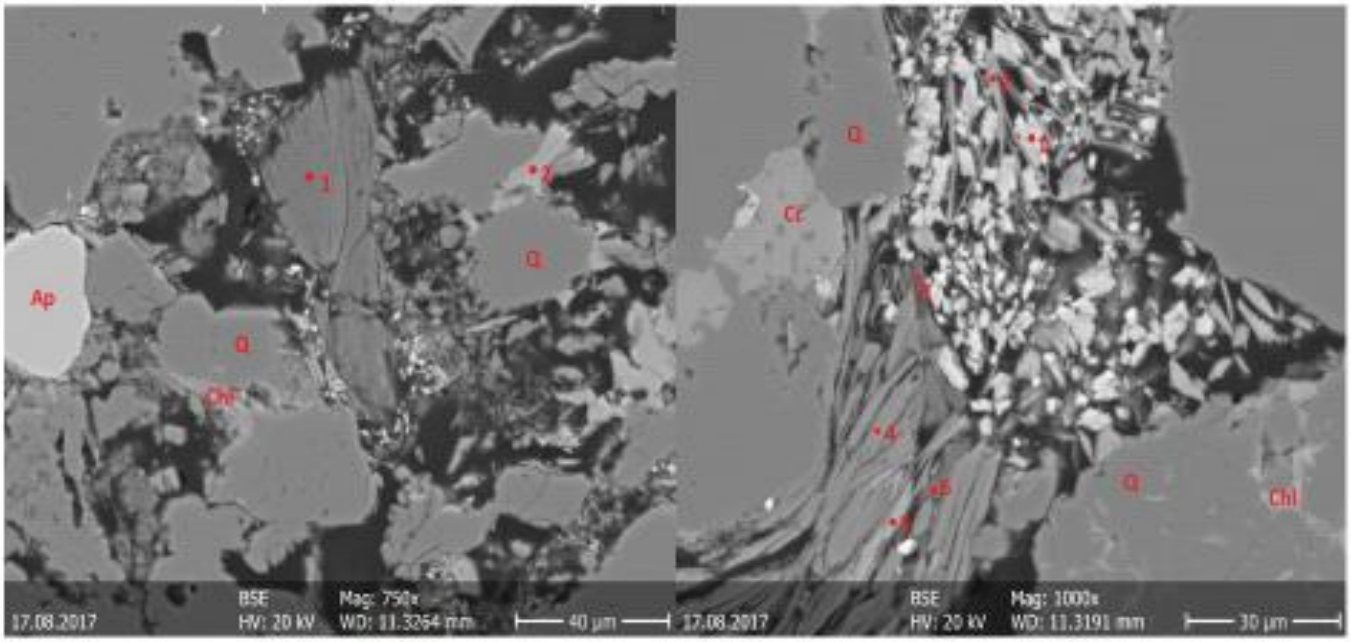

Appendix G

Sample D- 4- 1 (5%NaCl Brine)	size	Textural pos.	Associated	micro p.
kaolinite booklets	<10	pore filling	pure	not
Chlorite grains	< 20	Pore filling	With other clay minerals	Might be
illite	<15	pore filling	With other clay minerals	Might be
Exfoliated muscovite	30- 100	Pore filling	Fe, Mg carb with other clay minerals	developed
Quartz grain	20- 300	Grain and between the pores	Ms, chl, bio, cc, ca carbonate	Might be
ill=illite, cc=calcite, si=silica, kao= kaolinite, chl= chlorite, carb= carbonate, Ms= muscovite, bio= biotite, cc= calcite				

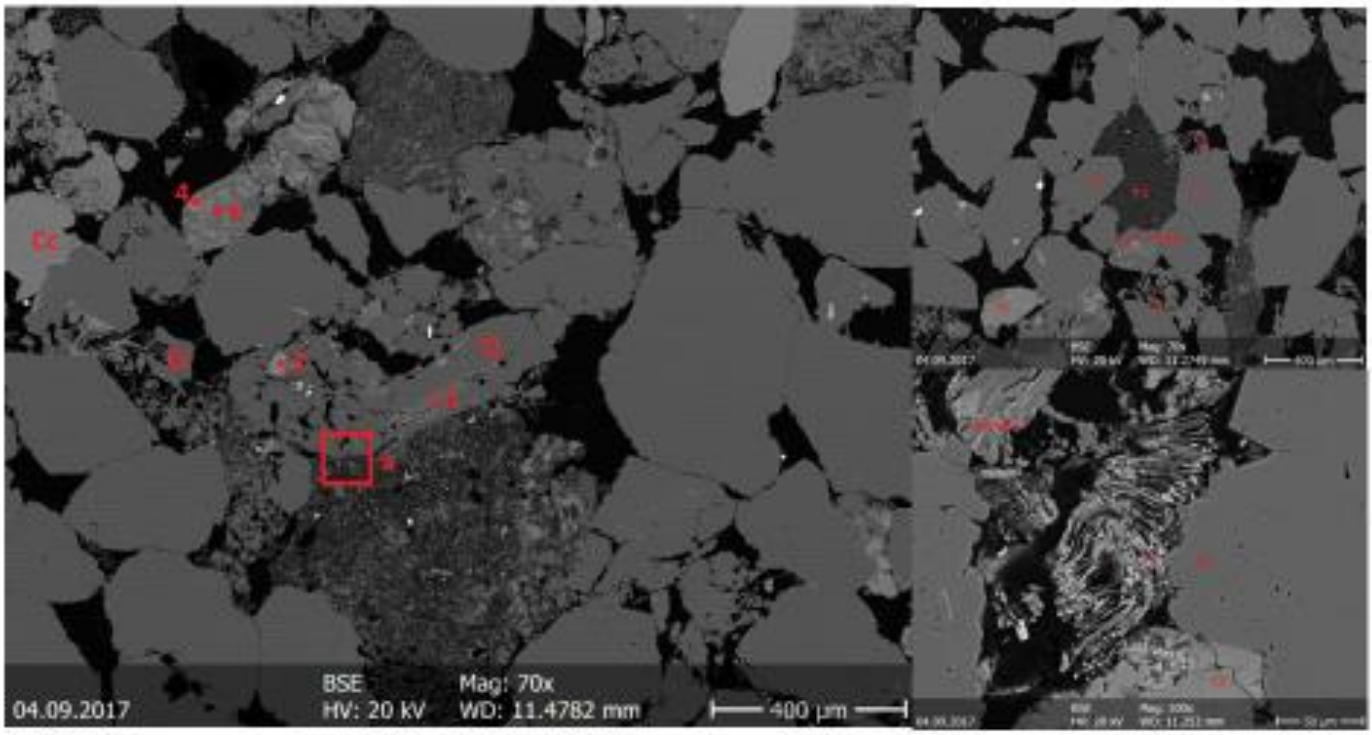

Appendix G

Sample D- 3- 2 (5%NaCl Brine)	Size µm	Textural pos.	Associated	micro p.
kaolinite booklets	<10	pore filling	pure	Not develpoed
kaolinite paltelets	< 8	Pore filling	Between chl and Ms lamella	Might be
chlorite	20*30	pore filling	Ill/chl, g, si	Not generated
Illite lamella	50* 100	Pore bridging and pore filling	Chl, si, Ca carb,cc g, Ms	Might be
Illite/ chlorite	10*30	Pore filling	Kao, si, Ca carb	not
K-feldspar and albite	100- 200	Pore	Between the quartz grains	not
Micaceous flakes	50- 200	Pore filling	Ill, chl, fine grain quartz and Fe Ca carbonates	developed
Fe, Mg Carbonate	<5	Pore filling	Exist between micaceous flakes	developed
ill=illite, cc=calcite, si=silica, kao= kaolinite, ill/chl= interstratified illite/ chlorite, Ms= muscovite, g= glass, carb= carbonate, cc= calcite				

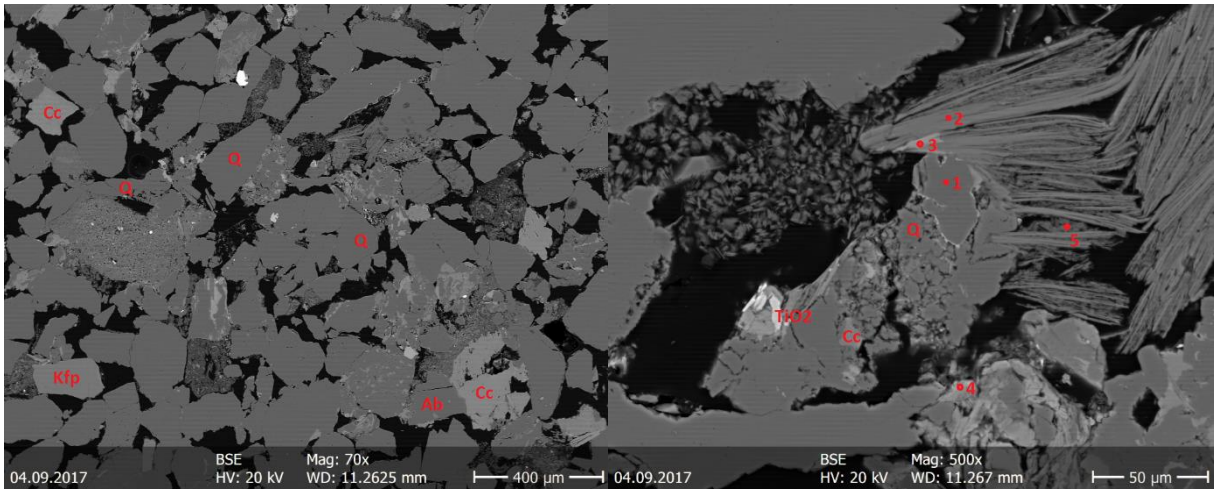

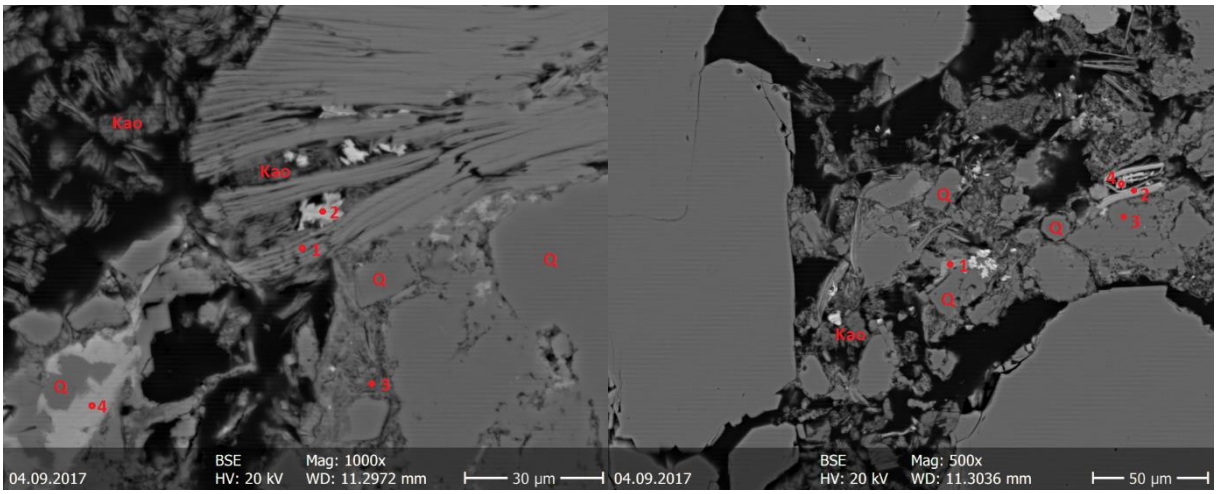

Appendix G

Sample D- 3- 1 (5%NaCl Brine)	Size	Textural pos.	Associated	micro p.
kaolinite booklets	<10	pore filling	pure	developed
kaolinite coating	<8	Pore filling	no	developed
Exfoliated chlorite	100*150	pore filling	Fe,Ca carb	Might be
illite	<10	Pore filling	Chl and fine grain quartz	Might be developed
Chlorite	<50	Pore filling	Ill, carbonates between muscovite flakes	Developed
Quartz	50- 400	Pore grains	not	Not developed
Fe- Mg carbonates	<10	Pore filling	Between micaceous flakes	developed
Micaceous flakes	50- 200	Pore filling	Fe, Mg carb	developed
ill=illite, cc=calcite, si=silica				

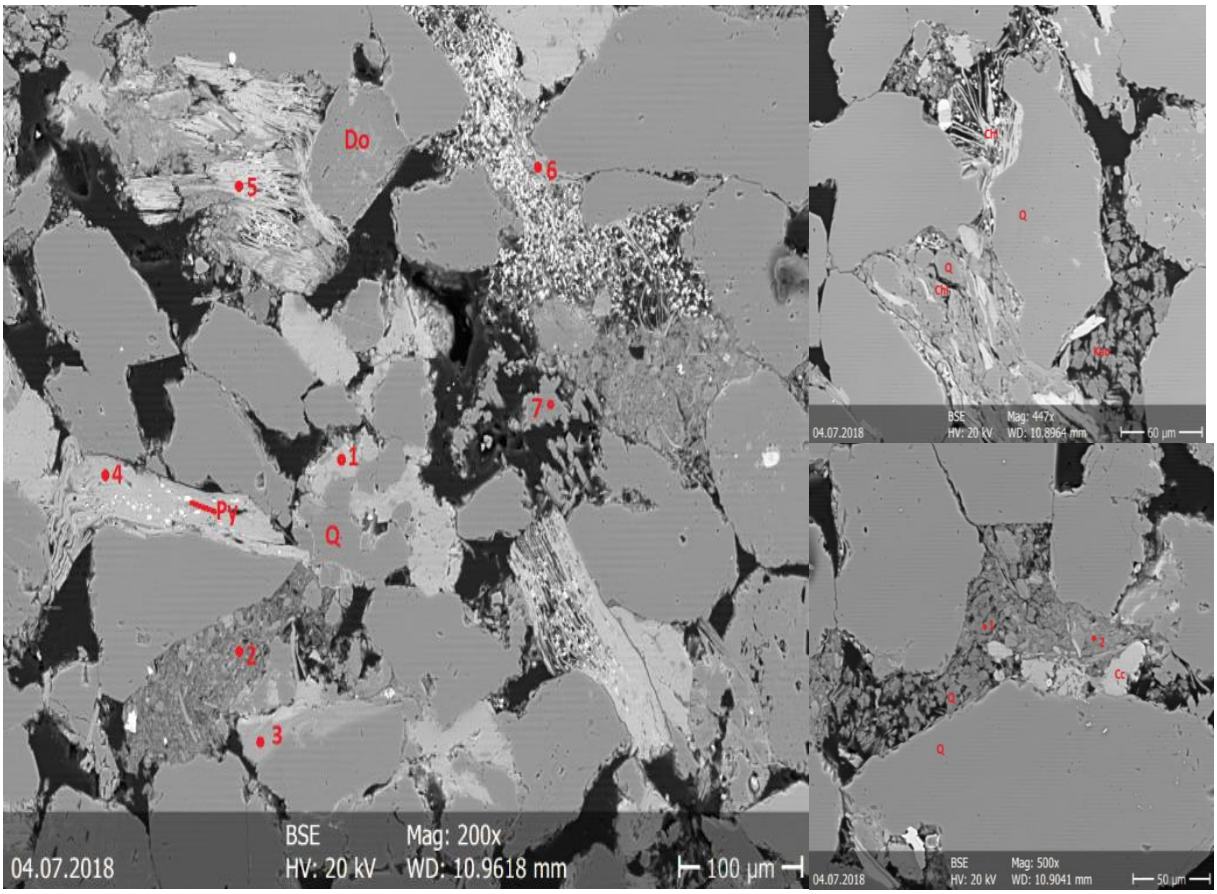

Appendix G

SME images and Tables of core characteristics After Flooding

Sample D- 2- 6 (pH9)	Size µm	Textural pos.	Associated	micro p.
kaolinite booklets	<10	pore filling	Ill, chl. And carbonated	developed
kaolinite coating	<10	Pore filling	no	developed
Chlorite and illite	<10- 50	partially filling the pores	Fine grain Q	Developed
Micaceous flakes	100*150	pore filling	Fe, Ca carb some of fine grains migrated	Developed and partially blocked some pores.
carbonates	<5- 50	Totally filling the pores	Chl, micaceous flakes and fine grain quartz	Developed
Quartz grains	<10- 200	grains	no	Not developed
ill=illite, cc=calcite, si=silica, apatite, carbonate, Q: quartz				

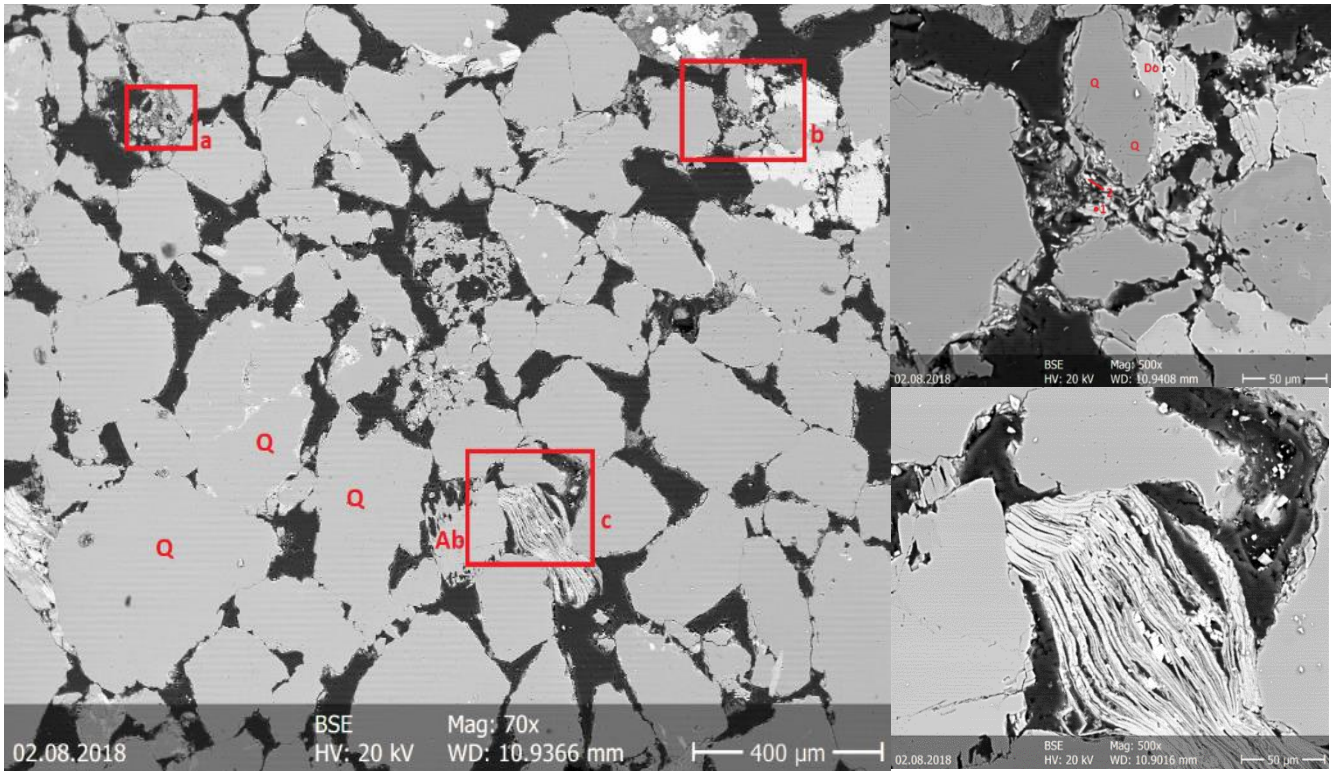

Appendix G

Sample D- 2- 5 (pH11)	Size µm	Textural pos.	Associated	micro p.
kaolinite booklets	<20-100	pore filling	With fine grain quartz, carbonates	Possibly developed
kaolinite platelets	< 10	Pore filling	With chl, ill and fine grain quartz	Might be
exfoliated chlorite	100*150	pore filling	Fe, Ca carb which is partially mobilized	generated
Chlorite and illite	< 20	Pore filling	Ill + si	generated
Kfp and Ab	100- 200	Between the quartz grains	not	Not developed
Flaky muscovite	20- 50	Filling the pores	not	generated
ill=illite, cc=calcite, si=silica, Ap= apatite, chl= chlorite, Kfp= K- feldspar, Ab= albite				

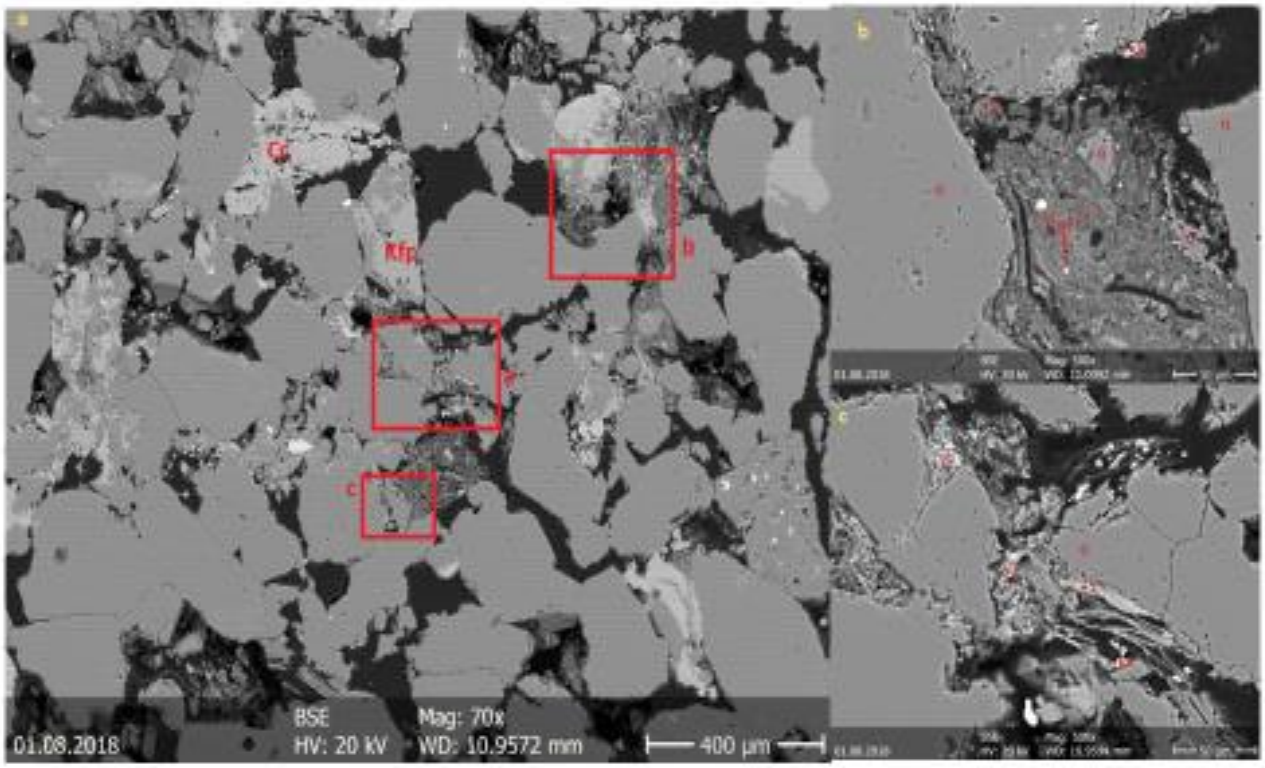

Appendix G

Sample D- 2- 4 (pH3)	Size µm	Textural pos.	Associated	micro p.
kaolinite booklets	<5- 50	pore filling	ill, cc, si, partially mobilsed	developed
kaolinite coating	< 20	Pore filling		Not developed
exfoliated chlorite	100-150	Bridging the interconnected pore channels	Fe, Ca carb partially moves from their original position.	Developed
illite flakes	<10- 100	Pore filling	With si and cc and chloite	Partially generated
Flaky muscovite	30- 80	Pore filling	As an individual grains	Not generate
Illite/ chlorite	<10	Pore filling	With Fe, Ca carb	developed
ill=illite, cc=calcite, si=silica, Ab= albite, kao= kaolinite, chl= chlorite, Ms= muscovite, cc= calcite, Kfp= k- feldspar, Ep, epidote				

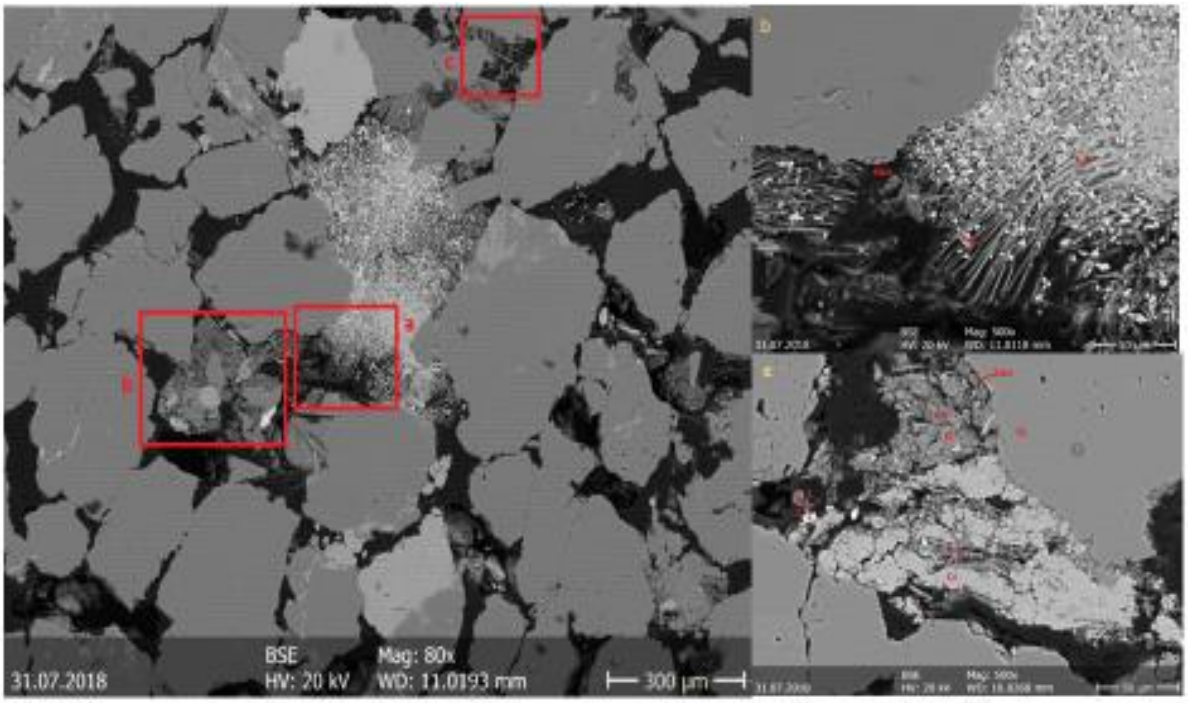

Appendix G

Sample D- 4- 2 (pH9)	Size µm	Textural pos.	Associated	micro p.
kaolinite booklets	<5-30	pore filling	ill, cc, si	developed
kaolinite coating	<30	Pore filling	no	developed
chlorite	<30	pore filling	no	Might be developed
illite	<10	Pore filling	no	Might be developed
Exfoliated muscovite	5- 20	Pore filling	Fe, Ca carb partially mobiles	developed
Quartz	20- 120	Pore grains	no	Might be developed
carbonates	<8	Pore filling	Fe, Ca carb mobilsed during flooding	developed
ill=illite, cc=calcite, si=silica, carb: carbonate				

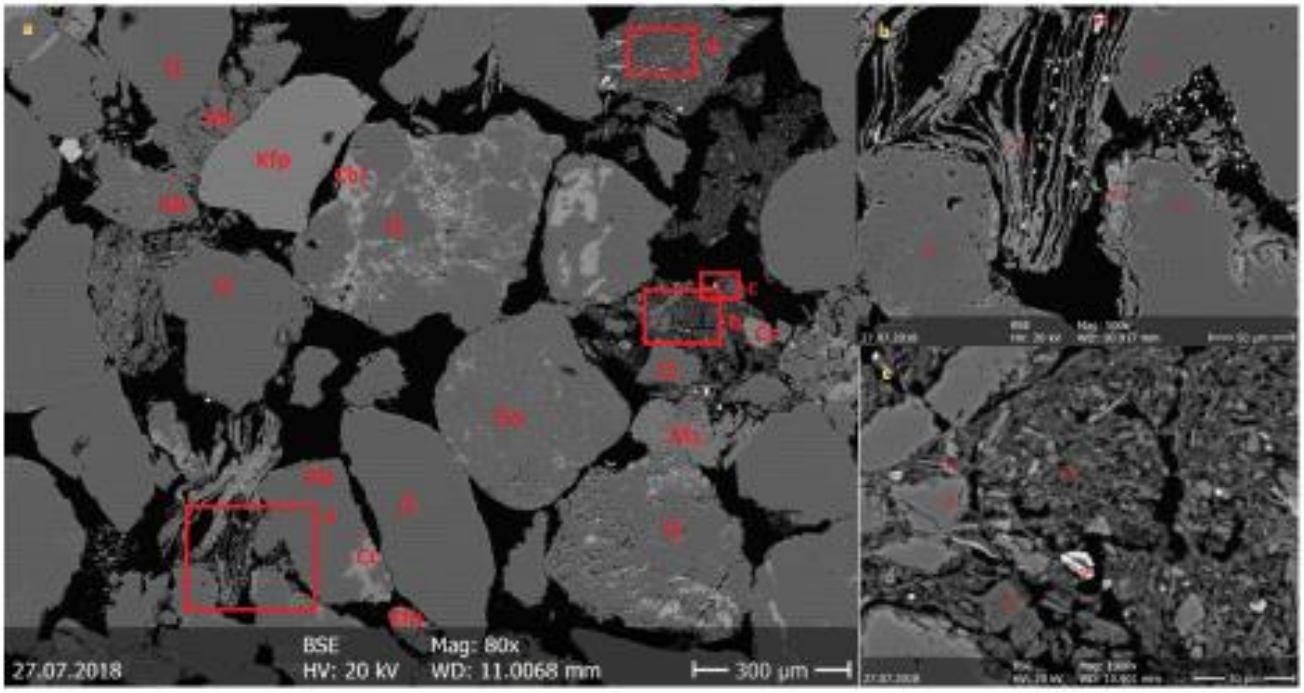

Appendix G

Sample D- 4- 1 (pH9)	Size µm	Textural pos.	Associated	micro p.
kaolinite booklets	<10	pore filling, partially mobilised	Clay mineral and FE, Mg carbonates	developed
Chlorite grains	< 20	pore filling	With other clay minerals	Might be
illite	<15	pore filling	With other clay minerals	Might be
Exfoliated muscovite	30- 100	Pore filling	Fe, Mg carb with other clay minerals, moved form their position	developed
Quartz grain	20- 300	Grain and between the pores	Ms, chl, bio, cc, ca carbonate, fine grains <5 **µm mobilized**	Might be
ill=illite, cc=calcite, si=silica, kao= kaolinite, chl= chlorite, carb= carbonate, Ms= muscovite, bio= biotite, cc= calcite				

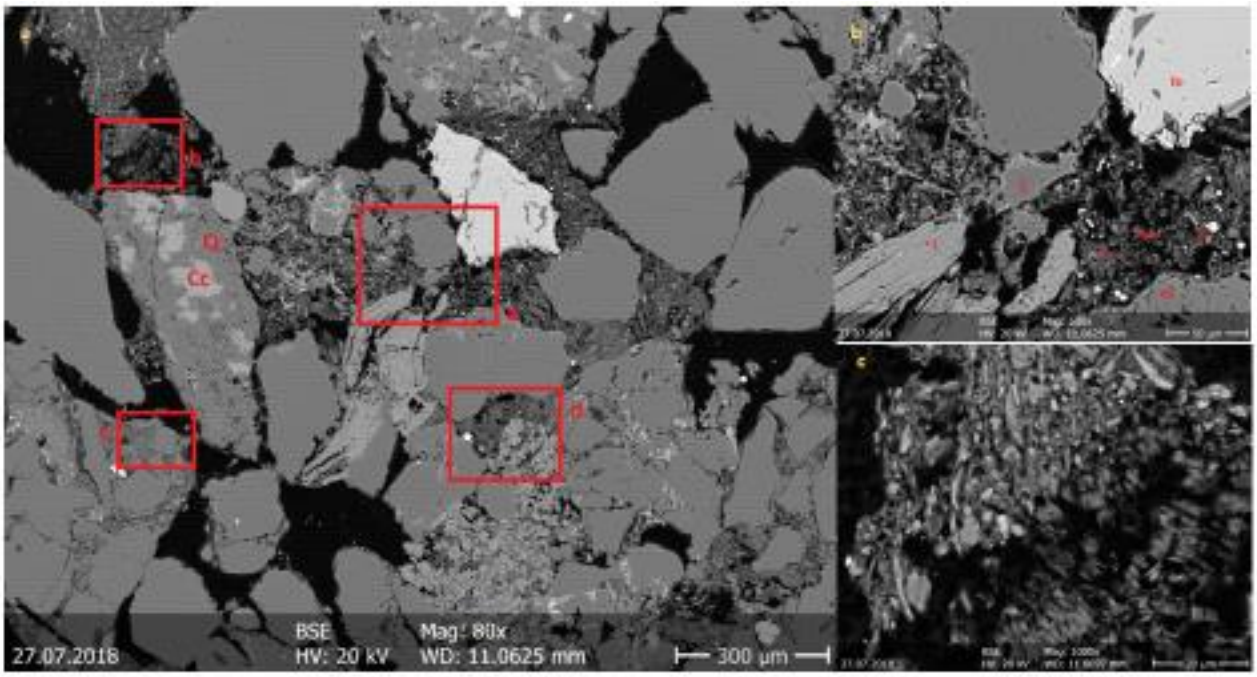

Appendix G

Sample D- 3- 2 (pH9)	Size µm	Textural pos.	Associated	micro p.
kaolinite booklets	<10	pore filling	Pure mobilized	Not developed
kaolinite paltelets	< 8	Pore filling	Between chl and Ms lamella, migrated partially	Possibly developed
chlorite	20*30	pore filling	Ill/chl, g, si, contributed fines migration	Might be generated
Illite lamella	50* 100	Pore bridging and pore filling	Chl, si, Ca carb,cc g, Ms, mobilized	Might be
Illite/ chlorite	10*30	Pore filling	Kao, si, Ca carb	Might be
K-feldspar and albite	100- 200	Pore	Between the quartz grains	not
Micaceous flakes	50- 200	Pore filling	Ill, chl, fine grain quartz and Fe Ca carbonates, not contributed fines migration	developed
Fe, Mg Carbonate	<5	Pore filling	Exist between micaceous flakes, partially mobilised	developed
ill=illite, cc=calcite, si=silica, kao= kaolinite, ill/chl= interstratified illite/ chlorite, Ms= muscovite, g= glass, carb= carbonate, cc= calcite				

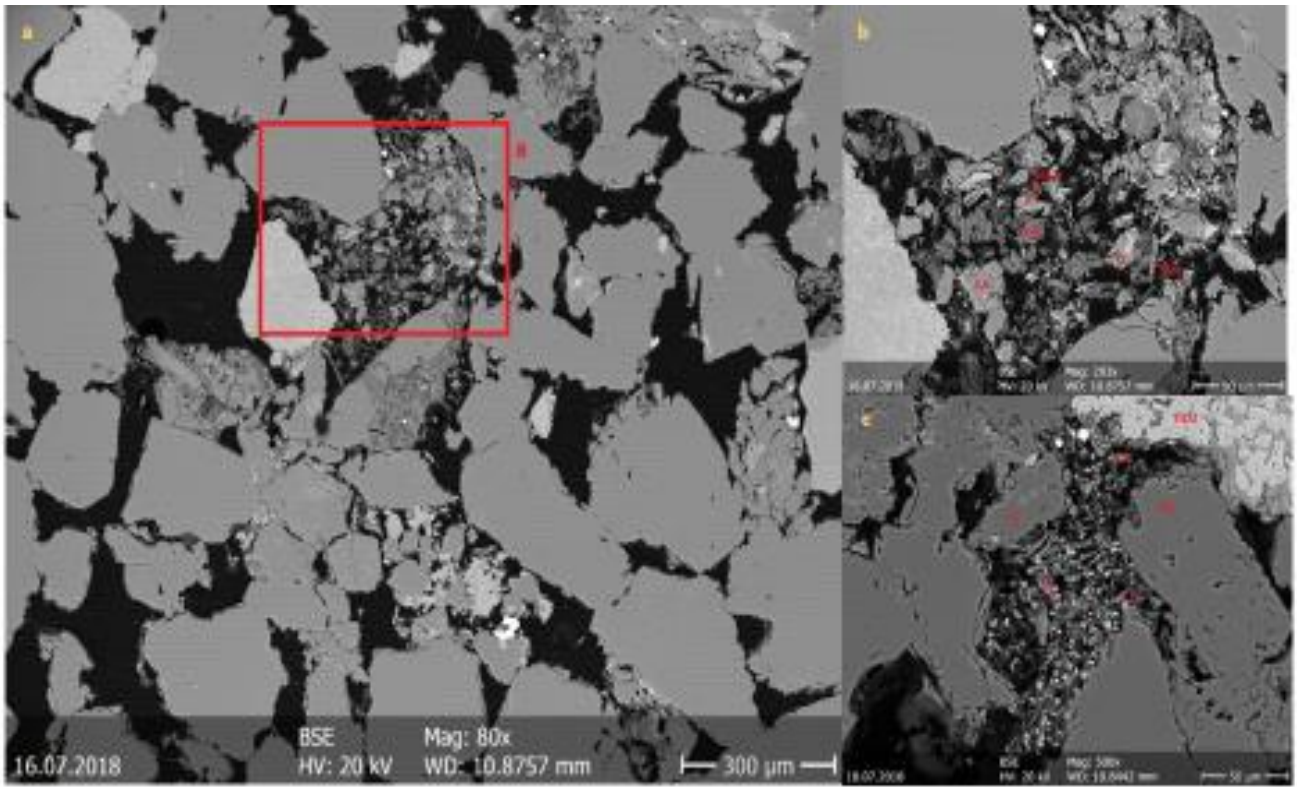

Appendix G

Sample D- 3- 1 (pH9)	Size µm	Textural pos.	Associated	micro p.
kaolinite booklets	<10	pore filling	Associate with other clay minerals, partially migrated	developed
kaolinite coating	<8	Pore filling	Clay minerals	Might be developed
Exfoliated chlorite	100*150	pore filling	Fe,Ca carb, partially mobilized form their original position	developed
illite	<10	Pore filling	Chl and fine grain quartz	Might be developed
Chlorite	<50	Pore filling	Ill, carbonates between muscovite flakes	Developed
Quartz	50- 400	Pore grains	not	Not developed
Fe- Mg carbonates	<10	Pore filling	Between micaceous flakes, partially mobilized.	developed
Micaceous flakes	50- 200	Pore filling	Fe, Mg carb	developed
ill=illite, cc=calcite, si=silica				

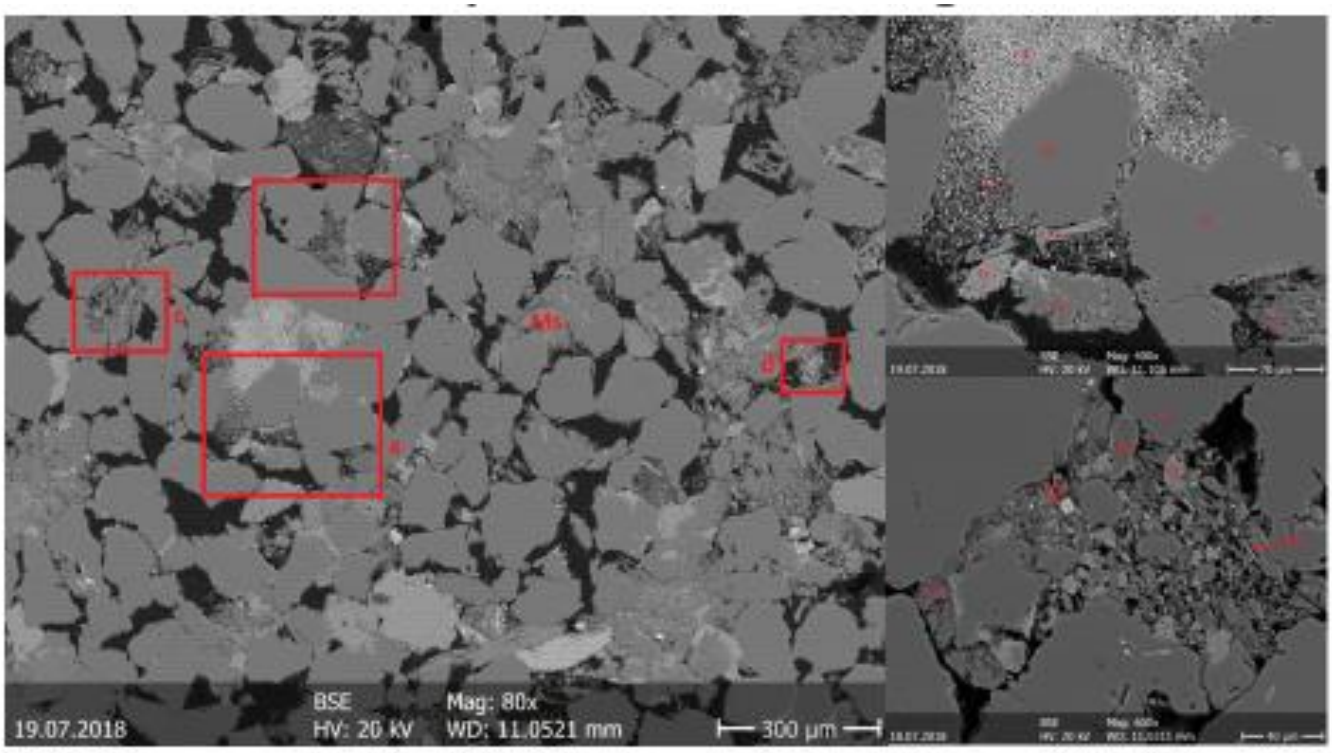

Appendix H

SEM Quantitative Result- Before Flooding

D-2-6

Quantitative Result

Elt	W%	A%	Formula	Ox%
O	47.32	62.25		0
Na	0.22	0.2	Na2O	0.3
Mg	1.39	1.2	MgO	2.3
Al	14.51	11.32	Al2O3	27.42
Si	27.08	20.29	SiO2	57.94
Cl	0.22	0.13		0.22
K	6.61	3.56	K2O	7.96
Ca	0.16	0.08	CaO	0.23
Ti	0.35	0.15	TiO2	0.59
Fe	2.13	0.8	Fe2O3	3.05
	100	100		100

D-2-5

Quantitative Result

Elt	W%	A%	Formula	Ox%
O	46.14	61.78		0
Mg	2.65	2.33	MgO	4.39
Al	17.09	13.57	Al2O3	32.29
Si	22.02	16.8	SiO2	47.11
Cl	0.13	0.08		0.13
K	5	2.74	K2O	6.02
Ti	0.37	0.17	TiO2	0.62
Fe	6.6	2.53	Fe2O3	9.44
	100	100		100

D-2-4

Quantitative Result

Elt	W%	A%	Formula	Ox%
O	48.47	62.48		0
Na	0.42	0.38	Na2O	0.57
Mg	0.62	0.53	MgO	1.03
Al	21.5	16.44	Al2O3	40.63
Si	24.1	17.7	SiO2	51.56
S	0.11	0.07	SO3	0.28
Cl	0.11	0.06		0.11
K	3.87	2.04	K2O	4.67
Ti	0.14	0.06	TiO2	0.24
Fe	0.64	0.24	Fe2O3	0.92
	100	100		100

D-4-2				
Quantitative Result				
Elt	W%	A%	Formula	Ox%
O	46.74	61.45		0
Na	0.56	0.51	Na2O	0.75
Mg	0.82	0.71	MgO	1.36
Al	19.5	15.2	Al2O3	36.84
Si	23.38	17.51	SiO2	50.01
K	7.53	4.05	K2O	9.07
Ti	0.17	0.08	TiO2	0.29
Fe	1.31	0.49	FeO	1.69
	100	100		100

D-4-1				
Quantitative Result				
Elt	W%	A%	Formula	Ox%
O	48.15	62.91		0
Mg	1.5	1.29	MgO	2.49
Al	10.62	8.23	Al2O3	20.07
Si	31.7	23.59	SiO2	67.81
Cl	1.61	0.95		1.61
K	3.84	2.05	K2O	4.63
Ti	0.22	0.09	TiO2	0.36
Fe	2.35	0.88	FeO	3.03
	100	100		100

D-3-2				
Quantitative Result				
Elt	W%	A%	Formula	Ox%
O	47.16	61.77		0
Na	0.27	0.25	Na2O	0.36
Mg	0.95	0.82	MgO	1.58
Al	19.77	15.35	Al2O3	37.35
Si	23.69	17.68	SiO2	50.68
K	6.54	3.5	K2O	7.87
Ca	0.01	0.01	CaO	0.02
Ti	0.16	0.07	TiO2	0.26
Fe	1.45	0.54	FeO	1.86
	100	100		100

D-3-1				
Quantitative Result				
Elt	W%	A%	Formula	Ox%
O	29.14	50.43		0
Mg	1.19	1.36	MgO	1.98
Si	0.7	0.69	SiO2	1.5
Ca	68.31	47.2	CaO	95.58
Fe	0.66	0.33	Fe2O3	0.94
	100	100		100

SEM Quantitative Result- After Flooding

D- 2- 6 (pH 9)

Quantitative Result

Elt	W%	A%	Formula	Ox%
O	50.97	64.81		0
Mg	1.31	1.09	MgO	2.17
Al	7.5	5.65	Al2O3	14.17
Si	37.44	27.12	SiO2	80.1
K	1.83	0.95	K2O	2.2
Ca	0.19	0.1	CaO	0.27
Fe	0.76	0.28	Fe2O3	1.09
	100	100		100

Quantitative Result

Elt	W%	A%	Formula	Ox%
O	44.34	61.22		0
Mg	8.11	7.37	MgO	13.45
Al	13.26	10.86	Al2O3	25.05
Si	17.67	13.9	SiO2	37.81
K	0.28	0.16	K2O	0.34
Ca	0.18	0.1	CaO	0.25
Fe	16.15	6.39	Fe2O3	23.1
	100	100		100

Quantitative Result

Elt	W%	A%	Formula	Ox%
O	43.79	61.18		0
Na	0.46	0.44	Na2O	0.61
Mg	6.35	5.84	MgO	10.53
Al	14.8	12.26	Al2O3	27.96
Si	16.12	12.83	SiO2	34.49
K	0.1	0.06	K2O	0.12
Ca	0.12	0.07	CaO	0.17
Fe	18.27	7.31	Fe2O3	26.12
	100	100		100

D- 2- 5 (pH 11)				
Quantitative Result				
Elt	W%	A%	Formula	Ox%
O	42.96	61.03		0
Mg	9.54	8.92	MgO	15.82
Al	9.51	8.01	Al2O3	17.97
Si	16.37	13.25	SiO2	35.02
P	0.18	0.13	P2O5	0.41
K	0.12	0.07	K2O	0.14
Ca	0.56	0.32	CaO	0.78
Fe	19.04	7.75	Fe2O3	27.23
As	1.71	0.52	As2O5	2.62
	100	100		100

Quantitative Result				
Elt	W%	A%	Formula	Ox%
O	47.64	62.16		0
Na	0.44	0.4	Na2O	0.6
Mg	0.92	0.79	MgO	1.53
Al	19.04	14.74	Al2O3	35.98
Si	24.52	18.23	SiO2	52.45
K	5.46	2.91	K2O	6.57
Ca	0.11	0.06	CaO	0.15
Ti	0.16	0.07	TiO2	0.27
Fe	1.71	0.64	Fe2O3	2.45
	100	100		100
Quantitative Results				
Elt	W%	A%	Formula	Ox%
O	32.98	60.03		0
Mg	1.02	1.22	MgO	1.68
Al	1.26	1.36	Al2O3	2.38
Si	5.24	5.43	SiO2	11.21
S	0.22	0.2	SO3	0.55
K	0.2	0.15	K2O	0.24
Ca	3.76	2.73	CaO	5.26
Mn	3.1	1.64	MnO	4
Fe	52.23	27.24	Fe2O3	74.68
	100	100		100

D- 2- 4 (pH 3)				
Quantitative Result				
Elt	W%	A%	Formula	Ox%
O	47.17	61.78		0
Na	0.6	0.55	Na2O	0.81
Mg	1.14	0.98	MgO	1.89
Al	19.41	15.08	Al2O3	36.68
Si	23.51	17.54	SiO2	50.29
K	6.21	3.33	K2O	7.48
Ti	0.18	0.08	TiO2	0.31
Fe	1.78	0.67	Fe2O3	2.54
	100	100		100

Quantitative Result				
Elt	W%	A%	Formula	Ox%
O	42.37	60.52		0
Mg	8.47	7.96	MgO	14.04
Al	13.83	11.71	Al2O3	26.13
Si	13.23	10.76	SiO2	28.3
Mn	0.54	0.22	MnO	0.7
Fe	21.57	8.83	Fe2O3	30.84
	100	100		100
Quantitative Results				
Elt	W%	A%	Formula	Ox%
O	49.86	64.09		0
Mg	1.17	0.99	MgO	1.95
Al	10.14	7.73	Al2O3	19.16
Si	33.91	24.83	SiO2	72.54
K	2.96	1.56	K2O	3.56
Ca	0.49	0.25	CaO	0.69
Fe	1.47	0.54	Fe2O3	2.1
	100	100		100

D- 2- 4 (pH 9)				
Quantitative Result				
Elt	W%	A%	Formula	Ox%
O	32.69	58.33		0
Na	1.36	1.69	Na2O	1.84
Mg	3.32	3.89	MgO	5.5
Al	2.09	2.21	Al2O3	3.95
Si	2.92	2.97	SiO2	6.24
P	0.57	0.53	P2O5	1.31
Ca	6.02	4.28	CaO	8.42
Mn	1.57	0.82	MnO	2.03
Fe	49.47	25.28	Fe2O3	70.72
	100	100		100

Quantitative Result				
Elt	W%	A%	Formula	Ox%
O	30.08	59.14		0
Mg	0.6	0.78	MgO	1
Al	0.12	0.15	Al2O3	0.24
Si	0.25	0.28	SiO2	0.53
K	0.09	0.07	K2O	0.1
Ca	3.55	2.79	CaO	4.97
Mn	1.53	0.87	MnO	1.97
Fe	63.78	35.93	Fe2O3	91.19
	100	100		100

Quantitative Results				
Elt	W%	A%	Formula	Ox%
O	51.68	65.33		0
Na	0.3	0.26	Na2O	0.4
Mg	0.81	0.67	MgO	1.34
Al	5.21	3.91	Al2O3	9.85
Si	40.32	29.04	SiO2	86.26
K	1.13	0.58	K2O	1.36
Fe	0.55	0.2	Fe2O3	0.79
	100	100		100

D- 4. 1 (pH 9)				
Quantitative Result				
Elt	W%	A%	Formula	Ox%
O	52.88	66.4		0
Al	1.19	0.88	Al2O3	2.24
Si	45.28	32.39	SiO2	96.87
S	0.06	0.04	SO3	0.16
Cl	0.11	0.06		0.11
K	0.3	0.15	K2O	0.36
Ti	0.02	0.01	TiO2	0.03
Fe	0.15	0.05	Fe2O3	0.22
	100	100		100

Quantitative Result				
Elt	W%	A%	Formula	Ox%
O	49.8	64.12		0
Mg	1.19	1	MgO	1.97
Al	9.65	7.37	Al2O3	18.23
Si	34.17	25.06	SiO2	73.09
K	3.32	1.75	K2O	4
Ti	0.12	0.05	TiO2	0.21
Fe	1.75	0.65	Fe2O3	2.5
	100	100		100

Quantitative Results				
Elt	W%	A%	Formula	Ox%
O	47.17	63.14		0
Na	0.18	0.17	Na2O	0.24
Mg	1.88	1.65	MgO	3.12
Al	13.74	10.91	Al2O3	25.97
Si	23.51	17.92	SiO2	50.29
S	1.46	0.97	SO3	3.64
K	3.18	1.74	K2O	3.83
Ca	0.19	0.1	CaO	0.27
Ti	0.97	0.43	TiO2	1.61
Fe	7.72	2.96	Fe2O3	11.04
	100	100		100

D-3-2 (pH 9)				
Quantitative Result				
Elt	W%	A%	Formula	Ox%
O	44.75	61.38		0
Mg	7.2	6.49	MgO	11.93
Al	14.42	11.73	Al2O3	27.25
Si	18.22	14.23	SiO2	38.98
K	0.52	0.29	K2O	0.63
Ca	0.15	0.08	CaO	0.21
Mn	0.47	0.19	MnO	0.6
Fe	14.27	5.61	Fe2O3	20.4
	100	100		100

Quantitative Result				
Elt	W%	A%	Formula	Ox%
O	47.84	62.2		0
Na	0.31	0.28	Na2O	0.42
Mg	1.91	1.64	MgO	3.17
Al	17.24	13.29	Al2O3	32.58
Si	25.86	19.15	SiO2	55.32
K	5.57	2.97	K2O	6.71
Fe	1.26	0.47	Fe2O3	1.8
	100	100		100

Quantitative Results				
Elt	W%	A%	Formula	Ox%
O	46.48	62.85		0
Mg	4.87	4.34	MgO	8.08
Al	11.18	8.97	Al2O3	21.13
Si	24.31	18.73	SiO2	52.01
K	0.12	0.06	K2O	0.14
Fe	13.04	5.05	Fe2O3	18.64
	100	100		100

D-3-1 (pH 9)				
Quantitative Result				
Elt	W%	A%	Formula	Ox%
O	37.86	59.67		0
Na	0.36	0.39	Na2O	0.48
Mg	4.8	4.98	MgO	7.96
Al	6.05	5.65	Al2O3	11.43
Si	10.46	9.39	SiO2	22.37
P	0.2	0.16	P2O5	0.46
S	0.3	0.24	SO3	0.75
Cl	0.03	0.02		0.03
K	1.34	0.86	K2O	1.61
Ca	6.71	4.22	CaO	9.39
Ti	0.18	0.09	TiO2	0.29
Mn	0.86	0.4	MnO	1.12
Fe	30.85	13.93	Fe2O3	44.11
	100	100		100

Quantitative Result				
Elt	W%	A%	Formula	Ox%
O	34.94	59.26		0
Mg	4.17	4.66	MgO	6.92
Al	4.22	4.24	Al2O3	7.97
Si	6.05	5.85	SiO2	12.95
P	0.15	0.13	P2O5	0.35
K	0.73	0.51	K2O	0.88
Ca	6	4.06	CaO	8.4
Ti	0.38	0.21	TiO2	0.63
Mn	0.6	0.3	MnO	0.77
Fe	42.76	20.78	Fe2O3	61.14
	100	100		100

Note: The flow rate condition would not be able to specify at each table above because after measured the initial poro-perm the flooding exepriments were codnucted, the selected core plugs first were run at 50 ml/h; after that siwtched to 100ml/h and finally chnaged to 200ml/h continuously. After the flooding exepriments conducted the flooded core plugs took to further XRD and SEM investigation at the laboratory in order to investigate the influence of the degree of alkalanity (pH value), flow rate and the percentage of clay content. it means after flooding the SEM has taken.